Lipid antigens and immunoregulatory iNKT cells in the prevention and treatment of type 1 diabetes and related autoimmune diseases

A thesis submitted to the

University of Birmingham

for the degree of Doctor of Philosophy

September 2007

Faye Reddington, BSc (HONS)

For the

Pickety Mon Ficketies

Abstract

Invariant natural killer T (iNKT) cells constitute an important regulatory arm of the immune system. Defects in the number and activities of iNKT cells have been linked to the development of autoimmune diseases. The glycoprotein CD1d plays an integral part in the recognition and presentation of lipid antigens such as α-galactosylceramide (α-GalCer) to iNKT cells, producing a variety of anti-inflammatory (T_H2) cytokines, such as interleukin-4 (IL-4), and pro-inflammatory (T_H1) cytokines, such as interferon-γ (IFN-γ). A decreased number of iNKT cells and defects in their capacity to produce T_H2 cytokines is associated with autoimmune diseases, such as type 1 diabetes (T1D). α-GalCer stimulates both T_H1 and T_H2 responses. Some analogues of α-GalCer preferentially induce the production of T_H2 cytokines, highlighting the possibility that such compounds could have therapeutic potential with regards to T_H1 cell-mediated autoimmune diseases, such as T1D and SLE.

A library of α-GalCer analogues was synthesised and their ability to modulate immune responses analysed. Altering the length of the phytosphingosine chain in α-GalCer analogues was shown to drastically affect the T_H1:T_H2 response, with truncated phytosphingosine chains of 9 carbons skewing the response towards a predominantly T_H2 response. Substituting the galactose sugar head for glucose (α-GlcCer) or L-fucose (α-L-FucCer) also elicited differences in the immunological profile of α-GalCer analogues, with lymphocytic proliferation being greatest in the galactose analogue, followed by L-fucose, followed by a glucose analogue. These differences in activity were also mirrored in the cytokine responses of the analogues, suggesting the C4' hydroxyl group plays a key part in antigen recognition and activity. Analogues incorporating 2 double bonds in the *N*-acyl chain exhibited T_H2 cytokine profiles on a par with α-GalCer, yet dramatically decreased T_H1 responses were observed. They also considerably delayed the clinical presentation of glucosuria in NOD mice. These results have provided important insights into the nature of antigen binding with CD1d, recognition of the antigen by iNKT cell receptors, and how such factors play a role in skewing the immune response, thus highlighting areas where structural diversity could be introduced in order to exploit immunomodulating potential, and find a possible prophylactic therapy for the prevention and treatment of autoimmune diseases, such as T1D.

Declaration

The work recorded in this thesis was carried out in the School of Biosciences at the University of Birmingham, U.K. during the period of October 2003 to September 2006. The work in this thesis is original except where acknowledged by reference.

No portion of this work is being, or has been submitted for a degree, diploma or any other qualification at any other university.

Acknowledgements

Being diagnosed with type 1 diabetes in 1987 undoubtedly influenced my choice of PhD. There have been moments when I have wondered what prompted me to dedicate a further 3 plus years to post-graduate study, but like any challenging task, the ups have most certainly outweighed the downs. Not only did this PhD afford me the opportunity to work with some first-class researchers, it has vastly expanded my knowledge of autoimmune diseases, reignited my passion for biomedical science, and provided me with some treasured memories.

I would like to take this opportunity to thank Professor Gurdyal S Besra for granting me the opportunity to study for this PhD, and for his help and support over the past few years. I would also like to express my appreciation to Lynn, Sid and Ali for being there in times of scientific turmoil. The support, friendship and generosity from the Besra lab has led to countless giggles and good times, and I will look back at this time with fond memories. I must also thank Lynn for his unprecedented patter, top-notch jokes, numerous drinks and the dance(s).

I'd like to express my gratitude to Professor Steven A. Porcelli, who helped me secure a travel scholarship to his laboratory in New York, USA and for being so helpful during my time in the US. I felt it to be an extremely worthwhile experience, and gained a great deal from it.

I count myself truly lucky to have trodden the path of this PhD alongside four others from the Besra Lab: Luke, Veemal, Raju and Jess. V – I am honoured to have shared a fume-hood with you. Chemistry has, and will never be the same again. Lukey boy – you have provided me with hours of entertainment and advice, and if you ever fancy a career change, I'm sure you'd be snapped up as founding member of Out of Sync*. Jess – where do I start? You've

been there for rants, raves, and red wine, and have been a true rock. I could not have done this without you.

And last, but by no means least, I am sending monumental thanks to my family, for their love, support and encouragement throughout my PhD, and always.

Contents

Abstract	ii
Declaration	iii
Acknowledgements	iv
Table of contents	vi
List of figures	xvi
List of tables	xxi
List of abbreviations	xxii
Published work associated with this thesis	xxvi

Table of contents

Chapter 1

1.1	Cluster of Differentiation (CD1)	2
1.2	Group 1 CD1 proteins and associated antigens	3
1.3	CD1d microbial and self-lipid antigens	7
1.4	CD1d and α-GalCer	11
1.5	CD1 crystal structure	12
1.6	CD1 assembly	17
1.7	Invariant natural killer T (iNKT) cells	18
1.8	iNKT cell effector functions	27
1.9	The T_H1/ T_H2 response	27
1.10	Type 1 diabetes (T1D)	31
1.11	Systemic lupus erythematosus (SLE)	34
1.12	iNKT cells: TCRs, down-regulation, and expansion	35
1.13	Aims and objectives	38

Chapter 2

2.1.	Hydroxyl group variations	41
2.2.	Hydroxyl group variations	43
2.3.	Base chain length	45

2.4. Chemical synthesis 46
2.4.1. Protection of D-lyxose 46
2.4.2. Wittig reaction 48
2.4.3. Fluorinated Wittig salts 50
2.4.4. Catalytic hydrogenation 52
2.4.5. Mesylation and azidation 54
2.4.6. Silyl ether and benzoate protecting groups 55
2.5. Glycosylation and *N*-acylation products with varying base chains. 57
2.5.1. Glycosylation 58
2.5.2. Basic transesterification; removing benzoyl protecting groups 59
2.5.3. Reduction of the azide group 60
2.5.3.1. Trimethylphosphine and the Staudinger reaction 60
2.5.3.2. Reduction using hydrogen sulphide 61
2.6. Biological results and interpretation 62

Chapter 3

3.1. Introduction 74
3.2. α vs. β anomeric linkage 75
3.3. *O*- and *C*-glycosidic linkage 77
3.4. Variation of the hydroxyl group on the sugar 79
3.5. Results and Discussion 87
3.5.1. Chemical Methods 87
3.5.1.1. Glycosylation 87
3.5.1.2. Glycosylation using a glycosyl fluoride 87
3.5.1.3. Activated glycosyl fluoride donors 88
3.5.1.4. *N*-acylation using hexacosanoic acid 90
3.5.1.5. Removal of the benzyl ether protecting groups 91
3.5.1.6. Glycosylation using a glycosyl iodide 92
3.5.1.7. Variations on the C-6' hydroxyl group 95
3.6. Biological evaluation of glycolipid antigens α-GalCer (44), α-GlcCer (50) and α-L-FucCer (53). 96

Chapter 4

4.1. Introduction 108
4.2. Fluorescent analogues of α-GalCer 109
4.3. *N*-acyl chain length and saturation 113
4.4. Microbial glycolipid antigens 118

4.5. Results and discussion 121
4.5.1. Chemical synthesis 121
4.5.1.1. *N*-Hydroxysuccinimide esters of carboxylic acids and their use in *N*-acylation 121
4.5.2. PEGylation 123
4.6. Biological evaluation of glycolipid antigens varying in the *N*-acyl chain. 127

Chapter 5

5.1. Chemical synthesis 140
5.1.1. General chemical procedures 140
5.1.1.1. The formation of Wittig salts and subsequent olefination 140
5.1.1.2. Addition of a mesyl group 140
5.1.1.3. Deprotection of the mesylated base 141
5.1.1.4. General procedure for catalytic reduction 141
5.1.1.5. Introduction of an azide group 141
5.1.1.6. Addition of a TBDPS protecting group 142
5.1.1.7. Addition of benzoate groups 142
5.1.1.8. Removal of the TBDPS group 143
5.1.1.9. Preparation of pertrimethylsilyl-D-pyranoses 143
5.1.1.10. Coupling of pertrimethylsilylated sugars with benzoate-protected azido-phytosphingosine analogues 143
5.1.1.11. Removal of benzoate protecting groups 144
5.1.1.12. Preparation of *N*-hydroxy succinimide esters of various carboxylic acids 144
5.1.1.13. Azide reduction and subsequent *N*-acylation 145
5.2. Protection of D-lyxose 145
5.3. The Wittig reaction 147
5.3.1. (R)-1-[(4S,5R)-2,2-Dimethyl-5-(undec-1-enyl)-1,3-dioxolan-4-yl]-2-trityloxy-ethanol (3) 147
5.3.2. (R)-1-[(4S,5R)-2,2-Dimethyl-5-(oct-1-enyl)-1,3-dioxolan-4-yl]-2-trityloxy-ethanol (4) 148
5.3.3. (R)-1-[(4S,5R)-2,2-Dimethyl-5-(pent-1-enyl)-1,3-dioxolan-4-yl]-2-trityloxy-ethanol (5) 149
5.4. Addition of a mesylate group 150
5.4.1. Methanesulfonic acid (R)-1-[(4R,5R)-2,2-dimethyl-5-(undec-1-enyl)-1,3-dioxolan-4-yl]-2-trityloxy-ethyl ester (7) 150

5.4.2. Methanesulfonic acid (R)-1-[(4R,5R)-2,2-dimethyl-5-(oct-1-enyl)-1,3-dioxolan-4-yl]-2-trityloxy-ethyl ester (8) 151
5.4.3. Methanesulfonic acid (R)-1-[(4R,5R)-2,2-dimethyl-5-(pent-1-enyl)-1,3-dioxolan-4-yl]-2-trityloxy-ethyl ester (9) 152
5.5. Deprotection of the phytosphingosine base 153
5.5.1. Methanesulfonic acid (1R,2R,3R)-2,3-dihydroxy-1-hydroxymethyl-tetradec-4-enyl ester (10) 153
5.5.2. Methanesulfonic acid (1R,2S,3S)-2,3-dihydroxy-1-hydroxymethyl-undec-4-enyl ester (11) 154
5.5.3. Methanesulfonic acid (1R,2R,3R)-2,3-dihydroxy-1-hydroxymethyl-oct-4-enyl ester (12) 155
5.6. Reduction of the double bond 156
5.6.1. Methanesulfonic acid (1R,2R,3R)-2,3-dihydroxy-1-hydroxymethyl-tetradecyl ester (13) 156
5.6.2. Methanesulfonic acid (1R,2R,3R)-2,3-dihydroxy-1-hydroxymethyl-undecyl ester (14) 157
5.6.3. Methanesulfonic acid (1R,2R,3R)-2,3-dihydroxy-1-hydroxymethyl-octyl ester (15) 158
5.7. Azidation 159
5.7.1. (2S,3S,4R)-2-Azido-octadecane-1,3,4-triol (16) 159
5.7.2. (2S,3S,4R)-2-Azido-pentadecane-1,3,4-triol (17) 160
5.7.3. (2S,3S,4R)-2-Azido-dodecane-1,3,4-triol (18) 161
5.7.4. (2S,3S,4R)-2-Azido-nonane-1,3,4-triol (19) 161
5.8. Addition of *tert*-butyldiphenyl silyl protecting group 162
5.8.1. (2S,3S,4R)-2-azido-1-(*tert*-butyl-diphenyl-silanyloxy)-octadecane-3,4-diol (20) 162
5.8.2. (2S,3S,4R)- 2-Azido-1-(*tert*-butyl-diphenyl-silanyloxy)-pentadecane-3,4-diol (21) 163
5.8.3. (2S,3S,4R)- 2-Azido-1-(*tert*-butyl-diphenyl-silanyloxy)-dodecane-3,4-diol (22) 164
5.8.4. (2S,3S,4R)-2-Azido-1-(*tert*-butyl-diphenyl-silanyloxy)-nonane-3,4-diol (23) 165
5.9. Adding benzoate protecting groups 166
5.9.1. ((2S,3S,4R)-2-Azido-3,4-*bis*-benzoyloxy-octadecyloxy)-*tert*-butyl-diphenyl-silane (24) 166
5.9.2. ((2S,3S,4R)-2-Azido-3,4-*bis*-benzoyloxy-pentadecyloxy)-*tert*-butyl-diphenyl-silane (25) 167

5.9.3. ((2S,3S,4R)-2-Azido-3,4-*bis*-benzoyloxy-dodecyloxy)-*tert*-butyl-diphenyl-silane (26) 167
5.9.4. ((2S,3S,4R)-2-Azido-3,4-*bis*-benzoyloxy-nonyloxy)-*tert*-butyl-diphenyl-silane (27) 168
5.10. Removing the TBDPS group 169
5.10.1. (2S,3S,4R)-2-Azido-3,4-*bis*-benzoyloxy-octadecan-1-ol (28) 169
5.10.2. (2S,3S,4R)-Azido-3,4-*bis*-benzoyloxy-pentadecan-1-ol (29) 170
5.10.3. (2S,3S,4R)-2-Azido-3,4-*bis*-benzoyloxy-dodecan-1-ol (30) 171
5.10.4. (2S,3S,4R)-2-Azido-3,4-*bis*-benzoyloxy-nonan-1-ol (31) 172
5.11. Glycosyl iodide precursors 173
5.11.1. (3R,4S,5S,6R)-2,3,4,5-Tetrakis-trimethylsilanyloxy-6-trimethylsilanyloxymethyl-tetrahydropyran (32) 173
5.11.2. (3R,4S,5R,6R)-2,3,4,5-Tetrakis-trimethylsilanyloxy-6-trimethylsilanyloxymethyl-tetrahydropyran (33) 174
5.11.3. (2S,3R,4R,5S)-2-Methyl-3,4,5,6-tetrakis-trimethylsilanyloxy-tetrahydropyran (34) 175
5.12. Glycosylation 176
5.12.1. (2S,3R,4S,5R,6R)-2-((2S,3S,4R)-2-Azido-3,4-*bis*-benzoyloxy-octadecyloxy)-6-hydroxymethyl-tetrahydro-pyran-3,4,5-triol (35) 176
5.12.2. (2S,3R,4S,5R,6R)-2-((2S,3S,4R)-2-Azido-3,4-*bis*-benzoyloxy-pentadecyloxy)-6-hydroxymethyl-tetrahydro-pyran-3,4,5-triol (36) 177
5.12.3. (2S,3R,4S,5R,6R)-2-((2S,3S,4R)-2-Azido-3,4-*bis*-benzoyloxy-dodecyloxy)-6-hydroxymethyl-tetrahydro-pyran-3,4,5-triol (37) 178
5.12.4. (2S,3R,4S,5R,6R)-2-((2S,3S,4R)-2-Azido-3,4-*bis*-benzyloxy-nonyloxy)-6-hydroxymethyl-tetrahydro-pyran-3,4,5-triol (38) 179
5.13. Removal of benzoate protecting groups 181
5.13.1. 2-(2-Azido-3,4-dihydroxy-octadecyloxy)-6-hydroxymethyl-tetrahydro-pyran-3,4,5-triol (39) 181
5.13.2. (2S,3R,4S,5R,6R)-2-((2S,3S,4R)-2-Azido-3,4-dihydroxy-pentadecyloxy)-6-hydroxymethyl-tetrahydro-pyran-3,4,5-triol (40) 182
5.13.3. (2S,3R,4S,5R,6R)-2-((2S,3S,4R)-2-Azido-3,4-dihydroxy-dodecyloxy)-6-hydroxymethyl-tetrahydro-pyran-3,4,5-triol (41) 183
5.13.4. (2S,3R,4S,5R,6R)-2-((2S,3S,4R)-2-Azido-3,4-dihydroxy-nonyloxy)-6-hydroxymethyl-tetrahydro-pyran-3,4,5-triol (42) 184
5.14. Synthesis of *N*-hydroxy succinimide esters 185
5.14.1. Hexacosanoic acid 2,5-dioxo-pyrrolidin-1-yl ester (43) 185
5.15. Addition of an *N*-acyl chain 186

5.15.1. Hexacosanoic acid [(1S,2S,3R)-2,3-dihydroxy-1-((2S,3R,4S,5R,6R)-3,4,5-trihydroxy-6-hydroxymethyl-tetrahydro-pyran-2-yloxymethyl)-heptadecyl]-amide (44) 186
5.15.2. Hexacosanoic acid [(1S,2S,3R)-2,3-dihydroxy-1-((2S,3R,4S,5R,6R)-3,4,5-trihydroxy-6-hydroxymethyl-tetrahydro-pyran-2-yloxymethyl)-tetradecyl]-amide (45) 187
5.15.3. Hexacosanoic acid [(1S,2S,3R)-2,3-dihydroxy-1-((2S,3R,4S,5R,6R)-3,4,5-trihydroxy-6-hydroxymethyl-tetrahydro-pyran-2-yloxymethyl)-undecyl]-amide (46) 188
5.15.4. Hexacosanoic acid [(1S,2S,3R)-2,3-dihydroxy-1-((2S,3R,4S,5R,6R)-3,4,5-trihydroxy-6-hydroxymethyl-tetrahydro-pyran-2-yloxymethyl)-octyl]-amide (47) 189
5.16. Glycosylation with glucose 190
5.16.1. (2S,3R,4S,5S,6R)-2-((2S,3S,4R)-2-Azido-3,4-*bis*-benzyloxy-octadecyloxy)-6-hydroxymethyl-tetrahydro-pyran-3,4,5-triol (48) 190
5.17. Removal of benzoate protecting groups 192
5.17.1. (2S,3R,4S,5S,6R)-2-(2-Azido-3,4-dihydroxy-octadecyloxy)-6-hydroxymethyl-tetrahydro-pyran-3,4,5-triol (49) 192
5.18. Addition of an *N*-acyl chain 193
5.18.1. Hexacosanoic acid [(1S,2S,3R)-2,3-dihydroxy-1-((2S,3R,4S,5S,6R)-3,4,5-trihydroxy-6-hydroxymethyl-tetrahydro-pyran-2-yloxymethyl)-heptadecyl]-amide (50) 193
5.19. Glycosylation with L-fucose 194
5.19.1. (2R,3S,4R,5S,6S)-2-((2S,3S,4R)-2-Azido-3,4-*bis*-benzyloxy-octadecyloxy)-6-methyl-tetrahydro-pyran-3,4,5-triol (51) 194
5.20. Removal of benzoate protecting groups 195
5.20.1. (2R,3S,4R,5S,6S)-2-((2S,3S,4R)-2-Azido-3,4-dihydroxy-octadecyloxy)-6-methyl-tetrahydro-pyran-3,4,5-triol (52) 195
5.21. Addition of an *N*-acyl chain 196
5.21.1. Hexacosanoic acid [(1S,2S,3R)-2,3-dihydroxy-1-((2R,3S,4R,5S,6S)-3,4,5-trihydroxy-6-methyl-tetrahydro-pyran-2-yloxymethyl)-heptadecyl]-amide (53) 196
5.22. Synthesis of *N*-hydroxy succinimide esters 197
5.22.1. Tetracosanoic acid 2,5-dioxo-pyrrolidin-1-yl ester (54) 197
5.22.2. (15Z)-Tetracos-15-enoic acid 2,5-dioxo-pyrrolidin-1-yl ester (55) 198
5.22.3. (4Z,7Z,10Z,13Z,16Z,19Z)-Docosa-4,7,10,13,16,19-hexaenoic acid 2,5-dioxo-pyrrolidin-1-yl ester (56) 199

5.22.4. (5Z,8Z,11Z,14Z,17Z)-Eicosa-5,8,11,14,17-pentaenoic acid 2,5-dioxo-pyrrolidin-1-yl ester (57) 200
5.22.5. (5Z,8Z,11Z,14Z)-Eicosa-5,8,11,14-tetraenoic acid 2,5-dioxo-pyrrolidin-1-yl ester (58) 201
5.22.6. (11Z,14Z)-Eicosa-11,14-dienoic acid 2,5-dioxo-pyrrolidin-1-yl ester (59) 202
5.22.7. (11E)-Eicos-11-enoic acid 2,5-dioxo-pyrrolidin-1-yl ester (60) 202
5.22.8. (11Z)-Eicos-11-enoic acid 2,5-dioxo-pyrrolidin-1-yl ester (61) 203
5.22.9. Eicosanoic acid 2,5-dioxo-pyrrolidin-1-yl ester (62) 204
5.22.10. (9Z, 12Z)-Octadeca-9,12-dienoic acid 2,5-dioxo-pyrrolidin-1-yl ester (63) 204
5.22.11. Octanoic acid 2,5-dioxo-pyrrolidin-1-yl ester (64) 205
5.22.12. m-Tolyl-acetic acid 2,5-dioxo-pyrrolidin-1-yl ester (65) 206
5.23. Addition of an *N*-acyl chain 207
5.23.1. Tetracosanoic acid [(1S,2S,3R)-2,3-dihydroxy-1-((2S,3R,4S,5R,6R)-3,4,5-trihydroxy-6-hydroxymethyl-tetrahydro-pyran-2-yloxymethyl)-heptadecyl]-amide (68) 207
5.23.2. (15Z)-Tetracos-15-enoic acid [2,3-dihydroxy-1-(3,4,5-trihydroxy-6-hydroxymethyl-tetrahydro-pyran-2-yloxymethyl)-heptadecyl]-amide (69) 208
5.23.3. (4Z,7Z,10Z,13Z,16Z,19Z)-Docosa-4,7,10,13,16,19-hexaenoic acid [(1S,2S,3R)-2,3-dihydroxy-1-((2S,3R,4S,5R,6R)-3,4,5-trihydroxy-6-hydroxymethyl-tetrahydro-pyran-2-yloxymethyl)-heptadecyl]-amide (70) 209
5.23.4. (5Z,8Z,11Z,14Z,17Z)-Eicosa-5,8,11,14,17-pentaenoic acid [(1S,2S,3R)-2,3-dihydroxy-1-((2S,3R,4S,5R,6R)-3,4,5-trihydroxy-6-hydroxymethyl-tetrahydro-pyran-2-yloxymethyl)-heptadecyl]-amide (71) 210
5.23.5. (5Z,8Z,11Z,14Z)-Eicosa-5,8,11,14-tetraenoic acid [(1S,2S,3R)-2,3-dihydroxy-1-((2S,3R,4S,5R,6R)-3,4,5-trihydroxy-6-hydroxymethyl-tetrahydro-pyran-2-yloxymethyl)-heptadecyl]-amide (72) 211
5.23.6. (11Z,14Z)-Eicosa-11,14-dienoic acid [(1S, 2S, 3R)-2,3-dihydroxy-1-((2S, 3R, 4S, 5R, 6R)-3,4,5-trihydroxy-6-hydroxymethyl-tetrahydro-pyran-2-yloxymethyl)-heptadecyl]-amide (73) 212
5.23.7. (11Z,14Z)-Icosa-11,14-dienoic acid [(1S,2S,3R)-2,3-dihydroxy-1-((2S,3R,4S,5R,6R)-3,4,5-trihydroxy-6-hydroxymethyl-tetrahydro-pyran-2-yloxymethyl)-tetradecyl]-amide (74) 214
5.23.8. (11Z,14Z)-Eicosa-11,14-dienoic acid [(1S,2S,3R)-2,3-dihydroxy-1-((2S,3R,4S,5R,6R)-3,4,5-trihydroxy-6-hydroxymethyl-tetrahydro-pyran-2-yloxymethyl)-undecyl]-amide (75) 215

5.23.9. (11Z,14Z)-Eicosa-11,14-dienoic acid [(1S,2S,3R)-2,3-dihydroxy-1-((2S,3R,4S,5R,6R)-3,4,5-trihydroxy-6-hydroxymethyl-tetrahydro-pyran-2-yloxymethyl)-octyl]-amide (76) 216
5.23.10. (11E)-Eicos-11-enoic acid [(1S, 2S, 3R)-2,3-dihydroxy-1-((2S, 3R, 4S, 5R, 6R)-3,4,5-trihydroxy-6-hydroxymethyl-tetrahydro-pyran-2-yloxy-methyl)-heptadecyl]-amide (77) 217
5.23.11. (11Z)-Eicos-11-enoic acid [(1S, 2S, 3R)-2,3-dihydroxy-1-((2S, 3R, 4S, 5R, 6R)-3,4,5-trihydroxy-6-hydroxymethyl-tetrahydro-pyran-2-yloxy-methyl)-heptadecyl]-amide (78) 218
5.23.12. Eicosanoic acid [(1S, 2S, 3R)-2,3-dihydroxy-1-((2S, 3R, 4S, 5R, 6R)-3,4,5-trihydroxy-6-hydroxymethyl-tetrahydro-pyran-2-yloxymethyl)-heptadecyl]-amide (79) 220
5.23.13. (9Z, 12Z)-Octadeca-9,12-dienoic acid [(1S, 2S, 3R)-2,3-dihydroxy-1-((2S, 3R, 4S, 5R, 6R)-3,4,5-trihydroxy-6-hydroxymethyl-tetrahydro-pyran-2-yloxymethyl)-heptadecyl]-amide (80) 221
5.23.14. (9Z,12Z)-Octadeca-9,12-dienoic acid [(1S,2S,3R)-2,3-dihydroxy-1-((2S,3R,4S,5R,6R)-3,4,5-trihydroxy-6-hydroxymethyl-tetrahydro-pyran-2-yloxymethyl)-tetradecyl]-amide (81) 222
5.23.15. (9Z,12Z)-Octadeca-9,12-dienoic acid [(1S,2S,3R)-2,3-dihydroxy-1-((2S,3R,4S,5R,6R)-3,4,5-trihydroxy-6-hydroxymethyl-tetrahydro-pyran-2-yloxymethyl)-undecyl]-amide (82) 223
5.23.16. (9Z,12Z)-Octadeca-9,12-dienoic acid [(1S,2S,3R)-2,3-dihydroxy-1-((2S,3R,4S,5R,6R)-3,4,5-trihydroxy-6-hydroxymethyl-tetrahydro-pyran-2-yloxymethyl)-octyl]-amide (83) 224
5.23.17. Octanoic acid [(1S, 2S, 3R)-2,3-dihydroxy-1-((2S, 3R, 4S, 5R, 6R)-3,4,5-trihydroxy-6-hydroxymethyl-tetrahydro-pyran-2-yloxymethyl)-heptadecyl]-amide (84) 225
5.23.18. *N*-[(1S,2S,3R)-2,3-Dihydroxy-1-((2S,3R,4S,5R,6R)-3,4,5-trihydroxy-6-hydroxymethyl-tetrahydro-pyran-2-yloxymethyl)-heptadecyl]-3-propionamide (85) 227
5.23.19. *N*-[(1S,2S,3R)-2,3-Dihydroxy-1-((2S,3R,4S,5R,6R)-3,4,5-trihydroxy-6-hydroxymethyl-tetrahydro-pyran-2-yloxymethyl)-heptadecyl]-3-(2-ethoxy)-ethoxy]-ethoxy}-ethoxy)-propionamide (86) 228
5.23.20. *N*-[(1S,2S,3R)-2,3-Dihydroxy-1-((2S,3R,4S,5R,6R)-3,4,5-trihydroxy-6-hydroxymethyl-tetrahydro-pyran-2-yloxymethyl)-heptadecyl]-2-*m*-tolyl-acetamide (87) 229

5.23.21. Tetracosanoic acid [(1S,2S,3R)-2,3-dihydroxy-1-(3,4,5-trihydroxy-6-hydroxymethyl-tetrahydro-pyran-2-yloxymethyl)-heptadecyl]-amide (88) 230
5.23.22. (4Z,7Z,10Z,13Z,16Z,19Z)-Docosa-4,7,10,13,16,19-hexaenoic acid [(1S,2S,3R)-2,3-dihydroxy-1-(3,4,5-trihydroxy-6-hydroxymethyl-tetrahydro-pyran-2-yloxymethyl)-heptadecyl]-amide (89) 231
5.23.23. (5Z,8Z,11Z,14Z)-Eicosa-5,8,11,14-tetraenoic acid [(1S, 2S, 3R)-2,3-dihydroxy-1-(3,4,5-trihydroxy-6-hydroxymethyl-tetrahydro-pyran-2-yloxymethyl)-heptadecyl]-amide (90) 232
5.23.24. Eicosa-11,14-dienoic acid [(1S, 2S, 3R)-2,3-dihydroxy-1-(3,4,5-trihydroxy-6-hydroxymethyl-tetrahydro-pyran-2-yloxymethyl)-heptadecyl]-amide (91) 233
5.23.25. (11Z)-Eicos-11-enoic acid [2,3-dihydroxy-1-(3,4,5-trihydroxy-6-hydroxymethyl-tetrahydro-pyran-2-yloxymethyl)-heptadecyl]-amide (92) 234
5.23.26. (11E)-Eicos-11-enoic acid [2,3-dihydroxy-1-(3,4,5-trihydroxy-6-hydroxymethyl-tetrahydro-pyran-2-yloxymethyl)-heptadecyl]-amide (93) 235
5.23.27. Eicosanoic acid [2,3-dihydroxy-1-(3,4,5-trihydroxy-6-hydroxymethyl-tetrahydro-pyran-2-yloxymethyl)-heptadecyl]-amide (94) 236
5.23.28. Octadeca-9,12-dienoic acid [2,3-dihydroxy-1-(3,4,5-trihydroxy-6-hydroxymethyl-tetrahydropyran-2-yloxymethyl)-heptadecyl]-amide (95) 237
5.23.29. (11Z,14Z)-Nonadeca-11,14-dienoic acid [(1S,2S,3R)-2,3-dihydroxy-1-((2R,3S,4R,5S,6S)-3,4,5-trihydroxy-6-methyl-tetrahydro-pyran-2-yloxymethyl)-heptadecyl]-amide (96) 239
5.23.30. (9Z,12Z)-Octadeca-9,12-dienoic acid [(1S,2S,3R)-2,3-dihydroxy-1-((2R,3S,4R,5S,6S)-3,4,5-trihydroxy-6-methyl-tetrahydro-pyran-2-yloxymethyl)-heptadecyl]-amide (97) 240
5.24. Biological assays 241
5.24.1. Materials and methods 241
5.24.1.1. Protein expression and purification 241
5.24.1.2. Preparation of soluble heterodimeric TCRs 242
5.24.1.3. Surface Plasmon Resonance (SPR) 243
5.24.1.4. iNKT TCR tetramer staining 244
5.24.1.5. Enzyme-linked immunsorbent assay (ELISA) 244
5.24.1.6. iNKT cell expansion 245
5.24.1.7. Structural modeling 245
5.24.1.8. T cell proliferation 246
5.24.1.9. Measurement of cytokine secretion by *in vitro*-activated iNKT cells 246

5.24.1.10. Preparation of soluble CD1d fusion proteins and tetramers 246
5.24.1.11. Derivation of CD1d-restircted T cell clones 247
5.24.1.12. T cell responses to APCs 247
5.24.1.13. T cell responses to lipid Ags presented by plate-bound CD1d molecules 248

Chapter 6
Conclusions 251

Chapter 7
References 257

List of figures

Chapter 1

Figure 1.1	Examples of Group 1 CD1 ligands	4
Figure 1.2:	Lipoarabinomannan (LAM)	6
Figure 1.3:	The structure of *Borrelia burgdorferi* glycolipid II (BbGL-II)	8
Figure 1.4:	CD1d self-lipid antigens	9
Figure 1.5:	Structures of galactosyl ceramides	12
Figure 1.6:	The CD1d protein	13
Figure 1.7:	CD1d crystal structure	14
Figure 1.8:	Hydrogen bonding between residues of CD1d and the glycolipid antigen α-GalCer	14
Figure 1.9:	Crystal structure of α-GalCer loaded human CD1d	15
Figure 1.10:	Schematic representation of CD1 assembly and trafficking	18
Figure 1.11:	TCR - CD1d interaction	22
Figure 1.12:	Schematic of iNKT cell development	25
Figure 1.13:	Schematic representation of how IL-4/ IFN-γ can skew T_H cell development	28
Figure 1.14:	Model of T_H1/T_H2 cell development and the prevention of T_H1-mediated autoimmunity	29
Figure 1.15:	Potential mode of iNKT cell-mediated regulation of DC maturation in autoimmune diabetes	32
Figure 1.16:	iNKT cell response to α-GalCer activation	37

Chapter 2

Figure 2.1:	Functionality of α-Galactosyl Ceramide (α-GalCer)	41
Figure 2.2:	The relationship between the structure of α-GalCer analogues and bio-reactivity	43
Figure 2.3:	3-α-Galactosylated variant of α-GalCer	44

Figure 2.4:	Variations between the naturally occurring sphingosine (left) and phytosphingosine (right).	45
Figure 2.5:	Scheme showing the protection of **D**-lyxose using acetone and trityl chloride	47
Figure 2.6:	The mechanism of **D**-lyxose acetonide formation, compound (1)	47
Figure 2.7:	The olefination of protected D-lyxose with various Wittig salts	49
Figure 2.8:	The formation of a Wittig reagent and subsequent olefination	49
Figure 2.9:	The hydrogenation of a Wittig product	52
Figure 2.10:	Mesylation, deprotection, reduction and azidation of Wittig compounds	54
Figure 2.11:	Reprotection of C1, C3 and C4 hydroxyl groups of the developing phytosphingosine base and C1 deprotection	56
Figure 2.12:	Glycosylation, deprotection, azide reduction and *N*-acylation of varying phytosphingosine bases	57
Figure 2.13:	Nucleophilic attack on a glycosyl donor	59
Figure 2.14:	Mechanism of base-catalysed transesterification	60
Figure 2.15:	The general mechanism of the Staudinger reaction	61
Figure 2.16:	Changes in serum cytokine levels after injection of α-GalCer (44) or OCH9 (47)	63
Figure 2.17:	Binding affinities of α-GalCer analogues to hCD1d	65
Figure 2.18:	Affinity and kinetics of iNKT TCR binding to hCD1d-α-GalCer complexes	66
Figure 2.19:	iNKT cell activation in vitro is modulated by the length of the phytosphingosine base chain in α-GalCer analogues	68
Figure 2.20:	iNKT cell expansion in vitro is modulated by the length of the α-GalCer phytosphingosine chain	69
Figure 2.21:	Modelling of the effects of variations in lipid chain length on the structure of hCD1d	70

Chapter 3

Figure 3.1:	The relationship between the structure of α-GalCer analogues and bio-reactivity	74
Figure 3.2:	The structures of α- and β-anomeric positions in three sugars	75
Figure 3.3:	Cytokine production in human iNKT cells and DCs by α-GalCer (44) and its *C*-glycoside analogue	78
Figure 3.4:	Plakoside A. One of the β-galactosylceramides isolated from *Plakortis simplex*	81
Figure 3.5:	Analogues with C6' hydroxyl group alterations	83
Figure 3.6:	α-GalCer analogues with variations on the sugar hydroxyl groups	84
Figure 3.7:	An α-GalCer analogue of bacterial origin (GSL-1) incorporating varied C6' functionality	84
Figure 3.8:	iNKT cell activation with α-GalCer (44) and GSL-1	86
Figure 3.9:	The proposed mechanism for the formation of a glycosyl fluoride using DAST	88
Figure 3.10:	Activation of a glycosyl fluoride by tin (II) chloride	89
Figure 3.11:	Solvent influence on the stereochemical outcome of glycosylation	89
Figure 3.12:	Acetylation of azido-phytosphingosine base	90
Figure 3.13:	Synthesis of α-GalCer, α-GlcCer and α-L-FucCer	91
Figure 3.14:	Halide-catalysed in-situ anomerisation	93
Figure 3.15:	Glycosylation, deprotection, azide reduction and *N*-acylation of varying phytosphingosine bases	94
Figure 3.16:	Glycosylation, deprotection, azide reduction and *N*-acylation in the synthesis of L-fucosylceramide	95
Figure 3.17:	The proliferation of NKT cells by various α-GalCer analogues	96
Figure 3.18:	Cytokine profiles of α-GalCer analogues with variations in the sugar head group	98
Figure 3.19:	T_H2 skewing properties of α-L-FucCer (53)	99

Figure 3.20: Vα24-positive and Vα24–negative clones in response to α-GalCer (44) and α-GlcCer (50) 100
Figure 3.21: Cytometric staining of Vα24-positive and Vα24–negative clones in response to α-GalCer and α-GlcCer 102
Figure 3.22: Side and top view of the crystal structure of human CD1d complexed with α-GalCer (44) 103
Figure 3.23: Cytokine secretion by Vα24-positive (left hand panels) and Vα24-negative (right hand panels) clones in response to glycolipid-pulsed APCs 105

Chapter 4

Figure 4.1: The relationship between the structure of α-GalCer analogues and bio-reactivity 108
Figure 4.2: Fluorescence-labelled α-GalCer analogues 110
Figure 4.3: The effects of α-GalCer (44) and biotinylated-α- and β-GalCer (biotin-α-GalCer and biotin-β-GalCer, respectively) on the proliferation of murine spleen cells 111
Figure 4.4: The effects of α-GalCer (44), NBD-α-GalCer and biotin-α-GalCer on the proliferation of murine spleen cells 112
Figure 4.5: α-GalCer analogues varying in the length and saturation of the *N*-acyl chain and their immunological activity 116
Figure 4.6: Bacterial glycosphingolipids 119
Figure 4.7: Cytokine production by iNKT cells in response to bacterial glycolipids 119
Figure 4.8: General mechanism of *N*-acylation using a water-soluble carbodiimide 122
Figure 4.9: Schematic representation of the reaction between *N*-hydroxy-succinimide and a fatty acid to produce an *N*-hydroxysuccinimide ester 122
Figure 4.10: Two α-GalCer analogues incorporating PEG molecules, (85) and (86) 124

Figure 4.11: Azide reduction and *N*-acylation with *N*-hydroxysuccinimide esters of fatty acids to produce a library of α-GalCer analogues 126
Figure 4.12: *In vivo* cytokine skewing by α-GalCer analogues 128
Figure 4.13: Prevention of diabetes in female NOD mice by α-GalCer analogues 128
Figure 4.14: iNKT cell expansion in vitro is modulated by the *N*-acyl chain of α-GalCer 130
Figure 4.15: Binding affinities of α-GalCer analogues to hCD1d 132
Figure 4.16: Affinity and kinetics of iNKT TCR binding to hCD1d-α-GalCer complexes 133
Figure 4.17: Modeling of the effects of variation in lipid chain length on the hCD1d structure 136

List of tables

Chapter 1

Table 1.1: Comparison of mouse and human iNKT cells 33

Chapter 2

Table 2.1: Affinity and kinetic measurements of hCD1d-α-GalCer complexes with iNKT TCR 67

Chapter 3

Table 3.1: Proliferation of spleen cells by α-GalCer (44) and α-GlcCer (50) 80

Chapter 4

Table 4.1: Compound classification of α-GalCer, α-GlcCer and α-L-FucCer analogue library 125

Table 4.2: Affinity and kinetic measurements of hCD1d-α-GalCer complexes with iNKT TCR 134

List of Abbreviations

%	percent
°C	degrees centigrade
Å	angstrom
Ag	antigen
ANA	antinuclear antibodies
APC	antigen presenting cell
Ar	aromatic
Asp	aspartic acid
β_2m	beta 2 microglobulin
B-CLL	B cell chronic leukaemia
Bn	benzyl (CH_2-Ph)
BODIPY	boron dipyrromethane difluoride
b.p.	boiling point
Bq	becquerel
Br	bromine
Bz	benzoyl (O=CPh)
CC	column chromatography
CD1	cluster of differentiation 1
$CDCl_3$	deuterated chloroform
CDR	complimentarity determining region
Ci	curie
CIA	collagen-induced arthritis
CNS	central nervous system
CNX	calnexin
CRN	calreticulin
CSF	colony stimulating factor
Cys	cysteine
d_4-methanol	deuterated methanol
DAST	diaminosulfurtrifluoride
DC	dendritic cell
DCC	dicyclohexylcarbodiimide
DCM	dichloromethane
DDM	didehydroxymycobactin
DMF	dimethylformamide
DMSO	dimethylsulfoxide
DN	double negative: $CD4^-CD8^-$
DP	double positive
EAE	experimental autoimmune encephalomyelitis
EDTA	ethylenediaminetetra-acetate
ELISA	enzyme-linked immunosorbent assay
ER	endoplasmic reticulum
Et_3N	triethylamine
EtOAc	ethyl acetate
FACS	fluorescence-activated cell sorting
FBS	fetal bovine serum

FCS	fetal calf serum
g	grams
GM-CSF	granulocyte-macrophage colony-stimulating factor
GMM	glucose monomycolate
GPI	glycosylphosphatidylinositol
GSL	glycosphingolipid
h	hours
HBS	HEPES buffered saline
HC	heavy chain
hCD1d	human CD1d
HEPES	*N*-2-hydroxyethylpiperazine-*N*'-2-ethanesulfonic acid
[^{3}H]TdR	tritiated thymidine
I	iodine
ip	intra peritoneal
iv	intra venous
IDDM	insulin dependent diabetes mellitus (or type 1 diabetes)
IFN	interferon
IgG	immunoglobulin G
IL	interleukin
iNKT Cell	invariant natural killer T cell. Also referred to as CD1d-restricted T cell
IR	Infrared
K_d	dissociation constant
KO	knock out
K-*t*-BuO	potassium-tert-butoxide
LAM	lipoarabinomannan
Leu	leucine
LHMDS	lithium bis(trimethylsilyl)amide
LM	lipomannan
LTP	lipid transfer protein
M	molar
m	milli
mAbs	monoclonal antibodies
mCD1	mouse CD1
MDC	myeloid dendritic cell
MeOD	deuterated methanol
MeOH	methanol
$MeSO_2Cl$	methanesulfonylchloride
mg	milligrams
MHC	major histocompatibility complex
MHz	mega-hertz
min	minute
ml	millilitres
mmol	millimolar
Mø	macrophage
MonoCer	monoglycosylceramide
MPD	mannosyl-β-1-phosphoisodolichol
MS	multiple sclerosis

MTP	microsomal triglyceride transfer protein
n	nano
N_2	nitrogen
NBD	7-nitrobenz-2-oxa-1,3-diazol
nBuLi	n-butyl lithium
NIDDM	non-insulin dependent diabetes mellitus
NK	natural killer
NKT	natural killer T
NMR	nuclear magnetic resonance
NOD	non-obese diabetic
PBL	peripheral blood lymphocyte
PBS	phosphate buffered solution
PCR	polymerase chain reaction
PE	1-palmitoyl-2-oleoyl-sn-glycero-3-phosphoethanolamine
PEG	polyethylene glycol
petrol	petroleum ether 40-60
PG	phosphatidylglycerol
Ph_3CCl	tritylchloride
Phe	phenylalanine
PI	phosphatidylinositol
PIM	phosphatidylinositol mannoside
PLN	pancreatic lymph node
PPh_3	triphenylphosphine
pyr	pyridine
RPMI	Roswell Park Memorial Institute medium
RT	room temperature
s	second
Saps	saposins
SD	standard deviation
SE	standard error
SLE	systemic lupus erythematosus
SPR	surface plasmon resonance
t	time
T1D	type 1 diabetes
T2D	type 2 diabetes
TBAF	tetrabutylammonium fluoride
TBAI	tetrabutylammonium iodide
TBDMS	tert butyl dimethylsilyl
TBDPS	tert butyl diphenylsilyl
TCR	T cell receptor
T_H	T helper
THF	tetrahydrofuran
Thr	threonine
TLC	thin layer chromatography
TNF	tumour necrosing factor
TPSH	2,4,6-tri-isopropylbenzenesulfonyl hydrazide
Tr	trityl

TrCl	tritylchloride
Trp	tryptophan
TsOH	p-toluenesulfonic acid
UV	ultra violet
w.t.	wild type
WSC-HCl	water soluble carbodiimide hydrochloride; *N*-(3-dimethylaminopropyl)-*N'*-ethylcarbodiimide hydrochloride
β-**L**-AraCer	beta-**L**-arabinosylceramide
α-**L**-FucCer	alpha-**L**-fucosylceramide
α-GalCer	alpha-galactosylceramide
α-GlcCer	alpha-glucosylceramide
α-ManCer	alpha-mannosylceramide
µ	micro

Published work associated with this thesis

Van Rhijn, I., Koets, A.P., Im, J.S., Piebes, D., Reddington, F., Besra, G.S., Porcelli, S.A., van Eden, W., and Rutten, V.P.M.G. (2006). The bovine CD1 family contains group 1 CD1 proteins, but no functional CD1d. *J. Immunol.* **176**(8)**:** 4888-4893

Brigl, M., van den Elzen, P., Chen, X., Meyers, J.H., Wu, D., Wong, C.-H., Reddington, F., Illarianov, P.A., Besra, G.S., Brenner, M.B., and Gumperz, J.E. (2006). Conserved and heterogeneous lipid antigen specificities of CD1d-restricted NKT cell receptors. *J. Immunol.* **176**(6)**:** 3625-3634

McCarthy, C., Shepherd, D., Fleire, S., Stronge, V.S., Koch, M., Illarionov, P.A., Bossi, G., Salio, M., Denkberg, G., Reddington, F., Tarlton, A., Reddy, B.G., Schmidt, R.R., Reiter, Y., Griffiths, G.M., van der Merwe, P.A., Besra, G.S., Jones, E.Y., Batista, F.D., and Cerundolo, V. (2007). The length of lipids bound to human CD1d molecules modulates the affinity of NKT cell TCR and the threshold of NKT cell activation. *J. Exp. Med.* **204**(5)**:** 1131-1144

Hegde, S., Chen, X., Keaton, J.M., Reddington, F., Besra, G.S., and Gumperz, J.E. (2007). NKT cells direct monocytes into a DC differentiation pathway. *J. Leukoc. Biol.* **81**(5)**:** 1224-1235

Chen, X., Wang, X., Keaton, J.M., Reddington, F., Illarionov, P.A., Besra, G.S., and Gumperz, J.E. (2007). Distinct endosomal trafficking requirements for presentation of autoantigens and exogenous lipids by human CD1d molecules. *J Immunol* **178**(10)**:** 6181-6190

Chapter 1

General Introduction

1. General Introduction

1.1 Cluster of Differentiation (CD1)

CD1 proteins are members of a group of molecules designated Cluster of Differentiation 1 (CD1) from their ability to stain leukocytes and the immunofluorescence of their monoclonal antibodies [1]. The CD1 family are transmembrane glycoproteins that can be divided into two sub-categories (group 1 and group 2 CD1), according to their predicted primary amino acid sequences, expression and functional diversities. The CD1 genes identified as members of group 1 are CD1A, CD1B, and CD1C encoding the three proteins CD1a, CD1b and CD1c, respectively. The CD1D gene corresponds to the CD1d protein which falls into the second group of the CD1 family [2]. The fifth CD1 gene, CD1E, has been transcribed, and the protein product is an intracellular protein that is thought to facilitate lipid presentation by other CD1 molecules [3]. CD1e is believed to be an intermediate isotype [4].

CD1 genes have been identified in the human [4-7], rodent [8-10], sheep [11], cow [12], rabbit [13, 14], guinea pig [15] and rhesus macaque [16], suggesting evolutionary preservation of the gene family [17]. The human CD1 isoforms are expressed as single examples (CD1A, B, C, D, and E), whilst in other species they are expanded or deleted; cattle lack intact CD1D genes, and rabbits express amongst others, two CD1A genes [12, 14]. In humans, the CD1 isoforms are differentially expressed with restricted tissue distribution. The proteins are expressed on a variety of professional antigen presenting cells (APCs) such as dendritic cells (DCs) located on both lymphoid and non-lymphoid tissues. Group 1 CD1 proteins are, for example, expressed on Langerhans cells, lymphoid follicles, B lymphocytes, and a subpopulation of circulating B cells in peripheral blood. CD1d can be found on gastrointestinal epithelia, haematopoietic cells, thymocytes, circulating T and B lymphocytes, and resting monocytes [2, 14, 18].

Group 1 CD1 proteins are expressed on derivatives of haemocytoblasts, and are especially induced on DCs of the myeloid lineage [19]. They are expressed on cortical thymocytes and the human CD1c protein can also be found on a specialised subset of B-cells, especially circulating B-cells of newborns and infants [20], B-cells of the tonsil and lymph nodes, and the marginal zone B-cells of the spleen [21]. Group 1 CD1 proteins are, however, not present on most other bone-marrow-derived cells [22].

1.2 Group 1 CD1 proteins and associated antigens

Diverse antigens are presented by the different isoforms. Despite their apparent diversity, there are structural similarities between the antigens presented by the CD1 proteins. Most notable is the fact that these antigenic compounds generally consist of a hydrophilic head group with two long hydrocarbon tails (Figure 1.1), supporting the notion that CD1 molecules successfully present lipid antigens. The interaction between CD1 proteins and lipids results in the antigen adopting an orientation that exposes the polar head at the protein surface for T cell receptor (TCR) recognition. The finely tuned differences observed in the structural organisation of the five CD1 isoforms can account for their varied antigen-binding preferences and capabilities [23-25].

The first antigens identified as being successfully presented to T cells by CD1 molecules were lipids [26]. The Group 1 CD1 proteins are involved in antimicrobial immunity and have to date been shown to present a number of foreign lipid antigens including a range of diverse microbial lipid antigens [26]. CD1a-restricted T cells have been recently shown to recognise the lipopeptide didehydroxymycobactin (DDM) [27] which is closely related to the mycobacterial lipopeptide mycobactin – an iron-scavenger derived from *Mycobacterium tuberculosis* (*M. tb.*) [28]. Contrary to the more classical CD1 antigens, DDM is composed of

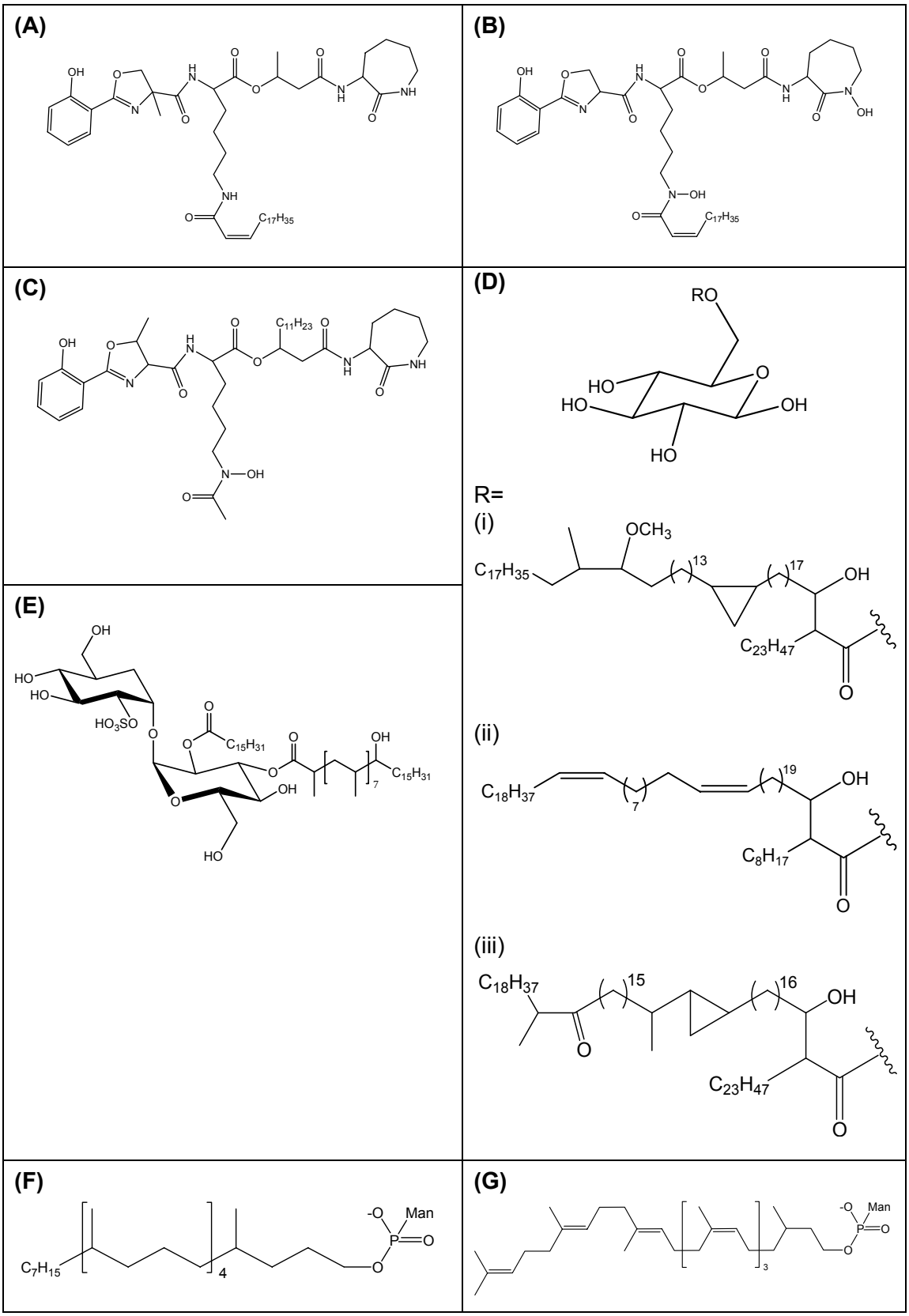

Figure 1.1 **Examples of Group 1 CD1 ligands**. CD1a ligands: (A) DDM; **(B)** Mycobactin; **(C)** Nocobactin; **CD1b ligands: (D)** Glucose mycolates; (i) Methoxy mycolate (ii) α-Mycolate from *Nocardia farcinica*; (iii) ketomycolate (glucose monomycolate; GMM); **(E)** Mycobacterial sulphoglycolipid (Ac_2GL); **CD1c ligands: (F)** Mannosyl-β-1-phosphopolyketide (MPI); **(G)** Mannosyl-β-1-phosphoisodolichol (MPD).

a complex head group of amino and organic acids linked to a single alkyl chain (Figure 1.1). CD1a proteins are established as binding with mycobactin in addition to the related structure nocobactin, which is produced by a number of *Nocardia* species, such as *Nocardia asteroides* that are most commonly associated with immunocompromised patients [29]. The latter compound differs structurally from a mycobactin in the positioning of the hydrocarbon chain (Figure 1.1B, Figure 1.1C). CD1a proteins also successfully present natural sulfatides (3-sulfated β-galactopyranosyl ceramides) with various *N*-acyl chains [30].

The diverse collection of antigens presented by CD1b include lipids derived from the mycobacterial cell wall, such as various mycolates (Figure 1.1D) (α-branched β-hydroxy long chain fatty acids) of which methoxy-mycolates and keto-mycolates are two examples [26]. Other CD1b lipids include GMM (a mycolic acid esterified to a single glucose sugar) [31], as well as the relatively recently defined *M. tb.* derived sulfoglycolipids (A_2SGL) (Figure 1.1). This particular sulfoglycolipid is found in the cell envelope of *M. tb strains* and has been shown to exert a number of immunological effects, such as antitumor activity [32, 33].

Phosphatidylinositol mannosides (PIMs) and lipoarabinomannan (LAM) (a non-peptide mycobacterial cell-wall constituent) (Figure 1.2) are also recognised and presented by CD1b proteins [34]. Both PIM and LAM are made up of a phosphatidylinositol core linked to additional glycans [34].

A group of compounds, based on isoprenoids, are found in a number of pathogenic mycobacterial species and are recognised by the Group 1 CD1c molecule [35, 36]. These antigens differ from what is deemed as the more conventional structure of CD1 antigens; in the fact it only contains a single short lipid tail linked to a mannose-phospholipid.

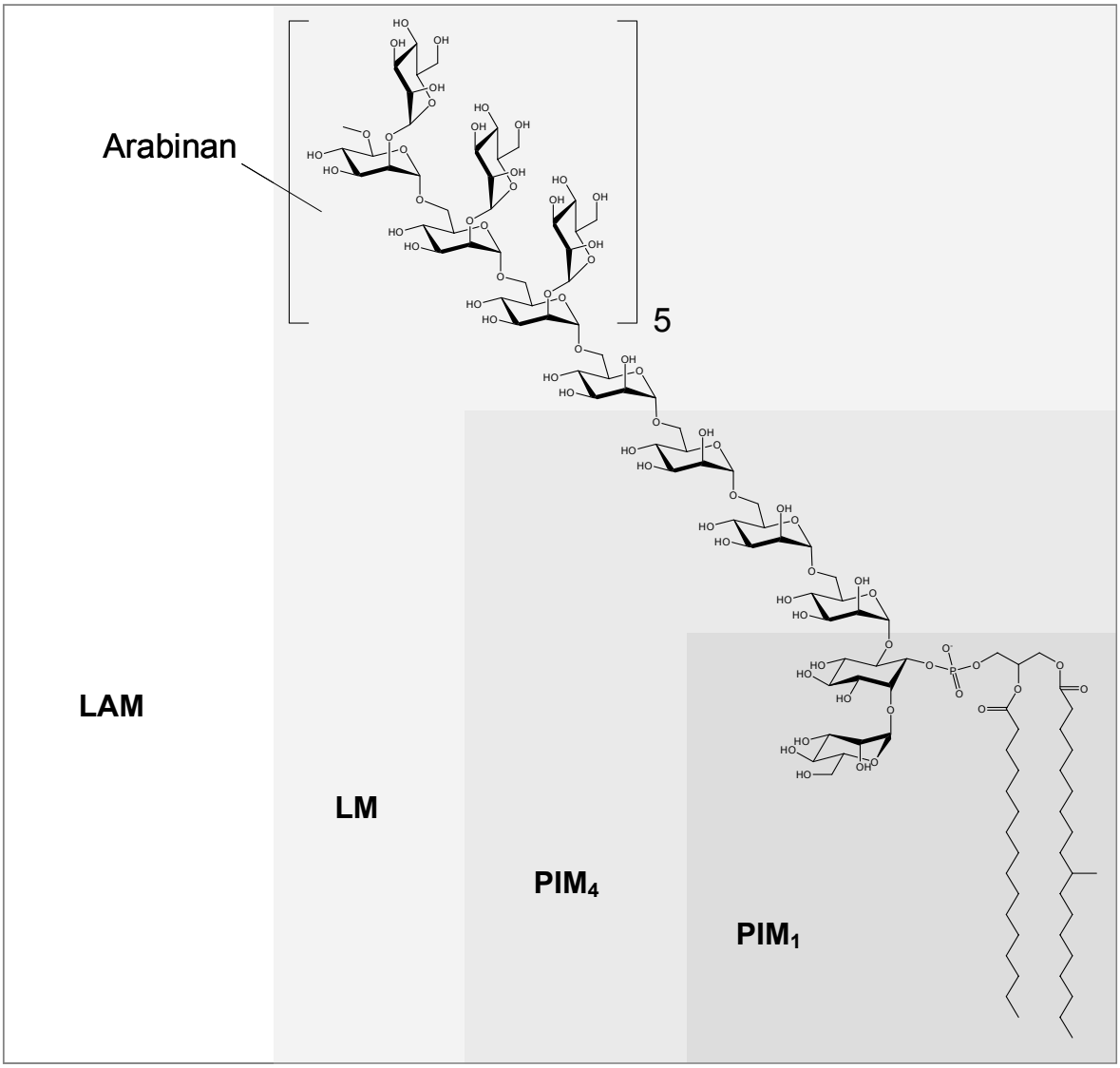

Figure 1.2: Lipoarabinomannan (LAM): Diagram showing the various mycobacterial glycophosphatidylinositols incorporated in the structure of LAM, highlighting the shared phosphatidyl inositol core of the constituent molecules, lipomannan (LM), and two different phosphatidyl inositol mannosides, PIM1 and PIM4. Adapted from [37].

It is structurally analogous to other isoprenoid-based compounds, such as MPD (Figure 1.1), which is an established carbohydrate donor in glycosylation pathways [38]. CD1c proteins also react with specific MPDs typical of eukaryotic cells [35].

1.3 CD1d microbial and self-lipid antigens

CD1d is a non-polymorphic, antigen-presenting molecule expressed on APCs, largely populated by DCs, which play a fundamental part in tolerisation to self-peptides and in the induction of immunity against foreign antigens [39]. DCs mediate interactions between lymphocyte populations, relaying and integrating a variety of signals through interactions with T, B, natural killer (NK) and natural killer T (NKT) cells [40]. Creusot *et al.* [41] stated that lymphocytes within a DC cluster both directly and indirectly instruct other lymphocytes by local cytokine secretion or by making a slight alteration in the DC function, respectively.

The presentation of microbial lipids by CD1 had until recently only been confirmed for CD1a, b, and c. However, there is evidence linking the group 2 protein CD1d with microbial immunity; CD1d-deficient mice have increased susceptibility to bacterial, fungal and parasitic infections [42]. A number of groups investigating CD1d microbial immunity have reported that murine CD1d-restricted invariant Natural Killer T (iNKT) cells recognise glycosylphosphatidylinositol (GPI)-anchored glycoproteins from *Plasmodium* or *Trypanosoma* species *in vitro* and *in vivo* [43-45].

Fischer *et al.* [46] discovered that the mycobacterial lipid PIM_4 (Figure 1.2) successfully binds CD1d and in doing so, activates iNKT cells. This was the only Group 1 mycobacterial antigens tested that proved to be antigenic towards murine iNKT cells via CD1d, further extending the role of CD1d in autoimmunity with respect to antimicrobial host defence.

Recently Kinjo *et al.* [47] have revealed that iNKT cells also recognise α-galactosyl diacylglycerols from the causative agent of Lyme disease, *Borrelia burgdorferi* (Figure 1.3).

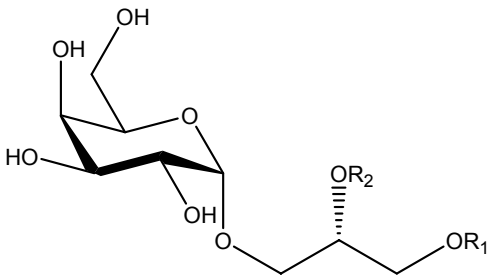

Figure 1.3: **The structure of *Borrelia burgdorferi* glycolipid II (BbGL-II).** This is a monogalactosyl diacylglycerol which represents 23% of the total bacterial glycolipid and consists of fatty acids ranging from C16:0 to C18:2 in both R_1 and R_2.

This has widened the scope for possible active antigens of iNKT cells, and could also aid in the understanding of the biology behind these lymphocytes, and their evolutionary specificity. Diacylglycerols, such as the one derived from *B. burgdorferi*, have also been found in mammalian cells, suggesting previously unknown self-antigens of iNKT cells.

Self-lipids that are naturally present in mammalian tissues have been observed to stimulate iNKT cells in the absence of foreign antigens [48, 49]. They are known to include phospholipids, such as phosphatidylinositol (PI), phosphatidylethanolamine (PE) and phosphatidylglycerol (PG) [50] (Figure 1.4). PI is a key membrane constituent and participates in essential metabolic processes in all plants, animals, and some bacteria. As shown in Figure 1.4, this form of phospholipid has one axial hydroxyl group at position 2, with the remaining hydroxyls remaining equatorial. In animals, stearic and arachidonic acid are found in high concentrations of PIs present, with the former acid linked to the *sn*-1 position, and the latter at *sn*-2 [51].

PE is frequently the main lipid component of microbial membranes, such as in *Escherichia coli*. Also when found in animal tissues, PE tends to have a higher proportion of arachidonic and docosahexaenoic acid. As with PI, the unsaturated fatty acids are concentrated at the

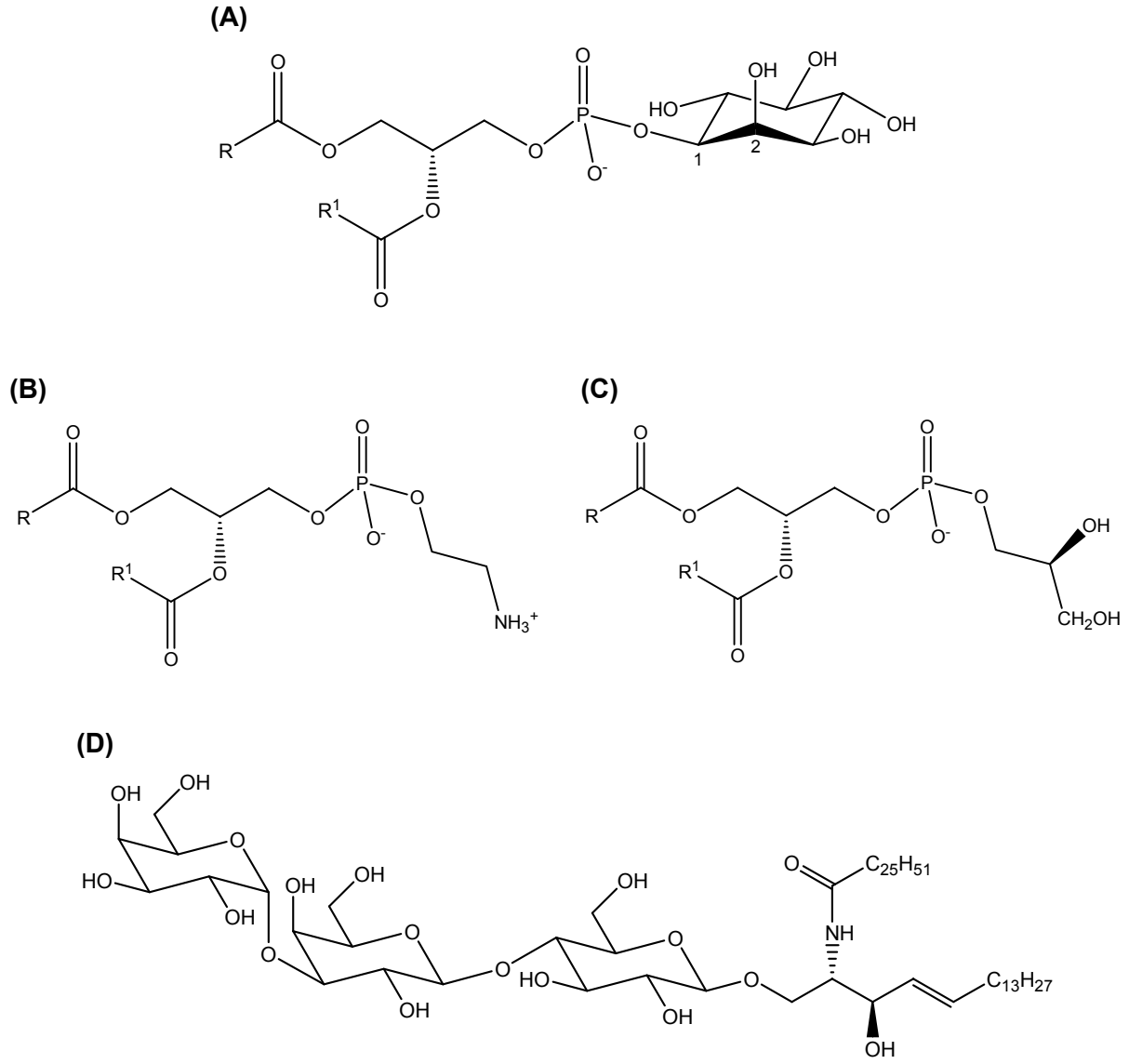

Figure 1.4: **CD1d self-lipid antigens: (A)** PI. R = generally fully saturated hydrocarbon chain, R^1 = generally unsaturated hydrocarbon chain. In animals, there is a high concentration of R=stearic acid, and R^1=arachidonic acid; **(B)** PE. R, R^1 = varying hydrocarbon chains. [51]; **(C)** PG. R, R^1 = varying hydrocarbon chains; **(D)** iGb3.

sn-1 position of the molecule [51]. PG is a ubiquitous lipid and is present in almost all types of bacteria. It can also be found in plant and animal cell membranes. Interestingly, in animal tissues the saturated and mono-unsaturated fatty acids are linked at the *sn*-1 position, which is in contrast to animal forms of PI and PE [51]. The fact that both PI and PG have been

isolated from CD1d proteins, suggests phospholipids may be naturally antigenic for CD1d [52, 53].

An endogenous ligand that has recently been identified as successfully binding to CD1d and stimulating iNKT cells, although showing similarities to α-GalCer, is in fact a β-linked ceramide. The compound in question is isoglobotrihexosylceramide (iGb3) [54]. It consists of a ceramide group with a sphingosine base and *N*-acylated hexacosanoic acid, β-linked with a Galα1-3Galβ1-4Glc saccharide unit (Figure 1.4). It is a natural product of the Hexb-dependant enzymes (β-hexosaminidase A and B) [55]. These enzymes remove β-linked GalNAc residues found in GSLs of the ganglio-, globo-, and isoglobo- series [56]. CD1d proteins also present self-lipid antigens such as glycosphingolipids (GSLs) and diacylglycerols, as well as a non-self lipid; α-galactosylceramide (α-GalCer) [18, 57].

iGb3 has been shown to be one of the only GSL products of the aforementioned ganglio-, globo-, and isoglobo- series that is able to stimulate iNKT cells, expanding the cell populations of IFN-γ and IL-4, respectively [58]. Interestingly, it has also been theorised that lysosomal iGb3 expression is dysregulated by iNKT cells in autoimmune disease, such as type 1 diabetes [54].

The fact that a naturally occurring ligand, successfully stimulating iNKT cells in a CD1d-dependent manner, has a β-anomeric link between the ceramide and sugar ‘head’ is unexpected with regards to the results gained from experiments carried out with β-versions of the parent glycolipid and the fact that it is un-stimulatory [59].

1.4 CD1d and α-GalCer

GSLs make up a variety of significant membrane lipids that exert important signalling functions. They range from cerebrosides with single sugar residues, to compounds incorporating complex carbohydrate patterns of which gangliosides and oligoglycosylceramides are two such examples [60]. The differential distribution and specific pattern of more complex GSLs in tissues, ardently suggests that they play important and specific functions in these tissues. The organisation of GSLs in the membrane provides specificity in the sorting of proteins destined for both the plasma membrane and for the melanosomes in pigmented cells [61]. GSLs contain chemical groups located between the sugar head and hydrophobic backbone that can function as both hydrogen bond acceptors and hydrogen bond donors. It is because of this that they may be able to form lateral hydrogen bonds and contribute to an increase in stability and decrease in permeability of the membrane layers [62].

GSLs are comprised of a ceramide backbone and a sugar head group. The former itself is made up of a sphingoid base and fatty acid. The ceramide portion is normally inserted in to the cellular membrane, whereas the polar head faces the non-cytosolic space [61].

The importance of GSLs in organism development and physiology has been exemplified by knockout studies in mice, where the deletion of an enzyme responsible for the synthesis of glucose-based GSLs proved to be embryonically lethal [61]. Other research has shown that GSL deficiency results in serious pathological conditions [63].

A group of relatively simple GSLs termed cerebrosides incorporate phytosphingosine in conjunction with either glucose or galactose, and are present in plant and animal tissues,

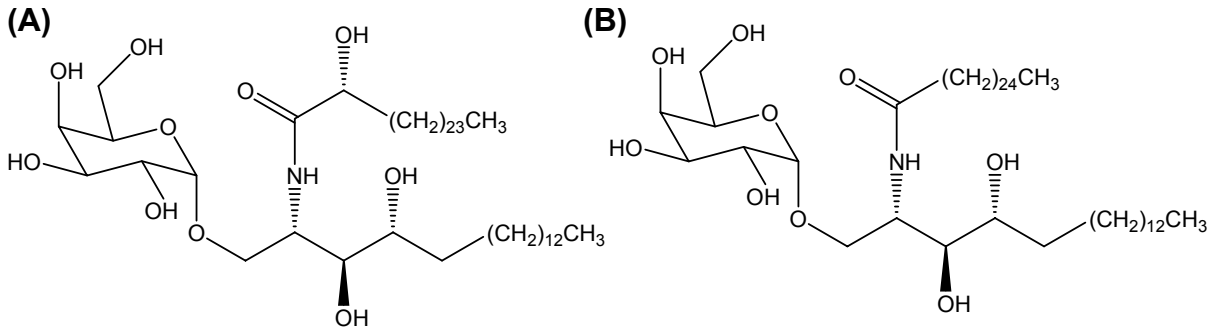

Figure 1.5: **Structures of galactosyl ceramides. (A)** 2-Hydroxy-hexacosanoic acid [2,3-dihydroxy-1-(3,4,5-trihydroxy-6-hydroxymethyl-tetrahydro-pyran-2-yloxymethyl)-heptadecyl]-amide. The GSL isolated from the marine sponge *Agelas mauritianus*, around which the parent glycolipid antigen α-GalCer is based. **(B)** α-Galactosylceramide (α-GalCer).

particularly human and bovine kidney, and the digestive tract of mammals [60]. α-GalCer (Figure 1.5) is a member of the GSL family and it is sometimes referred to as KRN7000 [64]. The structure of α-GalCer and other synthetic analogues is based around a naturally occurring GSL originally isolated from the marine sponge *Agelas mauritianus* [64]. α-GalCer is made up of a galactose sugar head, and linked ceramide tail composed of a phytosphingosine base chain and amine linked acyl chain (Figure 1.5), and like other GSLs exerts an effect on the immune system [60, 61].

1.5 CD1 crystal structure

CD1 molecules are structurally homologous to major histocompatibility complex (MHC) class I molecules. CD1 genes encode type 1 integral membrane proteins consisting of α1, α2 and α3 domains, much like MHC class I molecules, with the α3 domains being the most homologous across the five members of the CD1 family [18].

They also associate with β2-microglobulin (β2m) like the MHC class I molecules (Figure 1.6). CD1 molecules are expressed as heterodimers consisting of a heavy chain

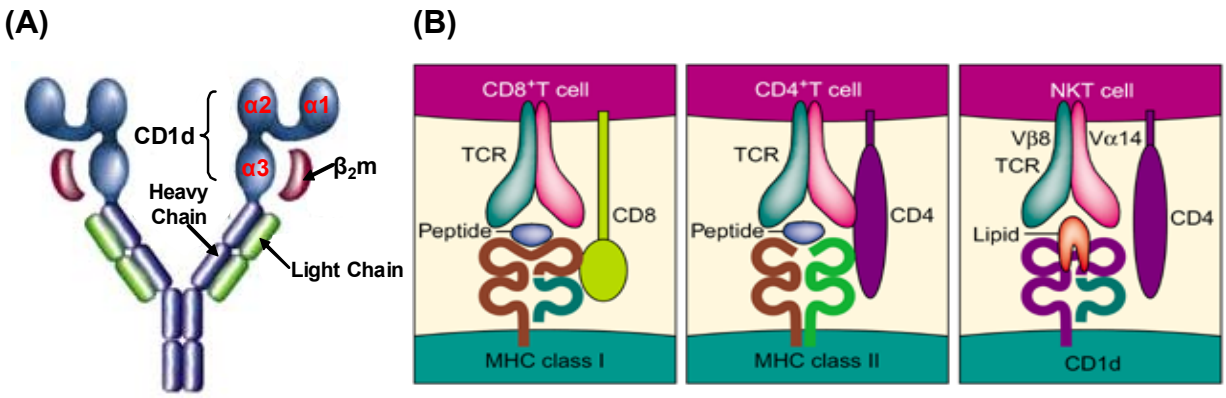

Figure 1.6: **The CD1d protein (A)** CD1 heterodimer consisting of an α1 and α2 domain forming the ligand binding groove, an α3 domain and associated β2-microglobulin (β2m). **(B)** Three different classes of antigen presenting cells and the distinct subsets of T cells they interact with, via peptide and lipid antigen recognition with the TCR. Adapted from [65, 66].

non-covalently linked with the β2m, which seems necessary for cell-surface expression of CD1. The human CD1 group is encoded by five nonpolymorphic genes that are closely linked and located on chromosome 1. MHC is encoded by genes located outside of chromosome 1 (namely on chromosome 6) and although MHC shows structural similarities to the CD1 family, it is genetically unrelated. These similarities could however be indicative of a common evolutionary origin [2, 17, 58, 67, 68].

CD1 polypeptides have predicted molecular masses nearing 33,000. However, the presence of at least three N-linked glycan components increases this value so that it falls between 41,000 and 55,000. Crystallographic studies have demonstrated that the groove structure of the CD1 protein is comprised of two large deep pockets, A' and F', that open between the two α-helixes: α1 and α2 (Figure 1.7). The pockets are lined almost exclusively by non-polar amino acids; the groove has only 10 amino acid residues that are capable of hydrogen bonding to bound antigenic ligands (Figure 1.8). Consequently, widespread hydrogen bonding at the termini of peptides as in class I MHC complexes, and bonding along the

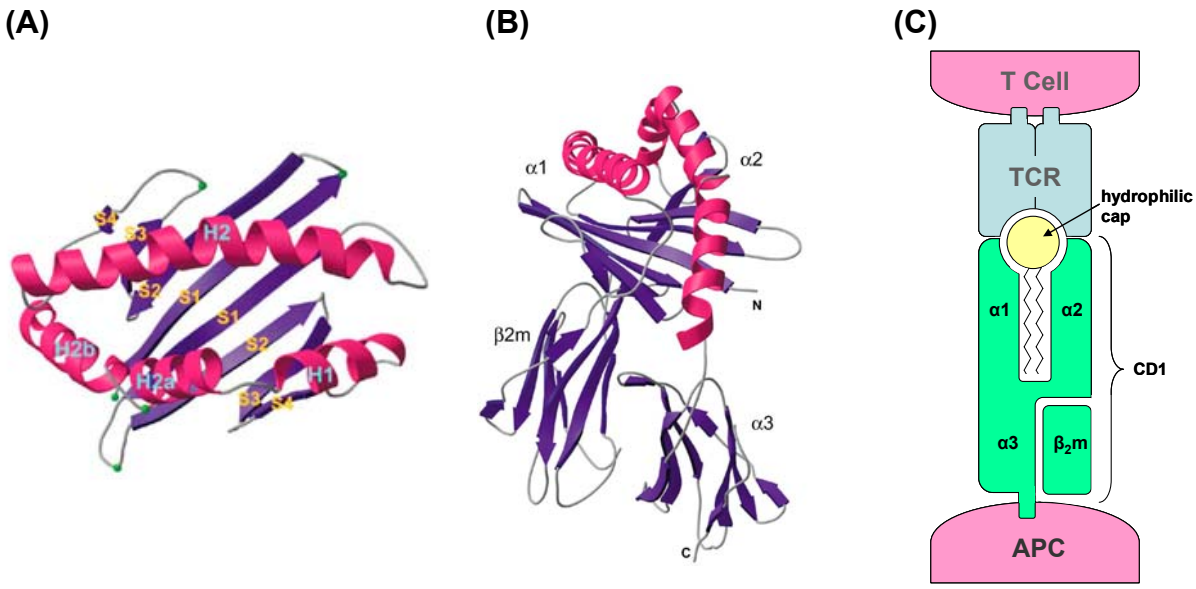

Figure 1.7: **CD1d crystal structure. (A)** Top view of ribbon diagram showing α1 and α2 domains, with the ligand binding groove. S (in blue) refers to a β strand and H (in pink) refers to an α helix. **(B)** Side view of ribbon diagram showing the α1, α2, α3 and β2m domains, with α helices in pink and β strands in blue. Figures adapted from [69, 70]. **(C)** Cartoon illustrating how the CD1 domains (green) from a binding groove to accommodate a lipid antigen (yellow) that is presented by a TCR (blue).

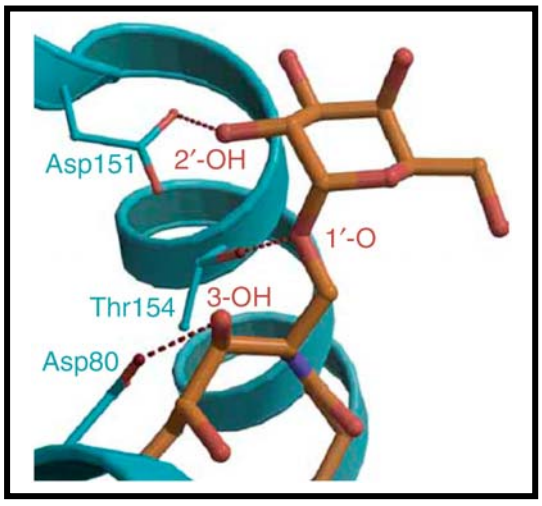

Figure 1.8: **Hydrogen bonding between residues of CD1d and the glycolipid antigen α-GalCer.** The CD1d residue is blue; α-GalCer is orange. The hydrogen atom of the hydroxyl (OH) group at the 2' position of the galactose ring bonds with the Cδ2 atom of the aspartic acid residue (Asp151). The anomeric oxygen atom at position 1' of the sugar forms a bond with the Cγ1 atom of threonine (Thr154), and the 3-OH of the sphingosine chain bonds with aspartic acid (Asp80) Cδ2. Figure adapted from [71].

sides of the longitudinal axis of the groove as in class II MHC complexes is not evident in CD1 proteins [2, 69-72].

Both Group 1 and Group 2 CD1 isoforms present antigens specific to them by securing the alkyl chain or chains of the ligand within their hydrophobic binding grooves. This allows the exposure of the polar head group or hydrophilic cap at the protein surface, together with surface sections of the CD1 heavy chain, enabling it to be recognised by the TCR (Figure 1.9) [57, 71]. Unlike the MHC class I and II molecules, the binding groove of the CD1 proteins, although considerably narrower (9-17 Å as opposed to measurements of over 22 Å), is significantly larger because of greater depth and the presence of only two pockets.

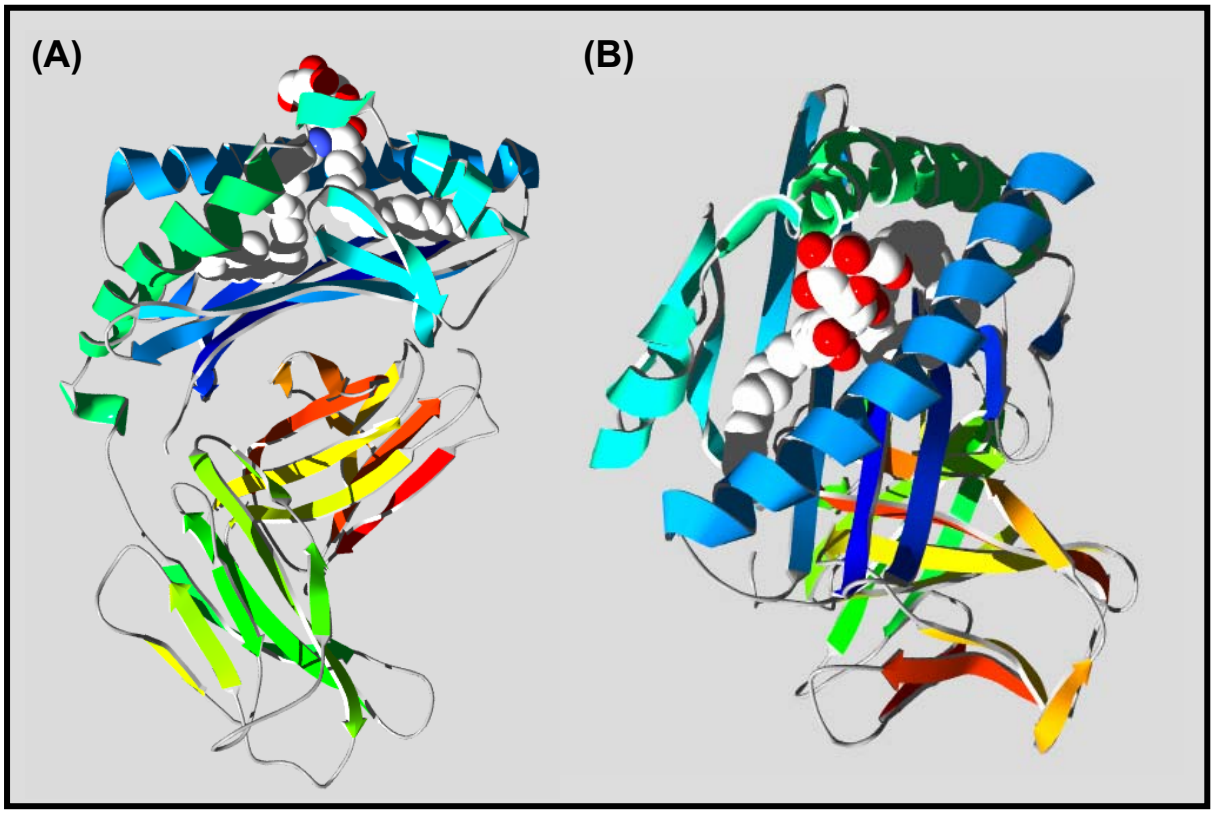

Figure 1.9: **Crystal structure of α-GalCer loaded human CD1d. (A)** Top view of CD1d loaded with α-GalCer **(B)** Front view of α-GalCer loaded CD1d. α-GalCer presented as Van der Waals spheres, white and red; α1 domain, light blue; α2 domain, dark blue; α3 domain, green; β_2m domain, yellow-red. Figure adapted from [71].

This is opposed to the several smaller pockets that are characteristic of MHC molecules. The fact that CD1 proteins fold in a different manner to MHC class I and class II molecules, suggests that they may have a different mode of antigen-presentation and T cell interaction [73].

The CD1d groove is larger than that of the CD1a protein, but does not accommodate as large molecules as the CD1b protein groove [18, 69, 74, 75]. The human CD1b (hCD1b) molecule has a binding groove volume of 2,200Å versus 1,400Å for hCD1d protein [18]. This significant difference allows antigens with maximal acyl chains of 80 carbon (C_{80}) atoms (such as mycolates from *M. tuberculosis*) to be bound in the CD1b pocket, whereas the CD1d channel can only bind antigens with shorter (C_{18}- C_{26}) lipid chains. Unlike the CD1b protein, the CD1d groove is closed at both ends and is only accessible from the top face of the protein molecule through a narrow opening extending from the centre of the groove to a point over the centre of the F' pocket [18, 71]. Also, the F' pocket of CD1a is shallower and wider than CD1d and can thus accommodate, for example, the N-aryl branch of the antigenic compound DDM (Figure 1.1).

Coupling the recently discovered knowledge of the intracellular trafficking of CD1 proteins with their crystallographic structures, has led to a greater understanding of the intricate workings of the immune system. This explains to why multiple CD1 isoforms have evolved to offer, amongst other things, immunoregulation with relevance to tumour immunity and autoimmunity. Sugita *et al.* [76] presented the hypothesis that the immune system has evolved diverse trafficking patterns to accomplish antigen sampling by CD1 isoforms and effective activation of the immunoregulatory T-cell populations that they stimulate.

1.6 CD1 assembly

The five human CD1 isoforms take different routes through the cell before being presented at the cell-surface of APCs, where they interact with specific TCRs [77]. CD1 heavy chains undergo translocation into the endoplasmic reticulum (ER) membrane positioning the α1, α2 and α3 domains in the ER lumen. A short while after translation into the ER the CD1 heavy chains associate with two protein-folding chaperones, calnexin (CNX) and calreticulin (CRN). This complex in turn engages a thiol oxidoreductase enzyme (Erp57) that promotes the formation of disulfide bonds in the heavy chain. This results in the proteins folding in such a way that the hydrophobic amino acids of the heavy chains are brought into close proximity, and the predominantly hydrophobic inner surface of the antigen-binding groove is formed. The oxidised protein then disassociates with the protein-folding complex, and forms a complex with β_2m. The five human CD1 isoforms bind to β_2m with varying degrees of affinity [57].

It has been suggested that in a similar manner to MHC class I and class II molecules, the CD1 isoforms undertake a similar pathway culminating in antigen presentation, and that the CD1 molecules require occupation of their antigen-binding pockets before exiting the ER [78]. Self-lipids, such as PI have been nominated as candidates that load into the CD1 groove during assembly in the ER. Following this assembly, the CD1 molecules are transported to the plasma membrane, where the protein is re-internalised, and traffics through the endocytic system exchanging and acquiring either self- or non-self-lipids, or microbial lipids. Lipid transfer proteins (LTPs), such as Saposins (Saps) and the G_{M2} activator ($G_{M2}A$) facilitate the exchange of the ER-loaded lipid for antigenic glycolipids that activate iNKT cells [79, 80] (Figure 1.10). Although re-internalising and endocytic trafficking is a necessity for the successful presentation of CD1d glycolipid antigens to invariant murine CD1d- restricted T cells, it is a dispensable commodity for human CD1d-restricted T cells,

thus indicating that CD1d can present a variety of glycolipid antigens acquired from both the endocytic system and from the plasma membrane. [2, 18, 57, 68, 73, 78, 79, 81, 82].

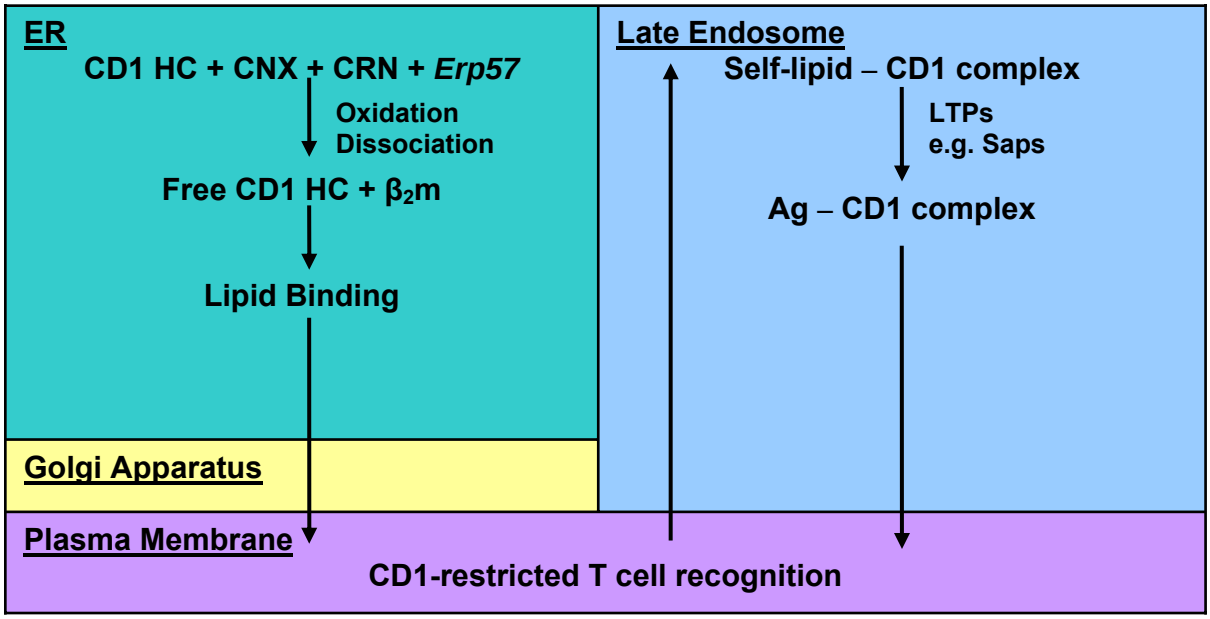

Figure 1.10: **Schematic representation of CD1 assembly and trafficking**. In the ER the CD1 heavy chain (HC) forms a complex with CNX and CRN in order to recruit the enzyme Erp57. The complex undergoes oxidation and dissociation, leaving the CD1 HC free to bind with β_2m, and associate with lipids. The CD1 complex traffics to the plasma membrane, via the Golgi apparatus, where it is recognised by CD1-restricted T cells. It is then re-internalised and LTPs such as Saps facilitate exchange of the ER-loaded lipid for other antigenic glycolipids.

1.7 Invariant natural killer T (iNKT) cells

The immune system is a complex organisation of protective mechanisms that ensure the body is defended against microbes and other so-called 'foreign-bodies'. It is an extremely intricate system which, if fails, can give rise to immunodeficiency. If it over-reacts against microbes, it can result in tissue damage [83].

There are two arms of the immune system; the innate and adaptive immune system. The former is the front-line in terms of microbial defence. It rapidly gives rise to the acute

inflammatory response, and although has some specificity in terms of the microbes it attacks, it has no so-called 'memory'; it fails to remember microbes it has previously encountered [83]. Distinct from this is the adaptive immune system, which although taking longer to develop and respond, is extremely specific and does show memory. The two systems work through direct immune cell contact and through a number of chemical mediations and cytokine interactions. Immune cells (lymphocytes) are specific for individual foreign antigens and proliferate and differentiate when bound to a particular antigen. The cells or their products then neutralise or eliminate the antigenic substance. It is the large number of antigen-specific immune cells present in the late immune response that are accountable for the memory of the adaptive immune system [84].

The two major immune cell types are T and B cells. The predominant maturation of the latter is governed by the bone marrow and gives rise to immunity involving the synthesis of immunoglobulins [83]. T cells mature under the influence of the thymus and induce cellular immunity upon stimulation by an antigen [83]. T cells express a number of complexes on the cell surface of which the cell-membrane bound antigen receptor is one. It consists of two polypeptide chains. More commonly these polypeptides are composed of an αβ dimer, yet some T cells have TCRs made up of γδ chains. The signalling complex, CD3 is also observed [85]. Once T cells have matured, specific subsets are formed after interactions with antigen-presenting molecules, and express the complexes CD4 and CD8 depending on the cell type [86]. CD4 is presented on T helper (T_H) cells, which provide help for B cell growth and differentiation, and CD8 expresses on cytotoxic T (Tc) cells involved in the recognition and destruction of virally infected cells. CD4 expressing cells recognise peptide antigens in MHC class II molecules, whereas $CD8^+$ T cells recognise peptides in MHC class I molecules [83].

Natural killer (NK) cells are large granular lymphocytes produced in the bone marrow and kill virus-infected self cells, in addition to some tumour cells. They function in an identical way to Tc cells, although they do not have true antigen specificity and memory like B and T cells [83]. Invariant natural killer T (iNKT) cells are an unusual subset of immune cells and their identification came about from the contributions of three experiments carried out in the late 1980s [87-89]. The cells express receptors typically present on both the T cell and NK cell lineage. They have been defined as immune cells with a semi-invariant TCR and are reactive to the non-self glycolipid antigen α-GalCer when it is presented by the CD1d protein. CD1d is an essential component with regards to ligand presentation and recognition by the iNKT cell TCRs [90].

Unlike conventional T cells, iNKT cell recognition of CD1d does not require co-receptors, such as CD4 or CD8, which are essential in successful TCR signalling of other T cells, although some iNKT cells do express CD4 markers. Park *et al.* [91] demonstrated that murine mCD1d is exclusively found in the lipid raft microdomains of the plasma membrane of eukaryotic APCs, and it is this specific localisation that is crucial in concentrating and transducing signals between CD1d and iNKT cell during immune responses [91].

In a manner similar to most other T cells, the TCR for CD1d-bound antigens located on the iNKT cell membrane is comprised of an αβ polypeptide dimer, plus a polypeptide-signalling complex. The invariant TCR α-chain of iNKT cells consists of a canonical Vα14-Jα18 chain in mice and a homologous Vα24-Jα18 chain in humans, coupled with a restricted β chain: Vβ8, Vβ2 or Vβ7 in mice and Vβ11 chain in humans [65, 92]. The iNKT cell can therefore also be referred to as the CD1d-restricted T cell or Vα14 NKT cell. Here, the term iNKT cells will be adopted.

T cell activation is mediated by the αβ TCRs. The fact that iNKT cells recognise and are subsequently activated by a diverse range of glycolipids is somewhat unconventional. The semi-invariant character of the TCR, with a fixed α-chain and restricted β-chain would suggest that only limited antigenic structures would effectively bind with the iNKT cell. However, glycolipids ranging from α-GalCer, PE [52], PIM_4 [37], α-glucuronyl ceramides [25], sulfated ceramides [93], gangliosides [25, 94], and isoglobotrihexosylceramide (iGb3) [54] are all presented by APCs to the TCR of iNKT cells. A β-galactosylceramide (β-GalCer) antigen complexed with CD1d, however, does not activate iNKT cells [95, 96], despite successfully binding with the CD1 protein itself [97]. This evidence suggests that the glycosyl head group of the glycolipid is a critical determinant in the recognition by and activation of iNKT cells; a conclusion reached by a number of research groups [92, 98, 99]. A possible explanation for this diverse antigen recognition is that the glycolipid head group binds with the TCR through a small cavity at the ligand-binding interface. This cavity envelopes the polar head group of the antigen positioning the α-chain of the complimentarity determining region (CDR3α) over the sugar ring. The walls of this cavity are comprised of unique amino acids present in the Vα domain and CDR3α region of the invariant TCR α-chain. In addition, CDR1β and CDR3β residues contribute to the structure [92].

The critical part played by the iNKT cell receptor α-chain is highlighted by the almost identical CDR3α sequences expressed in murine and human TCRs, both of which specifically bind the CD1d-αGalCer complex [100]. A specific α or β chain is not needed to recognise CD1d protein alone in human and murine iNKT cells, and this suggests the invariant CDR3α loop is intrinsic in antigenic recognition [100]. Figure 1.11 illustrates how the TCR of a human iNKT cell interacts with a CD1d-αGalCer complex with regards to the CDR loops. A specific α or β chain is not needed to recognise CD1d protein alone in human and murine iNKT cells, and this suggests the invariant CDR3α loop is intrinsic in antigenic recognition [100].

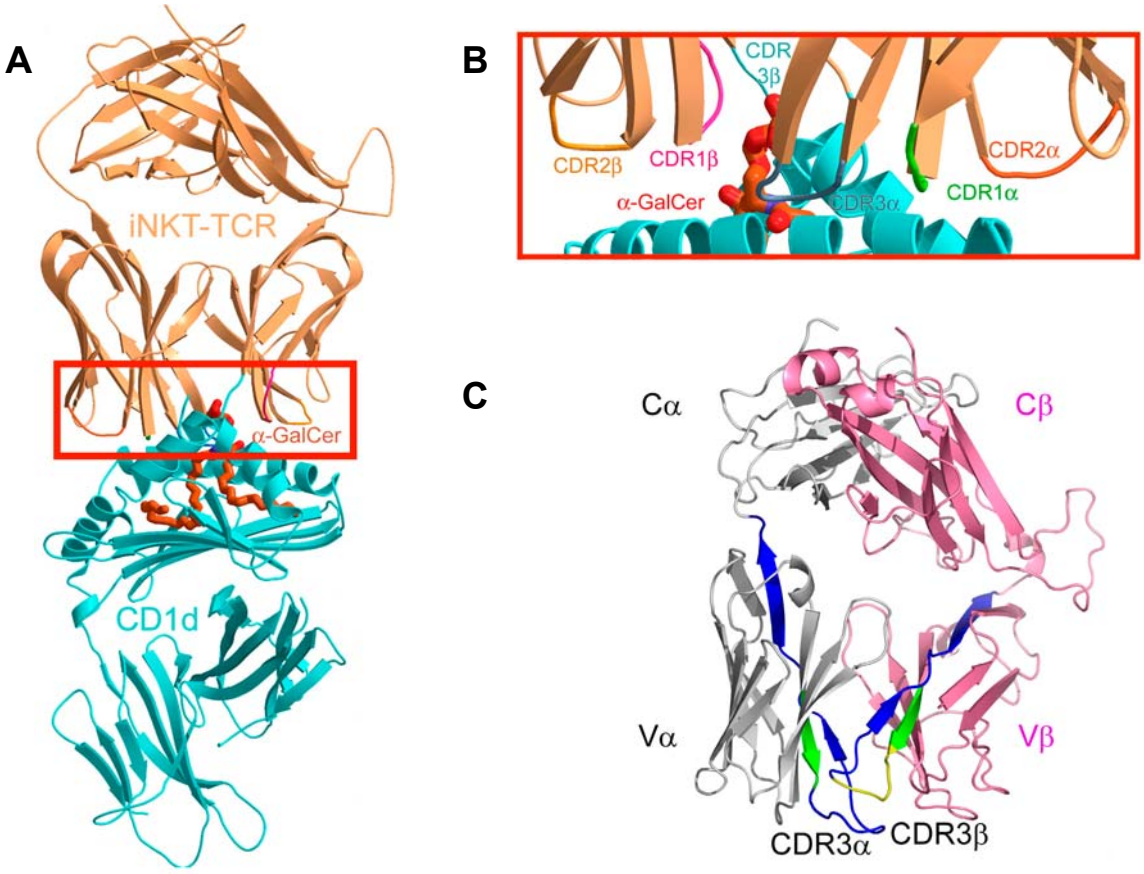

Figure 1.11: **TCR - CD1d interaction (A)** Ribbon structure model of the iNKT TCR-CD1d complex when bound with α-GalCer. The light blue area is representative of CD1d; the orange-yellow structure represents the iNKT TCR. The glycolipid α-GalCer is shown in red. **(B)** Expanded view of boxed region in (A), showing the CDR loops. Colours as in (A). The image has been rotated around the y axis 180°. **(C)** TCR structure showing the ligand binding interface. α-Chains are represented in grey and the β chains in pink. The CDR3 loops are coloured according to their genetic origin: Green, V-region; yellow, Dβ+N; blue, J-region. Adapted from [92, 100].

The efficacious accommodation of different sugar heads can be rationalised by a degree of plasticity within the CDR3 loops, particularly the CDR3β loop. The presence of CDRβ residues in the cavity wall provides a possible mechanism by which the CDR3β loop modulates antigen specificity. Variations in the CDR3β loop and the inherent ability of other CDR loops present at the binding surface of the TCR of different iNKT clones, results in preserved antigen recognition. This contributes to the idea that the CDR3 loops exhibit a conserved degree of flexibility across iNKT cell TCRs. This adjustability is usually typical of αβ TCR-MHC I interactions [101].

It is established that human and murine NKT cells expressing an invariant TCR α-chain are specific for CD1d molecules, such as α-GalCer [102], but the binding mechanism remains something of a mystery. Kang *et al*. [80] established that lysosomal binding of α-GalCer to CD1d molecules, and the subsequent presentation of the antigen-protein complex to T cells, is dependent on the expression of Saps. This is in contrast to cell-surface binding and the autoreactive recognition of CD1d by iNKT cells, which does not require Saps [78, 80]. More recently, Hava *et. al.* [57] demonstrated that the formation of stimulatory CD1-antigen complexes necessary for iNKT cell activation requires a spatial encounter between the CD1 protein and antigen. The group stated that candidate accessory molecules, such as microsomal triglyceride transfer protein (MTP) and Saps manipulate the antigen presentation and hypothesised that they act as lipid transfer proteins involved in CD1 loading [57].

Given the important role CD1d-lipid complexes hold in the activation of iNKT cells, CD1d tetramer/multimer studies have been employed in attempts to track the response of the iNKT cell receptor to glycolipid antigens [103-107]. Tetramer technology allows the direct exposure of a variety of T cell groups, which can be visualised, enumerated and characterised from unfractionated lymphocyte populations. It does not require *in vitro* culturing for amplification, and thus, is a very useful and powerful tool in the exploration of mechanisms in, for example, autoimmune diseases [104]. It was shown that the Vα region of the iNKT cell is not a key contributor in the recognition of α-GalCer when coupled with mCD1, but it has been hypothesised that, in humans, identification is more reliant on the β-chain [98]. Stanic *et al.* [108] discovered that the Vα repertoire of iNKT cells does in fact impact both recognition and antigen avidity. They went on to demonstrate that the Vα14-Jα18 iNKT cell receptor co-operatively engages with α-GalCer and analogue loaded multimers. Kjer-Neilsen *et al.* [92] concurred with this concept and although a number of studies state that the CDR3β loops do not take part in iNKT cell antigen recognition, the

Kjer-Neilsen group recently showed that CDR3β loops that do not recognise CD1d-glycolipid complexes are likely to result from either steric hindrance from obstructing CDR3β loops at the cavity surface or interference from the CDR3α loop conformation [92].

iNKT cells present as either double negative (DN) or $CD4^+$ T lymphocytes that co-express an intermediate level of the αβTCR along with a number of other receptor characteristics from the NK cell lineage. That is, approximately 60% of all NKT cells express the CD4 marker ($CD4^+$), and the majority of the remaining cells lack both CD4 and CD8 expression; they are defined as DN cells [65, 109, 110]. The iNKT cell developmental pathway is initially the same as that of conventional $CD4^+$ and $CD8^+$ T cells. A number of genes identified as affecting iNKT cell development have also been identified as regulating NK and T cell function and development, further substantiating the hypothesis that the iNKT cell maturation lineage diverges from the conventional T cell pathway [111].

DN thymocyte progenitor cells that do not express an antigen receptor enter the thymus and proliferate, before beginning gene rearrangement. This results in the cells having a pre-TCR and $CD4^+CD8^+$ co-receptor; the cells are now double positive (DP) [112]. As the cells mature, the α-chain genes rearrange and undergo positive or negative selection [112]. Positive selection is the process by which DP thymocytes are salvaged from apoptosis by TCR engagement with a ligand. In the case of conventional T cells, thymocytes whose receptors can interact with self-peptide:self-MHC complexes are positively selected allowing them to mature into conventional $CD4^+$ or $CD8^+$ T cells. Thymocytes whose TCRs recognise self-ligand complexes too well are induced to undergo programmed cell death, thus removing potentially self-reactive cells before they reach maturation [83].

It has been suggested that the unique iNKT cell lineage occurs on or after the DP stage of T cell development through the mechanism of α-chain gene rearrangement and positive selection by specific self-ligands, analogous of the MHC class I-restricted $CD8^+$ and MHC class II-restricted $CD4^+$ T lymphocyte lineages [86]. The self-ligands of iNKT cells are CD1d-expressing thymocytes originating from bone marrow [86]. Based on the expression of DX5 (a cell surface marker), iNKT cell development has been separated into four stages [111] (Figure 1.12). In the most immature stage the iNKT cells are highly $CD4^+$ and lack both the DX5 and NK1.1 cell markers. iNKT cells are also highly $CD4^+$ in the second of the first two immature stages, but at this point do express the cell surface marker DX5 ($DX5^+$/ $NK1.1^-$). Mature iNKT cells are then equally divided into $DX5^+$/$NK1.1^+$ cells and $DX5^-$/$NK1.1^+$ cells. It is thus following the random TCR α-chain rearrangement that the iNKT cell lineage gains its distinctive signalling features [86, 90, 111, 113].

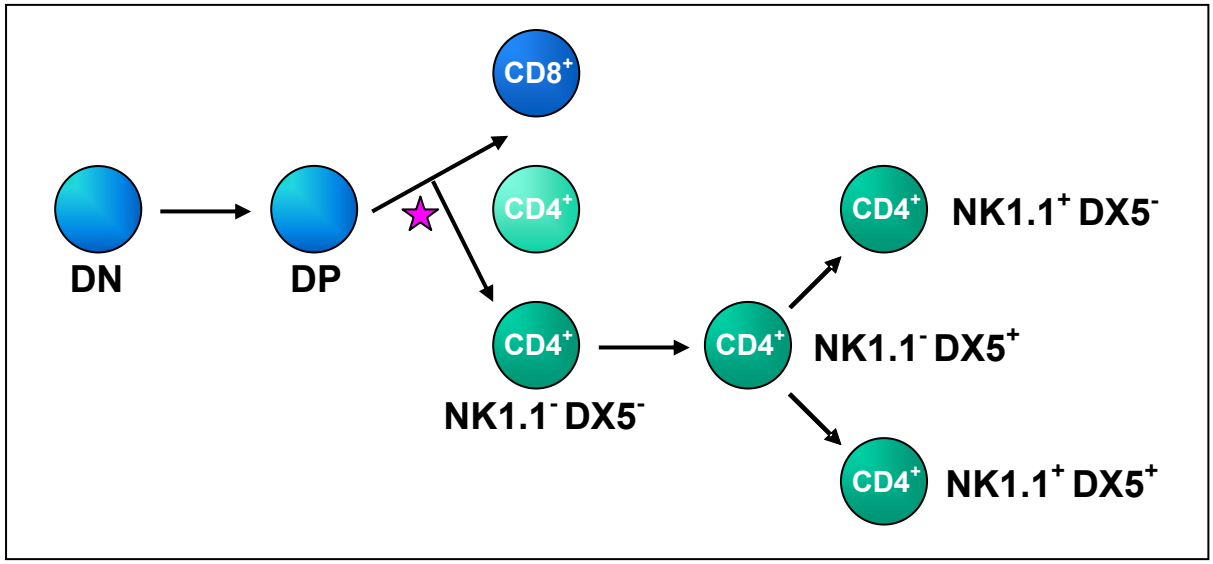

Figure 1.12: **Schematic of iNKT cell development.** Double negative (DN) T cells go through gene rearrangement expressing CD4+CD8+ – they are now double positive (DP) T cells. In conventional T cell development, the cells become sensitive to peptide:MHC complexes and undergo positive and negative selection, the former resulting in the production of CD8+ and CD4+ T cells. Positive selection by CD1d-expressing thymocytes, on or after the DP stage (indicated by ★), together with TCR Vα14 and Jα18 gene rearrangement leads to the development of iNKT cells, by the expression of various cell surface markers, namely DX5 and NK1.1.

iNKT cells exercise a key influence on an array of immune responses and pathologic conditions and upon TCR cross-linking rapidly secrete an assortment of cytokines such as interferon-γ (IFN-γ) and interleukin-4 (IL-4) within a few hours. Interestingly, they are stimulated to produce only IFN-γ upon cross-linking with C-lectin type NK receptors, such as the NK1.1 molecules NKR-P1 and CD161c [110, 114, 115].

IL-4 is a multi-functional cytokine that plays a critical role in regulating immune responses within the body, as well as being a key component in tissue adhesion and inflammation. It is produced by T_H2 cells, basophils and mast cells and regulates the differentiation of antigen-stimulated naïve T cells [116]. iNKT cells have been linked to a variety of immune responses including responses to pathogens, tumours, tissue grafts, allergens and autoantigens. Thus iNKT cells bridge the gap between the innate and adaptive immune systems; a characteristic also attributed to innate B and T cells [117, 118].

Ontogenic programming of the unique features of iNKT cell function occurs at the stage involving Vα14-Jα18 TCR α-chain rearrangement and after interaction with the positively selecting CD1d-self-lipid ligand complex [113]. This is presumably why the iNKT cell lineage precursor in the thymus undergoes a major expansion upon contact with a CD1d-lipid compound, before the expression of the NK1.1 marker molecule.

Soon after stimulation, the iNKT cell population dramatically decreases and the cells remain dormant for a short period of time, before eventually proliferating [119]. The cell's effector functions, such as cytokine production remain very much intact even after down-regulation of the Vα14 receptor, indicating that Vα14 NKT cells resist becoming anergic upon receptor activation [119]. Matsuda *et. al.* [86] state that the differences expressed in the surface molecules and/ or the cytokines produced by the MHC molecules or the CD1d proteins is

likely to be responsible for the activation of cascade pathways that add to or result in the diverse phenotypes of iNKT cells in comparison to typical $CD4^+$ and $CD8^+$ T cells.

1.8 iNKT cell effector functions

The immune system is able to produce an immune response to virtually all molecules or cells [83]. The capacity of the human body to respond to self-antigens is ever-present, but more often than not results in anergy - a state of tolerance involving non-responsiveness to antigen rather than cell deletion [120]. This implies that mechanisms, such as, either the inactivation or deletion of autoreactive T and B cells or the suppression of autoimmunity by cells or cytokines exist to subdue autoimmune responses [121]. In certain individuals, these mechanisms are either absent or are overridden, culminating in a breakdown of self-tolerance and the development of autoimmune disease, such as type 1 diabetes (T1D) and lupus (systemic lupus erythematosus; SLE) [122].

1.9 The T_H1/ T_H2 response

There are two forms of $CD4^+$ helper T (T_H) cells, which play an integral part in the immune response to protein antigens [123]. They also aid in the production of antibodies by B cells. T_H cells can be discriminated into two groups: T_H1 and T_H2. Each type of T_H cell develops from uncommitted T_H0 cells (naïve $CD4^+$ T cells) [124, 125]. When initially stimulated by antigen loaded APCs, naïve $CD4^+$ T cells begin to secrete an array of cytokines which manipulates their polarisation to either the T_H1 or T_H2 pathways [126]. Other influences include antigen concentration, the presence of certain hormones and the type of APC itself. T_H1 cells release pro-inflammatory cytokines, such as IL-2, TNF-α and IFN-γ, all of which are involved in killing intracellular microbes, generating Tc cells, and potentially stimulating

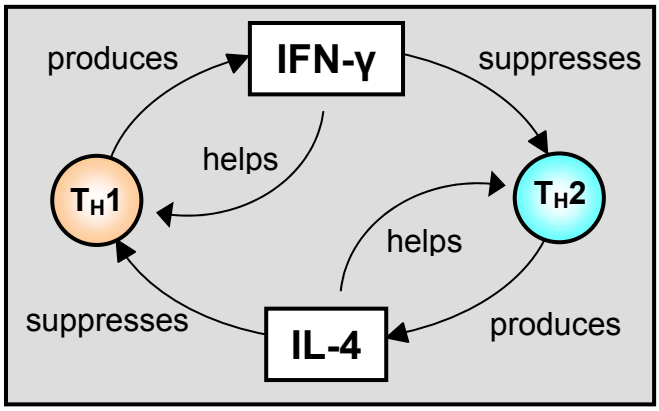

Figure 1.13: Schematic representation of how IL-4/ IFN-γ can skew T_H cell development.

the phagocytic action of macrophages [125]. The anti-inflammatory cytokines IL-4, IL-10 and IL-13 are produced by T_H2 cells and amongst other things are important in helping eradicate parasitic infections, and for B cell proliferation and differentiation [125]. T_H cytokines are self-regulating and can inhibit each other's functions; both T_H1 and T_H2 are antagonists for each other (Figure 1.13). The initial response to infection involves T_H1 or T_H2 cytokines. The T_H1 response leads to the release of the pro-inflammatory cytokines, followed by the production of the T_H2 anti-inflammatory cytokines. Activated APCs, such as DCs and macrophages produce IL-12, which is critical in the development of T_H1 cells. The production of IL-12 stimulates IFN-γ production by iNKT cells, and NK cells, of which the latter in turn induces more IFN-γ production by APCs. iNKT cells produce large concentrations of IL-4 when stimulated through their TCR by CD1d-antigen complexes. IL-4 brings about the polarisation of T_H0 cells towards the T_H2 pathway. T_H2 cells themselves secrete IL-4. The production of IL-6 by APCs triggers the secretion of IL-4 by naïve $CD4^+$ T cells (Figure 1.14) [105, 115, 125, 127, 128].

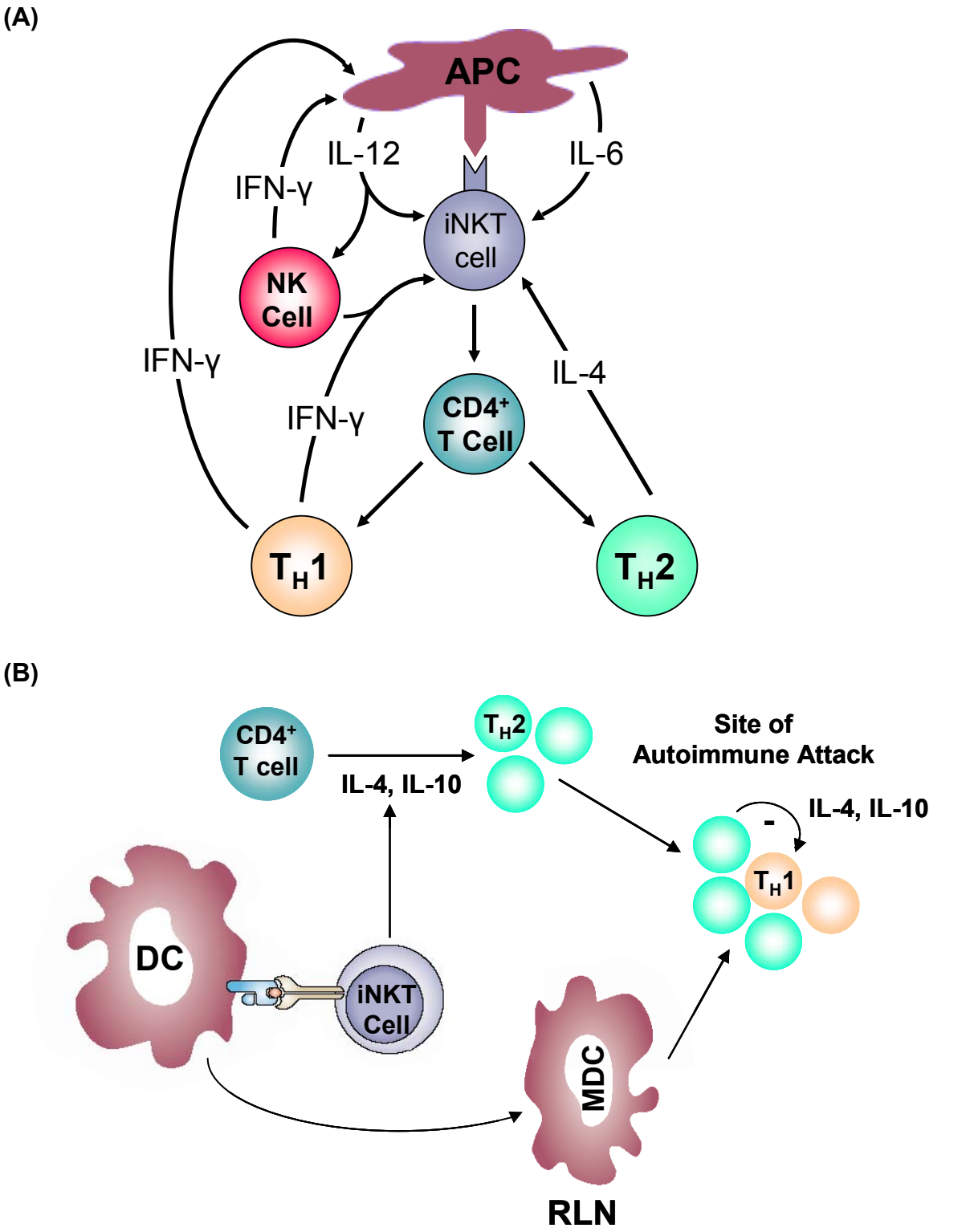

Figure 1.14: **Model of T_H1/T_H2 cell development and the prevention of T_H1-mediated autoimmunity.** **(A)** iNKT cells are activated by antigen-loaded CD1d-expressing APCs. This stimulates the production of cytokines such as IL-4, IL-6, IL-12, TGF-β, IFN-γ. These cause differentiation of naïve $CD4^+$ iNKT cells into T_H1 or T_H2 cells. An increase in a particular cytokine can skew the immune response towards T_H1 or T_H2, depending on the cytokine environment. **(B)** α-GalCer-loaded DCs interact with iNKT cells, promoting T_H cells to produce cytokines such as IL-4, IL-10 and IL-12. Myeloid dendritic cells (MDCs) that prevent tissue damage are then recruited and activated in the regional lymph nodes (RLN) under the influence of IL-12. Regulatory T_H2 cells may suppress the activities of pathogenic T_H1 cells at the site if the autoimmune attack thus preventing ongoing autoimmune attack.

An increase in a particular cytokine can skew the immune response towards either a T_H1 or T_H2 type depending on which is associated with protection [128]. High concentrations of IL-4 (or IL-6) obstruct the T_H1 cell developmental pathway, even if the cytokine IL-12 is present [129]. In a similar manner, IFN-γ secreted by T_H1 cells blocks the proliferation of T_H2 cells, but leaves the T_H1 population unaffected (Figure 1.13). This is due to a lack of β-chain IFN-γ receptor expression. The production of IL-10 by T_H2 cells also inhibits APC production of IL-12 [130].

Defective regulation of the anti-self response through T_H1 and T_H2 cells can lead to a breakdown of self-tolerance, which in turn can trigger the development of an autoimmune disease (Figure 1.14) [129, 131].The discrete T-cell population of iNKT cells is stimulated to secrete cytokines, such as IL-4 and IFN-γ, by a T_H1/T_H2 response and is mediated by a CD1d:antigen complex [132, 133]. Glycolipids such as α-GalCer bind with CD1d proteins forming a compound that activates iNKT cells [95, 134]. The atypical ability to rapidly produce such cytokines suggests that iNKT cells are able to manipulate adaptive immune responses. α-GalCer has become an increasingly attractive analogue since the realisation of the important role it plays in regulating the development of a number of autoimmune diseases, such as systemic sclerosis, T1D and SLE [135]. α-GalCer polarises the differentiation of naïve $CD4^+$ T cell precursors in mice towards the development of a T_H2 phenotype, and therefore highlights the exciting possibility that glycolipid antigens could prevent T_H1 cell-mediated autoimmunity [102, 136-139]. Although, the glycolipid antigen also produces the T_H1 lymphocyte IFN-γ, repeated exposure of murine spleen cells both *in vitro* and *in vivo* to α-GalCer. This is in contrast to exposure with LAM or other glycolipid antigens which results in a dramatic decrease in the production of IFN-γ and enhancement of the T_H2 cytokines IL-10 and IL-4 [109].

1.10 Type 1 diabetes (T1D)

Type 1 diabetes (T1D) is characterised by lymphocyte-mediated destruction of insulin-producing β-cells in the pancreatic islets of Langerhans. This process is mediated by T cells specific for β-cell antigens [140]. Antibodies to β-cell proteins can be simultaneously generated and used for predicting the occurrence of the condition in at-risk populations (see [141] for a review of β-cell protein and lipid autoantigens implicated in the development of type 1 diabetes). In a healthy individual, insulin increases the synthesis of glycogen from glucose by binding with insulin receptors allowing the cellular uptake of glucose from the blood stream [142]. Glycogen is the chief polysaccharide store of cells. The process of islet destruction culminating in inhibited insulin-production, leads to severe hyperglycaemia (raised blood glucose levels). Hepatic overproduction of glucose by glycogenolysis and gluconeogenesis leasd to subsequent impaired cellular uptake of blood glucose. Gluconeogenesis is the production of glucose gained from a source other than glycogen. If left untreated, hyperglycaemia can lead to central nervous system (CNS) depression, coma and eventually death [142].

Organ-specific autoimmune diseases, such as T1D and multiple sclerosis (MS) are governed by uncontrolled T_H1-cell reactions [128]. Destructive insulitis is paralleled by predominant secretion of IFN-γ, IL-2, IL-12, TNF-α, and IL-18, while the T_H2 cytokine, IL-4 is associated with non-destructive insulitis [140, 143].

The modulation of immune reactions from a T_H1- to T_H2-dominant reaction can successfully prevent autoimmunity [139, 144, 145]. Systemic treatment with the T_H1 cell promoter IL-12, has been recorded as accelerating the onset of diabetes in non-obese diabetic (NOD) mice, whereas treatment with anti-IFN-γ, or IL-12 antagonists delays the development of T1D (Figure 1.15) [146-148]. NOD mice are genetically predisposed to develop the autoimmune

disease T1D [149]. The development of diabetes is initiated by the infiltration of lymphocytes into the islets of Langerhans at approximately 4 weeks of age. The majority of female NOD mice clearly develop diabetes by 30 weeks of age; in the NOD mouse model, the incidence of diabetes is more prevalent in the female of the species [117].

Antigen recognition by inactivated $CD4^+$ T lymphocytes leads them to differentiate into T_H1 or T_H2 effector cells, depending on the tissue-specific microenvironment and cytokine milieu in which they develop, thus indicating that cytokine imbalance plays a vital part in the emergence of autoimmune diseases [115].

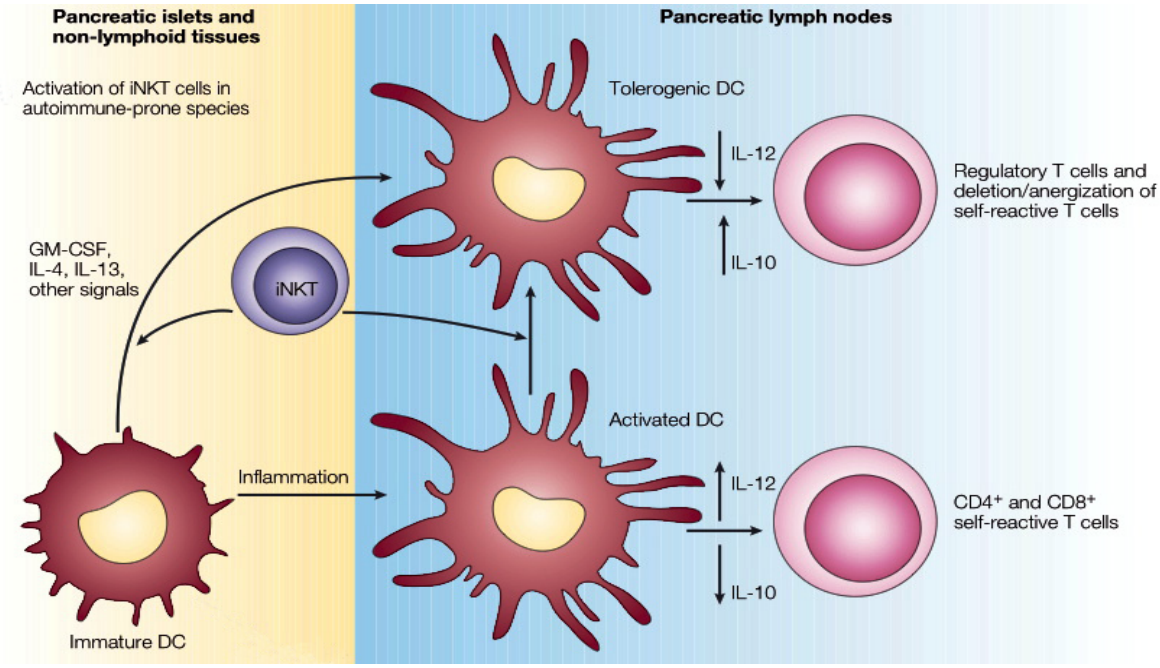

Figure 1.15: **Potential mode of iNKT cell-mediated regulation of DC maturation in autoimmune diabetes**. During the onset of type 1 diabetes, CD1d-expressing DCs activate iNKT cells under the influence of pro-inflammatory cytokines such as IL-12. This results in a change of the activated phenotype of DCs in pancreatic lymph nodes, suppressing pro-inflammatory cytokine production and thus preventing ongoing autoimmunity. In a host prone to T1D, impaired iNKT cell function results in continual pro-inflammatory autoimmune attack. Adapted from [150].

NOD mice are often used as models for T1D as the cell system involving CD1d proteins and NKT cells is phylogenetically conserved among mammals (Table 1.1) and thus pre-clinical studies carried out in mice are expected to have a direct correlation in humans. The human body, however, has a decreased number of iNKT cells in comparison to mice. The NOD

	Mouse	Human
TCR Repertoire: (α-chain)	Vα14-Jα18	Vα24-Jα18
TCR Repertoire: (β-chain)	Vβ8.2, Vβ7, Vβ2	Vβ11
Co-Receptor	$CD4^+$ or DN	$CD4^+$, $CD8\alpha\beta^+$, $CD8\alpha\alpha^+$ or DN
Cognate Antigen	α-GalCer	α-GalCer
Antigen-presenting molecule	mCD1d	hCD1d
Frequency (as a proportion of lymphocytes)	Thymus (0.3-0.6%); Spleen (0.6-1%); Liver (12-20%); Bone Marrow (0.3-0.5%); Blood (0.5-0.8%)	Blood (0.01-1%); Liver <0.5%)
Cytokine profile	IL-4, IFN-γ, TNF-α, IL-13*	IFN-γ, TNF-$\alpha^{\dagger}$, IL-4, IL-13, IL-2, GM-CSF, IL-6, IL-10, IFN-γ, TNF-$\alpha^{\ddagger}$
NK Receptors	Mostly NK1.1 $(CD161)^+$	Mostly NK1.1 $(CD161)^+$. Some $CD4^{neg}$ express 2B4, CD94, NKG2A

*Vα14 iNKT cells have not been shown to differentially secrete cytokines. †Preferential cytokine production by $CD4^{neg}$ subset. ‡Preferential cytokine production by $CD4^+$ subset.

Table 1.1: Comparison of mouse and human iNKT cells. Adapted from [66, 102]

mouse strain spontaneously develops diabetes with many features common to those presented by humans with the same condition. Studies have found that NOD mice are **Table** .specifically deficient in iNKT cells in comparison to other strains, thus suggesting that iNKT cells may be involved in the development of T1D [66].

It has been implied that results gained from utilising NOD murine cells could be biased towards a T_H1-mediated autoimmunity. However, this was disproved by Araujo *et al.* [146], when the group successfully induced experimental allergic asthma in NOD mice, a typical T_H2-mediated disease.

1.11 Systemic lupus erythematosus (SLE)

Systemic lupus erythematosus (SLE) is a multi-system fluctuating inflammatory disease that is extremely variable with regards to its clinical presentation [151]. It is an immune complex-mediated disease characterised by chronic IgG antibody production directed at ubiquitous self-antigens present in all nucleated cells; SLE patients almost invariably express antinuclear antibodies (ANA). Symptoms can range from a mild disease associated with rashes and arthritis to a devastating illness coupled with renal failure and profound nervous system disturbances. Regardless of these clinical manifestations, it has been suggested that T cells are the driving force in the pathogenesis of this and other autoimmune diseases [152-154].

IFN-γ contributes to tissue injury in lupus and Sieling *et al.* [155] demonstrated that DN T cells, incorporating CD1-restricted APCs derived from SLE patients, produce the T_H2 cytokine IL-4, which aids in B cell production of IgG and consequently dramatically decreases the activity of this antibody mediated disease. Oishi *et al.* [156] showed that the selective reduction of DN iNKT cells is related to the disease progression of SLE.

The effects of α-GalCer on both the hereditary and induced models of SLE have been explored. Injection of α-GalCer in to the murine model for hereditary SLE, the MRL-*lpr/lpr* mouse, lessens inflammatory dermatitis, but has no effect on kidney disease [157]. This particular strain of mouse has a naturally decreased iNKT cell population [158]. Repeated α-GalCer administration caused a marked clonal expansion of iNKT cells and an increase in serum immunoglobulin E (IgE) concentration, suggesting that α-GalCer polarises the immune system towards a T_H2 response, inducing the suppression of SLE dermatitis. α-GalCer also induces a T_H2 response in BALB/c mice, protecting the mouse from pristine-induced SLE . This is in contrast to the SJL/L mouse, where the α-GalCer injection is seen

to exacerbate SLE caused by the hydrocarbon oil pristine, which can be correlated to the production of T_H1 cytokines [117]. Miyamoto *et al.* [144] reported that an α-GalCer derivative (termed OCH) with a truncated aliphatic chain preferentially induced NKT cells to secrete the T_H2 cytokine IL-4.

Treatment of NZB/W mice (another murine model for hereditary SLE) with α-GalCer produces dichotomous results, according to the age of the animal. Van Kaer *et al.* [117] observed that a T_H1 response exacerbating the disease, is induced in old NZB/W mice, yet a T_H2 response is seen in younger mice of the same strain. Zeng *et al.* [159] have also noted that the activation of NKT cells in adult NZB/W mice by α-GalCer augments T_H1-type responses (the secretion of IFN-γ) and autoantibody production, both of which contribute to lupus development. These findings give rise to the theory that SLE-like autoimmunity can be attributed to changes in the balance of T_H1/T_H2 immune response.

1.12 iNKT cells: TCRs, down-regulation, and expansion

The majority of iNKT cells (incorporating all Vα14 NKT cells and NK1.1-expressing T lymphocytes) recognise a glycolipid antigen:protein complex, comprising α-GalCer or related structure, and a CD1d molecule. In addition to cytokine production on activation, iNKT cells down-regulate immunity, including the suppression of anti-tumour responses *via* a mechanism involving the cytokine IL-13 and the promotion of tolerance induction [160]. Soon after stimulation (approximately 2 hours) by α-GalCer for example, TCRs are down-regulated, with their levels eventually being restored after approximately 24 hours (Figure 1.16). After activation, the iNKT cell population dramatically decreases and the cells remain dormant for a while, before eventually proliferating. All the while, the cell's effector functions such as cytokine production remain very much intact, even after down-regulation

of the TCR Vα14 receptor; this indicates that Vα14 NKT cells resist becoming anergic upon receptor activation [117, 119].

In addition to iNKT cells being less functional in terms of IL-4 production in patients with T1D, the frequency of $V\alpha24^+$ $CD4^-CD8^-$ DN T cells has been exhibited to be lower in diabetic than in non-diabetic identical multiplets (i.e. twins or triplets). In the case of diabetes in the NOD mouse, a reduction in the numbers of iNKT cells is observed in the thymus, spleen, bone marrow and liver, and is controlled by a number of genetic loci [102, 161-165]. A reduction of iNKT cells in newly diagnosed insulin-dependent diabetics has also been reported, and although some patients of type 2 diabetes (T2D) have a lower level of NKT cells than non-diabetic counterparts (yet still not as low as patients with T1D), their $CD4^+CD25^+$ T cell numbers are normal [166]. The incidence of iNKT cells has also shown to be lower in patients suffering from other autoimmune diseases, such as MS (a chronic inflammatory disease of the CNS), SLE and systemic sclerosis, thus indicating that iNKT cells regulate autoimmune responses and play a crucial role in controlling the development of autoimmune diseases [114, 135, 167-170].

Hammond *et al*. [165] have been researching the effects of NKT cells in autoimmune disease therapy and iNKT cell deficiency in NOD mice which was found to be directly related to T1D propensity. This was demonstrated by the inhibition of the development of the spontaneous disease after transferral of as few as 1.5×10^5 thymic αβ+ DN cells.

Administration of α-GalCer to female NOD mice has been revealed to ameliorate the development of diabetes, and results in the accumulation of iNKT cells and DCs in pancreatic lymph nodes (PLN). Injection of myeloid DC isolated from PLN, but not inguinal

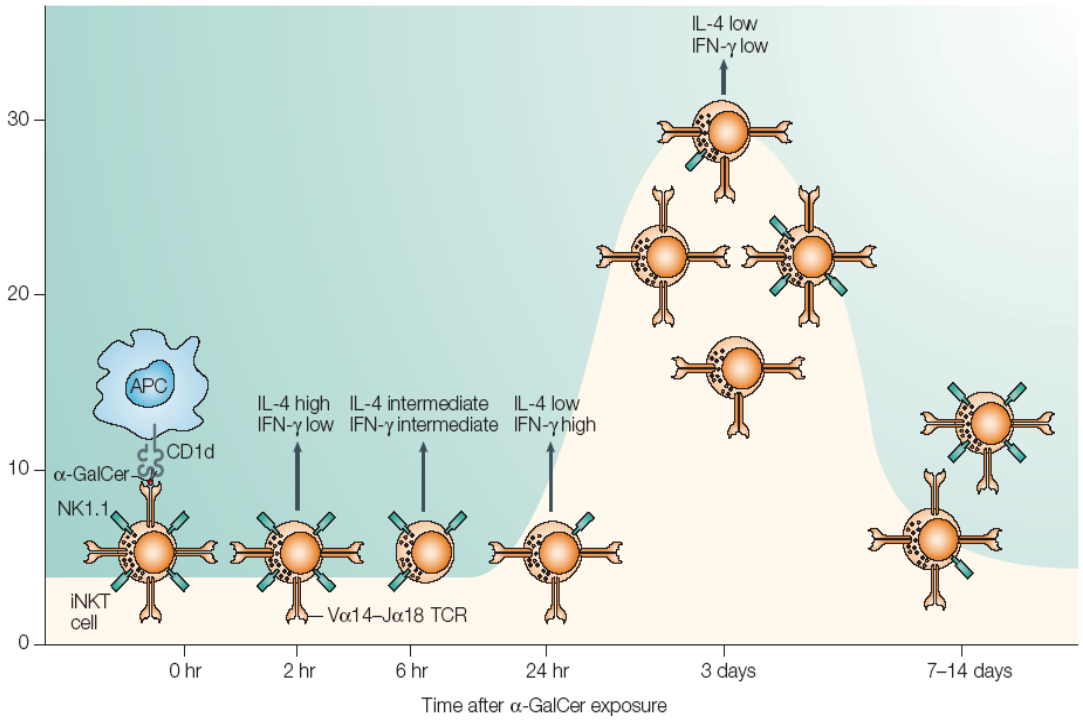

Figure 1.16: **iNKT cell response to α-GalCer activation.** Within hours of administration to mice, α-GalCer binds to CD1d on APC surfaces and activates iNKT cells, initiating the secretion of cytokines such as IL-4 and IFN-γ. During the first few hours of activation, iNKT cells mainly produce IL-4. At this time, TCR expression is downregulated, returning to relatively normal levels at approximately 24h. It is at this point that iNKT cells produce higher concentrations of IFN-γ and undergo rapid proliferation. ~3days after injection, the iNKT cell population is maximal, and cytokine production is much decreased, although still detectable. Adapted from [117].

lymph nodes (lymph nodes isolated from the groin region) completely prevented the occurrence of diabetes in the female NOD mouse [162]. Interestingly, it has been reported that sulfatide-reactive T cells (T cells reactive to the myelin-derived lipid sulfatide, presented by CD1d) and not iNKT cells are increased several-fold in CNS tissue in EAE, the murine model for human MS [171]. Mercer *et al.* [111] commented on the number of studies to have shown that treating NOD mice with α-GalCer injections, or injecting iNKT cells activated *ex vivo* with α-GalCer, prevents both the development and recurrence of the condition. It is worth noting, however, that although agreeing that iNKT cells have a general role in natural protection against destructive autoimmunity, Lee *et al.* [172] contradicted the general consensus that patients with T1D have decreased NKT cell frequency and decreased IL-4 production.

Additional studies have concluded that transgenic over expression of iNKT cells improves diabetes. It has been shown that α-GalCer effectively stimulates the number of detectable iNKT cells, before causing the number to deplete and that repeated stimulation with α-GalCer and various structures based around this compound, expands the human $V\alpha24^{+}V\beta11^{+}$ populous, whilst retaining their $CD4^{+}$ or $CD4^{-}$ phenotype [96, 136, 173-175].

1.13 Aims and objectives

The importance of α-GalCer in the medical world is apparent from studies carried out relating to cytokine production, immune cell proliferation and autoimmune disease therapy. However, as previously discussed it does not provide the definitive solution for the prevention and treatment of conditions such as T1D.

In conjunction with the induction of the anti-inflammatory T_H2 cytokine IL-4, a substantial amount of the unfavourable T_H1 cytokine IFN-γ is produced upon activation of iNKT cells by the CD1d:α-GalCer complex resulting in, for example, continued self or autoimmune attack. The aim of this thesis has been to synthesise a library of GSLs that are structurally analogous to the parent antigen α-GalCer, but with variations in the acyl chain, phytosphingosine base and sugar head, and to investigate the effects some of these compounds have on the immune system. By carrying out *in vitro* and *in vivo* assays, it was hoped that an antigen that provokes a skewed T_H2 immune response could be found, and thus lead to a potential therapeutic regime that can be implemented as part of the care and treatment of patients with autoimmune disease, such as T1D.

Recently, analogues with greater deviations from the parent GSL α-GalCer have been investigated. Modulation of the 6' carbon on the sugar head from a hydroxyl group to an amine or amide, linked with small molecules or incorporation of fatty acids have been scrutinized [72, 176]. Such analogues thus far have for the most part been based on the C18 base chain coupled with galactose. Therefore, the possibility of synthesising analogues with shorter base chains, such as the C9 analogue, with the inclusion of C6' modulations could prove exciting in terms of their immunostimulatory properties. The incorporation of a sulfate group at C3' of the sugar and a di-unsaturated fatty acid chain [177-180] could also heighten the immunomodulating character. Experimental results gained so far, and from other group's data have reported that analogues entailing either a sulfate group or unsaturated acyl chain are successful activators of iNKT cells. Including both variations could lead to the discovery of a so-called super-antigen.

Chapter 2

Variations in the phytosphingosine base

2. Variations in the phytosphingosine base

2.1. Hydroxyl group variations

α-GalCer **(44)** can be sub-divided into 3 main portions: a sugar ring, an *N*-acyl chain, and sphingosine derived base, of which the latter two components constitute the ceramide or lipid moiety (Figure 2.1). Diversity and variability can be introduced into all three sections in order to produce novel antigenic compounds.

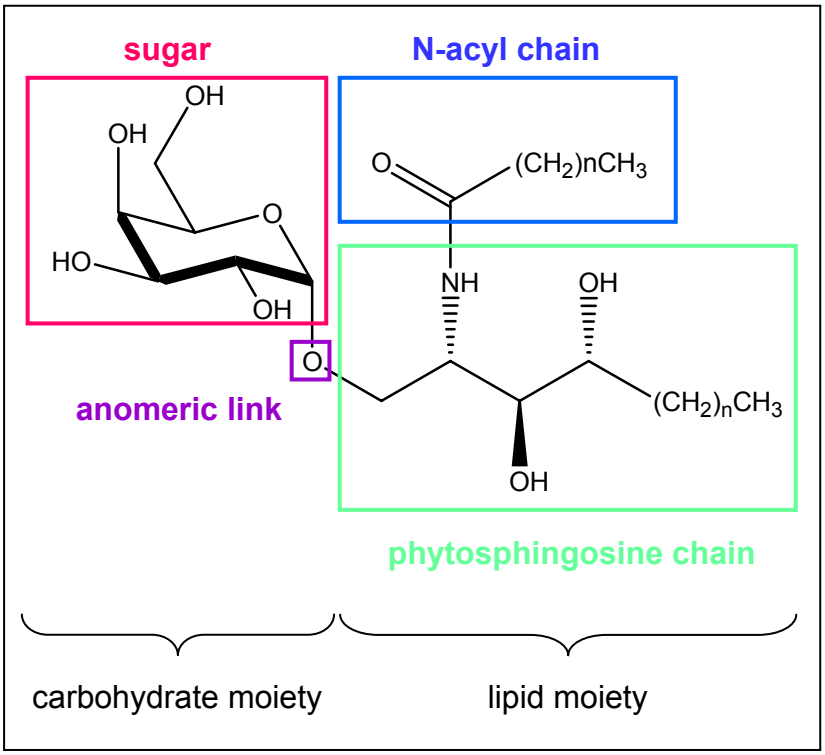

Figure 2.1: **Functionality of α-Galactosyl Ceramide (α-GalCer).** The GSL is comprised of a polar sugar head group, anomerically linked to a ceramide portion which itself is made up of an *N*-acylated phytosphingosine base.

There is now interest in synthesising analogues of the parent glycolipid antigen that vary in the carbohydrate and lipid portions to investigate their immunostimulatory properties, in the hope of discovering more potent agents for specifically activating iNKT cells in different disease states.

Although the discovery of α-GalCer **(44)** has had a great impact on the immunological world, it does not provide a fault-free solution to the treatment and prevention of autoimmune diseases. Alongside the T_H2 cytokine IL-4, a single dose of α-GalCer **(44)** induces the production of greater concentrations of the potentially detrimental T_H1 cytokine IFN-γ [95, 139, 181]. Thus, the development of analogues that have significantly greater T_H2-inducing properties is an exciting prospect and one undertaken in this project.

A negative effect exhibited in NZB/W mice (the mouse model of experimental autoimmune encephalitis, EAE) by α-GalCer **(44)** is the induction of an abnormal T_H1-type immune response, resulting in intensified SLE [159]. The administration of α-GalCer **(44)** to $apoE^{-/-}$ mice (a hypercholesterolemic mouse model prone to the development of atherosclerosis) has been shown to induce a 50% increase in atherosclerotic lesion size, highlighting another problem associated with α-GalCer **(44)** [182]. However, no change was seen to lesion size of $apoE^{-/-}CD1d^{-/-}$ mice showing that it is the CD1d protein that is needed to present α-GalCer **(44)**.

Another concern regarding the use of α-GalCer **(44)** encompasses side effects, such as significant liver toxicity, the triggering of abortion and even death have been induced by the injection of α-GalCer **(44)** into mice. On a more positive note, clinical trials of the compound in human cancer patients did not produce any detrimental side effects, possibly due to the naturally decreased population of iNKT cells in humans [65]. Nonetheless, it has become apparent that one cannot wholly rely on animal models to determine the effectiveness of immuno-intervention studies, due to quite profound differences between experimental murine models and human conditions [183].

Two main areas of the parent α-GalCer structure with regards to the phytosphingosine base have been scrutinized; namely the chain length and the inclusion/ exclusion of the hydroxyl groups at positions C3 and C4. Figure 2.2 highlights the variations that can be introduced into the phytosphingosine base, and the effect they have on the antigenic activity of the GSL.

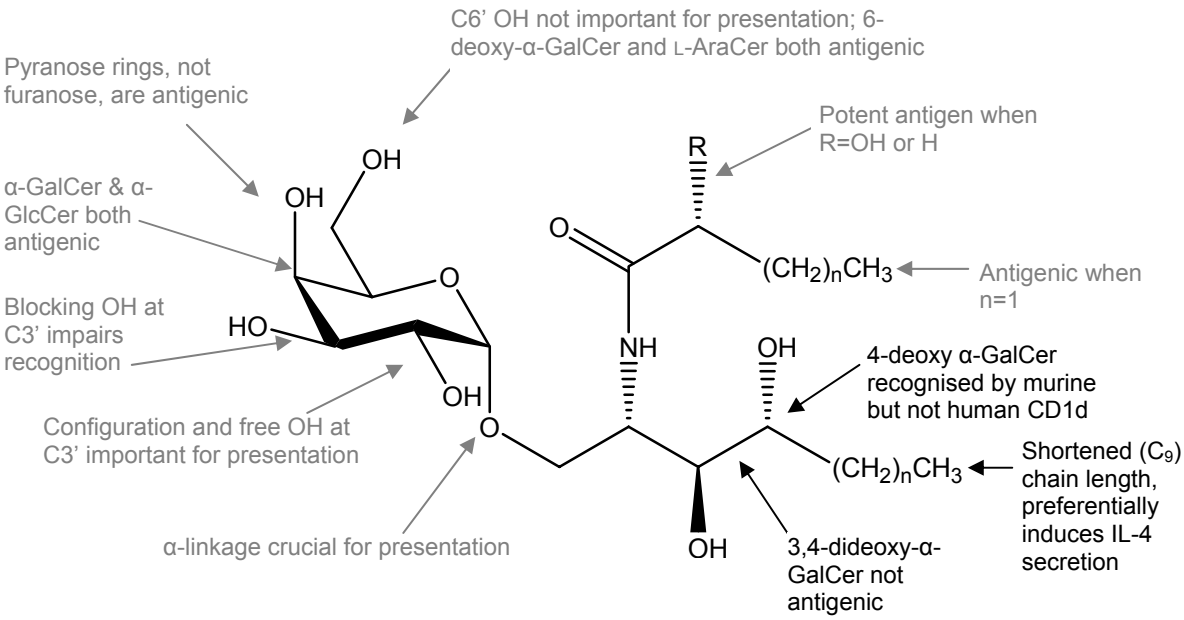

Figure 2.2: The relationship between the structure of α-GalCer analogues and bio-reactivity.

2.2. Hydroxyl group variations

The effect hydroxyl groups have on achieving iNKT cell activation has been in the spotlight. It has been reported that the lack of a hydroxyl group at position 4 of the phytosphingosine base portion does not hinder α-GalCer **(44)** binding by mCD1, but does affect the binding of antigenic analogues to hCD1d [98]. However, when hydroxyl groups are absent from both carbon-3 and -4 of the phytosphingosine base, the antigen/protein complex does not significantly activate murine or human iNKT cells [98]. This could simply be a matter of

decreased solubility, or could be indicative that hydroxyl groups may interact with both CD1 protein molecules and the T-cell receptors that are present on the surface of NKT cells. The binding of the antigens to CD1 molecules has been shown to be independent of the presence of hydroxyl groups in the C3 and C4 positions of the phytosphingosine base, suggesting that the hydroxyl groups are an integral part of activating NKT cells, but not essential for the binding of α-GalCer **(44)** with CD1d molecules [98, 184, 185].

Varying the position of the coupled sugar with the ceramide portion of the CD1d ligand affects the NKT activation. When a galactose group was glycosylated at the 3-hydroxyl group of the ceramide in an α-configuration (Figure 2.3), a greater proliferation of murine spleen cells was observed than from α-GalCer **(44)**, but with no immunostimulatory activity. Incidentally, the β-form of the analogue coupled at the C3 of the phytosphingosine base exhibited a weaker proliferative response [185].

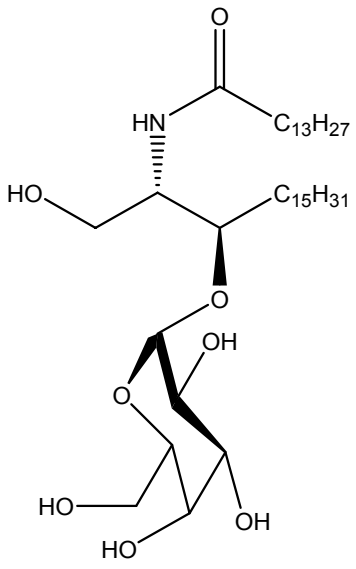

Figure 2.3: **3-α-Galactosylated variant of α-GalCer.** This derivative has been shown to have a stronger proliferative response than the parent glycolipid, but no immunostimulatory activity.

2.3. Base chain length

Sphingolipids comprise a group of approximately 400 naturally occurring compounds and are recognised as bioactive lipid molecules [186]. They are primarily signalling molecules, but also function as building blocks, forming the basis of the plasma membrane in eukaryotic cells [186]. Structurally, they are typified by a long chain base backbone, often comprising of 18-20 carbon atoms with several hydroxyl functional groups. The naturally occurring sphingosine is a C_{18} hydrocarbon chain with a hydroxyl function at C1, an amine at C2, a hydroxyl group at C3 and a *trans* double bond between C4 and C5 [187]. Phytosphingosine is fully saturated with an additional hydroxyl group at C4, as opposed to the double bond (Figure 2.4). When coupled with a polar sugar head, such as galactose or glucose, and acylated at the amine group with a fatty acid, sphingolipids become GSLs, and can affect physiological processes, such as embryogenesis, neuronal cell and leukocyte differentiation, cell adhesion, and signal transduction [61]. GSLs are recognised by the immune system and individual GSLs are specific blood group antigens that can be detected in autoimmune diseases, such as Guillain-Barre Syndrome and T1D [188].

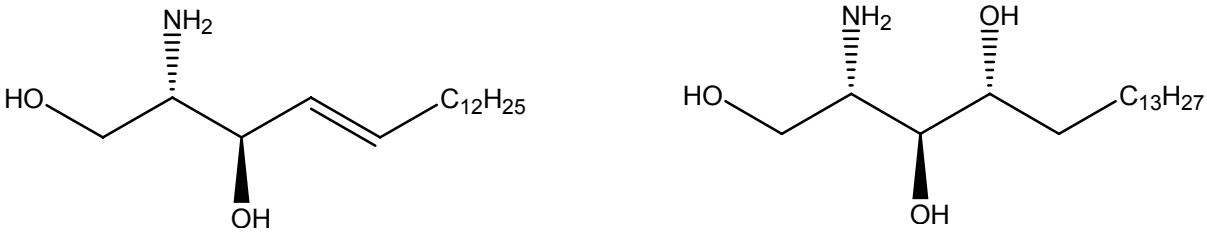

Figure 2.4: Variations between the naturally occurring sphingosine (left) and phytosphingosine (right).

α-GSLs are potent immunostimulants [186, 189]. When Brossay *et al*. [98] tested the cytokine production of α-GalCer analogues with variations in the phytosphingosine chain length, they discovered that both a 15-carbon and 11-carbon chain successfully stimulated cells to release IL-2, although on a somewhat less effective scale than the parent glycolipid.

This is not the case for hCD1d, which only presented the tested analogues with C_{18} and C_{15} phytosphingosine chains to any effect.

Miyamoto *et al.* [144] reported that an α-GalCer derivative, with a truncated aliphatic chain (termed OCH9) **(47),** preferentially induced iNKT cells to secrete the T_H2 cytokine IL-4. Studies in IFN-γR$^{-/-}$ mice suggested that IFN-γ is not a pre-requisite for the adjuvant effect of α-GalCer **(44)**. In conjunction with this finding, results illustrated enhanced T cell responses when using OCH9 **(47)**, and reduced ability to secrete IFN-γ [144, 190, 191].

Oki *et al.* [192] demonstrated IFN-γ production upon activation of iNKT cells by CD1d associated glycolipids, is more susceptible to the length of the phytosphingosine chain moiety, than that of IL-4. Their team also concluded that the number of carbon atoms in the chain shapes the duration of iNKT cell stimulation, and that IFN-γ expression requires longer T cell receptor stimulation than IL-4 secretion. More recently, OCH9 **(47)** has been shown by means of T_H2 cell polarisation, to suppress collagen-induced arthritis (CIA, a murine model for the autoimmune disease rheumatoid arthritis) in SJL mice, which are characteristically prone to the development of autoimmune diseases and have a deficiency in their NKT cell population and function [193].

2.4. Chemical synthesis

2.4.1. Protection of D-lyxose

The general procedure for producing deviations in the phytosphingosine base moiety of α-GalCer **(44)** was based on the procedures of Lin et al. [194]. This method, in contrast to many others reported, was concise with moderately high yields of the final phytosphingosine

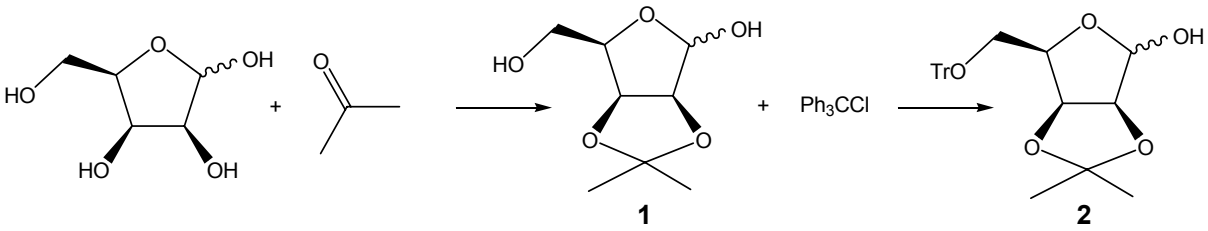

Figure 2.5: **Scheme showing the protection of d-lyxose using acetone and trityl chloride**

product. The starting sugar (D-lyxose) used is relatively inexpensive with the desired required stereochemistry found in phytosphingosine (Figure 2.5). The isopropylidene ketal group is commonly used to protect 1,2- and 1,3-diols, especially in carbohydrates where it can selectively mask the hydroxyl groups. In compounds containing three hydroxyl groups on neighbouring carbon atoms, the 1,2-derivative of the acetonide (Figure 2.6) is generally favoured over 1,3- and 1,4-derivatives. However, this preference does depend quite heavily on the actual structure of the triol. In compounds where there is more than one acetonide possibility, the thermodynamically more favoured structure dominates. Secondary alcohols preferentially form cyclic acetals compared with primary alcohols. Conversely, when two *trans* secondary alcohols are present, the primary alcohol is preferred in forming the acetal

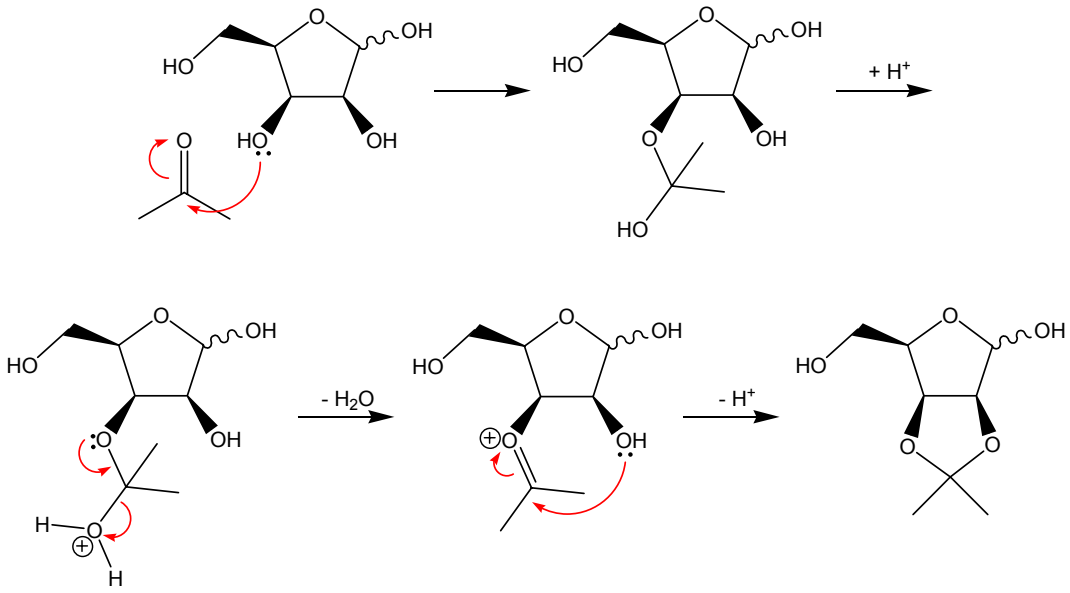

Figure 2.6: **The mechanism of D-lyxose acetonide formation, compound (1).**

as this is thermodynamically more stable [195].

Triphenylmethyl ethers (Tr-OR) are used as protecting groups of alcohols as they are able to selectively protect primary alcohols in the presence of secondary alcohols, due to their bulky nature. Due to the fact that these protecting groups can be removed by mild acid hydrolysis, the acetal protecting group was introduced first.

2.4.2. Wittig reaction

There is a wide variety of commercially available Wittig salts and it is relatively easy to prepare non-commercial products from triphenylphosphine and a halogenated alkane (Figure 2.7). Several attempts at synthesising the Wittig reagent and resulting olefination product were undertaken (Figure 2.8).

In the first instance, 2 M eq of triphenylphosphine, haloalkane and base were used, with the protected form of **D**-lyxose. Lithium *bis*(trimethylsilyl)amide (LHMDS) was the chosen base as stated by Lin *et al*. [194]. However, TLC analysis showed a significant amount of unreacted starting material. Several factors could have contributed to this, such as the presence of moisture in the reaction vessel or reagents, or simply the base being too weak ($pK_a \approx 30$ [196]. The reaction was thus repeated, substituting LHMDS with n-butyl lithium (n-BuLi), which although is a stronger base ($pK_a = 42$) [197] still proved unsuccessful. An alternative method based around [198] was adopted in order to synthesise the various Wittig reagents and condensation products as reported in the experimental section (Figure 2.8). Using the method described by Plettenburg *et al*. [198], compounds **(3)**, **(4)** and **(5)** were synthesised.

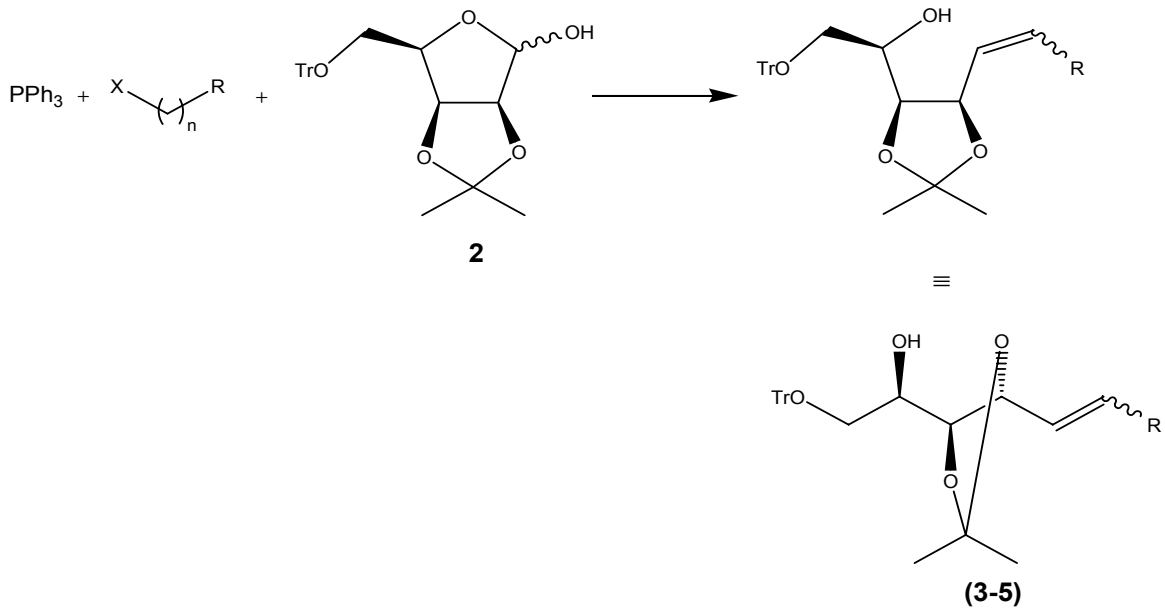

Figure 2.7: **The olefination of protected D-lyxose with various Wittig salts.** Haloalkanes used: 1-bromotridecane (X=Br, n=12), 1-bromooctane (X=Br, n=7), 1-bromodecane (X=Br, n=9), 1-iodobutane (X=I, n=3). R=C_9H_{19} **(3)**; R=C_6H_{13} **(4)**; R=C_3H_7 **(5)**.

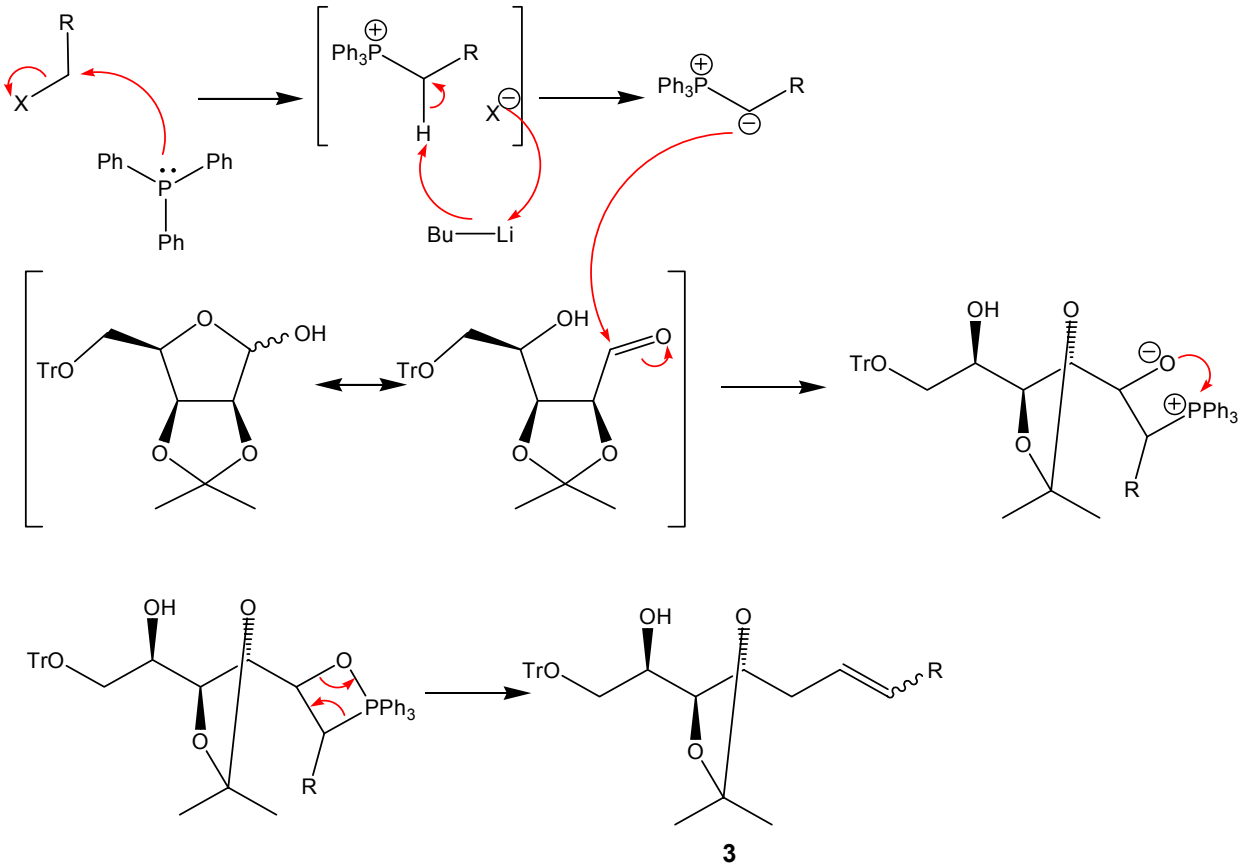

Figure 2.8: **The formation of a Wittig reagent and subsequent olefination.** R=C_8H_{17} **(4)**; R=C_5H_{11} **(5)**; R=C_2H_5 **(6).**

2.4.3. Fluorinated Wittig salts

This project aims to investigate analogues of α-GalCer **(44)**, with variability introduced into the three different portions of the compound, in order to alter the immunomodulatory properties of the analogues. Fluorescent versions of these antigens can aid in tracking the intracellular distribution of GSLs and their metabolites [199, 200]. Fluorinated ceramide and dihydroceramide analogues have been shown to have increased apoptogenic activity, increasing the biological value and interest in fluorine-containing analogues of such compounds [201]. Thus, fully saturated, highly fluorinated versions of the phytosphingosine base portion were investigated. Using an experimental procedure by Buchanan *et al.* (2003) [202], an attempt to synthesise fluorinated versions of two of the Wittig reagents previously prepared was undertaken. Buchanan *et al.* (2003) [202] synthesised highly fluorinated fatty acids to be used in the synthesis of novel delivery agents in hyperpolarized xenon magnetic resonance imaging. The key step in their synthesis was the Wittig reaction between highly fluorinated phosphonium salts and an aldehyde. Highly fluorinated phosphonium salts can be prepared, provided that solvents with high boiling points (such as xylene) and an inert atmosphere (argon) are employed. Successfull Wittig reactions occurred when polar aprotic solvents, such as THF, non-lithiated bases and low reaction temperatures were employed. Potassium-*tert*-butoxide has also been shown to be a preferable base over either n-BuLi or sodium ethoxide-ethanol ($NaOC_2H_5C_2H_5OH$) in the Wittig reaction where an ylide is formed as an intermediate in the production of an alkene (for a review of K-*t*-BuO in synthesis, see [203]). Thus, 1,1,1,2,2,3,3,4,4,5,5,6,6,7,7,8,8-heptadecafluoro-10-iododecane, and triphenylphosphine were refluxed in anhydrous xylene for ~18h under argon in order to produce the fluorinated Wittig salt, which could then be coupled with (3aS,6R,6aS)-2,2-dimethyl-6-trityloxymethyl-tetrahydro-furo[3,4-*d*]-1,3-dioxol-4-ol **(3)** as for the non-fluorinated Wittig salts. However, this did not prove successful, as after 48h, unreacted **(2)** was still present. Therefore the reaction was repeated using potassium-*tert*-butoxide, as a non-lithiated base (pK_a = 19 [204]). This reaction attempt was also unsuccessful.

Caesium carbonate (Cs_2CO_3) is an established inorganic base that can be successfully used in organic synthesis. This powerful base (pK_a = 10.25 [205]) has been utilised in Horner-Wittig reactions in the presence of isopropanol yielding the required unsaturated product in good yields, when other more common bases have not proved competent or give unsatisfactory yields [206]. Yamanoi *et al*. [207] effectively produced an *E*-olefin on reaction of a phosphonate with aldehyde in the presence of Cs_2CO_3. Owing to the fact that the Wittig reactions involving fluorinated reagents and bases, such as nBuLi and K-t-BuO were unsuccessful, a Horner-Wittig type reaction was attempted. The method was based around [207], using a pre-prepared fluorinated Wittig reagent with Cs_2CO_3 and isopropyl alcohol. Compound **(2)** (1.1eq) was added at 0°C and stirred for 18h whilst gradually being warmed to room temperature. NMR and TLC analysis indicated the disappearance of the fluorinated Wittig salt, but unfortunately, the desired fluorinated Wittig olefin had not formed. The reaction was repeated with 2 molecular equivalents of Cs_2CO_3, yet still the desired reaction had not proceeded.

One problem surrounding the use of fluorinated Wittig salts is their insolubility. This could have contributed to the reaction failure, and thus a Wittig reaction was carried out, using 1,4-dioxane as the solvent and n-BuLi as the corresponding base. The reaction was carried out at room temperature due to the relatively high freezing point of the solvent. The reaction was continued as for the reaction of **(2)** with the various unfluorinated Wittig salts, and NMR analysis showed a peak corresponding to possible ethylene protons, which were shifted slightly more downfield in comparison to unfluorinated olefins.

The use of fluorinated Wittig reagents is of great interest, but yet also of frustration; it could prove to be a route to incorporate exciting functionality into the GSL analogues and this is a possible area for further investigation.

2.4.4. Catalytic hydrogenation

In order to produce an active α-GalCer analogue, it is necessary to reduce the double bond resulting from the Wittig reaction at carbon 5 and 6 of the sphingosine base. Lin *et al.* [194] described a synthetic route to phytosphingosine from lyxose in 6 steps; with the double bond being catalytically reduced with a very high yield (91%) whilst the acetonide and trityl protecting groups remained intact (Figure 2.9). Taking this method, a Wittig reagent was subjected to treatment with palladium-barium sulfate under a hydrogen atmosphere. However, after a total of 72h ^{1}H-NMR analysis showed the presence of ethylene protons, indicating the reduction had not succeeded. Palladium barium sulfate (Pd-Ba$(SO_4)_2$) was substituted with palladium-hydroxide ($Pd(OH)_2$) on carbon, and stirred under a hydrogen atmosphere.

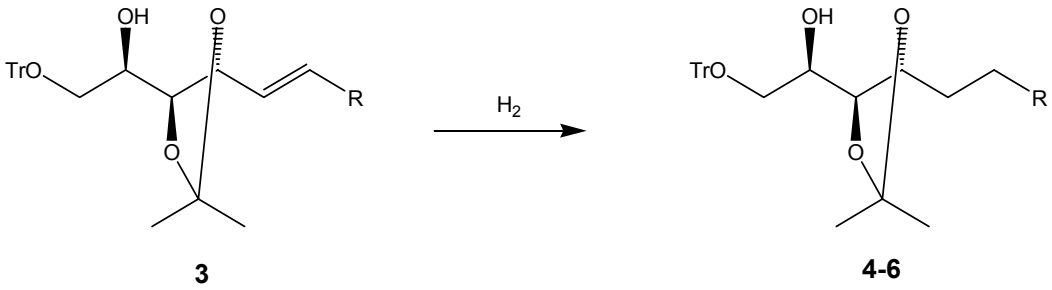

3 **4-6**

Figure 2.9: **The hydrogenation of a Wittig product.** R=$(CH_2)_8CH_3$ **(4)**; R=$(CH_2)_5CH_3$ **(5)**; R=$(CH_2)_2$ CH_3 **(6)**.

After 48h, ethylene protons were still apparent in the ^{1}H-NMR and thus ammonium formate and isopropanol were added. After a further 48h, ^{1}H-NMR indicated the cleavage of the protecting groups. The spectroscopic analyses showed partial reduction of the double bond (1 ethylene proton still present). This suggests that one isomer of **(3)** used was successfully catalytically reduced, whilst the other is possibly hindered by the presence of the isopropylidene protecting group on the 3,4-diol of compound **(3)**.

Although catalytic hydrogenation reactions are more than adequate in many cases, they tend to require relatively expensive equipment and the handling of hydrogen gas. This type of reduction procedure also has a tendency to be unspecific with regards to the stereochemistry and position of the hydrogenation owing to the reversible addition and abstraction of hydrogen to and from the alkene-based compound adsorbed onto the surface of the metal catalyst. The prevalent backbone in sphingolipids is sphingosine, a biologically active molecule that is unsaturated between the 4^{th} and 5^{th} carbon of the base (and thus is missing a hydroxyl group at position 4). Owing to this fact, the possibility of incorporating aromatic rings into α-GalCer analogues, and the fact that unsaturated *N*-acylated chains are deemed more active than their saturated counterparts [208], a method of selectively reducing the double bond formed after Wittig reaction would be an extremely useful tool, and would open up the extent of GSL analogues that could be produced. Diimide reductions can be carried out in readily available laboratory equipment and are selective in as much as a single double bond can be reduced in a compound containing a number of unsaturations, such as a naturally derived fatty acid. In addition, allylic and benzylic groups do not experience hydrogenolysis with diimide reductions [209]. Hünig *et al*. [210] show that hydrogenation by di-imine/ hydrazine (the result of 2 molecules of diimide reacting with nitrogen gas) proceeds with at least 97-98% stereo-specificity.

Diimide can be generated in a number of ways, of which the oxidation of hydrazines and the decarboxylation of benzenesulfonyl hydrazide are just a couple of examples [211, 212]. Cusack *et al*. [213] found that 2,4,6-tri-isopropylbenzenesulfonyl hydrazide (TPSH) in the presence of a base quite readily generates diimide. A synthetic procedure as outlined in [214] was used as a method of generating diimide and theoretically goes on to selectively reduce a double bond, such as that present in the olefins produced after Wittig reaction. However, ^{1}H-NMR analysis indicated that although the double bond had been reduced, the isopropylidene and trityl protecting groups had also been cleaved.

2.4.5. Mesylation and azidation

Due to the unsuccessful reduction involving both catalytic hydrogenation and diimide reduction, it was decided that the Wittig reaction product would have to be deprotected in order to rule out steric hindrance of the isopropylidene protecting group. The hydroxyl group at C2 first had to be protected with a group that would be suitable to azidation at a slightly later stage in the synthesis. This group also had to be stable to the reaction conditions used to remove the acetonide and trityl groups.

A mesylate group was added to the hydroxyl group at C2 of the phytosphingosine base by the addition of methanesulfonylchloride ($MeSO_2Cl$) before the isopropylidene and trityl groups could be cleaved by the addition of hydrochloric acid and methanol (MeOH) (Figure 2.10).

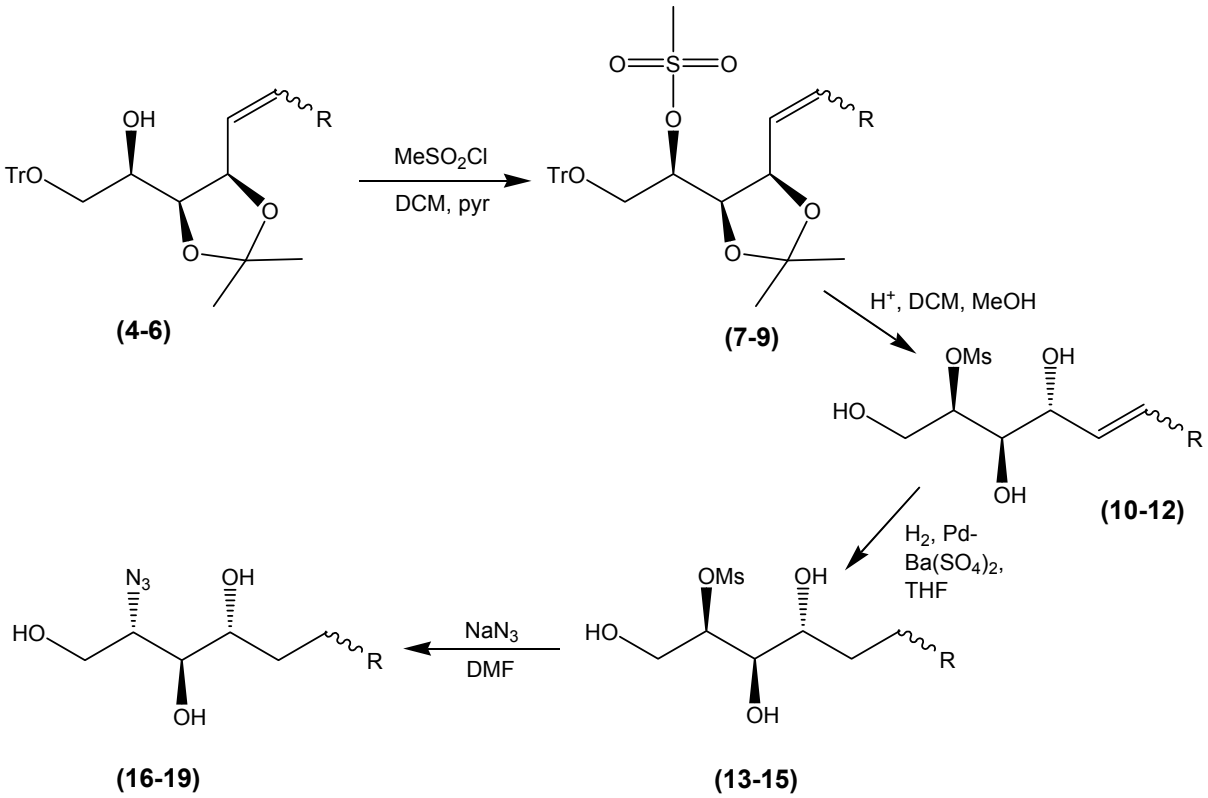

Figure 2.10: **Mesylation, deprotection, reduction and azidation of Wittig compounds.** R=$C_{12}H_{25}$ **(16)**; R=C_9H_{19} **(4)**, **(7)**, **(10)**, **(13)**, **(17)**; C_6H_{13} **(5)**, **(8)**, **(11)**, **(14)**, **(18)**; C_3H_7 **(6)**, **(9)**, **(12)**, **(15)**, **(19)**.

Catalytic hydrogenation of the double bond then proceeded without complication using 5% palladium barium-sulfate as the catalyst. The addition of sodium azide resulted in the mesylate group being replaced with an azide group, with an inversion of stereochemistry at C2 (Figure 2.10).

2.4.6. Silyl ether and benzoate protecting groups

Silyl ethers are some of the most common protecting groups for hydroxyl groups, due to the fact that the reactivity of their formation and cleavage can be modified by altering the substituents on the silicon atom; their steric and electronic effects modulate the ease of cleavage in multiply functionalised substrates. Silyl groups can be easily removed by the addition of a chemical containing a fluoride ion. This is due to the high affinity that fluoride ions have for silicon atoms. This is quantified by the fact that a silicon-fluoride bond is 30kcal/mol greater than a silicon-oxygen bond. Silyl ethers do have the ability to migrate between hydroxyl groups within a compound. Occasionally this can be advantageous, but more often than not is troublesome. *Tert*-butyldiphenylsilyl (TBDPS) groups are more stable than *tert*-butyldimethylsilyl (TBDMS) groups, which are frequently seen to migrate, and although the former is less stable to base, it is approximately 100 times more stable towards acidic hydrolysis than the TBDMS group. *Tert*-butyldiphenylsilyl chloride was used to introduce this group and is selective for primary hydroxyl groups i.e. the OH at C1, due to its bulky nature (Figure 2.11). The remaining two free hydroxyl groups were then protected using benzoyl chloride, the most common reagent used for the introduction of benzoyl groups, resulting in the formation of acid-stable, base-labile benzoate ester groups (Figure 2.11).

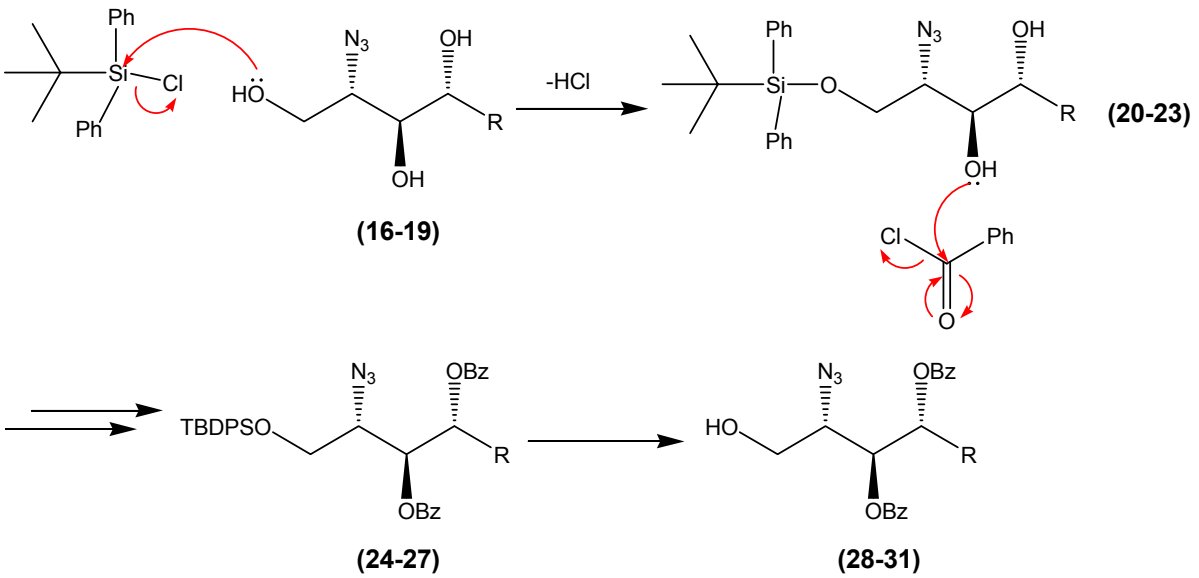

Figure 2.11: **Reprotection of C1, C3 and C4 hydroxyl groups of the developing phytosphingosine base and C1 deprotection.** R=$C_{14}H_{29}$ **(16)**, **(20)**, **(24)**, **(28)**; R=$C_{11}H_{23}$ **(17)**, **(21)**, **(25)**, **(29)**; R=C_8H_{17} **(18)**, **(22)**, **(26)**, **(30)**; R=C_5H_{11} **(19)**, **(23)**, **(27)**, **(31)**.

The benzoate ester is one of the more common esters used in the protection of alcohols, due to it being more stable to hydrolysis than acetates and its tendency to migrate to adjacent hydroxyl groups is not nearly as strong as the migrating nature of acetate groups. Nevertheless, the benzoate group can be forced to migrate if their resulting position is more thermodynamically stable.

After removal of the TBDPS group, using acetic acid and 1M tetrabutylammonium fluoride (TBAF) solution (due to the high affinity of silicon with a fluoride ion, as discussed above), the benzoyl-protected azido compound could undergo glycosylation specifically at C1 of the phytosphingosine-derived group, without the protecting groups being cleaved.

2.5. Glycosylation and *N*-acylation products with varying base chains.

In order to synthesise analogues of α-GalCer (44), a number of chemical obstacles had to be overcome. Several groups have reported the synthesis of the parent glycolipid analogue, yet when these were investigated, problems were encountered and thus adaptations were made and in some steps of the chemical synthesis, alternative methods were sought out. These are discussed in some detail throughout the next chapters and possible explanation considered as to why certain reactions did not proceed according to the literature and/ or general chemical know-how. Figure 2.12 shows the general reactions involved in coupling the phytosphingosine base with sugar, and subsequent deprotection, reduction and *N*-acylation.

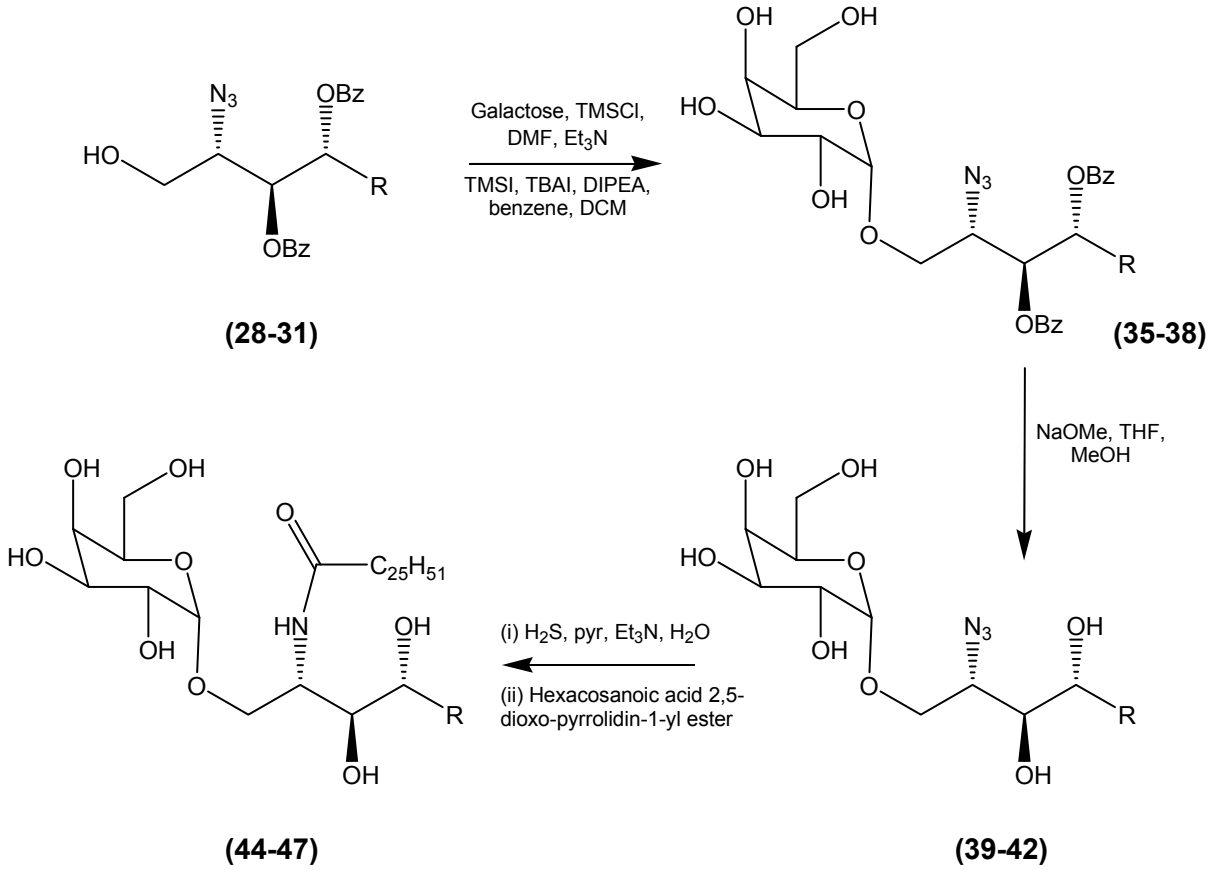

Figure 2.12: **Glycosylation, deprotection, azide reduction and *N*-acylation of varying phytosphingosine bases.** R=$C_{14}H_{29}$ **(28)**, **(32)**, **(36)**, **(40)**; R=$C_{11}H_{23}$ **(29)**, **(33)**, **(37)**, **(41)**; R=C_8H_{17} **(30)**, **(34)**, **(38)**, **(42)**; R=C_5H_{11} **(31)**, **(35)**, **(39)**, **(43)**.

2.5.1. Glycosylation

Glycosylation involves the displacement of the anomeric leaving group on one sugar (termed the glycosyl donor) and the subsequent coupling with the free hydroxyl group of the glycosyl acceptor. In the presence of water, hydrolysis products are formed where a hydroxyl group replaces the leaving group on the glycosyl donor; water molecules act as competitive nucleophiles. The reaction therefore must be performed under anhydrous conditions, with molecular sieves being added to scavenge for any remaining water molecules. Molecular sieves are zeolites that consist of a three-dimensional network of silica, aluminia tetrahedral. Water, naturally present in the zeolite network, is removed by heating, leaving cavities that can selectively absorb molecules of a specific size. 4Å molecular sieves absorb water, which once absorbed is trapped and thus can not affect the reaction mixture.

Regioselectivity is a problem when the glycosyl acceptor has more than one hydroxyl group as any free alcohol can act as the nucleophile. Thus protecting groups are vital. As some glycosylations using glycosyl fluorides use a hard Lewis acid to activate the glycosyl donor, the protecting group must be acid-stable as discussed earlier. Hindered secondary hydroxyl groups of partially protected glycosyl acceptors are less efficient nucleophiles, but should still be protected to obtain the required regioselectivity.

The presence of the ring oxygen facilitates a S_N1 type reaction; its lone pairs aid the departure of the leaving group at the anomeric carbon, and they also help stabilize the resulting carbonium ion intermediate by resonance. Nucleophilic attack can occur from either the top or bottom face of the sugar ring structure (Figure 2.13). The nature of the solvent and protecting group on the neighbouring C2 hydroxyl group play important roles in determining the relative amounts of the two possible (α or β) products.

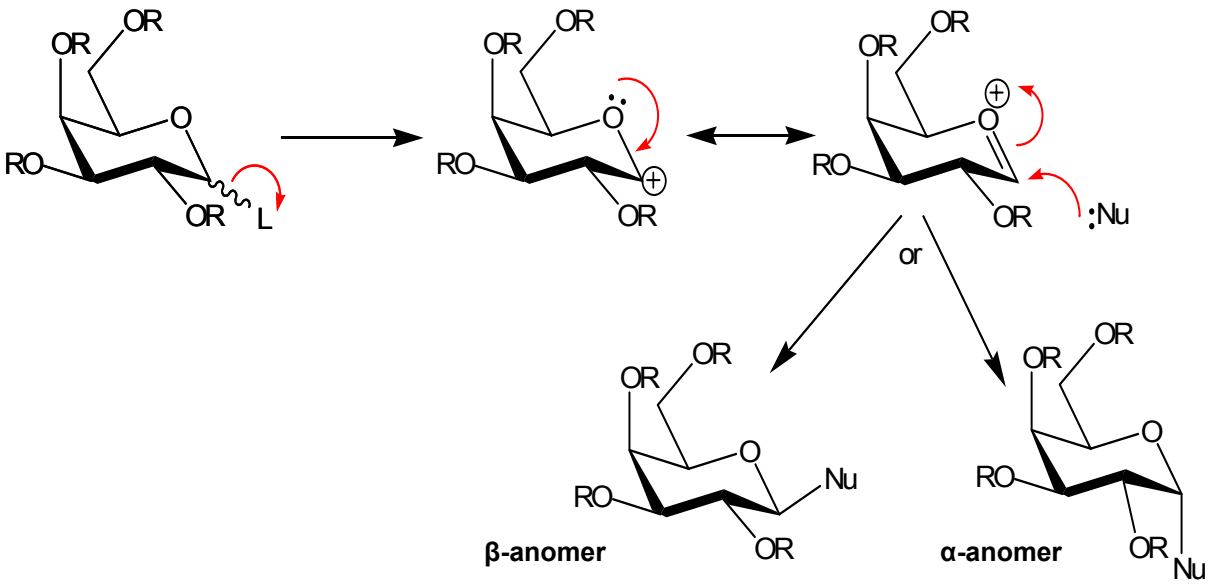

Figure 2.13: **Nucleophilic attack on a glycosyl donor.** The reaction can lead to two possible anomers on an anomeric glycosyl donor, where L indicates a leaving group and Nu represents the nucleophile.

2.5.2. Basic transesterification; removing benzoyl protecting groups

A benzoate ester can be cleaved by the addition of methanolic sodium hydroxide at room temperature. Addition of acetic acid prevents the migration of the benzoyl group, ensuring the desired compound is produced. Esters in the presence of an alcoholate anion base undergo base-catalysed transesterification, forming an anionic intermediate that can either dissociate back to the original ester or a new ester and alcohol. If there is a sufficiently large excess of sodium methoxide, the equilibrium point of the reaction will be displaced until virtually all the product is the new ester and alcohol, which in this case is a benzoic acid methyl ester and the glycosylated azido diol (Figure 2.14). The reaction must be carried out under strictly anhydrous conditions as the presence of water irreversibly dissociates the intermediate compound to the free acid. 0.5M to 2M sodium methoxide in anhydrous MeOH is one of the most common reagents used for basic transesterification (Figure 2.14).

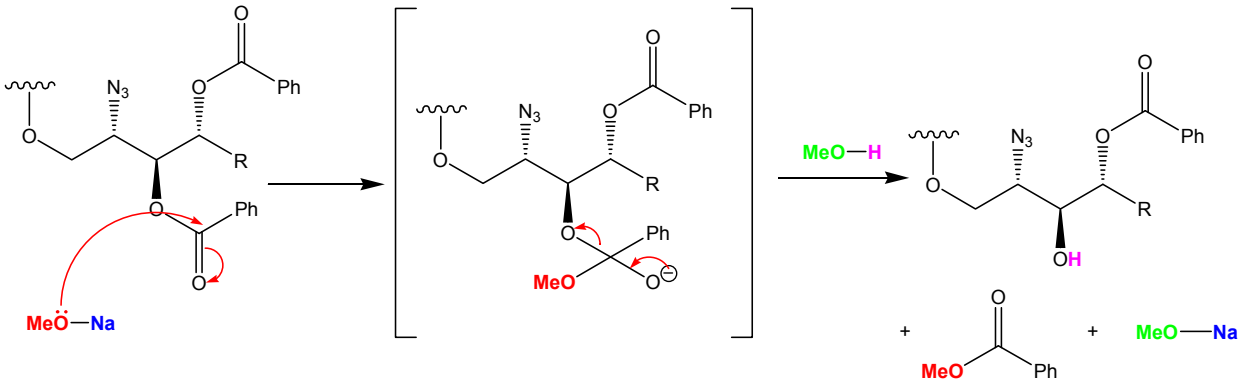

Figure 2.14: **Mechanism of base-catalysed transesterification.** Sodium methoxide acts as a base attacking the carbonyl of the benzoate group, forming an anionic intermediate with the benzoate ester protecting group on the sphingosine hydroxyl groups. In the presence of a large excess of methanolic sodium methoxide, this forms the new benzoic acid methyl ester and free hydroxyl groups on the C3 and C4 positions of the sphingosine base. (C4 deprotection not shown, but occurs in an identical manner).

2.5.3. Reduction of the azide group

In order for an *N*-acyl group to be introduced producing a glycosyl ceramide, the azide functional group needs be converted to a reactive amine group. Traditionally, the azide group has been reduced to the amine by using hydrogen sulfide. Two methods conventionally used to reduce the azide are via the Staudinger reaction and also by employing hydrogen sulfide.

2.5.3.1. Trimethylphosphine and the Staudinger reaction

An effective method of reducing an azide group to an amine group is by the Staudinger reaction, which is a very mild azide reduction. The reaction involves triphenylphosphine reacting with the azide to generate a phosphazide, which then loses nitrogen gas to form an iminophosphorane. Aqueous work up leads to the amine and the very stable phosphine oxide (Figure 2.15). An alternative reagent which has been successfully employed in the

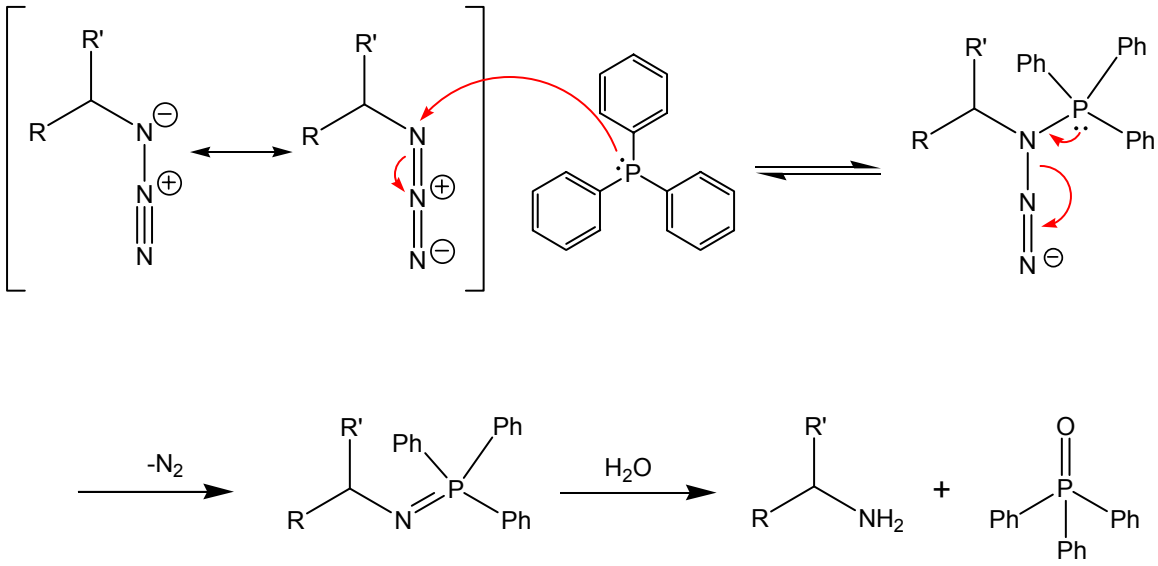

Figure 2.15: **The general mechanism of the Staudinger reaction.** The triphenylphosphine forms a phosphazide intermediate which produces nitrogen gas as a by-product in the formation of an iminophosphorane. This is then hydrolysed to give the amine and phosphine oxide.

Staudinger reaction in place of triphenylphosphine, is trimethyphosphine [215]. Although the triphenyl phosphineoxide bi-product of the reaction using triphenylphosphine is stable, it has to be removed by chromatographic methods.

Employing trimethylphosphine results in a volatile bi-product that is easily removed along with the reaction solvent by rotary evaporation, thus reducing potential loss of product during purification [216]. However the reactant itself is pyrophoric, with the potential to react violently when it comes into contact with humid air or water. Thus handling requirements are more stringent than with triphenylphosphine, and the azido compound must be moisture-free.

2.5.3.2. Reduction using hydrogen sulphide

Although hydrogen sulfide is a toxic substance, its use in the azide reduction proceeded well and any residual sulfur containing compounds were successfully removed following the

addition of the *N*-acyl group and during purification. This method was employed because the Staudinger reaction, although successful in reducing the azide group, proved to interfere in some way at the later stages of *N*-acylation when the glycosyl iodide method of glycosylation was employed. Other groups had reported similar problems, and had overcome them by using hydrogen sulfide [217].

2.6. Biological results and interpretation

A number of groups have shown that an α-GalCer analogue with a truncated phytosphingosine chain, (OCH9) **(47)** exhibits a less stable binding interaction with CD1d than α-GalCer [144, 192]. The two pockets of the hCD1d protein adopt different conformations when empty, than when occupied by a lipid [71]. One theory is that the shortened phytosphingosine chain does not completely 'fill' the F' pocket of the protein, possibly resulting in the phytosphingosine base chain of α-GalCer **(44)** being repositioned in the F' channel which in turn affects the orientation of the α-linked sugar. Alternatively, sections of the F' pocket could collapse if only partially filled, altering the internal structure of the CD1d α-helices, which in turn could modify the orientation of the sugar head group [218]. The effect of an altered sugar orientation is likely to result in a less prolonged TCR stimulation, and thus a possible skewing of the immune response. As shown by Miyamoto *et al.* [144], the immune response of B6 mice after an intra-peritoneal injection of α-GalCer **(44)**, results in a rapid secretion of the T_H2 cytokine IL-4, followed by a prolonged secretion of the T_H1 cytokine IFN-γ. If an altered glycolipid antigen binds less stably with the TCR, and thus for a decreased amount of time, it was hypothesised that the immune response could effectively be altered to bias the initial T_H2 response. Miyamoto *et al.* [144] went on to demonstrate this with murine cells and OCH9 **(47)**, showing greater concentrations of the cytokine IL-4 being secreted and decreased IFN-γ production by iNKT cells over time, when compared with control and α-GalCer **(44)** (Figure 2.16).

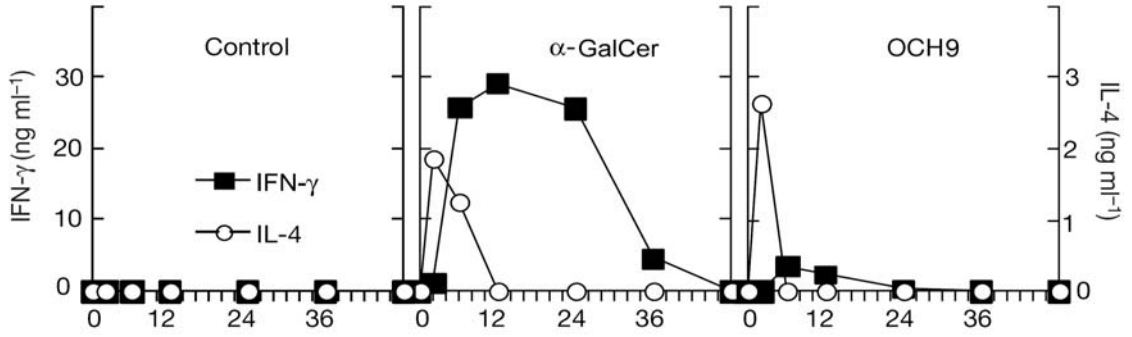

Figure 2.16: **Changes in serum cytokine levels after injection of α-GalCer (44) or OCH9 (47)**. B6 mice were injected intraperitoneally with 100μg kg^{-1} of glycolipid, and serum samples were obtained at indicated times after injection. Serum levels of IL-4 and IFN-γ were determined by a sandwich enzyme-linked immunosorbent assay (ELISA). Figure adapted from [144].

Taking this theory further, a number of biological evaluations were performed by McCarthy *et al.* at the Weatherall Institute of Molecular Medicine, University of Oxford, UK using a small library of α-GalCer analogues synthesised during this project, that varied in the chain length of the phytosphingosine base [218]. These included the affinity of hCD1d binding and the TCR binding affinity to hCD1d. A Fab antibody that specifically binds to C1R-hCD1d molecules loaded with α-GalCer **(44)** and other associated analogues (Fab 9B) was used to measure the dissociation of the analogues from soluble hCD1d over a period of time. The Fab 9B antibody fails to stain unpulsed C1R-hCD1d cells, or cells loaded with β-GalCer, which was used as a negative control. The rate of dissociation of each α-GalCer analogue from C1R-hCD1d cells over time, as measured by surface plasmon resonance (SPR) studies is shown in Figure 2.17A [218]. It is clear from these results that a decreased number of carbon atoms in the phytosphingosine chain of α-GalCer **(44)** increases the rate of dissociation from hCD1d molecules; the analogue OCH9 **(47)** has a half-life approximately 4 times shorter than α-GalCer **(44)**.

The dissociation constants (K_d) of α-GalCer **(44)** and three analogues (OCH15 **(45)**, OCH12 **(46)** and OCH9 **(47)**), that vary in the phytosphingosine chain length, were also determined.

The equilibrium constant K_d measures the tendency of a larger object to separate reversibly into smaller components. It corresponds to the concentration of antigen, at which the concentration of protein with antigen bound is equal to the concentration of protein with no antigen bound. A smaller dissociation constant results in a higher affinity between antigen and protein. In this case, it is a measure of the propensity of α-GalCer **(44)** to dissociate from the CD1d protein to which it is bound. The data in Figure 2.17B corresponds with the affinity measurements of the four GSLs tested (Figure 2.17A) and shows that analogues with truncated phytosphingosine bases have a greater degree of dissociation from CD1d than α-GalCer **(44)**. The results also indicate that this effect dramatically increases with reduced chain length, and this is exemplified by K_d values of 123μM for OCH9 **(47)**, compared with 1.29μM for α-GalCer **(44)** (Figure 2.17B). The affinity of complexed hCD1d-α-GalCer with iNKT TCR was also investigated, and the results demonstrated that the binding of the hCD1d-α-GalCer complex was much more stable than that of the analogues with shortened phytosphingosine bases (Figure 2.18). The complex incorporating OCH15 **(45)** had an affinity for the TCR similar to that of α-GalCer **(44)**, whereas the OCH12 **(46)** and OCH9 **(47)** analogues, respectively, had dramatically decreased affinities. This implies that optimal iNKT TCR binding requires the hCD1d F' channel to be occupied by an α-GalCer analogue with a phytosphingosine chain of 15 to 18 carbons.

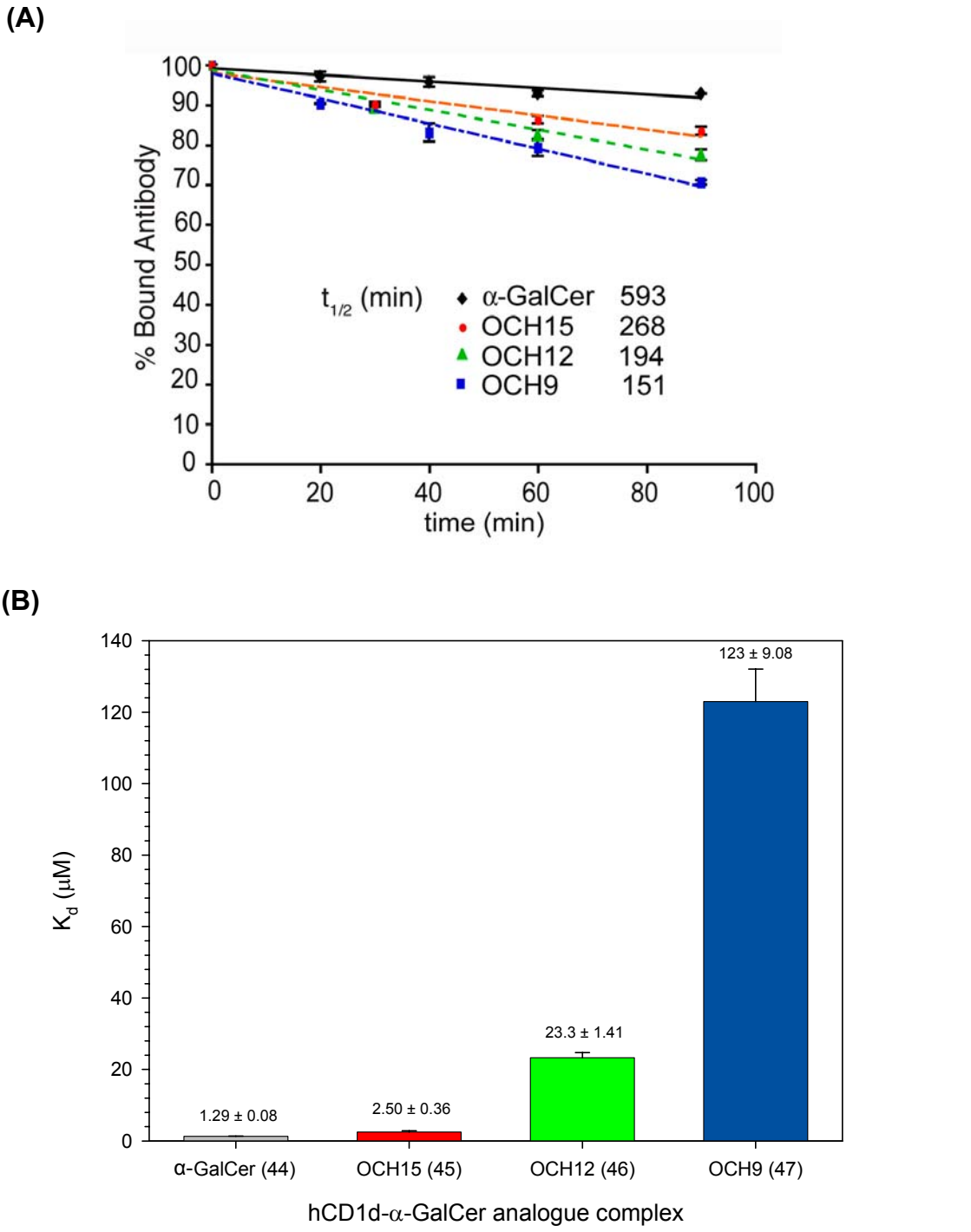

Figure 2.17: **Binding affinities of α-GalCer analogues to hCD1d. (A)** Dissociation of α-GalCer analogues from hCD1d.The antigen-hCD1d complexes were loaded onto a sensor surface at t = 0. The amount of remaining hCD1d at given time points was measured using Fab 9B antibody and SPR. Dissociation values only shown for the first 100 mins, but with half-life values listed. Figure adapted from [218] **(B)** The mean dissociation constants from hCD1d of α-GalCer **(44)** and three analogues varying in the length of the phytosphingosine base chain: OCH15 **(45)**, OCH12 **(46)**, OCH9 **(47)**. Experiments carried out at the Weatherall Institute of Molecular Medicine, University of Oxford, UK using analogues synthesized during this project. All compounds produced by methods outlined in Chapter 5.

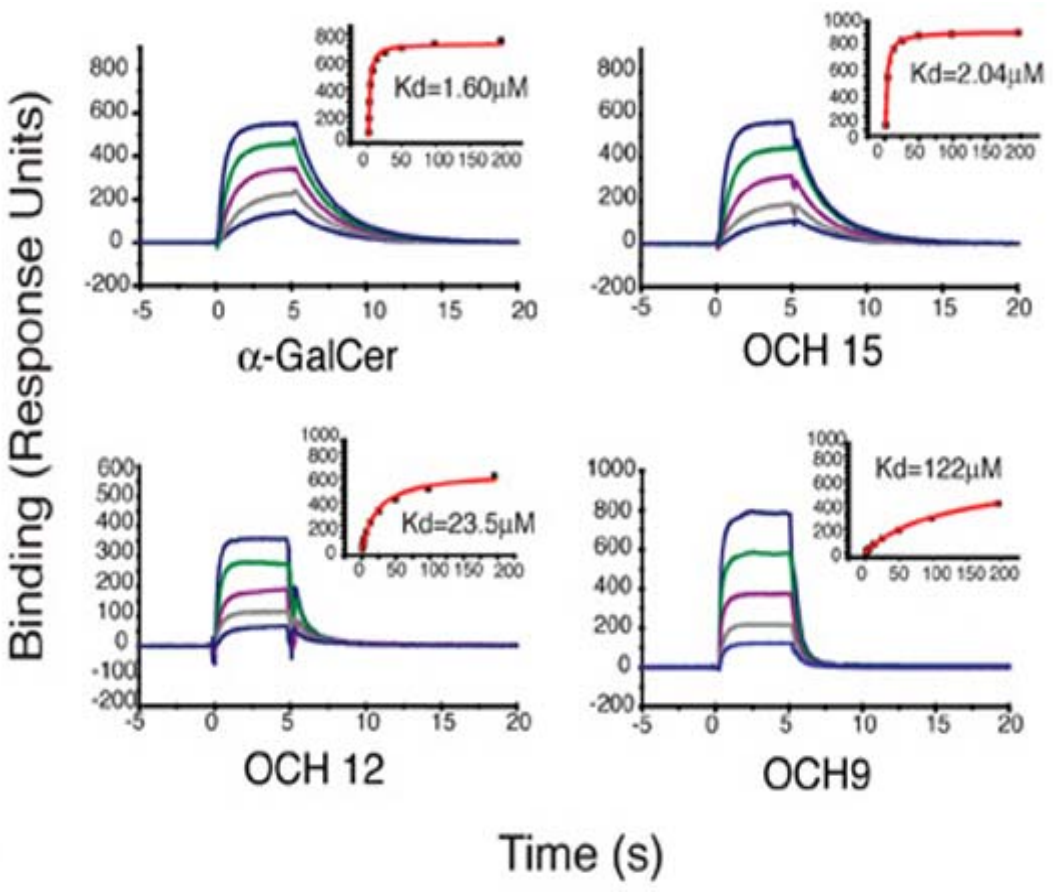

Figure 2.18: **Affinity and kinetics of iNKT TCR binding to hCD1d-α-GalCer complexes.** The binding responses of 5 concentrations (increasing from 0.4 – 194μM) of hCD1d-α-GalCer complex injected with iNKT TCR for 5s are shown, with the equilibrium binding response (K_d) shown in the insets. Experiments carried out at the Weatherall Institute of Molecular Medicine, University of Oxford, UK using analogues synthesized during this project. Figure adapted from [218].

To demonstrate that the binding affinities of the hCD1d-α-GalCer complexes with the TCR were not as a result of hCD1d loading with the α-GalCer analogues described, the rate constants k_{on} and k_{off} were determined by direct measurements of the TCR with hCD1d-α-GalCer analogues complexed with α-GalCer **(44)**, OCH15 **(45)**, OCH12 **(46)**, with the exception of OCH9 **(47)**. Due to its exceptionally fast k_{off} value (2.67 S^{-1} compared with 0.39 S^{-1} of α-GalCer **(44)**) (Table 2.1), the k_{on} value of OCH9 **(47)** was difficult to determine experimentally, but was instead calculated from k_{off}/ K_d values gained.

hCD1d-α-GalCer complex	**k_{off} (S^{-1})**	**k_{on} ($M^{-1}S^{-1}$)**
α-GalCer **(44)**	0.39 ± 0.01†	$3.31 \times 10^5 \pm 2.5 \times 10^{4}$†
OCH15 **(45)**	0.47 ± 0.06	$2.04 \times 10^5 \pm 1.6 \times 10^4$
OCH12 **(46)**	1.00 ± 0.12	$3.7 \times 10^4 \pm 5 \times 10^3$
OCH9 **(47)**	2.67 ± 0.12	$2.3 \times 10^4 \pm 1 \times 10^{3*}$

Table 2.1: **Affinity and kinetic measurements of hCD1d-α-GalCer complexes with iNKT TCR.** Unless stated, all values are the mean of two experiments. †Mean of three or more experiments. *Calculated from experimentally derived K_d and k_{off} values. Experiments carried out at the Weatherall Institute of Molecular Medicine, University of Oxford, UK using analogues synthesized during this project. [218].

From the smaller K_d values in Figure 2.18 and the smaller k_{off} values in Table 2.1, one can surmise that α-GalCer analogues with longer phytosphingosine chains have a greater affinity for the iNKT TCR when complexed with the CD1d protein. A smaller K_d value is indicative of a stronger binding interaction. In relation to this, a much faster k_{off} results in an increased K_d and thus indicates a weaker binding between the hCD1d-α-GalCer complex and the iNKT TCR.

As hypothesised, a less stable binding interaction between α-GalCer **(44)**, CD1d and the TCR has an effect on the immunological response of the iNKT cell. Unlike the results obtained using murine iNKT cells, the cytokine profile of OCH9 **(47)** was not biased towards a T_H2 response when hCD1d was employed, but instead resulted in a decrease of both IL-4 and IFN-γ production (Figure 2.19). However, the amounts of T_H1 and T_H2 cytokine were much more similar in OCH12 **(46)** and OCH9 **(47)**, than in the parent glycolipid, α-GalCer **(44)** and OCH15 **(45)**.

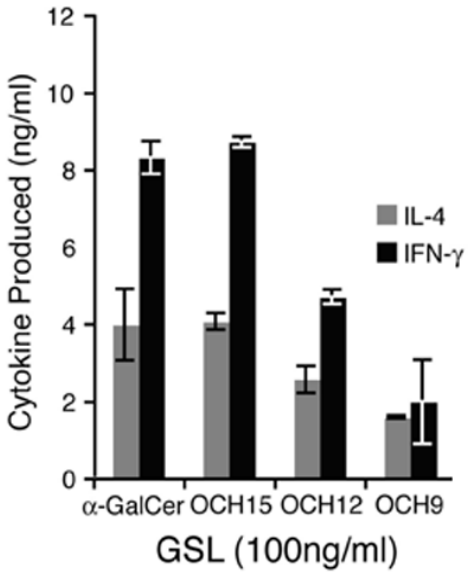

Figure 2.19: **iNKT cell activation in vitro is modulated by the length of the phytosphingosine base chain in α-GalCer analogues.** C1R-hCD1d cells were pulsed with 4 α-GalCer analogues as shown and used to stimulate human iNKT cells. The supernatant was assayed for IL-4 and IFN-γ production by ELISA. SD (error bars) from the mean of two duplicate experiments is shown. Experiments carried out at the Weatherall Institute of Molecular Medicine, University of Oxford, UK using analogues synthesized during this project. Figure adapted from [218].

The ability of α-GalCer **(44)** and OCH9 **(47)** to stimulate the expansion of iNKT cells from peripheral blood lymphocytes (PBLs) from healthy donors was demonstrated at the Weatherall Institute of Molecular Medicine, University of Oxford, UK by McCarthy *et al.* [218] and by G. Bricard, J.S. Im and myself at the Albert Einstein College of Medicine, New York, USA using the analogues synthesised during this project. The frequency of iNKT cells was measured 21 days after stimulation of PBLs with mature autologous DCs, pulsed with either α-GalCer **(44)** or OCH9 **(47)** at various concentrations, and repeated on three different PBL samples. As shown in Figure 2.20, the parent glycolipid antigen α-GalCer **(44)** was much more successful at stimulating iNKT cell expansion than OCH9 **(47)** at all concentrations.

Assuming OCH9 **(47)** adopts the same orientation as α-GalCer **(44)**, the crystal structures of unloaded hCD1d and α-GalCer-loaded hCD1d can be used as comparative models. Both crystal structures have bee reported previously [71] and one can surmise from the results

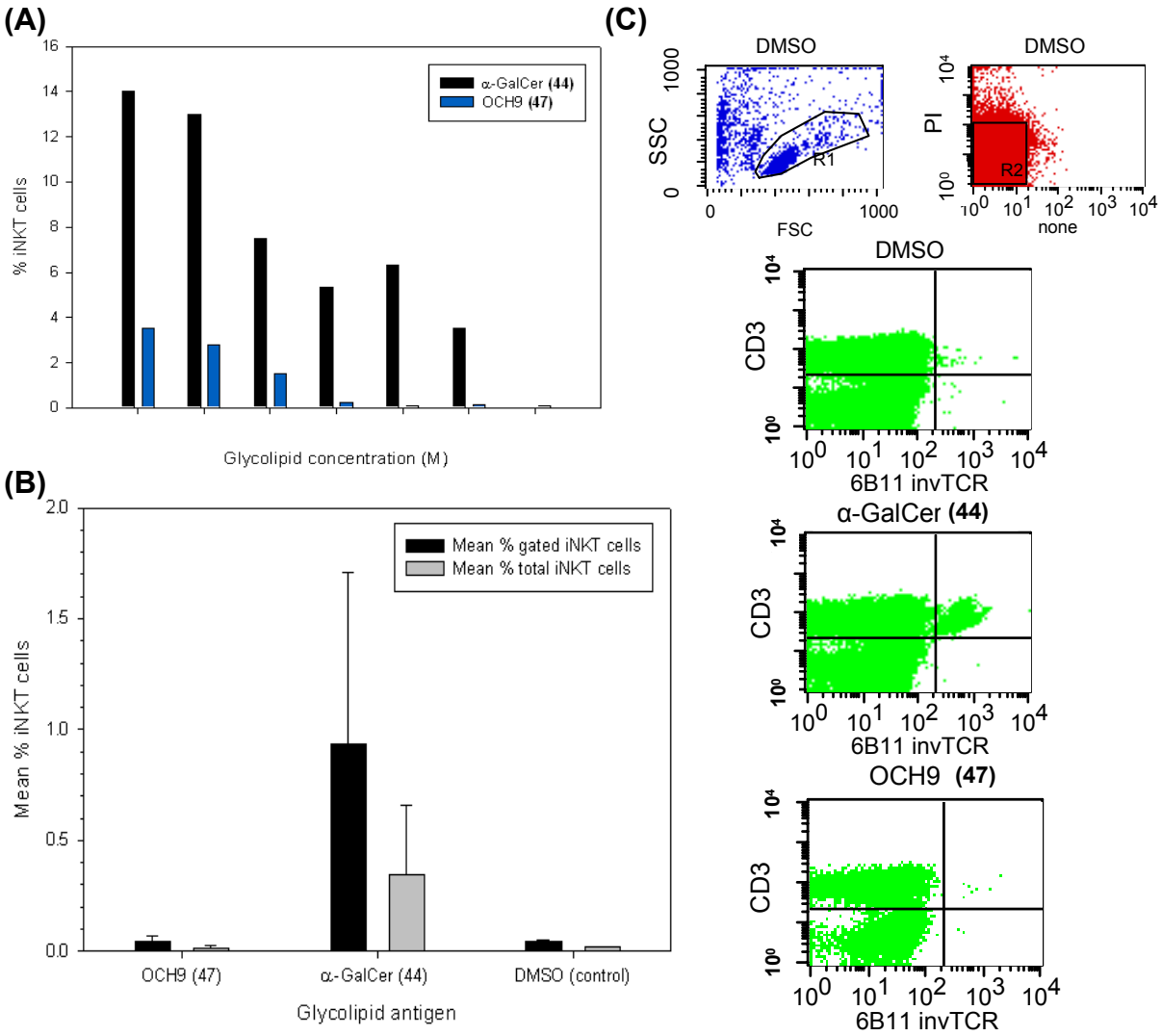

Figure 2.20: **iNKT cell expansion in vitro is modulated by the length of the α-GalCer phytosphingosine chain. (A)** iNKT ($V\alpha24^{+}$hCD1d-tetramer^{+}) cell frequency from treatment with varying concentrations of α-GalCer analogues. The results are shown as the percentage of gated cells as determined by fluorescence-activated cell sorting (FACS) analysis. Experiments carried out at the Weatherall Institute of Molecular Medicine, University of Oxford, UK using analogues synthesized during this project. Data from [218]. **(B)** Mean percentage of gated and total iNKT cell (HDD.11 cells) frequency from ex vivo treatment with 100nM α-GalCer analogue. Procedures completed at Albert Einstein College of Medicine, New York, USA using analogues synthesised during this project. **(C)** FACS analysis plots showing the gating of iNKT cells and the differences in cell expansion of HDD.11 cells after stimulation with α-GalCer **(44)** and OCH9 **(47)** compared with a control of DMSO after ex vivo 100nM GSL stimulation. Experiments carried out at Albert Einstein College of Medicine, New York, USA using analogues synthesised during this project.

that the OCH9 **(47)** only partially fills the F' channel of hCD1d, due to its shorter phytosphingosine chain.

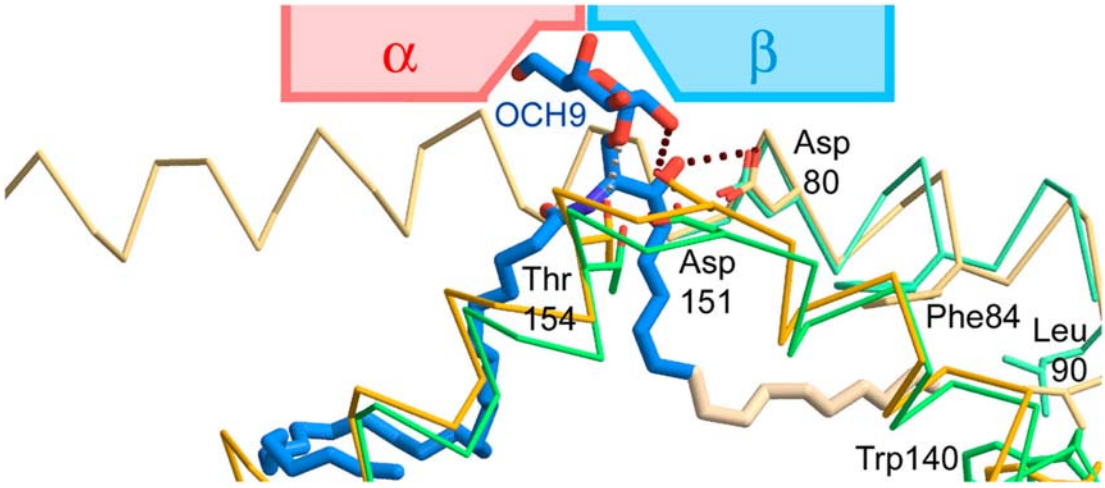

Figure 2.21: **Modelling of the effects of variations in lipid chain length on the structure of hCD1d.** A Cα trace and selected side chains are shown in yellow for the hCD1d crystal structure with bound α-GalCer **(44)**. Relevant regions of the structure of hCD1d in the absence of bound ligand are shown in green. Hydrogen bonds are depicted as dotted lines, and the assumed position of bound TCR is depicted schematically. The portion of α-GalCer corresponding to OCH9 **(47)**, is drawn in blue. Side chains are positioned differently in the empty and partially-filled structures. Based on these differences, residues within the F' channel that are predicted to alter when hCD1d is bound with OCH9 **(47)**, as opposed to α-GalCer **(44)**, have been highlighted. Modelling carried out at the Weatherall Institute of Molecular Medicine, University of Oxford, UK. Adapted from [218].

Two residues that hydrogen bond to the sugar head of α-GalCer antigens are Asp151 and Thr154, as shown by mutagenesis studies by Burdin *et al.* [219] and Sidobre *et al.* [220].

Any substantial alterations in the positions of these residues would be expected to impact the network of hydrogen bonds, thus affecting the recognition of the antigen by the iNKT cell TCR, as it is the hydrogen bonding that dictates the position of the polar head-group.

Modification of the phytosphingosine chain and the subsequent partially filled conformation of the F' channel of hCD1d, results in predicted differences between hCD1d-OCH9 and hCD1d-α-GalCer structure of approximately 2Å between residues Leu139 and Thr154 in the main chain of the α2 helix of the CD1d molecule.

It is in this same putative TCR binding region that the two hydrogen-bonding residues are found. Thus, a shift in the α2 helix residue position directly correlates to a shift in the hydrogen bonding network position, which in turn affects the recognition of α-GalCer **(44)** antigen by the TCR. The model shown (Figure 2.21) and the experimental data gained, support the hypothesis that a conformational change in the hCD1d molecule and the extent of filling of the hCD1d F' channel, both affect the TCR recognition of α-GalCer analogues.

Differences between PBLs stimulated with α-GalCer **(44)** and OCH9 **(47),** in their cytokine profiles (Figure 2.16, Figure 2.19) and cell proliferation (Figure 2.20), can be attributed to the weaker binding of OCH9 **(47)** within the CD1d pocket and consequently with the TCR of iNKT cells, compared with that of the parent glycolipid, α-GalCer **(44)**. It has been shown that *in vivo* activation of iNKT cells can assist in priming of antigen-specific immune responses [191]. Reduced lysis of DCs pulsed with shorter phytosphingosine chain α-GalCer analogues suggests that more attention should be paid to the use of so-called 'weaker' iNKT cell agonists, such as OCH9 **(47)**, which, unlike α-GalCer **(44)**, may ensure a longer lifespan of APCs which is paramount in clinical settings.

The fact that the hypothetical model of OCH9 **(47)** bound hCD1d complexes mirrors the experimental results gained using glycolipids varying in the length of the phytosphingosine chain, effectively highlights the fact that α-GalCer **(44)** structure, with regards to the base chain length, does play a part in fine-tuning the affinity of the TCR to the hCD1d-GSL complex. This directly affects the downstream immunological processes, such as cytokine release and cell proliferation. Further experimentation is needed in order to broaden and expand these results, and investigate the mechanisms behind them in a fuller manner. However, these structural differences, and the observed effects they have on CD1d-TCR

binding, could play a vital part in the search for an antigen that could successfully prevent or treat autoimmune diseases such as type 1 diabetes.

Chapter 3

Variations in the sugar head

3. Variations in the sugar head

3.1. Introduction

There are a number of possible variations of the sugar head of an α-GalCer antigen that can be adjusted to produce novel antigenic compounds, whilst still retaining their desired immunological properties. Figure 3.1 summarises some of the structural requirements that have previously been explored, how they relate to the reactivity of the resulting glycolipid antigen, and which features are vital for activation of iNKT cells [54, 95, 178, 180, 185, 221-225], some of which have been investigated throughout this project.

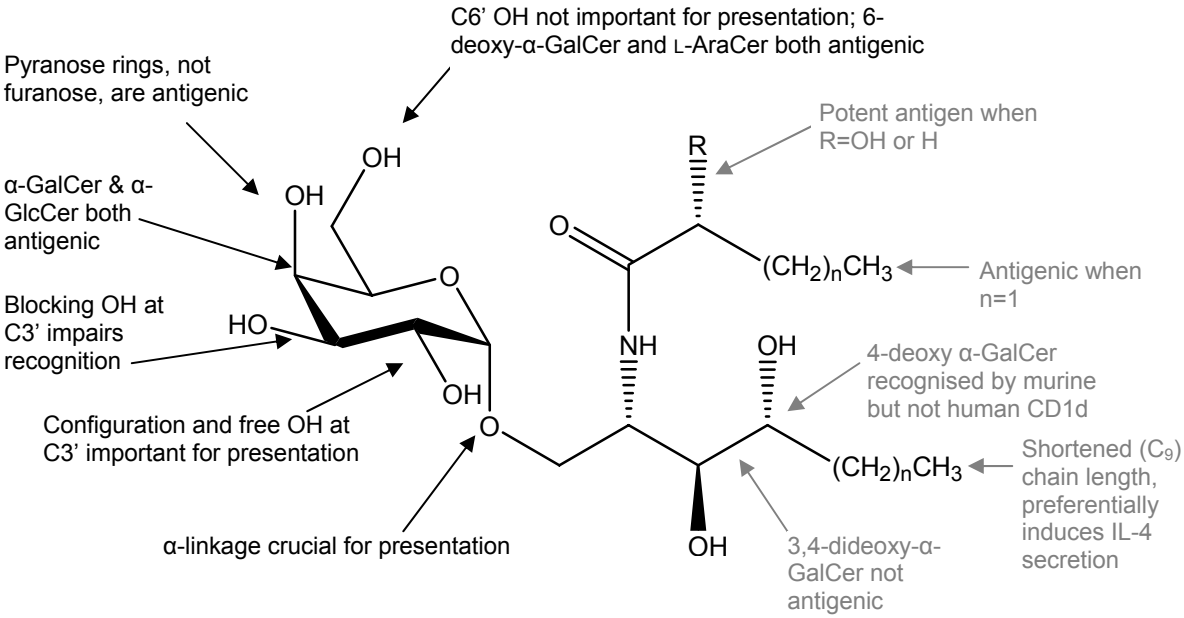

Figure 3.1: The relationship between the structure of α-GalCer analogues and bio-reactivity.

3.2. α vs. β anomeric linkage

An α-anomer of a sugar refers to a pyranosyl or furanosyl carbohydrate where the anomeric group (at C1) is on the opposite side of the ring to the C6 carbon group; the CH_2OH unit in the case of galactose and glucose, CH_3 in the case of fucose. Hence a β-anomer has the anomeric group on the same side of the ring as the C6 functionality (Figure 3.2).

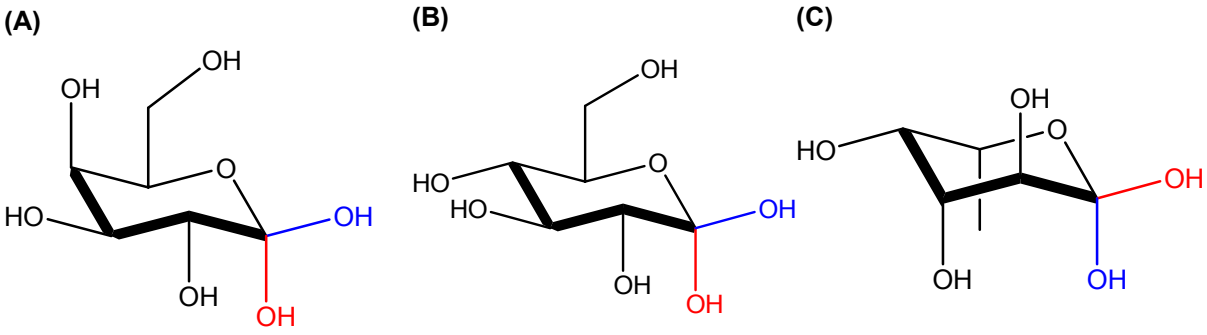

Figure 3.2: **The structures of α- and β-anomeric positions in three sugars. (A)** D-Galactose **(B)** D-Glucose **(C)** L-Fucose. The red hydroxyl groups indicate the α-positioning, and the blue hydroxyl groups indicate the β-positioning. Note that in the L-enantiomer of fucose, the C6 group sits below the ring, but the α-position is still on the opposite side of the ring to that group.

Mammalian cells produce a variety of glycosyl ceramides that are structurally related to α-GalCer **(44)**. However, these natural compounds have a β-anomeric link and are not known to activate iNKT cells [70].

The α-forms of D-GalCer **(44)** and D-GlcCer **(50)**, incorporating galactose and glucose as the sugar moiety respectively, have been shown to have stronger antitumour and immunostimulatory activities than their β-counterparts [59, 226]. β-Forms of the antigens do however bind to CD1d [227], suggesting that the orientation of the sugar on the analogue is more important for TCR stimulation than it is for CD1d contact. When the murine CD1 protein (mCD1) presents β-GalCer to iNKT cells, proliferative responses such as the release of IL-2 which is a typical T-cell response, ensuing activation, and cell-proliferation, are not observed [59, 96, 98, 224, 228]. Ortaldo *et al.* [96] concurred that the β-form of the α-GalCer

analogue does not stimulate cytokine production in C57BL/6 (B6) mice, and also showed that β-GalCer demonstrates lower intensity binding to iNKT cells compared with α-GalCer [96, 224].

Interestingly, the β-configuration of compounds like β-L-AraCer play a key part in the expression of strong immunostimulatory activity [226]. β-GalCer has also been shown to have a strong immunostimulatory profile, albeit by increasing the concentration of pro-inflammatory cytokines in the blood [229], revoking the beneficial effects of sulfatides. Sulfatide β-GSLs have been shown to be promiscuous CD1 ligands, successfully binding with CD1a, b and c [30, 93, 178]. They are present in pancreatic cells and are thought to play a part in islet pathology, decreasing the secretion of proinflammatory cytokines (IL-1β and TNF-α decreasing with a statistical significance), which are toxic to pancreatic β-cells at high concentrations [229]. This is a detrimental reaction, with regards to the conditions of both type 1 and type 2 diabetes (T1D and T2D, respectively), owing to the fact that the proinflammatory cytokines, such as IL-1β, IL-6, TNF-α and IFN-γ, are all known to influence pancreatic β-cells and have been implicated as pathogenic factors in both conditions [229, 230].

Singh *et al.* [227] went on to demonstrate that β-GalCer fails to stimulate iNKT cell responses with respect to T_H1/ T_H2 cytokine production, but does enhance another autoimmune disease, EAE, in mice. This could be though direct competition with an endogenous CD1d ligand, antagonising iNKT TCR recognition of the natural antigen. iNKT cells, activated by α-GalCer **(44),** are known to destroy leukaemic cell lines in a CD1d-dependent manner *in vitro* [231]. Rogers *et al.* [175] showed tumour cell lysis by $V\alpha24^+V\beta11^+$ NKT cells is a highly specific process that results in failure or a very poor response when the analogue β-GalCer is employed.

3.3. *O*- and *C*-glycosidic linkage

α-GalCer **(44)** is termed an *O*-glycoside due to the nature of the linkage between the sugar head and ceramide unit, via an oxygen atom. The majority of analogues of α-GalCer that have been synthesised and investigated to date, have also incorporated this *O*-glycosidic link. This possibly stems from the fact that the antigens, such as the naturally occurring sulfatide GSLs [30, 178], microbial ligands [46, 47, 179], KRN7000 [232] and the more recently discovered natural ligand of CD1d, iGb3 [54, 58], all have *O*-glycosidic linkages.

Recently, there has been increased attention to the possibility of synthesising *C*-glycoside analogues of α-GalCer [233, 234], where there is a carbon atom between the sugar and ceramide moiety, in place of more commonly found oxygen atom. The interest behind a *C*-glycosidic linkage has sprung from the train of thought suggesting *O*-linked glycosides are more susceptible to enzymatic degradation by enzymes such as α-galactosidases [233]. Glycosidases catalyse the hydrolysis of glycosidic linkages, generating two smaller sugar molecules from a larger more complex molecule. Amongst others, they are involved in normal cellular function and anti-bacterial defence strategies, and are a major constituent of the human body [235]. Therefore, a *C*-glycoside that is inert to such degradation by these enzymes could be beneficial in terms of potential drug administration.

When tested by Yang *et al.* [233], a *C*-glycoside analogue of α-GalCer **(44)** remained active in mice for a period of four days, whereas the corresponding *O*-glycoside analogue only remained active for one day. It was speculated that the endogenous enzymatic degradation of the *O*-glycoside, can be attributed to this difference in activity retention, although different binding mechanisms with the TCR or iNKT cells could also be a contributing factor [233].

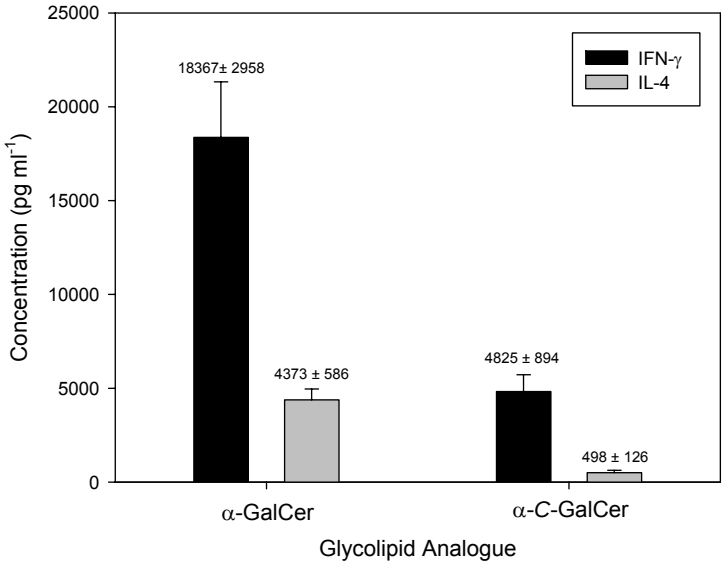

Figure 3.3: **Cytokine production in human iNKT cells and DCs by α-GalCer (44) and its *C*-glycoside analogue.** Supernatants from a 24h culture of DC and NKT cells with 100ng ml^{-1} of either α-GalCer **(44)** or α-C-GalCer were analyzed for cytokine secretion by Luminex multiplexing technology. Data are median standard deviations from five independent experiments. Raw data from [236].

Despite its increased activation times, the *C*-analogue of α-GalCer (α-*C*-GalCer) has been shown to have a skewed cytokine profile with a T_H1 bias (Figure 3.3) [236]. When directly compared with α-GalCer **(44)**, iNKT cells stimulated with 100ng ml^{-1} of α-*C*-GalCer had a cytokine profile with an IFN-γ:IL-4 ratio over twice that of the corresponding *O*-glycoside (ratios 9.6 and 4.2 respectively) (Figure 3.3) [236]; the *C*-glycoside shows a bias towards a T_H1 cytokine response, much like its *O*-glycoside counterpart. In the case of autoimmune diseases, such as T1D and SLE, this is detrimental.

The mechanism by which *C*-glycoside analogues of α-GalCer bind with CD1d proteins and stimulate iNKT cell responses is yet to be fully understood. One hypothesis is that the replacement of the anomeric oxygen with a carbon atom, results in a loss of one of the hydrogen bonds that are formed between the glycosidic head and CD1d protein, normally anchoring it in position [71, 234]. Removing one such hydrogen bond, could thus alter the orientation of the glycolipid within the protein, and subsequently alter the binding position of

the antigen: protein complex with the iNKT cell receptor. However, Lu *et al.* [236] disproved this with modeling studies that showed similar overall geometry of the bound *O*- and *C*-α-GalCer analogues within the CD1d protein. They suggested that the differences could be attributed to variations in the solubility of the molecules, access to lipid-transfer proteins and receptor-mediated uptake, all of which are involved in antigen-presentation [236].

The immunostimulatory activity of the *C*-analogue does suggest that this structural variation could provide another avenue to be explored through the synthesis of a *C*-glycoside analogue library, in the hope of discovering an antigen that could delay or prevent autoimmune diseases, without the T_H1 bias shown by the *C*-GalCer analogues investigated thus far.

3.4. Variation of the hydroxyl group on the sugar

A structural difference of α-GalCer analogues that has been investigated is the configuration of the hydroxyl group at carbon 4 (C4') of the sugar moiety [95, 223, 226]. When analysed by Motoki *et al.* [226], lymphocytic proliferation stimulatory activity of α-GalCer **(44)** was significantly greater than that of α-GlcCer **(50)**; the two analogues differ only in the configuration of the hydroxyl group at C4' of the sugar. This was also shown by Uchimara *et al.* [223] (Table 3.1).

These results indicate that the hydroxyl group at position 4' affects immunostimulatory activity. However, several years after Motoki's study [226], Kawano *et al.* [95] concluded that α-GalCer **(44)** and α-GlcCer **(50)** display no functional differences when stimulating iNKT cells. However, an analogue incorporating mannose as the sugar head (α-ManCer), and having altered stereochemistry at the C2' position of the carbohydrate portion compared

	^{3}H-TdR incorporation (cpm, mean ± standard deviation)			
Sample	**0.1 ng/ml**	**1 ng/ml**	**10 ng/ml**	**100 ng/ml**
Vehicle	2841 ± 285	3186 ± 423	2851 ± 290	2884 ± 238
α-GalCer (44)	9368 ± 1307*	15850 ± 644†	22733 ± 2862†	24535 ± 2331†
α-GlcCer (50)	4276 ± 626§	11381 ± 1510†	14634 ± 956†	17731 ± 2076†

Table 3.1: **Proliferation of spleen cells by α-GalCer (44) and α-GlcCer (50).** 2.5 x 10^5 murine spleen cells were plated in triplicate in 100μL wells and cultured with varying concentrations of glycolipid for 2 days at 37°C, before being pulsed with ^{3}H-TdR for 8h. ^{3}H-TdR uptake was counted using a liquid scintillation counter. $^{\S}P < 0.05$; $^*P < 0.01$; $^{\dagger}P < 0.001$ compared with vehicle-treated group. Experiments carried out by J.S. Im and myself at Albert Einstein College of Medicine, New York, USA using analogues synthesised during this project.

with α-GalCer **(44)** and α-GlcCer **(50)**, shows no immunostimulatory activity. Costantino *et al.* [237] showed that analogues of α-GalCer where the hydroxyl group at position 2 of the sugar is also glycosylated, are inactive, suggesting that it is the hydroxyl group at C2' that determines the activity of the antigen.

Cerebrosides with more complex sugar heads have been shown to exhibit immunostimulatory properties. Costantino *et al.* [224] investigated a number of novel glycosphingolipids with complex sugar heads. Two unique plakosides isolated from *Plakortis simplex* (β-galactosylceramides whose galactose residues are alkylated at the C2' hydroxyl group by a 3,3-dimethylallyl group, and incorporate a cyclopropane ring in the N-acetylated chain of the ceramide) (Figure 3.4) proved to be immunomodulating [224]. Not only were these compounds stimulatory, it was shown that their activity can be reversed, causing immunosuppression, which can be ascribed to the presence of the prenylated galactose [224]. This provides evidence that the hydrophilic carbohydrate-based portion of the antigen

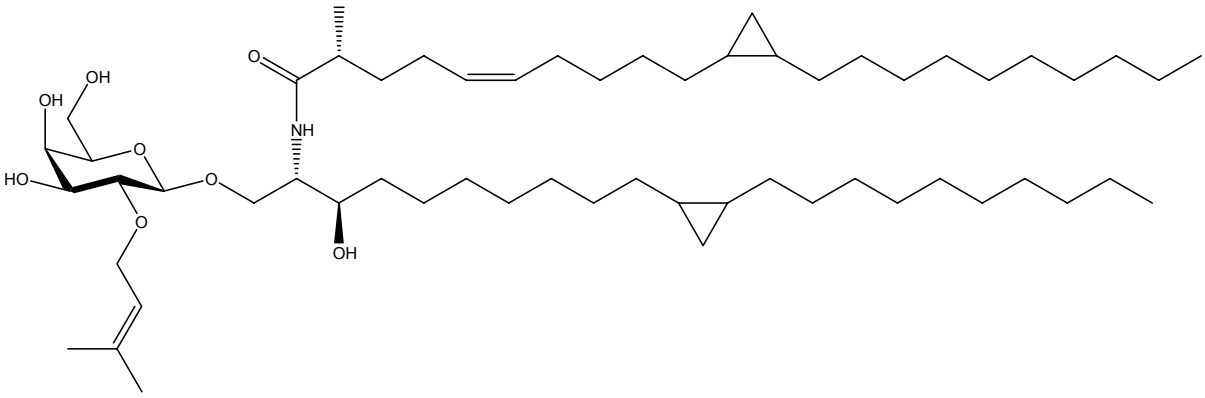

Figure 3.4: **Plakoside A.** One of the β-galactosylceramides isolated from *Plakortis simplex*. Plakoside B is identical, save for the base chain consisting of 24 carbons, with cis unsaturation at C7, and the cyclopropane ring at C13.

is accountable for the activation of the TCRs, and that iNKT cells can distinguish glycolipids that differ not only in the substituents coupled to the sugar hydroxyl groups, but also in the orientation of one hydroxyl group present in the sugar [31, 35, 185, 224, 228].

Wu *et al.* [179] also demonstrated that variations at the C2' position of the galactose head of α-GalCer alter the immunological activity of the analogues. However, the analysis inferred that unlike the plakosides, where immunological activity is preserved, substituting the hydroxyl group at C2' with a fluorine atom, a hydrogen atom, and an acylated amine, whilst preserving the stereochemistry of the sugar, results in no biological activity. This was demonstrated by the lack of IL-2 secretion by iNKT cells after stimulation with these analogues. Retaining the hydroxyl group functionality at C2', yet altering the conformation of the group from equatorial to axial also results in a distinct lack of biological activity [179].

Modulations in C2' resulting in no biological activity has also been observed when a second glycosylation of α-galactosyl or α-glucosyl is introduced [237]. Interestingly, adding a further sugar unit at C3' of the galactose of α-GalCer **(44)**, still retains immunostimulatory activity

and exhibits a statistically significant difference in lymphocyte proliferation compared with controls [237].

The introduction of other functional groups at the C6' position have been investigated [222, 238]. Replacing the hydroxyl group at C6' of the sugar with amino functionality, and then coupling biotin and fluorophores with this amino group provides a means of observing antigenic compounds both *in vivo* and *in vitro*, thereby allowing quantification of the association between the glycolipid-bound protein CD1d and the iNKT cell receptor [238].

Kamada *et al.* [72] suggested that the hydroxyl groups at the C4' and C6' positions of the sugar head group are not intrinsic to the recognition and subsequent formation of the CD1d-glycolipid-iNKT cell complex. Consequently, incorporating a small molecule, such as biotin, or a fluorophore, such as prodan, at C6' of the sugar (Figure 3.5) as means of a label should not affect the immunostimulatory properties of the glycolipid antigen.

When IL-2 production by iNKT cell stimulation was compared between α-GalCer **(44)** and the biotin- and prodan-labelled analogues, there was similar production of IL-2 by the two labelled analogues. The former analogue was in fact reproducibly more efficient than the parent analogue α-GalCer **(44)** and the fluorophore analogue [238].

Substituting the hydroxyl group at C6' with an amide linked to a small molecule such as a methyl group has also been shown to be effective in the activation of iNKT cells and subsequent cytokine secretion [222]. Liu *et al.* [222] synthesised an example of such molecule, with the addition of a double bond in the *N*-acyl chain of the ceramide moiety. This compound (PBS-57) successfully binds with CD1d and stimulates iNKT cells in a manner

(A) **(B)**

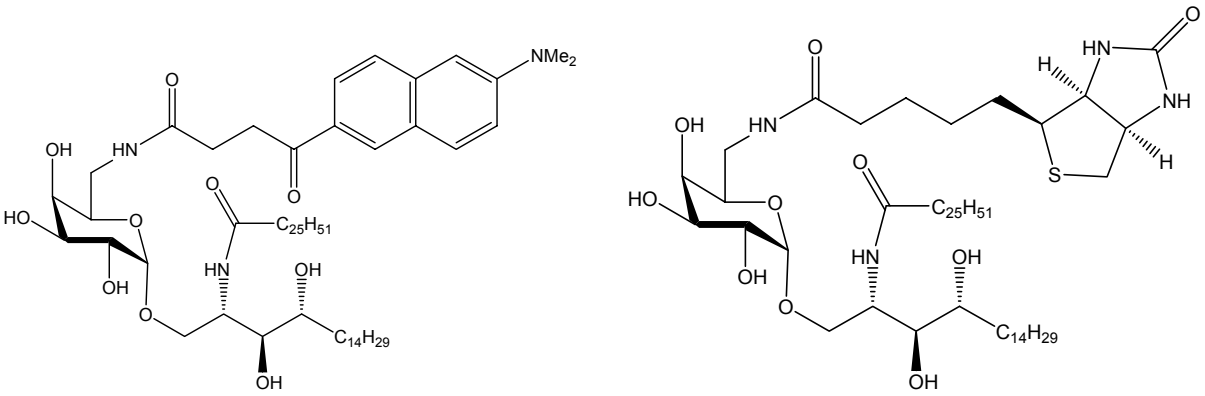

Figure 3.5: **Analogues with C6' hydroxyl group alterations (A)** α-GalCer labelled with the fluorophore prodan **(B)** α-GalCer labelled with biotin.

comparable to that of α-GalCer **(44)** [222]. In addition, lower concentrations of PBS-57 were more active than α-GalCer **(44)**, and this could be attributed to its increased solubility. One of the difficulties faced when using α-GalCer **(44)** is its solubility; therefore antigens modified in such a manner with an amide at C6' of the sugar head, thereby increasing their solubility, could prove to be extremely useful in terms of possible therapeutics.

Further, adding to the evidence that glycolipid antigens modified at the C6' position of the sugar successfully activate iNKT cells has been demonstrated by Mattner *et al.* [176]. These workers reported that analogues incorporating a carboxylic acid at C6' of a galactose or glucose head group (Figure 3.6A) strongly induced both mouse and human iNKT cell proliferation and IFN-γ cytokine secretion with a profile very similar to that of α-GalCer **(44)**. The secretion of the T_H1 cytokine IFN-γ is not completely unexpected when one examines the nature of the analogues. Glycosphingolipids incorporating a carboxylic group at C6' originate from the Gram-negative bacterial genus *Sphingomonas* and IFN-γ production by iNKT cells is stimulated during microbial infection. Interestingly, in a manner similar to that of α-GalCer **(44)**, the β-analogue of the glucuronosyl ceramide compound has been shown not to activate iNKT cells [179, 180].

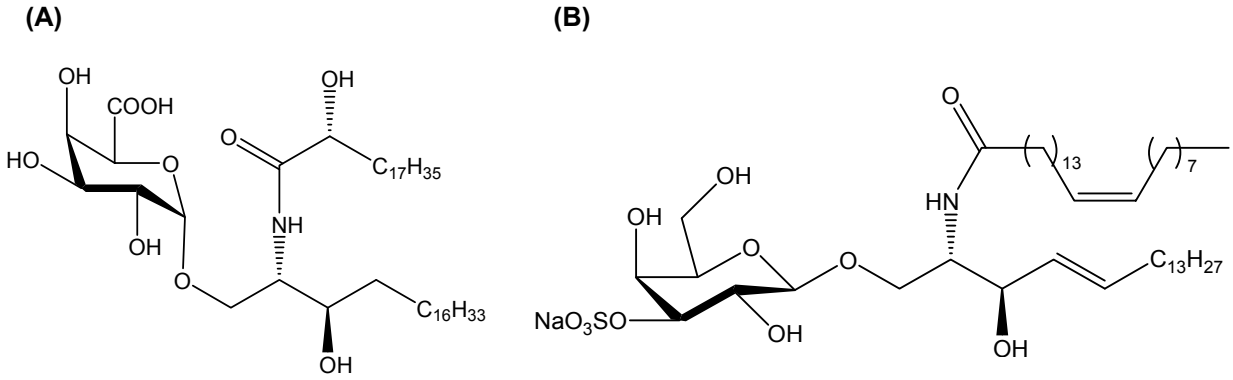

Figure 3.6: **α-GalCer analogues with variations on the sugar hydroxyl groups. (A)** α-Galacturonosylceramide. A glycolipid antigen isolated from *Sphingomonas* cell wall with variations at the C6' position, the inclusion of a hydroxyl group at C2''of the fatty acid and deletion of a hydroxyl group on the phytsphingosine base chain; **(B)** A Sulfatide glycolipid antigen with a sulphate group at the C3' position of β-linked galactose, an unsaturated fatty acid group, and a sphingosine base chain.

Wu *et al.* [179] also investigated the effect varying the functionality at C6' of an α-GalCer analogue would have on the recognition and resulting activity of the antigen. A galacturonic acid analogue of bacterial origin, with a structure similar to that investigated by Mattner *et al.* [176], incorporating carbonyl functionality at C6' in addition to the hydroxyl group, but without the presence of a hydroxyl group at C2'' of the *N*-acyl chain (GSL-1) (Figure 3.7), retains some of α-GalCer's stimulatory activity, albeit to a lesser extent [179]. Computer modelling of GSL-1 (Figure 3.7), docked to the crystal structure of murine CD1d protein,

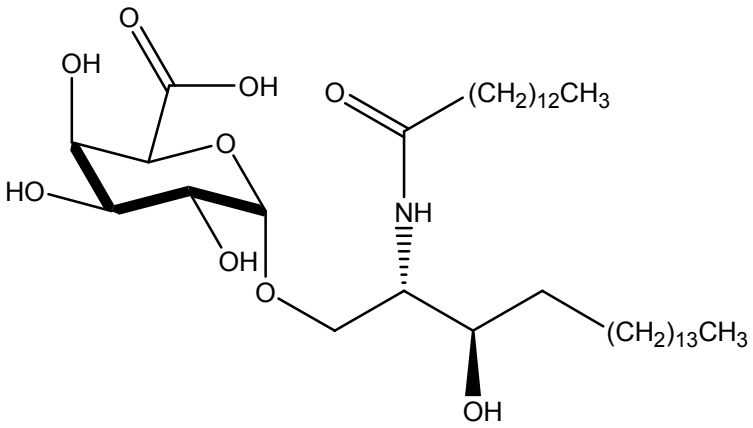

Figure 3.7: **An α-GalCer analogue of bacterial origin (GSL-1) incorporating varied C6' functionality.** The oxidation of the alcohol to a carboxylic acid at C6', and the lack of hydroxyl group at C4 of the phytosphingosine base can alter the antigen's biological profile [179, 180].

allows the sugar head group to be exposed and presented for iNKT cell recognition [179]. Combining the oxidation of the alcohol to a carboxylic acid at C6', with the deleted 4-OH on the phytosphingosine chain, results in shifts both within the lipid binding groove (due to the lack of hydrogen bonding between the OH at C4, and an aspargine residue within the pocket), and above the A' and F' channels where the sugar head is exposed [180]. These effects have been shown by Wu *et al.* [180] through electron density and modelling studies. A distinct lack of definition in the electron density map of GSL-1 bound within the CD1d protein implies that the analogue has a greater degree of flexibility within the binding pocket than α-GalCer **(44)**, and can result in an altered orientation of the sugar head [180]. The 6'-COOH substituent does not directly bind within the CD1d pockets and, therefore, the flexibility of the analogue within the binding grooves of CD1d can be attributed to the lack of OH at position 4 of the phytosphingosine chain [180].

Although not directly involved in binding within the groove structure of CD1d, the sugar head group does play a large part in antigenic recognition, as it is this moiety that is identified by, and binds with, the TCR of the iNKT cell. Therefore, a conformational change in this part of the antigen could vary the degree of recognition and conversely affect the antigenic profile of the compound [180]. This has been shown by the decreased production of cytokines, such as IL-2, IL-4 and IFN-γ by iNKT cells, when exposed to α-galacturonosylceramide (Figure 3.6) and GSL-1 (Figure 3.7) compared with α-GalCer **(44)** (Figure 3.8) [179, 180].

Sulfatides naturally exist in mammalian serum and are successfully presented by CD1a, CD1b and CD1c [30, 93, 177, 178, 229]. The endogenous sulfatide ligand, has structural similarities to α-GalCer (44) (Figure 3.6B) and is recognised by iNKT cells. A modulation of the C3' hydroxyl group of α-GalCer to incorporate a sulfate group has proved successful in terms of iNKT cell stimulation [178-180]. This was in fact shown by Xing *et al.* [177] who

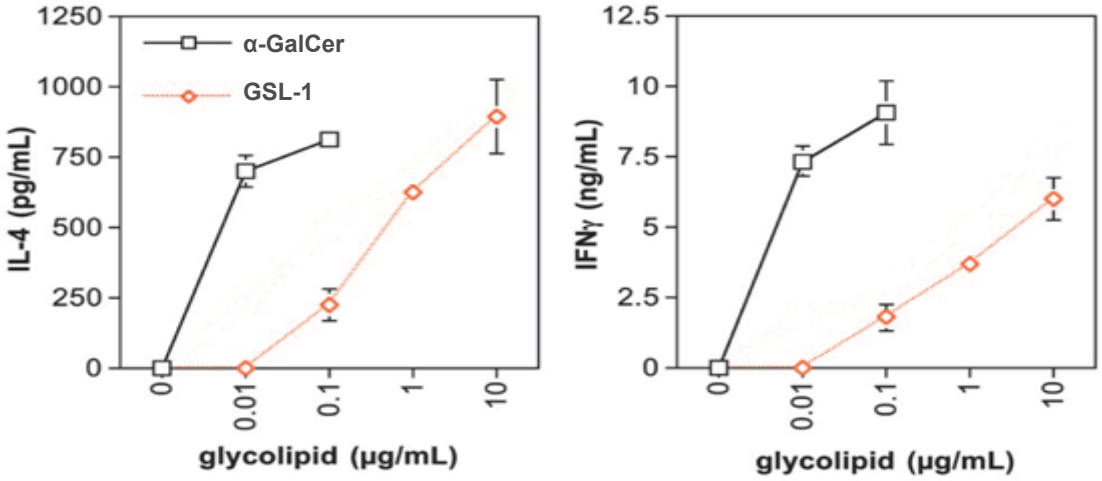

Figure 3.8: **iNKT cell activation with α-GalCer (44) and GSL-1.** Production of IL-4 and IFN-γ by lymphocytes stimulated with glycolipid pulsed DCs. Adapted from [180].

demonstrated that an α-linked sulfatide analogue identical to α-GalCer except for the inclusion of a sulfate group, was a better immuno-stimulator than α-GalCer.

Removal of the hydroxyl group at C6' results in 6-deoxy galactose (fucose). Both the **D**- and **L**- enantiomers of fucose are found in nature, with the former occurring widely in plants and the latter being found in bacterial, plant and human glycosides, including several families of blood-group antigens [239]. **L**-Fucose is the immunodominant sugar of many complex carbohydrate antigens and its presence can increase the strength of antigenic responses [239]. Incorporating an α-**L**-fucosyl moiety, has been demonstrated to delay progression of lupus-like symptoms (lupus or SLE is an autoimmune disease characterized by IFN-γ cytokine tissue injury) in NZB/W F1 mice [240]. Conversely, α-GalCer **(44)** exacerbates the same symptoms in the same mouse model. NZB/W F1 mice have been found to have detectable levels of circulating IFN-γ, and the production of this cytokine is dramatically decreased *in vitro* when α-fucosylceramide (α-**L**-FucCer) **(53)** is introduced [240].

Motoki *et al.* [226] have also demonstrated the immunostimulatory activities of α-L-FucCer **(52)**, showing that it produces a markedly higher immune response in terms of lymphocyte proliferation than α-GalCer **(44)**. It was also compared to analogues incorporating sugars in the furanose form, and it was clear to see that pyranosyl-antigens gave a far stronger immune response than their furanosyl counterparts [226].

3.5. Results and Discussion

3.5.1. Chemical Methods

3.5.1.1. Glycosylation

The synthesis of α-GalCer analogues involves having to overcome a number of chemical obstacles. Regioselectivity is a problem when the glycosyl acceptor has more than one hydroxyl group, as any free alcohol can act as the nucleophile. Thus protecting groups are vital. As the glycosylation uses a hard Lewis acid to activate the glycosyl donor, the protecting group must be stable to acidic conditions.

3.5.1.2. Glycosylation using a glycosyl fluoride

Glycosyl fluorides are more stable donors than the corresponding bromides or chlorides and can be readily synthesised from thioglycosides by treatment with diethylaminosulfurtrifluoride (DAST). This converts the free unprotected anomeric hydroxyl group to a fluoride, giving an α/β anomeric mix, the ratio of which is often solvent dependent (Figure 3.9).

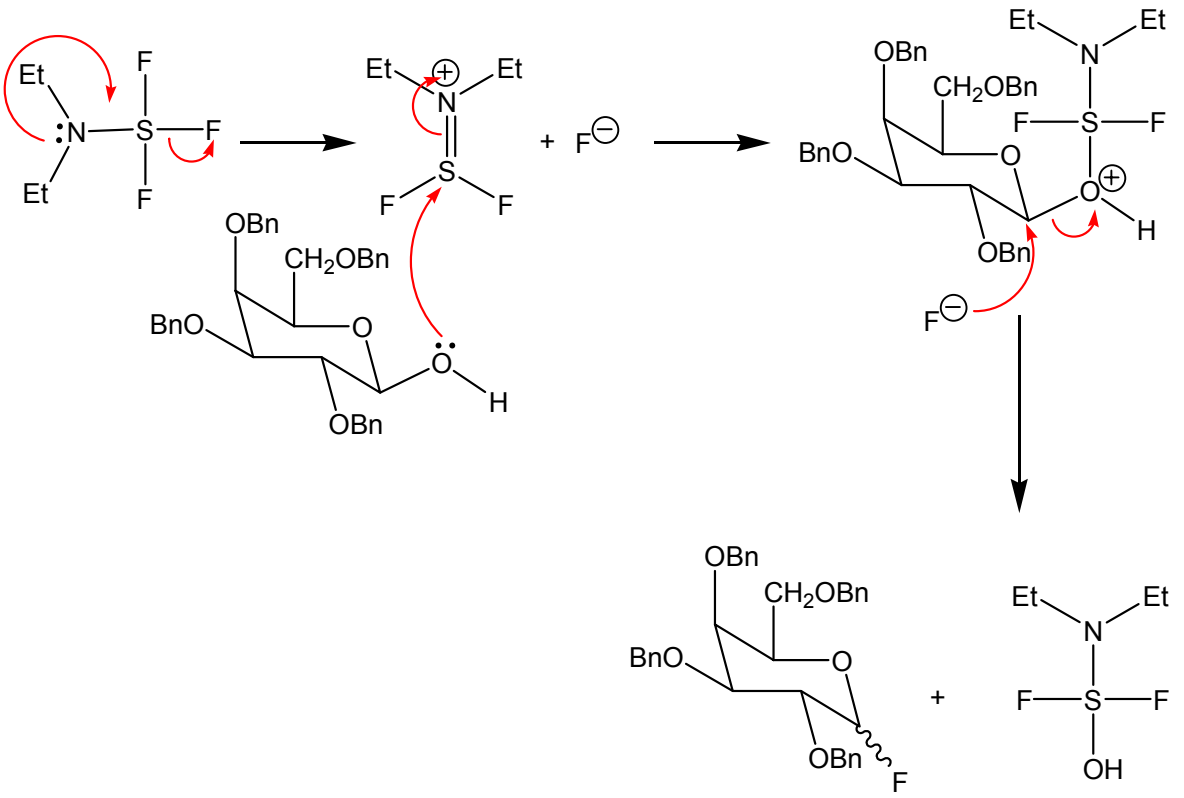

Figure 3.9: **The proposed mechanism for the formation of a glycosyl fluoride using DAST.**

3.5.1.3. Activated glycosyl fluoride donors

In order for glycosylation to proceed successfully, the glycosyl donor must be activated. In the case of the benzyl ether protected galactosyl fluoride, this can be achieved by the addition of a hard Lewis acid, such as boron trifluroetherate or tin (II) chloride. Selective activation can be achieved by adding silver perchlorate to the reaction mixture. Tin (II) chloride acts as a base, causing the carbon-fluorine bond to become polarised, imparting electrophilic characteristics to the fluorine atom. The nucleophile (glycosyl acceptor), which in this case is the benzoyl protected azido alcohol compound, then attacks the δ-positive anomeric carbon atom (Figure 3.10).

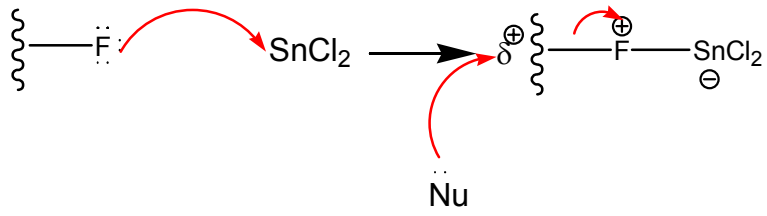

Figure 3.10: **Activation of a glycosyl fluoride by tin (II) chloride.**

When using a glycosyl fluoride, THF is the preferred solvent, in addition to diethyl-ether [241]. Due to the bulky nature of the benzyl ether on C2', THF co-ordinates with the glycosyl donor from the top face forming a β-intermediate. This results in the free hydroxyl group of the glycosyl acceptor molecule, attacking from the bottom face, producing an α-glycosylated compound (Figure 3.11).

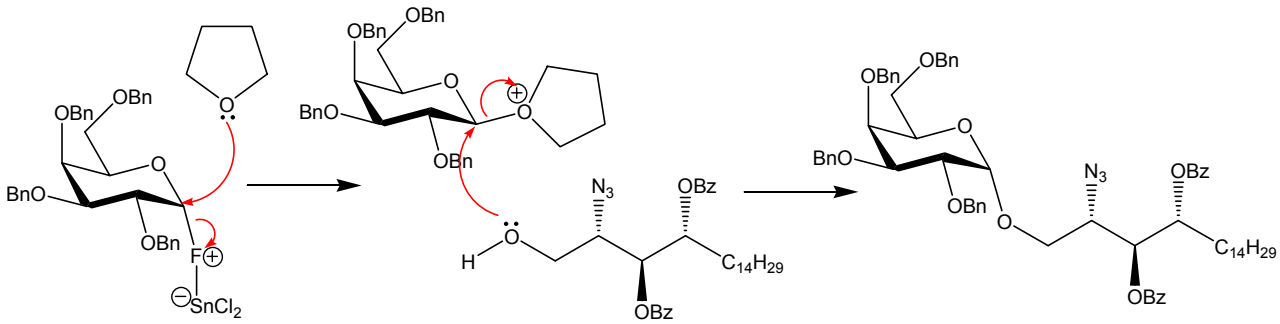

(28)

Figure 3.11: **Solvent influence on the stereochemical outcome of glycosylation.**

One alternative synthesis would be using a phytosphingosine base protected by an isopropylidene group at C3-OH and C4-OH. This method was applied to compound **(16)**; using 2,2-dimethoxypropane, the cyclic acetal was formed at C3, C4, along with the formation of a hemiacetal at the hydroxyl group of C1. Being much less stable than the cyclic form, this terminal hemiacetal was easily cleaved by washing with cold 1M HCl, leaving the desired protected azido compound (Figure 3.12). However, when this compound

was used in glycosylation reactions with galactosyl fluoride, the isopropylidene group was not stable to the acidic conditions produced when using tin (II) chloride and silver perchlorate.

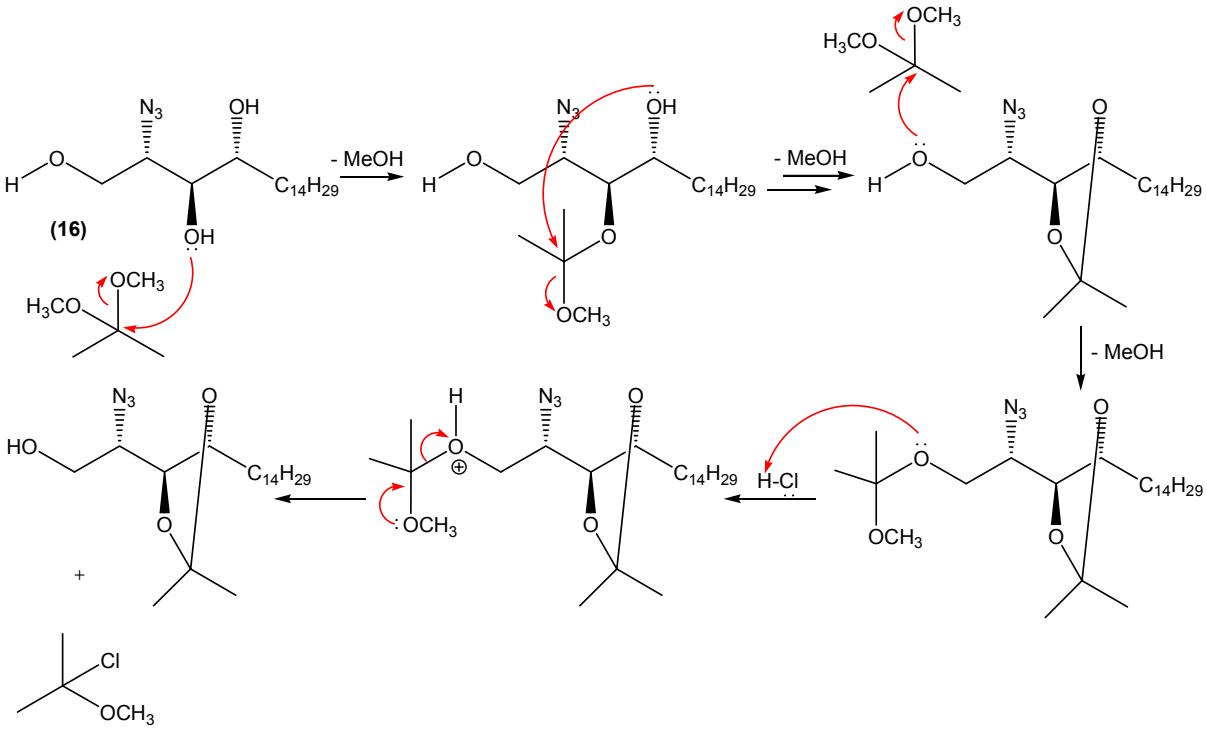

Figure 3.12: **Acetylation of azido-phytosphingosine base.** Compound **(16)** was reacted with 2,2-dimethoxypropane, forming the desired acetal and hemi-acetal at position C1. This was then removed by the addition of HCl, leaving the protected azido-phytosphingosine base.

3.5.1.4. *N*-acylation using hexacosanoic acid

Several groups have reported the synthesis of the parent glycolipid analogue, yet when these were investigated, problems were encountered and thus adaptations were made and in some steps of the chemical synthesis, alternative methods were sought out. These are discussed in some detail in chapters 2, 3 and 4 and possible explanations considered as to why certain reactions did not proceed according to the literature and/ or established

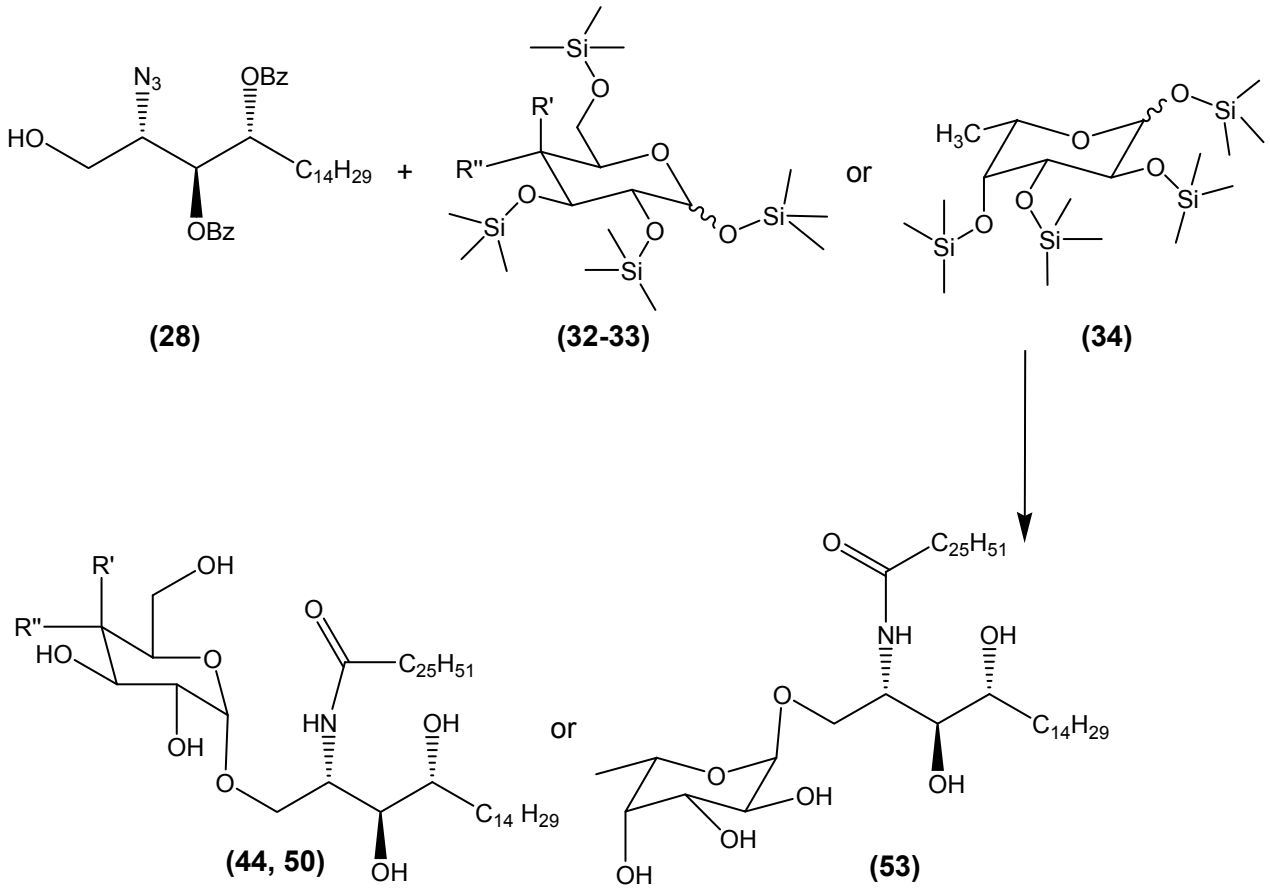

Figure 3.13: **Synthesis of α-GalCer, α-GlcCer and α-L-FucCer.** R'=OH, R''=H **(32)**, **(44)**; R'=H, R''=OH **(33)**, **(50)**.

chemistry. Figure 3.13 shows the general reactions involved in coupling the phytosphingosine base with sugar, and subsequent deprotection, reduction and *N*-acylation.

3.5.1.5. Removal of the benzyl ether protecting groups

After incorporating the C_{26} *N*-acyl chain, the final step in the synthesis using a glycosyl fluoride, is the deprotection of the pyranose ring. Benzyl ethers can be removed by catalytic hydrogenation, with palladium on carbon being the preferred catalyst. Platinum catalysed reactions can result in hydrogenation of the aromatic rings, as opposed to removal of the benzyl groups. The reaction is solvent dependent, with the reaction rates (mmH_2/min/0.1g

catalyst) being as follows: THF (40) > hexanol (25) > hexane (6) > MeOH (5) > toluene (2) [195]. The presence of a non-aromatic amine can hinder *O*-debenzylation. When this synthetic method was employed in the laboratory, the desired compound (i.e. the unprotected glycosyl ceramide) was not produced and analysis by TLC showed numerous sugar-positive spots, suggesting the compound had been broken down during the debenzylation reaction. This was the catalyst for investigating an alternative glycosylation technique.

3.5.1.6. Glycosylation using a glycosyl iodide

The development of glycosylation methods that employ milder reaction conditions and do not make use of alkylating agents, oxidising agents or heavy-metal salts has becoming increasingly desirable, especially given the need to synthesise tailor-made glycosides that can be used within the body to study and influence biological mechanisms [242, 243]. The use of glycosyl halides in glycosylation reactions is well-established, and a wide variety of glycosyl donors are available for use in these reactions. Anomeric halosugars, such as glycosyl bromides and glycosyl fluorides activated by heavy-metal salts are the more traditionally utilised compounds in glycosylations [244]. Over the past decade or so, the introduction of glycosyl iodides as effective glycosyl donors has been noted [245]. This is somewhat contradictory to the supposedly established view that glycosyl iodides are unsuitable agents due to their intense reactivity and unstable nature [246]. Studies by Hadd *et al.* [247] demonstrated the successful use of glycosyl iodides in the synthesis of *O*-linked glycosidic compounds, with high α-stereoselectivity. The group also showed that glycosyl iodides are highly efficient donors even under neutral conditions, and that the advantages of glycosyl iodides over corresponding bromides includes increased reaction rates, and successful reaction with sterically demanding acceptors, all of which add to the attractiveness of this method [247].

The use of glycosyl iodides to produce α-linked glycosides originated from work by Lemieux *et al.* [248, 249] who showed that glycosylations with glycosyl bromides produced α-glycosides in good yields when bromide ions were employed. By treating α-glycosyl halides with quaternary ammonium halides, such as tetrabutylammonium iodide (TBAI), the established equilibrium between the α- and β-glycoside halides could be driven towards the more reactive β-glycosyl halides, which when attacked by a glycosyl acceptor, resulted in the formation of an α-linked glycoside (Figure 3.14) [246, 250]. van Well *et al.* [251] also demonstrated this using glycosyl iodide, and concluded that the decreased thermodynamic stability of the β-glycoside halide renders it more reactive than its α-analogue, and reacts with the glycosyl acceptor in an S_N2 fashion to produce an α-linked glycosidic product.

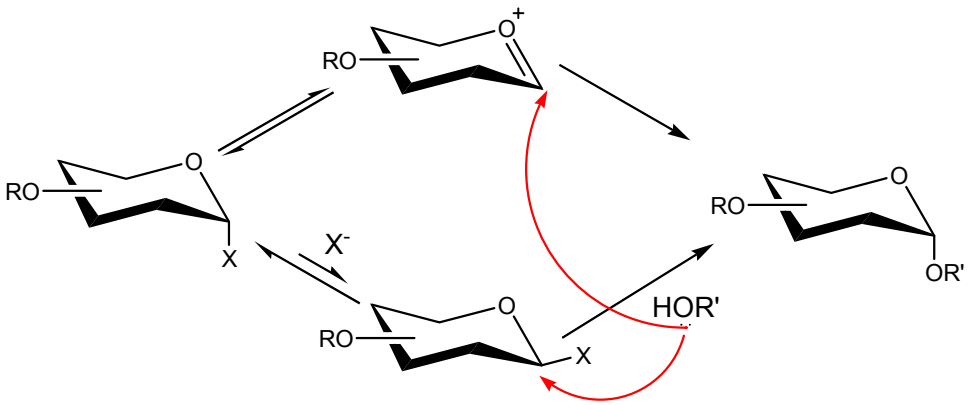

Figure 3.14: **Halide-catalysed in-situ anomerisation.** The addition of quaternary ammonium halide, results in the production of a β-glycosyl halide, which in turn produces an α-linked glycoside. X = Br or I [246].

The difficulties encountered when using glycosyl fluorides led to the use of a method employing a glycosyl iodide as the donor. Not only did this overcome the issues faced when trying to separate the α- and β-glycosyl fluorides, it also enabled different protecting groups to be used on the sugar instead of the benzyl ethers that proved difficult to remove. Bickley *et al.* [244] reported that among several methods that can be used for the preparation of glycosyl iodides, one of the more efficient reactions employs trimethylsilyl iodide, generating stable glycosyl iodides in high yields (91% versus 67% with KI). Du *et al.* [217] showed that

per-*O*-silylated sugars are very good precursors to glycosyl iodides, undergoing nucleophilic addition in a ready and facile manner, thus providing a stereoselective and efficient route to α-GalCer **(44)** and its analogues.

The anomeric silyl ethers were generated by the reaction of the unprotected sugar with trimethylsilyl chloride, producing the per-*O*-trimethylsilylgalactopyranose. Reacting this compound with iodo trimethylsilane produced the glycosyl iodide, which was then reacted with TBAI (to produce the β-glycosyl iodide) and the glycosyl donor (azido-protected phytosphingosine), giving the α-linked galactosylceramide pre-cursor (Figure 3.15).

The same method was used when synthesising the glucosylceramide intermediates **(48)**, **(49)**, and the final ceramide antigen **(50)**, substituting the galactose starting material for glucose.

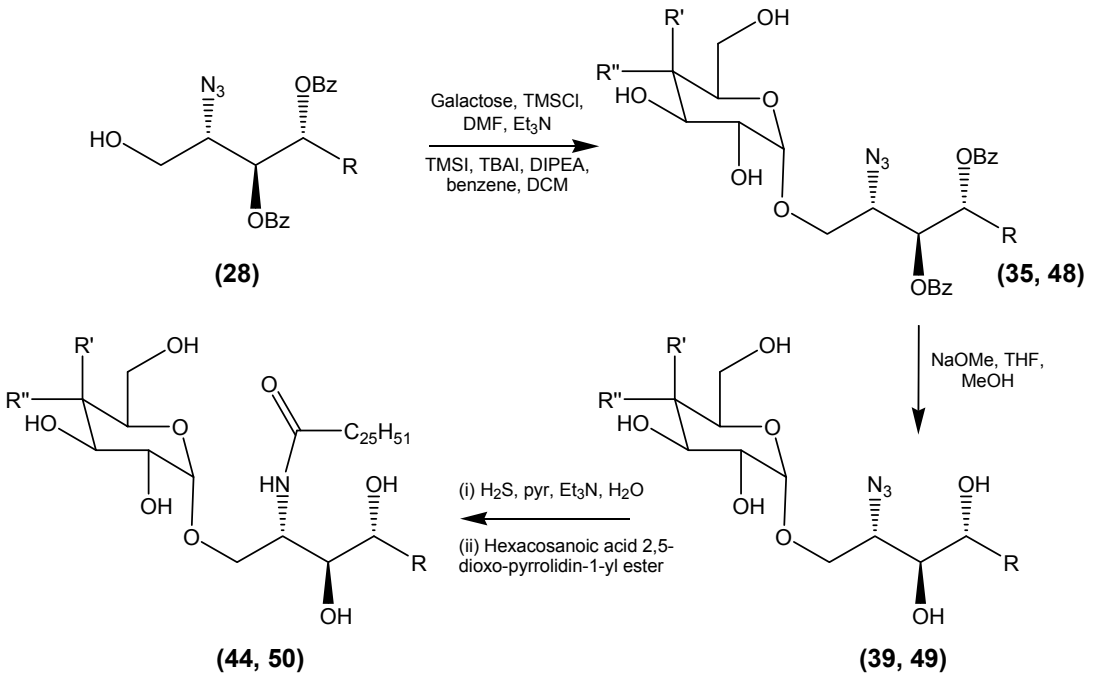

Figure 3.15: **Glycosylation, deprotection, azide reduction and *N*-acylation of varying phytosphingosine bases. (28)** R=$C_{14}H_{29}$; **(35), (39), (44)** R=$C_{14}H_{29}$, R'=OH, R''=H; **(48)**, **(49)**, **(50)** R=$C_{14}H_{29}$, R'=H, R''=OH.

3.5.1.7. Variations on the C-6' hydroxyl group

α-Fucosylated oligosaccharides can be found in mammals. Fucose-containing glycans play a key part in a variety of physiological processes, such as blood transfusion reactions, host-microbe interactions, and numerous ontogenic events, including signalling events [252]. Until recently, α-fucosyl compounds were almost exclusively chemically synthesised using 2,3,4-tri-*O*-benzyl fucopyranosyl donors [253]. With the issues raised and encountered during the benzyl-protected galactosyl ceramide synthesis, an alternative method was sought to incorporate a fucose ring into the α-GalCer analogues. Fortunately, Uchiyama et al. [254] found a simple alternative to the use of tri-*O*-benzylfucopyranosyl donors for α-fucosylation, which was not too dissimilar to the methods employed in the glycosyl iodide glycosylation reactions described above. In a similar manner to the synthetic methods used for the protection of both galactose and glucose, L-fucose was reacted with trimethylsilyl chloride, triethylamine and dimethylformamide (DMF). The per-*O*-trimethylsilyl fucose was then treated with one equivalent of iodotrimethylsilane, producing the per-*O*-trimethylsilyl-α-fucopyranosyl iodide. This glyscosyl iodide was then taken on and reacted in a similar manner to the glycosylation reactions for galactose and glucose (Figure 3.16).

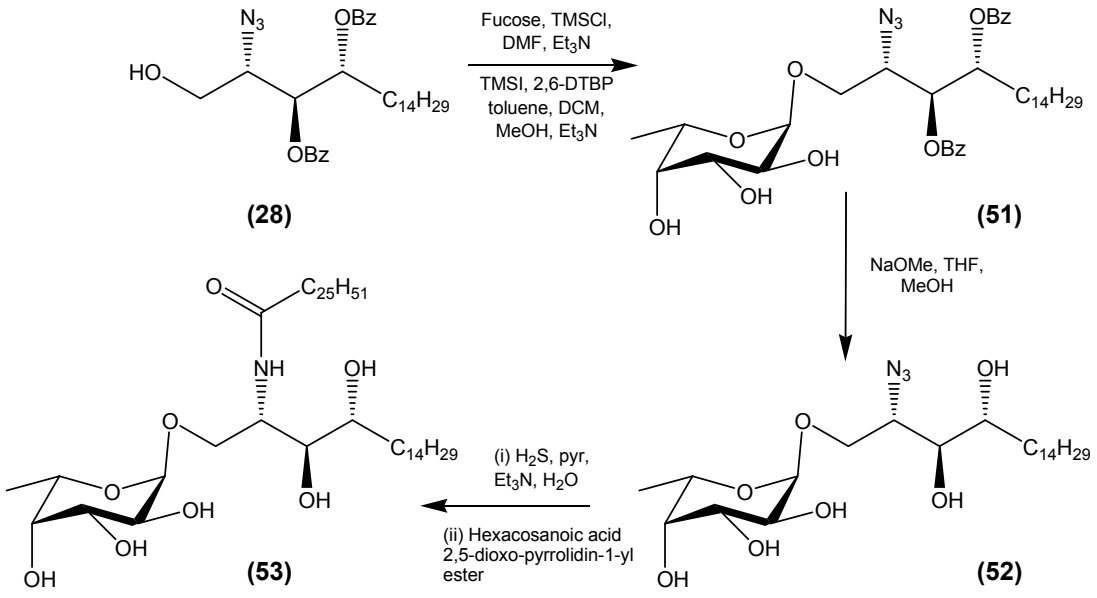

Figure 3.16: Glycosylation, deprotection, azide reduction and *N*-acylation in the synthesis of L-fucosylceramide.

3.6. Biological evaluation of glycolipid antigens α-GalCer (44), α-GlcCer (50) and α-L-FucCer (53).

The results, shown by Uchimara *et al.* [223], demonstrate that the configuration of the hydroxyl group at C4' of the sugar head has a profound affect on the biological activity of α-GalCer analogues. Figure 3.17 shows the decreased activity with regards to cell proliferation of α-GlcCer **(50)**, from experimental procedures carried out by J.S. Im and myself at Albert Einstein College of Medicine, New York, USA using compounds synthesised throughout this project. The graph also shows the effect modifying the C6' position of the sugar has on cell proliferation, and although the effect is not as pronounced as that of α-GalCer **(44)**. An analogue without a hydroxyl group at C6' of the sugar head group (α-L-FucCer, **(53)**), does

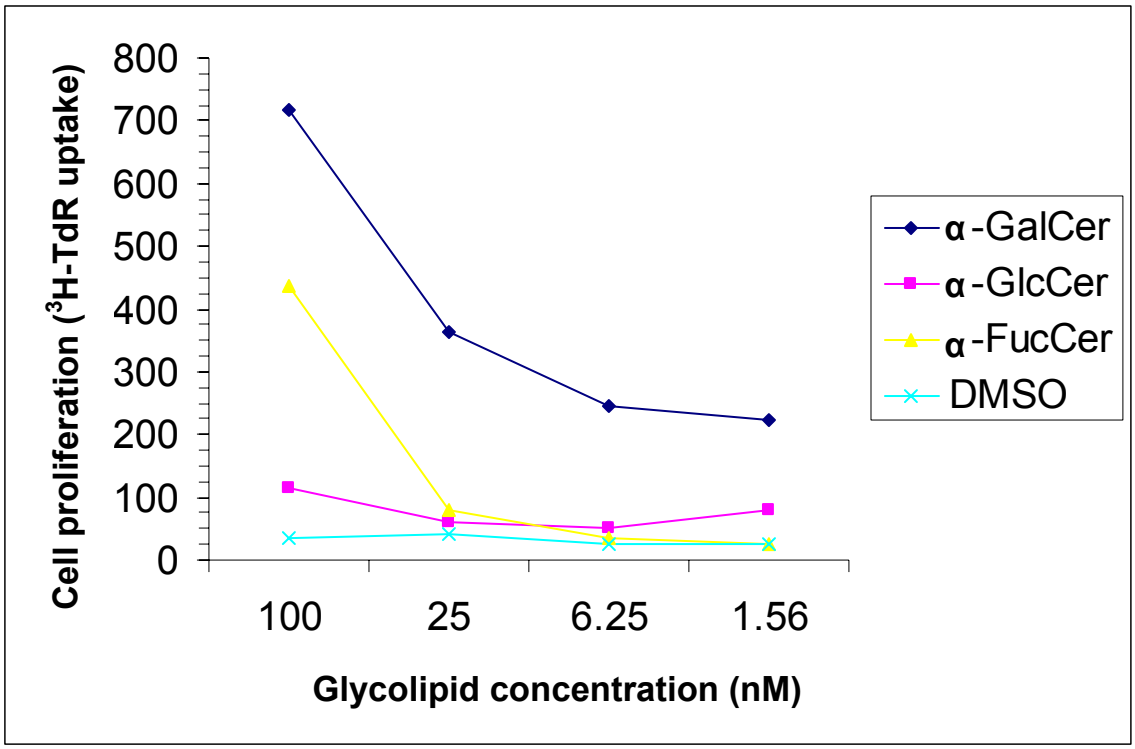

Figure 3.17: **The proliferation of NKT cells by various α-GalCer analogues.** HDD.D11 NKT cells (50000 cells/200 µL) were plated in a 96-well plate in triplicate and cultured with glycolipid samples at 37°C for two days, and were pulsed for additional 8 h with ^{3}H -TdR. ^{3}H –TdR uptake into cells was counted using a liquid scintillation counter. The results shown are the mean values from each triplicate, with the exception of α-GalCer **(44)** which was the mean of 6 wells. Experiment carried out at Albert Einstein College of Medicine, New York, USA using analogues synthesized during this project.

stimulate iNKT cell proliferation in a concentration dependent manner and is more active than α-GlcCer **(50)**.

The fact that a modification at C6' seems to affect the biological activity of α-GalCer analogues less than a modification at C4', is also shown by the cytokine stimulation profiles of analogues prepared during this project. As depicted in Figure 3.18, the analogue, which is modified at C4' of the sugar (α-GlcCer **(50)**), has a much weaker stimulatory profile than the parent α-GalCer **(44)** or the C6' modified analogue, α-**L**-FucCer **(53)**. It is also interesting to note that the cytokine response of iNKT cells upon stimulation with 100nM of α-**L**-FucCer **(53)** seems to favour the release of the T_H2 cytokine IL-13. The ratio of T_H1:T_H2 cytokines upon activation by α-GalCer **(44)** is 1:1.62, whereas the ratio is 1:2.35 for T_H1:T_H2 cytokines after α-**L**-FucCer **(53)** stimulation. This shows that although the release of both the T_H1 and T_H2 cytokines is diminished with respect to α-GalCer **(44)**, the α-**L**-FucCer analogue **(53)** seems to skew the immune response more towards that of a T_H2 profile, as shown by the greater difference between the two different cytokines (Figure 3.19).

The apparent differences between α-GalCer analogues with varying sugar heads have also been exhibited by Brigl *et al.* [255]. Previous experiments have implied that reactivity to α-GalCer **(44)** is dependent on the TCR α-chain [256, 257]. However, the ability of the TCR α-chain to recognise lipids outside the GSL family varies. Canonical iNKT cell clones vary in their autoreactive responses to CD1d-positive APCs, thus suggesting that recognition is not always conferred by the TCR α-chain.

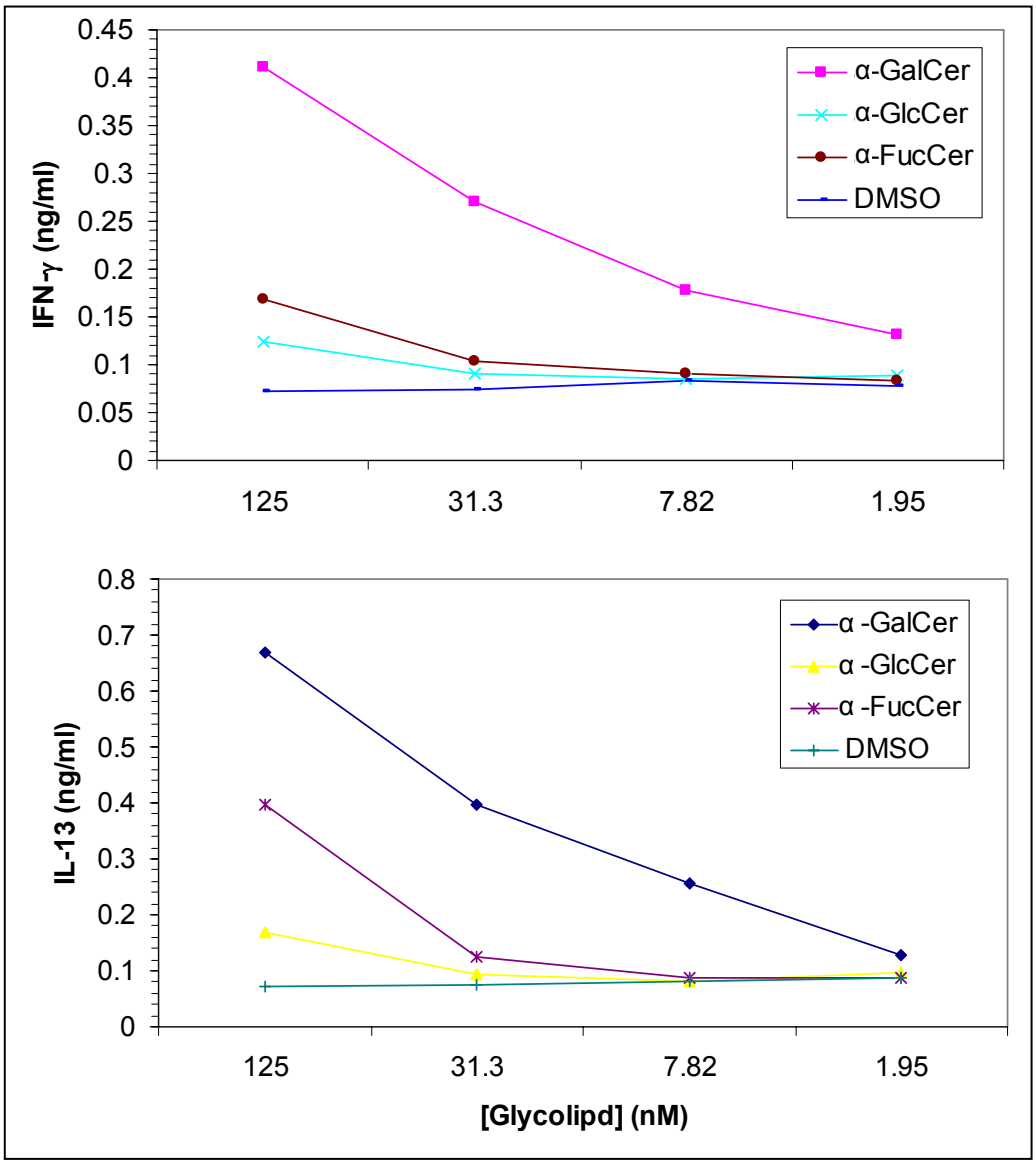

Figure 3.18: **Cytokine profiles of α-GalCer analogues with variations in the sugar head group.** The top panel shows the IFN-γ (T_H1 cytokine) response and the bottom panel shows the IL-13 (T_H2 cytokine) response of iNKT cells to various α-GalCer analogues. Experiments carried out at Albert Einstein College of Medicine, New York, USA using analogues synthesized during this project

Brigl *et al.* [255] showed that a variety of novel Vα24-negative/ Vβ11-positive CD1d-restricted T cell clones respond differently to antigens such as α-GalCer **(44)**, iGb3 and α-GlcCer **(50)**, due to their noncanonical TCR α-chains, thus shedding light on the features that influence lipid antigen recognition.

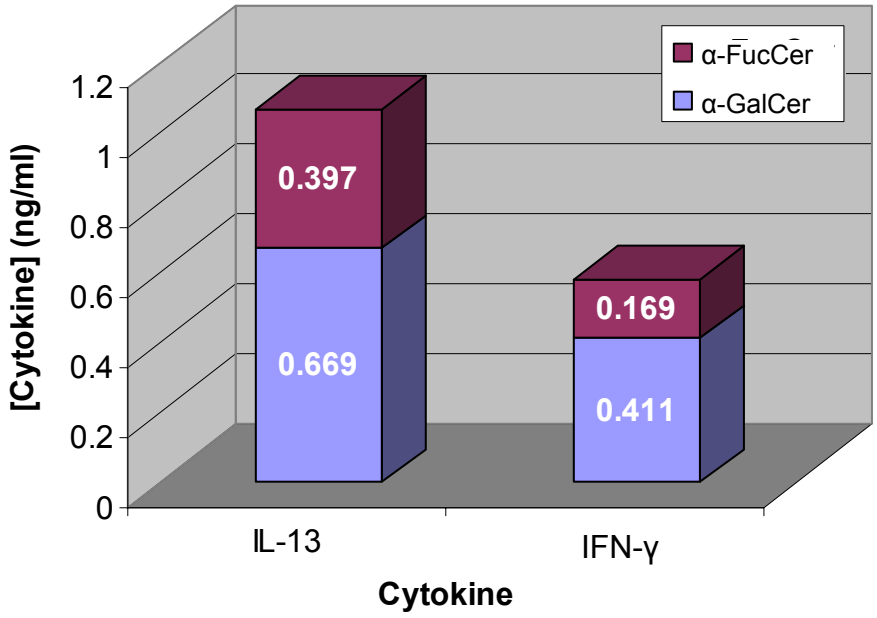

Figure 3.19: **T_H2 skewing properties of α-L-FucCer (53)**. HDD.11 NKT cells (50,000 cells per well) and immature DCs (25,000 cells per well) were incubated with 125nM of analogue in DMSO and the cytokine production measured by ELISA. α-L-FucCer **(53)** skews the immune response towards a T_H2 response, as shown by the greater proportion of the T_H2 cytokine IL-13, than the T_H1 cytokine IFN-γ, when compared with α-GalCer **(44)**. Experiments carried out at Albert Einstein College of Medicine, New York, USA using analogues synthesized during this project.

Five novel Vα24-negative/Vβ11-positive and 13 canonical Vα24-positive/Vβ11-positive human NKT cell clones were generated using α-GalCer-loaded CD1d tetramers. iNKT cells with Vα14- or Vα24-invariant TCRα-chains have been previously characterised as responding similarly to α-GalCer **(44)** and α-GlcCer **(50),** but failing to respond to α-ManCer [95, 258]. Strikingly, the Vα-chains of the Vα24-negative clones had highly conserved Jα18 regions, resulting in CD3Rα loops practically identical to those of the canonical TCRs [255]. The Vα24-negative and Vα24-positive T cell clones generated were tested in parallel for their ability to respond to the α-GalCer **(44)** and α-GlcCer **(50)** analogues prepared during this project and tested by Brigl *et al.* [42]. All of the Vα24-positive CD1d-restricted T cell clones responded robustly to both α-GalCer **(44)** and α-GlcCer **(50)**, whereas all of the Vα24-negative clones responded strongly to α-GalCer **(44)** but showed markedly lower responses to α-GlcCer **(50)** (Figure 3.20). There was little or no cytokine secretion in

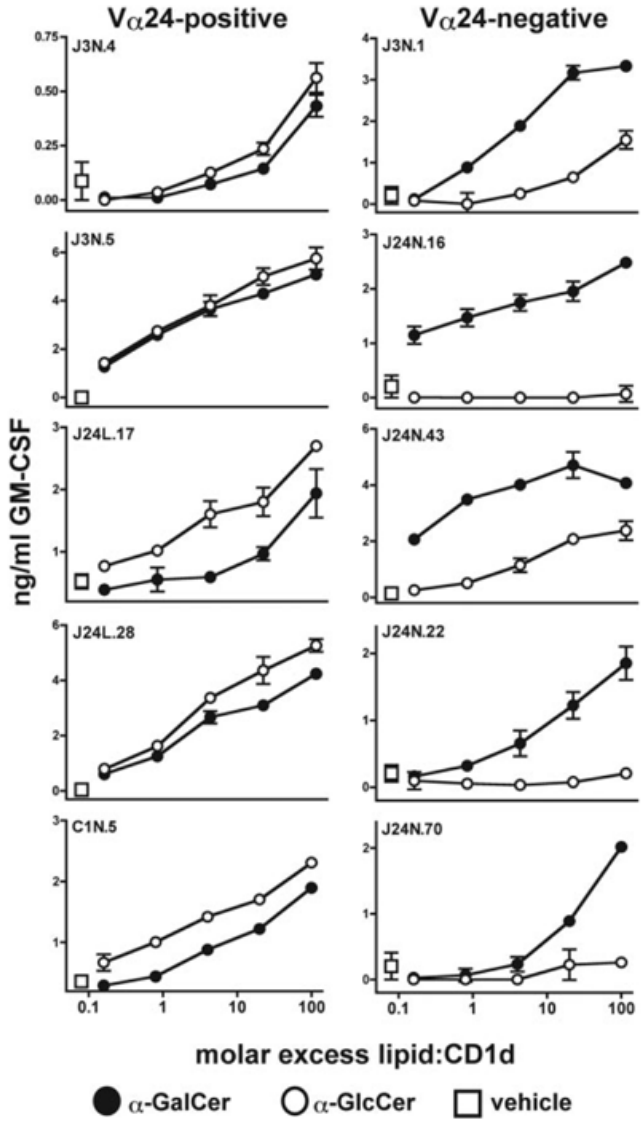

Figure 3.20: **Vα24-positive and Vα24–negative clones in response to α-GalCer (44) and α-GlcCer (50).** Cytokine secretion by Vα24-positive and Vα24–negative clones in response to plate-bound recombinant CD1d molecules pretreated with two analogues synthesized throughout this project (α-GalCer **(44)** [filled circles], α-GlcCer **(50)** [open circles]), or vehicle alone (open squares). Assays were performed in triplicate, and error bars show the SD values of the mean. Similar results were obtained in three independent experiments. Experiments carried out by Brigl *et al.* at Department of Rheumatology, Immunology, and Allergy, Brigham and Women's Hospital, Boston, USA. [255]

response to vehicle-treated CD1d molecules by any of the clones, and no detectable response was observed when they were exposed to a negative control protein treated with α-GalCer **(44)**, thus demonstrating the specificity and CD1d-dependence of the α-GalCer **(44)** and α-GlcCer **(50)** responses. These results indicated that the Vα24-negative and

Vα24-positive T cell clones differ in their specificity for sugar residues of α-GalCer analogues.

To investigate this sugar specificity difference further, three Vα24-positive and three Vα24-negative T cell clones were tested for staining by human CD1d-Fc dimers loaded with either α-GalCer **(44)** or α-GlcCer **(50)** or treated with vehicle alone. The Vα24-positive T cells stained similarly with α-GalCer- and α-GlcCer-loaded CD1d dimers, whereas the Vα24-negative T cells showed significant positive staining only with the α-GalCer-loaded CD1d dimer (Figure 3.21). The titration curves for clones J3N.1 and J24N.70 appeared to approach saturation at a similar concentration of the α-GalCer-loaded CD1d dimer as that observed for the Vα24-positive clones tested, suggesting that the affinity of these Vα24-negative TCRs for α-GalCer **(44)** may be close to that of canonical Vα24-positive TCRs (Figure 3.21). In contrast, the titration curve for clone J24N.22 reproducibly appeared to require higher dimer concentrations to reach saturation, suggesting that the TCR of this clone may have a lower affinity for α-GalCer **(44)** (Figure 3.21). Thus, variation in Vα-encoded TCR α-chain regions may affect the strength of the interaction with α-GalCer **(44)**, but the most significant effect appears to be on the ability to bind α-GlcCer **(50)**. These results suggest that the weaker functional response of the Vα24-negative T cell clones to α-GlcCer **(50)** is due to lower TCR affinity for this glycolipid compared with α-GalCer **(44)**, whereas Vα24-positive TCRs appear to have similar affinity for both glycolipids.

The results from the clone experiments provide new insights into TCR elements that determine lipid antigen specificity. Analysis of the five Vα24-negative T cell clones suggests that conservation of the CDR3α loop may be sufficient to permit recognition of α-GalCer (44) and related bacterial α-glycosphingolipids, despite substantial variation in the sequences and predicted conformations of the CDR1α and CDR2α loops. The finding that the Vα24-

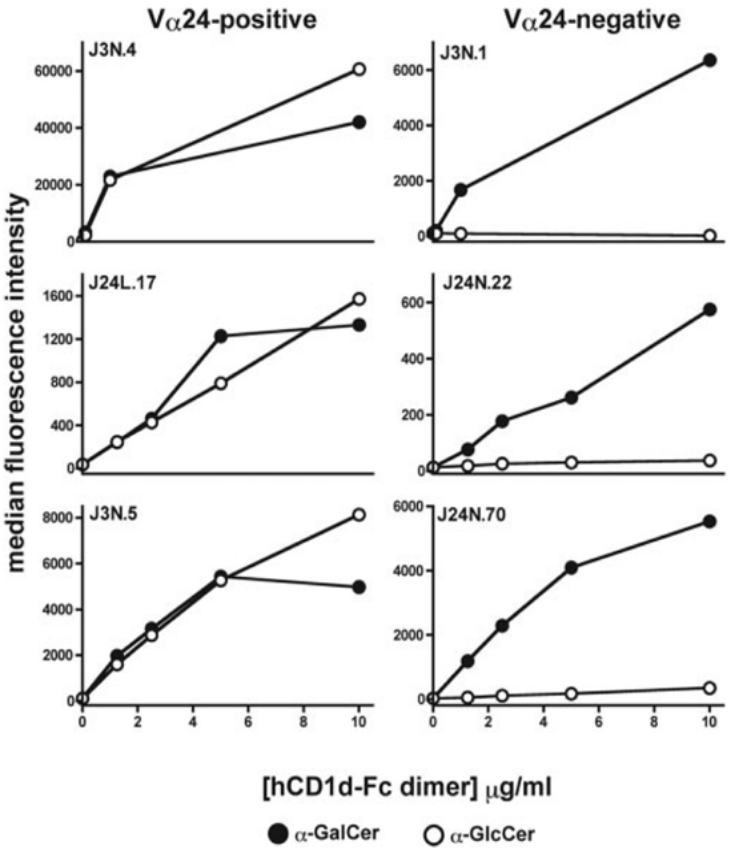

Figure 3.21: **Cytometric staining of Vα24-positive and Vα24–negative clones in response to α-GalCer and α-GlcCer.** Flow cytometric staining of Vα24-positive and Vα24-negative T cell clones by CD1d-Fc dimers loaded with α-GalCer **(44)** (filled circles) or α-GlcCer **(50)** (open circles). Similar results were obtained in three independent experiments. Experiments carried out by Brigl *et al.* at Department of Rheumatology, Immunology, and Allergy, Brigham and Women's Hospital, Boston, USA, using analogues synthesized during this project. Adapted from [255].

negative clones differed from their Vα24-positive counterparts, showing a reduced response to α-GlcCer **(50)**, indicates that Vα-encoded TCR features affect glycan specificity, and suggests that the α-chain of the TCR plays a key part in the recognition of, and specificity for, α-GSLs.

Crystal structures have been solved for human CD1d complexed with α-GalCer **(44)**, and murine CD1d with a short-chain form of α-GalCer [71, 259, 260]. In these structures, the polar head group of α-GalCer **(44)** emerges from the CD1d binding pocket in a relatively

central location, and the sugar ring is angled toward the C-terminal end of the CD1d α_2-helix (Figure 3.22). Previous crystal structures of TCRs complexed with MHC class I and II molecules have shown that the TCR α-chain docks over this end of the Ag-presenting molecule [261, 262]. Analyses of NKT cell responses to mutagenised CD1d molecules has suggested that their TCRs bind the Ag-presenting molecule in an overall similar manner to that observed for MHC class I and II-restricted TCRs [219], this positioning is consistent with the possibility that TCR α-chains play a dominant role in recognising α-GSLs.

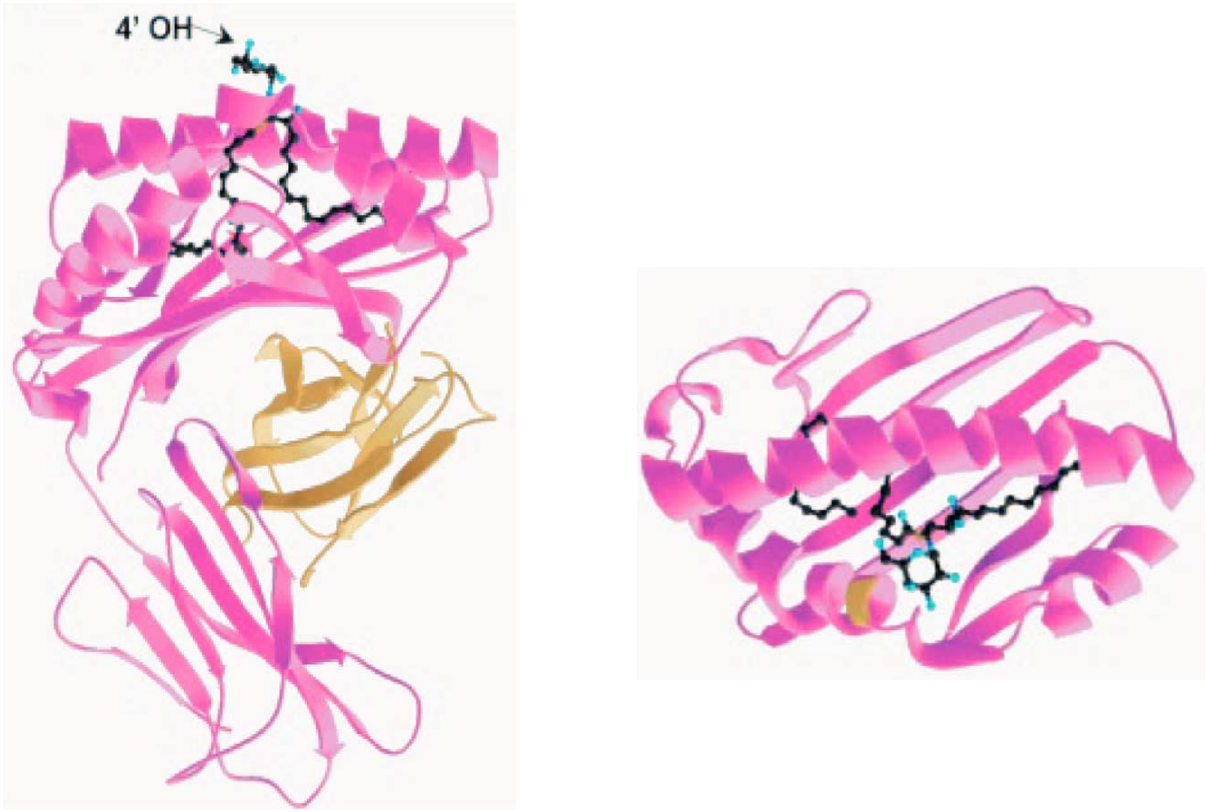

Figure 3.22: **Side and top view of the crystal structure of human CD1d complexed with α-GalCer (44).** CD1d heavy chains are shown as pink ribbons and the bound lipids are shown as ball-and-stick representations with carbon atoms shown in black, oxygen in blue, nitrogen in orange. Left-hand side diagram β_2-microglobulin is shown as a gold ribbon. Right-hand side diagram, for clarity only the α1 and α2 domains are shown, and Thr157 on the α2 helix has been coloured gold to provide a point of reference. Experiments carried out at the Department of Rheumatology, Immunology, and Allergy, Brigham and Women's Hospital, Boston, USA, using analogues synthesized during this project. Adapted from [255].

Crystalographic visualisation techniques (Figure 3.22) carried out at the department of Rheumatology, Immunology, and Allergy, Brigham and Women's Hospital, Boston, USA , using compounds synthesized during this project, shows that the positioning of a key hydroxyl group of the galactose sugar is consistent with the finding that the Vα24-negative, CD1d-restricted TCRs can distinguish between α-GalCer **(44)** and α-GlcCer **(50)**. The configuration of the 4'-OH of the sugar ring is the only structural difference between galactose and glucose, and thus appears highly accessible for TCR recognition. Since the position of this prominent hydroxyl would be altered in α-GlcCer **(44)**, it seems reasonable that this difference might be able to affect TCR binding. The data suggests that the presence of a conserved amino acid motif at the beginning of the CDR1α loop may allow canonical NKT TCRs to accommodate the difference caused by the change in the positioning of this hydroxyl in galactose and glucose, in contrast to the Vα24-negative TCRs.

The finding that the Vα24-negative T cell clones did not respond to iGb3 (Figure 3.23) shows that the ability to recognise α-GSLs is separate from the ability to respond to iGb3. This observation raises intriguing questions about which ligands drive the positive selection of human TCRs that can recognise α-GSLs. iGb3 has been proposed to be the major self antigen responsible for thymic selection of canonical Vα14-positive murine NKT cells [54], but whether this compound plays a similar role in selecting human NKT cells remains unknown. Since the Vα24-negative T cells were all isolated from peripheral blood of healthy adult donors, they are presumed to have undergone positive selection and may have been expanded *in vivo* because of their antigen-recognition properties. Moreover, since these clones resemble canonical Vα24-positive clones by using a TCRα rearrangement that has strictly maintained the germline Jα18 sequence and conserved the overall CDR3α loop length, they may have been selected *in vivo* by a process similar to that which selects Vα24-positive NKT cells. Thus, although the requirement for iGb3 in the positive selection of canonical human Vα24-positive NKT cells remains unclear, our results suggest there are

additional mammalian antigens that can select human CD1d-restricted TCRs that are specific for α-GSLs.

The possibility that multiple self antigens select CD1d-restricted T cells could explain the observation that NKT cell clones differ in their autoreactive responses. An ability to monitor a heterogeneous selection of self lipids could also have important implications for the

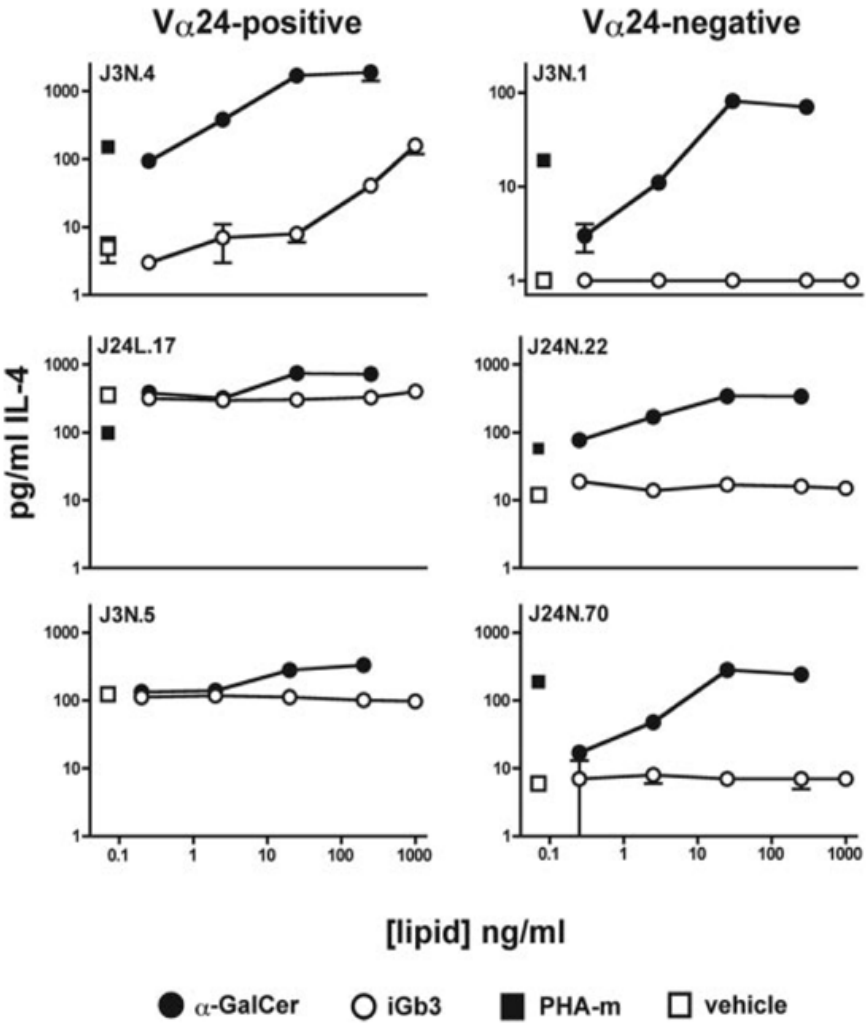

Figure 3.23: **Cytokine secretion by Vα24-positive (left hand panels) and Vα24-negative (right hand panels) clones in response to glycolipid-pulsed APCs.** IL-4 production by the T cell clones was measured in response to APCs pulsed with the indicated concentration of α-GalCer **(44)** (filled circles), iGb3 (open circles), or vehicle alone (open squares). The filled squares indicate the response of the clones to the non-specific stimulator phytohaemaglutinin m (PHA-m). Experiments carried out by Brigl *et al.* at the Department of Rheumatology, Immunology, and Allergy, Brigham and Women's Hospital, Boston, USA, partly using analogues sythesised during this project. Adapted from [255]

physiological functions of NKT cells. For example, different NKT cell clones could be sensitive to lipids loaded in distinct intracellular compartments, allowing them to become activated under differing circumstances. The finding that a human NKT cell clone exhibits a similar reactivity to phospholipids, as that observed previously for a murine NKT cell hybridoma [50], suggests that this lipid Ag specificity is evolutionarily conserved. Because CD1d has been shown to bind phospholipids in the endoplasmic reticulum (ER), this specificity may permit NKT cell monitoring of ER-derived lipids and, thus, perhaps monitoring of the integrity of ER biosynthetic processes. Such ability could be particularly valuable in viral infections; because NKT cells having autoreactive specificity for ER-derived lipids may be broadly sensitive to changes that occur upon viral subversion of cellular processes.

Chapter 4

Variations in the *N*-acyl chain

4. Variations in the *N*-acyl chain

4.1. Introduction

Variations in the *N*-acyl chain of α-GalCer analogues have become of particular interest over recent years, with interest focusing on a number of aspects of ceramide diversity. This includes antigens with *N*-acyl chains derived from bacterial glycolipids [179, 180], more complex groups incorporated into the structure *via* *N*-acylation [184, 263, 264], and the length and degree of saturation of straight-chain hydrocarbon-based *N*-acyl chains [64, 98, 237, 265-267].

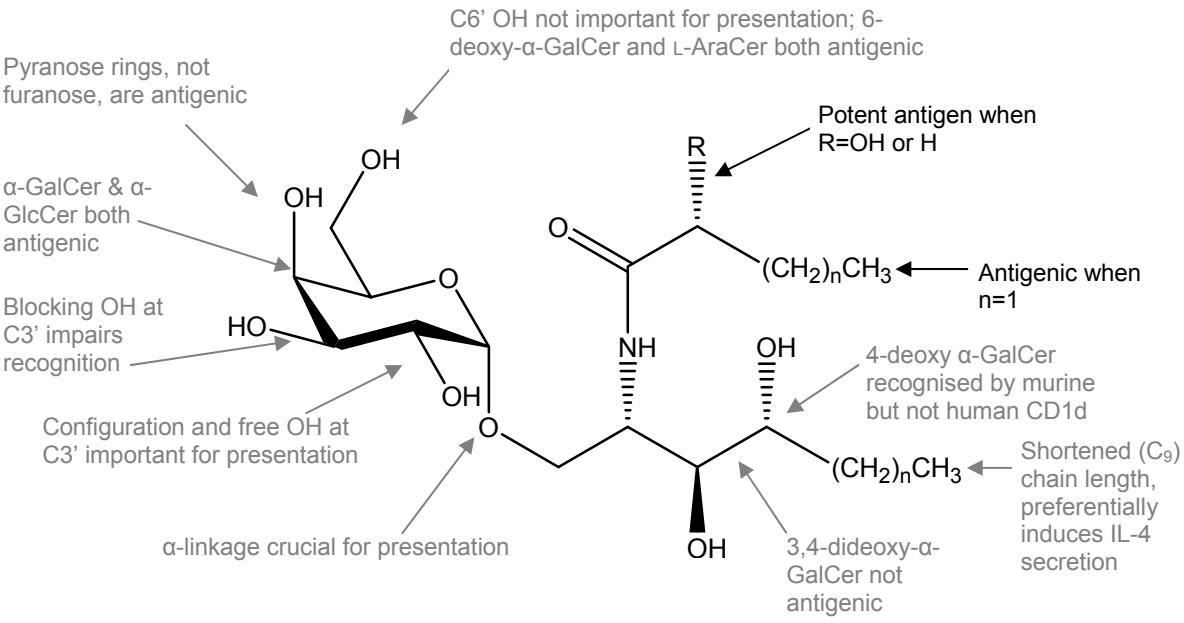

Figure 4.1: The relationship between the structure of α-GalCer analogues and bio-reactivity.

Figure 4.1 summarises some of the structural requirements that have previously been explored, how they relate to the reactivity of the resulting glycolipid antigen and which features are vital for activation of iNKT cells [64, 98, 179, 180, 184, 237, 263-267]; some of these features have been investigated throughout this project.

4.2. Fluorescent analogues of α-GalCer

Several studies have centred themselves around the synthesis of fluorescence-labelled antigens and CD1d tetramers [106, 107, 264, 268]. A novel glycolipid antigen labelled with the fluorescent group boron dipyrromethane difluoride (4,4-difluoro-5,7-dimethyl-4-bora-3a,4a-diaza-*s*-indacene-3-propionic acid; BODIPY) was prepared and proved to be biologically active in the same typical test as α-GalCer **(44)** (Figure 4.2A) [264]. The BODIPY fluorescent probe was administered by intra-peritoneal (ip) injection to 8-week old mice and the biological activity monitored by the activation-induced disappearance of liver iNKT cells, reflecting the overall *in vivo* activation of the cells, with no prejudice for the specific cytokine released [264]. In fact, the type of cytokine produced may be dependant on the *N*-acyl chain of the α-GalCer analogue [139].

Sakai *et al.* [184] synthesised both α- and β-biotinylated analogues of α-GalCer, and showed that only the biotinylated α-analogue of α-GalCer (biotin-α-GalCer) (Figure 4.2B) exhibited statistically significant binding to mCD1and hCD1d molecules compared to a control ($P < 0.05$) (Figure 4.3). Not only does this further add to the evidence that analogues of α-GalCer with altered acyl chains can be successfully presented by CD1d to iNKT cells in a manner comparable to α-GalCer **(44)** (Figure 4.3), it also concurs with the findings by Motoki *et al*. [226], Kobayashi *et al*. [59] and Ortaldo *et al.* [96], who showed that iNKT cells

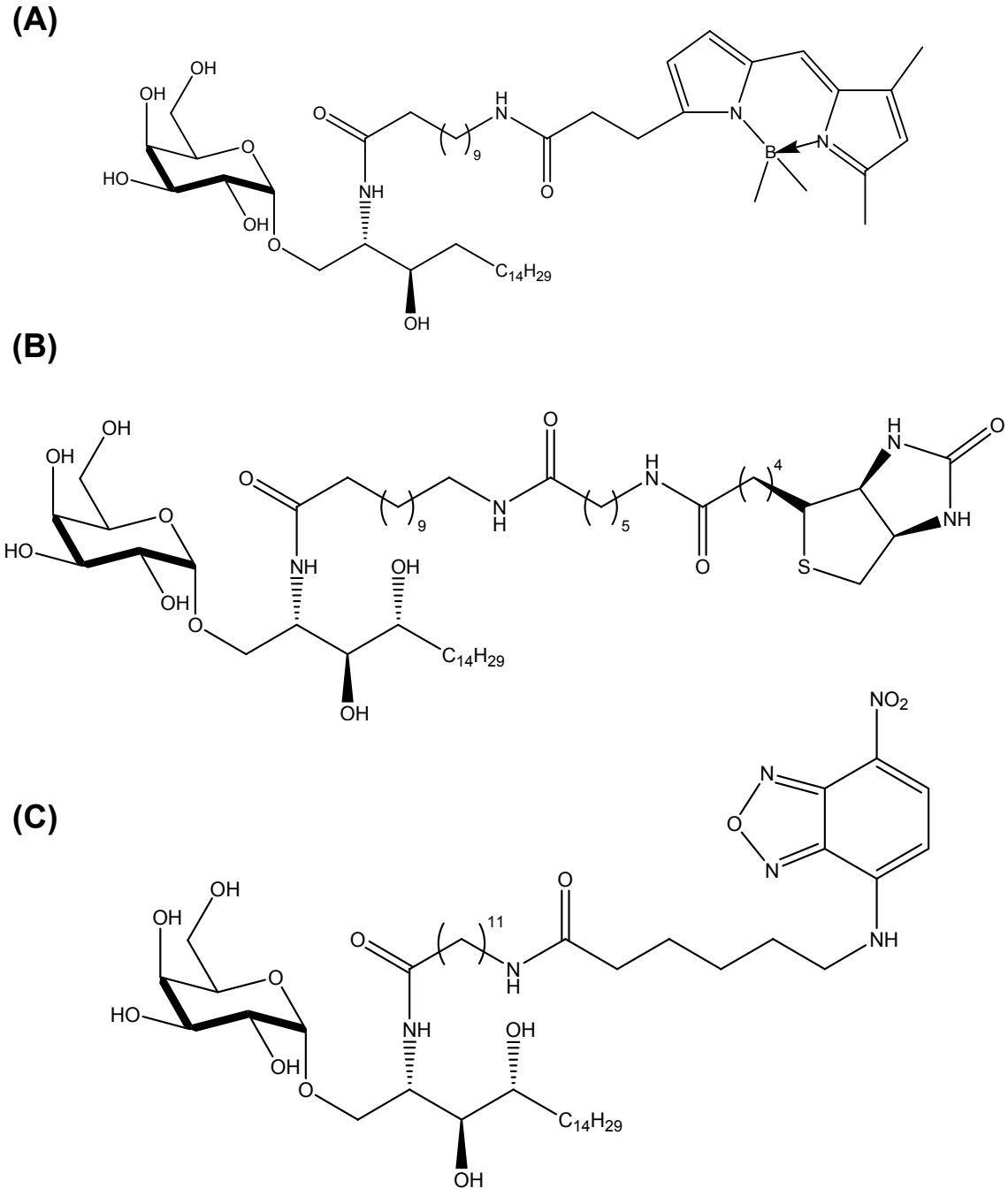

Figure 4.2: **Fluorescence-labelled α-GalCer analogues. (A)** 5,7-dimethyl-4-bora-3a,4a-diaza-s-indacene-3-propionic acid-α-GalCer (BODIPY-α-GalCer) **(B)** 11- (Bi-undecanoic acid [2,3-dihydroxy-1-(3,4,5-trihydroxy-6-hydroxymethyl-tetrahydro-pyran-2-yloxymethyl)-heptadecyl]-amide(biotin-α-GalCer) **(C)** 6-7-Nitro-benzo(1,2,5)oxadiazol-4-ylamino-α-GalCer (NBD-α-GalCer).

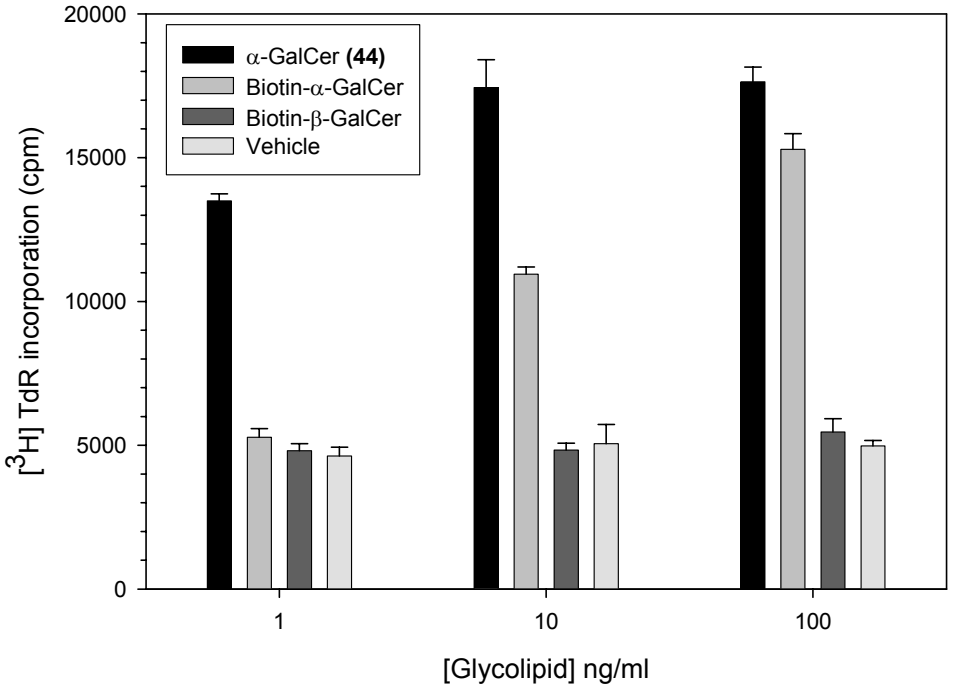

Figure 4.3: **The effects of α-GalCer (44) and biotinylated-α- and β-GalCer (biotin-α-GalCer and biotin-β-GalCer, respectively) on the proliferation of murine spleen cells.** 2.5 x 10^5 cells/ 100µl/ well of murine spleen cells were cultured with various concentrations of glycolipid antigen, before 0.5µCi/well [^{3}H]TdR was added into each well and the resulting [^{3}H]TdR uptake into the cells was measured by liquid scintillation. Each bar represents the mean count ± S.D. $P < 0.05$ α-GalCer and biotin-α-GalCer vs. vehicle-treated group. Adapted from [184].

can differentiate between the different glycosidic links when presented with a CD1d/ α-GalCer complex.

Although, the ability of biotin-α-GalCer to stimulate iNKT cells has been demonstrated, its capacity to successfully stimulate cytokines has been questioned. Naidenko *et al*. [97] showed that the addition of a biotin group did not eliminate the ability of the α-GalCer analogue to be presented to NKT cells by mCD1 protein, but they did demonstrate the antigen incorporating a biotin group is a weaker antigen. The ineffectual ability of biotin-α-GalCer at secreting IL-2 was shown by a 3- to 5-fold lower cytokine release when incubated with either murine or human CD1d molecules [97]. These experiments also clarified that both β-GalCer and a biotinylated version of β-GalCer display little or no immunostimulatory

activity and do not enhance the APC function of DCs in mice and humans, even at concentrations as high as 100ng/ml [97].

In a similar investigation, Sakai *et al.* [263] synthesised a fluorescent analogue of α-GalCer incorporating a 7-nitrobenz-2-oxa-1,3-diazole (NBD) group at the terminus of the *N*-acyl chain (Figure 4.2C). This proved to be significantly potent at spleen cell proliferation stimulatory activity (Figure 4.4) [263]. In fact, at lower concentrations the NBD-α-GalCer analogue was notably more potent than α-GalCer **(44)** at spleen cell proliferation (Figure 4.4), illustrating the fact that the immunostimulatory properties of α-GalCer **(44)** are dependent on the chemical structure of the fatty acid side chain in the ceramide portion of the molecule. In conjunction with these findings, one can surmise that the lack of recognition

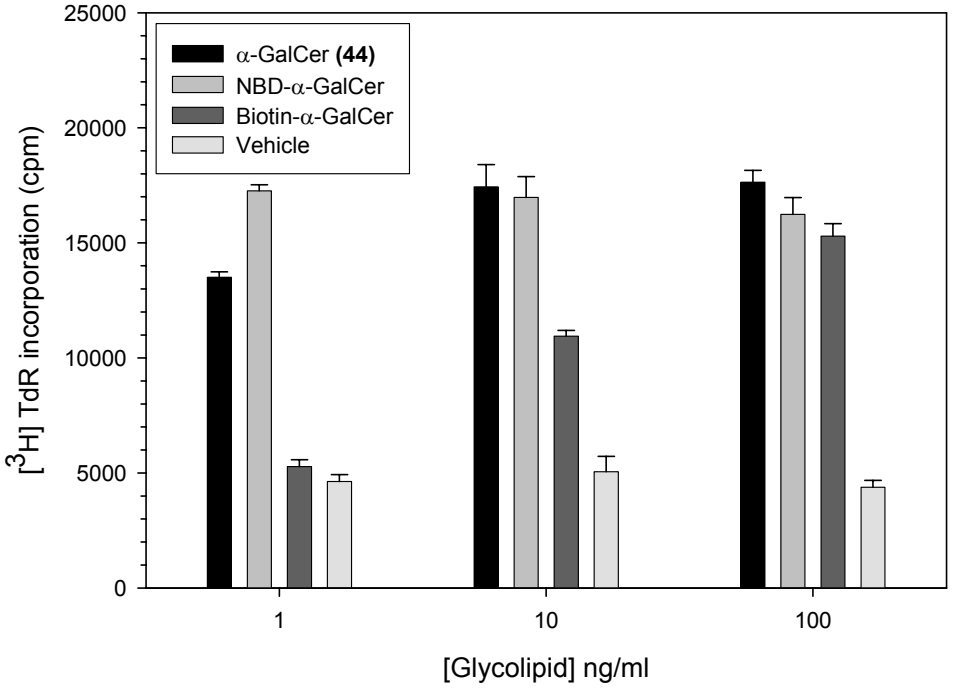

Figure 4.4: **The effects of α-GalCer (44), NBD-α-GalCer and biotin-α-GalCer on the proliferation of murine spleen cells.** 2.5 x 10^5 cells/ 100µl/ well of murine spleen cells were cultured with various concentrations of glycolipid antigen, before 0.5µCi/well of [^{3}H]TdR was added into each well and the resulting [^{3}H]TdR uptake into the cells was measured by liquid scintillation. Each bar represents the mean count ± S.D. $P < 0.05$ α-GalCer and biotin-α-GalCer vs. vehicle-treated group. Adapted from [263].

between biotin-α-GalCer (Figure 4.2B) and CD1d in transfected cells is due to the limited binding capacity, expressed by weaker stimulatory activity in comparison with α-GalCer **(44)** and NBD-α-GalCer [263]. The analogue containing an NBD group may have a higher affinity of interaction with CD1d, thus being a potential agent for use in studying the mechanism of CD1d presentation.

4.3. *N*-acyl chain length and saturation

The *N*-acyl chain of α-GalCer **(44)** sits in one of the pockets of the antigen binding site of the CD1d protein [218]. Studies have shown that analogues with acyl chains consisting of 26 carbons are optimal for stimulating CD1d-restricted T cell responses [95]. Acyl chain lengths that are shorter, by as little as two carbons, are significantly less active, illustrating that the acyl chain configuration plays a key part in their recognition by CD1d [228]. Brossay *et al*. [98] however, established that an α-GalCer analogue that differed only from the parent by incorporating an acyl chain length totalling two carbons was successfully presented by mCD1 to the iNKT cell receptor. This was exemplified by the release of high concentrations of the cytokine IL-2. The successful presentation of a short-chain fatty acids suggests that only one of the CD1 protein pockets needs to be filled by the aliphatic hydrocarbon chain of the antigen, rendering the hydrophilic sugar-based head of the antigen available to adequately stimulate the TCR of the iNKT cell [98]. However, when the acyl chain was substituted for a bulky aromatic group, the analogue failed to produce an antigenic response in mCD1 cells [98].

Altering the lipid chain length of the α-GalCer **(44)** molecule has gained interest over recent years. Moody *et al.* [269] hypothesised and subsequently demonstrated that the size of the lipid moiety controls the kinetics, sub-cellular localisation, efficiency of antigen loading into

the CD1 groove, and ultimately the presentation by different types of CD1 expressing APCs. The perceptible distinctions in cellular requirements for the presentation of antigens can be explained by alkyl chain length controlling the entry of long-chain lipids into efficient endosomal antigen-presentation pathways and short-chain lipids into less efficient non-endosomal pathways. The X-ray crystal structure of murine CD1d indicates that the groove in the protein structure is big enough to maximally house 31 or 32 methylene units. This figure correlates with the lipid moiety size of PI eluted directly from cellular CD1d molecules [269].

α-GalCer **(44)** is well established as an antigenic molecule that binds with CD1d molecules and activates iNKT cells [181], yet the biology surrounding this phenomenon and endogenous antigen coupling is still somewhat of a mystery. It is known that phospholipids such as PI (Figure 1.1B) are naturally occurring and are antigenic, binding to CD1d molecules and stimulating iNKT cells [70]. mCD1d has been shown to specifically bind the PI fraction of cellular GPI, which is a natural ligand of the protein [52]. One hypothesis is that PI acts as a chaperone in the assembly of the CD1 family of molecules in the ER, and conserves the integrity of the hydrophobic groove in the protein structure. The hypothesis by Park *et al.* [270] proceeds by suggesting that PI remains in the ER until the protein binds an antigenic glycolipid. Rauch *et al.* [208] demonstrated that recognition of one phospholipid, phosphatidylethanolamine (1-palmitoyl-2-oleoyl-sn-glycero-3-phosphoethanolamine; PE) is dependent on the degree of unsaturation within the acyl chain length, and the double-bond configuration of the unsaturated bonds. From an iNKT 24.8.Å cell hybridoma study, it has been shown that increasing unsaturation in synthetic PEs with 18-carbon acyl chains resulted in strong recognition by the iNKT cell hybridoma [271]. The PE with greatest recognition incorporated two double bonds in each of the two acyl chains, but at the same time it was also shown that synthetic PEs containing only one unsaturated fatty acid chain resulted in 24.8.A iNKT cell hybridoma stimulation [271]. Although, this particular cell line

fails to recognise α-GalCer **(44)** and is instead specific for phospholipids, it simply represents one end of the scale of CD1d-restricted iNKT cells. Sitting at the opposite end, are iNKT cells that are not autoreactive but are stimulated by α-GalCer **(44)**. In the central core of this band sit iNKT cells that are autoreactive and recognise both α-GalCer **(44)** and phospholipids. This implies that α-GalCer analogues with two *cis* double bonds in the acyl chain are going to be significantly more active than those incorporating saturated fatty acid chains.

The suggestion that unsaturated α-GalCer analogues are more active than saturated ones was demonstrated by Yu *et al.* [266]. A number of *N*-acyl variants of α-GalCer were synthesised and subsequently tested for their iNKT cell stimulatory properties. It was found that a synthetic analogue incorporating a C20 fatty acid with four *cis* double bonds (C20:4) **(71)** induced proliferation and cytokine secretion by murine splenocytes [266].

In response to these results, a panel of synthetic analogues were produced and tested in a similar manner [266]. Various analogues of α-GalCer with *N*-acyl substituents incorporating varying degrees of unsaturation and carbon-chain length were synthesised (Figure 4.5A). These were then subjected to screening for their ability to activate an iNKT cell hybridoma and their ability to induce cytokine production (Figure 4.5B).

Truncating the acyl chain from 26 carbons to 20 carbons (C20:0) **(79)** resulted in a marked decrease in cytokine production. However, incorporating double bonds into the C20 chain amplified activity similar to that of α-GalCer **(44),** with a C_{20} chain with one **(78)**, two **(73)** and four **(72)** *cis* double bonds providing the greatest activity of the C20 library.

Administration of the C20:2 analogue **(73)** (incorporating unsaturation at C11'' and C14'') resulted in a slightly smaller concentration of IL-4 and the IFN-γ response was drastically reduced, compared to C20:1 (*cis* double bond) **(78)** and α-GalCer **(44)** (Figure 4.5). It seems that the insertion of two double bonds into the acyl chain is accountable for this increased

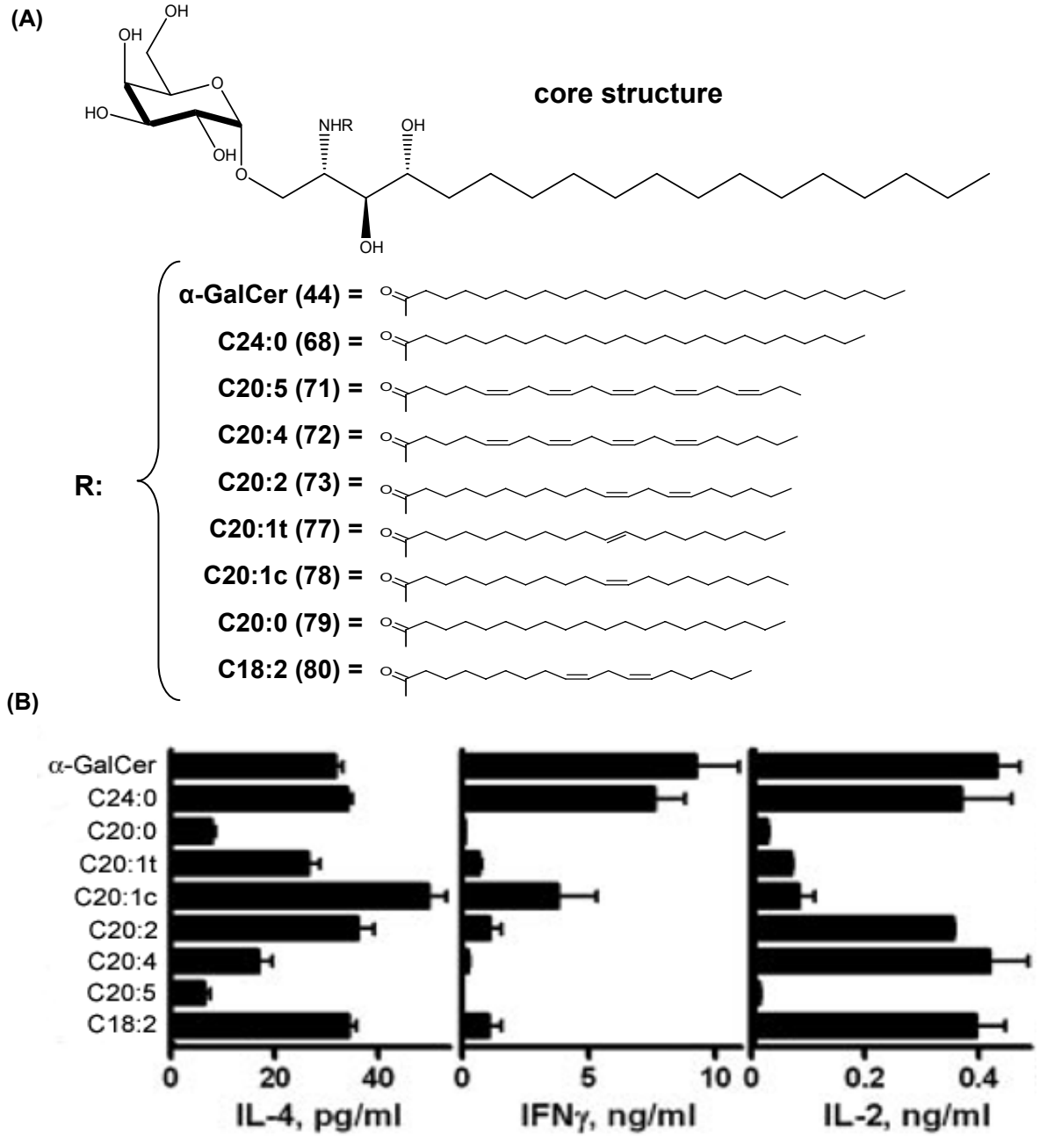

Figure 4.5: **α-GalCer analogues varying in the length and saturation of the *N*-acyl chain and their immunological activity (A)** *N*-acyl variant analogue structures. Using the core structure, various fatty acids were synthesised with altered carbon chain lengths and degrees of unsaturation in order to analyse their recognition by iNKT cell hybridomas **(B)** C57BL/6 splenocyte cultures. IL-4, IFN-γ, and IL-2 cytokine levels were recorded in response to 3.2 nM of the various glycolipid analogues depicted in **(A).** Figure adapted from [266].

potency as an analogue with 18 carbons and 2 double bonds in the acyl chain (C18:2) **(80)**, exhibited similar potency to the C20:2 analogue **(73)**.

Interestingly, an analogue with *trans* orientation around the double bond (C20:1t **(77)**) showed a considerably lower stimulatory cytokine profile compared with the corresponding *cis* analogue (C20:1c **(78)**), suggesting that *cis* orientation of the double bond has a greater stimulatory effect on iNKT cells.

The difference exhibited between the beneficial effects of C20:2 **(73)** and C24:0 **(68)** with regards to T1D in mice has been highlighted by Forestier *et al.* [272]. Using two different α-GalCer analogues, these workers demonstrated that there was a significant difference between the incidence of glucosuria (P = 0.0424 C24:0 **(68)** vs. C20:2 **(73)**) and the survival rate of female NOD mice (P = 0.0318 C24:0 **(68)** vs. vehicle, and P = 0.0006 C20:2 **(73)** vs vehicle). There was a significant difference in survival between mice injected with the two analogues at 30 weeks (P = 0.0049), and at 53 weeks of age the insulinitis index of the C20:2 **(73)** group compared to vehicle was statistically significant (P = 0.002) [272].

The incorporation of a polyethylene glycol (PEG) molecule as an alternative to a hydrocarbon-based fatty acid has a number of possible advantages over the usual hydrocarbon based fatty acid. Not only would PEG vastly improve the aqueous solubility of the analogues, rendering them far easier in terms of handling and administration, but it has also been proved to be inert towards most biological macromolecules [273]. Polymeric biomaterials incorporating structures, such as PEG have been extensively used in the medical world since the 1950s [273].

PEG is a hydroxyl-terminated linear polyether with a repeating unit within the general structure -$(CH_2CH_2O)_n$- which accounts for the hydrophilicity of such compounds. PEG-bound biomaterials form the basis of preparations such as laxatives, sexual lubricants, skin creams, bowel preparations, and drug regimes for such conditions as hepatitis C [274]. Together with its status as an FDA approved compound, its aforementioned physical and commercial properties are highly favourable in terms of investigating potential new drug therapies for human use. It has also been shown that drugs that have modified protein, peptide or non-peptide molecules by the linking of one of more PEG chains, so called PEGylated drugs, have increased body-residence time [273, 275], another attractive quality of a PEG-incorporated glycolipid antigen.

4.4. Microbial glycolipid antigens

The diverse group of α-GalCer analogues that have been found to bind to each of the human CD1 isoforms encompasses both mammalian and bacterial lipids [2, 37], suggesting a role for CD1 proteins in bacterial immunity. Wu *et al.* [179] synthesised and isolated a number of α-GalCer analogues and tested them for their immunological activity. Bacterial glycolipids from the outer membrane of *Sphingomonas wittichii* and from the causative agent of Lyme disease, *Borrelia burgorferi*, were isolated and analysed (Figure 4.6) [179]. Of the bacterial glycolipids analysed, those derived from the *Sphingomonas* species showed considerable activity, although they were not as potent α-GalCer **(44)** (Figure 4.7). Although, these analogues have been shown to bind with CD1d and stimulate iNKT cells, one can not conclusively state this is due to the altered *N*-acyl chain, as the structures of both GSL-1 and GSL-2 vary in other parts of the antigen structure compared to α-GalCer **(44)**.

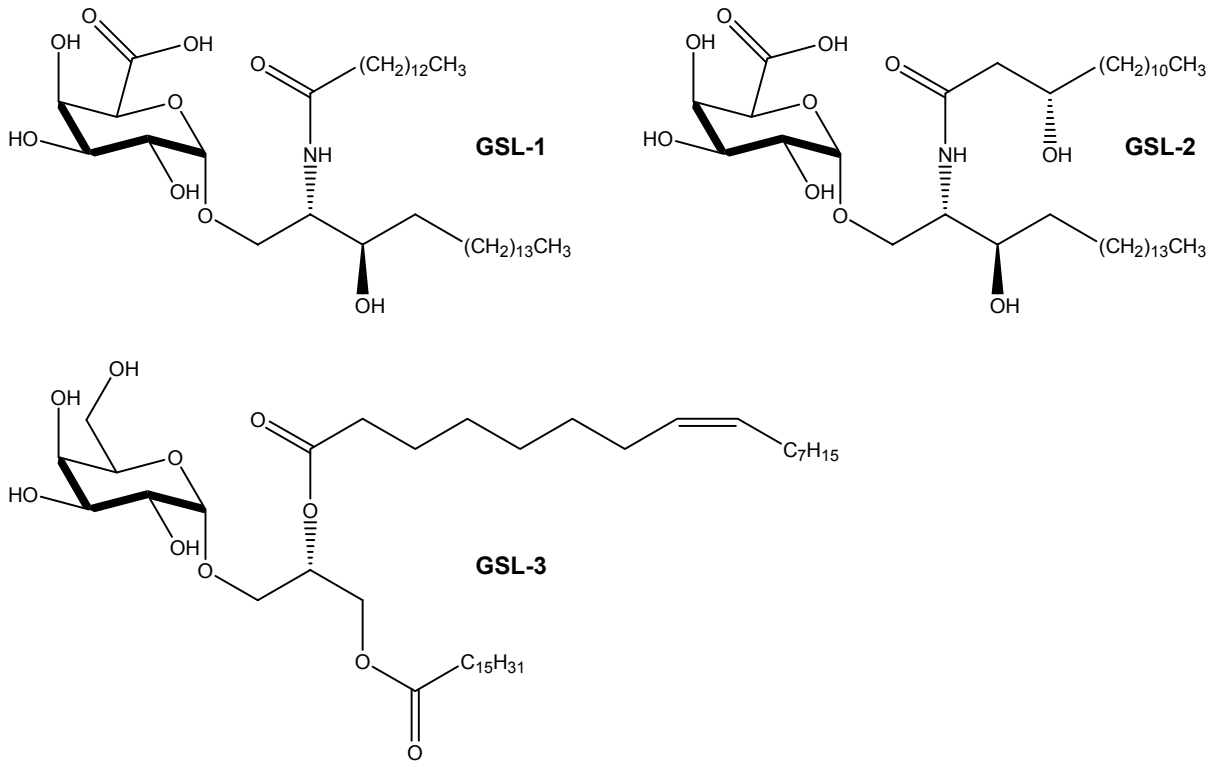

Figure 4.6: **Bacterial glycosphingolipids.** GSL-1 and GSL-2 are derived from *Sphingomonas wittichiia* and GSL-3 from *Borrelia burgorferi* [179].

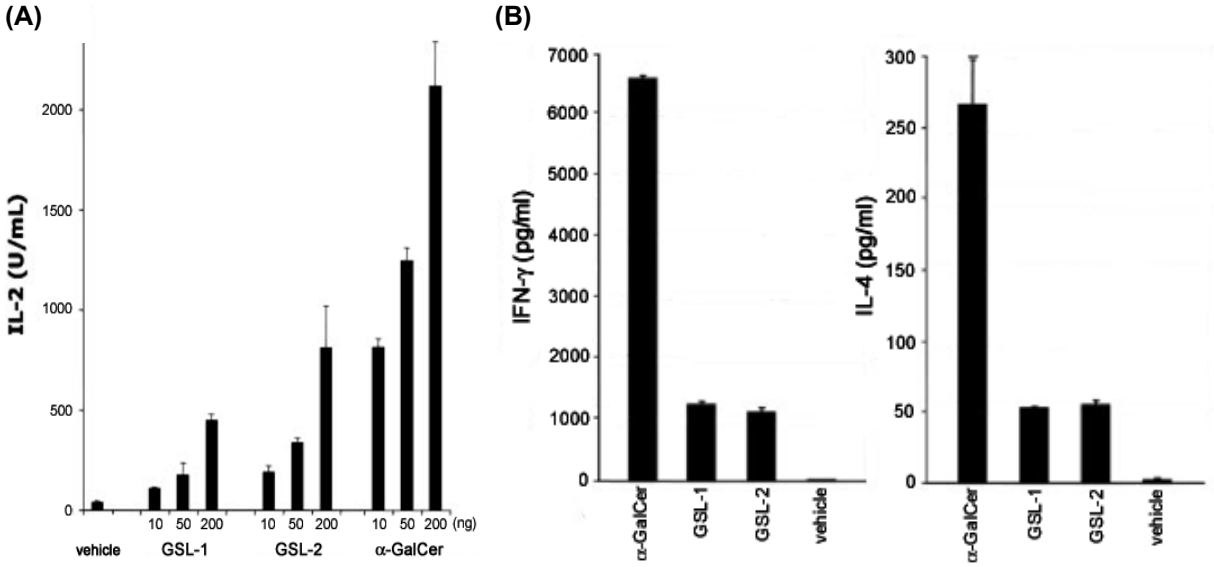

Figure 4.7: **Cytokine production by iNKT cells in response to bacterial glycolipids. (A)** Dose-dependent IL-2 secretion by *Sphingomonas* GSLs (GSL-1 and GSL-2) compared with α-GalCer, as determined by ELISA. **(B)** IFN-γ and IL-4 release by human iNKT cells after stimulation with10µg/mlglycopid antigen and determined by ELISA. Figure adapted from [179].

Wu *et al.* [180] went on to investigate further the effect bacterial glycolipids have on the activation of iNKT cells. A synthetic analogue of the *Sphingomonas* derived GSL-1, which more closely resembled α-GalCer **(44)** (a galactose head coupled to a ceramide with a C_{18} sphingosine base and a C_{14} *N*-acyl chain) was analysed for IL-4 and IFN-γ production against GSL-1 and α-GalCer **(44)** [180]. The results showed that this synthetic analogue of GSL-1 gave a cytokine production profile for both IL-4 and IFN-γ more similar to α-GalCer than GSL-1 [180]. This suggests that the *N*-acyl chain, as opposed to the other subtle variations in the structure of GSL-1, is the contributing factor in its ability to activate iNKT cells.

It has recently been reported that diacylglycerol lipids from *Borrelia burgdorferi* are recognised by iNKT cells and that their antigenic potency is dependent on acyl chain length and saturation [47]. It was demonstrated that murine iNKT cells more efficiently recognise mCD1d molecules loaded with diacylglycerol analogues with C_{16} acyl chains. This is in contrast to human iNKT cells that recognise hCD1d proteins loaded with diacylglycerol analogues of 18 carbons in length [47]. This is more than likely due to the shorter length of the mCD1d F' channel [69, 71].

The results gained do not however provide an answer as to whether the enhanced potency of diacylglycerol analogues is caused by their more stable binding to the CD1d protein, or because of a higher affinity with the TCR of the iNKT cell. Thus, different length acyl chains were incorporated into the structure of α-GalCer and varying degrees of unsaturation were added, in order to analyse the role of the lipid chain occupying the A' channel of hCD1d molecules in modulating TCR affinity and/ or stability of hCD1d-GSL complexes.

4.5. Results and discussion

4.5.1. Chemical synthesis

In order for *N*-acylation to take place, an activating agent is required. 1-(3-Dimethylaminopropyl)-3-ethylcarbodiimide hydrochloride is a water soluble condensing reagent used as a carboxyl group activating agent for amide bonding with primary amines. Typically it is utilised in the pH range 4.0-6.0 without buffers. The first step in the reaction is the addition of the carboxylic acid to one of the C=N bonds of the carbodiimide, generating an *O*-acylated derivative of urea. This is a reactive acylating agent; there is a strong preference for eliminating the substituted urea unit. The result is formation of a stable amide carbonyl group (Figure 4.8).

4.5.1.1. *N*-Hydroxysuccinimide esters of carboxylic acids and their use in *N*-acylation

N-Hydroxysuccinimide esters of the appropriate carboxylic acids needing to be *N*-acylated onto the developing GSL were prepared and activated by the carbodiimide. Hammarstrom *et al.* [276] described the synthesis of ceramides using direct coupling of fatty acids and mixed carbodiimide. However, the product yields were relatively low (30-37.5%). The selective *N*-acylation of unprotected aminosugars with esters derived from *N*-hydroxysuccinimide as activated acylating agents has proven to be a versatile and general approach to acylamidosugars [277]. A wide range of acyl groups can be introduced along with other functionalities, such as labile phosphate groups [278]. Several years after Hammarstrom reacted fatty acids directly with ceramides in the presence of mixed carbodiimides [276], Ong *et al.* [279] successfully acylated the amino group of a number of ceramides employing *N*-hydroxysuccinimide esters of fatty acids in high yield and purity with

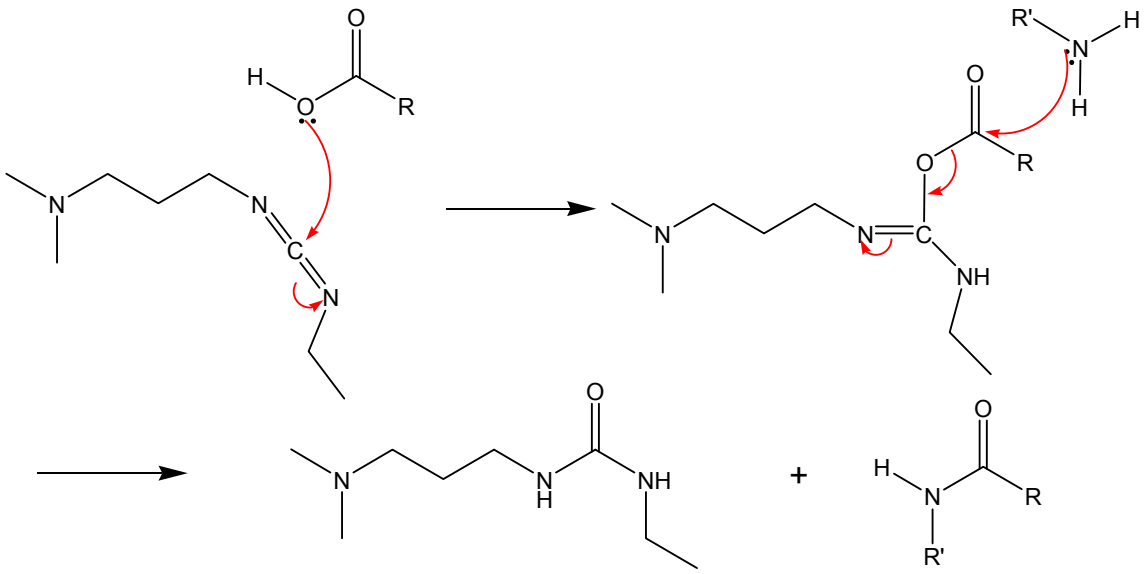

Figure 4.8: **General mechanism of *N*-acylation using a water-soluble carbodiimide.**

no visible side-products. This was also true in the reactions carried out by Lazarevic *et al.* [278], who also showed that no *O*-acylation products were observed despite the presence of several unprotected hydroxyl groups. In the synthesis of α-GalCer analogues that vary in the *N*-acyl chain, the *N*-hydroxysuccinimide ester route was adopted, with the ester being prepared if they weren't commercially available (Figure 4.9).

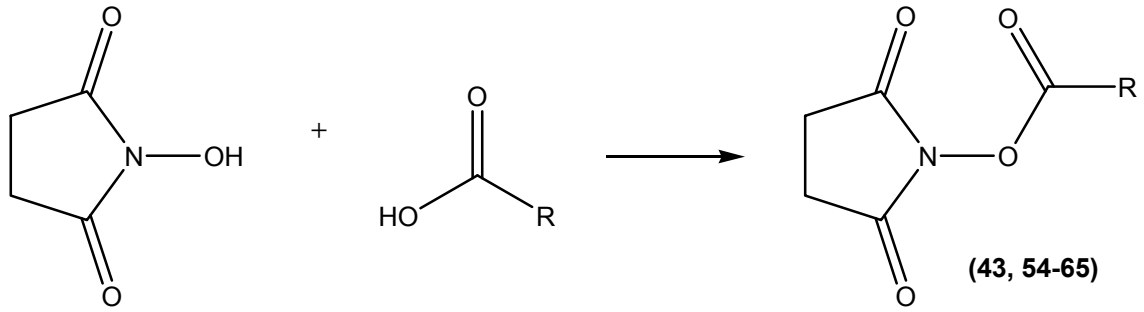

Figure 4.9: **Schematic representation of the reaction between *N*-hydroxysuccinimide and a fatty acid to produce an *N*-hydroxysuccinimide ester.** R = $C_{25}H_{51}$ **(43)**; $C_{23}H_{47}$ **(54)**; $(CH_2)_{13}CH{=}CH(CH_2)_7CH_3$ **(55)**; $(CH_2)_2(CH{=}CHCH_2)_6CH_3$ **(56)**; $(CH_2)_3(CH{=}CHCH_2)_5CH_3$ **(57)**; $(CH_2)_3(CH{=}CHCH_2)_4(CH_2)_3CH_3$ **(58)**; $(CH_2)_9(CH{=}CHCH_2)_2(CH_2)_3CH_3$ **(59)**; Z-$(CH_2)_9CH{=}CH(CH_2)_7CH_3$ **(60)**; E-$(CH_2)_9CH{=}CH(CH_2)_7CH_3$ **(61)**; $C_{19}H_{39}$ **(62)**; $(CH_2)_7(CH{=}CHCH_2)_2(CH_2)_3CH_3$ **(63)**; C_8H_{15} **(64)**; CH_2PhCH_3 **(65)**

4.5.2. PEGylation

PEGylation, the incorporation of one or more PEG groups into a protein, peptide or non-peptide molecule was first described in the 1970s, when two scientists successfully modified the enzyme catalase, whilst retaining its biological activity [275]. Since that time, a large number of chemical and enzymatic procedures for conjugating PEG have been discovered [275].

Amino groups were the first targets of PEGylation by acylation or alkylation, but now thiol, hydroxyl and amide groups can all be successfully conjugated with PEG [275]. Amine conjugation by acylation is a commonly used method of incorporating PEG into a molecule [275]. One method of carrying out this acylation is by producing a PEG derivative with a succinimide group. The carboxylic group of the PEG molecule is activated as an *N*-hydroxy succinimidyl ester, which can then acylate an amine [275]. It is this method that was employed in this project to incorporate PEG chains into the glycolipid antigen, in place of a saturated or unsaturated hydrocarbon acyl chains.

The inclusion of polyethylene glycol $(PEG)_n$ as a component of a protein reagent imparts improved solubility, improved stability, protection from proteolytic digestion, increased half-life in biological applications, reduced aggregation, reduced immunogenicity to the modified protein and minimized interference for both *in vitro* and *in vivo* applications [273, 275]. With these advantages in mind two analogues of α-GalCer were synthesised using two *N*-acylated PEG chains in place if the *N*-acyl hydrocarbon chain (Figure 4.10).

Using the *N*-hydroxysuccinimide method of introducing an *N*-acyl chain to the GSL, a library of α-GalCer analogues was synthesised as outlined in Table 4.1 and Figure 4.11. In addition to varying the sugar head group and phytosphingosine base chain length, the *N*-acyl chain was varied not only on the parent antigenic structure (α-GalCer **(44)**), but also on α-GlcCer **(50)** and α-L-FucCer **(53)** both with C_{18} phytosphingosine bases, and with α-GalCer with C_{18}, C_{15}, C_{12} and C_9 bases. The latter analogues had only the key *N*-acyl chains coupled to them, namely C26, C20:2 and C18:2. These *N*-acyl chains are of particular interest with regards to iNKT stimulation and CD1d recognition, when coupled with α-GalCer **(44)**, and have exhibited strong immunostimulatory profiles [266, 269, 272].

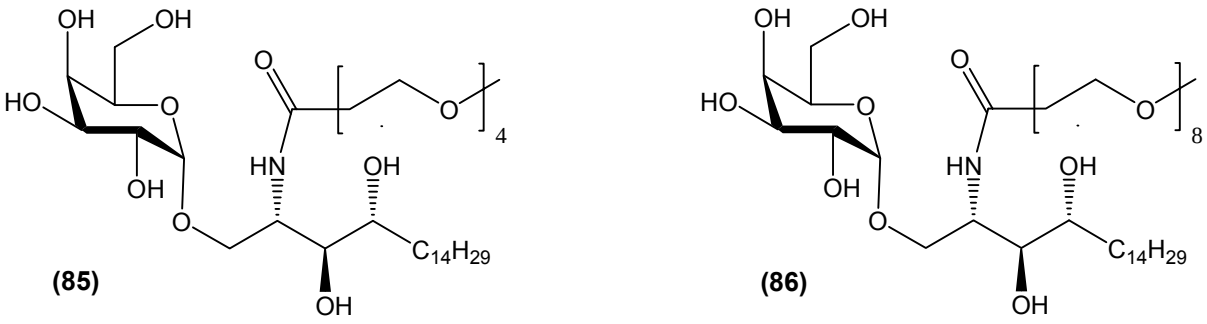

Figure 4.10: Two α-GalCer analogues incorporating PEG molecules, (85) and (86).

	Parent GSL					
	α-GalCer (44)	**α-GlcCer (50)**	**α-GalCer (44)**	**α-GalCer (44)**	**α-GalCer (44)**	**α-L-FucCer (53)**
	R=$C_{14}H_{29}$ R'=OH R''=H	**R=$C_{14}H_{29}$ R'=H R''=OH**	**R=$C_{11}H_{23}$ R'=OH R''=H**	**R=C_8H_{17} R'=OH R''=H**	**R=C_5H_{11} R'=OH R''=H**	**R=$C_{14}H_{29}$**
R'''	**(39)**	**(49)**	**(40)**	**(41)**	**(42)**	
$C_{25}H_{51}$	**(44)**	**(50)**	**(45)**	**(46)**	**(47)**	**(53)**
$C_{23}H_{47}$	**(68)**	**(88)**				
$(CH_2)_{13}CH{=}CH(CH_2)_7CH_3$	**(69)**					
$(CH_2)_2(CH{=}CHCH_2)_6CH_3$	**(70)**	**(89)**				
$(CH_2)_3(CH{=}CHCH_2)_5CH_3$	**(71)**					
$(CH_2)_3(CH{=}CHCH_2)_4(CH_2)_3CH_3$	**(72)**	**(90)**				
$(CH_2)_9(CH{=}CHCH_2)_2(CH_2)_3CH_3$	**(73)**	**(91)**	**(74)**	**(75)**	**(76)**	**(96)**
E-$(CH_2)_9CH{=}CH(CH_2)_7CH_3$	**(77)**	**(93)**				
Z-$(CH_2)_9CH{=}CH(CH_2)_7CH_3$	**(78)**	**(92)**				
$C_{19}H_{39}$	**(79)**	**(94)**				
$(CH_2)_7(CH{=}CHCH_2)_2(CH_2)_3CH_3$	**(80)**	**(95)**	**(81)**	**(82)**	**(83)**	**(97)**
C_7H_{15}	**(84)**					
$(CH_2CH_2O)_4CH_3$	**(85)**					
$(CH_2CH_2O)_8CH_3$	**(86)**					
CH_2PhCH_3	**(87)**					

Table 4.1: **Compound classification of α-GalCer, α-GlcCer and α-L-FucCer analogue library. See Figure 4.11 for definition of R, R', R'' and R'''.**

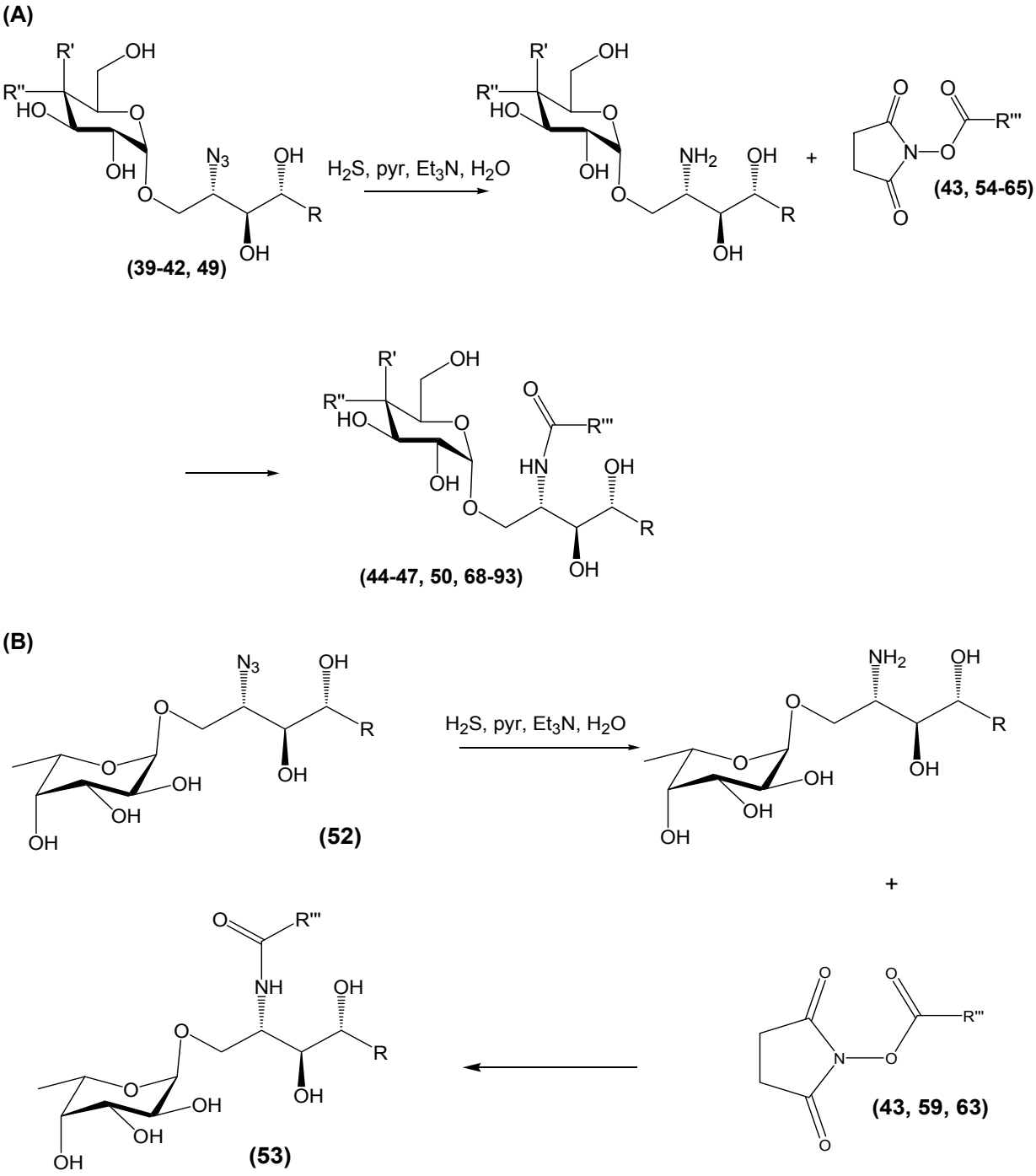

Figure 4.11: **Azide reduction and *N*-acylation with *N*-hydroxysuccinimide esters of fatty acids to produce a library of α-GalCer analogues. (A)** Synthesis using galactose and glucose coupled compounds. **(B)** Synthesis using fucosylated compound. For explanation of R, R', R'' and R''' see Table 4.1.

4.6. Biological evaluation of glycolipid antigens varying in the *N*-acyl chain.

Altering the length, degree of unsaturation and functionality of the *N*-acyl chain of α-GalCer analogues exhibits profound effects on the immunological response [64, 97, 98, 179, 180, 184, 263, 264, 267, 271]. In the hunt for a so-called 'super antigen', it has been demonstrated that analogues incorporating *cis* double bonds in the *N*-acyl chain skews the immune response towards a predominantly T_H2 effect [266, 272].

The effect two analogues of α-GalCer (C20:2 **(73)** and C20:4 **(71)**) have on *in vivo* cytokine production was investigated by S. Porcelli and co-workers at the Albert Einstein College of Medicine, New York, USA using analogues prepared during this project and C57BL/6 female mice obtained from the Jackson Laboratory, Maine, USA (Figure 4.12). This particular strain of mouse is a general purpose strain, particularly suited for use in diabetes-related investigations, due to its susceptibility to hyperglycaemia and hyperinsulinaemia [280]. The results clearly show that treatment with C20:2 **(73)** skews the immunological profile of C57BL/6 mice towards a T_H2 response, with comparable IL-4 (a T_H2 cytokine) production, and dramatically reduced IFN-γ (a T_H1 cytokine) release.

As shown by Forestier *et al*. [272], novel analogues of α-GalCer varying in the *N*-acyl chain have a profound effect on the development of diabetes in NOD mice and can elicit more selective expression of iNKT cell functions. C20:2 **(73)** show greater IL-4 production and decreased IFN-γ production in comparison to α-GalCer **(44)** (Figure 4.12), and the analogue C24:0 **(68)** (incorporating a fully saturated C24 fatty acid chain) (C24:0). It has also been shown to exhibit a dramatic effect on glucosuria incidence in NOD mice, preventing the condition in 100% of animals treated up to 25 weeks of age (Figure 4.13). The results gained after the treatment of female NOD mice (predisposed to developing clinical symptoms of T1D [149]) with either α-GalCer **(44)**, C20:2 **(73)** or vehicle alone, clearly show

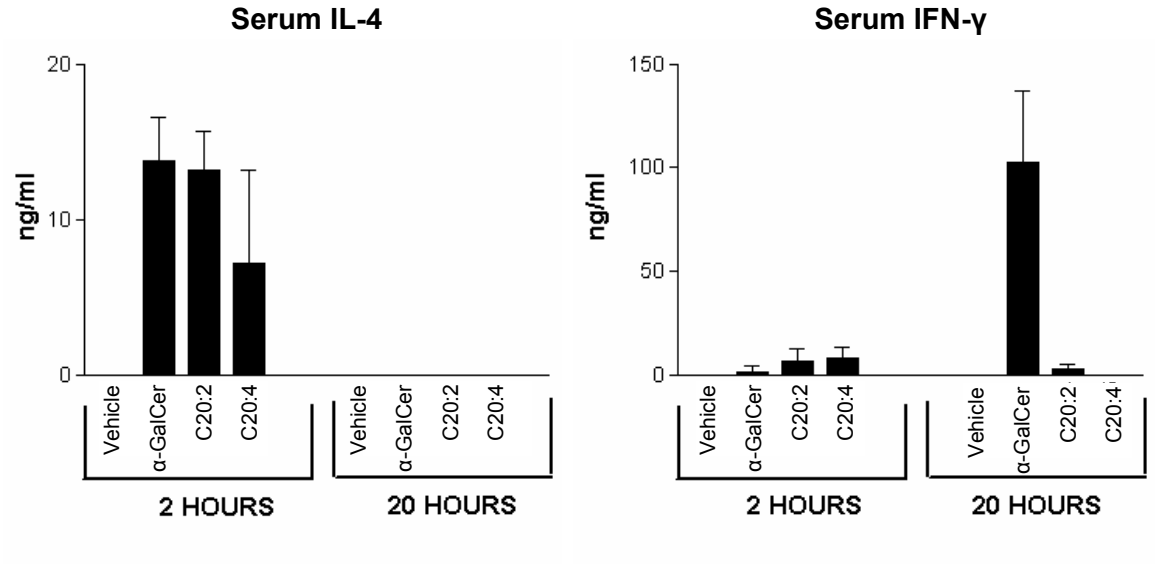

Figure 4.12: ***In vivo* cytokine skewing by α-GalCer analogues.** Serum levels of IL-4 and IFN-γ after a single injection of α-GalCer **(44)**, C20:4 **(71)** or C20:2 **(72)**. C57BL/6 mice (11-13 weeks old) were given a single i.p. injection of 4.8nmol of the analogues or phosphate buffered solution (PBS)/vehicle (VEHI) control. Serum levels were assayed 2 and 20 hours later using ELISA. Bars show means of three mice with standard deviation. Experiments carried out by S. Porcelli and co-workers at Albert Einstein College of Medicine, New York, USA using analogues synthesized during this project.

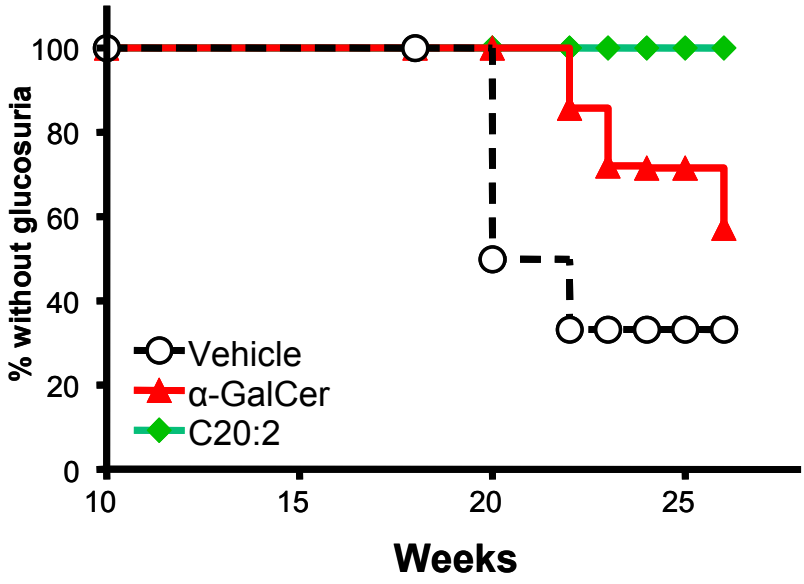

Figure 4.13: **Prevention of diabetes in female NOD mice by α-GalCer analogues.** Female NOD wild type (w.t.) mice were treated with α-GalCer **(44)** and C20:2 **(73)** and the percentage of animals not presenting with glucosuria, in comparison to an untreated animal, was recorded. Starting at 4–6 weeks of age, female NOD mice received seven weekly i.p. injections of glycolipid at a concentration of 4μg/mouse in 250μl of vehicle (PBS plus 0.04% Tween 20) or vehicle alone. T1D was assessed from 10 weeks by monitoring mice weekly for the presence of glucose in the urine (glucosuria) determined using Diastix reagent strips (Bayer). Mice were considered diabetic when two consecutive positive measurements were obtained and the time of onset of diabetes was recorded as the date of the first of the two consecutive readings. Experiments carried out by S. Porcelli and co-workers at Albert Einstein College of Medicine, New York, USA using analogues synthesized during this project

the protective effect of the C20:2 **(73)** analogue in the context of the development of glucosuria, a physiological indication of the development of T1D (Figure 4.13). In addition to the beneficial effects on glucosuria, treatment with C20:2 **(73)** displayed a huge percentage increase in mouse survival, with no mortality up to approximately 37 weeks, and 70% survival after 40 weeks. This is compared to a steady decline in surviving mice treated with α-GalCer **(44)** after approximately 20 weeks, with only 40% survival after 40 weeks.

These results demonstrate that variation within the structure of the *N*-acyl chain of α-GalCer analogues plays a part in modifying their antigenic activity. Figure 4.14A shows the expansion of iNKT cells from PBLs 21 days after stimulation with mature DCs pulsed with analogues, varying in the length and saturation of the *N*-acyl chain. One can see decreased activity with regard to iNKT cell expansion of the analogue with 4 double bonds, C20:4 **(72)**, similar to the results gained from α-GalCer **(44)**, and C20:2 **(73)**. The latter analogue has already shown its ability to skew the immune response (Figure 4.12) and the fact that is able to stimulate iNKT cell expansion in a similar vein to α-GalCer **(44)** widens its scope as an effective immuno-modulator. From the FACS analysis plots (Figure 4.14B), one can see also that C20:2 **(73)** stimulates greater iNKT cell expansion than C20:4 **(72)**, as shown by the greater density in the upper right quadrant of the FACS plots. However, one can not conclude that this is directly related to the unsaturated *N*-acyl chain, as C20:4 **(68)** had a dramatically decreased effect on iNKT cell expansion.

The antigen-binding site of mouse and human CD1d (hCD1d) molecules is composed of two channels: A′ and F′ which connect directly to the surface. The F' channel accommodates the phytosphingosine chain, and the A' channel contains the *N*-acyl chain of α-GalCer **(44)** [69, 178, 259, 260, 281]. Although the A′ channel can accommodate an alkyl chain up to 26

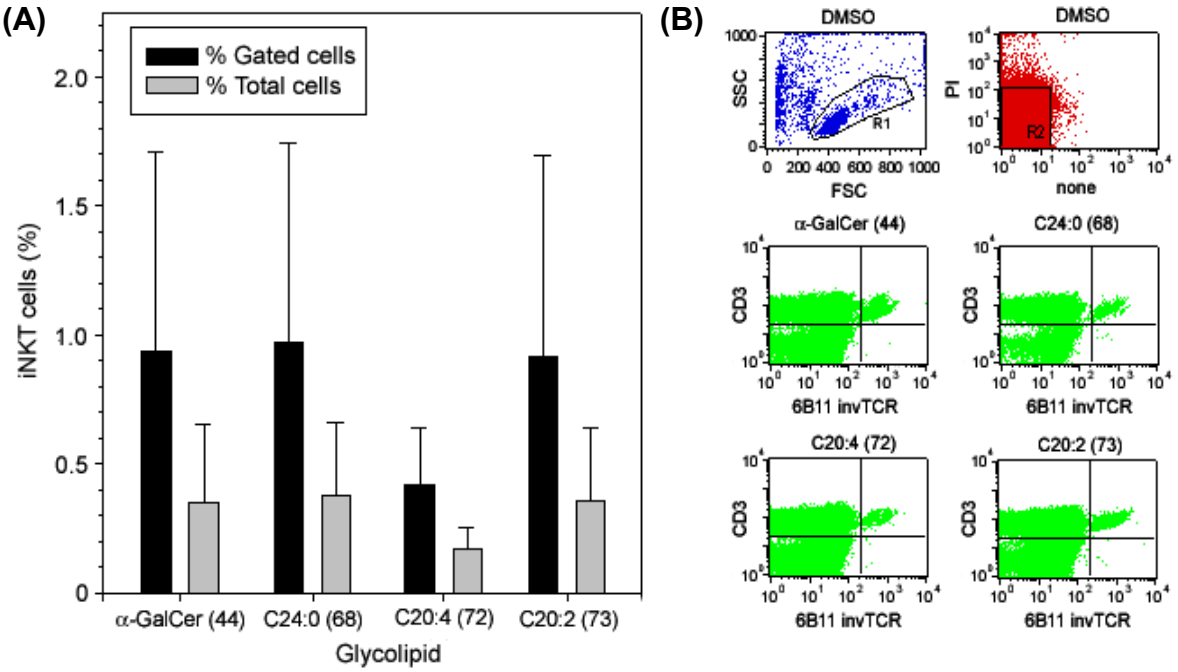

Figure 4.14: **iNKT cell expansion in vitro is modulated by the *N*-acyl chain of α-GalCer. (A)** Mean percentage of gated and total iNKT cell (HDD.11 cells) frequency from ex vivo treatment with 100nM α-GalCer analogues measured by FACS analysis. **(B)** FACS analysis plots showing the gating of iNKT cells and the differences in cell expansion of HDD.11 cells after stimulation with α-GalCer **(44)**, C24:0 **(68)**, C20:4 **(72)** and C20:2 **(73)** compared with a control of DMSO after ex vivo 100nM GSL stimulation. Experiments carried out by G. Bricard and myself at Albert Einstein College of Medicine, New York, USA using analogues synthesized during this project

carbon atoms long, the F′ channel has a decreased capacity with a maximum chain length of 18 carbons long. hCD1d molecules in which the A′ and F′ channels are not filled (they are in the nonlipid-bound state) have an altered conformation compared to hCD1d proteins bound to a glycolipid antigen such as α-GalCer **(44)** [71]. Whereas the entrance of the cavity is wider in the empty conformation, the volumes of the A′ and F′ channels are reduced, due to the conformational shifts in the side chains of several tryptophan residues [218]. The recently solved crystal structures of CD1d–α-GalCer–specific TCR and docking models are consistent with the TCR binding footprint encompassing the polar head of the lipid ligand and portions of the CD1d α1 and α2 helices but do not support direct interactions between the TCR and the lipid alkyl chains [92, 100].

In order to further examine the role of each alkyl chain in α-GalCer **(44)** and related compounds, McCarthy *et al.* [218] carried out kinetic experiments to assess the degree of control exhibited by both the phytosphingosine chain (Chapter 2) and the *N*-acyl chain of α-GalCer on the dissociation rate. A small library of lipids prepared during the course of this project and varying in the *N*-acyl chain, were analysed for their rate of dissociation from their complexed state with hCD1d, thus giving the affinity each analogue has for TCR binding [218].

In the same manner that the affinity of phytosphingosine analogues were tested, Fab 9B was used by McCarthy *et al.* [218] to measure dissociation of *N*-acyl chain analogues prepared during this project from soluble hCD1d over a period of time (Figure 4.15). These results show that decreasing the length of the *N*-acyl chain does have an affect on the rate of dissociation from hCD1d molecules; the rate of dissociation of C20:0 **(79)** is 2.15-fold faster than that of C20:2 **(73)** (half-life of 170 min and 367 min respectively at 25°C) and approximately 3.5 times slower than α-GalCer **(44)**. However, the rate of dissociation of an unsaturated analogue is raised compared to its corresponding fully saturated analogue [218]. The analogue incorporating an *N*-acyl chain with 11 carbons and one double bond (C11:1), although having a chain length more than half as long as α-GalCer **(44)**, has a greater half-life than C20:0 **(79)**, suggesting that a double-bond in the *N*-acyl chain may play a part in retaining the bonding association between the analogue and CD1d protein.

The dissociation constants (K_d) of α-GalCer **(44)** and three analogues (C20:2 **(73)**, C20:0 **(79)** and C11:1) that vary in the *N*-acyl chain length and saturation were also determined, measuring the tendency of α-GalCer **(44)** to dissociate from the CD1d protein to which it is bound. The data in Figure 4.16 corresponds with the affinity measurements of the four GSLs tested (Figure 4.15A) and shows that analogues with truncated *N*-acyl chains do affect the

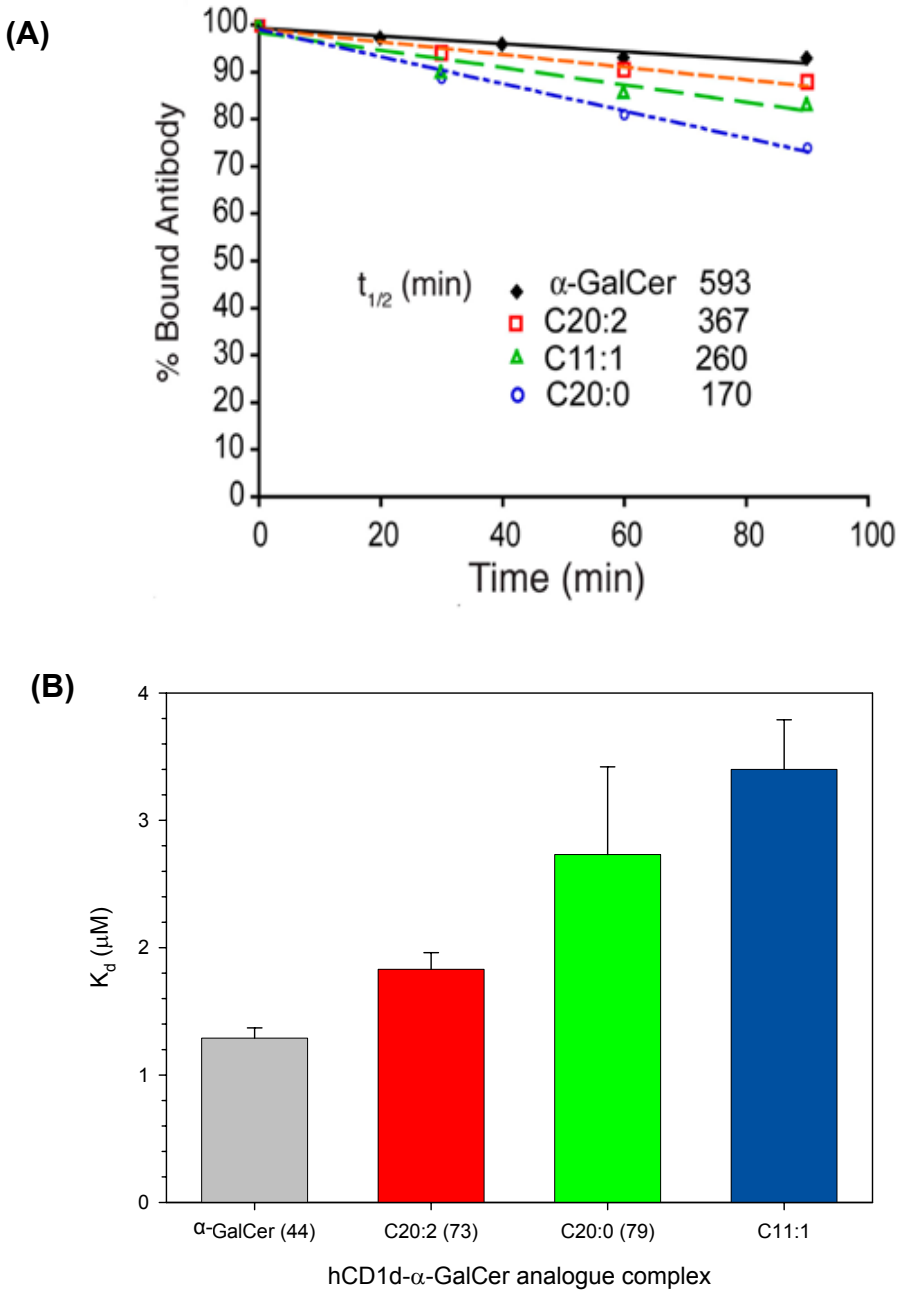

Figure 4.15: **Binding affinities of α-GalCer analogues to hCD1d. (A)** Dissociation of α-GalCer analogues from hCD1d.The antigen-hCD1d complexes were loaded onto a sensor surface at t=0. The amount of remaining hCD1d at given time points was measured using Fab 9B antibody and SPR. Dissociation values only shown for the first 100 mins, but with half-life values listed. Figure adapted from [218] **(B)** The mean dissociation constants from hCD1d of α-GalCer **(44)** and three analogues varying in the length and degree if unsaturation of the *N*-acyl chain: C20:2 **(73)**, C20:0 **(79)**, C11:1. Experiments carried out by McCarthy *et al.* at the Weatherall Institute of Molecular Medicine, University of Oxford, UK using in part, analogues synthesized during this project.

degree of dissociation from CD1d compared with α-GalCer **(44)**. The results also indicate that the effect of incorporating unsaturated *N*-acyl chains reverts the dissociation rate back to a value nearer to α-GalCer **(44)**. This is illustrated by K_d values of 2.73μM for C20:0 **(79)** and 1.81μM for C20:2 **(73)**, compared with 1.29μM for α-GalCer **(44)** (Figure 4.15B). Although, the *N*-acyl variants of α-GalCer do show some degree of difference in binding affinities compared with α-GalCer **(44)**, the phytosphingosine analogues OCH15 **(45)**, OCH12 **(46)**, and OCH9 **(47)**, exhibit a greater level of control over the affinity of TCR binding to hCD1d-glycolipid complexes and subsequent iNKT cell activation. The affinity of complexed hCD1d-α-GalCer with iNKT TCR was also investigated (Figure 4.16) and showed that C20:2 **(73)** has an affinity for the TCR similar to that of α-GalCer **(44)**, whereas C11:1 and C20:0 **(79)** exhibited decreased affinities for the iNKT cell receptor.

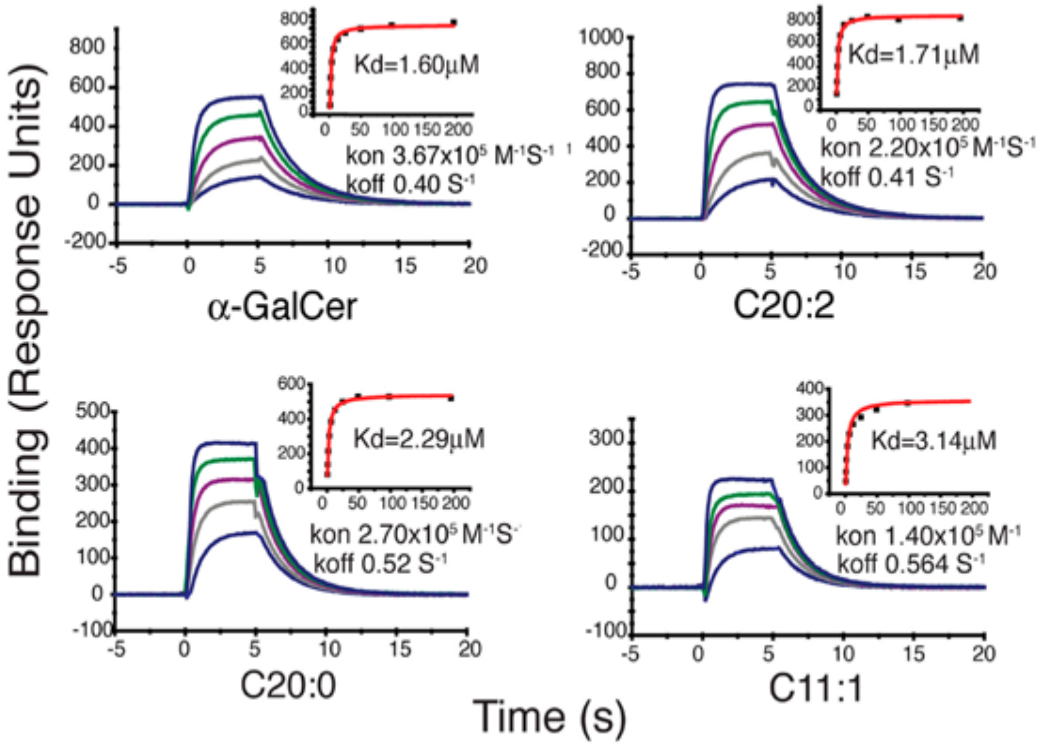

Figure 4.16: **Affinity and kinetics of iNKT TCR binding to hCD1d-α-GalCer complexes.** The binding responses of 5 concentrations (increasing from 0.4 – 194μM) of hCD1d-α-GalCer complex injected with iNKT TCR for 5s are shown, with the equilibrium binding response (K_d) shown in the insets. Experiments carried out by McCarthy *et al.* at the Weatherall Institute of Molecular Medicine, University of Oxford, UK using in part, analogues synthesized during this project. Figure adapted from [218].

Surprisingly, the difference between C11:1 and C20:0 was not as large as expected, despite the truncation of the *N*-acyl chain. This could be attributed to the double bond at C10 of the acyl chain and implies that optimal iNKT TCR binding require the hCD1d A' channel to be occupied by an α-GalCer analogue with an *N*-acyl chain, incorporating some degree of unsaturation around C10 (C20:2) **(73)** has two double bonds at C11 and C14). To test this hypothesis further, the experiment would need to be repeated using a larger library of analogues incorporating one or two double bonds at various carbon atoms along the *N*-acyl chain, but the results thus far (Figure 4.15 and Figure 4.16) suggest that unsaturation of bonds in the *N*-acyl chain of α-GalCer favours the formation of more stable hCD1d-glycolipid complexes.

To demonstrate that the binding affinities of the hCD1d-α-GalCer complexes with the TCR were not a result of hCD1d loading with the α-GalCer analogues described, the rate constants k_{on} and k_{off} were determined by direct measurements of the TCR with hCD1d-α-GalCer analogues complexed with α-GalCer **(44)**, C20:2 **(73)**, C20:0 **(79)**, and C11:1 (Table 4.2). From the smaller K_d values in Figure 4.16 and the smaller k_{off} values in

hCD1d-α-GalCer complex	**k_{off} (s^{-1})**	**k_{on} ($M^{-1}s^{-1}$)**
α-GalCer **(44)**	$0.39 \pm 0.01^{\dagger}$	$3.31 \times 10^5 \pm 2.5 \times 10^{4\dagger}$
C20:2 **(73)**	0.46 ± 0.06	$2.46 \times 10^5 \pm 2.3 \times 10^4$
C20:0 **(79)**	0.58 ± 0.07	$2.38 \times 10^4 \pm 4.6 \times 10^4$
C11:1	0.59 ± 0.04	$1.65 \times 10^4 \pm 3.5 \times 10^4$

Table 4.2: **Affinity and kinetic measurements of hCD1d-α-GalCer complexes with iNKT TCR.** Unless stated, all values are the mean of two experiments. †Mean of three or more experiments. Experiments carried out by McCarthy *et al.* at the Weatherall Institute of Molecular Medicine, University of Oxford, UK using in part, analogues synthesized during this project. Table adapted from [218].

Table 4.2 one can surmise that α-GalCer analogues with at least one double bond have a greater affinity for the iNKT TCR when complexed with the CD1d protein.

The binding of hCD1d molecules with analogues of α-GalCer that have shorter lipid chains may result in the partial collapse of unfilled portion of the A' and F' channels, which in turn could result in surface-exposed structural changes. Thus, analogues containing identical polar heads and varied acyl chains were synthesised in this project to study the affinity of soluble iNKT TCR to hCD1d molecules loaded with the synthetic analogues. In a similar manner, the partial filling of F' channel of hCD1d was investigated by shortening the *N*-acyl chain in an α-GalCer analogue using modelling exercises. This predicted changes in the position of the α1 helix from residues Phe58 through to Phe70, but in contrast to the differences resulting from using a truncated phytosphingosine chain, the changes using shortened *N*-acyl chains are in a region that is peripheral to the iNKT cell TCR docking area and have no influence on the orientation of the polar head group of the analogue (Figure 4.17) [218]. This further suggests that, although a structural variation in the *N*-acyl chain affects the binding of the analogue to the CD1d molecule, it does not play a part in modulating TCR recognition.

By demonstrating that the presence of two *cis* double bonds in the *N*-acyl chain at positions C11 and C14 (C20:2 **(73)**) [178], reduces the rate of dissociation from hCD1d molecules as compared with its fully saturated analogue, one can surmise that the *N*-acyl chain plays a pivotal role in the stability of the hCD1d-glycolipid stability. Unlike C20:0 **(79)**, C20:2 **(73)** has been shown to successfully load into mCD1d molecules that lack an endosomal targeting motif, further suggesting that double bonds at C11 and C14 facilitate the lipid binding to CD1d molecules [266].

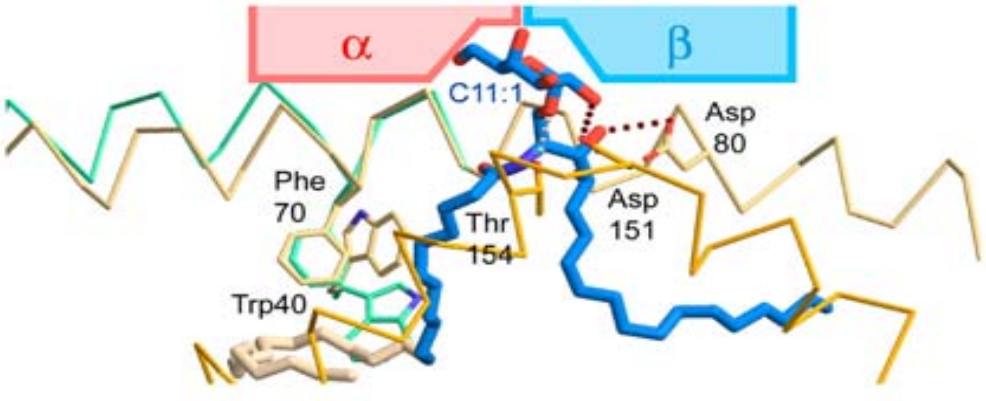

Figure 4.17: **Modeling of the effects of variation in lipid chain length on the hCD1d structure.** A Cα trace and selected side chains are shown for the hCD1d crystal structure with bound α-GalCer (44) (yellow), and relevant regions of the structure of hCD1d in the absence of bound ligand are shown in green. Hydrogen bonds are depicted as dotted lines. The putative position of bound TCR is indicated schematically. The portion of α-GalCer that corresponds to a ligand with a shortened acyl chain (C11:1) is highlighted in blue, and the side chains that are predicted to shift positions are highlighted, based on a comparison of the empty and fully occupied (i.e., α-GalCer bound) hCD1d A′ channel. Figure adapted from [218].

The *N*-acyl chain of α-GalCer **(44)** and associated analogues is anchored within the A' channel of the CD1d protein. By circumnavigating a central pole made up of Phe70, Trp40 and Cys12 residues at the junctions of the A' and F' channels, the acyl chain enters the A' channel [71] and secures the position of the analogue within the CD1d molecule. The observed differences between the dissociation rates of C20:0 **(79)** and C20:2 **(73)** (Figure 4.15 and Figure 4.16) suggests that the preformed kink in the *N*-acyl chain of the latter analogue (caused by the presence of the unsaturated bonds) may stabilise binding of the glycolipid by favouring the tightly curved conformation required for binding in the A' channel [218].

A less stable binding interaction between an α-GalCer analogue, CD1d and the TCR has an effect on the immunological response of the iNKT cell. The cytokine profile of C20:2 **(73)** is biased towards a T_H2 response when coupled with hCD1d (Figure 4.12). This could be attributed to the binding differences within the hCD1d channel (as compared with α-GalCer **(44)**), and thus could open up the possibility that more analogues incorporating such

unsaturated functionality could prove to be a vital characteristic of a glycolipid analogue that could prevent and treat autoimmune diseases such as T1D. Although both the *N*-acyl chain and phytosphingosine chain control the stability of lipids bound to hCD1d molecules, it is the latter chain that seems to control the affinity of TCR binding to hCD1d-glycolipid complexes.

Chapter 5

Materials and methods

5. Materials and methods

Chemical reagents were obtained from Aldrich, Lancaster, Fischer and Pierce. All solvent extractions from reaction work-up were dried over anhydrous sodium sulfate, prior to evaporation *in situ*. Nuclear Magnetic Resonance (NMR) spectra chemical shift values (δ) are given in ppm and were obtained using deuterated chloroform ($CDCl_3$) and deuterated methanol (D_3COD). ^1H NMR spectra were measured on a Bruker AC300 spectrometer operating at 300MHz, Bruker AV400 operating at 400MHz and a Bruker DRX500 operating at 500MHz. The references used were the residual solvent signals of: $CDCl_3$ at 7.25ppm and D_3COD at 3.30ppm. ^{13}C NMR spectra were run on a Bruker AV300 spectrometer, operating at 75MHz. The references were the residual solvent signals of $CDCl_3$ at 77.0ppm and D_3COD at 49.0ppm. The spectra were run ^1H decoupled, using the PENDANT sequence, which edits CH and CH_3 signals from the quaternary and CH_2 signals. Mass spectrometric data was analysed using an electrospray (Micromass LCT time-of-flight mass spectrometer) and an electron impact (VG ZabSpec magnetic sector mass spectrometer). Anhydrous acetone was prepared by mixing with dry $CaSO_4$ for ~2h, followed by filtration and distillation. Anhydrous THF was prepared by distillation with $LiAlH_4$. Anhydrous DCM was prepared by distillation with P_2O_5. All CC was performed on Silica Gel 60 (Fluka 60741, particle size 0.063-0.2mm). All TLC was performed on TLC aluminium sheets silica gel 60 F_{254} (Merck Z293024). Molecular sieves used were 4Å powder < 5 micron, and molecular sieve 4 Å beads 4-8 Mesh (both purchased from Aldrich).

5.1. Chemical synthesis

5.1.1. General chemical procedures

Specific amounts are given in each individual synthesis

5.1.1.1. The formation of Wittig salts and subsequent olefination

Triphenylphosphine (3M eq) and 1-bromoalkane were stirred together at 140°C for 4.5h. The flask was gradually cooled and the compound dissolved in THF. The solution was cooled (-10°C) and the nBuLi (2.5M solution in hexanes; 2.8M eq) was added drop wise. The reaction mixture was stirred for 30mins, before a solution of (3aS, 4R, 6R, 6aS)-2,2-dimethyl-6-trityloxymethyl-tetrahydro-furo[3, 4-*d*]-1,3-dioxol-4-ol **(2)** (1M eq) in THF was added and stirred for 18h whilst the temperature was gradually raised to RT. The reaction was quenched with MeOH, followed by 80% MeOH in H_2O, and the reaction mixture was extracted with heptane (4 x 20ml). The organic portions were combined, dried ($NaSO_4$), concentrated and dried *in vacuo*. Purification by CC (heptane: ethyl acetate [EtOAc], 20:1) [198].

5.1.1.2. Addition of a mesyl group

The 1-trityl-3,4-ispropylidene protected base (1M eq) prepared using the procedure outlined in section 5.1.1.1 was dissolved in dry dichloromethane and pyridine (3:1). Methanesulfonylchloride (1.6M eq) was added and the solution was stirred overnight at 31°C under argon. TLC was used to monitor the reaction 8:1 (petrol:EtOAc). Ethanol was added and the mixture stirred for 1h at RT. The solution was concentrated and a mixed solvent of heptane:MeOH:water (10:7:3) was added. The aqueous portion was thrice re-

extracted with heptane. The organic layers combined, dried ($NaSO_4$), concentrated and dried *in vacuo* [282].

5.1.1.3. Deprotection of the mesylated base

The mesylated base was dissolved in dry DCM:MeOH (2:1). Concentrated HCl (~1/8 volume of DCM:MeOH) was added drop wise and the mixture stirred at RT for 1.5h. $NaHCO_3$ powder was added until the solution was neutral, followed by filtration and washing with EtOAc. The organic extract was concentrated, and washed with saturated brine and EtOAc. The aqueous layer was thrice re-extracted with EtOAc. The organic layers were combined, dried ($NaSO_4$), concentrated, dried *in vacuo*, and purified by CC (silica gel 60), (15% EtOAc in petrol as the starting eluting solvent system) [282].

5.1.1.4. General procedure for catalytic reduction

The deprotected mesylated base was dissolved in minimal THF. 5% Pd-$Ba(SO_4)_2$ (10% of the weight of mesylated base) was added to the solution, and degassed three times. The solution was stirred for 24h at RT under a H_2 atmosphere. The mixture was filtered through Celite and washed with chloroform ($CHCl_3$):MeOH (1:1). The filtrate was concentrated and dried *in vacuo* [282].

5.1.1.5. Introduction of an azide group

The reduced mesylated base (1M eq) was dissolved in DMF (~10ml per gram of reduced mesylated base). Sodium azide (2M eq) was added and the solution stirred at 95°C for 6h.

The solution was concentrated and EtOAc was added to the residue and the mixture extracted with H_2O. The organic layers were combined, washed with saturated brine, dried (Na_2SO_4), concentrated and dried *in vacuo*. The resulting compound was purified by CC (silica gel 60) 9:1 (heptane:EtOAc) [282].

5.1.1.6. Addition of a TBDPS protecting group

The azido-triol base (8 M eq) was dissolved in DCM:pyridine (6.25:1). 4-(4-dimethylaminopyridine) (1M eq). *Tert*-butyldiphenylsilylchloride (14.4 M eq) was added at 0˚C and stirred for 36h at RT. Hydrochloric acid (1M) was added at 0˚C and the reaction mixture diluted with $CHCl_3$. The organic portion was extracted, dried (Na_2SO_4) and concentrated. The residue was purified by column chromatography (petrol:EtOAc [20:1]) [283].

5.1.1.7. Addition of benzoate groups

To a solution of TBDPS-protected azido-diol (1M eq) in pyridine was added benzoyl chloride (6M eq) and DMAP (catalytic amount). The solution was stirred at RT for 18h. Cooled water was added to the reaction mixture and extracted with $CHCl_3$. The organic layer was washed with water, dried (Na_2SO_4) and concentrated, before being purified by CC (2% EtOAc in petrol) [284].

5.1.1.8. Removal of the TBDPS group

Acetic acid (1.1M eq) and a 1M solution of tetrabutylammonium fluoride (TBAF) (1.1M eq) were added to a solution of TBDPS benzoyl protected azido-diol (1M eq) in dry THF. The mixture was stirred at RT and monitored by TLC (petrol:EtOAc, 9:1). After 2h the solution was passed through a 200ml silica gel 60 column and washed with THF. The solution was then concentrated and purified by CC (starting eluting solvent 100% petrol, gradually increasing proportion of EtOAc) [195].

5.1.1.9. Preparation of pertrimethylsilyl-D-pyranoses

A solution of free pyranose in dry DMF was prepared. Triethylamine (1.1M eq for each free hydroxyl group) was added and the solution cooled to 0°C. Redistilled chlorotrimethylsilane (1.1M eq for each free hydroxyl group) was added and stirred at RT for 6h. Pentane and crushed ice were added and the aqueous layer thrice extracted with pentane. The combined organic portions were washed twice with water, saturated NaCl solution, dried (Na_2SO_4) and concentrated [285].

5.1.1.10. Coupling of pertrimethylsilylated sugars with benzoate-protected azido-phytosphingosine analogues

The pertrimethylsilylated pyranose (3M eq) was dissolved in dry DCM. Iodotrimethylsilane (3M eq) was added at RT and the solution stirred under argon for 20min. After concentration, dry benzene was added and azeotroped twice with benzene. The yellow-orange residue was dissolved in benzene and kept under argon. Meanwhile, activated MS 4Å, tetrabutylammonium iodide (6M eq), the benzoate protected azido phytosphingosine

analogue (1M eq) and diisopropylethylamine (4.5M eq) were added to a 2-necked flask fitted with a condenser. Benzene was added and the solution stirred at 70°C for 20min. The glycosyl iodide solution was cannulated into the two-necked flask and stirred for a further hour at 70°C. The reaction was monitored by TLC (petrol: EtOAc) (3:1). EtOAc was added and the solution cooled to 0°C, before being filtered through Celite. The filtrate was twice washed with saturated $Na_2S_2O_3$ solution, and then saturated NaCl solution, before being dried (Na_2SO_4) and concentrated. The residue was dissolved in MeOH. Dowex 50 WX8-200 ion exchange resin was added and the mixture refluxed for 45min. The resin was removed from the residue by filtration, and the residue washed with MeOH and concentrated, before being purified by CC (80% EtOAc in petrol) [217].

5.1.1.11. Removal of benzoate protecting groups

The 2-(2-azido-3,4-*bis*-benzoyloxy-alkyloxy)-sugar (1M eq) was dissolved in minimal dry THF and MeOH. 0.5M Sodium methoxide solution in MeOH (1.5M eq) was added and stirred at room temperature and monitored by TLC (9:1 petrol: EtOAc). Upon completion, Dowex© 50WX8-200 resin (washed with 1M HCl, H_2O and MeOH) was added until the solution reached pH7. The resin was then removed by filtration and the filtrate concentrated before being purified by FCC ($CHCl_3$: MeOH) [286].

5.1.1.12. Preparation of *N*-hydroxy succinimide esters of various carboxylic acids

The carboxylic acid was dissolved in dry DCM. N-(3-dimethylaminopropyl)-N'-ethyl carbodiimide hydrochloride (1.1M eq), *N*-hydroxysuccinimide (1.2M eq), and dimethylamino pyridine DMAP (10% of acid weight) were added and the solution stirred at 40°C and monitored by TLC (pet ether 40-60: Et_2O) (6:4). On completion, the reaction mixture was

poured into water and extracted with Et_2O. The organic layer washed with saturated NaCl solution, dried (Na_2SO_4), filtered and concentrated [287].

5.1.1.13. Azide reduction and subsequent *N*-acylation

The azido compound (1M eq) was dissolved in pyridine:Et_3N:H_2O (18:5:8). Hydrogen sulfide was bubbled through the mixing solution for ~24h. The solution was concentrated. The crude amine was dissolved in pyridine:H_2O (9:1). The *N*-hydroxysuccinimide ester of a fatty acid (1.4M eq) was added and the solution stirred overnight at 50°C. EtOAc was added and the solution washed with H_2O, then saturated NaCl solution, before being dried ($MgSO_4$), concentrated and purified by FCC ($CHCl_3$: MeOH, 2:1) and preparative TLC [288, 289].

5.2. Protection of D-lyxose

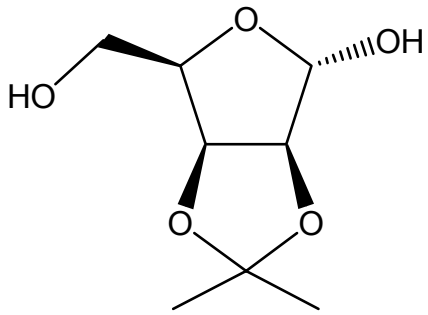

$C_8H_{14}O_5$

Mol. Wt.: 190.1938 g mol^{-1}

(3aS, 4R, 6R, 6aS)-6-hydroxymethyl-2,2-dimethyl-tetrahydro-furo [3, 4-*d*]-1,3-dioxol-4-ol **(1)**

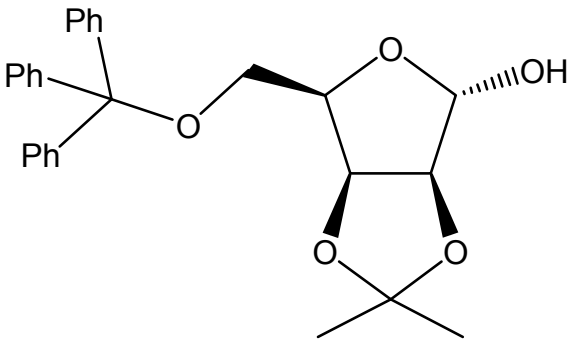

$C_{27}H_{28}O_5$

Mol. Wt.: 432.5082 g mol^{-1}

(3aS, 4R, 6R, 6aS)-2,2-dimethyl-6-trityloxymethyl-tetrahydro-furo [3, 4-*d*]-1,3-dioxol-4-ol **(2)**

D-Lyxose (20g, 0.133mol) was suspended in acetone (300ml). Conc. H_2SO_4 (a few drops) was added and the mixture stirred at RT for 18h. Molecular Sieve 4 Å (Aldrich) (10g) was

added and the mixture filtered. The residue was washed with acetone. The washes were combined, concentrated and dried *in vacuo*, producing (3aS, 4R, 6R, 6aS)-6-hydroxymethyl-2,2-dimethyl-tetrahydro-furo [3, 4-*d*]-1,3-dioxol-4-ol **(1)**, which was recrystallised using anhydrous toluene. The resulting crystals (25.29g, 0.133mol) were dissolved in anhydrous pyridine (160ml). Trityl chloride (25.95g, 0.093mol) was added and the solution stirred for 18h under argon at RT. The solution was concentrated *in vacuo* and the resulting solid (3aS, 4R, 6R, 6aS)-2,2-dimethyl-6-trityloxymethyl-tetrahydro-furo[3, 4-*d*]-1,3-dioxol-4-ol **(2)** purified by CC (petrol:EtOAc [20:1]), affording a colourless syrup. Yield 42.85g, 74.37%.

(3aS, 4R, 6R, 6aS)-6-hydroxymethyl-2,2-dimethyl-tetrahydro-furo [3, 4-*d*]-1,3-dioxol-4-ol (1) [282]

δ ^{1}H ($CDCl_3$): 5.43 (1H, s), 4.82-4.79 (1H, q, J=3.80, 2.10, 3.79 Hz), 4.63-4.61 (1H, d, J=5.92 Hz), 4.30-4.25 (1H, dd, J=4.95, 4.22, 5.22 Hz), 3.93-3.90 (2H, dd, J=2.73, 1.72 Hz), 1.45 (3H, s), 1.31 (3H, s) δ ^{13}C ($CDCl_3$): 113.85 (QC), 102.01 (C-1), 86.76 (C-4), 81.43, 80.97 (C-2,3) 62.27 (C-5), 27.00, 25.61 (Acetonide methyl C).

(3aS, 4R, 6R, 6aS)-2,2-dimethyl-6-trityloxymethyl-tetrahydro-furo [3, 4-*d*]-1,3-dioxol-4-ol (2) [282]

δ ^{1}H ($CDCl_3$): 7.19-7.5 (15H, m), 5.37 (1H, s), 4.77 (1H, dd, J=3.71 Hz), 4.58 (1H, d, J=5.90 Hz), 4.29-4.37 (1H, m), 3.35-3.47 (2H, m), 1.3 (3H, s), 1.27 (3H, s). δ ^{13}C ($CDCl_3$): 144.00 (QC), 128.86, 127.77, 126.97 (Aromatic C), 101.25 (C-1), 85.46 (C-4), 80.15, 79.73 (C-2,3) 61.88 (C-5), 26.56, 25.01 (Acetonide methyl C). m/z (ES) 455.1 (M^+ + $[Na]^+$ 100%). α_D-16.10° IR:3200-3400cm^{-1} (br OH stretch), 3100-3160 (Ar stretch)

5.3. The Wittig reaction

5.3.1. (R)-1-[(4S,5R)-2,2-Dimethyl-5-(undec-1-enyl)-1,3-dioxolan-4-yl]-2-trityloxy-ethanol (3)

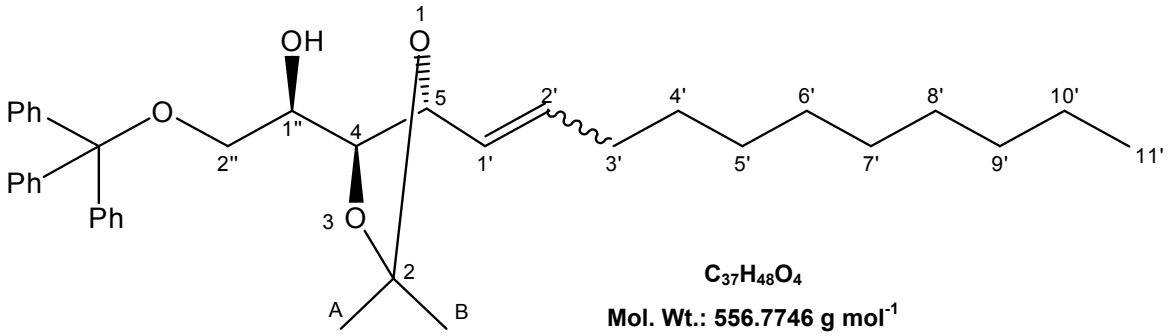

$C_{37}H_{48}O_4$

Mol. Wt.: 556.7746 g mol^{-1}

Prepared by the general procedure for Wittig salt and subsequent olefination **(5.1.1.1)**, using triphenylphosphine (1.822g, 6.945mmol), 1-bromodecane (1.536g, 6.945mmol), nBuLi (2.58ml, 6.482mmol), and (3aS, 4R, 6R, 6aS)-2,2-dimethyl-6-trityloxymethyl-tetrahydro-furo[3, 4-*d*]-1,3-dioxol-4-ol **(2)** (1g, 2.315mmol), affording a colourless syrup. Yield 712mg, 55.24%. δ ^{1}H ($CDCl_3$): 7.19-7.48 (Ar-H, 15H, m), 5.47-5.58 (H-1', H-2', 2H, m), 4.91 (H-5 *trans*, 0.7H, m), 4.40-4.46 (H-5 *cis*, 0.3H, m), 4.25 (H-4 *cis*, 0.3H, dd, J=4.63, 4.65 Hz), 4.21 (H-4 *trans*, 0.7H, dd, J=4.39, 4.40 Hz), 3.72-3.79 (H-1'' *trans, 0*.7H, m), 3.68-3.70 (H-1'' *cis*, 0.3H, m), 3.22 (H-2''$_a$ *cis*, 0.3H, dd, J=5.07, 5.14 Hz), 3.15 (H-2''$_a$ *trans*, 0.7H, dd, J=5.27, 9.47Hz), 3.08-3.13 (H-2''$_b$ *cis* [0.7H], H-2''$_b$ *trans* [0.3H], m), 1.71-2.03 (H-3'$_{ab}$, 2H, m), 1.56 (H-A_{abc} *trans* 3H, s), 1.47 (H-B_{abc} *trans*, 3H, s), 1.39, 1.38 (H-A_{abc} H-B_{abc} *cis*, 3H, each s), 1.11-1.35 (H-4'$_{ab}$ – H-10'$_{ab}$, 14H, m), 0.87 (H-11'$_{abc}$, 3H, t, J=6.65 Hz). δ ^{13}C ($CDCl_3$): 145.73 (C-2), 137.17 (C-1'), 130.56, 129.65, 128.87 (Aromatic C), 126.84 (C-2'), 79.54 (C-1''), 74.88 (C-4), 70.8 (C-5), 66.51 (C-2''), 34.02, 31.34, 31.17, 30.01 (C-3' – C-10') 29.25, 27.01 (C-A, -B), 16.04(C-11'). m/z (ES): 580.4 (M^+ + $[Na]^+$ + $[H]^+$ 30%), 579.1 (M^+ + $[Na]^+$ 100%).

HRMS: Calculated for $C_{37}H_{48}O_4$ [M + Na]+, 579.3450, found 579.3454. $\alpha_{D:}$-47.6°. IR: 3200-3400cm^{-1} (br OH), 3100-3160cm^{-1} (Ar), 1650-1680 cm^{-1} (alkene).

5.3.2. (R)-1-[(4S,5R)-2,2-Dimethyl-5-(oct-1-enyl)-1,3-dioxolan-4-yl]-2-trityloxy-ethanol (4)

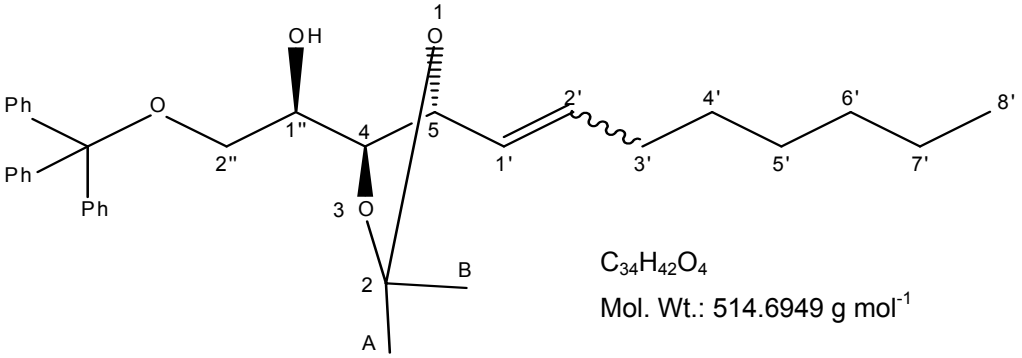

$C_{34}H_{42}O_4$
Mol. Wt.: 514.6949 g mol^{-1}

n-Hepyltriphenylphosphonium bromide (9.269g, 21mmol) was dissolved in dry THF (100ml). nBuLi (2.5M solution in hexanes) (7.7ml, 19.2mmol) was added to the solution and stirred at -50°C for 40mins. A solution of (3aS, 4R, 6R, 6aS)-2,2-dimethyl-6-trityloxymethyl-tetrahydro-furo[3, 4-*d*]-1,3-dioxol-4-ol **(2)** (3.32g, 7.68mmol) in dry THF (15ml) was added to the reaction mixture which was allowed to warm to RT overnight. The general procedure for olefination **(5.1.1.1)** was then followed. This afforded a colourless syrup. Yield 2.594g, 66%. δ ^{1}H ($CDCl_3$): 7.19-7.48 (Ar-H, 15H, m), 5.47-5.58 (H-1', H-2', 2H, m), 4.91 (H-5 *trans*, 0.7H, m), 4.43 (H-5 *cis*, 0.3H, m), 4.25 (H-4 *cis*, 0.3H, m), 4.21 (H-4 *trans*, 0.7H, m), 3.68-3.81 (H-1'' *trans*, 0.7H, m), 3.51-3.56 (H-1'' *cis*, 0.3H, m), 3.22 (H-2''$_a$ *cis*, 0.3H, dd , J=4.92, 9.52), 3.18 (H-2''$_a$ *trans*, 0.7H, m), 3.07-3.17 (H-2''$_b$ *cis*, H-2''$_b$ *trans*, 1H, m), 1.91-2.09 (H-3'$_{ab}$, 2H, m), 1.54 (H-A$_{abc}$ *trans* 3H, s), 1.49 (H-B$_{abc}$ *trans*, 3H, s), 1.39, 1.38 (H-A$_{abc}$ H-B$_{abc}$ *cis*, 3H, each s), 1.19-1.39 (H-4'$_{ab}$ – H-7'$_{ab}$, 8H, m), 0.88 (H-8'$_{abc}$ 3H, t, J= 5.68). δ ^{13}C ($CDCl_3$): 145.9 (C-2), 137.3 (C-1'), 129.1, 129.9, 130.8 (Aromatic C), 127.1 (C-2'), 79.5 (C-1''), 75.1 (C-4), 71.3 (C-5), 67.1 (C-2''), 34.2, 31.3, 31.1, 29.7, 25.0 (C-3' – C7') 29.8, 27.1 (C-A, -B), 17.1

(C-8'). m/z (ES) 538.5 (M^+ + $[Na]^+$ + $[H]^+$ 10%), 537.5 (M^+ + $[Na]^+$ 100%), 243.2 (M^+ - $CH_3(CH_2)_5$-CH=CH-CH($OC(CH_3)_2O$)CH-CH(OH)-CH_2-O 80%). α_D: -50.5°. IR: 3200-3400cm^{-1} (br OH), 3100-3160cm^{-1} (Ar), 1600-1680 cm^{-1} (alkene).

5.3.3. (R)-1-[(4S,5R)-2,2-Dimethyl-5-(pent-1-enyl)-1,3-dioxolan-4-yl]-2-trityloxy-ethanol (5)

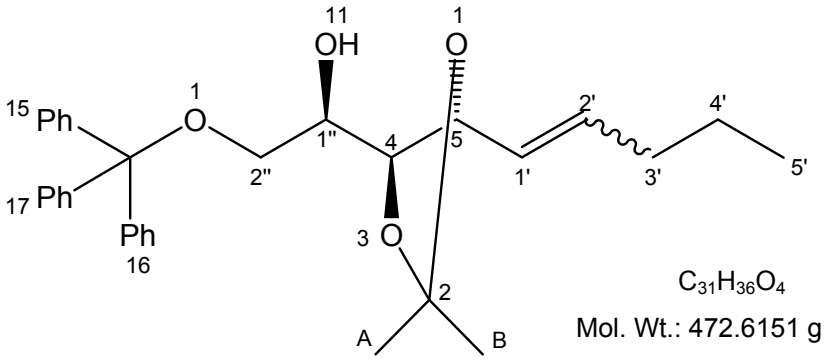

$C_{31}H_{36}O_4$

Mol. Wt.: 472.6151 g mol^{-1}

Triphenylphosphine (18.36g, 70mmol) and 1-iodobutane (10.73g, 58.34mmol) were stirred together in refluxing toluene for 8h. Then as general procedure for Wittig salt and subsequent olefination **(5.1.1.1)**, using nBuLi (18.05ml, 45.11mmol), and (3aS, 4R, 6R, 6aS)-2,2-dimethyl-6-trityloxymethyl-tetrahydro-furo[3, 4-*d*]-1,3-dioxol-4-ol **(2)** (6.97g, 16.11mmol) affording a white solid [290]. Yield 6.455g, 84.78%. δ ^{1}H ($CDCl_3$): 7.19-7.49 (Ar-H, 15H, m), 5.57-5.61 (H-1', H-2' *trans*, 1.4H, m), 5.53-5.56 (H-1', H-2' *cis*, 0.6H, m), 4.93 (H-5, *trans*, 0.7H, m), 4.45 (H-5, *cis*, 0.3H, t, J=7.4), 4.28 (H-4, *cis*, 0.3H, m), 4.22 (H-4, *trans*, 0.7H, m), 3.77 (H-1'', *trans*, 0.7H, m), 3.69 (H-1'', *cis*, 0.3H, m), 3.25 (H-2_a'', *cis*, 0.3H, dd, J=5.13, 9.48Hz), 3.18 (H-2_a'', *trans*, 0.7H, m), 3.07-3.15 (H-2_b'', 1H, m), 1.92-2.06 (H-3_{ab}', *trans*, 1.4H, m), 1.75-1.86 (H-3_{ab}', *cis*, 0.6H, m), 1.58 (H-A_{abc} *trans* 3H, s), 1.52 (H-B_{abc} *trans*, 3H, s), 1.39, 1.37 (H-A_{abc} H-B_{abc} *cis*, 3H, each s), 1.22-1.32 (H-4'$_{ab}$, 2H, m), 0.87 (H-5'$_{abc}$, 3H, t, J=7.3Hz). δ ^{13}C ($CDCl_3$): 144.1 (C-2), 135.8 (C-1'), 127.3, 128.0, 128.9

(Aromatic C), 125.5 (C-2'), 79.5 (C-1''), 73.3 (C-4), 69.4 (C-5), 65.2 (C-2''), 30.6, 30.1 (C-3', -4') 28.5, 25.7 (C-A, -B), 14.9 (C-5'). **m/z** (ES): 496.3 (M^+ +$[Na]^+$ + $[H]^+$ 10%), 495.3 (M^+ + $[Na]^+$ 100%). HRMS: Calculated for $C_{31}H_{36}O_4$ [M + Na]+ 495.2511, found 495.2511. $\alpha_{D:}$ -7.0° m.p. 101-107°C IR: 3200-3400cm^{-1} (br OH), 3100-3160cm^{-1} (Ar), 1650-1680 cm^{-1} (alkene).

5.4. Addition of a mesylate group

5.4.1. Methanesulfonic acid (R)-1-[(4R,5R)-2,2-dimethyl-5-(undec-1-enyl)-1,3-dioxolan-4-yl]-2-trityloxy-ethyl ester (7)

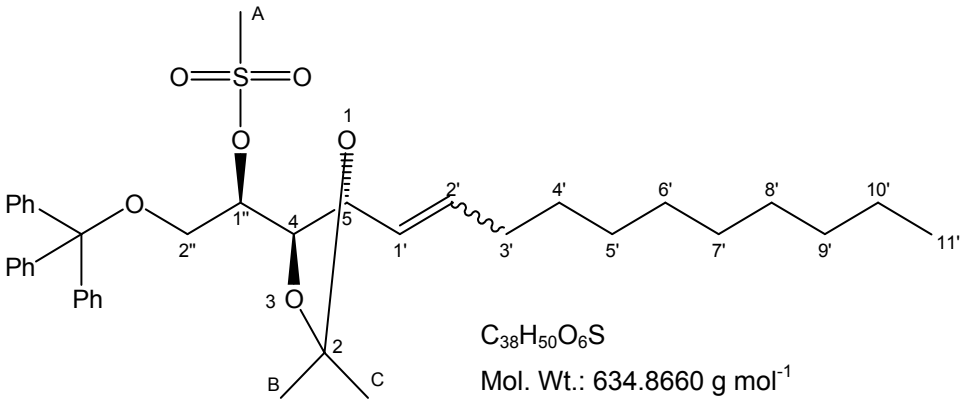

$C_{38}H_{50}O_6S$

Mol. Wt.: 634.8660 g mol^{-1}

Prepared by the general procedure for mesylation **(5.1.1.2)** using (R)-1-[(4S,5R)-2,2-dimethyl-5-(undec-1-enyl)-1,3-dioxolan-4-yl]-2-trityloxy-ethanol **(3)** (10.77g, 19.34mmol), dichloromethane (90ml), pyridine (30ml), methanesulfonylchloride (2.5ml, 32.19mmol), ethanol (3ml), heptane:MeOH:water (10:7:3) (100ml), affording an opaque oil. Yield 12.19g, 99.3%. δ ^1H ($CDCl_3$): 7.19-7.48 (Ar-H, 15H, m), 5.40-5.48 (H-2' *trans*, 0.7H, m), 5.28-5.37 (H-1' *trans*, 0.7H, m), 5.20-5.25 (H-2' *cis*, 0.3H, m), 4.97-5.06 (H-1' *cis*, 0.3H, m), 4.79-4.85 (H-1'', 0.7H, m), 4.74 (C-5 *trans*, 0.7H, m), 4.62-4.66 (H-1'' *cis*, 0.3H, m), 4.61 (C-5 *cis*, 0.3H, m), 4.49 (C-4 *trans*, 0.7H, dd, J=5.63, 8.66Hz), 4.2 (C-4 *cis*, 0.3H, dd, J=4.22, 9.40Hz), 3.56

(H-2''$_a$, 1H, dd, J=1.58, 11.36Hz), 3.45 (H-2''$_b$, 1H, dd, J=2.91, 10.83Hz), 3.04-3.17 (H-A$_{abc}$, 3H, m), 1.59-1.82 (H-3', 2H, m), 1.48 (H-B$_{abc}$, *trans*, 3H, s), 1.47 (H-C$_{abc}$, *trans*, 3H, s), 1.38, 1.36 (H-A$_{abc}$ H-B$_{abc}$ *cis*, 3H, each s), 1.08-1.32 (H-4'$_{ab}$-H-10'$_{ab}$, 14H, m), 0.88 (H-11'$_{abc}$, 3H, t, J=6.45Hz). δ ^{13}C ($CDCl_3$): 144.27 (C-2), 137.26 (C-2'), 129.70, 128.93, 128.19 (Ar C), 124.55 (C-1'), 81.97 (C-1''), 77.10 (C-5), 73.19 (C-4), 64.12 (C-2''), 40.13 (C-A), 33.1, 32.4, 30.47, 30.25, 30.18 (C-3'-10') 26.77, 26.60 (C-B, C), 23.89 (C-11') **m/z** (ES): 673.2 (M^+ + $[K]^+$ 40%), 657.2 (M^+ + $[Na]^+$ 100%), 617.2 (M^+ + $[Na]^+$ - $CH=CHCH_2$ 7%), 561.2 (M^+ + $[Na]^+$ - OMs 35%), 503.2 (M^+ + $[Na]^+$ - $CH=CH(CH_2)_8CH_3$ 8%), 415.1 (M^+ + $[Na]^+$ - Tr 15%), 319.2 (M^+ - ($TrOCH_2$ + $CH_2CH_2CH_3$) 7%), 243.1 (M^+ - $OCH_2CH(OMs)CHOC(CH_3)_2OCHCH=CH(CH_2)_8CH_3$ 63%). α_D: -50.0°. IR: 3200-3400cm^{-1} (br OH), 3100-3160cm^{-1} (Ar), 1650-1680 cm^{-1} (alkene), 1000-1350cm^{-1} (S=O).

5.4.2. Methanesulfonic acid (R)-1-[(4R,5R)-2,2-dimethyl-5-(oct-1-enyl)-1,3-dioxolan-4-yl]-2-trityloxy-ethyl ester (8)

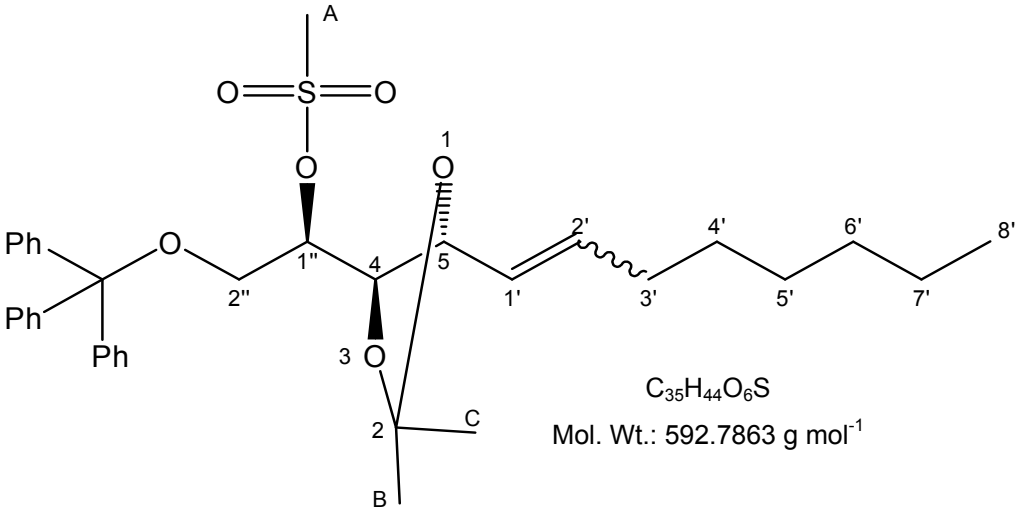

$C_{35}H_{44}O_6S$

Mol. Wt.: 592.7863 g mol^{-1}

Prepared by the general procedure for mesylation **(5.1.1.2)** using (R)-1-[(4S,5R)-2,2-Dimethyl-5-(oct-1-enyl)-1,3-dioxolan-4-yl]-2-trityloxy-ethanol **(4)** (2.594g, 5.04mmol), dichloromethane (25ml), pyridine (7.5ml), methanesulfonylchloride (0.624ml, 8.064mmol),

ethanol (0.75ml), heptane:MeOH:water (10:7:3) (100ml), affording an opaque oil. Yield 3.02g, 100%. δ ^{1}H ($CDCl_3$): 7.17-7.52 (Ar-H, 15H, m), 5.27-5.52 (C-1', C-2' *trans*, 2H, m), 5.17-5.25 (C-2' *cis*, 0.3H, m), 5.03 (C-1' *cis*, 0.3H, m), 4.82 (C-1'', 1H, m), 4.75 (H-5, 1H, m), 4.58-4.69 (H-4, 1H, m), 4.48 (H-2''$_a$ *trans*, 0.7H, dd, J=5.96, 8.42Hz), 4.24 (H-2''$_a$ *cis*, 0.3H, dd, J=6.97, 14.03Hz), 3.57 (H-2''$_b$ *cis*, 0.3H, m), 3.45 (H-2''$_b$ *trans*, 0.7H, dd, J=2.68, 10.75Hz), 2.99-3.18 (H-A_{abc}, 3H, m), 1.57-1.82 (H-3'$_{ab}$, 2H, m), 1.48 (H-B_{abc}, *trans*, 3H, s), 1.41 (H-C_{abc}, *trans*, 3H, s), 1.39, 1.38 (H-A_{abc} H-B_{abc} *cis*, 3H, each s), 1.10-1.33 (H-4'$_{ab}$-H-7'$_{ab}$, 10H, m), 0.85 (H-8'$_{abc}$, 3H, t, J=6.77Hz). δ ^{13}C ($CDCl_3$): 144.8 (C-2), 137.8 (C-2'), 130.2, 129.4, 128.7 (Ar C), 125.1 (C-1'), 82.5 (C-1''), 77.6 (C-4), 73.7 (C-5), 64.61 (C-2''), 39.9 (C-A), 35.1, 30.9, 30.2 (C-3'-5') 29.5 (C-B), 29.0 (C-6'), 28.1 (C-C), 24.5 (C-7') 16.8 (C-8'). **m/z** (ES): 633.2 (M^+ + $[K]^+$ + $[H]^+$ 70%), 315.1 (M+ - Ph_3C-O -$(CH_2)_4$- 100%), 219.1 (M^+ + [Na]+ - Ph_2COCH_2 82%). α_D: -47.6°. IR: 3200-3400cm^{-1} (br OH), 3100-3160cm^{-1} (Ar), 1650-1680 cm^{-1} (alkene), 1000-1350cm^{-1} (S=O).

5.4.3. Methanesulfonic acid (R)-1-[(4R,5R)-2,2-dimethyl-5-(pent-1-enyl)-1,3-dioxolan-4-yl]-2-trityloxy-ethyl ester (9)

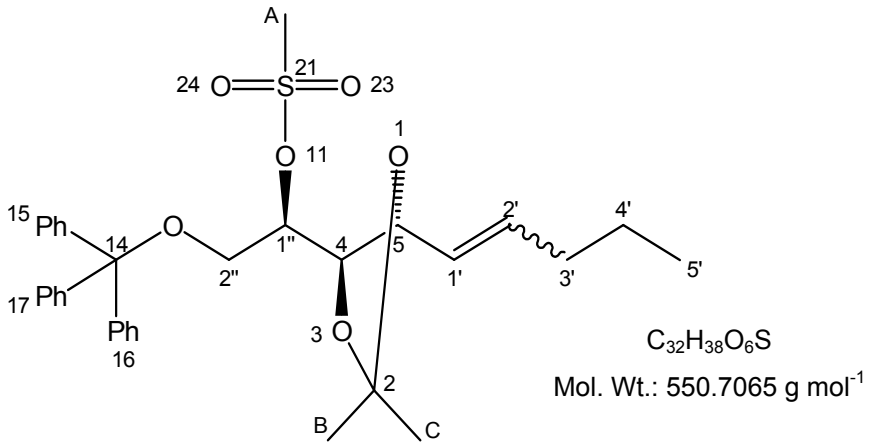

$C_{32}H_{38}O_6S$

Mol. Wt.: 550.7065 g mol^{-1}

Prepared by the general procedure for mesylation **(5.1.1.2)** using (R)-1-[(4S,5R)-2,2-dimethyl-5-(pent-1-enyl)-1,3-dioxolan-4-yl]-2-trityloxy-ethanol **(5)** (6.46g, 13.66mmol), dichloromethane (45ml), pyridine (20.3ml), methanesulfonylchloride (1.8ml, 22.74mmol), ethanol (2ml), heptane:MeOH:water (10:7:3) (70ml), affording an off-white solid. Yield 6.125g, 81.4%. δ ^{1}H ($CDCl_3$): 7.21-7.49 (Ar-H, 15H, m), 5.89 (H-2' *trans*, 0.7H, m), 5.75 (H-2' *cis*, 0.3H, m), 5.52 (H-1' *trans*, 0.7H, m), 5.48 (H-1' *cis*, 0.3H, m), 5.07 (H-1'' *trans*, 0.7H, m), 4.78 (H-1'' *cis*, 0.3H, m), 4.50 (H-5, 1H, m), 4.34 (H-4, 1H, m), 4.26 (H-2''$_a$, 1H, dd, J=5.94, 9.13Hz), 3.92 (H-2''$_b$, 1H, dd, J= 2.53, 10.72), 3.14 (H-A_{abc}, 3H, d, J=4.85Hz), 2.12 (H-3'$_{ab}$, 1H, m), 1.44 (H-4'$_{ab}$, 2H, m) 0.82 (H-5'$_{abc}$, 3H, t). δ ^{13}C ($CDCl_3$): 141.4 (C-2), 135.3 (C-2'), 126.9, 126.8, 126.1 (Ar C), 121.9 (C-1'), 79.2 (C-1''), 74.3 (C-5), 70.2 (C-4), 61.3 (C-2''), 37.2 (C-A), 34.6 (C-3'), 22.1 (C-4'), 13.65 (C-5'). **m/z** (ES): 589.1 (M^+ + $[K]^+$ 18%), 573.1 (M^+ + $[Na]^+$ 75%), 477.2 (M^+ + $[Na]^+$ - OMs 47%), 419.1 (M^+ + $[Na]^+$ - $CHOC(CH_3)_2OCHCH=CH(CH_2)_2$ 35%), 243.1 (M^+ - $OCH_2CH(OMs)CHOC(CH_3)_2OCHCH=CH(CH_2)_8CH_3$ 100%). α_D: -5.4°. m.p.: 97-100°C. IR: 3200-3400cm^{-1} (br OH), 3100-3160cm^{-1} (Ar), 1650-1680 cm^{-1} (alkene), 1000-1350cm^{-1} (S=O).

5.5. Deprotection of the phytosphingosine base

5.5.1. Methanesulfonic acid (1R,2R,3R)-2,3-dihydroxy-1-hydroxymethyl-tetradec-4-enyl ester (10)

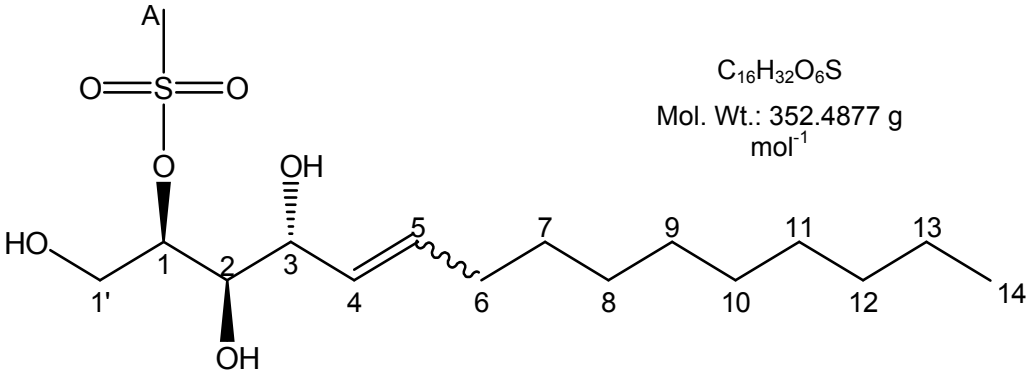

$C_{16}H_{32}O_6S$

Mol. Wt.: 352.4877 g mol^{-1}

Prepared by the general procedure for deprotection of mesylated base **(5.1.1.3)** using methanesulfonic acid (R)-1-[(4R,5R)-2,2-dimethyl-5-(undec-1-enyl)-1,3-dioxolan-4-yl]-2-trityloxy-ethyl ester **(7)** (12.918g, 0.02mol), DCM (100ml), MeOH (70ml), conc. HCl (10.5ml, 12M), affording an off-white solid. Yield 3.142g, 46.1%. δ ^{1}H ($CDCl_3$): 5.71-5.89 (H-4, 1H, m), 5.43-5.59 (H-5, 1H, m), 4.89-4.96 (H-1, 1H, m), (H-3 *trans*, 0.7H, t, J=8.3Hz), 4.08-4.13 (H-3 *cis*, 0.3H, t, J=7.2Hz), 4.0-3.94 (H-1'$_a$, H-2, 2H, m), 3.75-3.68 (H-1$_b$, 1H, m), 3.2 and 3.19 (H-A$_{abc}$, 3H, each s), 2.53 (OH-2,-3,-1', 3H, br s), 2.05-2.25 (H-6$_{ab}$, 2H, m), 1.18-1.49 (H-7$_{ab}$ – H-13$_{ab}$, 14H, m), 0.89 (H-14$_{abc}$, 3H, t, J=6.2Hz). δ ^{13}C ($CDCl_3$): 137.88 (C-5), 127.78 (C-4), 82.29 (C-1), 74.39 (C-3), 67.64 (C-2), 63.93 (C-1'), 39.32 (C-A), various signals 32.59-23.38 (C-6 -13), 14.81 (C-14). **m/z** (ES): 376.1 (M^+ + $[Na]^+$ 5%), 375.1 (M^+ + $[Na]^+$ 100%), 279.2 (M^+ + $[Na]^+$ - OMs, 68%) α_D: -54.0°. m.p.: 72-90°C. IR: 3200-3400cm^{-1} (br OH), 1650-1680 cm^{-1} (alkene), 1000-1350cm^{-1} (S=O).

5.5.2. Methanesulfonic acid (1R,2S,3S)-2,3-dihydroxy-1-hydroxymethyl-undec-4-enyl ester (11)

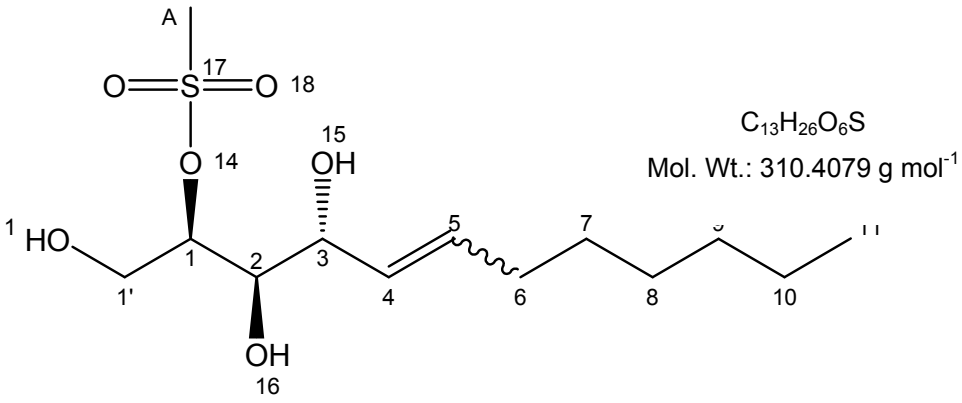

$C_{13}H_{26}O_6S$

Mol. Wt.: 310.4079 g mol^{-1}

Prepared by the general procedure for deprotection of mesylated base **(5.1.1.3)** using methanesulfonic acid (R)-1-[(4R,5R)-2,2-dimethyl-5-(oct-1-enyl)-1,3-dioxolan-4-yl]-2-trityloxy-ethyl ester **(8)** (4.375g, 7.38mmol), dry DCM (45ml), MeOH (20ml), and

concentrated HCl (5ml, 12M), affording an cream-coloured oil. Yield 1.092g, 47.67%. δ ^{1}H ($CDCl_3$): 5.71-5.91 (H-5, 1H, m), 5.43-5.59 (H-4, 1H, m), 4.95 (H-1, 1H, m), 4.32-4.38 (H-3, 1H, m), 4.06-4.13 (H-1'$_a$, 1H, m), 3.95-4.02 (H-2, 1H, m), 3.68-3.71 (H-1'$_b$, 1H, dd, J=3.1, 7.1Hz), 3.21 (H-A$_{abc}$, 3H, s), 3.19 (H-A$_{abc}$, 3H, s), 2.41 (OH-2, -3, -1', 3H, br s), 2.01-2.24 (H-6$_{ab}$, 2H, m), 1.2-1.49 (H-7$_{ab}$ – 10$_{ab}$, 8H, m), 0.9 (3H, t, J=6.5Hz). δ ^{13}C ($CDCl_3$): 137.3 (C-5), 127.3 (C-4), 81.6 (C-1), 74.8 (C-3), 67.1 (C-2), 63.4 (C-1'), 38.8 (C-A), 31.8, 29.6, 29.1, 28.0, 22.7 (C-6-10), 24.9 (C-11). **m/z** (ES): 311.1 (M^+ + $[H]^+$ 100%). α_D: -52.8°. IR: 3200-3400cm^{-1} (br OH), 1650-1680 cm^{-1} (alkene), 1000-1350cm^{-1} (S=O).

5.5.3. Methanesulfonic acid (1R,2R,3R)-2,3-dihydroxy-1-hydroxymethyl-oct-4-enyl ester (12)

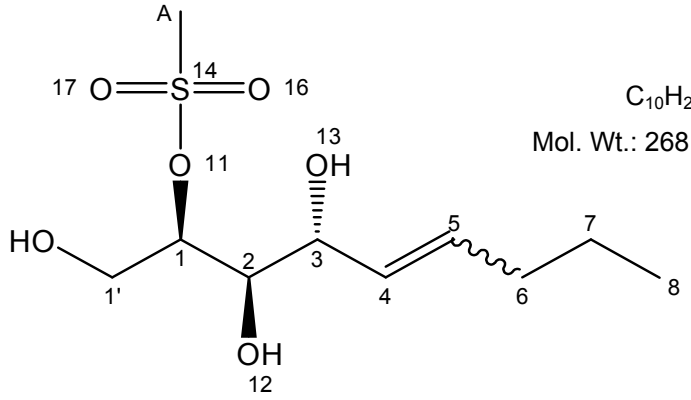

$C_{10}H_{20}O_6S$

Mol. Wt.: 268.3282 g mol^{-1}

Prepared by the general procedure for deprotection of mesylated base (5.1.1.3) using methanesulfonic acid (R)-1-[(4R,5R)-2,2-dimethyl-5-(pent-1-enyl)-1,3-dioxolan-4-yl]-2-trityloxy-ethyl ester **(9)** (6.125g, 11.1 mmol), DCM (80ml), MeOH (40ml), conc. HCl (7ml, 12M), affording an off-white wax. Yield 1.957g, 65.7%. δ ^{1}H ($CDCl_3$): 5.74-5.86 (H-5 *trans*, 1H, m), 5.68-5.72 (H-5 *cis*, 0.2H, m), 5.50-5.58 (H-4, 1H, m), 4.96-5.02 (H-1, 1H, m), 4.32-4.38 (H-3, 1H, dd, J=6.8, 14.1Hz), 4.24-4.28 (H-1'$_a$, 1H, dd, J=2.3, 4.8Hz), 4.16-4.20 (H-1, 1H, d, J=3.3Hz), 3.84-3.88 (H-1'$_b$, 1H, dd, J=2.5, 4.6Hz), 3.10-3.14 (H-A$_{abc}$, 3H, d, J=3.1),

1.88-2.06 (H-6_{ab}, 2H, m), 1.34-1.44 (H-7_{ab}, 2H, m), 0.82-0.92 (H-8_{abc}, 3H, t, J=6.9Hz). δ ^{13}C ($CDCl_3$): 137.32 (C-5), 124.12 (C-4), 85.88 (C-1), 82.86 (C-3), 76.41 (C-2), 70.99 (C-1'), 38.40 (C-A), 34.98 (C-6), 22.49 (C-7), 13.79 (C-8). **m/z** (ES): 291.2 (M^+ + $[Na]^+$ 100%). α_D: -90°. mp: 79-81°C. IR: 3200-3400cm^{-1} (br OH), 1650-1680 cm^{-1} (alkene), 1000-1350cm^{-1} (S=O).

5.6. Reduction of the double bond

5.6.1. Methanesulfonic acid (1R,2R,3R)-2,3-dihydroxy-1-hydroxymethyl-tetradecyl ester (13)

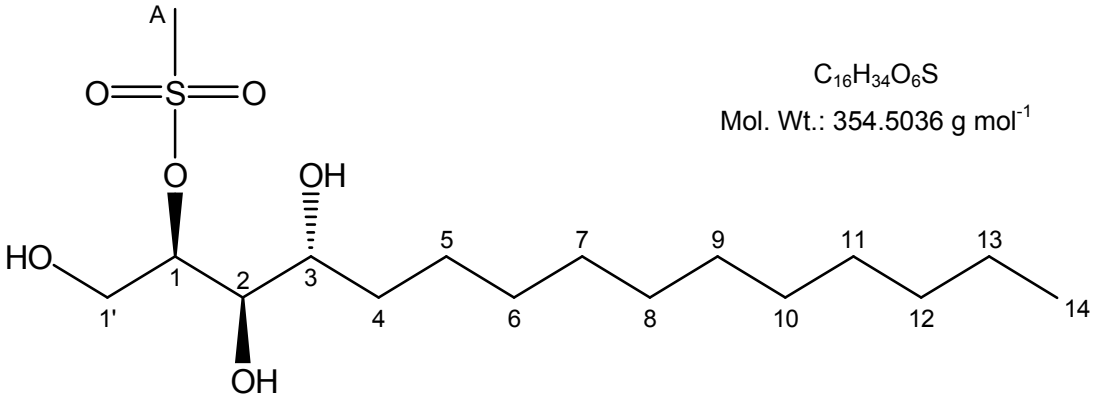

$C_{16}H_{34}O_6S$

Mol. Wt.: 354.5036 g mol^{-1}

Prepared by the general procedure for catalytic reduction **(5.1.1.4)** using methanesulfonic acid (1R,2R,3R)-2,3-dihydroxy-1-hydroxymethyl-tetradec-4-enyl ester **(10)** (3.142g, 8.9mmol), Pd-$Ba(SO_4)_2$ (0.3g), affording creamy-white crystals. Yield, 2.789g, 88%. δ ^{1}H (MeOD): 4.99-5.05 (H-1, 1H, m), 3.98- 4.04 (H-1'$_{ab}$, 2H, m), 3.55-3.62 (H-3, 1H, m), 3.45-3.49 (H-2, 1H, m), 3.15 (H-A_{abc}, 3H, s), 1.48-1.86 (H-4_a, H-6_a, 2H, m), 1.22-1.43 (H-5_b, H-6_{ab}, H-7_b, H-8_{ab}-H13_{ab}, 18H, m), 0.89 (H-14_{abc}, 3H, t, J=6.8Hz). δ ^{13}C (MeOD): 85.36 (C-1), 75.63 (C-2), 72.83 (C-3), 64.13 (C-1'), 40.14 (C-A), various peaks 36.8 – 25.9 (C-4-13), 16.2 (C-14). **m/z** (ES): 377.2 (M^+ + $[Na]^+$ 100%), 281.2 (M^+ +$[Na]^+$ - OMs 95%). HRMS:

Calculated for $C_{16}H_{34}O_6S$ [M + Na]+ 377.1974, found 377.1980. α_D: -180°. m.p.: 124-130°C. IR: 3200-3400cm^{-1} (br OH), 1000-1350cm^{-1} (S=O).

5.6.2. Methanesulfonic acid (1R,2R,3R)-2,3-dihydroxy-1-hydroxymethyl-undecyl ester (14)

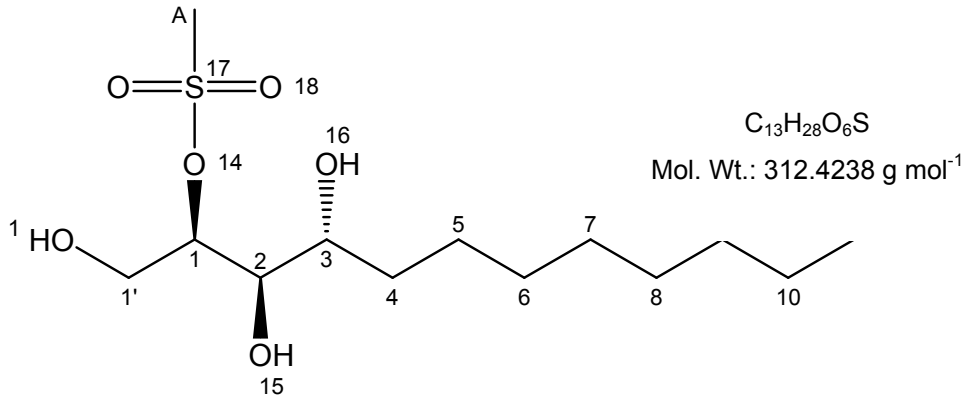

Prepared by the general procedure for catalytic reduction **(5.1.1.4)** using methanesulfonic acid (1R,2S,3S)-2,3-dihydroxy-1-hydroxymethyl-undec-4-enyl ester **(11)** (1.092g, 3.52mmol), Pd-Ba$(SO_4)_2$ (110mg), affording a colourless syrup. Yield 0.946g, 86%. δ ^{1}H (MeOD): 4.74-4.78 (H-1, 1H, m), 3.62-3.78 (H-1'$_{ab}$, 2H, m), 3.31-3.47 (H-3, 1H, m), 3.18-3.21 (H-2, 1H, m), 3.06 (H-A$_{abc}$, 3H, s), 1.48-1.56 (H-4$_a$, H-6$_a$, 2H, m), 1.22-1.43 (H-4$_b$, H-5$_{ab}$, H-6$_b$, H7$_{ab}$-H-10$_{ab}$, 12H, m), 0.73 (H-11$_{abc}$, 3H, t, J=6.5Hz). δ ^{13}C ($CDCl_3$): 83.9 (C-1), 74.7 (C-2), 71.5 (C-3), 63.3 (C-1'), 40.1 (C-A), 34.2, 33.1, 30.9, 30.8, 30.5, 26.5, 23.8 (C- 4-10), 15.1 (C-11). **m/z** (ES): 335.2 (M^+ + $[Na]^+$ 100%), 239.2 (M^+ + $[Na]^+$ - OMs 30%). HRMS: Calculated for $C_{13}H_{28}O_6S$ $[M + Na]^+$ 335.1504, found 335.1520. α_D: -32.2°. IR: 3200-3400cm^{-1} (br OH), 1000-1350cm^{-1} (S=O).

5.6.3. Methanesulfonic acid (1R,2R,3R)-2,3-dihydroxy-1-hydroxymethyl-octyl ester (15)

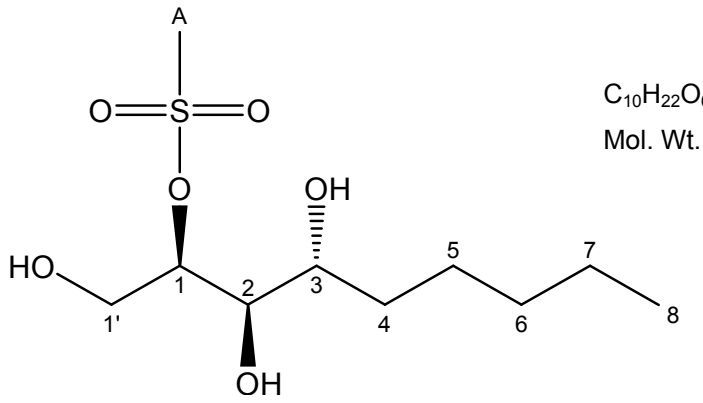

$C_{10}H_{22}O_6S$
Mol. Wt.: 270.3441 g mol^{-1}

Prepared by the general procedure for catalytic reduction **(5.1.1.4)** using methanesulfonic acid (1R,2R,3R)-2,3-dihydroxy-1-hydroxymethyl-oct-4-enyl ester **(12)** (1.957g, 7.29mmol), Pd-$Ba(SO_4)_2$ (200mg), affording a cream-coloured wax. Yield 1.906g 97.4%. δ ^1H ($CDCl_3$): 4.84-4.88 (H-1, 1H, m), 3.78-3.88 (H-$1'_{ab}$, 2H, m), 3.49-3.55 (H-3, 1H, m), 3.43-3.47 (H-2, 1H, dd, J=2.2, 8.3), 3.15 (H-A_{abc}, 3H, s), 2.76 (OH-1', -2, -3, 3H, br s), 1.75-1.67 (H-4_a, 1H, m,) 1.53-1.46 (H-6_a, 1H, m), 1.38- 1.19 (H-4_b, H-5_{ab}, H-6_b, H-7_{ab}, 6H, m,), 0.88 (H-8_{abc}, 3H, t, J=6.8). δ ^{13}C ($CDCl_3$): 82.90 (C-1), 73.61 (C-2), 70.47 (C-3), 62.25 (C-1'), 38.35 (C-A), 33.14 (C-4), 32.03 (C-5), 25.19 (C-6), 22.74 (C-7), 14.01 (C-8). **m/z** (ES): 293.4 (M^+ + $[Na]^+$ 100%). HRMS: Calculated for $C_{10}H_{22}O_6S$ [M^+ + Na^+] 293.1035, found 293.1026. α_D: -80.0°. m.p.: 71-78°C. IR: 3200-3400cm^{-1} (br OH), 1000-1350cm^{-1} (S=O).

5.7. Azidation

5.7.1. (2S,3S,4R)-2-Azido-octadecane-1,3,4-triol (16)

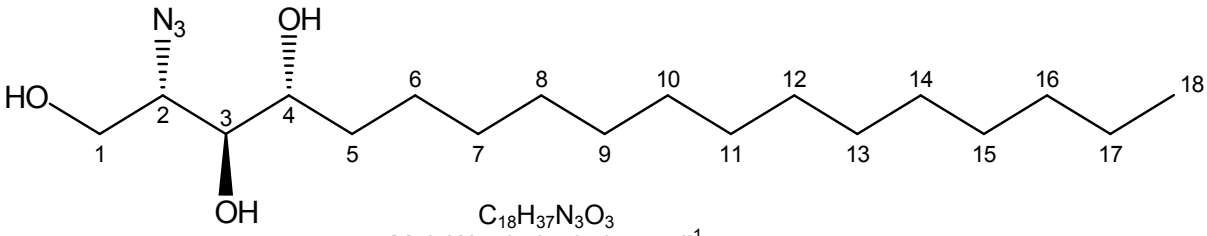

$C_{18}H_{37}N_3O_3$
Mol. Wt.: 343.5048 g mol^{-1}

A solution of sodium azide (1.19g, 18.3mmol) in water (3ml) was cooled to 0°C. Dichloromethane (5ml) was added and the resulting biphasic mixture stirred vigorously and treated with trifluoromethanesulfonic anhydride (1.046, 3.7mmol). The reaction was stirred at 0°C for 2h, the organic phase was separated and the aqueous phase washed thrice with DCM. The organic extracts were combined, washed with saturated sodium chloride solution, and dried (Na_2SO_4) yielding the trifluoromethanesulfonic azide solution in DCM. Phytosphingosine (590mg, 1.86mmol) was dissolved in water (6ml) and potassium carbonate (384mg, 2.78mmol) and copper sulfate ($CuSO_4.5H_2O$) (2.8mg, 16µmol) were added to the solution, followed by MeOH (12ml) and the TfN_3 solution. More MeOH was added until the solution was homogenous, and the reaction mixture stirred overnight at RT. The organic phase was extracted, washed with NaCl, dried (Na_2SO_4), and concentrated *in vacuo*. The resulting (2S,3S,4R)-2-azido-octadecane-1,3,4-triol **(16)** was purified by column chromatography (heptane:EtOAc) (9:1), affording a solid. Yield: 490mg, 76.7%. δ ^{1}H (MeOD): 3.81-3.86 (H-1_a, 1H, dd, J=3.0, 11.1), 3.64-3.71 (H-1_b, 1H, dd, J=7.9, 11.2), 3.36-3.54 (H-3, -4, 2H, m), 3.22-3.55 (H-2, 1H, m), 1.42-1.65 (H-5_{ab}, H-7_a, 3H, m), 1.21-1.47 (H-6_{ab}, H-7_b, H-8_{ab}-H17_{ab}, 23H, m), 0.89 (H-18_{abc}, 3H, t, J=6.5). δ ^{13}C (MeOD): 76.4 (C-3), 73.2 (C-4), 67.0 (C-2), 62.9 (C-1), 33.4, 31.2, 30.8, 27.1, 24.1 (C-5 - 17), 14.8 (C-18). **m/z** (ES): 366.3 (M^+ + $[Na]^+$ 100%). HRMS: Calculated for $C_{18}H_{37}N_3O_3$: $[M + Na]^+$ 366.2733,

found 366.2727. α_D:+5.7°. m.p.: 92-93°C. IR: 3200-3400cm^{-1} (br OH), 2040-2080cm^{-1} (azide).

5.7.2. (2S,3S,4R)-2-Azido-pentadecane-1,3,4-triol (17)

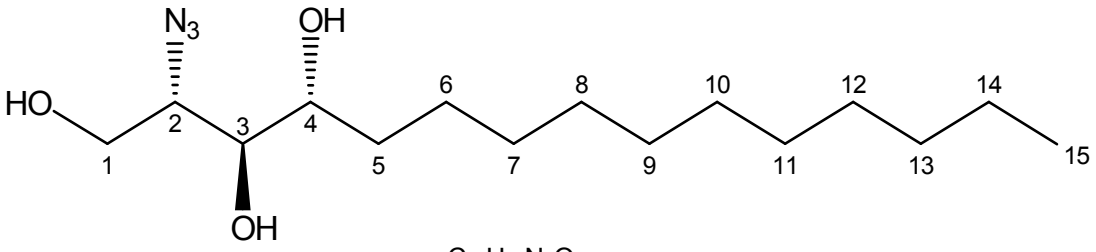

$C_{15}H_{31}N_3O_3$

Mol. Wt.: 301.4251 g mol^{-1}

Prepared by the general procedure for the introduction of an azide group **(5.1.1.5)**, using methanesulfonic acid (1R,2R,3R)-2,3-dihydroxy-1-hydroxymethyl-tetradecyl ester **(13)** (2.642g, 7.45mmol), DMF (20ml), sodium azide (0.969g, 14.91mmol), affording a translucent oil. Yield: 1.609g, 71.65%. δ ^{1}H (MeOD): 3.92-3.98 (H-1$_a$, 1H, dd, J=3.3, 11.4), 3.74-3.84 (H-1$_b$, 1H, m), 3.58-3.66 (H-4, 1H, m), 3.1-3.58 (H-3, 1H, m), 3.32-3.36 (H-2, 1H, m), 1.51-1.76 (H-5$_{ab}$, H-7$_a$, 3H, m), 1.18-1.47 (H-6$_{ab}$, H-7$_b$, H-8$_{ab}$-H14$_{ab}$, 17H, m), 0.91 (H-15$_{abc}$, 3H, t, J=6.6). δ ^{13}C (MeOD): 73.9 (C-3), 70.8 (C-4), 64.6 (C-2), 60.4 (C-1), 31.8, 31.0, 28.7, 28.4, 24.7, 21.7 (C-5 - 14). **m/z** (ES): 325.3 (M^+ + $[Na]^+$ + $[H]^+$ 5%), 324.2 (M^+ + $[Na]^+$ 100%). HRMS: Calculated for $C_{15}H_{31}N_3O_3$ $[M + Na]^+$ 324.2263, found 324.2275. α_D: +31.4°. IR: 3200-3400cm^{-1} (br OH), 2040-2080cm^{-1} (azide).

5.7.3. (2S,3S,4R)-2-Azido-dodecane-1,3,4-triol (18)

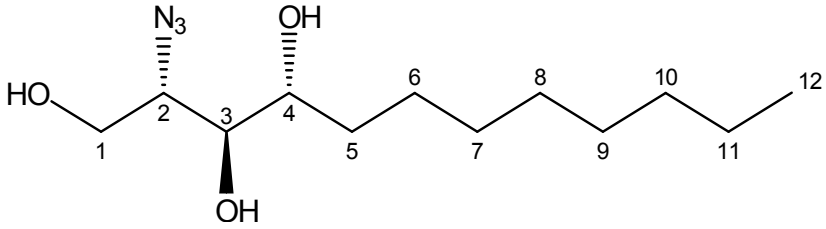

$C_{12}H_{25}N_3O_3$

Mol. Wt.: 259.3453 g mol^{-1}

Prepared by the general procedure for the introduction of an azide group **(5.1.1.5)**, using methanesulfonic acid (1R,2R,3R)-2,3-dihydroxy-1-hydroxymethyl-undecyl ester **(14)** (0.946g, 3.03mmol), DMF (10ml), sodium azide (0.39g, 6.06mmol), affording a colourless syrup. Yield: 690mg, 87%. δ ^{1}H (MeOD): 3.88-3.95 (H-1_a, 1H, dd, J=3.3, 11.1), 3.71-3.8 (H-1_b, 1H, m), 3.54-3.63 (H-4, 1H, m), 3.48-3.53 (H-3, 1H, m), 3.28-3.32 (H-2, 1H, m), 1.47-1.73 (H-5_{ab}, H-7_a, 3H, m), 1.20-1.45 (H-6_{ab}, H-7_b, H-8_{ab}-H-11_{ab}, 11H, m), 0.89 (H-12_{abc}, 3H, t, J=6.2). δ ^{13}C (MeOD): 75.9 (C-3), 72.8 (C-4), 66.2 (C-2), 62.4 (C-1), 33.8, 32.9, 30.7, 30.3, 26.6, 23.6 (C-5 - 11). **m/z** (ES): 282.2 (M^+ + $[Na]^+$ 100%). HRMS: Calculated for $C_{12}H_{25}N_3O_3$ $[M + Na]^+$ 282.1794, found 282.1794. α_D: +45.0°. IR: 3200-3400cm^{-1} (br OH), 2040-2080cm^{-1} (azide).

5.7.4. (2S,3S,4R)-2-Azido-nonane-1,3,4-triol (19)

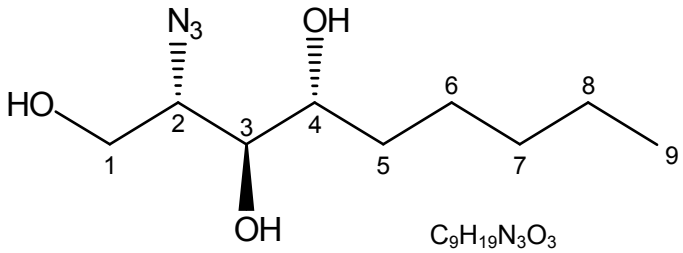

$C_9H_{19}N_3O_3$

Mol. Wt.: 217.2656 g mol^{-1}

Prepared by the general procedure for the introduction of an azide group **(5.1.1.5)**, using methanesulfonic acid (1R,2R,3R)-2,3-dihydroxy-1-hydroxymethyl-octyl ester **(15)** (0.744g, 2.75mmol), DMF (10ml), sodium azide (0.36g, 5.5mmol), affording a white solid. Yield: 297mg, 49.7%. δ ^{1}H (MeOD): 3.82-3.86 (H-1_a, 1H, dd, J=4.9, 11.5Hz), 3.71-3.77 (H-1_b, 1H, m), 3.58-3.64 (H-3, H-4, 2H, m), 3.44-3.47 (H-2, 1H, q, J=4.5, 9.9Hz), 1.45-1.56 (H-5_a, H-7_a, 2H, m), 1.38-1.44 (H-5_b, 1H, m), 1.27-1.14 (H-6_{ab}, H-7_b, H-8_{ab}, 5H, m), 0.79 (H-9_{abc}, 3H, t, J=6.1). δ ^{13}C (MeOD): 74.02 (C-3), 71.87 (C-4), 62.71 (C-2), 60.95 (C-1), 31.47 (C-5), 31.29 (C-6), 24.95 (C-7), 22.09 (C-8), 13.49 (C-9). **m/z** (ES): 240 (M^+ + $[Na]^+$ 100%). HRMS: Calculated for $C_9H_{19}N_3O_3$ [M + Na^+] 240.1324, found 240.1315. α_D: +144.0°. m.p.: 71-78°C. IR: 3200-3400cm^{-1} (br OH), 2040-2080cm^{-1} (azide).

5.8. Addition of *tert*-butyldiphenyl silyl protecting group

5.8.1. (2S,3S,4R)-2-azido-1-(*tert*-butyl-diphenyl-silanyloxy)-octadecane-3,4-diol (20)

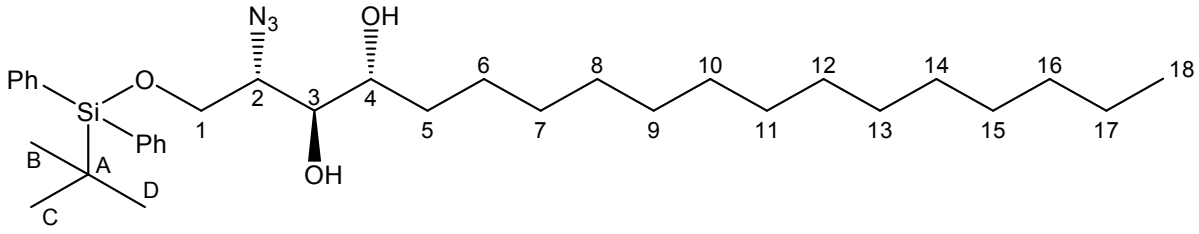

$C_{34}H_{55}N_3O_3Si$

Mol. Wt.: 581.9044 g mol^{-1}

Prepared by the general procedure for the addition of a *tert*-butyldiphenyl silyl protecting group **(5.1.1.6)** using (2S,3S,4R)-2-azido-octadecane-1,3,4-triol **(16)** (5.878g, 17.1mmol), dichloromethane (200ml), pyridine (30ml), 4-DMAP (300mg), *tert*-butyldiphenylsilylchloride (6.58g, 6.23ml, 23.94mmol), affording a colourless oil. Yield: 9.095g (91%). δ ^{1}H ($CDCl_3$):

7.35-7.70 (Ar-H, 10H, m), 4.01 (H-1_a, 1H, dd, J=3.7, 10.5Hz), 3.89 (H-1_b, 1H, dd, J=5.6, 10.9Hz), 3.68 (H-3, H-4, 2H, m), 3.54 (H-2, 1H, m), 2.02 (OH-3, -4, 2H, br s), 1.36-1.55 (H-5_a, H-7_a, 2H, m), 1.19-1.34 (H-5_b, H-6_{ab}, H-7_b, H-8_{ab}-H17_{ab}, 24H, m), 1.06 (H-B_{abc}, H-C_{abc}, H-D_{abc}, 9H, s), 0.82 (H-18_{abc}, 3H, t, J=6.4Hz). δ ^{13}C ($CDCl_3$): 133.6, 128.1, 125.9 (Ar C), 72.6 (C-3), 70.4 (C-4), 62.2 (C-1), 61.4 (C-2), 27.7, 27.4, 24.8, 23.7 (C-5 – 17). **m/z** (ES): 605.5 (M^+ + $[Na]^+$ + $[H]^+$ 20%) 604.4 (M^+ + $[Na]^+$ 100%). HRMS: Calculated for $C_{34}H_{55}N_3O_3Si$ $[M + Na]^+$ 604.3915, found 604.3910. α_D: +2.8°. IR: 3200-3400cm^{-1} (br OH), 3100-3000 (Ar), 2040-2080cm^{-1} (azide).

5.8.2. (2S,3S,4R)- 2-Azido-1-(*tert*-butyl-diphenyl-silanyloxy)-pentadecane-3,4-diol (21)

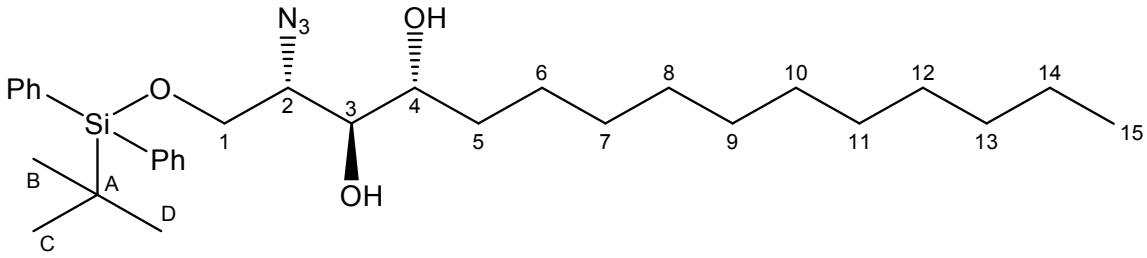

$C_{31}H_{49}N_3O_3Si$

Mol. Wt.: 539.8247 g mol^{-1}

Prepared by the general procedure for the addition of a *tert*-butyldiphenyl silyl protecting group **(5.1.1.6)** using (2S,3S,4R)-2-azido-pentadecane-1,3,4-triol **(17)** (1.574g, 5.22mmol), dichloromethane (50ml), pyridine (8ml), 4-DMAP (80mg), *tert*-butyldiphenylsilylchloride (2.574g, 2.43ml, 9.37mmol)., affording a colourless oil. Yield: 1.2g (42.6%). δ ^{1}H ($CDCl_3$): 7.37-7.69 (Ar-H, 10H, m), 3.99-4.03 (H-1_a, 1H, dd, J=4.1, 11.1Hz), 3.87-3.92 (H-1_b, 1H, dd, J=5.5, 10.9Hz), 3.66-3.68 (H-3, H-4, 2H, m), 3.51-3.57 (H-2, 1H, m), 1.19-1.57 (H-5_{ab} – H14_{ab}, 22H, m) 1.06 (H-B_{abc}, H-C_{abc}, H-D_{abc}, 9H, s), 0.84-0.88 (H-15_{abc}, 3H, t, J=6.7).

δ ^{13}C ($CDCl_3$): 136.204, 130.601, 128.473 (Ar-C), 74.689 (C-3), 72.910 (C-4), 64.724 (C-1), 63.940 (C-2), 32.494 – 26.235 multiple signals (C-5 – 14), 27.318 (C-A,B,C). **m/z** (ES): 563.4 (M^+ + $[Na]^+$ + $[H]^+$ 30%), 562.3 (M^+ + $[Na]^+$ 100%). HRMS: Calculated for $C_{31}H_{49}N_3O_3Si$ $[M + Na]^+$ 562.3441, found 562.3459. α_D: +35.7°. IR: 3200-3400cm^{-1} (br OH), 3100-3000 (Ar), 2040-2080cm^{-1} (azide).

5.8.3. (2S,3S,4R)- 2-Azido-1-(*tert*-butyl-diphenyl-silanyloxy)-dodecane-3,4-diol (22)

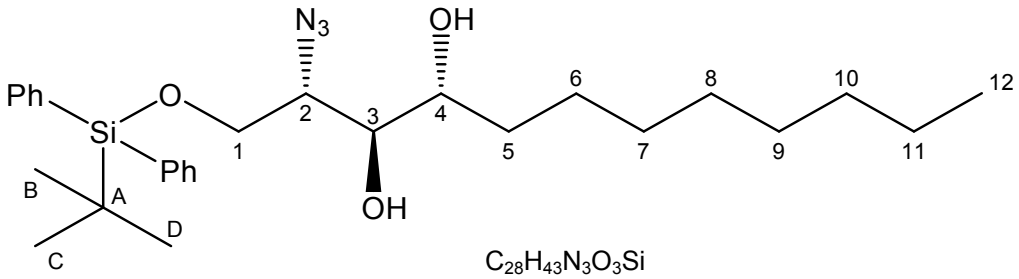

$C_{28}H_{43}N_3O_3Si$

Mol. Wt.: 497.7449 g mol^{-1}

Prepared by the general procedure for the addition of a *tert*-butyldiphenyl silyl protecting group **(5.1.1.6)** using (2S,3S,4R)-2-azido-dodecane-1,3,4-triol **(18)** (577mg, 2.22mmol), dichloromethane (20ml), pyridine (2ml), 4-dimethylaminopyridine (35mg), *tert*-butyldiphenylsilylchloride (1.094mg, 1.04ml, 4mmol), affording a colourless oil. Yield: 450mg (40.7%). δ ^{1}H ($CDCl_3$): 7.66-7.69 (Ar-H, 10H, m), 3.99-4.04 (H-1_a, 1H, dd, J=4.2, 11.0Hz), 3.86-3.92 (H-1_b, 1H, dd, J=5.4, 10.9Hz), 3.65-3.67 (H-3, H-4, 2H, m), 3.54-3.58 (H-2, 1H, m), 2.03 (OH-3, -4, 2H, br s), 1.35-1.54 (H-5_{ab}, H-7_a, 3H, m), 1.20-1.32 (H-6_{ab}, H-7_b, H-8_{ab} – H-11_{ab}, 11H, m), 1.06 (H-B_{abc}, H-C_{abc}, H-D_{abc}, 9H, s), 0.84-0.86 (H-12_{abc}, 3H, t, J=6.8Hz). δ ^{13}C ($CDCl_3$): 136.705, 131.103, 128.973 (Ar C), 75.213 (C-3), 73.425 (C-4), 65.226 (C-1), 64.460 (C-2), 32.932 – 23.741 (multiple signals, C-5 – 11), 27.824 (C-B,C,D), 16.150 (C-12). **m/z** (ES): 521.75 (M^+ + Na^+ + H^+ 8%), 520.74 (M^+ + Na^+ 100%). HRMS:

Calculated for $C_{28}H_{43}N_3O_3Si$ [M + Na]$^+$ 520.7447, found 520.7460. α_D: +45°. IR: 3200-3400cm^{-1} (br OH), 3100-3000 (Ar), 2040-2080cm^{-1} (azide).

5.8.4. (2S,3S,4R)-2-Azido-1-(*tert*-butyl-diphenyl-silanyloxy)-nonane-3,4-diol (23)

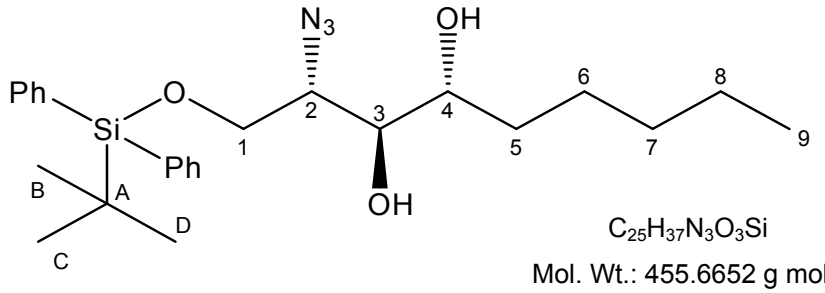

$C_{25}H_{37}N_3O_3Si$

Mol. Wt.: 455.6652 g mol^{-1}

Prepared by the general procedure for the addition of a *tert*-butyldiphenyl silyl protecting group **(5.1.1.6)** using (2S,3S,4R)-2-azido-nonane-1,3,4-triol **(19)** (352mg, 1.62mmol), dichloromethane (75ml), pyridine (7.5ml), 4-DMAP (20mg), and *tert*-butyldiphenylsilylchloride (0.62g, 0.59ml, 2.268mmol), affording a colorless oil. Yield 168mg, 23%. δ ^{1}H ($CDCl_3$): 7.37-7.68 (Ar-H, 10H, m), 3.99-4.02 (H-1$_a$, 1H, dd, J=4.4, 11.4), 3.88-3.91 (H-1$_b$, 1H, dd, J=5.8, 11.4), 3.66-3.68 (H-3, H-4 2H, m), 3.53-3.56 (H-2, 1H, q, J=4.5, 6.2, 10.3), 2.45-2.46 (OH-3, 1H, d, J=4.8) 1.93-1.94 (OH-4, 1H, d, J= 4.4), 1.46-1.54 (H-5$_a$, H-7$_a$, 2H, m), 1.38-1.44 (H-5$_b$, 1H, m), 1.23-1.34 (H-6$_{ab}$, H-7$_b$, H-8$_{ab}$, 5H, m), 1.06 (H-B$_{abc}$, H-C$_{abc}$, H-D$_{abc}$, 9H, s), 0.89-0.86 (H-9$_{abc}$, 3H, t, J=6.7). δ ^{13}C ($CDCl_3$): 135.58 (C-Ar), 132.56, 132.50 (QC-Ar), 129.99 (C-Ar), 127.87 (C-Ar), 74.14 (C-3), 72.34 (C-4), 64.13 (C-1), 63.39 (C-2), 3.82, 31.72 (C-5,6), 26.72 (C-B, -C, -D), 25.28 (C-7), 22.56 (C-8), 13.99 (C-9). **m/z** (ES): 479.7 (M$^+$ + [Na]$^+$ + [H]$^+$ 12%), 478.7 (M$^+$ + [Na]$^+$ 100%). HRMS: Calculated for $C_{25}H_{37}N_3O_3Si$ [M + Na]$^+$ 478.2502, found 478.2507. α_D: +19.5°. IR: 3200-3400cm^{-1} (br OH), 3100-3000cm^{-1} (Ar), 2040-2080cm^{-1} (azide).

5.9. Adding benzoate protecting groups

5.9.1. ((2S,3S,4R)-2-Azido-3,4-*bis*-benzoyloxy-octadecyloxy)-*tert*-butyl-diphenyl-silane (24)

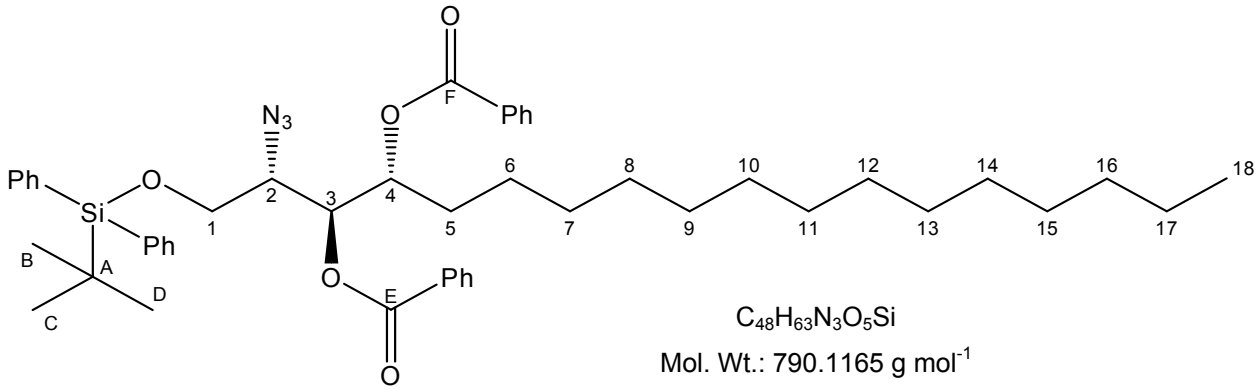

$C_{48}H_{63}N_3O_5Si$

Mol. Wt.: 790.1165 g mol^{-1}

Prepared by the general procedure for addition of benzoate groups **(5.1.1.7)** using (2S,3S,4R)-2-azido-1-(*tert*-butyl-diphenyl-silanyloxy)-octadecane-3,4-diol **(20)** (9.095g, 15.6mmol), pyridine (60ml), benzoyl chloride (13.16g, 10.86ml, 93.6mmol), and DMAP (65.97mg, 0.54mmol), affording a colourless oil. Yield: 10.379g, 84%. δ ^{1}H ($CDCl_3$): 7.19-7.95 (Ar-H, 20H, m), 5.49 (H-3, H-4, 2H, m), 3.98 (H-1_a, 1H, m), 3.84 (H-1_b, H-2, 2H, m), 1.73-1.86 (H-5_{ab}, 2H, m), 1.19-1.41 (H-6_{ab} – H-17_{ab}, 24H, m), 1.04 (H-B_{abc}, H-C_{abc}, H-D_{abc}, 9H, s), 0.87 (H-18_{abc}, 3H, t, J=6.9Hz). δ ^{13}C ($CDCl_3$): 165.3 (C-E, -F), 135.2, 132.6, 129.4, 129.3, 128.1, 128.0, 127.3 (Ar C), 72.7 (C-3), 71.9 (C-4), 63.8 (C-1), 62.8 (C-2), 31.6, 29.3, 29.1, 29.0 (C-5 – 17). **m/z** (ES): 813.6 (M^+ + $[Na]^+$ + $[H]^+$ 20%), 812.6 (M^+ + $[Na]^+$ 100%). HRMS: Calculated for $C_{48}H_{63}N_3O_5Si$ $[M + Na]^+$ 812.4435, found 812.4443. α_D: +6.8°. IR: 3100-3000cm^{-1} (Ar), 2040-2080cm^{-1} (azide), 1750-1750cm^{-1} (C=O).

5.9.2. ((2S,3S,4R)-2-Azido-3,4-*bis*-benzoyloxy-pentadecyloxy)-*tert*-butyl-diphenyl-silane (25)

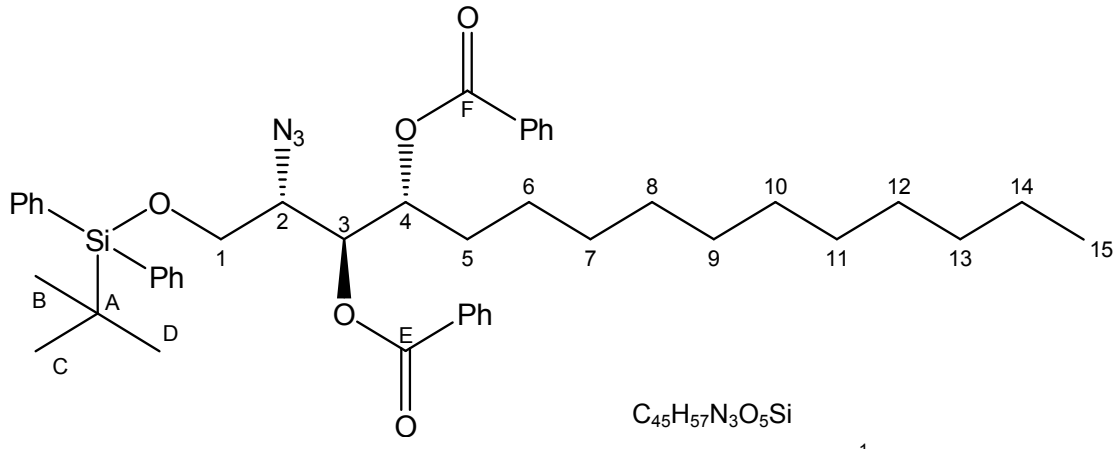

$C_{45}H_{57}N_3O_5Si$

Mol. Wt.: 748.0368 g mol^{-1}

Prepared by the general procedure for addition of a benzoate group **(5.1.1.7)** using (2S,3S,4R)- 2-azido-1-(*tert*-butyl-diphenyl-silanyloxy)-pentadecane-3,4-diol **(21)** (902mg, 1.67mmol), pyridine (10ml), DMAP (6.1mg, 0.05mmol), benzoylchloride (1. 26g, 1.04ml, 8.98mmol). This was then taken crude onto the next step **(5.10.2)**.

5.9.3. ((2S,3S,4R)-2-Azido-3,4-*bis*-benzoyloxy-dodecyloxy)-*tert*-butyl-diphenyl-silane (26)

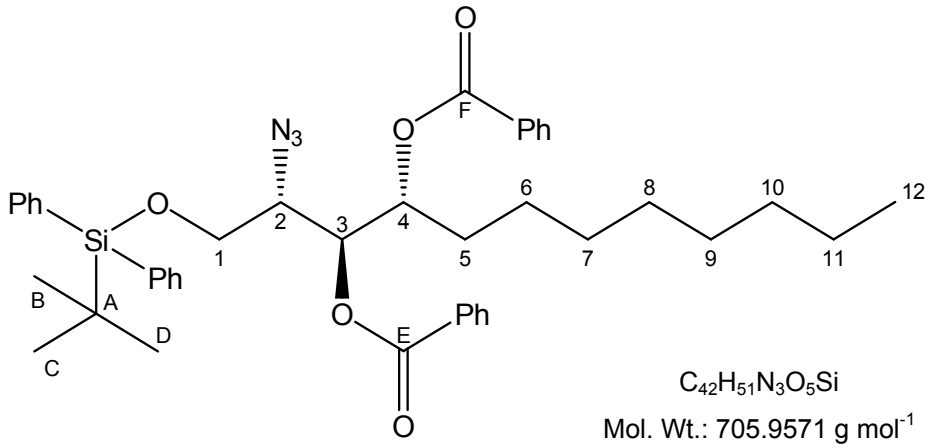

$C_{42}H_{51}N_3O_5Si$

Mol. Wt.: 705.9571 g mol^{-1}

Prepared by the general procedure for addition of benzoate groups **(5.1.1.7)** using (2S,3S,4R)- 2-azido-1-(*tert*-butyl-diphenyl-silanyloxy)-dodecane-3,4-diol **(22)** (413mg, 829µmol), pyridine (5ml), DMAP (3.1mg, 25µmol) and benzoylchloride (55mg, 0.45ml, 4.46mmol). This was taken crude onto the next step **(5.10.3)**.

5.9.4. ((2S,3S,4R)-2-Azido-3,4-*bis*-benzoyloxy-nonyloxy)-*tert*-butyl-diphenyl-silane (27)

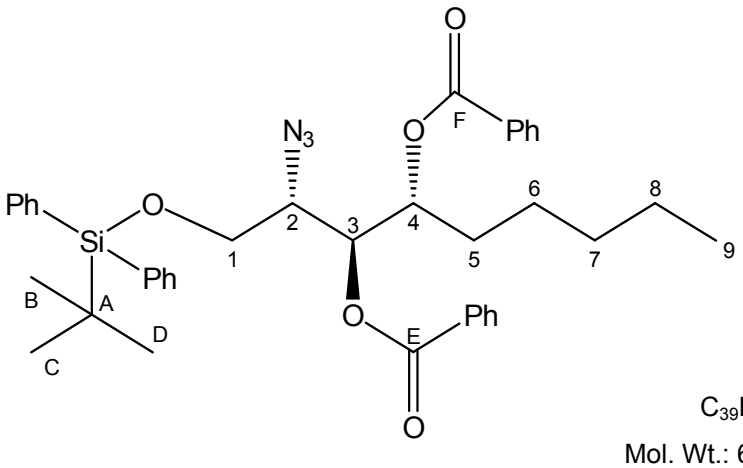

$C_{39}H_{45}N_3O_5Si$

Mol. Wt.: 663.8773 g mol^{-1}

Prepared by the general procedure for addition of benzoate groups **(5.1.1.7)** using (2S,3S,4R)-2-azido-1-(*tert*-butyl-diphenyl-silanyloxy)-nonane-3,4-diol **(23)** (168mg, 0.37mmol) in pyridine (5ml), benzoyl chloride (0.312g, 0.26ml, 2.22mmol), and DMAP (1.6mg, 13µmol), affording a ceamy-white syrup. Yield: 214mg, 87.12%. δ ^{1}H ($CDCl_3$): 8.16-7.30 (Ar-H [TBDPS and Bz PGs), 20H, m), 5.52-5.48 (H-3, H-4, 2H, m), 3.98-3.94 (H-1_a, 1H, m), 3.87-3.82 (H-1_b, H-2, 2H, m), 1.83-1.78 (H-5_{ab}, 2H, m), 1.42-1.23 (H-6_{ab}, H-7_{ab}, H-8_{ab}, 6H, m), 1.04 (H-B_{abc}, H-C_{abc}, H-D_{abc}, 9H, s), 0.85-0.83 (H-9_{abc}, 3H, t, J=6.70). δ ^{13}C ($CDCl_3$): 165.63, 165.03 (C-E, -F), 135.52-132.98 (multiple signals, C-Ar), 132.71, 132.45 (QC-Ar), 130.56-129.64 (multiple signals, C-Ar), 129.45, 129.25, (QC-Ar), 128.85-128.35 (multiple signals, C-Ar), 73.11 (C-3), 72.25 (C-4), 64.11 (C-1), 63.18 (C-2), 31.51 (C-7), 29.74 (C-5), 26.62 (C-B, -C, -D) 25.04 (C-6), 22.41 (C-8), 19.02 (C-A), 13.91 (C-9). **m/z** (ES): 687.4

(M^+ + $[Na]^+$ + $[H]^+$ 20%), 686.4 (M^+ + $[Na]^+$ 100%), 249.1 (M^+ + $[K]^+$ - ^{t}BuSi(Ph)$_2$-O-CH_2-CH(N_3)-CH(O)-CH(O)-$(CH_2)_4$-CH_3 35%). HRMS: Calculated for $C_{39}H_{45}N_3O_5Si$ $[M + Na]^+$ 686.3026, found 686.3030. α_D: +13.6°. IR: 3100-3000cm^{-1} (Ar), 2040-2080cm^{-1} (azide), 1750-1750cm^{-1} (C=O).

5.10. Removing the TBDPS group

5.10.1. (2S,3S,4R)-2-Azido-3,4-*bis*-benzoyloxy-octadecan-1-ol (28)

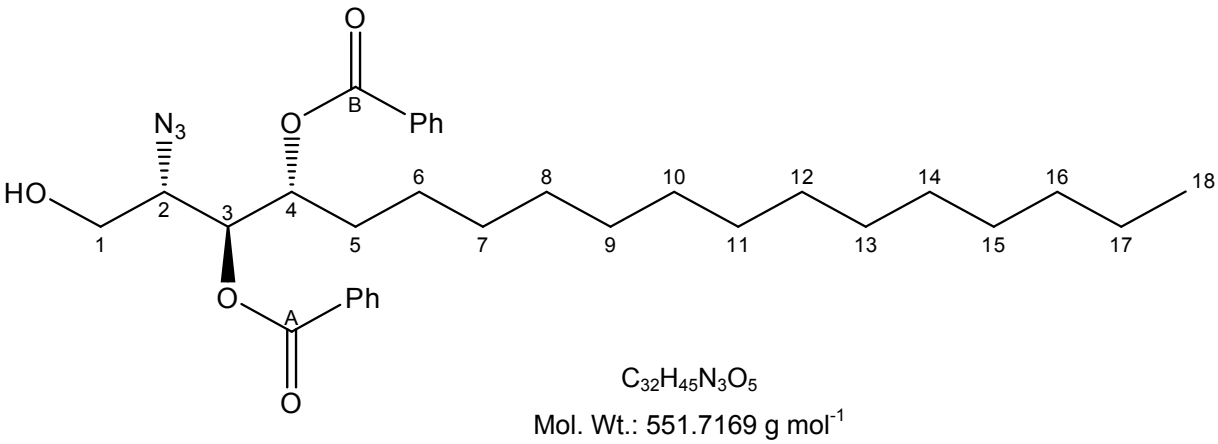

$C_{32}H_{45}N_3O_5$

Mol. Wt.: 551.7169 g mol^{-1}

Prepared by the general procedure for the removal of a TBDPS group **(5.1.1.8)** using acetic acid (0.87g, 14.454mmol, 0.563ml), TBAF (14.454mmol, 14.454ml), and ((2S,3S,4R)-2-azido-3,4-*bis*-benzoyloxy-octadecyloxy)-*tert*-butyl-diphenyl-silane **(24)** (10.379g, 13.14mmol) in dry THF (30ml), affording a white solid. Yield: 4.419g, 60.95%. δ ^{1}H ($CDCl_3$): 7.48-8.07 (Ar-H, 10H, m), 5.56 (H-3, H-4, 2H, m), 3.98 (H-1_a, 1H, m), 3.8 (H-1_b, H-2, 2H, m), 1.82-1.99 (H-5_{ab}, 2H, m), 1.18-1.51 (H-6_{ab} – H17_{ab}, 24H, m), 0.89 (H-9_{abc}, 3H, t, J=6.4). δ ^{13}C ($CDCl_3$): 165.5 (C=O), 133.4, 133.0, 129.7, 129.5 (Ar C), 128.9 (Ar QC), 128.4, 128.2 (Ar C), 73.0 (C-3), 72.7 (C-4), 62.8 (C-2), 61.9 (C-1), 31.7, 29.4, 29.3, 29.1, 22.4 (C-5 - 17). **m/z** (ES): 575.4 (M^+ + $[Na]^+$ + $[H]^+$ 15%), 574.3 (M^+ + $[Na]^+$ 100%). HRMS: Calculated for

$C_{32}H_{45}N_3O_5$ [M + Na]$^+$ 574.3257, found 574.3265. α_D: +2.2°. m.p.: 48-50°C. IR: 3200-3400cm^{-1} (br OH), 3100-3000cm^{-1} (Ar), 2040-2080cm^{-1} (azide), 1750-1750cm^{-1} (C=O).

5.10.2. (2S,3S,4R)-Azido-3,4-*bis*-benzoyloxy-pentadecan-1-ol (29)

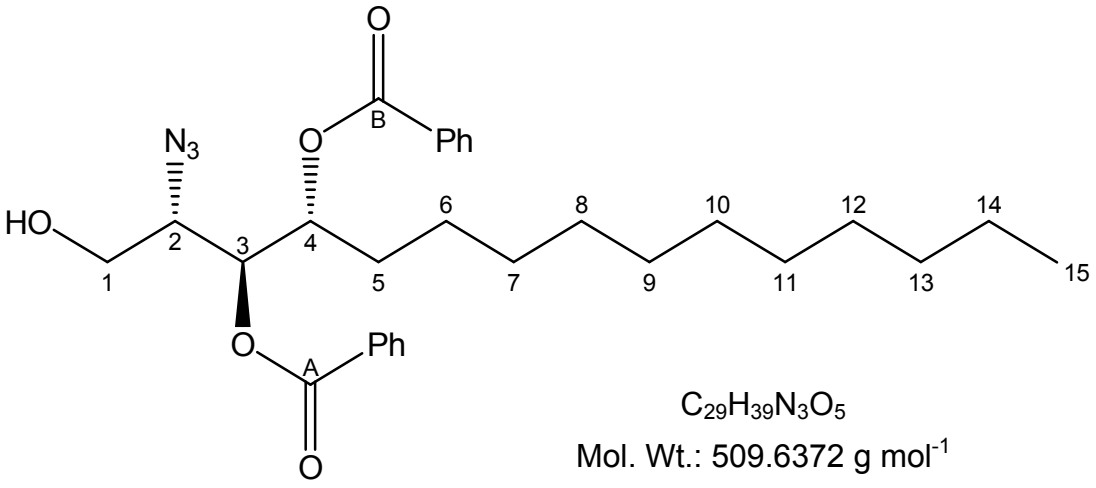

$C_{29}H_{39}N_3O_5$

Mol. Wt.: 509.6372 g mol^{-1}

Prepared by the general procedure for removal of a TBDPS group **(5.1.1.8)** using crude ((2S,3S,4R)-2-azido-3,4-*bis*-benzoyloxy-pentadecyloxy)-*tert*-butyl-diphenyl-silane **(25)** (1g, 1.34mmol), THF (20ml), acetic acid (0.088ml, 1.47mmol), TBAF (384mg, 0.426ml, 1.47mmol), affording an opaque oil. Yield 504mg, 74%. δ ^{1}H ($CDCl_3$): 7.25-8.11 (Ar-H, 10H, m), 5.54 (H-3, H-4, 2H, m), 4.80-4.84 (H-1_a, 1H, q, J=7.3, 14.6), 3.67-4.03 (H-1_b, H-2, 2H, m), 1.77-1.97 (H-5_{ab}, 2H, m), 1.09-1.46 (H-6_{ab} – H-14_{ab}, 18H, m), 0.83-0.88 (H-9_{abc}, 3H, t, J=6.6Hz). δ ^{13}C ($CDCl_3$): 162.5 (C-A, -B), 135.798- 130.603 (multiple signals, Ar C), 75.425 (C3), 75.059 (C4), 65.288 (C2), 64.276 (C1), 34.021-27.598 (multiple signals, C5 - 14), 16.235 (C15). **m/z** (ES): 532.7 (M$^+$ + [Na]$^+$ 100%). HRMS: Calculated for $C_{29}H_{39}N_3O_5$ [M + Na]$^+$ 532.6370, found 532.6361. α_D: +157.9°. IR: 3200-3400cm^{-1} (br OH), 3100-3000cm^{-1} (Ar), 2040-2080cm^{-1} (azide), 1750-1750cm^{-1} (C=O).

5.10.3. (2S,3S,4R)-2-Azido-3,4-*bis*-benzoyloxy-dodecan-1-ol (30)

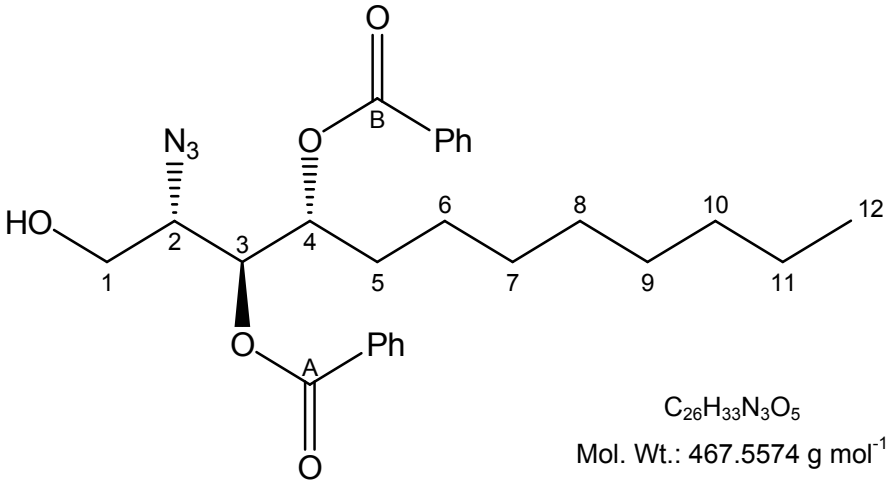

$C_{26}H_{33}N_3O_5$

Mol. Wt.: 467.5574 g mol^{-1}

Prepared as the general procedure for removal of a TBDPS group **(5.1.1.8)** using crude ((2S,3S,4R)-2-azido-3,4-*bis*-benzoyloxy-dodecyloxy)-*tert*-butyl-diphenyl-silane **(26)** (812mg, 1.15mmol), THF (20ml), acetic acid (75.96mg, 75.96µml, 1.265mmol), TBAF (0.766ml, 0.766mmol), affording a colourless oil. Yield 246mg, 45.7%. δ ^{1}H ($CDCl_3$): 7.26-7.89 (Ar-H, 10H, m), 5.32-5.39 (H-3, H-4, 2H, m), 3.65-3.82 (H-1_a, 1H, m), 3.54.3.60 (H-1_b, H-2, 2H, m), 1.62-1.82 (H-5_{ab}, 2H, m), 1.06-1.30 (H-6_{ab} – H-11_{ab}, 12H, m), 0.65-0.70 (H-12_{abc}, 3H, t, J=6.7). δ ^{13}C ($CDCl_3$): 136.434- 131.057 (multiple signals, Ar C), 76.149 (C3), 75.355 (C4), 66.187 (C2), 64.756 (C1), 34.519-25.318 (multiple signals, C5 - 11), 16.676 (C12). **m/z** (ES): 491.2 (M^+ + $[H]^+$ 10%), 490.2 (M^+ + $[Na]^+$ 100%) HRMS: Calculated for $C_{26}H_{33}N_3O_5$ $[M + Na]^+$ 490.2318, found 490.2308. α_D: +8.8°. IR: 3200-3400cm^{-1} (br OH), 3100-3000cm^{-1} (Ar), 2040-2080cm^{-1} (azide), 1750-1750cm^{-1} (C=O).

5.10.4. (2S,3S,4R)-2-Azido-3,4-*bis*-benzoyloxy-nonan-1-ol (31)

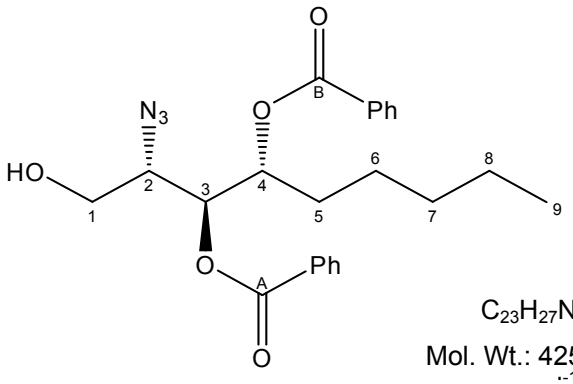

$C_{23}H_{27}N_3O_5$

Mol. Wt.: 425.4777 g

Prepared by the general procedure for the removal of a TBDPS group **(5.1.1.8)** using acetic acid (20mg, 19µl, 0.354mmol), TBAF (454µl, 454µmol), and ((2S,3S,4R)-2-azido-3,4-*bis*-benzoyloxy-nonyloxy)-*tert*-butyl-diphenyl-silane **(27)** (214mg, 322µmol) in dry THF (10ml), affording an opaque oil. Yield: 124mg, 90.5%. δ ^{1}H ($CDCl_3$): 7.48-8.07 (Ar-H, 10H, m), 5.49-5.56 (H-3, H-4, 2H, m), 3.98-4.01 (H-1_a, 1H, m), 3.75-3.82 (H-1_b, H-2, 2H, m), 1.82-1.99 (H-5_{ab}, 2H, m), 1.18-1.51 (H-6_{ab} – H-8_{ab}, 6H, m), 0.89 (H-9_{abc}, 3H, t, J=6.8). δ ^{13}C ($CDCl_3$): 166.07, 165.74 (C-A, -B), 133.74-129.71 (multiple signals, C-Ar), 129.26, 129.11 (QC-Ar), 128.61, 128.46 (C-Ph), 73.28 (C-3), 72.94 (C-4), 63.11 (C-2), 62.13 (C-1), 31.50 (C-7), 29.73 (C-5), 25.21 (C-6), 22.42 (C-8), 13.91 (C-9). **m/z** (ES): 449.3 (M^+ + $[Na]^+$ + $[H]^+$ 10%), 448.2 (M^+ + $[Na]^+$ 100%). HRMS: Calculated for $C_{23}H_{27}N_3O_5Na$ $[M + Na]^+$ 448.1848, found 448.1829. α_D: +81.4°. IR: 3200-3400cm^{-1} (br OH), 3100-3000cm^{-1} (Ar), 2040-2080cm^{-1} (azide), 1750-1750cm^{-1} (C=O).

5.11. Glycosyl iodide precursors

5.11.1. (3R,4S,5S,6R)-2,3,4,5-Tetrakis-trimethylsilanyloxy-6-trimethylsilanyloxymethyl-tetrahydropyran (32)

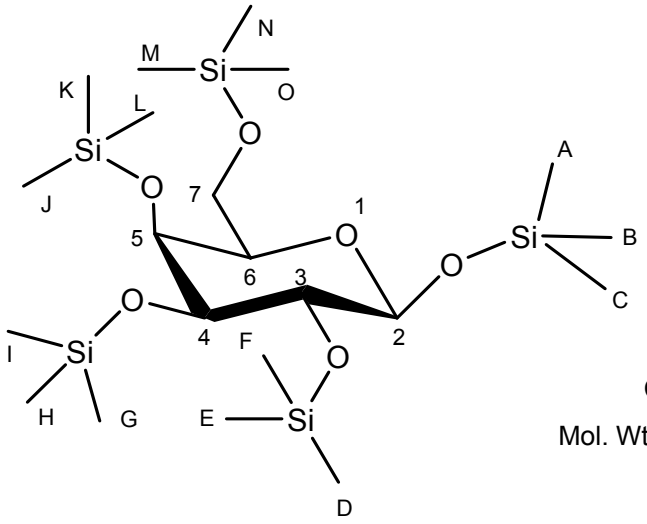

$C_{21}H_{52}O_6Si_5$

Mol. Wt.: 541.0615 g mol^{-1}

Prepared by the general procedure for trimethly silylation **(5.1.1.9)** using **D**-galactose (1.8g, 10mmol), DMF (80ml), Et_3N (5.57g, 7.67ml, 55mmol) and chlorotrimethylsilane (5.98g, 6.96ml, 55mmol), affording a colourless viscous syrup. Yield 5.12g (94.63%). δ ^1H ($CDCl_3$): 5.03 (H-2, 1H, d, J=7.3Hz), 3.48-3.91(H-3, H-4, H-5 H-6, H-7ab, 6H, m), 0.08-0.14 (H-TMS, 45H, m) δ ^{13}C ($CDCl_3$): 94.2978 (C-1) 72.0191, 70.8496, 70.2041, 69.6680 (C-2 - C-5), 60.9238 (C-6), 0.3304 – 0.7958 (multiple signals, C-TMS). **m/z** (ES): 564.4 (M^+ + $[H]^+$ + $[Na]^+$ 25%), 563.1 (M^+ + $[Na]^+$ 100%). HRMS: Calculated for $C_{21}H_{52}O_6Si_5$ $[M + Na]^+$ 563.2508, found 563.2500. α_D: -98.0°.

5.11.2. (3R,4S,5R,6R)-2,3,4,5-Tetrakis-trimethylsilanyloxy-6-trimethylsilanyloxymethyl-tetrahydropyran (33)

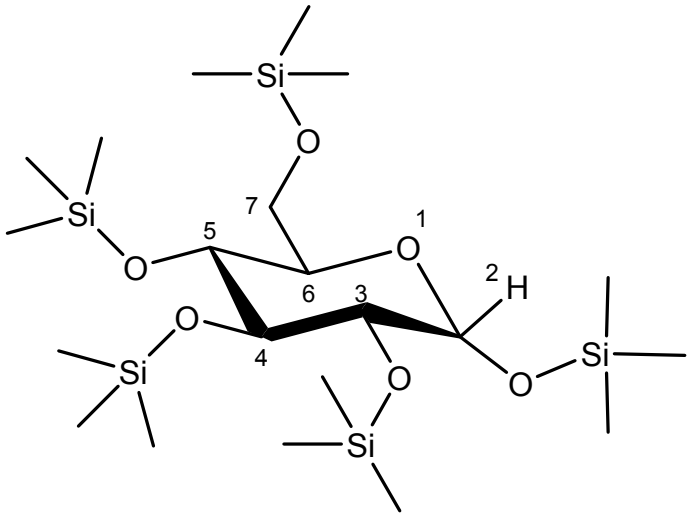

$C_{21}H_{52}O_6Si_5$

Mol. Wt.: 541.0615 g mol^{-1}

Prepared by the general procedure for trimethly silylation **(5.1.1.9)** using **D**-glucose (1.8g, 10mmol), DMF (80ml), Et_3N (5.57g, 7.67ml, 55mmol), and chlorotrimethylsilane (5.98g, 6.96ml, 55mmol), affording a yellow-tinged translucent syrup. Yield 4.62g, 85.39%. δ ^1H ($CDCl_3$): 4.97-4.98 (H-2, 1H, d, J=3.24Hz), 3.28-3.77 (H-3, H-4, H-5 H-6, H-7ab 6H, m), 0.04-0.16 (H-TMS, 45H, m). δ ^{13}C ($CDCl_3$): 93.38 (C1) 71.25, 69.98, 69.70, 68.76 (C2-5), 59.38 (C6), 0.32 – -0.78 (multiple signals C-TMS). **m/z** (ES): 564.3 (M^+ + $[H]^+$ 15%), 563.1 (M^+ + $[Na]^+$ 100%), 491.3 (M^+ + $[H]^+$ + $[Na]^+$ - TMS 25%). HRMS: Calculated for $C_{21}H_{52}O_6Si_5$ $[M + Na]^+$ 563.2508, found 563.2501. α_D: +82.0°.

5.11.3. (2S,3R,4R,5S)-2-Methyl-3,4,5,6-tetrakis-trimethylsilanyloxy-tetrahydropyran (34)

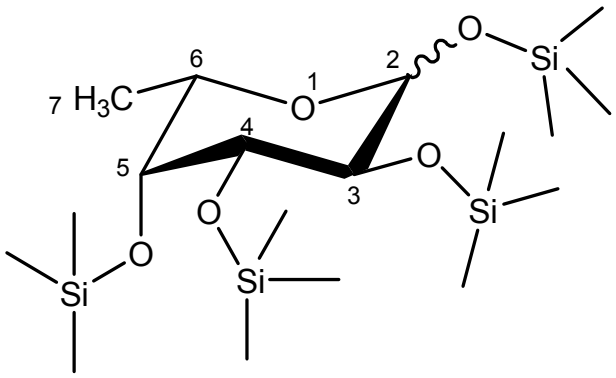

$C_{18}H_{44}O_5Si_4$
Mol. Wt.: 452.2266g mol^{-1}

L-Fucose (1g, 6.09mmol) and triethylamine (4.4ml, 31.55mmol, 5.18M eq) were dissolved in dry DMF (50ml). Trimethylsilyl chloride (3.44g, 4ml, 31.55mmol) was added at 0°C and the reaction stirred at room temperature overnight. The solution was diluted with pentane (100ml), and extracted with water (3 x 30ml). The organic portions were combined, dried ($MgSO_4$), filtered and concentrated, affording a white solid [291]. Yield 2.363g, 85.65%. δ ^1H ($CDCl_3$): 4.98-5.01 (H-2, 1H, m), 3.87-4.05 (H-2, 1H, m), 3.76-3.80 (H-3, H-4, 2H, m), 3.56-3.58 (H-6, 1H, m), 1.07-1.11 (H-7_{abc}, 3H, m), 0.04-0.15 (H-TMS, 36H, m). δ ^{13}C ($CDCl_3$): 93.83 (C2) 75.33, 69.90, 68.89, 65.92 (C3-6), 16.06 (C7), 0.00 – -0.50 (multiple signals C-TMS). **m/z** (ES): 564.3 (M^+ + $[H]^+$ 15%), 563.1 (M^+ + $[Na]^+$ 100%), 491.3 (M^+ + $[H]^+$ + $[Na]^+$ - TMS 25%). HRMS: Calculated for $C_{18}H_{44}O_5Si_4$ $[M + Na]^+$ 475.2264, found 475.2280. α_D: -210.0°. m.p.: 109-115°C.

5.12. Glycosylation

5.12.1. (2S,3R,4S,5R,6R)-2-((2S,3S,4R)-2-Azido-3,4-*bis*-benzoyloxy-octadecyloxy)-6-hydroxymethyl-tetrahydro-pyran-3,4,5-triol (35)

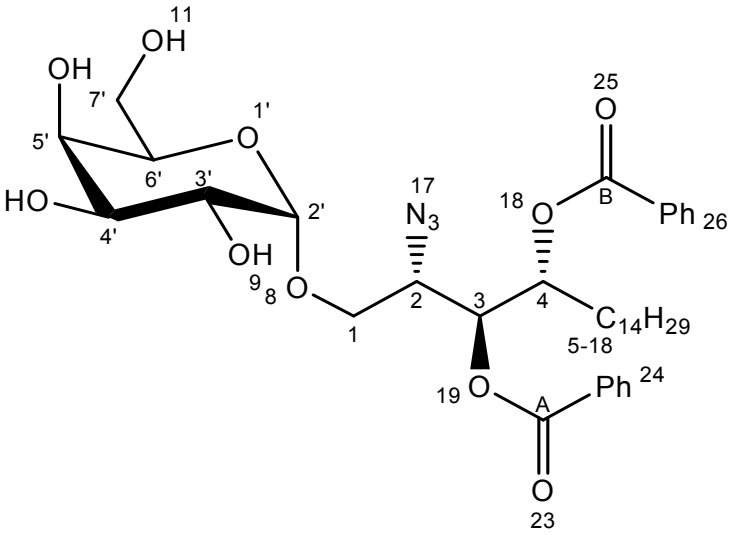

$C_{38}H_{55}N_3O_{10}$

Mol. Wt.: 713.8575 g mol^{-1}

Prepared by the general procedure for the coupling of sugars with phytosphingosine analogues **(5.1.1.10)** using pertrimethylsilylated galactose **(32)** (2.94g, 5.44mmol), DCM (40ml), iodotrimethylsilane (1.09g, 0.77ml, 5.44mmol), benzene (6ml, then 2 x 1ml, then 3ml), MS 4Å (1.5g), tetrabutylammonium iodide (4.02g, 10.88mmol), (2S,3S,4R)-2-Azido-3,4-*bis*-benzoyloxy-octadecan-1-ol **(28)** (1g, 1.81mmol), diisopropylethylamine (1.05g, 1.42ml, 8.16mmol), benzene (6ml), MeOH (30ml), and Dowex© 50WX8-200 resin (10g), affording a yellow-tinged oil. Yield 740mg, 57.3%. δ ^{1}H ($CDCl_3$): 7.47-8.14 (Ar-H, 10H, m), 5.78-5.84 (H-3, 1H, q, J=4.5, 2.7, 6.6Hz), 5.59-5.67 (H-4, 1H, m), 4.94-4.98 (H-2', 1H, d, J=2.4), 4.26-4.33 (H-7_a, 1H, dd, J=2.7, 10.5Hz), 4.01-4.09 (H-2, H-5', 2H, m), 3.95-3.99 (H-4', 1H, m), 3.87-3.95 (H-1_{ab}, H-3', H-6', 4H, m), 3.71-3.79 (H-7_b, 1H, dd, J=5.1, 10.5), 2.36 (OH-3, -4, -5, -7, 4H, br s), 1.82-2.03 (H-5_{ab}, 2H, m), 1.21-1.53 (H-6_{ab} – H17_{ab}, 34H, m), 0.91-0.98 (H-18_{abc}, 3H, t, J=6.7). δ ^{13}C ($CDCl_3$): 129.74-135.11 (multiple signals, Ar-C), 100.39 (C-2'), 69.01-74.14 (C-4, C-3, C-4', C-6', C-5', C-3'), 61.62 (C-7'), 21.59-30.86

(C-5 – C17), 15.40 (C-18). **m/z** (ES): 737.8 (M^+ + $[Na]^+$ + $[H]^+$ 15%), 736.8 (M^+ + $[Na]^+$ 100%), HRMS: Calculated for $C_{38}H_{55}N_3O_{10}$ $[M + Na]^+$ 736.8573, found 736.8591. α_D: +54.0°. IR: 3200-3400cm^{-1} (br OH), 3100-3000cm^{-1} (Ar), 2040-2080cm^{-1} (azide), 1750-1750cm^{-1} (C=O).

5.12.2. (2S,3R,4S,5R,6R)-2-((2S,3S,4R)-2-Azido-3,4-*bis*-benzoyloxy-pentadecyloxy)-6-hydroxymethyl-tetrahydro-pyran-3,4,5-triol (36)

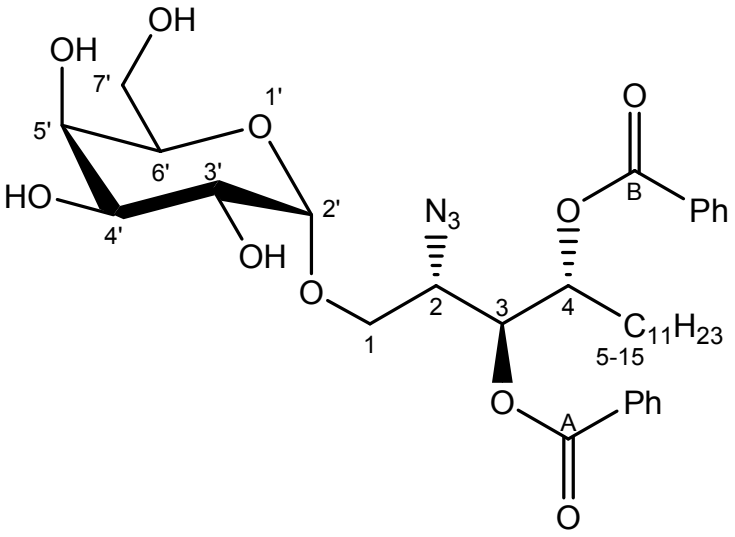

$C_{35}H_{49}N_3O_{10}$
Mol. Wt.: 671.7778 g mol^{-1}

Prepared by the general procedure for the coupling of sugars with phytosphingosine analogues **(5.1.1.10)** using pertrimethylsilylated galactose **(32)** (1.606g, 2.97mmol), DCM (20ml), iodotrimethylsilane (594mg, 0.43ml, 2.97mmol), benzene (5ml, then 2 x 1ml, then 2ml), MS 4Å (800mg), tetrabutylammonium iodide (2.19g, 5.94mmol), (2S,3S,4R)-azido-3,4-*bis*-benzoyloxy-pentadecan-1-ol **(29)** (504mg, 0.991mmol), diisopropylethylamine (576mg, 0.78ml, 4.45mmol), benzene (10ml), MeOH (30ml), and Dowex© 50WX8-200 resin (7g), affording a pale yellow oil. Yield 175mg, 26.29%. δ ^1H ($CDCl_3$): 7.37-8.02 (Ar-H, 10H, m), 5.62-5.66 (H-3, 1H, m), 5.48-5.55 (H-4, 1H, m), 4.80 (H-2', 1H, d, J=2.41Hz), 4.16-4.12 (H-$7'_a$, 1H, m), 3.90-3.95 (H-2, H-5', 2H, m), 3.83-3.85 (H-4', 1H, m), 3.71-3.74 (H-1_{ab}, H-3', H-

6', 4H, m), 3.63-3.69 (H-7'$_b$, 1H, m), 1.82-1.92 (H-5$_{ab}$, 2H, m), 1.15-1.30 (H-6$_{ab}$ – H-14$_{ab}$, 16H, m), 0.81-0.85 (H-15$_{abc}$ 3H, t, J=6.9Hz). δ ^{13}C ($CDCl_3$): 139.5 – 135.1 (multiple signals, Ar C), 106.5 (C-1'), 79.5 (C-4), 78.1(C-3), 77.8 (C-3'), 76.1 (C-5'), 75.5(C-4'), 75.2 (C-2'), 73.6 (C-6'), 68.0 (C-1), 66.5 (C-2), 40.5 – 28.9 (multiple signals, C-5 –C-14), 19.5 (C-15). **m/z** (ES): 711.9 (M^+ + $[K]^+$ + $[H]^+$ 10%), 694.7 (M^+ + $[Na]^+$ 100%). HRMS: Calculated for $C_{35}H_{49}N_3O_{10}$ $[M + Na]^+$ 694.7675, found 694.7686. α_D: +81.4°. IR: 3200-3400cm^{-1} (br OH), 3100-3000cm^{-1} (Ar), 2040-2080cm^{-1} (azide), 1750-1750cm^{-1} (C=O).

5.12.3. (2S,3R,4S,5R,6R)-2-((2S,3S,4R)-2-Azido-3,4-*bis*-benzoyloxy-dodecyloxy)-6-hydroxymethyl-tetrahydro-pyran-3,4,5-triol (37)

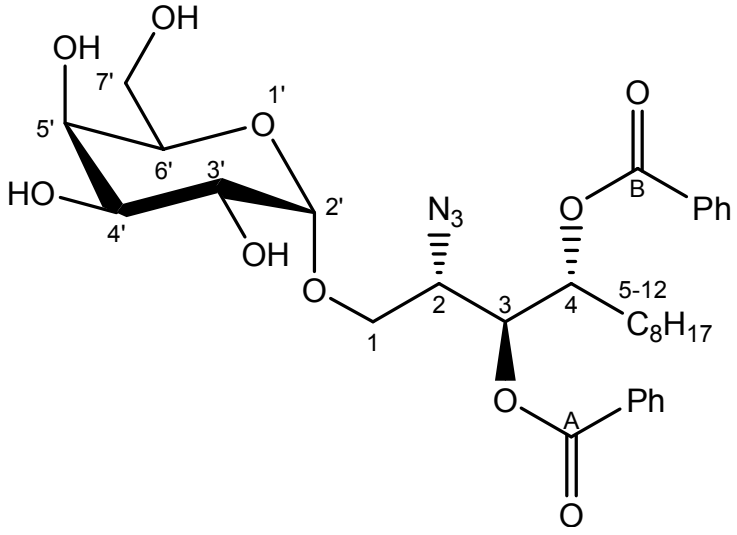

$C_{32}H_{43}N_3O_{10}$
Mol. Wt.: 629.6980 g mol^{-1}

Prepared by the general procedure for the coupling of sugars with phytosphingosine analogues **(5.1.1.10)** using pertrimethylsilylated galactose (32) (852mg, 1.578mmol), DCM (15ml), iodotrimethylsilane (316mg, 0.23ml, 1.578mmol), benzene (3ml, then 2 x 1ml, then 1ml), MS 4Å (500mg), tetrabutylammonium iodide (1.17g, 3.156mmol), (2S,3S,4R)-azido-3,4-*bis*-benzoyloxy-dodecan-1-ol **(30)** (246mg, 0.53mmol), diisopropylethylamine

(1.05g, 1.42ml, 8.16mmol), benzene (6ml), MeOH (20ml), and Dowex© 50WX8-200 resin (5g), producing an off-white solid. Yield 110 mg, 32.96%. δ ^{1}H ($CDCl_3$): 7.38-7.98 (Ar-H, 10H, m), 5.61-5.64 (H-3, 1H, m), 5.48-5.52 (H-4, 1H, m), 4.79 (H-2', 1H, s), 4.11-4.13 (H-7'$_a$, 1H, dd, J=2.9, 8.0Hz), 3.90-3.93 (H-2, H-5', 2H, m), 3.82-3.85 (H-4', 1H, m), 3.71-3.75 (H-1$_{ab}$, H-3', H-6', 4H, m), 3.63-3.67 (H-7'$_b$, 1H, q, J=6.0, 10.4, 4.8Hz), 1.81-1.94 (H-5$_{ab}$, 2H, m), 1.18-1.42 (H-6$_{ab}$ – H-11$_{ab}$ 12H, m), 0.78-0.81 (H-12$_{abc}$, 3H, t, J=6.7Hz) δ ^{13}C ($CDCl_3$): 166.8, 166.286 (C-A, -B), 134.238-128.683 (multiple signals, Ar C), 100.219 (C-2'), 73.696 (C-4), 72.563 (C-3), 71.407 (C-4'), 70.598 (C-6'), 70.227 (C-5'), 69.456 (C-3'), 67.867 (C-7'), 62.160 (C-1), 61 164 (C-2), 32.136-22.933 (multiple signals, C-5 –C-11), 14.176 (C-12). **m/z** (ES): 668.1 (M^+ + $[K]^+$ 5%), 653. 1 (M^+ + $[Na]^+$ + $[H]^+$ 10%), 652.1 (M^+ + $[Na]^+$ 100%). HRMS: Calculated for $C_{32}H_{43}N_3O_{10}$ [M + Na]$^+$ 652.2846, found 652.2840. α_D: +92.4°. m.p.: 53-65°C. IR: 3200-3400cm^{-1} (br OH), 3100-3000cm^{-1} (Ar), 2040-2080cm^{-1} (azide), 1750-1750cm^{-1} (C=O).

5.12.4. (2S,3R,4S,5R,6R)-2-((2S,3S,4R)-2-Azido-3,4-*bis*-benzyloxy-nonyloxy)-6-hydroxymethyl-tetrahydro-pyran-3,4,5-triol (38)

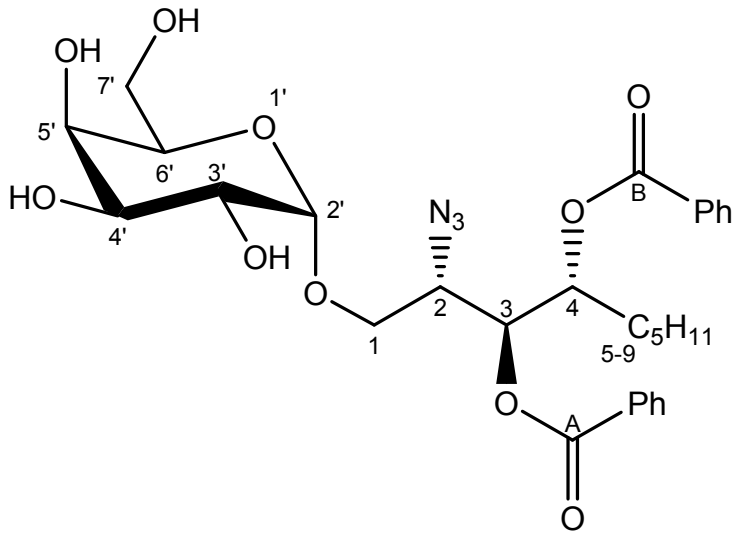

$C_{29}H_{37}N_3O_{10}$

Mol. Wt.: 587.6183 g mol^{-1}

Prepared by the general procedure for the coupling of sugars with phytosphingosine analogues **(5.1.1.10)** using pertrimethylsilylated galactose **(32)** (0.266g, 0.494mmol), DCM (5ml), iodotrimethylsilane (97mg, 0.07ml, 0.494mmol), benzene (2ml, then 2 x 1ml, then 2ml), MS 4Å (200mg), tetrabutylammonium iodide (3.65mg, 0.988mmol), (2S,3S,4R)-2-azido-3,4-*bis*-benzoyloxy-nonan-1-ol **(31)** (0.7mg, 0.16mmol), diisopropylethylamine (97.5mg, 0.13ml, 0.741mmol), benzene (3ml), MeOH (5ml), and Dowex© 50WX8-200 resin (2g), affording a pale yellow translucent oil. Yield: 0.043g, 45.73%. δ ^{1}H ($CDCl_3$): 7.38-7.96 (Ar-H, 10H, m), 5.59-5.61 (H-3, 1H, m), 5.40-5.50 (H-4, 1H, m), 4.80 (H-2', 1H, s), 4.10-4.13 (H-7'$_a$, 1H, dd, J=3.0, 7.9Hz), 3.91-3.94 (H-2, H-5', 2H, m), 3.80-3.84 (H-4', 1H, t, J=6.0Hz), 3.70-3.75 (H-1$_{ab}$, H-3', H-6', 4H, m), 3.62-3.67 (H-7'$_b$, 1H, m), 1.81-1.91 (H-5$_{ab}$, 2H, m), 1.15-1.41 (H-6$_{ab}$ – H-8$_{ab}$ 6H, m), 0.80-0.85 (H-9$_{abc}$, 3H, t, J=6.4Hz). δ ^{13}C ($CDCl_3$): 167.12, 167.00 (C-A, -B), 127.44-133.37 (multiple signals, Ar C), 101.36 (C-2'), 73.15 (C-4), 72.01 (C-3), 70.98 (C-4'), 70.56 (C-6'), 70.21 (C-5'), 69.69 (C-3'), 68.10 (C-7'), 62.41 (C-1), 61.00 (C-2), 21.94-33.34 (multiple signals, C-5 – C-8), 13.92 (C-9). **m/z** (ES): 611.62 (M^+ + $[Na]^+$ + $[H]^+$ 10%), 610.62 (M^+ + $[Na]^+$ 100%). HRMS: Calculated for $C_{29}H_{37}N_3O_{10}$ $[M + Na]^+$ 610.6183, found 610.9192. α_D: +36.1°. IR: 3200-3400cm^{-1} (br OH), 3100-3000cm^{-1} (Ar), 2040-2080cm^{-1} (azide), 1750-1750cm^{-1} (C=O).

5.13. Removal of benzoate protecting groups

5.13.1. 2-(2-Azido-3,4-dihydroxy-octadecyloxy)-6-hydroxymethyl-tetrahydro-pyran-3,4,5-triol (39)

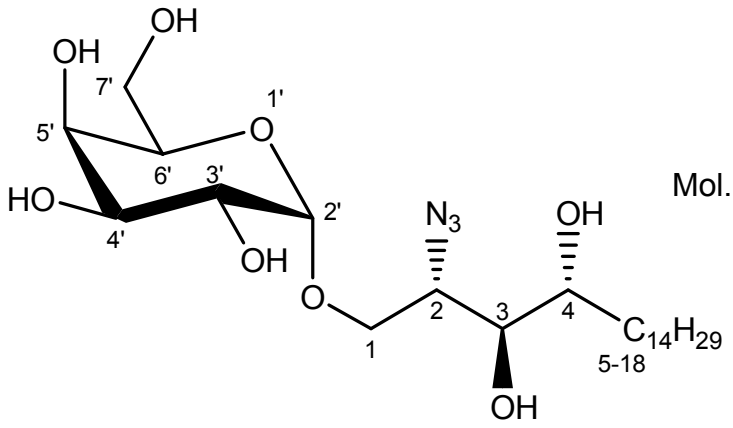

$C_{24}H_{47}N_3O_8$

Mol. Wt.: 505.6454 g mol^{-1}

Prepared by the general procedure for the removal of benzoyl protecting groups **(5.1.1.11)** using 2-(2-azido-3,4-*bis*-benzoyloxy-octadecyloxy)-6-hydroxymethyl-tetrahydro-pyran-3,4,5-triol **(35)** (740mg, 1.04mmol), THF (20ml), MeOH (10ml), 0.5M NaOMe in MeOH (84mg, 3.12ml, 1.56mmol; then 54mg, 2ml, 1mmol), affording a white solid. Yield 417mg, 79.3%. δ ^{1}H ($CDCl_3$): 4.71-4.81 (H-2', 1H, d, J=3.6Hz), 3.99-4.05 (H-1_a, 1H, dd, J=3.4, 10.5Hz), 3.84-3.87 (H-6', 1H, d, J=3.0), 3.71-3.78 (H-5', 1H, m), 3.56-3.71 (H-1_b, H-3', H-4', H7'$_{ab}$, 5H, m), 3.42-3.55 (H-2, H-3, H-4, 3H, m), 1.33-1.53 (H-5_a, H-7_a, 2H, m), 1.05-1.32 (H-5_b, H-6_{ab}, H-7_b, H-8_{ab}– H17_{ab}, 24H, m), 0.73-0.79 (H-18_{abc}, 3H, t, J=6.6Hz). δ ^{13}C ($CDCl_3$): 100.25 (C-2'), 74.89 (C-3), 71.73 (C-4), 71.09 (C-5'), 69.98 (C-3') 68.55 (C-6'), 68.01 (C-4'), 67.64 (C-1), 64.93, 64.36 (C-2, C-6'), 35.19 (C-5), 32.75 (C-6), 31.31 (C-8 – C-16), 26.24 (C-7), 15.71 (C-18). **m/z** (ES): 529.4 (M^+ + $[Na]^+$ + $[H]^+$ 5%), 528.4 (M^+ + $[Na]^+$ 100%), 242.3 (M^+ + $[Na]^+$ + $[Na]^+$ - Gal-O-CH_2-$CH(N_3)$-CH(OH)-CH(OH) 25%). HRMS: Calculated for $C_{24}H_{47}N_3O_8$ [M + Na]$^+$ 528.3261, found 528.3238. α_D: +44.0° m.p.: 121-137°C. IR: 3200-3400cm^{-1} (br OH), 2040-2080cm^{-1} (azide).

5.13.2. (2S,3R,4S,5R,6R)-2-((2S,3S,4R)-2-Azido-3,4-dihydroxy-pentadecyloxy)-6-hydroxymethyl-tetrahydro-pyran-3,4,5-triol (40)

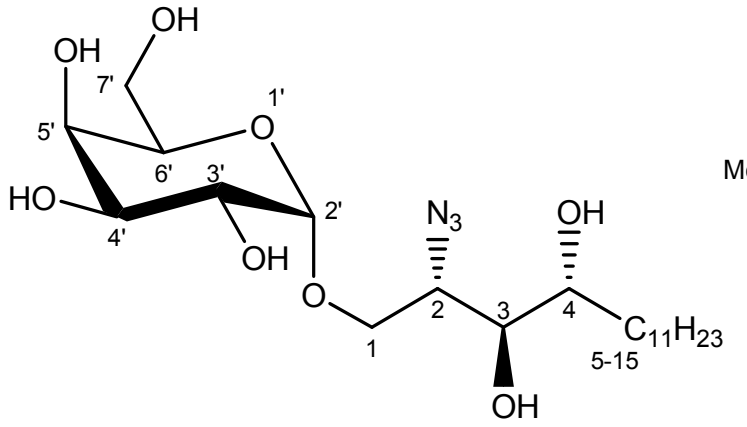

$C_{21}H_{41}N_3O_8$

Mol. Wt.: 463.5657 g mol^{-1}

Prepared by the general procedure for the removal of benzoyl protecting groups using **(5.1.1.11)** 2-(2-azido-3,4-*bis*-benzoyloxy-pentadecyloxy)-6-hydroxymethyl-tetrahydro-pyran-3,4,5-triol **(36)** (156mg, 0.23mmol), THF (5ml), MeOH (2ml), 0.5M NaOMe in MeOH (27.6mg, 1.02ml, 0.51mmol), affording a yellow oil. Yield 21mg, 20.9%. δ ^{1}H ($CDCl_3$:MeOD, 2:1): 4.86-4.88 (H-2', 1H, d, J=3.7 Hz), 4.06-4.13 (H-1_a, 1H, dd, J=3.4, 10.8Hz), 3.91-3.92 (H-6', 1H, d, J= 2.8Hz), 3.83-3.85 (H-5', 1H, t, J=5.6), 3.69-3.80 (H-1_b, 3', 4', 7'$_{ab}$, 5H, m), 3.60-3.65 (H-2, H-3, 2H, m), 3.54-3.59 (H-4, 1H, m), 1.60-1.67 (H-5_a 1H, m), 1.49-1.58 (H-7_a 1H, m), 1.20-1.43 (H-5_b, H-6_{ab}, H-7_b, H-8_{ab} – H-14_{ab}, 18H, m,), 0.82-0.86 (H-15_{abc}, 3H, t, J=6.8Hz). δ ^{13}C ($CDCl_3$:MeOD, 2:1): 100.25 (C-2'), 74.84 (C-3), 72.37 (C-4), 71.59 (C-5'), 70.72 (C-3'), 70.36 (C-6'), 69.42 (C-4'), 68.09 (C-1), 62.39, 62.39 (C-2, 7'), 33.09 (C-5), 32.38 (C-6), 30.19-29.79 (multiple signals, C-8-13), 26.20 (C-7), 23.09 (C-14), 14.25 (C-15). **m/z** (ES): 487.66 (M^+ + $[Na]^+$ + $[H]^+$ 5%), 486.66 (M^+ + $[Na]^+$ 100%). HRMS: Calculated for $C_{24}H_{47}N_3O_8$ [M + Na]$^+$ 486.6357, found 586.6364. α_D: +81.4° IR: 3200-3400cm^{-1} (br OH), 2040-2080cm^{-1} (azide).

5.13.3. (2S,3R,4S,5R,6R)-2-((2S,3S,4R)-2-Azido-3,4-dihydroxy-dodecyloxy)-6-hydroxymethyl-tetrahydro-pyran-3,4,5-triol (41)

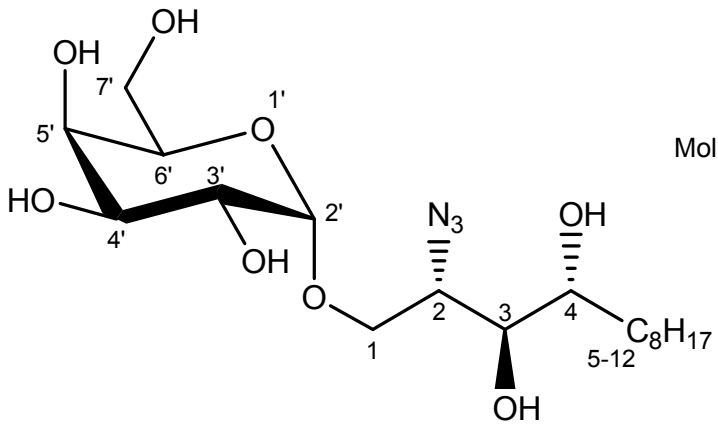

$C_{18}H_{35}N_3O_8$

Mol. Wt.: 421.4859 g mol^{-1}

Prepared by the general procedure for the removal of benzoate protecting groups **(5.1.1.11)** using 2-(2-azido-3,4-*bis*-benzoyloxy-dodecyloxy)-6-hydroxymethyl-tetrahydro-pyran-3,4,5-triol **(37)** (95mg, 0.15mmol), THF (5ml), MeOH (2ml), 0.5M NaOMe in MeOH (1.8eq, 14.6mg, 0.54ml, 0.27mmol), affording a colourless oil. Yield 55.6mg, 88%. δ ^{1}H ($CDCl_3$:MeOD, 2:1): 4.84-4.87 (H-2', 1H, d, J=3.6 Hz), 4.06-4.10 (H-1_a, 1H, dd, J=3.6, 10.6Hz), 3.91 (H-6', 1H, s), 3.79-3.83 (H-5', 1H, t, J=5.5), 3.74-3.78 (H-1_b, 3', 4', 7'$_{ab}$, 5H, m), 3.67-3.64 (H-2, H-3, 2H, m), 3.58-3.66 (H-4, 1H, m), 1.46-1.59 (H-5_a 1H, m), 1.33-1.43 (H-7_a 1H, m), 1.19-1.32 (H-5_b, H-6_{ab}, H-7_b, H-8_{ab} – H-11_{ab}, 12H, m,), 0.79-0.84 (H-12_{abc}, 3H, t, J=6.7Hz). δ ^{13}C ($CDCl_3$:MeOD, 2:1):101.45 (C-2'), 75.67 (C-3), 71.21 (C-4), 71.15 (C-5'), 69.33 (C-3'), 69.16 (C-6'), 68.58 (C-4'), 68.09 (C-1), 62.59, 62.29 (C-2, 7'), 30.09 (C-5), 29.14 (C-6), 29.01-27.98 (multiple signals, C-8-11), 25.30 (C-7), 13.15 (C-12). **m/z** (ES): 445.4937 (M^+ + $[Na]^+$ + $[H]^+$ 5%), 444.4857 (M^+ + $[Na]^+$ 100%). HRMS: Calculated for $C_{24}H_{47}N_3O_8$ $[M + Na]^+$ 444.4857, found 444.4850. α_D: +198.4° IR: 3200-3400cm^{-1} (br OH), 2040-2080cm^{-1} (azide).

5.13.4. (2S,3R,4S,5R,6R)-2-((2S,3S,4R)-2-Azido-3,4-dihydroxy-nonyloxy)-6-hydroxymethyl-tetrahydro-pyran-3,4,5-triol (42)

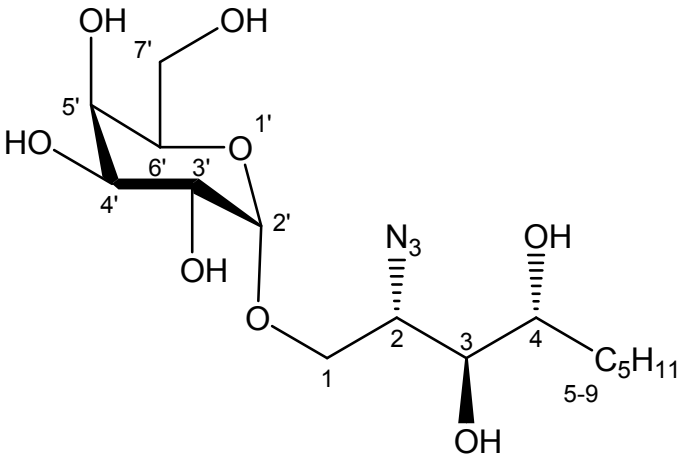

$C_{15}H_{29}N_3O_8$

Mol. Wt.: 379.4062 g mol^{-1}

Prepared by the general procedure for the removal of benzoyl protecting groups using 2-(2-azido-3,4-*bis*-benzoyloxy-nonyloxy)-6-hydroxymethyl-tetrahydro-pyran-3,4,5-triol **(38)** (43mg, 73.2µmol), THF (2ml), MeOH (1ml), 0.5M NaOMe in MeOH (2eq, 3.95mg, 0.146ml, 146.4µmol), affording a colourless oil. Yield 23.6mg, 85.0%. δ ^{1}H ($CDCl_3$:MeOD, 2:1): 4.81-4.86 (H-2', 1H, d, J=3.4 Hz), 4.05-4.10 (H-1_a, 1H, dd, J=3.5, 10.6Hz), 3.93-3.95 (H-6', 1H, d, J=2.7Hz), 3.79-3.82 (H-5', 1H, t, J=5.6), 3.71-3.76 (H-1_b, 3', 4', 7'$_{ab}$, 5H, m), 3.63-3.67 (H-2, H-3, 2H, m), 3.55-3.69 (H-4, 1H, m), 1.40-1.51 (H-5_a 1H, m), 1.35-1.44 (H-7_a 1H, m), 1.11-1.29 (H-5_b, H-6_{ab}, H-7_b, H-8_{ab} 12H, m,), 0.81-0.88 (H-9_{abc}, 3H, t, J=6.4Hz). δ ^{13}C ($CDCl_3$:MeOD, 2:1): 100.32 (C-2'), 76.57 (C-3), 72.77 (C-4), 71.45 (C-5'), 70.21 (C-3'), 69.86 (C-6'), 68.97 (C-4'), 68.01(C-1), 61.58, 61.49 (C-2, 7'), 32.61 (C-5), 30.08 (C-6), 29.01(C-8), 26.36 (C-7), 15.15 (C-8). **m/z** (ES): 403.4140 (M^+ + $[Na]^+$ + $[H]^+$ 10%), 402.406 (M^+ + $[Na]^+$ 100%). HRMS: Calculated for $C_{24}H_{47}N_3O_8$ [M + Na]$^+$ 402.4060, found 402.4064. α_D: +48.3° IR: 3200-3400cm^{-1} (br OH), 2040-2080cm^{-1} (azide).

5.14. Synthesis of *N*-hydroxy succinimide esters

5.14.1. Hexacosanoic acid 2,5-dioxo-pyrrolidin-1-yl ester (43)

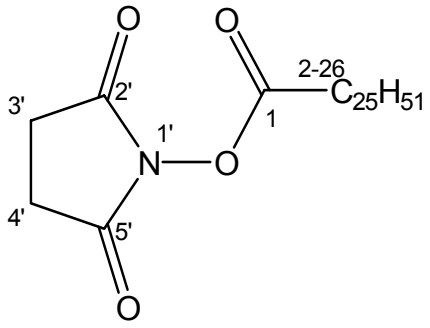

$C_{29}H_{53}NO_4$

Mol. Wt.: 479.7355 g mol^{-1}

Prepared by the general procedure for *N*-hydroxy succinimide carboxylic acid ester **(5.1.1.12)** using hexacosanoic acid (0.2g, 0.504mmol) dry DCM (6ml), *N*-(3-dimethylaminopropyl)-*N*'-ethyl carbodiimide hydrochloride (107mg, 0.558mmol) and *N*-hydroxysuccinimide (69.6mg, 0.604mmol). Yield 0.277g of a white foamy solid (92.88%). δ ^{1}H ($CDCl_3$): 2.80-2.86 (H-3'$_{ab}$, H-4'$_{ab}$, 4H, m), 2.56-2.63 (H-2$_{ab}$, 2H, t, J=7.49Hz) 1.68-1.79 (H-3$_{ab}$, 2H, m), 1.14-1.43 (H-4$_{ab}$ - H-25$_{ab}$, 44H, m), 0.84-0.90 (H-26$_{abc}$, 3H, t, J=6.6Hz). δ ^{13}C ($CDCl_3$): 67.33 (C-3', C-4', d), 23.60-27.71 (multiple signals, C-2-25), 12.44 (C-26). **m/z** (ES): 542.7 (M^+ + $[Na]^+$ + $[K]^+$ + $[H]^+$ 10%), 541.7 (M^+ + $[Na]^+$ + $[K]^+$ 100%).

5.15. Addition of an *N*-acyl chain

5.15.1. Hexacosanoic acid [(1S,2S,3R)-2,3-dihydroxy-1-((2S,3R,4S,5R,6R)-3,4,5-trihydroxy-6-hydroxymethyl-tetrahydro-pyran-2-yloxymethyl)-heptadecyl]-amide (44)

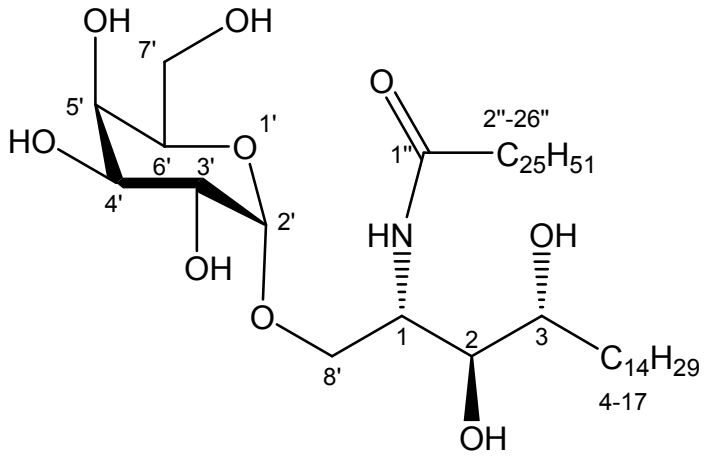

$C_{50}H_{99}NO_9$

Mol. Wt.: 858.3224 g mol^{-1}

Prepared by the general procedure for azide reduction and subsequent *N*-acylation **(5.1.1.13)** using (2S,3R,4S,5R,6R)-2-((2S,3S,4R)-2-azido-3,4-dihydroxy-octadecyloxy)-6-hydroxymethyl-tetrahydro-pyran-3,4,5-triol **(39)** (250mg, 0.494mmol), hexacosanoic acid 2,5-dioxo-pyrrolidin-1-yl ester **(43)** (325mg, 0.658mmol) affording a white solid. Yield: 203mg, 47.8%. δ ^{1}H ($CDCl_3$:MeOD, 2:1): 4.85-4.88 (H-2', 1H, d, J=3.8Hz), 3.96-3.98 (H-1, 1H, m), 3.70-3.75 (H-4', 1H, m), 3.61-3.67 (H-8_a, 1H, dd, J=4.7, 11.1Hz), 3.72-3.77 (H-3', H-6', 2H, m), 3.66-3.71 (H-5', H-$7'_{ab}$, 3H, m), 3.45-3.48 (H-8_b, 1H,dd, J=4.5, 10.8Hz), 3.31-3.34 (H-2, H-3, 2H, m), 2.01-2.06 (H-$2''_{ab}$, 2H, t, J=7.6Hz), 1.40-1.45 (H-$3''_a$, H-$4''_a$, H-4_a, 3H, m), 1.10-1.35 (H-$3''_b$, H-$4''_b$, H-4_b, H-5_{ab} – H13_{ab}, H-$5''_{ab}$ – H-$25''_{ab}$, 70H, m), 0.75-0.81 (H-14_{abc}, H-$26''_{abc}$, 6H, J=6.7Hz). δ ^{13}C ($CDCl_3$:MeOD, 2:1): 178.6 (C-1''), 103.8 (C-2'), 77.6 (C-2), 74.2 (C-3), 69.8 (C-6'), 68.5 (C-5'), 68.2 (C4'), 66.4 (C-3'), 65.1 (C-8), 63.5 (C-7'), 50.1 (C-1), 24.8-39.7(multiple signals C-2'' – C-25'', C-5 – C-16), 18.5, 17.9 (C-26'', C-17).

m/z (ES): 881.7 (M^+ + $[Na]^+$ + $[H]^+$ 45%), 880.6 (M^+ + $[Na]^+$ + 100%). HRMS: Calculated for $C_{50}H_{99}NO_9$ [M + Na]+ 880.7239, found 880.7218. α_D:+10.1° m.p.: 135-138°C IR: 3200-3400cm^{-1} (br OH), 1750-1750cm^{-1} (C=O)., 1500-1650cm^{-1} (N-H).

5.15.2. Hexacosanoic acid [(1S,2S,3R)-2,3-dihydroxy-1-((2S,3R,4S,5R,6R)-3,4,5-trihydroxy-6-hydroxymethyl-tetrahydro-pyran-2-yloxymethyl)-tetradecyl]-amide (45)

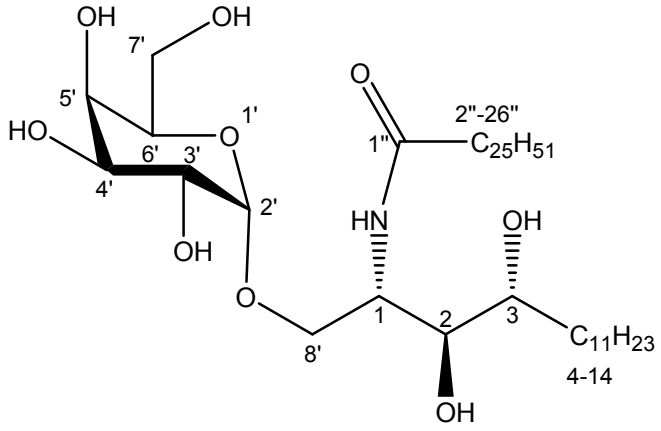

$C_{47}H_{93}NO_9$
Mol. Wt.: 816.2427 g mol^{-1}

Prepared by the general procedure for azide reduction and subsequent *N*-acylation **(5.1.1.13)** using (2S,3R,4S,5R,6R)-2-((2S,3S,4R)-2-azido-3,4-dihydroxy-pentadecyloxy)-6-hydroxymethyl-tetrahydro-pyran-3,4,5-triol **(40)** (45mg, 97.1µmol), hexacosanoic acid 2,5-dioxo-pyrrolidin-1-yl ester **(43)** (47.4mg, 0.134 mmol), affording a white solid. Yield: 41.2mg, 52%. δ ^{1}H ($CDCl_3$:MeOD, 2:1): 4.84-4.86 (H-2', 1H, d, J=3.7Hz), 4.13-4.16 (H-1, 1H, m), 3.87-3.89 (H-4', 1H, d, J=2.98Hz), 3.81-3.86 (H-8_a, 1H, dd, J=4.81, 11.0Hz), 3.72-3.77 (H-3', H-6', 2H, m), 3.66-3.71 (H-5', H-$7'_{ab}$, 3H, m), 3.61-3.66 (H-8_b, 1H, m), 3.46-3.51 (H-2, H-3, 2H, m), 2.13-2.17 (H-$2''_{ab}$, 2H, t, J=7.5Hz), 1.46-1.65 (H-$3''_a$, H-$4''_a$, H-4_a, 3H, m), 1.11-1.35 (H-$3''_b$, H-$4''_b$, H-4_b, H-5_{ab} – H13_{ab}, H-$5''_{ab}$ – H-$25''_{ab}$, 70H, m), 0.81-0.85 (H-14_{abc}, H-$26''_{abc}$, 6H, J=6.8Hz). δ ^{13}C ($CDCl_3$:MeOD, 2:1):102.50 (C-2'), 76.77 (C-2), 74.94 (C-3), 73.66 (C-6'),

73.12 (C-5'), 72.88 (C4'), 71.86 (C-3'), 70.76 (C-8), 65.02 (C-7'), 64.47 (C-1), 25.57-35.14 (multiple signals C-2'' – C-25'', C-4 – C-13), 16.93 (d, C-26'', C-14). **m/z** (ES): 853.7 (M^+ + $[H]^+$ + 2 x H_2O 5%), 852.7 (M^+ + 2 x H_2O 20%), 838.6 (M^+ + $[Na]^+$ + 100%). HRMS: Calculated for $C_{50}H_{99}NO_9$ [M + Na]+ 838.6760, found 838.6748. α_D: +26.7° m.p.: 127-132°C IR: 3200-3400cm^{-1} (br OH), 1750-1750cm^{-1} (C=O)., 1500-1650cm^{-1} (N-H).

5.15.3. Hexacosanoic acid [(1S,2S,3R)-2,3-dihydroxy-1-((2S,3R,4S,5R,6R)-3,4,5-trihydroxy-6-hydroxymethyl-tetrahydro-pyran-2-yloxymethyl)-undecyl]-amide (46)

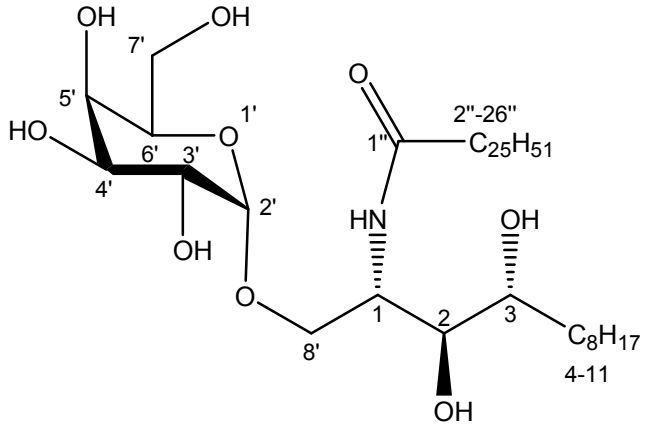

$C_{44}H_{87}NO_9$

Mol. Wt.: 774.1629 g mol^{-1}

Prepared by the general procedure for azide reduction and subsequent *N*-acylation **(5.1.1.13)** using (2S,3R,4S,5R,6R)-2-((2S,3S,4R)-2-azido-3,4-dihydroxy-dodecyloxy)-6-hydroxymethyl-tetrahydro-pyran-3,4,5-triol **(41)** (50mg, 0.119mmol), hexacosanoic acid 2,5-dioxo-pyrrolidin-1-yl ester **(43)** (71.7mg, 0.145mmol), affording a white solid. Yield: 3.32mg, 36%. δ ^1H ($CDCl_3$:MeOD, 2:1): 4.84-4.86 (H-2', 1H, d, J=3.8Hz), 4.12-4.16 (H-1, 1H, m), 3.87-3.89 (H-4', 1H, d, J=3.1Hz), 3.81-3.85 (H-8_a, 1H, dd, J=4.8, 10.5Hz), 3.72-3.77 (H-3', H-6', 2H, m), 3.66-3.72 (H-5', H-$7'_{ab}$, 3H, m), 3.61-3.66 (H-8_b, 1H, m), 3.47-3.51 (H-2, H-3, 2H, m), 2.14-2.18 (H-$2''_{ab}$, 2H, t, J=7.7Hz), 1.46-1.65 (H-$3''_a$, H-$4''_a$, H-4_a, 3H, m), 1.16-1.34

(H-3''$_b$, H-4''$_b$, H-4$_b$, H-5$_{ab}$ – H10$_{ab}$, H-5''$_{ab}$ – H-25''$_{ab}$, 57H, m), 0.81-0.85 (H-11$_{abc}$, H-26''$_{abc}$, 6H, J=6.6Hz). δ ^{13}C ($CDCl_3$:MeOD, 2:1): 101.80 (C-2'), 76.89 (C-2), 74.17 (C-3), 72.97 (C-6'), 73.00 (C-5'), 72.56 (C4'), 71.80 (C-3'), 70.13 (C-8), 65.54 (C-7'), 64.37 (C-1), 24.77-36.04 (multiple signals C-2'' – C-25'', C-4 – C-10), 17.03 (d, C-26'', C-11). **m/z** (ES): 797.6 (M^+ + $[Na]^+$ + $[H]^+$ 50%), 796.5 (M^+ + $[Na]^+$ 100%). HRMS: Calculated for $C_{44}H_{87}NO_9$ [M + Na]$^+$ 797.6289, found 797.6279. α_D: +15.6° m.p.: 115-120°C IR: 3200-3400cm^{-1} (br OH), 1750-1750cm^{-1} (C=O), 1500-1650cm^{-1} (N-H).

5.15.4. Hexacosanoic acid [(1S,2S,3R)-2,3-dihydroxy-1-((2S,3R,4S,5R,6R)-3,4,5-trihydroxy-6-hydroxymethyl-tetrahydro-pyran-2-yloxymethyl)-octyl]-amide (47)

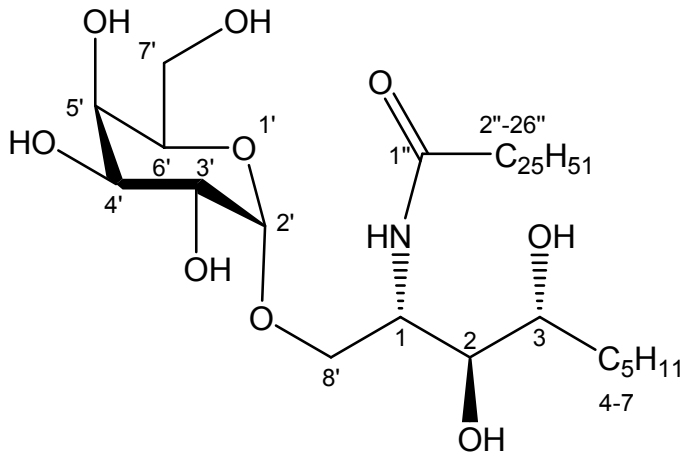

$C_{41}H_{81}NO_9$
Mol. Wt.: 732.0832 g mol^{-1}

Prepared by the general procedure for azide reduction and subsequent *N*-acylation **(5.1.1.13)** using (2S,3R,4S,5R,6R)-2-((2S,3S,4R)-2-azido-3,4-dihydroxy-nonyloxy)-6-hydroxymethyl-tetrahydro-pyran-3,4,5-triol **(42)** (15mg, 39.5μmol), hexacosanoic acid 2,5-dioxo-pyrrolidin-1-yl ester **(43)** (19.6mg, 39.6μmol), affording a white solid. Yield: 12.mg, 42.8%. δ ^{1}H ($CDCl_3$:MeOD, 2:1): 4.84-4.89 (H-2', 1H, d, J=3.4Hz), 4.13-4.16 (H-1, 1H, m), 3.86-3.89 (H-4', 1H, d, J=2.98Hz), 3.81-3.86 (H-8$_a$, 1H, dd, J=4.6, 10.5Hz), 3.72-3.78 (H-3',

H-6', 2H, m), 3.66-3.72 (H-5', H-7'$_{ab}$, 3H, m), 3.60-3.66 (H-8$_b$, 1H, m), 3.47-3.52 (H-2, H-3, 2H, m), 2.13-2.18 (H-2''$_{ab}$, 2H, t, J=7.9Hz), 1.53-1.67 (H-3''$_a$, H-4''$_a$, H-4$_a$, 3H, m), 0.94-1.46 (H-3''$_b$, H-4''$_b$, H-4$_b$, H-5$_{ab}$ – H6$_{ab}$, H-5''$_{ab}$ – H-25''$_{ab}$, 49H, m), 0.79-0.86 (H-7$_{abc}$, H-26''$_{abc}$, 6H, J=67.3Hz). δ ^{13}C ($CDCl_3$:MeOD, 2:1): 103.60 (C-2'), 77.67 (C-2), 75.49 (C-3), 73.66 (C-6'), 73.21 (C-5'), 72.68 (C4'), 71.68 (C-3'), 70.67 (C-8), 65.20 (C-7'), 64.74 (C-1), 23.75-33.41 (multiple signals C-2'' – C-25'', C-4 – C-6), 16.93 (d, C-26'', C-7). **m/z** (ES): 755.6 (M^+ + $[H]^+$ + $[Na]^+$ 25%), 754.5 (M^+ + $[Na]^+$ + 100%). HRMS: Calculated for $C_{41}H_{81}NO_9$ $[M + Na]^+$ 754.5809, found 754.5812. α_D: +12.6° IR: 3200-3400cm^{-1} (br OH), 1750-1750cm^{-1} (C=O)., 1500-1650cm^{-1} (N-H).

5.16. Glycosylation with glucose

5.16.1. (2S,3R,4S,5S,6R)-2-((2S,3S,4R)-2-Azido-3,4-*bis*-benzyloxy-octadecyloxy)-6-hydroxymethyl-tetrahydro-pyran-3,4,5-triol (48)

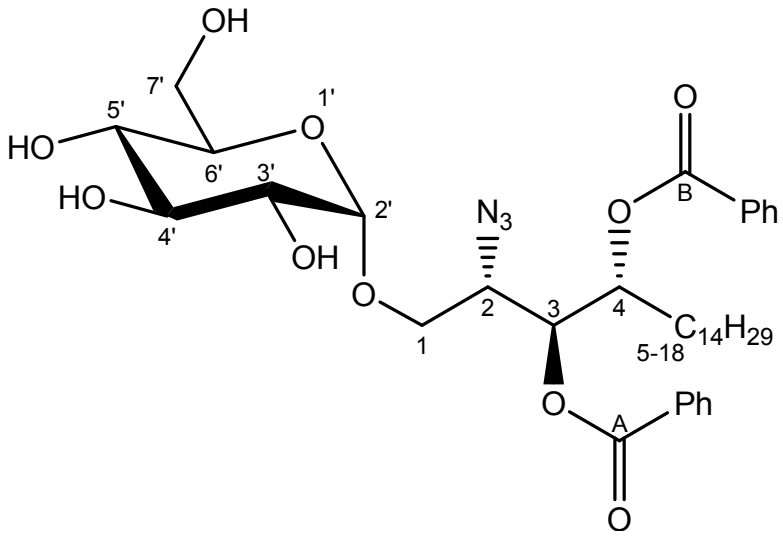

$C_{38}H_{55}N_3O_{10}$
Mol. Wt.: 713.8575 g mol^{-1}

Prepared by the general procedure for the coupling of sugars with phytosphingosine analogues **(5.1.1.10)** using pertrimethylsilylated glucose **(33)** (1g, 1.85mmol), DCM (15ml),

iodotrimethylsilane (370mg, 0.26ml, 1.85mmol), benzene (3ml, then 2 x 1ml, then 3ml), MS 4Å (600mg), tetrabutylammonium iodide (1.37g, 3.7mmol), (2S,3S,4R)-2-azido-3,4-*bis*-benzoyloxy-octadecan-1-ol **(28)** (340mg, 0.616mmol), diisopropylethylamine (360mg, 0.48ml, 2.775mmol), benzene (6ml), MeOH (10ml), and Dowex© 50WX8-200 resin (6g), affording a pale orange syrup. Yield 175mg, 39.79%, δ ^{1}H ($CDCl_3$): 7.25-8.22 (Ar-H, 10H, m), 5.59-5.65 (H-3, 1H, m), 5.45-5.53 (H-4, 1H, m), 4.72-4.75 (H-2', 1H, d, J=3.4Hz), 4.04-4.13 (H-7'$_a$, 1H, dd, J=3.1, 10.6Hz), 3.8-3.91 (H-2, H-5', 2H, m), 3.64-3.80 (H-4', 1H, m), 3.48-3,64 (H-1$_{ab}$, H-3', H-6', 4H, m), 3.37-3.48 (H-7'$_b$, 1H, m), 1.66-1.89 (H-5$_{ab}$, 2H, m), 1.11-1.31 (H-6$_{ab}$ – H-17$_{ab}$ 6H, m), 0.81-0.87 (H-18$_{abc}$, 3H, t, J=6.5Hz) δ ^{13}C ($CDCl_3$): 168.5, 168.09 (C-A, -B), 132.24-133.37 (multiple signals, Ar C), 131.99, 131.48 (QC-Ar), 101.70 (C-2'), 76.79 (C-4), 75.45 (C-3), 74.62 (C-4'), 74.48 (C-6'), 72.28 (C-5'), 69.74 (C-1), 64.18 (C-7') 63.09 (C-1), 63.00 (C-2), 25.19-34.41 (multiple signals, C-5 – C-17), 16.62 (C-18). **m/z** (ES): 737.1 (M^+ + $[Na]^+$ + $[H]^+$ 20%), 636.3 (M^+ + $[Na]^+$ 100%), HRMS: Calculated for $C_{38}H_{55}N_3O_{10}$ $[M + Na]^+$ 736.3785, found 736.3807. α_D: +80.0° IR: 3200-3400cm^{-1} (br OH), 3100-3000cm^{-1} (Ar), 2040-2080cm^{-1} (azide), 1750-1750cm^{-1} (C=O).

5.17. Removal of benzoate protecting groups

5.17.1. (2S,3R,4S,5S,6R)-2-(2-Azido-3,4-dihydroxy-octadecyloxy)-6-hydroxymethyl-tetrahydro-pyran-3,4,5-triol (49)

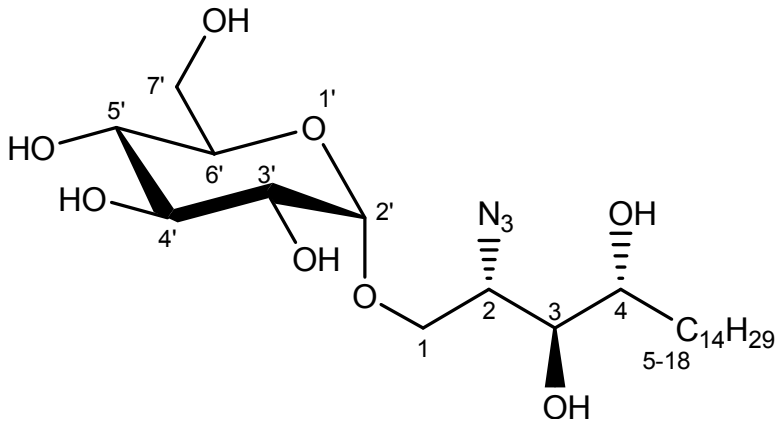

$C_{24}H_{47}N_3O_8$
Mol. Wt.: 505.6454 g mol^{-1}

Prepared by the general procedure for the removal of benzoyl protecting groups **(5.1.1.11)** using (2S,3R,4S,5S,6R)-2-((2S,3S,4R)-2-azido-3,4-*bis*-benzoyloxy-octadecyloxy)-6-hydroxymethyl-tetrahydro-pyran-3,4,5-triol **(48)** (150mg, 0.21mmol), THF (4ml), MeOH (2ml), 0.5M NaOMe in MeOH (1.5eq, 17.02mg, 0.63ml, 0.315mmol), affording an off-white solid. Yield 86mg, 80.99%. δ ^{1}H ($CDCl_3$:MeOD, 2:1): 4.56-4.62 (H-2', 1H, d, J=3.8 Hz), 3.81-3.91 (H-1_a, 1H, dd, J=2.9, 10.9Hz), 3.55-3.62 (H-6', 1H, dd, J= 2.3), 3.46-3.55 (H-5', 1H, m), 3.31-3.45 (H-1_b, 3', 4', 7'$_{ab}$, 5H, m), 3.18-3.24 (H-2, 1H, dd, J=3.7, 9.7Hz), 3.05-3.14 (H-3, H-4, 2H, m), 1.25-1.45 (H-5_a, H-7_a, 2H, m), 0.9-1.18 (H-5_b, H-6_{ab}, H-7_b, H-8_{ab} – H-17_{ab}, 12H, m,), 0.59-0.65 (H-18_{abc}, 3H, t, J=6.5Hz). δ ^{13}C ($CDCl_3$:MeOD, 2:1):105.47 (C-2'), 80.26 (C-3), 79.86 (C-4), 78.45 (C-5'), 78.08 (C-3'), 77.91 (C-6'), 76.38 (C-4'), 73.51 (C-1), 67.99 (C-7'), 67.67 (C-2), 31.79-38.58 (multiple signals C-5 – C-17), 19.89 (C-18). **m/z** (ES): 529.3 (M^+ + $[Na]^+$ + $[H]^+$ 20%), 528.3 (M^+ + $[Na]^+$ 100%). HRMS: Calculated for $C_{24}H_{47}N_3O_8$ [M + Na]$^+$ 528.3261, found 528.3249. α_D: +210.0° m.p.: 125-136°C IR: 3200-3400cm^{-1} (br OH), 2040-2080cm^{-1} (azide).

5.18. Addition of an *N*-acyl chain

5.18.1. Hexacosanoic acid [(1S,2S,3R)-2,3-dihydroxy-1-((2S,3R,4S,5S,6R)-3,4,5-trihydroxy-6-hydroxymethyl-tetrahydro-pyran-2-yloxymethyl)-heptadecyl]-amide (50)

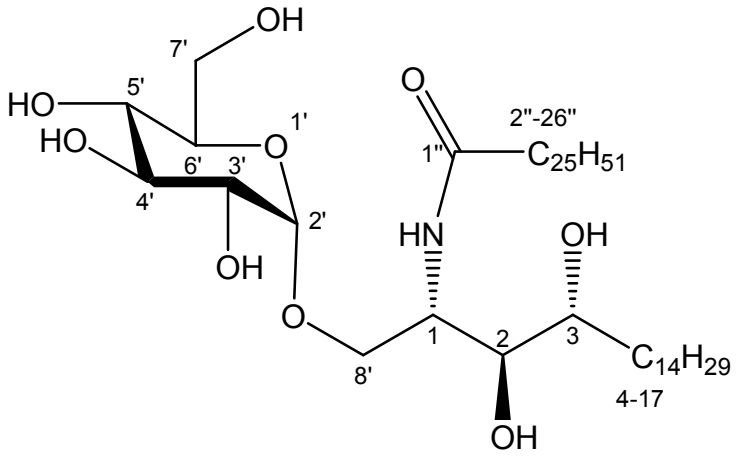

$C_{49}H_{97}NO_9$

Mol. Wt.: 844.2958

Prepared by the general procedure for azide reduction and subsequent *N*-acylation **(5.1.1.13)** using (2S,3R,4S,5S,6R)-2-((2S,3S,4R)-2-azido-3,4-dihydroxy-octadecyloxy)-6-hydroxymethyl-tetrahydro-pyran-3,4,5-triol **(49)** (45mg, 88.99µmol), hexacosanoic acid 2,5-dioxo-pyrrolidin-1-yl ester **(43)** (56.9mg, 115µmol), affording a white solid. Yield: 42mg, 56%. δ ^{1}H ($CDCl_3$:MeOD, 2:1): 4.80-4.82 (H-2', 1H, d, J=3.7Hz), 4.12-4.16 (H-1, 1H, m), 4.01-4.04 (H-4', 1H, m), 3.81-3.85 (H-8'$_a$, 1H, dd, J=4.6, 10.8Hz), 3.73-3.77 (H-5', 1H, dd, J=2.72Hz), 3.49-3.68 (H-6', H-7'$_{ab}$, H-8'$_{b,}$ H-2, H-3, 6H, m), 3.38-3.42 (H-3', 1H, dd, J= 3.7, 9.6Hz), 2.14-2.18 (H-2''$_{ab}$, 2H, m), 1.46-1.65 (H-3''$_a$, H-4''$_a$, H-4$_a$, 3H, m), 1.11-1.35 (H-3''$_b$, H-4''$_b$, H-4$_b$, H-5$_{ab}$ – H16$_{ab}$, H-5''$_{ab}$ – H-25''$_{ab}$, 69H, m), 0.81-0.85 (H-17$_{abc}$, H-26''$_{abc}$, 6H, J=6.8Hz). δ ^{13}C ($CDCl_3$:MeOD, 2:1): 102.50 (C-2'), 76.77 (C-2), 74.94 (C-3), 73.66 (C-6'), 73.12 (C-5'), 72.88 (C4'), 71.86 (C-3'), 70.76 (C-8'), 65.02 (C-7'), 64.47 (C-1), 25.57-35.14 (multiple signals C-2'' – C-25'', C-4 – C-13), 16.93 (d, C-26'', C-14). **m/z** (ES): 868.3 (M^+ + $[H]^+$ + $[Na]^+$ 10%), 867.3 (M^+ + $[Na]^+$ + 100%). HRMS: Calculated for $C_{49}H_{97}NO_9$ [M + Na]$^+$

867.2935, found 867.2947. α_D: +24.0° m.p. 135-139°C IR: 3200-3400cm^{-1} (br OH), 1750-1750cm^{-1} (C=O)., 1500-1650cm^{-1} (N-H).

5.19. Glycosylation with L-fucose

5.19.1. (2R,3S,4R,5S,6S)-2-((2S,3S,4R)-2-Azido-3,4-*bis*-benzyloxy-octadecyloxy)-6-methyl-tetrahydro-pyran-3,4,5-triol (51)

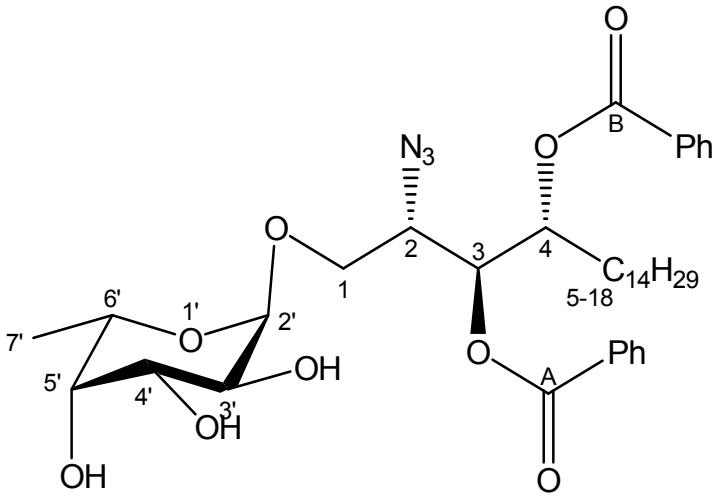

$C_{38}H_{55}N_3O_9$

Mol. Wt.: 697.8581 g mol^{-1}

Pertrimethylsilylated L-fucose **(34)** (1g, 2.21mmol) was dissolved in anhydrous DCM (10ml). Iodotrimethylsilane (442mg, 0.315ml, 2.21mmol) was added and the solution stirred at RT for 20min. A solution of (2S,3S,4R)-2-azido-3,4-*bis*-benzoyloxy-octadecan-1-ol **(28)** (0.3445g, 0.8096mmol) and 2,6-di-*tert*-di-butylphenol (0.493g, 0.597ml, 2.58mmol) in anhydrous toluene (5ml) was azeotroped thrice, before being dissolved in anhydrous DCM and added to the fucose solution and stirred at RT for 18h. MeOH (30ml) was added and stirred at RT for 30min. The solution was neutralised with triethylamine, before being concentrated. The compound was purified by CC (Petrol: EtOAc; 20:80) affording a pale yellow oil. Yield 181mg, 32.04%. δ ^{1}H ($CDCl_3$): 7.36-7.86 (Ar-H, 10H, m), 5.58-5.64 (H-3, 1H, m), 5.47-5.55 (H-4, 1H, m), 4.80-4.91 (H-2', 1H, d, J=2.8Hz), 3.88-4.00 (H-3', H-5', H-6',

3H, m), 3.62-3.80 (H-1_{ab}, H-2, H-4', 4H, m), 1.76-1.91 (H-5_{ab}, 2H, m), 1.10-1.43 (H-6_{ab} – H-17_{ab} 24H, m), 1.06-1.09 (H-$7'_{abc}$, 3H, d, J=6.6Hz), 0.81-0.88 (H-18_{abc}, 3H, t, J=6.6Hz). δ ^{13}C ($CDCl_3$): 130.45-135.64 (multiple signals, Ar C), 100.91 (C-2'), 62.60-74.99 (multiple signals C-2, C-3, C-4, C-3', C-4', C-5', C-6') 69.27 (C-1), 24.61-33.84 (multiple signals, C-5 – C-17), 31.93 (C-7'), 15.43 (C-18). **m/z** (ES): 721.5 (M^+ + $[Na]^+$ + $[H]^+$ 20%), 720.5 (M^+ + $[Na]^+$ 100%), HRMS: Calculated for $C_{38}H_{55}N_3O_{10}$ $[M + Na]^+$ 720.3836, found 720.3811. α_D: -20.0° IR: 3200-3400cm^{-1} (br OH), 3100-3000cm^{-1} (Ar), 2040-2080cm^{-1} (azide), 1750-1750cm^{-1} (C=O).

5.20. Removal of benzoate protecting groups

5.20.1. (2R,3S,4R,5S,6S)-2-((2S,3S,4R)-2-Azido-3,4-dihydroxy-octadecyloxy)-6-methyl-tetrahydro-pyran-3,4,5-triol (52)

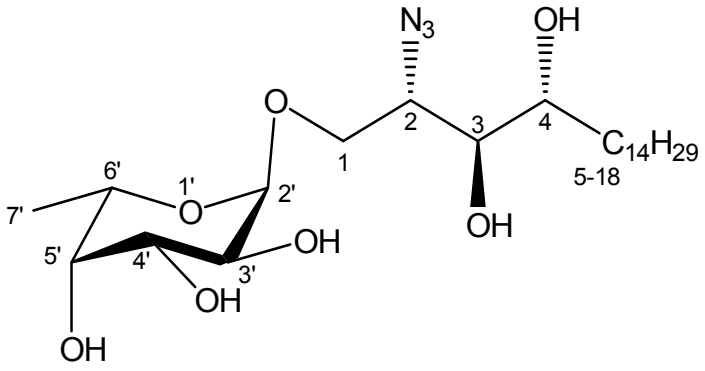

$C_{24}H_{47}N_3O_7$
Mol. Wt.: 489.6460 g mol^{-1}

Prepared by the general procedure for the removal of benzoyl protecting groups **(5.1.1.13)** using (2R,3S,4R,5S,6S)-2-((2S,3S,4R)-2-azido-3,4-*bis*-benzoyloxy-octadecyloxy)-6-methyl-tetrahydro-pyran-3,4,5-triol **(51)** (181mg, 0.259mmol), THF (5ml), MeOH (2ml), 0.5M NaOMe in MeOH (1.5eq, 20.99mg, 0.78ml, 0.3885mmol), affording an off-white solid. Yield 67mg, 52.8%. δ ^1H ($CDCl_3$:MeOD, 2:1): 4.55-4.57 (H-2', 1H, d, J=3.1 Hz), 3.03-3.71 (H-1ab, H-2 – H-4, H-2' – H-6', 10H, m) 1.34-1.45 (H-5_a, H-7_a, 2H, m), 0.93-1.26 (H-5_b,

H-6_{ab}, H-7_b, H-8_{ab} – H-17_{ab}, H-$7'_{abc}$, 27H, m), 0.57-0.63 (H-18_{abc}, 3H, t, J=6.6Hz). δ ^{13}C ($CDCl_3$:MeOD, 2:1): 100.60 (C-2'), 72.22-73.98 (C-3, C-4, C-3' C-6'), 70.27 (C-1), 68.16 (C-5'), 63.46 (C-2), 24.29-33.53 (multiple signals, C-8-17), 17.83 (C-7'), 15.39 (C-18). **m/z** (ES): 513.5 (M^+ + $[Na]^+$ + $[H]^+$ 8%), 512.5 (M^+ + $[Na]^+$ 100%) HRMS Calculated for $C_{24}H_{47}N_3O_7$ $[M + Na]^+$ 512.3312, found 512.3301. α_D: -168.0°. m.p.: 55-62°C IR: 3200-3400cm^{-1} (br OH), 2040-2080cm^{-1} (azide).

5.21. Addition of an *N*-acyl chain

5.21.1. Hexacosanoic acid [(1S,2S,3R)-2,3-dihydroxy-1-((2R,3S,4R,5S,6S)-3,4,5-trihydroxy-6-methyl-tetrahydro-pyran-2-yloxymethyl)-heptadecyl]-amide (53)

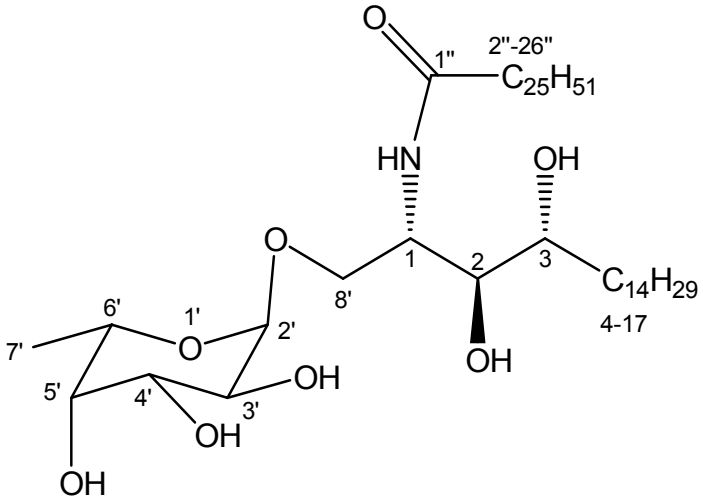

$C_{50}H_{99}NO_8$
Mol. Wt.: 842.3230 g mol^{-1}

Prepared by the general procedure for azide reduction and subsequent *N*-acylation **(5.1.1.13)** using (2R,3S,4R,5S,6S)-2-((2S,3S,4R)-2-azido-3,4-dihydroxy-octadecyloxy)-6-methyl-tetrahydro-pyran-3,4,5-triol **(42)** (35mg, 71.5μmol), hexacosanoic acid 2,5-dioxo-pyrrolidin-1-yl ester **(43)** (49.7mg, 0.101mmol), affording a white solid. Yield: 29.5mg, 49%. δ ^{1}H ($CDCl_3$:MeOD, 2:1): 4.71-4.74 (H-2', 1H, d, J=3.7Hz), 4.14-4.18 (H-1, 1H, m), 3.91-3.96

(H-4', H-5', 2H, m), 3.68-3.72 (H-8_a, 1H, dd, J=3.9, 9.9Hz), 3.61-3.68 (H-3, H-4, 2H, m), 3.52-3.55 (H-3', 1H, t, J=5.99Hz), 3.43-3.49 (H-6', 1H, m), 3.39-3.42 (H-8_b, 1H, dd, J=3.9, 9.9Hz), 2.12-2.17 (H-2''$_{ab}$, 2H, m), 1.43-1.62 (H-3''$_a$, H-4''$_a$, H-4_a, H-5_a, H-6_a, 5H, m), 1.14-1.31 (H-7'$_{abc}$, H-3''$_b$, H-4''$_b$, H-4_b, H-5_b, H-6_b, H-7_{ab} – H-16_{ab}, H-5''$_{ab}$ – H-25''$_{ab}$, 70H, m), 0.81-0.85 (H-14_{abc}, H-26''$_{abc}$, 6H, J=6.9Hz). δ ^{13}C ($CDCl_3$:MeOD, 2:1): 102.50 (C-2'), 76.77 (C-2), 74.94 (C-3), 73.66 (C-6'), 73.12 (C-5'), 72.88 (C4'), 71.86 (C-3'), 70.76 (C-8), 64.47 (C-1), 25.57-35.14 (multiple signals C-7', C-2'' – C-25'', C-4 – C-13), 16.93 (C-26'', C-14). **m/z** (ES): 865.8 (M^+ + $[H]^+$ + $[Na]^+$ 20%), 864.8 (M^+ + $[Na]^+$ 100%). HRMS: Calculated for $C_{50}H_{99}NO_8$ $[M + Na]^+$ 864.7268, found 864.7240. α_D: -10.0°. m.p.: 130-135°C. IR: 3200-3400cm^{-1} (br OH), 1750-1750cm^{-1} (C=O)., 1500-1650cm^{-1} (N-H).

5.22. Synthesis of *N*-hydroxy succinimide esters

5.22.1. Tetracosanoic acid 2,5-dioxo-pyrrolidin-1-yl ester (54)

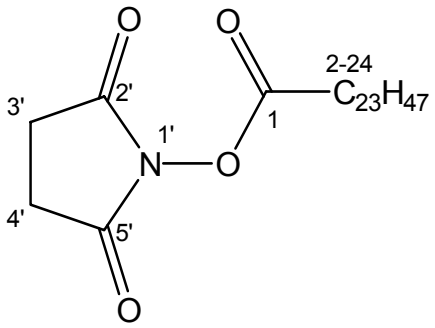

$C_{28}H_{51}NO_4$

Mol. Wt.: 465.7089 g mol^{-1}

Prepared by the general procedure for *N*-hydroxy succinimide carboxylic acid ester **(5.1.1.12)** using tetracosanoic acid (100mg, 0.27mmol), DCM (5ml), *N*-(3-dimethylaminopropyl)-*N*'-ethyl carbodiimide hydrochloride (55.9mg, 0.2916mmol), *N*-hydroxy succinimide (37.3mg, 0.324mmol) and DMAP (10mg), affording a whitish solid. Yield 76mg, 60.42%. δ ^{1}H ($CDCl_3$): 2.80-2.84 (H-3'$_{ab}$, H-4'$_{ab}$, 4H, m), 2.56-2.62 (H-2_{ab}, 2H, t, J=7.51Hz) 1.67-1.79 (H-3_{ab}, 2H, m), 1.20-1.44 (H-4_{ab} - H-23_{ab}, 40H, m), 0.84-0.89 (H-24_{abc}, 3H, t,

J=6.7Hz). δ ^{13}C ($CDCl_3$): 30.80-23.41 (multiple signals, C-2-23), 16.86 (C-29). **m/z** (ES): 489.4 (M^+ + $[Na]^+$ + $[H]^+$ 10%), 488.4 (M^+ + $[Na]^+$ 100%) HRMS: Calculated for $C_{28}H_{51}NO_4$ $[M + Na]^+$ 488.3710, found 488.3716.

5.22.2. (15Z)-Tetracos-15-enoic acid 2,5-dioxo-pyrrolidin-1-yl ester (55)

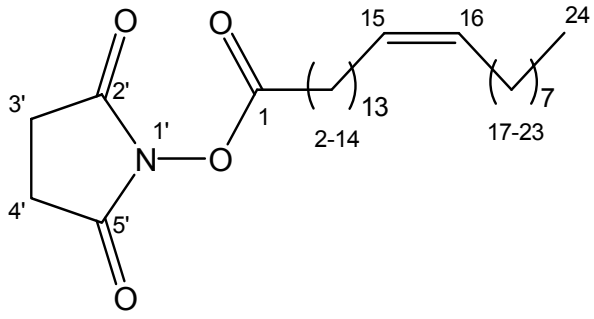

$C_{29}H_{51}NO_4$
Mol. Wt.: 477.7195 g mol^{-1}

Prepared by the general procedure for *N*-hydroxy succinimide carboxylic acid ester **(5.1.1.12)** using (15Z)-tetracos-15-enoic acid (500mg, 1.36mmol), DCM (10ml), *N*-(3-dimethylaminopropyl)-*N*'-ethyl carbodiimide hydrochloride (287mg, 1.49mmol), *N*-hydroxy succinimide (188mg, 1.63mmol), and DMAP (50mg), affording a white solid. Yield 510mg, 78.49%. δ ^1H ($CDCl_3$): 5.36-5.48 (H-15, H-16, 2H, m), 2.76-2.80 (H-3'$_{ab}$, H-4'$_{ab}$, 4H, m), 2.54-2.60 (H-7$_{ab}$, 2H, t, J=7.51Hz) 1.45-2.08 (H-2$_{ab}$ - H-14$_{ab}$, H-17$_{ab}$ – H-23$_{ab}$, 40H, m), 0.84-0.89 (H-24$_{abc}$, 3H, t, J=6.4Hz).δ ^{13}C ($CDCl_3$): 128.26, 127.89 (C-15, C16), 22.94-28.13 (multiple signals, C-2 – C14, C-17 – C23), 18.99 (C-24). **m/z** (ES): 500.7 (M^+ + $[Na]^+$ 100%), 478.7 (M^+ + 10%).

5.22.3. (4Z,7Z,10Z,13Z,16Z,19Z)-Docosa-4,7,10,13,16,19-hexaenoic acid 2,5-dioxo-pyrrolidin-1-yl ester (56)

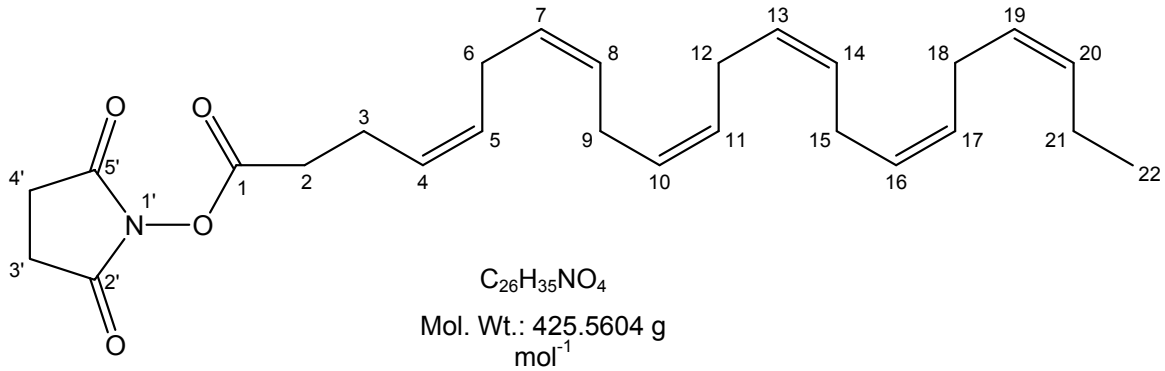

$C_{26}H_{35}NO_4$

Mol. Wt.: 425.5604 g mol^{-1}

Prepared by the general procedure for *N*-hydroxy succinimide carboxylic acid ester **(5.1.1.12)** using 4Z,7Z,10Z,13Z,16Z,19Z)-docosa-4,7,10,13,16,19-hexaenoic acid (100mg, 0.304mmol), DCM (5ml), *N*-(3-dimethylaminopropyl)-*N*'-ethyl carbodiimide hydrochloride (64.1mg, 0.334mmol), *N*-hydroxy succinimide (42.0mg, 0.365mmol) and DMAP (10mg). Yield 84mg, 64.9%. δ ^{1}H ($CDCl_3$): 5.23-5.34 (H-4, H-5, H-7, H-8, H-10, H-11, H-13, H-14, H-16, H-17, H-19, H-20, 12H, m), 2.76-2.80 (H-3'$_{ab}$, H-4'$_{ab}$, 4H, m), 2.70-2.80 (H-2$_{ab}$, H-3$_{ab}$, H-6$_{ab}$, H-9$_{ab}$, H-12$_{ab}$, H-15$_{ab}$, H-18$_{ab}$, H-21$_{ab}$, 16H, m) 0.84-0.91 (H-22$_{abc}$, 3H, t, J=7.4Hz). δ ^{13}C ($CDCl_3$): 128.26-127.02 (multiple signals, C-4, C-5, C-7, C-8, C-10, C-11, C-13, C-14, C-16, C-17, C-19, C-20), 31.35, 34.16 (C-3' C-4'), 20.46-29.9 (multiple signals, C-2, C-3, C-6, C-9, C-12, C-15, C-18, C-21), 14.01 (C-22). **m/z** (ES): 465.2 (M^+ + $[K]^+$ + $[H]^+$15%), 251.1 (M^+ + $[H]^+$ - CH=CH-CH_2-CH=CH-CH_2-CH=CH-CH_2-CH=CH-CH_2-CH_3 10%).

5.22.4. (5Z,8Z,11Z,14Z,17Z)-Eicosa-5,8,11,14,17-pentaenoic acid 2,5-dioxo-pyrrolidin-1-yl ester (57)

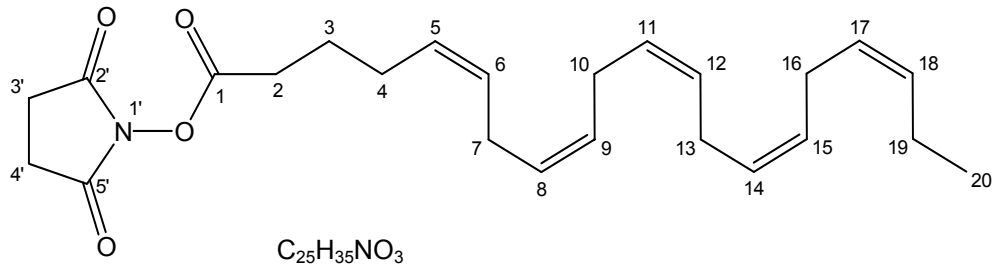

$C_{25}H_{35}NO_3$

Mol. Wt.: 397.5503 g mol^{-1}

Prepared by the general procedure for *N*-hydroxy succinimide carboxylic acid ester **(5.1.1.12)** using (5Z,8Z,11Z,14Z,17Z)-eicosa-5,8,11,14,17-pentaenoic acid (25mg, 82.66 µmol), DCM (2ml), *N*-(3-dimethylaminopropyl)-*N*'-ethyl carbodiimide hydrochloride (17.43mg, 90.9 µmol), *N*-hydroxy succinimide (11.43mg, 99.19 µmol) and DMAP (3mg), affording an creamy oil. Yield 32mg, 97.38%. δ ^{1}H ($CDCl_3$): 5.13-5.40 (H-5, H-6, H-8, H-9, H-11, H-12, H-14, H-15, H-17, H-18, 10H, m), 2.60-2.84 (H-3'$_{ab}$, H-4'$_{ab}$, 4H, m), 2.44-2.54 (H-2$_{ab}$, 2H, m) 0.96-2.22 (H-3$_{ab}$, H-4$_{ab}$, H-7$_{ab}$, H-10$_{ab}$, H-13$_{ab}$, H-16$_{ab}$, H-19$_{ab}$, 14H, m) 0.79-0.89 (H-20$_{abc}$, 3H, t, J=7.5Hz). δ ^{13}C ($CDCl_3$): 170.73, 159.19 (C-2', C-5', C-1), 118.62-133.36 (multiple signals, C-5, C-6, C-8, C-9, C-11, C-12, C-14, C-15, C-17, C-18), 32.35, 35.16 (C-3' C-4'), 29.1-29.6 (multiple signals, C-2, C-3, C-4, C-7, C-10, C-13, C-16, C-19), 8.40 (C-20). **m/z** (ES): 439.3 (M^+ + $[K]^+$ + $[H]^+$ 15%), 265.1 (M^+ + $[H]^+$ - CH=CH-CH_2-CH=CH-CH_2-CH=CH-CH_2-CH_3 90%), 237.1 (M^+ - CH-CH_2-CH=CH-CH_2-CH=CH-CH_2-CH=CH-CH_2-CH_3).

5.22.5. (5Z,8Z,11Z,14Z)-Eicosa-5,8,11,14-tetraenoic acid 2,5-dioxo-pyrrolidin-1-yl ester (58)

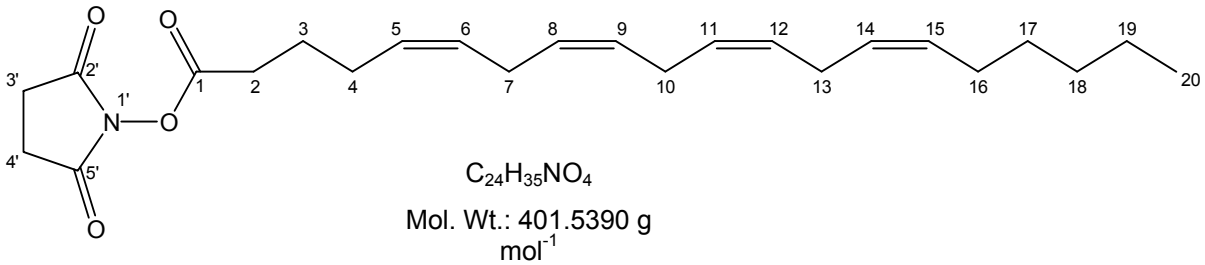

$C_{24}H_{35}NO_4$

Mol. Wt.: 401.5390 g mol^{-1}

Prepared by the general procedure for *N*-hydroxy succinimide carboxylic acid ester **(5.1.1.12)** using arachidonic acid ((5Z,8Z,11Z,14Z)-eicosa-5,8,11,14-tetraenoic acid) (100mg, 0.329mmol), DCM (5ml), *N*-(3-dimethylaminopropyl)-*N*'-ethyl carbodiimide hydrochloride (69.3mg, 0.361mmol), *N*-hydroxy succinimide (45.4mg, 0.394mmol) and DMAP (10mg), affording yellow-cream crystals. Yield 98mg, 74.18%. δ ^{1}H ($CDCl_3$): 5.15-5.32 (H-5, H-6, H-8, H-9, H-11, H-12, H-14, H-15, 8H, m), 2.63-2.77 (H-3'$_{ab}$, H-4'$_{ab}$, 4H, m), 1.01-2.32 (H-2$_{ab}$, H-3$_{ab}$, H-4$_{ab}$, H-7$_{ab}$, H-10$_{ab}$, H-13$_{ab}$, H-16$_{ab}$ – H-19$_{ab}$, 20H, m) 0.68-0.79 (H-20$_{abc}$, 3H, t, J=7.1Hz). δ ^{13}C ($CDCl_3$): 132.34-135.26 (multiple signals, C-5, C-6, C-8, C-9, C-11, C-12, C-14, C-15), 38.41-27.34 (multiple signals C-3', C-4', C-2, C-3, C-4, C-7, C-10, C-13, C-16, C-19), 18.73 (C-20). **m/z** (ES): 460.4 (M^+ + 2 x H_2O + $[Na]^+$ 100%), 400.3 (M^+ + $[H]^+$ + $[Na]^+$ + H_2O – $CH_3CH_2CH_2$ 40%), 389.3 (M^+ + $[H]^+$ + $[Na]^+$ + 2 x H_2O – $CH_2CH_2CH_2CH_2$-CH_3 60%), 375.3 (M^+ + H_2O + -O-C(O)- 10%).

5.22.6. (11Z,14Z)-Eicosa-11,14-dienoic acid 2,5-dioxo-pyrrolidin-1-yl ester (59)

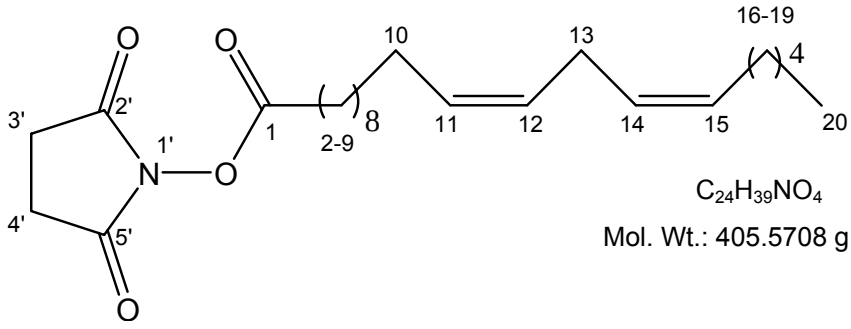

$C_{24}H_{39}NO_4$

Mol. Wt.: 405.5708 g mol^{-1}

Prepared by the general procedure for *N*-hydroxy succinimide carboxylic acid ester **(5.1.1.12)** using eicosadienoic acid (100mg, 0.324mmol), DCM (3ml), *N*-(3-dimethylaminopropyl)-*N*'-ethyl carbodiimide hydrochloride (68.4mg, 0.357mmol), *N*-hydroxy succinimide (44.7mg, 0.388mmol), DMAP (10mg), affording an off-white solid. Yield 124mg, 94.37%. δ ^{1}H ($CDCl_3$): 5.25-5.27 (H-11', H-12', H-14', H-15', 4H, m), 2.78-2.90 (H-3'$_{ab}$, H-4'$_{ab}$, 4H, m), 2.72-279 (C-13), 2.27-2.34 (H-2$_{ab}$), 1.89-2.09 (H-10$_{ab}$, H-16$_{ab}$, 4H, m), 1.65-1.78 (H-3$_{ab}$, 2H, m) 1.13-1.47 (H-4$_{ab}$ – H-9$_{ab}$, H-17$_{ab}$ – H-19$_{ab}$, 18H, m) 0.82-0.89 (H-20$_{abc}$, 3H, t, J=7.2Hz). δ ^{13}C ($CDCl_3$): 178.65 (C=O), 131.35, 129.13 (multiple signals, C-11, C-12, C-14, C-15), 76.4 (C-2), 23.73-40.48 (multiple signals C-3', C-4', C-3 - C-9, C-13, C16-C19), 15.21 (C-20). **m/z** (ES): 429.6 (M^+ + $[Na]^+$ + $[H]^+$ 5%), 428.6 (M^+ + $[Na]^+$ 100%). m.p. 105-111°C.

5.22.7. (11E)-Eicos-11-enoic acid 2,5-dioxo-pyrrolidin-1-yl ester (60)

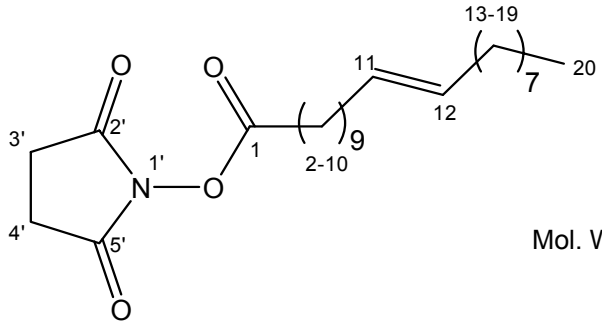

$C_{25}H_{43}NO_3$

Mol. Wt.: 405.6139 g mol^{-1}

Prepared by the general procedure for N-hydroxy succinimide carboxylic acid ester **(5.1.1.12)** using (11E)-eicos-11-enoic acid (50mg, 0.16mmol), DCM (2ml), N-(3-dimethylaminopropyl)-N'-ethyl carbodiimide hydrochloride (33.95mg, 0.117mmol), N-hydroxy succinimide (22.3mg, 0.19mmol), DMAP (5mg), affording a white solid. Yield 60.1mg, 92.61%. δ ^{1}H ($CDCl_3$): 5.21-5.31 (H-11', H-12', 2H, m), 2.64-2.81 (H-3'$_{ab}$, H-4'$_{ab}$, 4H, m), 2.42-2.51 (H-2), 0.79-2.09 (H-3$_{ab}$ – H-10$_{ab}$, H-13$_{ab}$ – H-19$_{ab}$, 30H, m), 0.69-0.77 (H-20$_{abc}$, 3H, t, J=7.4Hz). δ ^{13}C ($CDCl_3$): 131.96 (d, C-11, C-12), 27.21-34.21 (multiple signals C-2 - C-10, C-13-C19), 12.27 (C-20). m/z (ES): 466.3 (M^+ + $[Na]^+$ + $[H]^+$ + 2 x H_2O 5%), 465.3 (M^+ + $[Na]^+$ + 2 x H_2O 100%), 430.2 (M^+ + $[Na]^+$ 50%).

5.22.8. (11Z)-Eicos-11-enoic acid 2,5-dioxo-pyrrolidin-1-yl ester (61)

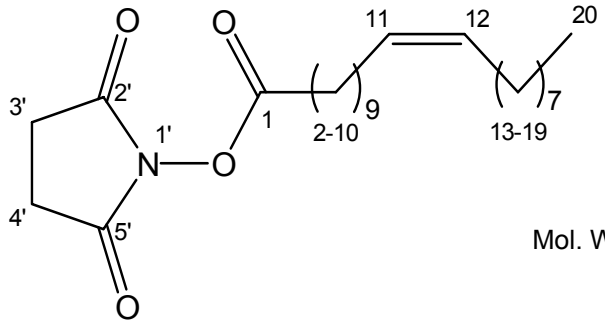

$C_{25}H_{43}NO_3$

Mol. Wt.: 405.6139 g mol^{-1}

Prepared by the general procedure for *N*-hydroxy succinimide carboxylic acid ester **(5.1.1.12)** using (11Z)-eicos-11-enoic acid (100mg, 0.32mmol), DCM (3ml), *N*-(3-dimethylaminopropyl)-*N*'-ethyl carbodiimide hydrochloride (67.67mg, 0.353mmol), *N*-hydroxy succinimide (44.1mg, 0.383 mmol), DMAP (10mg), affording a white solid. Yield 122mg, 93.5%. δ ^{1}H ($CDCl_3$): 5.30-5.39 (H-11', H-12', 2H, t, J=5.6Hz), 2.79-2.88 (H-3', H-4', 4H, m), 2.56-2.64 (H-2, m), 1.15-2.06 (H-3$_{ab}$ – H-10$_{ab}$, H-13$_{ab}$ – H-19$_{ab}$, 30H, m), 0.83-0.91 (H-20$_{abc}$, 3H, t, J=6.9Hz). δ ^{13}C ($CDCl_3$): 128.70, 128.62 (C-11, C-12), 23.33-29.70 (multiple signals C-2 – C-10, C-13 – C-19), 12.87 (C-20). **m/z** (ES): 447.3 (M^+ + $[K]^+$ + $[H]^+$ + 100%).

5.22.9. Eicosanoic acid 2,5-dioxo-pyrrolidin-1-yl ester (62)

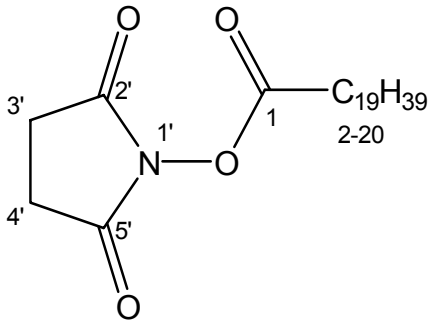

$C_{24}H_{43}NO_4$

Mol. Wt.: 409.6026 g mol^{-1}

Prepared by the general procedure for *N*-hydroxy succinimide carboxylic acid ester **(5.1.1.12)** using eicosanoic acid (200mg, 0.64mmol), DCM (10ml), *N*-(3-dimethylaminopropyl)-*N*'-ethyl carbodiimide hydrochloride (136mg, 0.708 mmol), *N*-hydroxysuccinimide (88.4mg, 0.767mmol) and DMAP (20mg), affording white solid. Yield: 240mg, 91.5%. δ ^{1}H ($CDCl_3$): 5.16-5.30 (H-9, H-10, H-12, H-13, 4H, m), 2.79-2.86 (H-3'$_{ab}$, H-4'$_{ab}$, 4H, m), 2.61-2.68 (H-2$_{ab}$, 2H, t, J=6.3Hz), 2.42-2.56 (H-11$_{ab}$, 2H, m) 1.87-2.03 (H-8$_{ab}$, H-14$_{ab}$, 4H, m), 0.99-1.69 (H-3$_{ab}$ – H-7$_{ab}$, H-15$_{ab}$ – H-17$_{ab}$, 16H, m), 0.69-0.81 (H-18$_{abc}$, 3H, t, J=67.2Hz). δ ^{13}C ($CDCl_3$): 174.39 (C=O), 132.69-134.69 (C-9, C-10, C-12, C13) 27.00-35.99 (multiple signals C-3', C-4', C-2 – C-8, C-11, C-14 – C-17), 19.37 (C-18). **m/z** (ES): 436.4 (M^+ + $[Na]^+$ + 2 x H_2O 100%), 365.3 (M^+ $[Na]^+$ + 2 x H_2O - CH_2-CH_2-CH_2-CH_2-CH_3)

5.22.10. (9Z, 12Z)-Octadeca-9,12-dienoic acid 2,5-dioxo-pyrrolidin-1-yl ester (63)

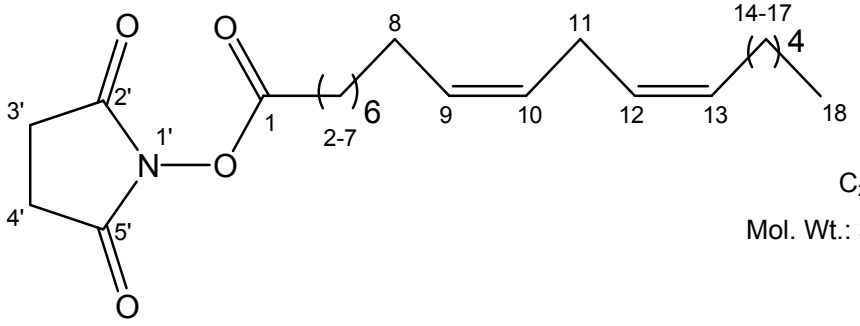

$C_{22}H_{35}NO_4$

Mol. Wt.: 377.5176 g mol^{-1}

Prepared by the general procedure for *N*-hydroxy succinimide carboxylic acid ester **(5.1.1.12)** using octadeca-9,12-dienoic acid (1g, 3.57mmol), DCM (10ml), *N*-(3-dimethylaminopropyl)-*N*'-ethyl carbodiimide hydrochloride (761mg, 3.97mmol), *N*-hydroxysuccinimide (494mg, 4.28mmol), and DMAP (100mg), affording an off-white solid . Yield 1.27g, 94.2%. δ ^{1}H ($CDCl_3$): 2.79-2.86 (H-3'$_{ab}$, H-4'$_{ab}$, 4H, m), 2.56-2.62 (H-2$_{ab}$, 2H, t, J=7.5Hz), 1.67-1.79 (H-3$_{ab}$, 2H, m), 1.20-1.44 (H-4$_{ab}$ – H-19$_{ab}$, 32H, m), 0.83-0.90 (H-20$_{abc}$, 3H, t, J=6.8Hz). δ ^{13}C ($CDCl_3$): 24.81-30.16 (multiple signals C-3', C-4', C-2 – C-19), 15.99 (C-20). **m/z** (ES): 432.2 (M^+ + $[Na]^+$ + 100%) HRMS: Calculated for $C_{24}H_{43}NO_4$ $[M + Na]^+$ 432.3088, found 432.3090.

5.22.11. Octanoic acid 2,5-dioxo-pyrrolidin-1-yl ester (64)

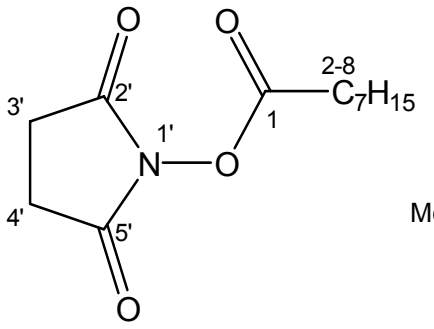

$C_{12}H_{19}NO_4$

Mol. Wt.: 241.2836 g mol^{-1}

Prepared by the general procedure for *N*-hydroxy succinimide carboxylic acid ester **(5.1.1.12)** using octanoic acid (100mg, 0.11ml, 0.69mmol), DCM (3ml), N-(3-dimethylaminopropyl)-*N*'-ethyl carbodiimide hydrochloride (146mg, 0.76mmol), *N*-hydroxy succinimide (95.3mg, 0.83mmol), affording white foamy solid. Yield 71mg, 42.6%. δ ^{1}H ($CDCl_3$): 2.76-2.93 (H-3'$_{ab}$, H-4'$_{ab}$, 4H, m), 2.54-2.66 (H-2$_{ab}$, 2H, t, J=7.8Hz), 2.27-2.40 (H-3$_{ab}$, 2H, t, J=7.8Hz) 1.59-1.83 (H-4$_{ab}$, H-5$_{ab}$, 4H, m), 1.12-1.51 (H-6$_{ab}$ – H-7$_{ab}$, 4H, m), 0.82-0.93 (H-8$_{abc}$, 3H, t, J=6.9Hz). δ ^{13}C ($CDCl_3$): 28.75-33.18 (multiple signals C-3', C-4', C-2 – C-7, 14.07 (C-8). **m/z** (ES): 308.2 (M^+ + $[Na]^+$ + $(CH_3)_2N$ (DMAP) 100%).

5.22.12. m-Tolyl-acetic acid 2,5-dioxo-pyrrolidin-1-yl ester (65)

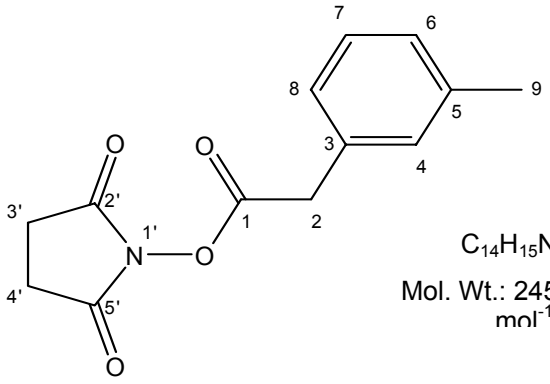

$C_{14}H_{15}NO_3$

Mol. Wt.: 245.2738 g mol^{-1}

Prepared by the general procedure for *N*-hydroxy succinimide carboxylic acid ester **(5.1.1.12)** using m-tolylacetic acid (500mg, 3.33mmol), DCM (10ml), *N*-(3-dimethylaminopropyl)-*N*'-ethyl carbodiimide hydrochloride (0.7g, 3.66mmol), *N*-hydroxysuccinimide (461mg, 3.99mmol) and DMAP (50mg), affording a yellow translucent oil. Yield 699mg, 84.9%. δ ^{1}H ($CDCl_3$): 7.01-7.24 (H-4, H-6, H-7, H-8, 4H, m), 3.86-3.91 (H-$3'_{ab}$, H-$4'_{ab}$, 4H, m), 2.59-2.84 (H-2_{ab}, 2H, m), 2.02-2.15 (H-9_{abc}, 3H, m) δ ^{13}C ($CDCl_3$): 127.53-131.28 (C-4, C-6, C-7, C-8) 38.79 (C-2), 26.84, 26.64 (C-3', C-4'), 22.58 (C-9). **m/z** (ES): 306.2 (M^+ + $[Na]^+$ + 2 x H_2O 100%).

5.23. Addition of an *N*-acyl chain

5.23.1. Tetracosanoic acid [(1S,2S,3R)-2,3-dihydroxy-1-((2S,3R,4S,5R,6R)-3,4,5-trihydroxy-6-hydroxymethyl-tetrahydro-pyran-2-yloxymethyl)-heptadecyl]-amide (68)

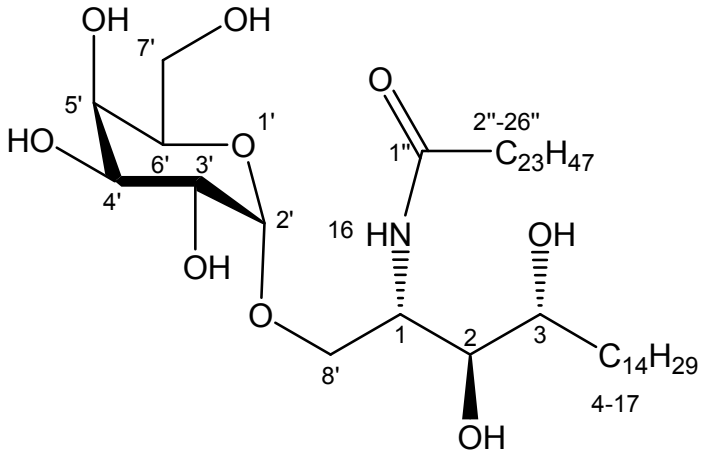

$C_{48}H_{95}NO_9$

Mol. Wt.: 830.2692 g mol^{-1}

Prepared by the general procedure for azide reduction and subsequent *N*-acylation **(5.1.1.13)** using (2S,3R,4S,5R,6R)-2-((2S,3S,4R)-2-azido-3,4-dihydroxy-octadecyloxy)-6-hydroxymethyl-tetrahydro-pyran-3,4,5-triol **(39)** (57mg, 112.7µmol), tetracosanoic acid 2,5-dioxo-pyrrolidin-1-yl ester **(54)** (76mg, 163µmol), affording a white solid. Yield: 74.8mg, 80%. δ ^{1}H ($CDCl_3$:MeOD, 2:1): 4.75-4.78 (H-2', 1H, d, J=3.6Hz), 3.95-3.98 (H-1, 1H, m), 3.79-3.81 (H-4', 1H, d, J=2.98Hz), 3.71-3.76 (H-8_a, 1H, dd, J=4.81, 11.0Hz), 3.56-3.58 (H-3', H-6', 2H, m), 3.50-3.54 (H-5', H-$7'_{ab}$, 3H, m), 3.47-3.49 (H-8_b, 1H, m), 3.31-3.46 (H-2, H-3, 2H, m), 2.13-2.15 (H-$2''_{ab}$, 2H, t, J=7.5Hz), 1.45-1.64 (H-$3''_a$, H-$4''_a$, H-4_a, 3H, m), 1.15-1.35 (H-$3''_b$, H-$4''_b$, H-4_b, H-5_{ab} – H16_{ab}, H-$5''_{ab}$ – H-$25''_{ab}$, 67H, m), 0.65-.80 (H-17_{abc}, H-$26''_{abc}$, 6H, J=6.8Hz). δ ^{13}C ($CDCl_3$:MeOD 2:1):96.66 (C-2'), 74.53 (C-2), 71.8 (C-3), 70.53 (C-6'), 70.03 (C-5'), 69.49 (C4'), 68.68 (C-3'), 67.23 (C-8), 61.55 (C-7'), 50.25 (C-1), 25.43-36.1 (multiple signals C-2'' – C-25'', C-4 – C-16), 13.40 (C-26'', C-17). **m/z** (ES): 853.7 (M^+ + $[Na]^+$ + $[H]^+$ 30%), 852.7 (M^+ + $[Na]^+$ + 100%). HRMS: Calculated for $C_{48}H_{95}NO_9$ $[M + Na]^+$ 852.6905,

found 852.6915. α_D: +2.5.0°. m.p.: 125-129°C IR: 3200-3400cm^{-1} (br OH), 1750-1750cm^{-1} (C=O)., 1500-1650cm^{-1} (N-H).

5.23.2. (15Z)-Tetracos-15-enoic acid [2,3-dihydroxy-1-(3,4,5-trihydroxy-6-hydroxymethyl-tetrahydro-pyran-2-yloxymethyl)-heptadecyl]-amide (69)

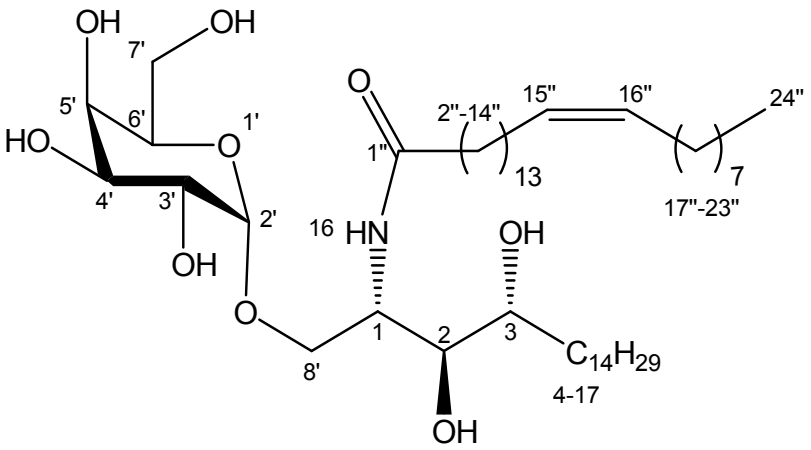

$C_{48}H_{93}NO_9$

Mol. Wt.: 828.25 g mol^{-1}

Prepared by the general procedure for azide reduction and subsequent *N*-acylation **(5.1.1.13)** using (2S,3R,4S,5R,6R)-2-((2S,3S,4R)-2-azido-3,4-dihydroxy-octadecyloxy)-6-hydroxymethyl-tetrahydro-pyran-3,4,5-triol **(39)** (470mg, 929µmol), tetracos-15-enoic acid 2,5-dioxo-pyrrolidin-1-yl ester **(55)** (717mg, 1.55mmol), affording a white solid. Yield: 371mg, 48.2%. δ ^{1}H ($CDCl_3$:MeOD, 2:1): 5.52-5.53 (H-15'', H-16'', 2H, m), 4.85-4.88 (H-2', 1H, d, J=3.7Hz), 4.14-4.19 (H-1, 1H, m), 3.87-3.90 (H-4', 1H, d, J=3.7Hz), 3.82-3.87 (H-8_a, 1H, dd, J=4.8, 10.3Hz), 3.74-3.82 (H-3', H-6', 2H, m), 3.69-3.74 (H-5', H-$7'_{ab}$, 3H, m), 3.63-3.68 (H-8_b, 1H, m), 3.49-3.57 (H-2, H-3, 2H, m), 2.15-2.21 (H-$2''_{ab}$, 2H, t, J=7.7Hz), 1.95-2.02 (H-$3''_a$, H-$4''_a$, H-4_a, 3H, m), 1.05-1.68 (H-$3''_b$, H-$4''_b$, H-4_b, H-5_{ab} – H16_{ab}, H-$5''_{ab}$ – H-$14''_{ab}$, H-$17''_{ab}$ – H-$23''_{ab}$, 61H, m), 0.81-0.87 (H-17_{abc}, H-$24''_{abc}$, 6H, J=7.5Hz). δ ^{13}C ($CDCl_3$:MeOD 2:1): 134.41 (C-15'', C-16''), 104.30 (C-2'), 78.67 (C-2), 75.37 (C-3), 74.85 (C-6'), 74.38 (C-5'), 73.52 (C4'), 71.90 (C-7'), 69.88 (C-3'), 66.41 (C-8'), 50.06 (C-1), 40.98 (C-2''), 27.18-37.01 (multiple signals C-3'' – C-14'', C-17'' – C-23'', C-4 – C-16), 13.40 (C-

24'', C-17). **m/z** (ES): 851.7 (M^+ + $[Na]^+$ + $[H]^+$ 40%), 850.7 (M^+ + $[Na]^+$ + 100%). HRMS: Calculated for $C_{48}H_{95}NO_9$ $[M + Na]^+$ 850.6748, found 850.6785. α_D: +7.6.0°. m.p.: 132-137°C IR: 3200-3400cm^{-1} (br OH), 1750-1750cm^{-1} (C=O), 1600-1675$_{cm}^{-1}$ (C=C), 1500-1650cm^{-1} (N-H).

5.23.3. (4Z,7Z,10Z,13Z,16Z,19Z)-Docosa-4,7,10,13,16,19-hexaenoic acid [(1S,2S,3R)-2,3-dihydroxy-1-((2S,3R,4S,5R,6R)-3,4,5-trihydroxy-6-hydroxymethyl-tetrahydro-pyran-2-yloxymethyl)-heptadecyl]-amide (70)

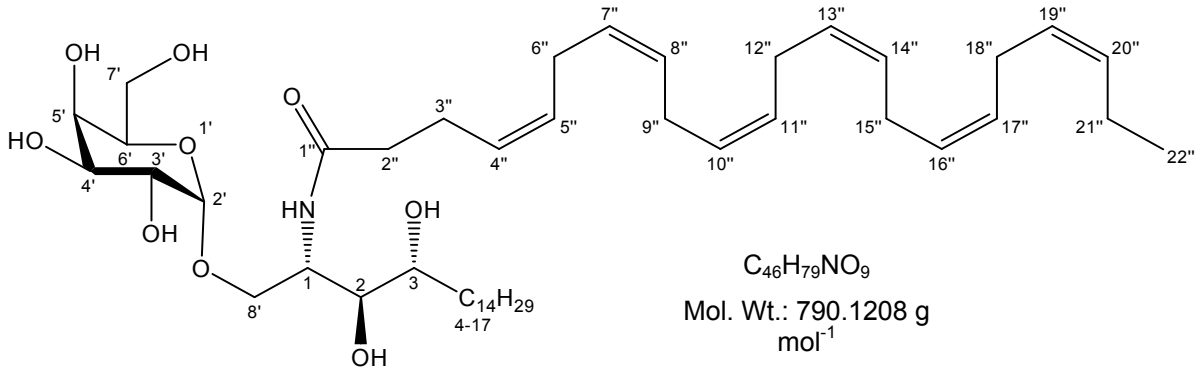

$C_{46}H_{79}NO_9$

Mol. Wt.: 790.1208 g mol^{-1}

Prepared by the general procedure for azide reduction and subsequent *N*-acylation **(5.1.1.13)** using (2S,3R,4S,5R,6R)-2-((2S,3S,4R)-2-azido-3,4-dihydroxy-octadecyloxy)-6-hydroxymethyl-tetrahydro-pyran-3,4,5-triol **(39)** (35mg, 69.2µmmol), docasa-4,7,10,13,16,19-hexaenoic acid 2,5-dioxo-pyrrolidin-1-yl ester **(56)** (42mg, 98.7µmol), affording a white solid. Yield: 5mg, 10%. δ ^{1}H ($CDCl_3$:MeOD, 2:1): 5.34-5.39 (H-4'', H-5'', H-7'', H-8'', H-10'', H-11'', H-13'', H-14'', H-16'', H-17'', H-19'', H-20'', 12H, m), 4.81-4.83 (H-2', 1H, d, J=3.75Hz), 4.02-4.04 (H-1, 1H, m), 3.75-3.81 (H-4', 1H, m), 3.71-3.74 (H-8_a, 1H, m), 3.58-3.62 (H-3', H-6', 2H, m), 3.51-3.55 (H-5', H-$7'_{ab}$, 3H, m), 3.45-3.48 (H-8_b, 1H, m), 3.35-3.42 (H-2, H-3, 2H, m), 2.56-2.80 (H-6'', H-9'', H-12'', H-15'', H-18'', 5H, m), 2.16-2.21 (H-$2''_{ab}$, 2H, t, J=7.3Hz), 1.45-1.60 (H-$3''_a$, H-4_a, H-5_a, 3H, m), 1.19-1.39 (H-$3''_b$, H-4_b, H-5_b, H-6_{ab} – H16_{ab}, H-$21''_{ab}$ 27H, m), 0.78-0.83 (H-17_{abc}, H-$22''_{abc}$, 6H, J=7.0Hz). **m/z** (ES): 813.1 (M^+ + $[Na]^+$ + 100%). HRMS: Calculated for $C_{48}H_{95}NO_9$ $[M + Na]^+$ 813.1105, found 813.1130.

α_D: +10.0°. m.p.: 135-139°C. IR: 3200-3400cm^{-1} (br OH), 1750-1750cm^{-1} (C=O), 1600-1675$_{cm}^{-1}$ (C=C), 1500-1650cm^{-1} (N-H).

5.23.4. (5Z,8Z,11Z,14Z,17Z)-Eicosa-5,8,11,14,17-pentaenoic acid [(1S,2S,3R)-2,3-dihydroxy-1-((2S,3R,4S,5R,6R)-3,4,5-trihydroxy-6-hydroxymethyl-tetrahydro-pyran-2-yloxymethyl)-heptadecyl]-amide (71)

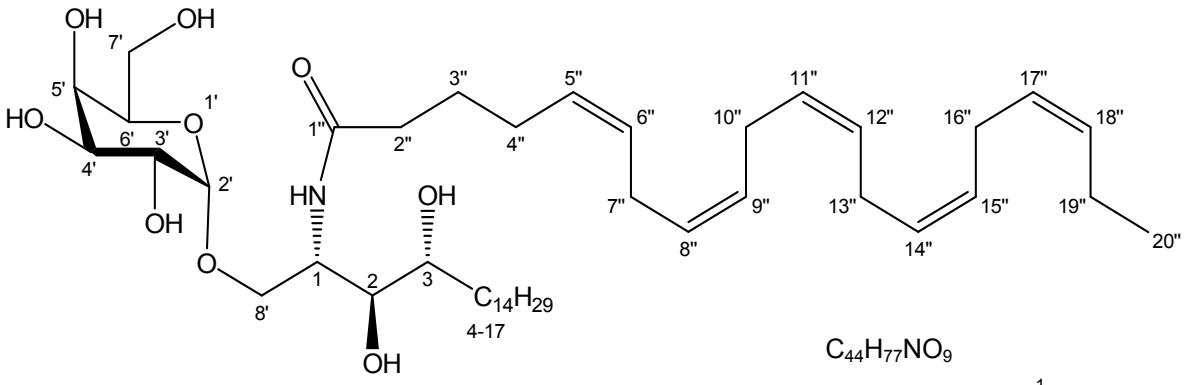

$C_{44}H_{77}NO_9$

Mol. Wt.: 764.0835 g mol^{-1}

Prepared by the general procedure for azide reduction and subsequent *N*-acylation **(5.1.1.13)** using (2S,3R,4S,5R,6R)-2-((2S,3S,4R)-2-azido-3,4-dihydroxy-octadecyloxy)-6-hydroxymethyl-tetrahydro-pyran-3,4,5-triol **(39)** (25mg, 49.4µmol), eicosa-5,8,11,14,17-pentaenoic acid 2,5-dioxo-pyrrolidin-1-yl ester **(57)** (31mg, 77.56µmol), affording white solid. Yield: 7.5mg, 20%. δ ^{1}H ($CDCl_3$:MeOD, 2:1): 5.28-5.40 (H-5'', H-6'', H-8'', H-9'', H-11'', H-12'', H-14'', H-15'', H-17'', H-18'', 10H, m), 4.35-4.38 (H-2', 1H, d, J=3.1Hz), 4.08-4.09 (H-1, 1H, m), 3.95-3.99 (H-4', 1H, m), 3.78-3.80 (H-8$_a$, 1H, dd, J=4.0, 10.5 Hz), 3.59-3.64 (H-3', H-6', 2H, m), 3.49-3.54 (H-5', H-7'$_{ab}$, 3H, m), 3.43-3.45 (H-8$_b$, 1H, m), 3.35-3.42 (H-2, H-3, 2H, m), 3.01-3.05 (H-7'', H-10'', H-13'', H-16'', 4H, m), 2.20-2.23 (H-2''$_{ab}$, 2H, t, J=7.4Hz), 1.48-1.62 (H-3''$_a$, H-4$_a$, H-5$_a$, 3H, m), 1.18-1.42 (H-3''$_b$, H-4$_b$, H-5$_b$, H-4''$_{ab}$, H-6$_{ab}$ – H16$_{ab}$, H-19''$_{ab}$ – H21''$_{ab}$ 33H, m), 0.78-0.81 (H-17$_{abc}$, H-20''$_{abc}$, 6H, J=7.3Hz). δ ^{13}C ($CDCl_3$:MeOD 2:1):

127.65-130.8 (multiple signals, C-5'', C-6', C-8'', C-9'', C-11'', C-12'', C-14'', C-15'', C-17'', C-18''), 101.60 (C-2'), 75.45 (C-2), 72.48 (C-3), 69.69 (C-6'), 69.55 (C-5'), 69.09 (C4'), 68.88 (C-3'), 65.37 (C-8), 60.14 (C-7'), 47.25 (C-1), 24.12-38.21 (multiple signals C-2'', C-3'', C-4'', C-7'', C-10'', C-13'', C-16'', C19'', C-4 – C-16), 13.40 (C-20'', C-17). **m/z** (ES): 788.1 (M^+ + $[Na]^+$ + $[H]^+$ 20%), 787.1 (M^+ + $[Na]^+$ 100%). HRMS: Calculated for $C_{44}H_{77}NO_9$ $[M + Na]^+$ 787.0732, found 787.0740. α_D: +7.1°. IR: 3200-3400cm^{-1} (br OH), 1750-1750cm^{-1} (C=O), 1600-1675$_{cm}^{-1}$ (C=C), 1500-1650cm^{-1} (N-H).

5.23.5. (5Z,8Z,11Z,14Z)-Eicosa-5,8,11,14-tetraenoic acid [(1S,2S,3R)-2,3-dihydroxy-1-((2S,3R,4S,5R,6R)-3,4,5-trihydroxy-6-hydroxymethyl-tetrahydro-pyran-2-yloxymethyl)-heptadecyl]-amide (72)

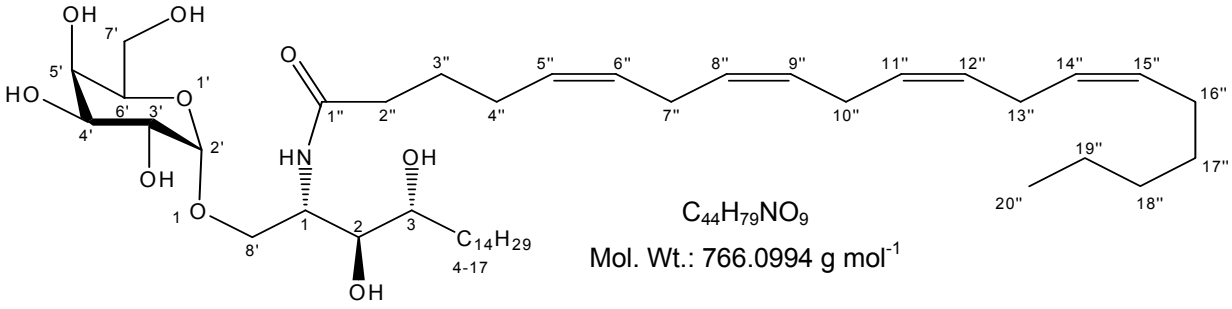

$C_{44}H_{79}NO_9$

Mol. Wt.: 766.0994 g mol^{-1}

Prepared by the general procedure for azide reduction and subsequent *N*-acylation **(5.1.1.13)** using (2S,3R,4S,5R,6R)-2-((2S,3S,4R)-2-azido-3,4-dihydroxy-octadecyloxy)-6-hydroxymethyl-tetrahydro-pyran-3,4,5-triol **(39)** (24mg, 47.46µmol), eicosa-5,8,11,14-tetraenoic acid 2,5-dioxo-pyrrolidin-1-yl ester **(58)** (27.7mg, 68.9µmol), affording a white solid. Yield: 9mg, 25%. δ ^1H ($CDCl_3$:MeOD, 2:1): 5.23-5.70 (H-5'', H-6'', H-8'', H-9'', H-11'', H-12'', H-14'', H-15'', 8H, m), 4.70-4.75 (H-2', 1H, m), 4.25-4.28 (H-1, 1H, m), 4.01-4.04 (H-4', 1H, m), 3.80-3.85 (H-8'$_a$, 1H, dd, J=3.9, 10.8 Hz), 3.54-3.68 (H-3', H-6', 2H, m), 3.49-3.54 (H-5', H-7'$_{ab}$, 3H, m), 3.41-3.46 (H-8'$_b$, 1H, m), 3.38-3.40 (H-2, H-3, 2H, m), 2.25-2.36 (H-7'',

H-10'', H-13'', 3H, m), 1.98-2.10 (H-2''$_{ab}$, 2H, m), 1.45-1.55 (H-3''$_a$, H-4$_a$, H-5$_a$, 3H, m), 1.15-1.40 (H-3''$_b$, H-4$_b$, H-5$_b$, H-4''$_{ab}$, H-6$_{ab}$ – H16$_{ab}$, H-16''$_{ab}$ – H19''$_{ab}$ 27H, m), 0.71-0.89 (H-17$_{abc}$, H-20''$_{abc}$, 6H, J=7.6Hz). δ ^{13}C ($CDCl_3$:MeOD 2:1): 129.45-130.80 (multiple signals, C-5'', C-6', C-8'', C-9'', C-11'', C-12'', C-14'', C-15''), 100.30 (C-2'), 77.55 (C-2), 73.98 (C-3), 70.19 (C-6'), 69.31 (C-5'), 69.00 (C4'), 67.97 (C-3'), 66.47 (C-8'), 59.53 (C-7'), 47.74 (C-1), 25.15-38.14 (multiple signals C-2'', C-3'', C-4'', C-7'', C-10'', C-13'', C-16'' – C19'', C-4 – C-16), 13.40 (C-20'', C-17). **m/z** (ES): 790.1 (M^+ + $[Na]^+$ + $[H]^+$ 50%), 789.1 (M^+ + $[Na]^+$ 100%), HRMS: Calculated for $C_{44}H_{77}NO_9$ $[M + Na]^+$ 789.0891, found 789.0905. α_D: +7.5°. m.p.: 126-129°C. IR: 3200-3400cm^{-1} (br OH), 1750-1750cm^{-1} (C=O), 1600-1675cm^{-1} (C=C), 1500-1650cm^{-1} (N-H).

5.23.6. (11Z,14Z)-Eicosa-11,14-dienoic acid [(1S, 2S, 3R)-2,3-dihydroxy-1-((2S, 3R, 4S, 5R, 6R)-3,4,5-trihydroxy-6-hydroxymethyl-tetrahydro-pyran-2-yloxymethyl)-heptadecyl]-amide (73)

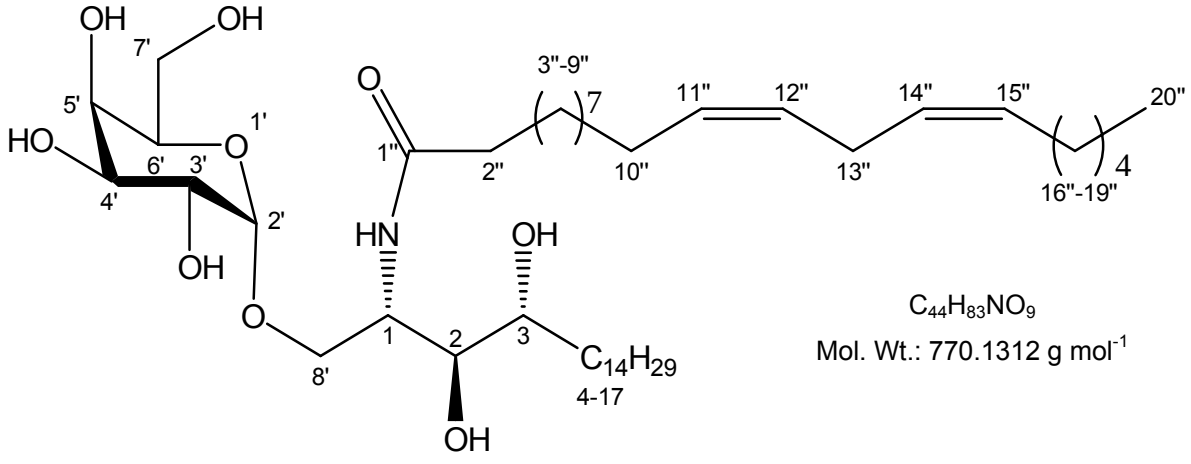

$C_{44}H_{83}NO_9$

Mol. Wt.: 770.1312 g mol^{-1}

Prepared by the general procedure for azide reduction and subsequent *N*-acylation **(5.1.1.13)** using (2S,3R,4S,5R,6R)-2-((2S,3S,4R)-2-azido-3,4-dihydroxy-octadecyloxy)-6-

hydroxymethyl-tetrahydro-pyran-3,4,5-triol **(39)** (110mg, 217.5µmol), eicosa-11,14-dienoic acid 2,5-dioxo-pyrrolidin-1-yl ester **(59)** (134mg, 330µmol), affording a white solid. Yield: 108mg, 65%. δ ^{1}H ($CDCl_3$: MeOD, 2:1): 5.03-5.13 (H11'', H12'', H14'', H15'', 4H, m), 4.64-4.66 (H-2', 1H, d, J=3.75Hz,), 3.93-3.97 (H-1, 1H, m), 3.66-3.67 (H-4', 1H, d, J=2.91Hz), 3.60-3.63 (H-8'$_a$, 1H, dd, J=4.67, 10.76Hz), 3.52-3.55 (H-6', H-3', 2H, m), 3.43-3.49 (H-5', H-7'$_{ab}$, 3H, m), 3.39-3.41 (H-8'$_b$, 1H, d, J=4.53Hz), 3.26-3.29 (H-2, H-3, 2H, m), 2.51-2.55 (H-13''$_{ab}$, 2H, t, J=6.60Hz), 1.90-1.94 (H-2''$_{ab}$, 2H, t, J=7.60Hz), 1.77-1.80 (H-10''$_{ab}$, H-16''$_{ab}$, 4H, q, J=6.82Hz), 1.27-1.42 (H-4$_a$, H-5$_a$, H-3''$_{ab}$, 4H, m), 0.99-1.12 (H-4$_b$, H-5$_b$, H-6$_{ab}$ – H-16$_{ab}$, H-4''$_{ab}$ – H-9''$_{ab}$, H-17''$_{ab}$ – H-19''$_{ab}$, 42H, m), 0.64-0.60 (H-17$_{abc}$, H-20''$_{abc}$, 6H, t, J=6.97Hz) δ ^{13}C ($CDCl_3$: MeOD, 2:1): 175.04 (C-1''), 130.52, 130.47, 128.41, 128.37 (C-11'', 12'', 14'', 15''), 100.26 (C-2'), 75.14 (C-2), 72.43 (C-3), 71.37 (C-6'), 70.77 (C-7'), 70.25 (C-4'), 69.44 (C-3'), 67.78 (C-8'), 62.26 (C-5'), 50.97 (C-1), 36.88 (C-2''), 32.92-29.77 (multiple signals, C-4 – C-15, C-3'' – C-9''), 27.64, 27.59 (C-10'', C-16''), 26.33, 26.29 (C-17'', C-18''), 26.02 (C-13''), 23.07, 22.96 (C-16, C-19''), 14.25, 14.31 (C-17, C-20''). **m/z** (ES): 793.6 (M^+ + $[Na]^+$ + $[H]^+$ 25%), 793.6 (M^+ + $[Na]^+$ + 100%) HRMS Calculated for $C_{44}H_{83}NO_9$ $[M + Na]^+$ 792.5966, found 792.5956. α_D: +13.2° m.p. 129-139°C IR: 3200-3400cm^{-1} (br OH), 1750-1750cm^{-1} (C=O), 1600-1675cm^{-1} (C=C), 1500-1650cm^{-1} (N-H).

5.23.7. (11Z,14Z)-Icosa-11,14-dienoic acid [(1S,2S,3R)-2,3-dihydroxy-1-((2S,3R,4S,5R,6R)-3,4,5-trihydroxy-6-hydroxymethyl-tetrahydro-pyran-2-yloxymethyl)-tetradecyl]-amide (74)

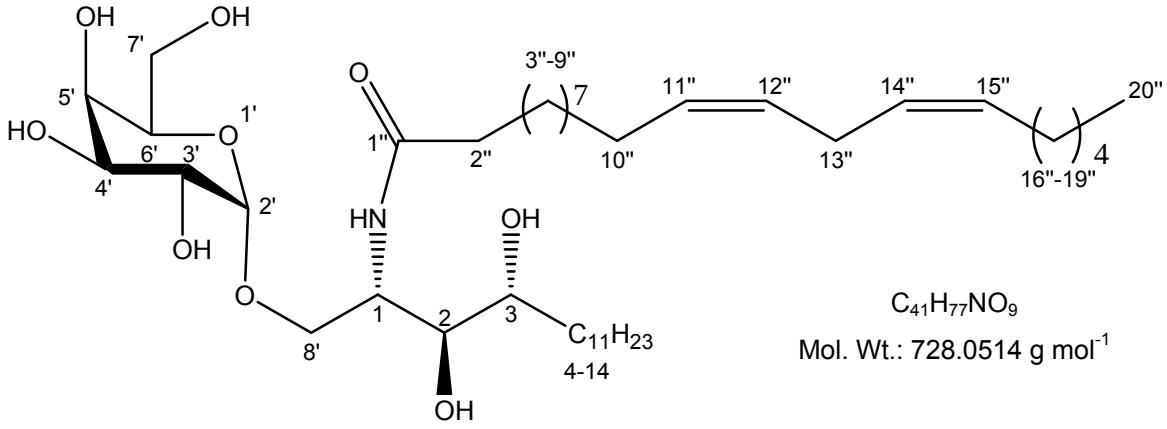

$C_{41}H_{77}NO_9$

Mol. Wt.: 728.0514 g mol^{-1}

Prepared by the general procedure for azide reduction and subsequent *N*-acylation **(5.1.1.13)** using (2S,3R,4S,5R,6R)-2-((2S,3S,4R)-2-azido-3,4-dihydroxy-pentadecyloxy)-6-hydroxymethyl-tetrahydro-pyran-3,4,5-triol **(40)** (45mg, 97.1µmol), eicosa-11,14-dienoic acid 2,5-dioxo-pyrrolidin-1-yl ester **(59)** (56.8mg, 140µmol), affording a white solid. Yield: 33.6mg, 47.5%. δ ^{1}H ($CDCl_3$: MeOD, 2:1): 5.25-5.32 (H11'', H12'', H14'', H15'', 4H, m), 4.75-4.77 (H-2', 1H, d, J=3.61Hz,), 4.10-4.18 (H-1, 1H, m), 3.86-3.88 (H-4', 1H, d, J=3.5Hz), 3.81-3.85 (H-8'$_a$, 1H, dd, J=4.8, 10.4Hz), 3.72-3.78 (H-6', H-3', 2H, m), 3.67-3.70 (H-5', H-7'$_{ab}$, 3H, m), 3.39-3.41 (H-8'$_b$, 1H, d, J=4.8Hz), 3.47-3.52 (H-2, H-3, 2H, m), 2.18-1.19 (H-13''$_{ab}$, 2H, t, J=6.5Hz), 1.90-2.04 (H-2''$_{ab}$, 2H, m), 1.42-1.65 (H-4$_a$, H-5$_a$, H-3''$_{ab}$, 4H, m), 1.18-1.39 (H-4$_b$, H-5$_b$, H-6$_{ab}$ – H-13$_{ab}$, H-4''$_{ab}$ – H-10''$_{ab}$, H-13''$_{ab}$, H-16''$_{ab}$ – H-19''$_{ab}$, 42H, m), 0.64-0.60 (H-14$_{abc}$, H-20''$_{abc}$, 6H, t, J=7.3Hz) δ ^{13}C ($CDCl_3$: MeOD, 2:1): 169.04 (C-1''), 128.82-130.74 (C-11'', 12'', 14'', 15''), 101.80 (C-2'), 74.91 (C-2), 72.56 (C-3), 71.09 (C-6'), 70.77 (C-7'), 70.33 (C-4'), 68.48 (C-3'), 67.17 (C-8'), 61.11 (C-5'), 48.73 (C-1), 34.42 (C-2''), 22.10-30.02 (multiple signals, C-4 – C-13, C-3'' – C-10'', C-13'', C-16'' – C-19''), 17.51, 18.16 (C-14, C-20''). **m/z** (ES): 752.0 (M^+ + $[Na]^+$ + $[H]^+$ 5%), 751.0 (M^+ + $[Na]^+$ + 100%). HRMS: Calculated

for $C_{44}H_{83}NO_9$ $[M + Na]^+$ 751.0411, found 751.0429. α_D: +26.0°. m.p.: 127-135°C IR: 3200-3400cm^{-1} (br OH), 1750-1750cm^{-1} (C=O), 1600-1675cm^{-1} (C=C), 1500-1650cm^{-1} (N-H).

5.23.8. (11Z,14Z)-Eicosa-11,14-dienoic acid [(1S,2S,3R)-2,3-dihydroxy-1-((2S,3R,4S,5R,6R)-3,4,5-trihydroxy-6-hydroxymethyl-tetrahydro-pyran-2-yloxymethyl)-undecyl]-amide (75)

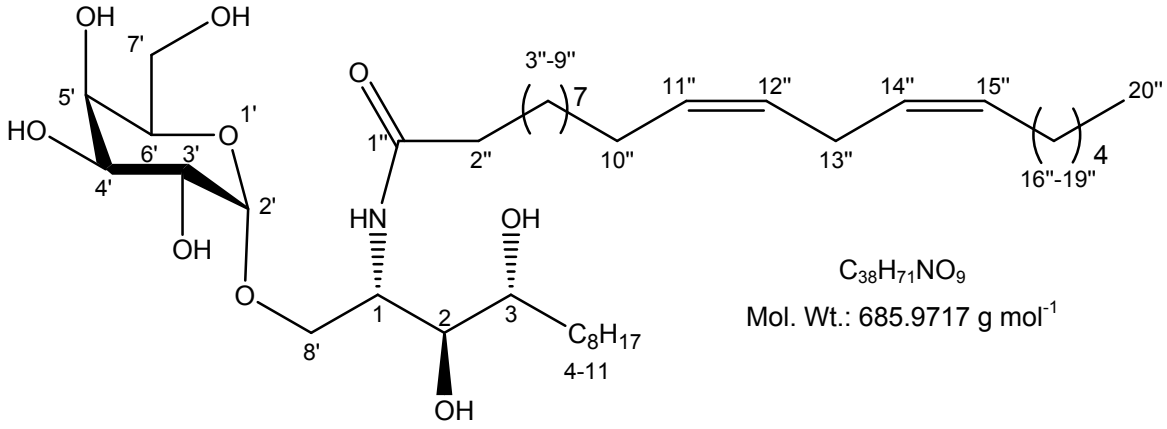

$C_{38}H_{71}NO_9$

Mol. Wt.: 685.9717 g mol^{-1}

Prepared by the general procedure for azide reduction and subsequent *N*-acylation using (2S,3R,4S,5R,6R)-2-((2S,3S,4R)-2-azido-3,4-dihydroxy-dodecyloxy)-6-hydroxymethyl-tetrahydro-pyran-3,4,5-triol **(41)** (54mg, 128.2µmol), Eicosa-11,14-dienoic acid 2,5-dioxo-pyrrolidin-1-yl ester **(59)** (77.3mg, 190µmol), affording a white solid. Yield: 55.4mg, 63%. δ ^{1}H ($CDCl_3$: MeOD, 2:1): 5.25-5.30 (H11'', H12'', H14'', H15'', 4H, m), 4.80-4.84 (H-2', 1H, d, J=3.7Hz,), 4.12-4.16 (H-1, 1H, m), 3.87-3.89 (H-4', 1H, d, J=3.7Hz), 3.79-3.85 (H-8'$_a$, 1H, dd, J=4.5, 10.5Hz), 3.72-3.77 (H-6', H-3', 2H, m), 3.67-3.69 (H-5', H-7'$_{ab}$, 3H, m), 3.49-3.65 (H-8'$_b$, 1H, m), 3.46-3.51 (H-2, H-3, 2H, m), 2.12-2.18 (H-13''$_{ab}$, 2H, t, J=6.5Hz), 1.95-2.02 (H-2''$_{ab}$, 2H, m), 1.46-1.66 (H-4$_a$, H-5$_a$, H-3''$_{ab}$, 4H, m), 1.16-1.32 (H-4$_b$, H-5$_b$, H-6$_{ab}$ – H-10$_{ab}$, H-4''$_{ab}$ – H-10''$_{ab}$, H-13''$_{ab}$, H-16''$_{ab}$ – H-19''$_{ab}$, 42H, m), 0.78-0.87 (H-11$_{abc}$, H-20''$_{abc}$, 6H, t, J=7.5Hz) δ ^{13}C ($CDCl_3$: MeOD, 2:1): 170.45 (C-1''), 130.65-133.13 (C-11'', 12'', 14'', 15''),

102.00 (C-2'), 75.71 (C-2), 72.99 (C-3), 72.09 (C-6'), 70.46 (C-7'), 70.03 (C-4'), 69.38 (C-3'), 68.17 (C-8'), 60.24 (C-5'), 45.62 (C-1), 34.20 (C-2''), 25.44-30.82 (multiple signals, C-4 – C-10, C-3'' – C-10'', C-13'', C-16'' – C-19''), 17.51, 18.16 (C-11, C-20''). **m/z** (ES): 725.9 (M^+ + $[K]^+$ + $[H]^+$ 2%), 724.9 (M^+ + $[K]^+$ + 100%), 301.2 (M^+ + $[H]^+$ + $[K]^+$ - $C_6H_{11}O_6$ (galactose) - $C_{20}H_{35}O$ (eicosa-11,14-dienoic acid) 25%). HRMS: Calculated for $C_{44}H_{83}NO_9$ $[M + Na]^+$ 708.9614, found 708.9624. α_D: +13.5° IR: 3200-3400cm^{-1} (br OH), 1750-1750cm^{-1} (C=O), 1600-1675cm^{-1} (C=C), 1500-1650cm^{-1} (N-H).

5.23.9. (11Z,14Z)-Eicosa-11,14-dienoic acid [(1S,2S,3R)-2,3-dihydroxy-1-((2S,3R,4S,5R,6R)-3,4,5-trihydroxy-6-hydroxymethyl-tetrahydro-pyran-2-yloxymethyl)-octyl]-amide (76)

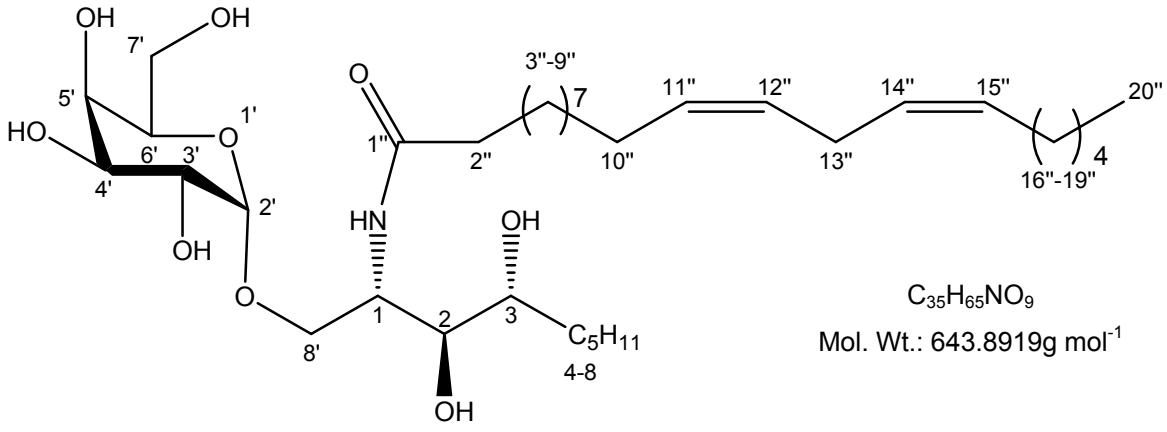

$C_{35}H_{65}NO_9$

Mol. Wt.: 643.8919g mol^{-1}

Prepared by the general procedure for azide reduction and subsequent *N*-acylation **(5.1.1.13)** using (2S,3R,4S,5R,6R)-2-((2S,3S,4R)-2-azido-3,4-dihydroxy-nonyloxy)-6-hydroxymethyl-tetrahydro-pyran-3,4,5-triol **(42)** (30mg, 79.1µmol), eicosa-11,14-dienoic acid 2,5-dioxo-pyrrolidin-1-yl ester **(59)** (46.3mg, 114µmol), affording a white solid. Yield: 27.5mg, 54%. δ ^1H ($CDCl_3$: MeOD, 2:1): 5.24-5.39 (H11'', H12'', H14'', H15'', 4H, m), 4.65-4.69 (H-2', 1H, d, J=3.5Hz,), 3.93-4.02 (H-1, 1H, m), 3.87-3.90 (H-4', 1H, m), 3.77-3.82 (H-8'$_a$, 1H, dd, J=4.6, 10.5Hz), 3.72-3.77 (H-6', H-3', 2H, m), 3.60-3.65 (H-5', H-7'$_{ab}$, 3H, m), 3.54-3.58

(H-8'$_b$, 1H, m), 3.50-3.53 (H-2, H-3, 2H, m), 2.15-2.20 (H-13''$_{ab}$, 2H, t, J=6.5Hz), 1.94-2.04 (H-2''$_{ab}$, 2H, m), 1.52-1.64 (H-4$_a$, H-5$_a$, H-3''$_{ab}$, 4H, m), 1.18-1.35 (H-4$_b$, H-5$_b$, H-6$_{ab}$ – H-7$_{ab}$, H-4''$_{ab}$ – H-10''$_{ab}$, H-13''$_{ab}$, H-16''$_{ab}$ – H-19''$_{ab}$, 30H, m), 0.85-0.88 (H-8$_{abc}$, H-20''$_{abc}$, 6H, t, J=6.9Hz) δ ^{13}C ($CDCl_3$: MeOD, 2:1): 131.54-133.15 (C-11'', 12'', 14'', 15''), 99.80 (C-2'), 74.76 (C-2), 72.38 (C-3), 71.99 (C-6'), 70.22 (C-7'), 69.75 (C-4'), 69.08 (C-3'), 67.89 (C-8'), 61.00 (C-5'), 46.51 (C-1), 33.80 (C-2''), 22.66-31.12 (multiple signals, C-4 – C-7, C-3'' – C-10'', C-13'', C-16'' – C-19''), 16.51, 18.16 (C-8, C-20''). **m/z** (ES): 667.9 (M^+ + $[Na]^+$ + $[H]^+$ 15%), 666.9 (M^+ + $[Na]^+$ 100%). HRMS: Calculated for $C_{35}H_{65}NO_9$ $[M + Na]^+$ 666.8816, found 666.8820. α_D:+13.8° m.p. 124-135°C IR: 3200-3400cm^{-1} (br OH), 1750-1750cm^{-1} (C=O), 1600-1675cm^{-1} (C=C), 1500-1650cm^{-1} (N-H).

5.23.10. (11E)-Eicos-11-enoic acid [(1S, 2S, 3R)-2,3-dihydroxy-1-((2S, 3R, 4S, 5R, 6R)-3,4,5-trihydroxy-6-hydroxymethyl-tetrahydro-pyran-2-yloxymethyl)-heptadecyl]-amide (77)

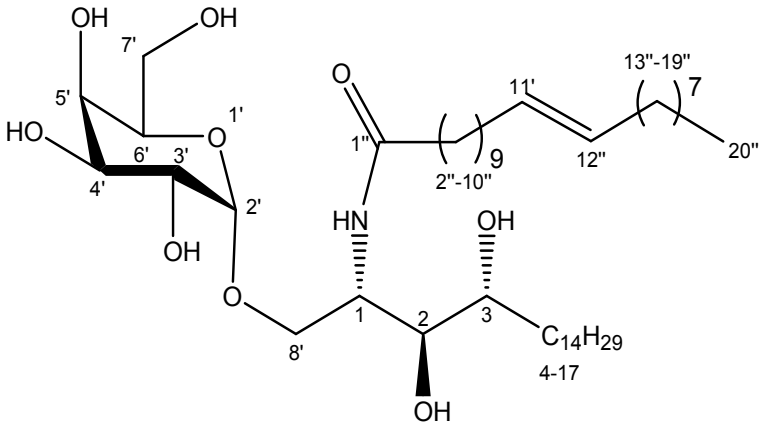

$C_{44}H_{85}NO_9$
Mol. Wt.: 772.1470 g mol^{-1}

Prepared by the general procedure for azide reduction and subsequent *N*-acylation **(5.1.1.13)** using (2S,3R,4S,5R,6R)-2-((2S,3S,4R)-2-azido-3,4-dihydroxy-octadecyloxy)-6-hydroxymethyl-tetrahydro-pyran-3,4,5-triol **(39)** (50.97mg, 100.7µmol), (11E)-eicosa-11-enoic acid 2,5-dioxo-pyrrolidin-1-yl ester **(61)** (49.5mg, 159µmol), affording a white solid.

Yield: 38.1mg, 49%. δ ^{1}H ($CDCl_3$: MeOD, 2:1): 5.31-5.34 (H11'', H12'', 2H, m), 4.84-4.86 (H-2', 1H, d, J=3.6Hz,), 4.12-4.15 (H-1, 1H, m), 3.88-3.89 (H-4', 1H, d, J=3.3Hz), 3.81-3.85 (H-8'$_a$, 1H, dd, J=4.6, 10.4Hz), 3.72-3.77 (H-6', H-3', 2H, m), 3.65-3.72 (H-5', H-7'$_{ab}$, 3H, m), 3.61-3.65 (H-8'$_b$, 1H, dd, J=4.6, 10.8Hz), 3.47-3.50 (H-2, H-3, 2H, m), 2.13-2.17 (H-2''$_{ab}$, 2H, t, J=7.4Hz), 1.87-1.93 (H-3''$_{ab}$, H-4$_{ab}$, 4H, m), 1.43-1.65 (H-4''$_{ab}$, H-10''$_{ab}$, H-13''$_{ab}$, 6H, m), 1.01-1.30 (H-5$_{ab}$ – H-16$_{ab}$, H-5''$_{ab}$ – H-9''$_{ab}$, H-14''$_{ab}$ – H-19''$_{ab}$, 46H, m), 0.80-0.84 (H-17$_{abc}$, H-20''$_{abc}$, 6H, t, J=6.8Hz) δ ^{13}C ($CDCl_3$: MeOD, 2:1):130.31-132.5 (C-11'', 12''), 100.08 (C-2'), 73.33 (C-2), 73.01 (C-3), 72.24 (C-6'), 70.56 (C-7'), 70.02 (C-4'), 69.87 (C-3'), 67.9 (C-8'), 62.38 (C-5'), 46.38 (C-1), 34.77 (C-2''), 21.87-30.20 (multiple signals, C-4 – C-16, C-3'' – C-10'', C-13'' – C-19''), 15.82, 16.41 (C-17, C-20''). **m/z** (ES): 795.6 (M^+ + $[Na]^+$ + $[H]^+$ 20%), 794.7 (M^+ + $[Na]^+$ 100%). HRMS Calculated for $C_{35}H_{65}NO_9$ $[M + Na]^+$ 794.6122, found 794.6115. α_D: +18.0° m.p. 122-138°C IR: 3200-3400cm^{-1} (br OH), 1750-1750cm^{-1} (C=O), 1600-1675cm^{-1} (C=C), 1500-1650cm^{-1} (N-H).

5.23.11. (11Z)-Eicos-11-enoic acid [(1S, 2S, 3R)-2,3-dihydroxy-1-((2S, 3R, 4S, 5R, 6R)-3,4,5-trihydroxy-6-hydroxymethyl-tetrahydro-pyran-2-yloxymethyl)-heptadecyl]-amide (78)

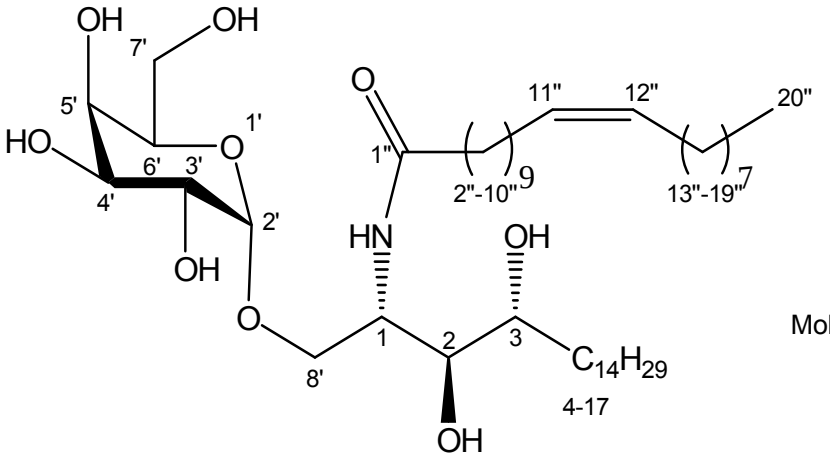

$C_{44}H_{85}NO_9$
Mol. Wt.: 772.1470 g mol^{-1}

Prepared by the general procedure for azide reduction and subsequent *N*-acylation **(5.1.1.13)** using (2S,3R,4S,5R,6R)-2-((2S,3S,4R)-2-azido-3,4-dihydroxy-octadecyloxy)-6-hydroxymethyl-tetrahydro-pyran-3,4,5-triol **(39)** (63.7mg, 125.9µmol), (11Z)-eicosa-11-enoic acid 2,5-dioxo-pyrrolidin-1-yl ester **(60)** (59.5mg, 191.6µmol), affording a white solid. Yield 67mg, 69%. δ ^{1}H ($CDCl_3$: MeOD, 2:1): 5.27-5.31 (H11'', H12'', 2H, t, J=4.6Hz), 4.84-4.86 (H-2', 1H, d, J=3.4Hz,), 4.13-4.17 (H-1, 1H, m), 3.87-3.89 (H-4', 1H, d, J=2.9Hz), 3.81-3.86 (H-8'$_a$, 1H, dd, J=4.7, 10.8Hz), 3.73-3.77 (H-6', H-3', 2H, m), 3.67-3.72 (H-5', H-7'$_{ab}$, 3H, m), 3.61-3.67 (H-8'$_b$, 1H, m), 3.47-3.52 (H-2, H-3, 2H, m), 2.13-2.18 (H-2''$_{ab}$, 2H, t, J=7.6Hz), 1.94-1.99 (H-3''$_{ab}$, H-4$_{ab}$, 4H, m), 1.46-1.65 (H-10''$_{ab}$, H-13''$_{ab}$, 4H, m), 1.17-1.32 (H-5$_{ab}$ – H-16$_{ab}$, H-4''$_{ab}$ – H-9''$_{ab}$, H-14''$_{ab}$ – H-19''$_{ab}$, 46H, m), 0.81-0.85 (H-17$_{abc}$, H-20''$_{abc}$, 6H, t, J=6.8Hz). δ ^{13}C ($CDCl_3$: MeOD, 2:1): 130.31-132.7 (C-11'', 12''), 101.80 (C-2'), 74.43 (C-2), 73.91 (C-3), 73.34 (C-6'), 71.66 (C-7'), 71.12 (C-4'), 69.97 (C-3'), 68.59 (C-8'), 63.88 (C-5'), 46.48 (C-1), 35.17 (C-2''), 20.26-32.10 (multiple signals, C-4 – C-16, C-3'' – C-10'', C-13'' – C-19''), 15.95, 16.31 (C-17, C-20''). **m/z** (ES): 795.8 (M^+ + $[Na]^+$ + $[H]^+$ 15%), 794.7 (M^+ + $[Na]^+$ 100%). HRMS: Calculated for $C_{35}H_{65}NO_9$ $[M + Na]^+$ 794.6122, found 794.6133. α_D: +20.0°. m.p.: 127-133°C IR: 3200-3400cm^{-1} (br OH), 1750-1750cm^{-1} (C=O), 1600-1675cm^{-1} (C=C), 1500-1650cm^{-1} (N-H).

5.23.12. Eicosanoic acid [(1S, 2S, 3R)-2,3-dihydroxy-1-((2S, 3R, 4S, 5R, 6R)- 3,4,5-trihydroxy-6-hydroxymethyl-tetrahydro-pyran-2-yloxymethyl)-heptadecyl]-amide (79)

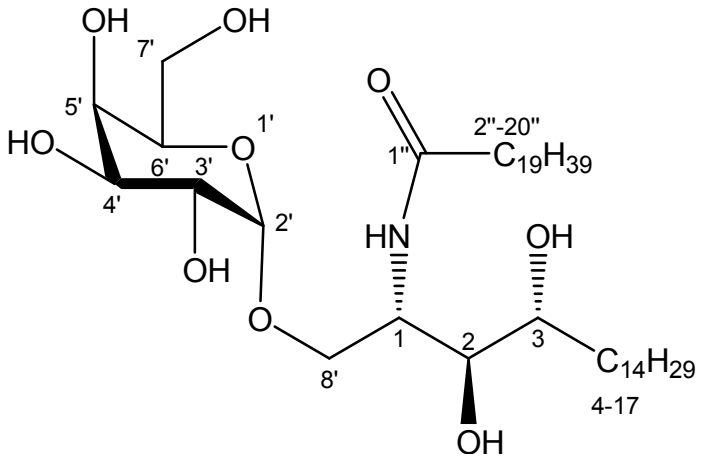

$C_{44}H_{87}NO_9$
Mol. Wt.: 774.1629 g mol^{-1}

Prepared by the general procedure for azide reduction and subsequent *N*-acylation **(5.1.1.13)** using (2S,3R,4S,5R,6R)-2-((2S,3S,4R)-2-azido-3,4-dihydroxy-octadecyloxy)-6-hydroxymethyl-tetrahydro-pyran-3,4,5-triol **(39)** (55mg, 98.9µmol), eicosanoic acid 2,5-dioxo-pyrrolidin-1-yl ester **(62)** (56.7mg, 138.5µmol), affording a white solid. Yield: 49mg, 64%. δ ^{1}H ($CDCl_3$:MeOD, 2:1): 4.78-4.82 (H-2', 1H, d, J=3.7Hz), 3.96-3.99 (H-1, 1H, m), 3.81-3.83 (H-4', 1H, d, J=3.1Hz), 3.72-3.76 (H-8_a, 1H, dd, J=4.8, 10.7Hz), 3.58-3.60 (H-3', H-6', 2H, m), 3.52-3.55 (H-5', H-$7'_{ab}$, 3H, m), 3.47-3.49 (H-8_b, 1H, m), 3.32-3.47 (H-2, H-3, 2H, m), 2.15-2.19 (H-$2''_{ab}$, 2H, t, J=7.6Hz), 1.48-1.63 (H-$3''_a$, H-$4''_a$, H-4_a, 3H, m), 1.19-1.40 (H-$3''_b$, H-$4''_b$, H-4_b, H-5_{ab} – H16_{ab}, H-$5''_{ab}$ – H-$19''_{ab}$, 57H, m), 0.80-0.83 (H-17_{abc}, H-$20''_{abc}$, 6H, J=6.9Hz). δ ^{13}C ($CDCl_3$:MeOD 2:1): 98.85 (C-2'), 76.52 (C-2), 73.49 (C-3), 71.88 (C-6'), 70.65 (C-5'), 69.17 (C4'), 68.24 (C-3'), 66.91 (C-8), 62.35 (C-7'), 51.26 (C-1), 26.30-36.10 (multiple signals C-2'' – C-19'', C-4 – C-16), 15.60 (C-20'', C-17). **m/z** (ES): 796.6 (M^+ + $[Na]^+$ + 100%). HRMS: Calculated for $C_{44}H_{87}NO_9$ $[M + Na]^+$ 796.6279, found 796.6276. α_D: +5.6°. IR: 3200-3400cm^{-1} (br OH), 1750-1750cm^{-1} (C=O), 1500-1650cm^{-1} (N-H).

5.23.13. (9Z, 12Z)-Octadeca-9,12-dienoic acid [(1S, 2S, 3R)-2,3-dihydroxy-1-((2S, 3R, 4S, 5R, 6R)-3,4,5-trihydroxy-6-hydroxymethyl-tetrahydro-pyran-2-yloxymethyl)-heptadecyl]-amide (80)

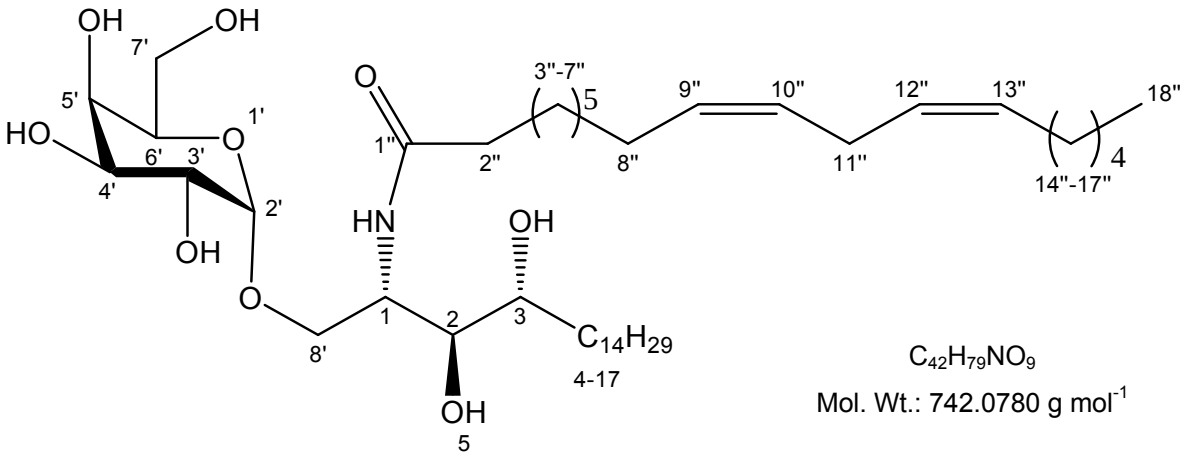

$C_{42}H_{79}NO_9$

Mol. Wt.: 742.0780 g mol^{-1}

Prepared by the general procedure for azide reduction and subsequent *N*-acylation **(5.1.1.13)** using (2S,3R,4S,5R,6R)-2-((2S,3S,4R)-2-azido-3,4-dihydroxy-octadecyloxy)-6-hydroxymethyl-tetrahydro-pyran-3,4,5-triol **(39)** (45mg, 88.99µmol), (9Z,12Z)-Octadeca-9,12-dienoic acid 2,5-dioxo-pyrrolidin-1-yl ester **(63)** (56.44mg, 0.149mmol), affording a white solid.Yield 27mg, 42%. δ ^{1}H ($CDCl_3$: MeOD, 2:1): 5.21-5.35 (H9'', H10'', H12'', H13'', 4H, m), 4.60-4.63 (H-2', 1H, d, J=3.65Hz,), 4.10-4.18 (H-1, 1H, m), 3.98-4.07 (H-4', 1H, d, J=3.2Hz), 3.79-3.83 (H-8'$_a$, 1H, dd, J=4.6, 10.8Hz), 3.62-3.75 (H-6', H-3', 2H, m), 3.58-361 (H-5', H-7'$_{ab}$, 3H, m), 3.46-3.52 (H-8'$_b$, 1H, m), 441-3.44 (H-2, H-3, 2H, m), 2.82-2.88 (H-11''$_{ab}$, 2H, m), 2.18-2.21 (H-2''$_{ab}$, 2H, t, J=7.8Hz), 1.82-2.01 (H-8''$_{ab}$, H-14''$_{ab}$, 4H, m), 1.43-1.66 (H-4$_a$, H-5$_a$, H-3''$_{ab}$, 4H, m), 1.15-1.39 (H-4$_b$, H-5$_b$, H-6$_{ab}$ – H-16$_{ab}$, H-4''$_{ab}$ – H-8''$_{ab}$, H-15''$_{ab}$ – H-17''$_{ab}$, 40H, m), 0.81-0.93 (H-17$_{abc}$, H-18''$_{abc}$, 6H, t, J=7.0Hz) δ ^{13}C ($CDCl_3$: MeOD, 2:1): 175.34 (C-1''), 131.02, 130.97, 128.91, 128.87 (C-9'', 10'', 12'', 13''), 100.76 (C-2'), 75.64 (C-2), 72.63 (C-3), 71.87 (C-6'), 70.27 (C-7'), 69.56 (C-4'), 69.04 (C-3'), 67.98 (C-8'), 62.56 (C-5'), 50.47 (C-1), 36.38 (C-2''), 29.77-31.57 (multiple signals, C-4 – C-16, C-3'' – C-8'', C-11'', C-14'' – C17''), 15.75, 14.81 (C-17, C-18''). **m/z** (ES): 64.0 (M^+ + $[Na]^+$ + $[H]^+$

30%), 763.0 (M^+ + $[Na]^+$ 100%). HRMS: Calculated for $C_{42}H_{79}NO_9$ $[M + Na]^+$ 763.0677, found 763.0686. α_D: 6.1° mp.: 121-135°C IR: 3200-3400cm^{-1} (br OH), 1750-1750cm^{-1} (C=O), 1600-1675cm^{-1} (C=C), 1500-1650cm^{-1} (N-H).

5.23.14. (9Z,12Z)-Octadeca-9,12-dienoic acid [(1S,2S,3R)-2,3-dihydroxy-1-((2S,3R,4S,5R,6R)-3,4,5-trihydroxy-6-hydroxymethyl-tetrahydro-pyran-2-yloxymethyl)-tetradecyl]-amide (81)

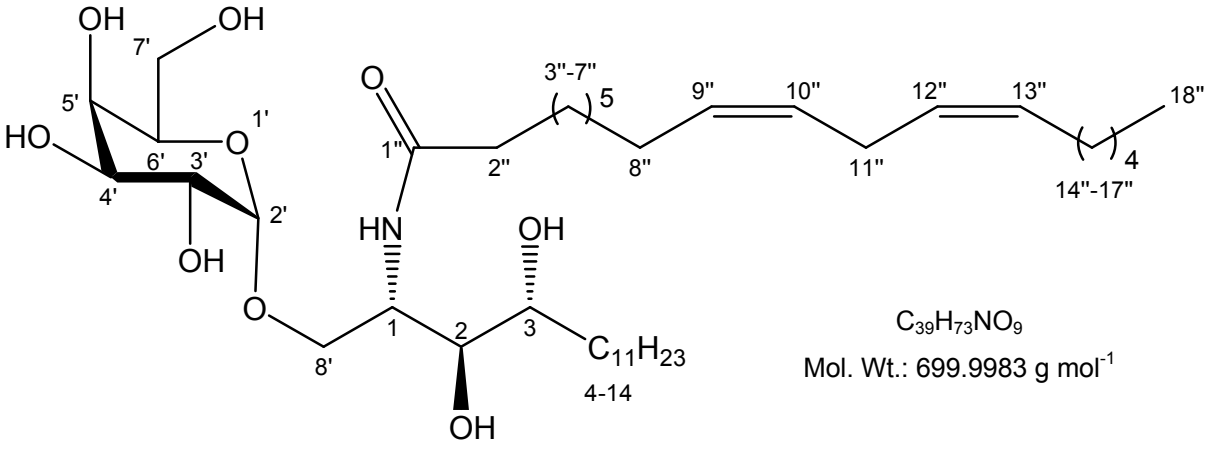

Prepared by the general procedure for azide reduction and subsequent *N*-acylation **(5.1.1.13)** using (2S,3R,4S,5R,6R)-2-((2S,3S,4R)-2-azido-3,4-dihydroxy-octadecyloxy)-6-hydroxymethyl-tetrahydro-pyran-3,4,5-triol **(40)** (49.5mg, 106.78µmol), (9Z,12Z)-Octadeca-9,12-dienoic acid 2,5-dioxo-pyrrolidin-1-yl ester **(63)** (66.3mg, 0.18mmol), affording a white solid. Yield: 35mg, 47.8%. δ ^1H ($CDCl_3$: MeOD, 2:1): 5.28-5.36 (H9'', H10'', H12'', H13'', 4H, m), 4.84-4.88 (H-2', 1H, d, J=4.0Hz,), 4.15-4.19 (H-1, 1H, m), 3.86-3.89 (H-4', 1H, d, J=2.8Hz), 3.81-3.85 (H-8'$_a$, 1H, dd, J=5.0, 11.1Hz), 3.74-3.77 (H-6', H-3', 2H, m), 3.67-3.72 (H-5', H-7'$_{ab}$, 3H, m), 3.62-3.67 (H-8'$_b$, 1H, m), 3.46-3.54 (H-2, H-3, 2H, m), 2.22-225 (H-11''$_{ab}$, 2H, t, J=7.8Hz), 2.15-2.18 (H-2''$_{ab}$, 2H, t, J=7.7Hz), 1.46-1.66 (H-18''$_{ab}$, H-14''$_{ab}$, 4H, m), 1.18-1.40 (H-4$_{ab}$ – H-13$_{ab}$, H-3''$_{ab}$ – H-7''$_{ab}$, H-15''$_{ab}$ – H-17''$_{ab}$, 36H, m), 0.80-0.87 (H-14$_{abc}$, H-18''$_{abc}$, 6H, t, J=6.9Hz). **m/z** (ES): 738.9 (M^+ + $[k]^+$ + $[H]^+$ 100%) HRMS: Calculated

for $C_{39}H_{73}NO_9$ $[M + Na]^+$ 722.988, found 722.9861. α_D: +24.6° m.p.: 128-137°C IR: 3200-3400cm^{-1} (br OH), 1750-1750cm^{-1} (C=O), 1600-1675cm^{-1} (C=C), 1500-1650cm^{-1} (N-H).

5.23.15. (9Z,12Z)-Octadeca-9,12-dienoic acid [(1S,2S,3R)-2,3-dihydroxy-1-((2S,3R,4S,5R,6R)-3,4,5-trihydroxy-6-hydroxymethyl-tetrahydro-pyran-2-yloxymethyl)-undecyl]-amide (82)

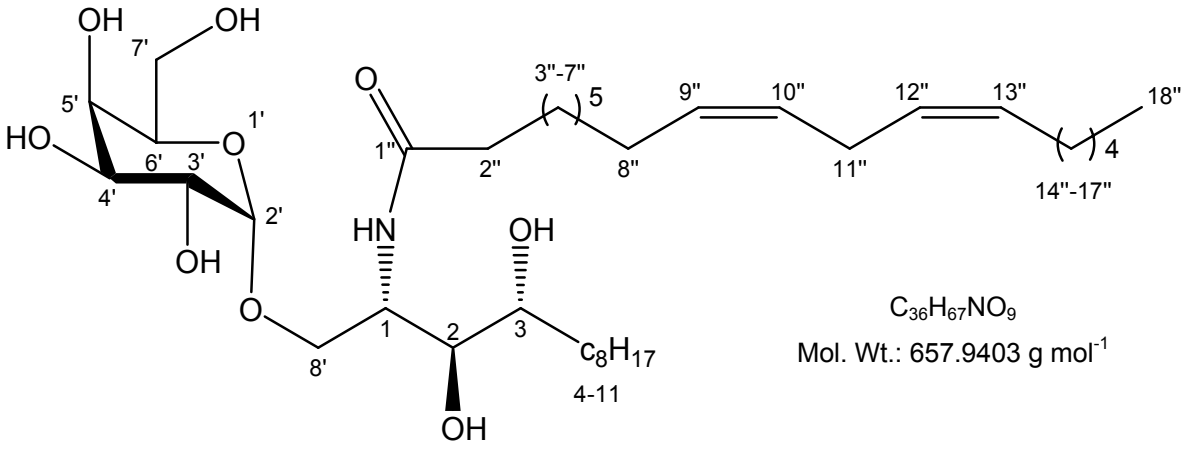

$C_{36}H_{67}NO_9$
Mol. Wt.: 657.9403 g mol^{-1}

Prepared by the general procedure for azide reduction and subsequent *N*-acylation **(5.1.1.13)** using (2S,3R,4S,5R,6R)-2-((2S,3S,4R)-2-azido-3,4-dihydroxy-dodecyloxy)-6-hydroxymethyl-tetrahydro-pyran-3,4,5-triol **(41)** (49mg, 116.3µmol), (9Z,12Z)-octadeca-9,12-dienoic acid 2,5-dioxo-pyrrolidin-1-yl ester **(63)** (73.3mg, 0.19mmol), affording a white solid. Yield: 31mg, 41%. δ ^{1}H ($CDCl_3$: MeOD, 2:1): 5.30-5.34 (H9'', H10'', H12'', H13'', 4H, m), 4.84-4.87 (H-2', 1H, d, J=3.7Hz,), 4.14-4.18 (H-1, 1H, m), 3.87-3.90 (H-4', 1H, d, J=2.87Hz), 3.82-3.86 (H-8'$_a$, 1H, dd, J=4.8, 10.9Hz), 3.7-3.76 (H-6', H-3', 2H, m), 3.66-3.72 (H-5', H-7'$_{ab}$, 3H, m), 3.61-3.66 (H-8'$_b$, 1H, m), 3.47-3.50 (H-2, H-3, 2H, m), 2.21-2.25 (H-11''$_{ab}$, 2H, t, J=8Hz), 2.14-2.18 (H-2''$_{ab}$, 2H, t, J=7.5Hz), 1.45-1.67 (H-8''$_{ab}$, H-14''$_{ab}$, 4H, m), 1.18-1.37 (H-4$_{ab}$ – H-10$_{ab}$, H-3''$_{ab}$ – H-7''$_{ab}$, H-15''$_{ab}$ – H-17''$_{ab}$, 30H, m), 0.80-0.88 (H-14$_{abc}$, H-18''$_{abc}$, 6H, t, J=7.0Hz). δ ^{13}C ($CDCl_3$: MeOD, 2:1): 127.57-131.49 (C-9'', 10'', 12'', 13''), 101.5 (C-2'),

75.14 (C-2), 73.36 (C-3), 72.85 (C-6'), 71.18 (C-7'), 70.92 (C-4'), 70.04 (C-3'), 68.31 (C-8'), 62.48 (C-5'), 51.11 (C-1), 37.00 (C-2''), 27.65-34.22- (multiple signals, C-4 – C-10, C-3'' – C-8'', C-11'', C14''-C17''), 15.06, 14.91 (C-11, C-18''). **m/z** (ES): 681.9 (M^+ + $[Na]^+$ + $[H]^+$ 10%), 680.9 (M^+ + $[Na]^+$ 100%). HRMS: Calculated for $C_{39}H_{73}NO_9$ $[M + Na]^+$ 680.9299, found 680.9305. α_D: +10.9°. m.p.: 126-136°C. IR: 3200-3400cm^{-1} (br OH), 1750-1750cm^{-1} (C=O), 1600-1675cm^{-1} (C=C), 1500-1650cm^{-1} (N-H).

5.23.16. (9Z,12Z)-Octadeca-9,12-dienoic acid [(1S,2S,3R)-2,3-dihydroxy-1-((2S,3R,4S,5R,6R)-3,4,5-trihydroxy-6-hydroxymethyl-tetrahydro-pyran-2-yloxymethyl)-octyl]-amide (83)

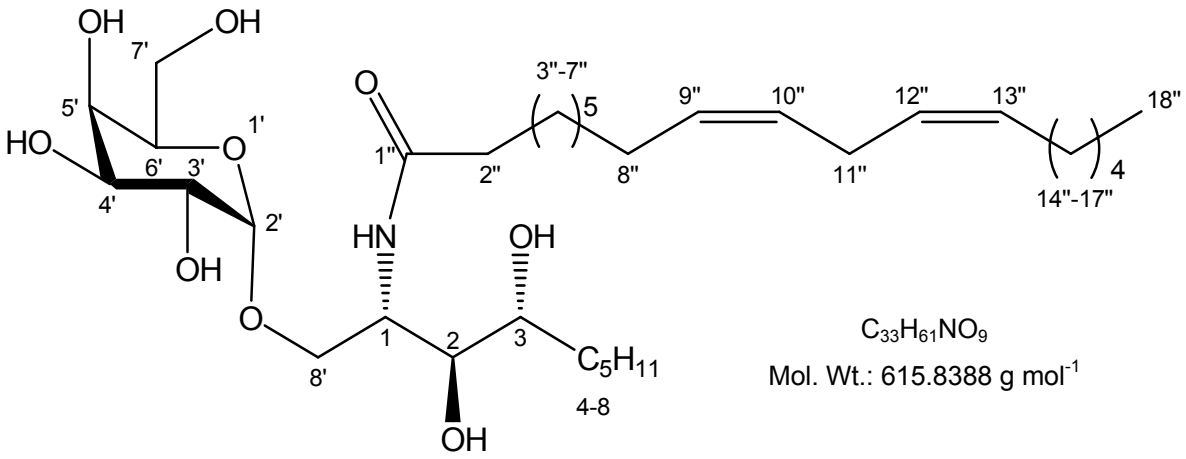

$C_{33}H_{61}NO_9$

Mol. Wt.: 615.8388 g mol^{-1}

Prepared by the general procedure for azide reduction and subsequent *N*-acylation **(5.1.1.13)** using (2S,3R,4S,5R,6R)-2-((2S,3S,4R)-2-azido-3,4-dihydroxy-nonyloxy)-6-hydroxymethyl-tetrahydro-pyran-3,4,5-triol **(42)** (27.4mg, 72.2µmol), (9Z,12Z)-octadeca-9,12-dienoic acid 2,5-dioxo-pyrrolidin-1-yl ester **(63)** (37.4mg, 99.04µmol), affording a white solid. Yield: 16mg, 36%. δ ^1H ($CDCl_3$: MeOD, 2:1): 5.31-5.38 (H9'', H10'', H12'', H13'', 4H, m), 4.83-4.87 (H-2', 1H, d, J=3.75Hz,), 4.14-4.18 (H-1, 1H, m), 3.86-3.89 (H-4', 1H, d, J=3.05Hz), 3.83-3.87 (H-8'$_a$, 1H, dd, J=4.9, 10.6Hz), 3.75-3.78 (H-6', H-3', 2H, m), 3.65-3.71

(H-5', H-7'$_{ab}$, 3H, m), 3.61-3.65 (H-8'$_b$, 1H, m), 3.47-3.50 (H-2, H-3, 2H, m), 2.22-2.24 (H-11''$_{ab}$, 2H, t, J=7.8Hz), 2.15-2.18 (H-2''$_{ab}$, 2H, t, J=7.65Hz), 1.40-1.69 (H-8''$_{ab}$, H-14''$_{ab}$, 4H, m), 1.21-1.40 (H-4$_{ab}$ – H-7$_{ab}$, H-3''$_{ab}$ – H-7''$_{ab}$, H-15''$_{ab}$ – H-17''$_{ab}$, 30H, m), 0.80-0.88 (H-8$_{abc}$, H-18''$_{abc}$, 6H, t, J=7.2Hz). δ ^{13}C ($CDCl_3$: MeOD, 2:1): 126.56-130.49 (C-9'', 10'', 12'', 13''), 100.8 (C-2'), 74.64 (C-2), 73.26 (C-3), 71.65 (C-6'), 71.20 (C-7'), 70.63 (C-4'), 70.01 (C-3'), 68.43 (C-8'), 62.38 (C-5'), 50.71 (C-1), 35.67 (C-2''), 27.55-35.22- (multiple signals, C-4 – C-7, C-3'' – C-8'', C-11'', C14''-C17''), 15.00, 13.21 (C-8, C-18''). **m/z** (ES): 655.8 (M^+ + $[K]^+$ + $[H]^+$ 28%), 654.8 (M^+ + $[K]^+$ 100%). HRMS: Calculated for $C_{33}H_{61}NO_9$ $[M + Na]^+$ 638.8285, found 638.8292. α_D: +15.1°. m.p.: 121-131°C. IR: 3200-3400cm^{-1} (br OH), 1750-1750cm^{-1} (C=O), 1600-1675cm^{-1} (C=C), 1500-1650cm^{-1} (N-H).

5.23.17. Octanoic acid [(1S, 2S, 3R)-2,3-dihydroxy-1-((2S, 3R, 4S, 5R, 6R)-3,4,5-trihydroxy-6-hydroxymethyl-tetrahydro-pyran-2-yloxymethyl)-heptadecyl]-amide (84)

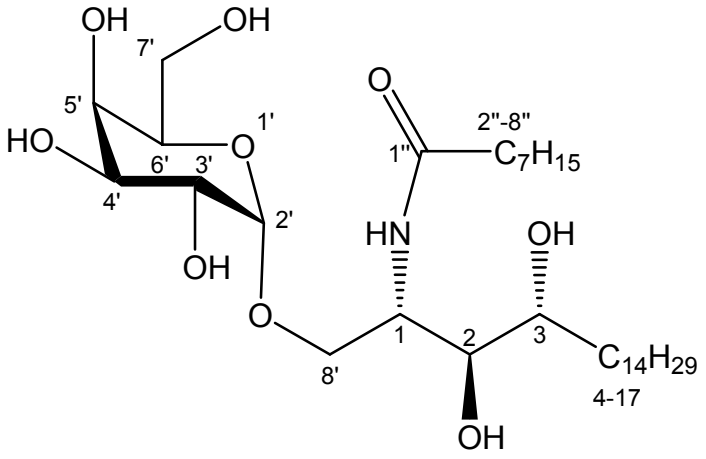

$C_{32}H_{63}NO_9$

Mol. Wt.: 605.8440 g mol^{-1}

Prepared by the general procedure for azide reduction and subsequent *N*-acylation **(5.1.1.13)** using (2S,3R,4S,5R,6R)-2-((2S,3S,4R)-2-azido-3,4-dihydroxy-octadecyloxy)-6-

hydroxymethyl-tetrahydro-pyran-3,4,5-triol **(39)** (125.5mg, 248.2µmol), Octanoic acid 2,5-dioxo-pyrrolidin-1-yl ester **(64)** (64.9mg, 269µmol), affording a white solid. Yield: 108mg, 72%. δ ^{1}H ($CDCl_3$:MeOD, 2:1): 4.84-4.88 (H-2', 1H, d, J=3.8Hz), 4.16-4.25 (H-1, 1H, m), 3.89-3.92 (H-4', 1H, d, J=3.0Hz), 3.83-3.87 (H-8'$_a$, 1H, dd, J=4.7, 10.7Hz), 3.74-3.79 (H-3', H-6', 2H, m), 3.68-3.72 (H-5', H-7'$_{ab}$, 3H, m), 3.63-3.67 (H-8'$_b$, 1H, dd, J=4.7, 10.7Hz), 3.49-3.55 (H-2, H-3, 2H, m), 2.16-2.2 (H-2'', 2H, t, J=7.7Hz), 1.48-1.66 (H-3''$_a$, H-4''$_a$, H-4$_a$, 3H, m), 1.17-1.38 (H-4$_b$, H-5$_{ab}$ – H-16$_{ab}$, H-3''$_b$, H-4''$_b$, H-5''$_{ab}$ – H -7''$_{ab}$, 33H, m), 0.88-0.82 (H-17$_{abc}$, H-8''$_{abc}$, 6H, m) δ ^{13}C ($CDCl_3$:MeOD, 2:1): 100.34 (C-2'), 75.15 (C-2), 72.55 (C-3), 71.41 (C-6'), 70.88 (C-5'), 70.48 (C-4'), 69.52 (C-3') , 67.82 (C-8'), 62.36 (C-7'), 51.05 (C-1), 36.93 (C-2''), 32.95 (C-4), 32.46-29.59 (multiple signals, C5-16, 6''-7''), 26.44, 26.40 (C-3'', 4''), 23.16 (C-5''), 14.29, 14.26 (C-18, C-8''). **m/z** (ES): 629.8 (M^+ + $[Na]^+$ + $[H]^+$ 8%), 628.7 (M^+ + $[Na]^+$ 100%). HRMS: Calculated for $C_{33}H_{61}NO_9$ $[M + Na]^+$ 628.4401, found 628.4389. α_D: +4.8° m.p.: 115-123°C. IR: 3200-3400cm^{-1} (br OH), 1750-1750cm^{-1} (C=O), 1500-1650cm^{-1} (N-H).

5.23.18. *N*-[(1S,2S,3R)-2,3-Dihydroxy-1-((2S,3R,4S,5R,6R)-3,4,5-trihydroxy-6-hydroxymethyl-tetrahydro-pyran-2-yloxymethyl)-heptadecyl]-3-propionamide (85)

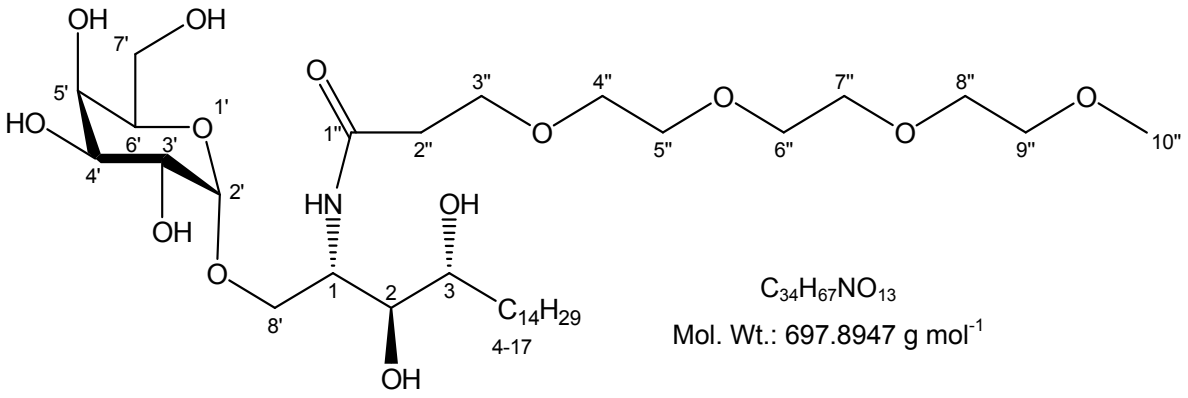

$C_{34}H_{67}NO_{13}$

Mol. Wt.: 697.8947 g mol^{-1}

Prepared by the general procedure for azide reduction and subsequent *N*-acylation **(5.1.1.13)** using (2S,3R,4S,5R,6R)-2-((2S,3S,4R)-2-azido-3,4-dihydroxy-octadecyloxy)-6-hydroxymethyl-tetrahydro-pyran-3,4,5-triol **(39)** (31mg, 631µmol), methyl-PEO_4-NHS ester (Pierce Biotechnology) (referred to here as **(66)**) (29.2mg, 88mmol). Butanol was used instead of EtOAc in the work up, affording an opaque oil. Yield: 374mg, 85%. δ ^{1}H ($CDCl_3$:MeOD, 2:1): 4.85-4.87 (H-2', 1H, d, J=3.8Hz), 4.23-4.27 (H-1, 1H, m), 3.90-3.93 (H-4', 1H, d, J=4.6Hz), 3.87-3.90 (H-8'$_a$, 1H, m), 3.79-3.82 (H-3', H-6', 2H, t, J=6.1Hz), 3.74-3.78 (H-8'$_b$, 1H, dd, J=4.2, 9.9Hz), 3.68-3.74 (H-5', H-7'$_{ab}$, 3H, m), 3.59-3.64 (H-3''$_{ab}$ – H-9''$_{ab}$, 14H, m), 3.51-3.55 (H-2, H-3, H-10''$_{abc}$, 5H, m), 2.45-2.49 (H-2'', 2H, t, J=6.1Hz), 1.48-1.72 (H-4$_a$, H-5$_a$, 2H, m), 1.21-1.33 (H-4$_b$, H-5$_b$, H-6$_{ab}$ – H-16$_{ab}$, 24H, m), 0.84-0.88 (H-17$_{abc}$, 3H, t, J=7.1Hz) δ ^{13}C ($CDCl_3$:MeOD, 2:1): 170.4 (C-1''), 98.9 (C-2'), 78.2 (C-2), 70.1 (C-3), 70.0 (C-8'), 69.8 (C-6'), 67.8 (C-4'), 65.4 (C-3'), 65.5-72.8 (multiple signals, C-3'' – C-9''), 61.5 (C-7'), 57.3 (C-5'), 53.2 (C-10''), 38.5 (C-2''), 29.59-31.8 (multiple signals, C4-16), 17.7 (C-18). **m/z** (ES): 721.8 (M^+ + $[Na]^+$ + $[H]^+$ 20%), 720.8 (M^+ + $[Na]^+$ 100%). HRMS Calculated for $C_{34}H_{67}NO_{13}$ $[M + Na]^+$ 720.4510, found 720.4491. α_D: +7.7°. IR: 3200-3400cm^{-1} (br OH), 1750-1750cm^{-1} (C=O), 1400-1420cm^{-1} (C-O), 1500-1650cm^{-1} (N-H).

5.23.19. *N*-[(1S,2S,3R)-2,3-Dihydroxy-1-((2S,3R,4S,5R,6R)-3,4,5-trihydroxy-6-hydroxymethyl-tetrahydro-pyran-2-yloxymethyl)-heptadecyl]-3-(2-ethoxy)-ethoxy]-ethoxy}-ethoxy)-propionamide (86)

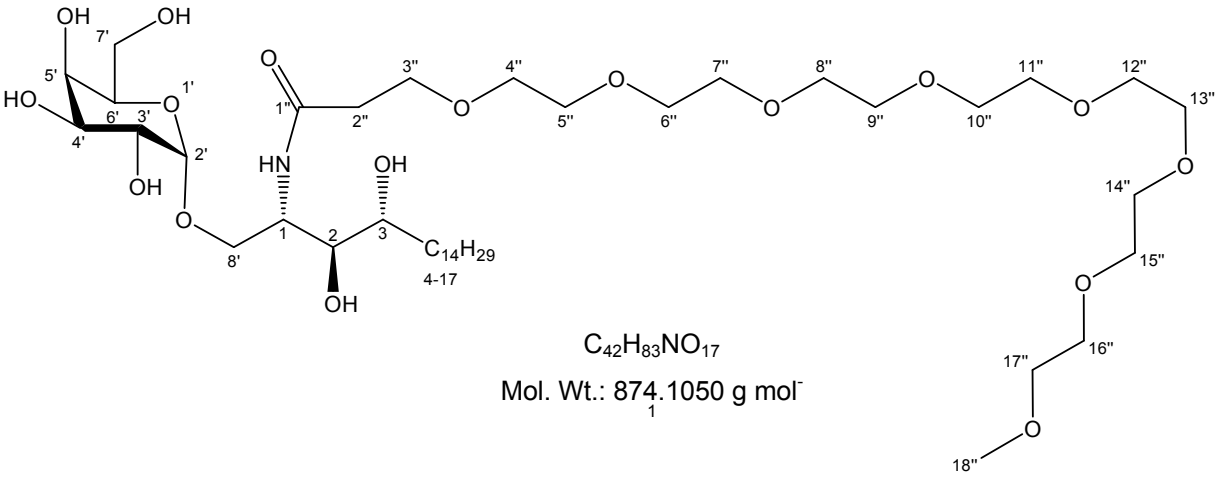

$C_{42}H_{83}NO_{17}$

Mol. Wt.: 874.1050 g mol^{-1}

Prepared by the general procedure for azide reduction and subsequent *N*-acylation **(5.1.1.13)** using (2S,3R,4S,5R,6R)-2-((2S,3S,4R)-2-azido-3,4-dihydroxy-octadecyloxy)-6-hydroxymethyl-tetrahydro-pyran-3,4,5-triol **(39)** (30mg, 59.3µmol), methyl-PEO_8-NHS ester (Pierce Biotechnology) (referred to as **(67)**) (44.62mg, 87.64mmol). Butanol was used instead of EtOAc in the work-up, affording an opaque oil. Yield: 38.4mg, 74%. δ ^{1}H ($CDCl_3$:MeOD, 2:1): 4.54-4.59 (H-2', 1H, d, J=3.75Hz), 4.15-4.20 (H-1, 1H, m), 3.92-3.94 (H-4', 1H, m), 3.88-3.93 (H-8'$_a$, 1H, m), 3.80-3.83 (H-3', H-6', 2H, m), 3.75-3.78 (H-8'$_b$, 1H, dd, J=4.2, 9.9Hz), 3.70-3.74 (H-5', H-7'$_{ab}$, 3H, m), 3.50-3.64 (H-3''$_{ab}$ – H-17''$_{ab}$, 30H, m), 3.49-3.50 (H-2, H-3, H-18''$_{abc}$, 5H, m), 2.43-2.48 (H-2'', 2H, t, J=6.1Hz), 1.50-1.67 (H-4$_a$, H-5$_a$, 2H, m), 1.181-1.35 (H-4$_b$, H-5$_b$, H-6$_{ab}$ – H-16$_{ab}$, 24H, m), 0.81-0.85 (H-17$_{abc}$, 3H, t, J=7.0Hz) δ ^{13}C ($CDCl_3$:MeOD, 2:1): 101.2 (C-2'), 80.4 (C-2), 78.8 (C-3), 78.5 (C-8'), 76.1 (C-6'), 76.0 (C-4'), 72.5 (C-3'), 68.5-75.5 (multiple signals, C-3'' – C-17''), 63.5 (C-7'), 59.8 (C-5'), 54.9 (C-18''), 39.7 (C-2''), 31.8-38.9 (multiple signals, C4-16), 19.9 (C-18). **m/z** (ES): 897.7 (M^+ + $[Na]^+$ + $[H]^+$ 30%), 896.6 (M^+ + $[Na]^+$ 100%). HRMS: Calculated for $C_{42}H_{83}NO_{17}$ [M + Na]$^+$ 896.5559,

found 896.5566. α_D: +5.8°. IR: 3200-3400cm^{-1} (br OH), 1750-1750cm^{-1} (C=O), 1400-1420cm^{-1} (C-O), 1500-1650cm^{-1} (N-H).

5.23.20. *N*-[(1S,2S,3R)-2,3-Dihydroxy-1-((2S,3R,4S,5R,6R)-3,4,5-trihydroxy-6-hydroxymethyl-tetrahydro-pyran-2-yloxymethyl)-heptadecyl]-2-*m*-tolyl-acetamide (87)

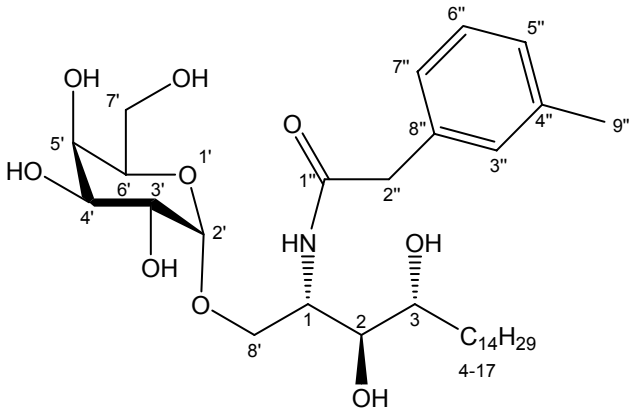

$C_{33}H_{57}NO_9$

Mol. Wt.: 611.8070 g mol^{-1}

Prepared by the general procedure for azide reduction and subsequent *N*-acylation **(5.1.1.13)** using (2S,3R,4S,5R,6R)-2-((2S,3S,4R)-2-azido-3,4-dihydroxy-octadecyloxy)-6-hydroxymethyl-tetrahydro-pyran-3,4,5-triol **(39)** (25mg, 49.44µmol), *m*-tolyl-acetic acid 2,5-dioxo-pyrrolidin-1-yl ester (17.04mg, 68.9µmol), affording an opaque oil. Yield: 21mg, 70%. δ ^{1}H ($CDCl_3$:MeOD, 2:1): 6.89-7.25 (H-3'', H-6'', H-7''), 4.66-4.70 (H-2', 1H, d, J=4.6Hz), 3.67-3.70 (H-1, 1H, m), 3.63-3.66 (H-4', 1H, d, J=3.8Hz), 3.55-3.61 (H-8'$_a$, 1H, dd, J=4.1, 9.9Hz), 3.49-3.54 (H-3', H-6', 2H, m), 3.45-3.49 (H-8'$_b$, 1H, m), 3.36-3.44 (H-5', H-7'$_{ab}$, 3H, m), 3.29-3.34 (H-2''$_{ab}$, H-9''$_{abc}$, 2H, m), 3.13-3.20 (H-2, H-3, 2H, m), 1.33-1.46 (H-4$_a$, H-5$_a$, 2H, m), 0.97-1.18 (H-4$_b$, H-5$_b$, H-6$_{ab}$ – H-16$_{ab}$, 24H, m), 0.65-0.73 (H-17$_{abc}$, 3H, t, J=7.3Hz). δ ^{13}C ($CDCl_3$:MeOD, 2:1): 178.5 (C-1''), 138.8, 140.2 (C-4'', C-8''), 129.1-132.9 (C-3'', C-5'', C-6'', C-7''), 102.7 (C-2'), 71.9-77.7 (C-2, C-3, C-3', C-4', C-5', C-6'), 70.35 (C-8'), 64.9 (C-7'), 53.5 (C-1), 46.3 (C-2''), 28.12-35.7 (C-4 – C-16), 24.12 (C-9''), 16.9 (C-17). **m/z** (ES): 635.3

(M^+ + $[Na]^+$ + $[H]^+$ 20%), 634.4 (M^+ + $[Na]^+$ 100%). HRMS: Calculated for $C_{33}H_{57}NO_9$ [M + Na]$^+$ 634.3931, found 634.3954. α_D: +17.7°. IR: 3200-3400cm^{-1} (br OH), 3000-3100cm^{-1} (Ar), 1750-1750cm^{-1} (C=O), 1500-1650cm^{-1} (N-H).

5.23.21. Tetracosanoic acid [(1S,2S,3R)-2,3-dihydroxy-1-(3,4,5-trihydroxy-6-hydroxymethyl-tetrahydro-pyran-2-yloxymethyl)-heptadecyl]-amide (88)

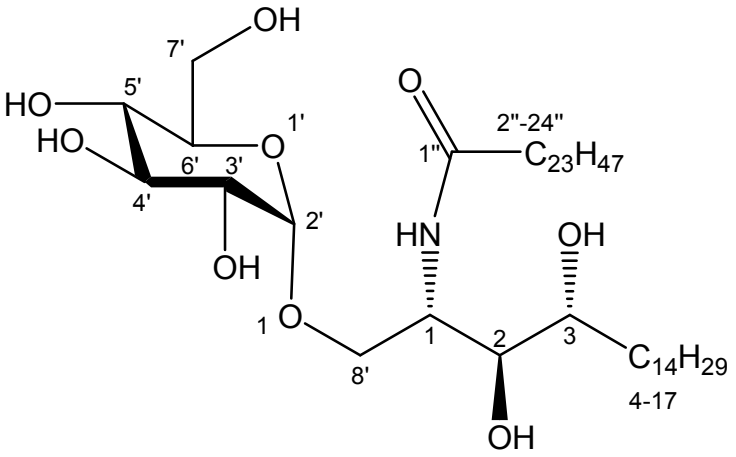

$C_{48}H_{95}NO_9$

Mol. Wt.: 830.2692 g mol^{-1}

Prepared by the general procedure for azide reduction and subsequent *N*-acylation using (2S,3R,4S,5S,6R)-2-((2S,3S,4R)-2-azido-3,4-dihydroxy-octadecyloxy)-6-hydroxymethyl-tetrahydro-pyran-3,4,5-triol **(49)** (55mg, 108.8µmol), tetracosanoic acid 2,5-dioxo-pyrrolidin-1-yl ester **(54)** (72.8mg, 160µmol), affording a white solid. Yield: 48.7mg, 54%. δ ^{1}H ($CDCl_3$:MeOD, 2:1): 4.8-4.82 (H-2', 1H, d, J=3.8Hz), 4.12-4.16 (H-1, 1H, m), 4.02-4.04 (H-4', 1H, m), 3.81-3.85 (H-8_a, 1H, dd, J=4.9, 10.6Hz), 3.73-3.77 (H-5', 1H, dd, J=2.4, 12Hz), 3.64-3.68 (H-3', H-6', H-5', 3H, m), 3.62-3.64 (H-7_{ab}, 2H, m), 3.49-3.55 (H-2, H-3, 2H, m), 3.38-3.42 (H-$8'_b$, 1H, dd, J=3.8, 9.8Hz), 2.13-2.18 (H-$2''_{ab}$, 2H, t, J=7.5Hz), 1.46-1.65 (H-$3''_a$, H-$4''_a$, H-4_a, 3H, m), 1.15-1.35 (H-$3''_b$, H-$4''_b$, H-4_b, H-5_{ab} – H16_{ab}, H-$5''_{ab}$ – H-$23''_{ab}$, 65H, m), 0.81-.85 (H-17_{abc}, H-$24''_{abc}$, 6H, J=6.9Hz). δ ^{13}C ($CDCl_3$:MeOD 2:1): 96.87 (C-2'), 74.51 (C-2), 71.0 (C-3), 70.53 (C-6'), 70.03 (C-5'), 69.49 (C4'), 68.68 (C-3'), 67.23 (C-8), 61.55 (C-7'), 51.25 (C-1), 25.43-36.1 (multiple signals C-2'' – C-23'', C-4 – C-16), 15.40 (C-24'', C-17).

m/z (ES): 853.9 (M^+ + $[Na]^+$ + $[H]^+$ 20%), 852.9 (M^+ + $[Na]^+$ + 100%) HRMS: Calculated for $C_{48}H_{95}NO_9$ $[M + Na]^+$ 852.6905, found 852.6920. α_D: +12.9°. m.p.: 125-129°C IR:3200-3400cm^{-1} (br OH), 1750-1750cm^{-1} (C=O), 1500-1650cm^{-1} (N-H).

5.23.22. (4Z,7Z,10Z,13Z,16Z,19Z)-Docosa-4,7,10,13,16,19-hexaenoic acid [(1S,2S,3R)-2,3-dihydroxy-1-(3,4,5-trihydroxy-6-hydroxymethyl-tetrahydro-pyran-2-yloxymethyl)-heptadecyl]-amide (89)

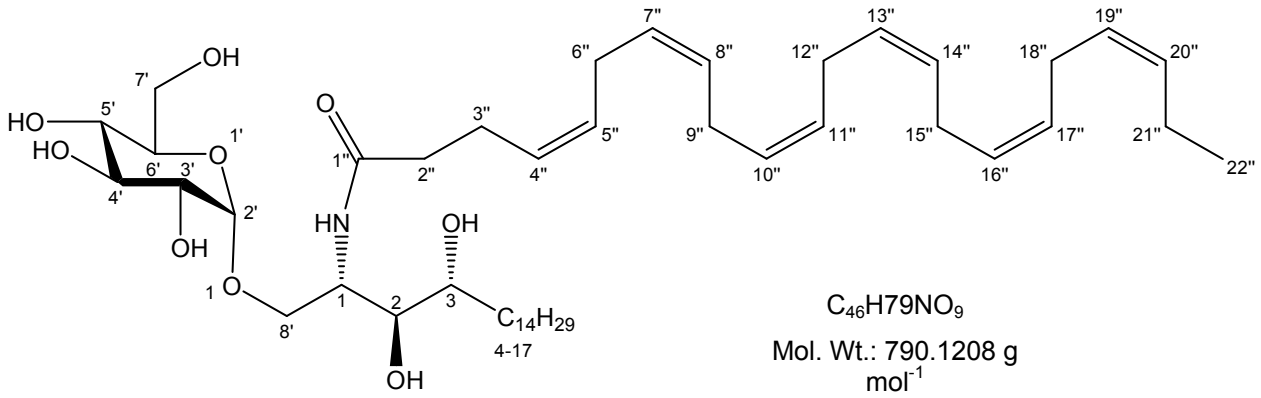

$C_{46}H79NO_9$

Mol. Wt.: 790.1208 g mol^{-1}

Prepared by the general procedure for azide reduction and subsequent *N*-acylation **(5.1.1.13)** using (2S,3R,4S,5S,6R)-2-((2S,3S,4R)-2-azido-3,4-dihydroxy-octadecyloxy)-6-hydroxymethyl-tetrahydro-pyran-3,4,5-triol **(49)** (33mg, 65.3µmol), (4Z,7Z,10Z,13Z,16Z,19Z) -docosa-4,7,10,13,16,19-hexaenoic acid 2,5-dioxo-pyrrolidin-1-yl ester **(56)** (42mg, 98.7µmol), affording a white solid. Yield: 3mg, 6% δ ^{1}H ($CDCl_3$:MeOD, 2:1): 5.55-5.49 (H-4'', H-5'', H-7'', H-8'', H-10'', H-11'', H-13'', H-14'', H-16'', H-17'', H-19'', H-20'', 12H, m), 4.91-4.94 (H-2', 1H, d, J=3.7Hz), 4.15-4.19 (H-1, 1H, m), 3.89-3.99 (H-4', 1H, m), 3.81-3.85 (H-8'$_a$, 1H, m), 3.62-3.66 (H-3', H-6', 2H, m), 3.58-3.61 (H-5', H-7'$_{ab}$, 3H, m), 3.50-3.57 (H-8'$_b$, 1H, m), 3.45-3.48 (H-2, H-3, 2H, m), 2.60-2.75 (H-6'', H-9'', H-12'', H-15'', H-18'', 5H, m), 2.26-2.31 (H-2''$_{ab}$, 2H, t, J=7.1Hz), 1.55-1.80 (H-3''$_a$, H-4$_a$, H-5$_a$, 3H, m), 1.25-1.42 (H-3''$_b$, H-4$_b$, H-5$_b$, H-6$_{ab}$ – H16$_{ab}$, H-21''$_{ab}$ 27H, m), 0.88-0.93 (H-17$_{abc}$, H-22''$_{abc}$, 6H, J=7.5Hz).

m/z (ES): 813.0 (M^+ + $[Na]^+$ + 100%). HRMS: Calculated for $C_{48}H_{95}NO_9$ $[M + Na]^+$ 813.1105, found 813.1113. α_D: +12°. m.p.: 135-141°C IR: 3200-3400cm^{-1} (br OH), 1750-1750cm^{-1} (C=O), 1600-1675cm^{-1} (C=C), 1500-1650cm^{-1} (N-H).

5.23.23. (5Z,8Z,11Z,14Z)-Eicosa-5,8,11,14-tetraenoic acid [(1S, 2S, 3R)-2,3-dihydroxy-1-(3,4,5-trihydroxy-6-hydroxymethyl-tetrahydro-pyran-2-yloxymethyl)-heptadecyl]-amide (90)

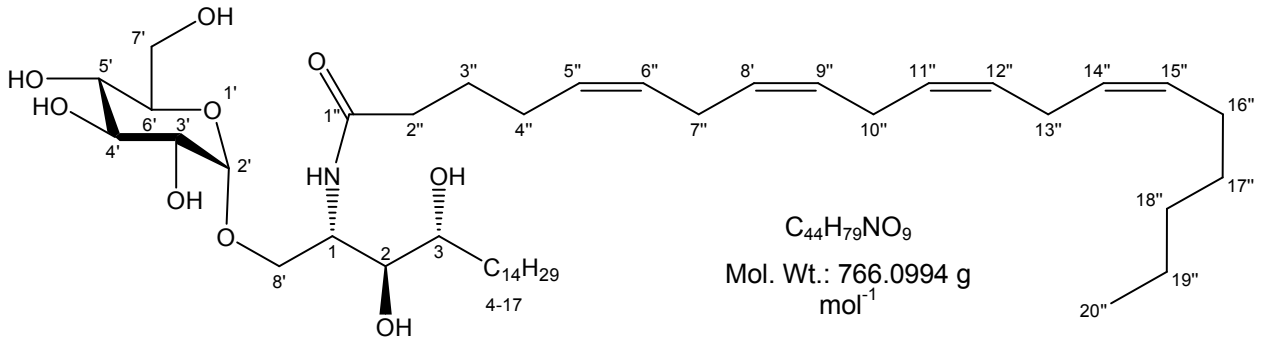

Prepared by the general procedure for azide reduction and subsequent *N*-acylation **(5.1.1.13)** using (2S,3R,4S,5S,6R)-2-((2S,3S,4R)-2-azido-3,4-dihydroxy-octadecyloxy)-6-hydroxymethyl-tetrahydro-pyran-3,4,5-triol **(49)** (20mg, 39.55µmol), (5Z,8Z,11Z,14Z)-eicosa-5,8,11,14-tetraenoic acid 2,5-dioxo-pyrrolidin-1-yl ester **(58)** (24.3mg, 60.49µmol), affording a white solid. Yield: 3mg, 10%. δ ^{1}H ($CDCl_3$:MeOD, 2:1): 5.34-5.75 (H-5'', H-6'', H-8'', H-9'', H-11'', H-12'', H-14'', H-15'', 8H, m), 4.75-4.81 (H-2', 1H, m), 4.31-4.35 (H-1, 1H, m), 4.11-4.16 (H-4', 1H, m), 3.90-3.96 (H-8'$_a$, 1H, dd, J=4.1, 10.6 Hz), 3.59-3.71 (H-3', H-6', 2H, m), 3.55-3.59 (H-5', H-7'$_{ab}$, 3H, m), 3.46-3.50 (H-8'$_b$, 1H, m), 3.41-3.44 (H-2, H-3, 2H, m), 2.32-2.37 (H-7'', H-10'', H-13'', 3H, m), 2.06-2.14 (H-2''$_{ab}$, 2H, m), 1.56-1.62 (H-3''$_a$, H-4$_a$, H-5$_a$, 3H, m), 1.22-1.49 (H-3''$_b$, H-4$_b$, H-5$_b$, H-4''$_{ab}$, H-6$_{ab}$ – H16$_{ab}$, H-16''$_{ab}$ – H19''$_{ab}$ 27H, m), 0.85-0.91 (H-17$_{abc}$, H-20''$_{abc}$, 6H, J=7.4Hz). δ ^{13}C ($CDCl_3$:MeOD 2:1): 131.6-135.4 (multiple signals, C-5'', C-6', C-8'', C-9'', C-11'', C-12'', C-14'', C-15''), 101.80 (C-2'), 78.62 (C-2),

74.98 (C-3), 71.90 (C-6'), 70.64 (C-5'), 69.98 (C4'), 68.39 (C-3'), 67.47 (C-8), 60.55 (C-7'), 49.21 (C-1), 26.61-39.54 (multiple signals C-2'', C-3'', C-4'', C-7'', C-10'', C-13'', C-16'' – C19'', C-4 – C-16), 15.55 (C-20'', C-17). **m/z** (ES): 790.2 (M^+ + $[Na]^+$ + $[H]^+$ 10%), 789.2 (M^+ + $[Na]^+$ 100%), HRMS: Calculated for $C_{44}H_{77}NO_9$ $[M + Na]^+$ 789.0891, found 789.0899. α_D: +2.8°. m.p.: 136-145°C IR: 3200-3400cm^{-1} (br OH), 1750-1750cm^{-1} (C=O), 1600-1675cm^{-1} (C=C), 1500-1650cm^{-1} (N-H).

5.23.24. Eicosa-11,14-dienoic acid [(1S, 2S, 3R)-2,3-dihydroxy-1-(3,4,5-trihydroxy-6-hydroxymethyl-tetrahydro-pyran-2-yloxymethyl)-heptadecyl]-amide (91)

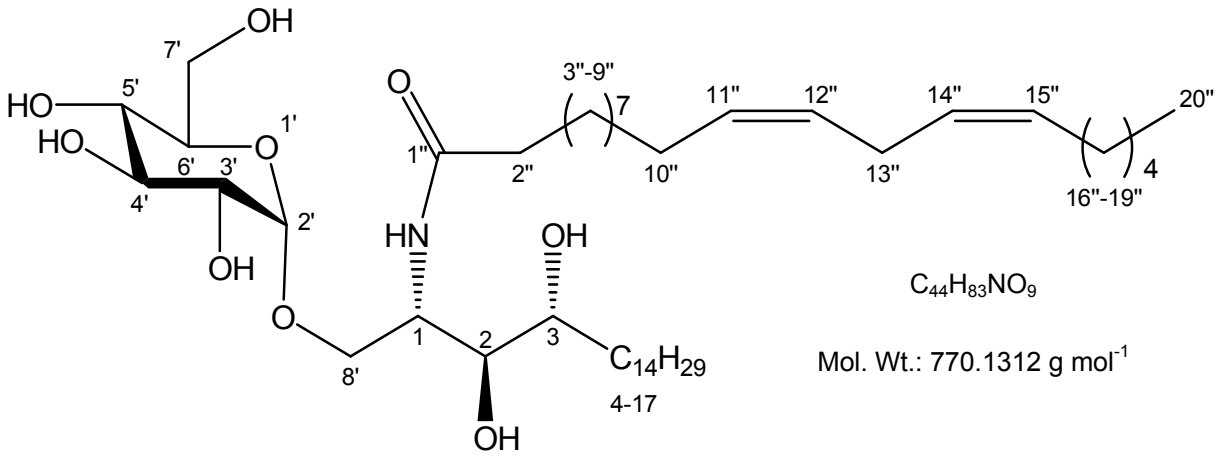

$C_{44}H_{83}NO_9$

Mol. Wt.: 770.1312 g mol^{-1}

Prepared by the general procedure for azide reduction and subsequent *N*-acylation **(5.1.1.13)** using (2S,3R,4S,5S,6R)-2-((2S,3S,4R)-2-azido-3,4-dihydroxy-octadecyloxy)-6-hydroxymethyl-tetrahydro-pyran-3,4,5-triol **(49)** (40mg, 79.1µmol), (11Z,14Z)-eicosa-11,14-dienoic acid 2,5-dioxo-pyrrolidin-1-yl ester **(59)** (46.3mg, 114µmol), affording a white solid. Yield: 24.9mg, 41%. δ ^1H ($CDCl_3$: MeOD, 2:1): 5.24-5.36 (H11'', H12'', H14'', H15'', 4H, m), 4.80-4.84 (H-2', 1H, d, J=4.4Hz,), 4.11-4.15 (H-1, 1H, m), 3.80-3.86 (H-8'$_a$, 1H, dd, J=4.9-10.3Hz), 3.73-3.78 (H-7'$_a$, 1H, dd, J=3, 11.3Hz), 3.61-3.70 (H-8'$_b$, H-7'$_b$, 2H, m), 3.56-3.70 (H-4', 1H, t, J=9.3), 3.48-3.55 (H-2, H-3, H-6', 3H, m), 3.48-3.53 (H-3', H-5', 2H, m), 2.70-

2.75 (H-13''$_{ab}$, 2H, t, J=7.4Hz), 2.13-2.19 (H-2''$_{ab}$, 2H, m), 1.54-1.69 (H-3''$_{ab}$, H-4''$_{ab}$, 4H, m), 1.05-1.44 (H-5''$_{ab}$ – H-19''$_{ab}$, H-5ab – H-16ab, 54H, m), 0.80-0.85 (H-17$_{abc}$, H-20''$_{abc}$, 6H, t, J=6.4, 7.1Hz). δ ^{13}C ($CDCl_3$: MeOD, 2:1): 169.04 (C-1''), 128.82-130.74 (C-11'', 12'', 14'', 15''), 101.80 (C-2'), 74.91 (C-2), 72.56 (C-3), 71.09 (C-6'), 70.77 (C-7'), 70.33 (C-4'), 68.48 (C-3'), 67.17 (C-8'), 61.11 (C-5'), 48.73 (C-1), 34.42 (C-2''), 22.10-30.02 (multiple signals, C-4 – C-16, C-3'' – C-10'', C-13'', C-16'' – C-19''), 17.51, 18.16 (C-17, C-20''). **m/z** (ES): 794.1 (M^+ + $[Na]^+$ + $[H]^+$ 10%), 793.1 (M^+ + $[Na]^+$ + 100%). HRMS: Calculated for $C_{44}H_{83}NO_9$ [M + $Na]^+$ 793.1209, found 793.1223. α_D: +6.4°. m.p.: 137-145°C. IR: 3200-3400cm^{-1} (br OH), 1750-1750cm^{-1} (C=O), 1600-1675cm^{-1} (C=C), 1500-1650cm^{-1} (N-H).

5.23.25. (11Z)-Eicos-11-enoic acid [2,3-dihydroxy-1-(3,4,5-trihydroxy-6-hydroxymethyl-tetrahydro-pyran-2-yloxymethyl)-heptadecyl]-amide (92)

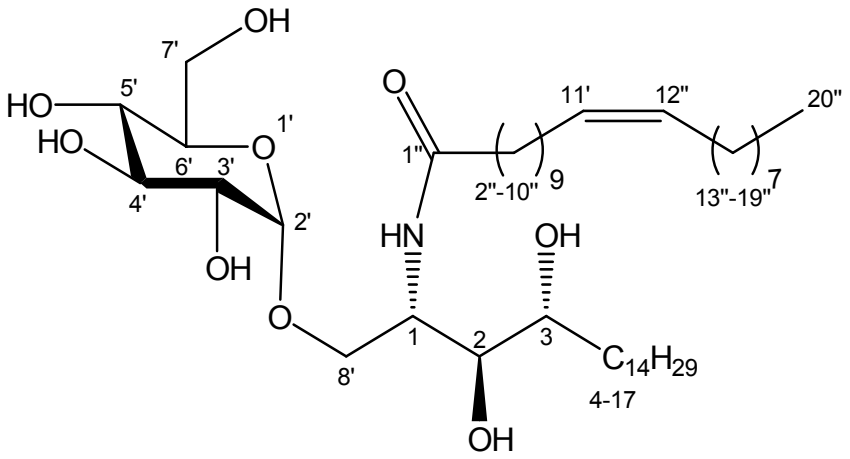

$C_{44}H_{85}NO_9$

Mol. Wt.: 772.1470 g mol^{-1}

Prepared by the general procedure for azide reduction and subsequent *N*-acylation **(5.1.1.13)** using (2S,3R,4S,5S,6R)-2-((2S,3S,4R)-2-azido-3,4-dihydroxy-octadecyloxy)-6-hydroxymethyl-tetrahydro-pyran-3,4,5-triol **(49)** (63mg, 124.6µmol), (11Z)-eicosa-11enoic acid 2,5-dioxo-pyrrolidin-1-yl ester **(60)** (59.5mg, 191.6µmol). Yield: 29.8mg, 31%. δ ^{1}H ($CDCl_3$: MeOD, 2:1): 5.28-5.31 (H11'', H12'', 2H, t, J=4.9Hz), 4.79-4.82 (H-2', 1H, d, J=3.4Hz,), 4.12-4.16 (H-1, 1H, m), 3.80-3.85, (H-8'$_a$, 1H, dd, J=4.9, 10.9Hz), 3.73-3.77 (H-

7'$_a$, 1H, dd, J=2.4, 11.4Hz), 3.61-3.68 (H-8'$_b$, H-7'$_b$, 2H, m), 3.56-3.61 (H-4', 1H, t, J=8.9Hz), 3.48-3.55 (H-2, H-3, H-6', 3H, m), 3.38-3.42 (H-5', 1H, dd, J=3.9, 9.9Hz), 2.13-2.18 (H-2''$_{ab}$, 2H, t, J=7.4Hz), 1.94-1.99 (H-3''$_{ab}$, H-4$_{ab}$, 4H, m), 1.45-1.65 (H-10''$_{ab}$, H-13''$_{ab}$, 4H, m), 1.18-1.32 (H-5$_{ab}$ – H-16$_{ab}$, H-4''$_{ab}$ – H-9''$_{ab}$, H-14''$_{ab}$ – H-19''$_{ab}$, 46H, m), 0.81-0.85 (H-17$_{abc}$, H-20''$_{abc}$, 6H, t, J=6.9Hz). δ ^{13}C ($CDCl_3$: MeOD, 2:1): 130.31-132.7 (C-11'', 12''), 101.80 (C-2'), 74.43 (C-2), 73.91 (C-3), 73.34 (C-6'), 71.66 (C-7'), 71.12 (C-4'), 69.97 (C-3'), 68.59 (C-8'), 63.88 (C-5'), 46.48 (C-1), 35.17 (C-2''), 20.26-32.10 (multiple signals, C-4 – C-16, C-3'' – C-10'', C-13'' – C-19''), 15.95, 16.31 (C-17, C-20''). **m/z** (ES): 795.6 (M^+ + $[Na]^+$ + $[H]^+$ 20%), 794.6 (M^+ + $[Na]^+$ 100%). HRMS: Calculated for $C_{35}H_{65}NO_9$ $[M + Na]^+$ 794.6122, found 794.6132. α_D: +18.2°. m.p.: 128-132°C IR: 3200-3400cm^{-1} (br OH), 1750-1750cm^{-1} (C=O), 1600-1675cm^{-1} (C=C), 1500-1650cm^{-1} (N-H).

5.23.26. (11E)-Eicos-11-enoic acid [2,3-dihydroxy-1-(3,4,5-trihydroxy-6-hydroxymethyl-tetrahydro-pyran-2-yloxymethyl)-heptadecyl]-amide (93)

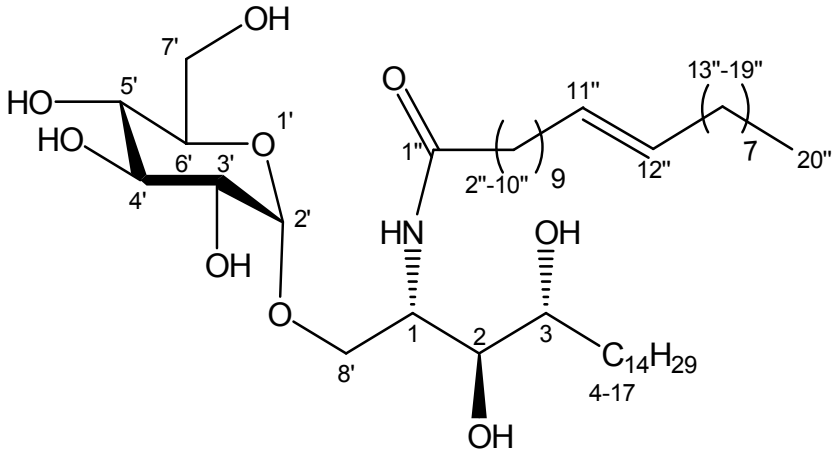

$C_{44}H_{85}NO_9$

Mol. Wt.: 772.1470 g mol^{-1}

Prepared by the general procedure for azide reduction and subsequent *N*-acylation **(5.1.1.13)** using (2S,3R,4S,5S,6R)-2-((2S,3S,4R)-2-azido-3,4-dihydroxy-octadecyloxy)-6-hydroxymethyl-tetrahydro-pyran-3,4,5-triol **(49)** (52mg, 102.8μmol), (11E)-eicosa-11enoic acid 2,5-dioxo-pyrrolidin-1-yl ester **(61)** (49.5mg, 159μmol), affording a white solid. Yield:

23mg, 29%. δ ^{1}H ($CDCl_3$: MeOD, 2:1): 5.28-5.31 (H11'', H12'', 2H, t, J=3.4Hz), 4.79-4.82 (H-2', 1H, d, J=3.4Hz,), 4.12-4.16 (H-1, 1H, m), 3.80-3.85, (H-8'$_a$, 1H, dd, J=4.9, 10.9Hz), 3.73-3.77 (H-7'$_a$, 1H, dd, J=2.4, 11.4Hz), 3.61-3.68 (H-8'$_b$, H-7'$_b$, 2H, m), 3.56-3.61 (H-4', 1H, t, J=8.9Hz), 3.48-3.55 (H-2, H-3, H-6', 3H, m), 3.38-3.42 (H-5', 1H, dd, J=3.9, 9.9Hz), 2.13-2.18 (H-2''$_{ab}$, 2H, t, J=7.4Hz), 1.94-1.99 (H-3''$_{ab}$, H-4$_{ab}$, 4H, m), 1.45-1.65 (H-10''$_{ab}$, H-13''$_{ab}$, 4H, m), 1.18-1.32 (H-5$_{ab}$ – H-16$_{ab}$, H-4''$_{ab}$ – H-9''$_{ab}$, H-14''$_{ab}$ – H-19''$_{ab}$, 46H, m), 0.81-0.85 (H-17$_{abc}$, H-20''$_{abc}$, 6H, t, J=6.9Hz). δ ^{13}C ($CDCl_3$: MeOD, 2:1): 130.31-132.7 (C-11'', 12''), 101.80 (C-2'), 74.43 (C-2), 73.91 (C-3), 73.34 (C-6'), 71.66 (C-7'), 71.12 (C-4'), 69.97 (C-3'), 68.59 (C-8'), 63.88 (C-5'), 46.48 (C-1), 35.17 (C-2''), 20.26-32.10 (multiple signals, C-4 – C-16, C-3'' – C-10'', C-13'' – C-19''), 15.95, 16.31 (C-17, C-20''). **m/z** (ES): 795.8 (M^+ + $[Na]^+$ + $[H]^+$ 30%), 794.8 (M^+ + $[Na]^+$ 100%). HRMS: Calculated for $C_{35}H_{65}NO_9$ [M + Na]$^+$ 794.6122, found 794.6108. α_D: +20° m.p.: 125-130°C. IR: 3200-3400cm^{-1} (br OH), 1750-1750cm^{-1} (C=O), 1600-1675cm^{-1} (C=C), 1500-1650cm^{-1} (N-H).

5.23.27. Eicosanoic acid [2,3-dihydroxy-1-(3,4,5-trihydroxy-6-hydroxymethyl-tetrahydro-pyran-2-yloxymethyl)-heptadecyl]-amide (94)

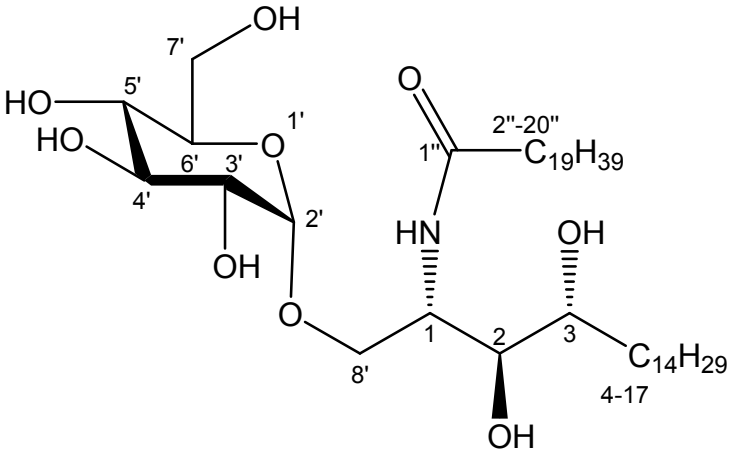

$C_{44}H_{87}NO_9$

Mol. Wt.: 774.1629 g mol^{-1}

Prepared by the general procedure for azide reduction and subsequent *N*-acylation **(5.1.1.13)** using (2S,3R,4S,5S,6R)-2-((2S,3S,4R)-2-azido-3,4-dihydroxy-octadecyloxy)-6-

hydroxymethyl-tetrahydro-pyran-3,4,5-triol **(49)** (50mg, 98.8µmol), eicosanoic acid 2,5-dioxo-pyrrolidin-1-yl ester **(62)** (59.8mg, 146µmol), affording a white solid. Yield: 46.6mg, 61%. δ ^{1}H ($CDCl_3$:MeOD, 2:1): 4.81-4.82 (H-2', 1H, d, J=4.6Hz), 4.11-4.16 (H-1, 1H, m), 3.83-3.85 (H-8'$_a$, 1H, dd, J=3.9, 10.7Hz), 3.74-3.77 (H-7'$_a$, 1H, dd, J=2.8, 12.2Hz), 3.63-3.68 (H-8'$_b$, H-7'$_b$, 2H, m), 3.58-3.61 (H-4', 1H, m,), 3.50-3.55 (H-2, H-3, H-6', 3H, m), 3.39-3.42 (H-3', 1H, dd, J=3.9, 9.7Hz), 3.31-3.35 (H-5', 1H, m), 2.15-2.19 (H-2''$_{ab}$, 2H, t, J=7.6Hz), 1.48-1.64 (H-3''$_a$, H-4''$_a$, H-4$_a$, H-5$_a$, 4H, m), 1.19-1.39 (H-4$_b$, H-5$_b$, H-6$_{ab}$ – H-16$_{ab}$, H-3''$_b$, H-4''$_b$, H-5''$_{ab}$ – H-19''$_{ab}$, 56H, m), 0.83-0.85 (H-17''$_{abc}$, H-20''$_{abc}$, 6H, t, J=6.7Hz) δ ^{13}C ($CDCl_3$:MeOD, 2:1):175.09 (C-1''), 99.88 (C-2'), 74.93 (C-2), 74.41 (C-4'), 72.83 (C-6'), 72.56, 72.47 (C-3, 3'), 67.64 (C-8'), 62.05 (C-7'), 50.93 (C-1), 49.84 (C-5') , 36.89 (C-2''), 32.81 (C-3''), 32.41 (C-4), 30.17-23.13 (various signals, C-5 – C-16, C-4'' – C-19''), 14.27, 14.25 (C-17, C-20''). **m/z** (ES): 797.80 (M^+ + $[Na]^+$ + $[H]^+$ 20%), 796.8 (M^+ + $[Na]^+$ + 100%). HRMS: Calculated for $C_{44}H_{87}NO_9$ $[M + Na]^+$ 796.6279, found 796.6288. α_D: +5.6°. m.p.: 132-138°C. IR: 3200-3400cm^{-1} (br OH), 1750-1750cm^{-1} (C=O), 1500-1650cm^{-1} (N-H).

5.23.28. Octadeca-9,12-dienoic acid [2,3-dihydroxy-1-(3,4,5-trihydroxy-6-hydroxymethyl-tetrahydropyran-2-yloxymethyl)-heptadecyl]-amide (95)

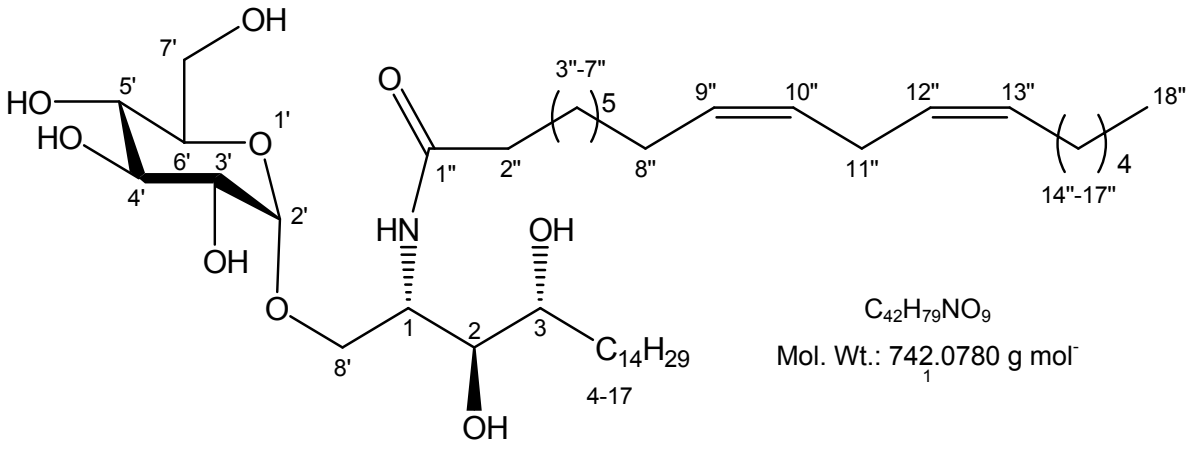

Prepared by the general procedure for azide reduction and subsequent *N*-acylation **(5.1.1.13)** using (2S,3R,4S,5S,6R)-2-((2S,3S,4R)-2-azido-3,4-dihydroxy-octadecyloxy)-6-hydroxymethyl-tetrahydro-pyran-3,4,5-triol **(49)** (50mg, 98.8µmol), Octadeca-9,12-dienoic acid 2,5-dioxo-pyrrolidin-1-yl ester **(63)** (59mg, 160µmol), affording a white solid. Yield: 22mg, 31%. δ ^{1}H ($CDCl_3$: d4-MeOH, 2:1): 5.23-5.27 (H11'', H12'', H14'', H15'', 4H, m), 4.79-4.84 (H-2', 1H, d, J=4.7Hz,), 4.11-4.15 (H-1, 1H, m), 3.80-3.87 (H-8'$_a$, 1H, d, J=2.91Hz), 3.73-3.78 (H-7'$_a$, 1H, dd, J=3.5, 11.8Hz), 3.63-3.69 (H-7'$_b$, H-8'b, 2H, dd, J=5.12, 12.12), 3.60-3.63 (H-4', 1H, m), 3.44-3.58 (H-2, H-3, H-6', 2H, m), 3.38-3.42 (H-3', 1H, dd, J=4.3, 9.8Hz), 3.31-3.33 (H-5', 1H, m), 2.6-2.75 (H11''$_{ab}$, 2H, t, J=7.8Hz), 2.13-2.20 (H-2''$_{ab}$, 2H, t, J=7.8), 1.97-2.04 (H-8''$_{ab}$, 2H, t, J=7.60Hz), 1.53-1.68 (H-14''$_{ab}$, H-4$_{ab}$, 4H, m), 1.27-1.42 (H-5$_a$, H-6$_a$, H-3''$_{ab}$, 4H, m), 1.09-1.25 (H-6$_b$ – H-16$_{ab}$, H-4''$_{ab}$ – H-9''$_{ab}$, H-17''$_{ab}$ – H-19''$_{ab}$, 40H, m), 0.80-0.85 (H-17$_{abc}$, H-18''$_{abc}$, 6H, t, J=6.3Hz) δ ^{13}C ($CDCl_3$: d4-MeOH, 2:1): 175.04 (C-1''), 130.52, 130.47, 128.41, 128.37 (C-11'', 12'', 14'', 15''), 99.88 (C-2'), 74.93 (C-2), 74.41 (C-3), 72.54 (C-6'), 72.01 (C-7'), 71.53 (C-4'), 70.84 (C-3'), 68.43 (C-8'), 60.31 (C-5'), 51.09 (C-1), 36.95 (C-2''), 29.77-35.72 (multiple signals, C-4 – C-16, C-3'' – C-8'', C-11'', C-14'' – C-17''), 14.25, 14.31 (C-17, C-18''). **m/z** (ES): 766.0 (M^+ + $[Na]^+$ + $[H]^+$ 15%), 765.0 (M^+ + $[Na]^+$ + 100%). HRMS: Calculated for $C_{42}H_{79}NO_9$ $[M + Na]^+$ 765.0677, found 765.0684. α_D: +35.0°. m.p.: 149-150°C. IR: 3200-3400cm^{-1} (br OH), 1750-1750cm^{-1} (C=O), 1600-1675cm^{-1} (C=C), 1500-1650cm^{-1} (N-H).

5.23.29. (11Z,14Z)-Nonadeca-11,14-dienoic acid [(1S,2S,3R)-2,3-dihydroxy-1-((2R,3S,4R,5S,6S)-3,4,5-trihydroxy-6-methyl-tetrahydro-pyran-2-yloxymethyl)-heptadecyl]-amide (96)

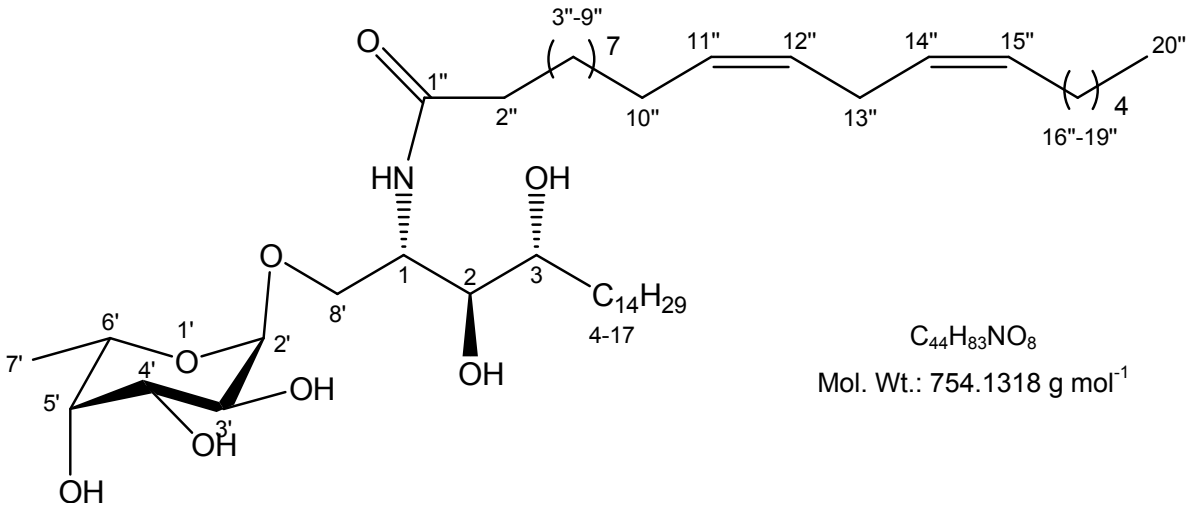

Prepared by the general procedure for azide reduction and subsequent *N*-acylation **(5.1.1.13)** using (2R,3S,4R,5S,6S)-2-((2S,3S,4R)-2-azido-3,4-dihydroxy-octadecyloxy)-6-methyl-tetrahydro-pyran-3,4,5-triol **(52)** (42mg, 85.78µmol), (11Z,14Z)-eicosa-11,14-dienoic acid 2,5-dioxo-pyrrolidin-1-yl ester **(59)** (46.3mg, 114µmol), affording a white syrup. Yield: 9.7mg, 15%. δ ^{1}H ($CDCl_3$: d4-MeOH, 2:1): 5.23-5.36 (H11'', H12'', H14'', H15'', 4H, m), 4.71-4.75 (H-2', 1H, d, J=3.88Hz,), 4.13-4.18 (H-1, 1H, m), 3.91-3.97 (H-2, H-3, 2H, m), 3.68-3.73 (H-3', 1H, dd, J=3.5, 9.9Hz), 3.66-3.68 (H-8'$_a$, 1H, d, J=3.5Hz), 3.60-3.65 (H-5', 1H, m), 3.51-3.56 (H-4', 1H, t, J=6.2Hz), 3.39-3.44 (H-8'$_b$, 1H, dd, J=3.8, 10.3Hz), 2.7-2.75 (H-13''$_{ab}$, 2H, t, J=7.3Hz), 2.12-2.20 (H-2''$_{ab}$, 2H, t, J=7.8Hz), 1.96-2.04 (H-10''$_{ab}$, H-16''$_{ab}$, 4H, m), 1.53-1.65 (H-3''$_{ab}$, H-4$_a$, H-5$_a$, 4H, m), 0.99-1.46 (H-4$_b$, H-5$_b$, H-6$_{ab}$ – H-16$_{ab}$, H-4''$_{ab}$ – H-9''$_{ab}$, H-17''$_{ab}$ – H-19''$_{ab}$, 42H, m), 0.81-0.85 (H-17$_{abc}$, H-20''$_{abc}$, 6H, t, J=7.3Hz). **m/z** (ES): 778.2 (M^+ + $[Na]^+$ + $[H]^+$ 45%), 777.2 (M^+ + $[Na]^+$ + 100%). HRMS: Calculated for $C_{44}H_{83}NO_8$ [M + $Na]^+$ 777.1215, found 777.1210. α_D:-4.4°. IR: 3200-3400cm^{-1} (br OH), 1750-1750cm^{-1} (C=O), 1600-1675cm^{-1} (C=C), 1500-1650cm^{-1} (N-H).

5.23.30. (9Z,12Z)-Octadeca-9,12-dienoic acid [(1S,2S,3R)-2,3-dihydroxy-1-((2R,3S,4R,5S,6S)-3,4,5-trihydroxy-6-methyl-tetrahydro-pyran-2-yloxymethyl)-heptadecyl]-amide (97)

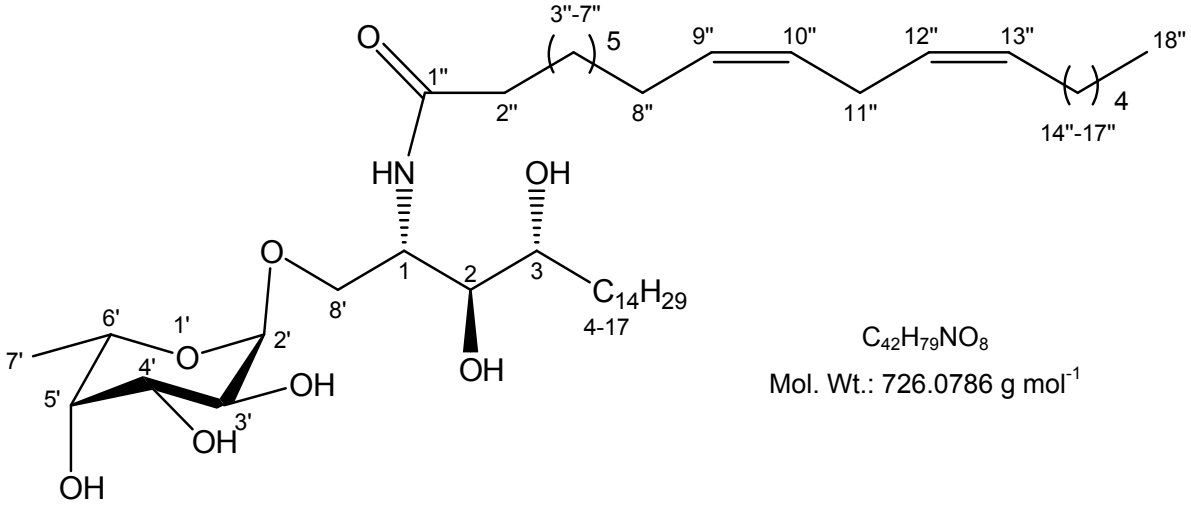

$C_{42}H_{79}NO_8$

Mol. Wt.: 726.0786 g mol^{-1}

Prepared by the general procedure for azide reduction and subsequent *N*-acylation **(5.1.1.13)** using (2R,3S,4R,5S,6S)-2-((2S,3S,4R)-2-azido-3,4-dihydroxy-octadecyloxy)-6-methyl-tetrahydro-pyran-3,4,5-triol **(52)** (125mg, 255.3µmol), (9Z,12Z)-octadeca-9,12-dienoic acid 2,5-dioxo-pyrrolidin-1-yl ester **(63)** (162mg, 430µmol), affording a white syrupy oil. Yield: 95.1mg, 51.3%. δ ^{1}H ($CDCl_3$: MeOD, 2:1): 5.23-5.36 (H9'', H10'', H12'', H13'', 4H, m), 4.71-4.75 (H-2', 1H, d, J=3.88Hz,), 4.13-4.18 (H-1, 1H, m), 3.91-3.97 (H-2, H-3, 2H, m), 3.68-3.73 (H-3', 1H, dd, J=3.5, 9.9Hz), 3.66-3.68 (H-8'$_a$, 1H, d, J=3.5Hz), 3.60-3.65 (H-5', 1H, m), 3.51-3.56 (H-4', 1H, t, J=6.2Hz), 3.39-3.44 (H-8'$_b$, 1H, dd, J=3.8, 10.3Hz), 2.7-2.75 (H-13''$_{ab}$, 2H, t, J=7.3Hz), 2.12-2.20 (H-2''$_{ab}$, 2H, t, J=7.8Hz), 1.96-2.04 (H-11''$_{ab}$, H-14''$_{ab}$, 4H, m), 1.53-1.65 (H-3''$_{ab}$, H-4$_a$, H-5$_a$, 4H, m), 0.99-1.46 (H-7'$_{abc}$, H-4$_b$, H-5$_b$, H-6$_{ab}$ – H-16$_{ab}$, H-4''$_{ab}$ – H-8''$_{ab}$, H-15''$_{ab}$ – H-17''$_{ab}$, 42H, m), 0.81-0.85 (H-17$_{abc}$, H-18''$_{abc}$, 6H, t, J=7.3Hz). **m/z** (ES): 750.1 (M^+ + $[Na]^+$ + $[H]^+$ 10%), 749.1(M^+ + $[K]^+$ + 100%). HRMS: Calculated for $C_{42}H_{79}NO_8$ $[M + Na]^+$ 749.0683, found 749.0671. α_D: -18°. IR: 3200-3400cm^{-1} (br OH), 1750-1750cm^{-1} (C=O), 1600-1675cm^{-1} (C=C), 1500-1650cm^{-1} (N-H).

5.24. Biological assays

5.24.1. Materials and methods

Human Vα24 iNKT cell lines were generated from healthy donors by Brigl *et al* [255], and McCarthy *et al* [218] at Brigham and Women's Hospital, Boston, USA and Weatherall Institute of Molecular Medicine, John radcliffe Hospital, Oxford, UK, respectively. PBMC were purified from patients' buffy coat by layering over Lymphoprep (Nycomed, Asker, Norway). Monocytes were then positively selected using magnetic beads coated with anti-CD14 monoclonal antibodies (mAbs) (MACS; Miltenyi Biotec, Bergisch Gladbach, Germany). and frozen in Roswell Park Memorial Institute medium (RPMI) medium (Sigma-Aldrich) until needed [218, 292].

5.24.1.1. Protein expression and purification

Purified hCD1d and β2M proteins were refolded with α-GalCer **(44)**, C20:0 **(79)**, C20:2 **(73)**, C11:1, OCH15 **(45)**, OCH12 **(46)**, OCH9 **(47),** by oxidative refolding chromatography, and the rate of dissociation from hCD1d molecules of each GSL was analysed. Purified CD1d heavy chain and β_2m were synthesized by using a prokaryotic expression system (pET, Novagen). Both recombinant proteins CD1d and β_2m were expressed in the *Escherichia coli* strain BL21 and purified from inclusion bodies. Soluble protein fractions were concentrated to a volume of 3 ml and biotinylated. Biotinylated monomeric CD1d–β_2m–glycolipid complexes were separated from soluble protein aggregates and free biotin by ÄKTA FPLC size exclusion chromatography by using a Superdex 75HR10/300 GL gel filtration column (Amersham Pharmacia) and conjugated to Streptavidin-PE (Sigma–Aldrich) [218, 292-294].

5.24.1.2. Preparation of soluble heterodimeric TCRs

Vα24 and Vβ11 iNKT cell TCR sequences were amplified by polymerase chain reaction (PCR) from the cDNA of an established iNKT cell clone. The α- and β-chains were individually cloned into pGMT7 bacterial expression vectors encoding the c-Jun and v-Fos fragments, respectively. TCR chains were expressed separately as inclusion bodies in the *E. coli* strain BL21-DE3 (pLysS) by induction in mid-log phase with 0.5mM isopropyl β-**D**-1-thiogalactopyranoside (IPTG). Inclusion bodies were isolated by sonication, followed by successive wash and centrifugation steps using 0.5% Triton X-100. Finally, the inclusion bodies were dissolved in 6M guanidine, 10mM dithiothreitol (DTT), 10mM ethylenediaminetetra-acetate (EDTA), buffered with 50mM tris(hydroxymethyl)aminomethane (Tris) pH 8.1 and stored at –80°C. Soluble TCR was refolded by rapid dilution of a mixture of the dissolved α- and β-chain inclusion bodies into 5M urea, 0.4M L-arginine, 100mM Tris pH 8.1, 3.7mM cystamine, 6.6mM β-mercaptoethylamine (4°C) to a final concentration of 60mg/l. The refold mixture was dialysed for 24 h against 10 vol of demineralized water, then against 10 vol of 10mM Tris pH 8.1 at 4°C. The refolded protein was then filtered and loaded onto a POROS 50HQ column (Applied Biosystems). The column was washed with 10mM Tris pH 8.1 prior to elution with a 0±500mM NaCl gradient in the same buffer. Fractions were analysed by Coomassie-stained sodium docecyl sulfate (SDS) ± 10% NuPAGE (Novagen, WI), and TCR-containing fractions were pooled and further purified by gel filtration on a Superdex 75PG 26/60 column (Amersham Biosciences, Uppsala, Sweden) pre-equilibrated in phosphate-buffered saline. Fractions comprising the main peak were pooled and analysed further. The final purified 1G4 dsTCR was analysed by Coomassie-stained SDS ± 10% NuPAGE under reducing and non-reducing conditions, and an aliquot of protein was buffer exchanged into HBSE (*N*-2-hydroxyethylpiperazine-*N*'-2-ethanesulfonic acid [HEPES] pH 7.4, 150mM NaCl, 3mM EDTA) and concentrated prior to activity determination by SPR. Soluble biotinylated TCR was made by inserting a 15–amino acid Avi-Tag recognition peptide (Avidity) after the c-Jun

fragment of the α-chain; the α-chain Jun fragment was amplified by PCR and sub-cloned into a pGMT7 vector encoding the AviTag peptide. This new α protein was expressed, refolded with the β- chain, and purified as before. The TCR heterodimer was biotinylated with BirA enzyme before the final SD75 gel filtration and were tetramerized by mixing at a 4:1 molar ratio with Extravidin-PE (Sigma-Aldrich) [218, 295].

5.24.1.3. Surface Plasmon Resonance (SPR)

The affinity and kinetic properties of Vα24 NKT TCR binding to hCD1d–lipid complexes were determined using BIAcore 2000 (BIAcore AB, St. Albans, UK) in HEPES buffered saline (HBS) (BIAcore). HBS contains 10mM HEPES (pH 7.4), 150mM NaCl, 3.4mM EDTA, and 0.005% Surfactant P20. Streptavidin (Sigma) and the JM22z TCR were covalently coupled to Research Grade CM5 sensor chips (BIAcore) via primary amines using the standard amine coupling kit (BIAcore). For coupling, streptavidin was injected at 0.5mg/ml in 10mM sodium acetate (pH 5.5). The purified biotinylated hCD1d–lipid complexes were immobilized onto streptavidin-coated CM5 sensor chips (Biacore) at a level of ~1,000 response U. Biotinylated proteins were immobilized at the indicated levels by injection at 50-150μg/ml for 0.5-10min over streptavidin-coupled surfaces. For coupling, JM22z was injected at 14μg/ml in 10mM sodium acetate (pH 5). Coupling levels ranged from 3200 to 11400 RU. To avoid multivalent aggregates, soluble proteins used in SPR experiments were purified by gel-filtration on a Superdex S-200 column, stored at 4°C, and used within 48 hr with minimum amounts of concentrating. In all experiments, hCD1d–β-GalCer molecules were used as negative controls. Equilibrium binding was performed at a flow rate of 10μl/min from the lowest TCR concentration. To exclude any effect of lipid dissociation, which would result in a gradual decrease in the level of immobilized CD1d–lipid during the course of the experiment, the affinity was determined with both increasing (from low to highest) and decreasing (from highest to lowest) concentrations of TCR. The affinity values obtained

were not significantly different, indicating that lipid dissociation during the course of the experiments had a negligible effect on the affinity measurements. The data was plotted using Origin software (OriginLab), and K_d values were calculated using the standard hyperbolic model. Kinetics of the TCR–hCD1d/lipid interactions was measured at 50µl/min. Equilibrium dissociation constants (K_d) and k_{on} and k_{off} were obtained by nonlinear curve fitting of the binding curves obtained after subtracting the response in the reference flow cells with equations derived from the simple 1:1 Langmuir binding model using the BIA evaluation program (version 3.02.2; Biacore). SPR was also used to estimate the dissociation rate of GSL from hCD1d molecules. 1,000 response U of hCD1d monomers loaded with either α-GalCer **(44)**, OCH9 **(47)**, OCH12 **(46)**, OCH15 **(45)**, C20:0 **(79)**, C20:2 **(73)**, or C11:1 were immobilized on a streptavidin-coated sensor chip. As a negative control, hCD1d–β-GalCer biotinylated monomers were used. The amount of hCD1d–GSL remaining at a particular time was measured by injecting saturating amounts (30 µl at 500 nM) of Fab 9B antibody [218, 296].

5.24.1.4. iNKT TCR tetramer staining

C1R-hCD1d cells were pulsed with 10µM, 5µM, 1µM, 500nM, and 100nM of lipid for 16h at 37°C and washed twice in RPMI. Cells were incubated with iNKT cell TCR tetramers at 37°C for 30min and washed again twice with ice-cold PBS/1% fetal calf serum (FCS). Samples were analyzed on a flow cytometer (FACSCalibur; BD Biosciences), and the data were processed using CellQuest software (BD Biosciences) [218].

5.24.1.5. Enzyme-linked immunsorbent assay (ELISA)

C1R-hCD1d cells were pulsed for 2h with GSLs and diluted to 10^6 cells/ml. 10^5 cell-pulsed targets were incubated at 37°C with 10^4 iNKT cells in a final volume of 200µl. After 18h, the

supernatants were harvested, and the concentrations of IFN-γ and IL-4 were determined by ELISA according to the manufacturer's instructions (Mabtech) [218].

5.24.1.6. iNKT cell expansion

Peripheral blod mononuclear cells (PBMCs) were isolated from healthy donors' buffy coats by density gradient centrifugation over Lymphoprep (Nycomed). Monocytes were positively selected using anti-CD14 mAb–coated magnetic beads (MACS; Miltenyi Biotec), and monocyte-depleted lymphocyte fractions (CD14 negative) were frozen until needed. Monocytes were cultured with 50ng/ml granulocyte-macrophage colony-stimulating factor (GM-CSF) (Novartis) and 1,000 U/ml IL-4 in six-well plates at 4×10^5 cells/ml (3ml/well). After 5d, maturation was induced using bacterial lipopolysaccharide (LPS) (1 µg/ml LPS of *Salmonella abortusequi*; Sigma-Aldrich). Immature and mature monocyte-derived DCs were phenotypically analyzed for maturation markers. 2×10^5 monocyte-derived DCs were pulsed with GSL for 2h in 24-well plates in 200µl RPMI 1640. 2×10^6 autologous lymphocytes were added in 1.8ml of medium (5% human serum). After 3d, 25 IU/ml IL-2 was added to cultures. Thereafter, cultures were fed every 3–4 d with fresh medium containing 1,000 U/ml IL-2. iNKT cell frequencies were determined using APC CD1d tetramer and Vα24 antibody (Serotec) [218].

5.24.1.7. Structural modeling

The structural effects of binding lipid chains of various lengths to hCD1d were assessed by comparison of the hCD1d–α-GalCer and empty hCD1d crystal structures (Protein Data Bank code 1ZT4). Structural superposition used the Structure Homology Program, and analysis was performed using the interactive graphics display program O [297].

5.24.1.8. T cell proliferation

For proliferation assays, 2 x 10^5 PBMC were plated per well in round-bottom 96-well plates. T cell medium was made by supplementing 500 ml of RPMI 1640 medium with 50 ml of FCS (HyClone), penicillin (Invitrogen Life Technologies), streptomycin (Invitrogen Life Technologies), 20 mM HEPES (Invitrogen Life Technologies), and 4 ml of 1 N NaOH solution. Proliferation was measured after culture for 3 days with α-GalCer or associated analogues at concentrations ranging 100mg/ml DMSO and diluted into culture mediam to the indicated final concentrations, followed by a 6-h pulse of 1 µCi of [^{3}H]thymidine before harvesting and counting β emissions using a Microbeta Trilux scintillation counter (Wallac).

5.24.1.9. Measurement of cytokine secretion by *in vitro*-activated iNKT cells

Human iNKT cell clones at 5 x 10^4/well were stimulated with 5 x 10^4 human DCs (derived by *in vitro* culture of peripheral blood monocytes for 3 days in medium supplemented with GM-CSF and IL-4) in the presence of the indicated concentrations of α-GalCer analogs. Levels of human IL-13 and IFN-γ, and were measured at 48h in culture supernatants by capture ELISA.

5.24.1.10. Preparation of soluble CD1d fusion proteins and tetramers

Single-chain β2m- CD1d-Fc fusion proteins were produced in mammalian cells and purified from culture supernatants by protein A affinity chromatography. The resulting dimeric CD1d-Fc fusion proteins were formed into complexes with fluorescently labeled soluble protein A molecules and purified by size exclusion chromatography on a Superose 6 column (Amersham Biosciences).

5.24.1.11. Derivation of CD1d-restircted T cell clones

T cells sorted using CD1d-tetramers were cultured at 37°C with 5% CO_2 in RPMI 1640 culture medium containing 10% fetal bovine serum (FBS), 2% human AB serum, 1% penicillin and streptomycin, and 1% L-glutamine in the presence of irradiated allogeneic PBMC and phytohaemagglutinin (PHA). After 5–10 days of culture, 200U/ml recombinant human IL-2 (Chiron) was added to the medium.

5.24.1.12. T cell responses to APCs

APCs were either CD1d-transfected 721.221 cells or *in vitro*-derived immature dendritic cells (DCs) generated from human peripheral blood monocytes purified by CD14-positive magnetic bead selection (Miltenyi Biotec) that were cultured for 3 days with 200 U/ml and 300 U/ml rIL-4 and GM-CSF, respectively. DCs were pulsed for 12–16 h with glycolipid antigens at the indicated concentrations or with vehicle (DMSO) alone and then washed and co-incubated with a 1:1 ratio of CD1d-restricted T cells (5 x 10^4 per well) in sterile 96-well plates in RPMI 1640 culture medium lacking IL-2 (i.e., RPMI 1640 containing 10% iron-supplemented bovine calf serum and penicillin/streptomycin) for 24 h at 37°C and 5% CO_2. Culture supernatants were then withdrawn and tested for the indicated cytokines using a standard, commercially available ELISA and purified recombinant cytokines as standards. Anti-CD1d mAb blocking experiments were performed by coincubating the CD1d59 murine IgM mAb (Prof. S. Porcelli, Albert Einstein College of Medicine, New York, USA) or the MOPC-104E negative control IgM mAb (Sigma-Aldrich) with the APCs and T cells. The I-B4 lectin from the plant *Griffonia simplicifolia* (Vector Laboratories; dissolved in 10 mM HEPES, 0.15MNaCl, 0.08% NaN3, and 0.1mMCa^{2+}) was co-incubated with the APCs and T cells at the indicated concentrations and compared with mock-treated (diluent buffer alone) APCs.

5.24.1.13. T cell responses to lipid Ags presented by plate-bound CD1d molecules

CD1-restricted T cell clones were tested for responses to glycoplid antigens presented by plate-bound CD1d fusion proteins: the CD1d-Fc fusion protein or an isotype-matched negative control mAb was coated in a 10:1 ratio with an anti-LFA-1 mAb onto 96-well microtiter plates. Glycolipid antigens dissolved in DMSO or vehicle alone were diluted into PBS and incubated with the CD1d fusion protein or negative control mAb at 37°C for 24–72 h. The plates were then thoroughly washed and CD1d-restricted T cell clones were added in RPMI 1640 culture medium, lacking IL-2. The plates were incubated for 24 h at 37°C and 5% CO_2, and the supernatants were then harvested and analyzed for cytokine content using a standard, commercially available ELISA.

Chapter 6

Conclusions

α-GalCer has shown remarkable activity in terms of iNKT cell activation when bound with CD1d [102, 136-139, 144, 145, 180] and in doing so has become increasingly attractive as a prophylactic agent for the treatment of autoimmune diseases, such as T1D and SLE [139]. One of its modes of action includes inducing iNKT cells to produce beneficial T_H2 cytokines, such as IL-4 [117]. In addition to cytokine stimulating properties, α-GalCer has been shown to stimulate iNKT cell expansion [163]; the diagnosis of T1D has been associated with a reduced number of circulating iNKT cells [144, 180, 298], thus providing further evidence of the therapeutics potential of α-GalCer.

Alongside the aforementioned effects of α-GalCer treatment, the potentially detrimental T_H1 cytokine IFN-γ is known to be released either at the same time, or immediately after T_H2 cytokines, and sometimes in far greater concentrations [128-130]. T_H1 and T_H2 cells, and the cytokines they produce, normally exist in an harmonious state [129, 131]. However, a disturbance in the equilibrium, and an increase in the pro-inflammatory cytokine IFN-γ, can lead to a breakdown of self-tolerance which in turn can trigger the development of an autoimmune disease [129, 131]. Destructive insulitis is paralled by predominant secretion of IFN-γ [140, 143] and treating NOD mice with anti-IFN-γ has been shown to delay the development of T1D [146, 148], both of which add to the mounting evidence that the over-production of T_H1 cytokines have a detrimental effect on the immune system.

The fact that α-GalCer produces both T_H2 and T_H1 cytokines is less than ideal in the context of conditions, such as T1D and SLE. In the hope of finding an antigen that could skew the immune system towards that of a predominantly T_H2 response, analogues of α-GalCer were synthesised and tested for their biological activity. Overcoming several chemical hurdles, a library of analogues varying in the phytosphingosine base, *N*-acyl chain and sugar head group were synthesised.

Following on from the work of Miyamoto *et al.* [144] who found that a truncated sphingosine base preferentially induced the production of T_H2 cytokines, analogues with base chains ranging from C_{18} (α-GalCer **(44)**) to C_9, OCH9 **(47)** were synthesised. These analogues were tested for their ability to produce IL-4 and IFN-γ in direct comparison with α-GalCer, and although the ratio of IL-4: IFN-γ produced by OCH9 **(47)** was dramatically reduced compared with α-GalCer **(44)**, OCH15 **(45)** and OCH12 **(46)**, the overall concentration of cytokines produced was also reduced [218]. This could be rationalised from the observation that the shortened phytosphingosine chain does not fully occupy one of the channels in the protein structure, thus allowing a degree of flexibility and rotation in the positioning of the sugar head, which in turn affects the binding of the antigen:CD1d complex with the TCR. The hypothesis that a truncated phytosphingosine chain lengths also affect the binding time of the antigen:protein complex with the TCR can also be attributed to the skewed immune response; IL-4 is rapidly produced by iNKT cells, followed by a more sustained release of IFN-γ [272]. If an antigen binds for a shorter time with the TCR, the chances of IFN-γ being produced in concentrations as great as a stable hCD1d-antigen:TCR complex, are reduced. Experimentally, the affinity of an hCD1d:OCH9 complex with the iNKT cell TCR was shown to be greatly reduced, with a dissociation constant of 122μM compared with 1.6μM for α-GalCer **(44)** [218]; a smaller dissociation constant is indicative of higher affinity between the two constituents.

Despite its capacity to skew the immune system towards that of a T_H2 response, OCH9 **(47)** is unable to stimulate iNKT cell expansion in a manner anywhere near α-GalCer **(44)** [218]. This could also be attributed to the decreased binding affinity between OCH9 **(47)** and the iNKT cell TCR, as iNKT cell proliferation is observed 24h after initial stimulation [117].

The immunostimulatory activity of analogues, with varying sugar head groups, was also investigated through the course of this project. Motoki *et al.* [226] showed that the

lymphocytic proliferation activity of α-GalCer **(44)** was greater than that of α-GlcCer **(50)**. The results from several experimental procedures mirrored the results gained by the Motoki group, and showed that α-GalCer **(44)** has greater lymphocytic proliferation activity than α-GlcCer **(50)**, but that α-L-FucCer **(53)** showed cell proliferation responses that were greater than the glucose analogue, but less efficient than the galactose analogue. This suggests that the positioning of the hydroxyl group at C4' plays a pivotal role in determining the biological response of the analogues. Interestingly, the cytokine profiles of the three analogues also positions the response of α-L-FucCer **(53)** between that of α-GalCer **(44)** and α-GlcCer **(50)**. The ratio of T_H1: T_H2 cytokine production by α-L-FucCer **(53)** is skewed toward that of a predominantly T_H2 response.

Research into variations in the *N*-acyl chain of α-GalCer in the context of GSLs and autoimmune diseases has been in the spotlight over recent months [64, 98, 179, 180, 237, 265-267]. Not only have a number of groups successfully incorporated fluorescent molecules into the *N*-acyl chain of α-GalCer [184, 185, 263], the length and saturation of the *N*-acyl chain of α-GalCer has been noted as having, in some cases, profound effects on the analogue's biological activity. In a manner similar to the conclusions regarding the truncated phytosphingosine base chain not fully occupying one of the CD1d protein tunnels, it has been speculated that alterations in the length and degree of unsaturation in an *N*-acyl chain also affect the analogue's activity due to altered binding and stability. Moody *et al.* [269] demonstrated that the size of the *N*-acyl chain controls many aspects of an analogue's interaction with CD1, such as the kinetics, sub-cellular localisation, efficiency of antigen loading into the groove and ultimately the presentation of the antigen. Yu *et al*. [266] showed that unsaturated analogues of α-GalCer are more biologically active than their fully saturated counterparts, with two *cis* orientated double-bonds being the most effective at skewing the immune response towards that of a T_H2 response. This was demonstrated by the IL-4/ IFN-γ response of α-GalCer **(44)** compared with C20:2 **(73)** and C20:4 **(71)**, which showed that

IL-4 production by C20:2 **(73)** was on a par with that of α-GalCer **(44)**, with drastically reduced concentrations of IFN-γ being detected. Although C20:4 **(71)** also showed minimal IFN-γ production at both 2 and 20 hours, the concentration of IL-4 released by *in* vivo iNKT cells was reduced.

The unsaturated analogue C20:2 **(73)** has also been shown to have a direct effect on delaying the development of T1D. NOD mice prone to the development of this autoimmune disease failed to present symptoms of the disease after treatment with C20:2 **(73)**. This is in contrast to those treated with α-GalCer **(44)**, which did not present with glucosuria as quickly as control animals, but showed a striking decrease in the number of animals without glucosuria after approximately 22 weeks.

The theories behind the varying affects of unsaturated *N*-acyl analogues of α-GalCer, suggest that the orientation of the polar head-group, and thus recognition by the TCR, is not influenced by a change in the *N*-acyl chain structure. Unlike variations in the phytosphingosine chain which can lead to partial collapse of one of the CD1d protein tunnels, a truncated *N*-acyl chain influences changes in residues peripheral to the iNKT cell TCR [218], suggesting that the structure of the *N*-acyl chain affects binding of the analogue with CD1d, but not TCR recognition. The observed differences in the rates of dissociation of unsaturated and fully saturated *N*-acyl chain variants, shows that unsaturations increase the stability of the binding of α-GalCer analogues with CD1d proteins, and that the natural kink featured in C20:2 **(73)** (formed from the two *cis* orientationed double bonds) favours the tightly curved conformation required for binding within the N-acyl chain channel.

Although these findings provide exciting insights into the elusive nature of CD1d-iNKT cell interactions, and add to the mounting knowledge of GSL antigens and the possibility of a ‘super-antigen’, a definitive answer to the prevention of autoimmune diseases has by no

means been unearthed. These results encourage the development of novel α-GalCer analogues in the search for a compound that could hold therapeutic potential in the successful modulation of the immune system for prevention and treatment of autoimmune diseases.

Chapter 7

References

1. **Bernard, A. and Boumsell, L. (1984).** The clusters of differentiation (CD) defined by the First International Workshop on Human Leucocyte Differentiation Antigens*. Hum. Immunol.* **11:** 1-10
2. **Porcelli, S.A. and Modlin, R.L. (1999).** The CD1 system: antigen-presenting molecules for T cell recognition of lipids and glycolipids*. Annu. Rev. Immunol.* **17:** 297-329
3. **de la Salle, H., Mariotti, S., Angenieux, C., Gilleron, M., Garcia-Alles, L.-F., Malm, D., Berg, T., Paoletti, S., Maitre, B., Mourey, L., Salamero, J., Cazenave, J.P., Hanau, D., Mori, L., Puzo, G., and De Libero, G. (2005).** Assistance of microbial glycolipid antigen processing by CD1e*. Science* **310:** 1321-1324
4. **Calabi, F., Jarvis, J.M., Martin, L., and Milstein, C. (1989).** Two classes of CD1 genes*. Eur. J. Immunol.* **19:** 285-92
5. **Martin, L.H., Calabi, F., Lefebvre, F.A., Bilsland, C.A., and Milstein, C. (1987).** Structure and expression of the human thymocyte antigens CD1a, CD1b, and CD1c*. Proc. Natl. Acad. Sci. USA* **84:** 9189-93
6. **Martin, L.H., Calabi, F., and Milstein, C. (1986).** Isolation of CD1 genes: a family of major histocompatibility complex-related differentiation antigens*. Proc. Natl. Acad. Sci. USA* **83:** 9154-8
7. **Calabi, F. and Milstein, C. (1986).** A novel family of human major histocompatibility complex-related genes not mapping to chromosome 6*. Nature* **323:** 540-3
8. **Balk, S.P., Bleicher, P.A., and Terhorst, C. (1991).** Isolation and expression of cDNA encoding the murine homologues of CD1*. J. Immunol.* **146:** 768-74
9. **Bradbury, A., Belt, K.T., Neri, T.M., Milstein, C., and Calabi, F. (1988).** Mouse CD1 is distinct from and co-exists with TL in the same thymus*. Embo. J.* **7:** 3081-6
10. **Matsuura, A., Hashimoto, Y., Kinebuchi, M., Kasai, K., Ichimiya, S., Katabami, S., Chen, H., Shimizu, T., and Kikuchi, K. (1997).** Rat CD1 antigen: structure, expression and function*. Transplant Proc.* **29:** 1705-6
11. **Rhind, S.M., Dutia, B.M., Howard, C.J., and Hopkins, J. (1996).** Discrimination of two subsets of CD1 molecules in the sheep*. Veterinary Immunology and Immunopathology.* **52:** 265-270
12. **Van Rhijn, I., Koets, A.P., Im, J.S., Piebes, D., Reddington, F., Besra, G.S., Porcelli, S.A., van Eden, W., and Rutten, V.P.M.G. (2006).** The bovine CD1 family contains group 1 CD1 proteins, but no functional CD1d*. J. Immunol.* **176:** 4888-4893
13. **Calabi, F., Belt, K.T., Yu, C.Y., Bradbury, A., Mandy, W.J., and Milstein, C. (1989).** The rabbit CD1 and the evolutionary conservation of the CD1 gene family*. Immunogenetics* **30:** 370-7

14. **Hayes, S.M. and Knight, K.L. (2001).** Group 1 CD1 genes in rabbit. *J. Immunol.* **166:** 403-10
15. **Dascher, C.C., Hiromatsu, K., Naylor, J.W., Brauer, P.P., Brown, K.A., Storey, J.R., Behar, S.M., Kawasaki, E.S., Porcelli, S.A., Brenner, M.B., and LeClair, K.P. (1999).** Conservation of a CD1 multigene family in the guinea pig. *J. Immunol.* **163:** 5478-88
16. **Angenieux, C., Salamero, J., Fricker, D., Wurtz, J.M., Maitre, B., Cazenave, J.P., Hanau, D., and de la Salle, H. (2003).** Common characteristics of the human and rhesus macaque CD1e molecules: conservation of biochemical and biological properties during primate evolution. *Immunogenetics* **54:** 842-9
17. **Matsuura, A., Kinebuchi, M., Katabami, S., Hong-Zhi, C., Kasai, K., Ichimiya, S., Yamada, K., Yoshida, M.C., Horie, M., and Sato, N. (2000).** Comparative analysisof the structure and chromosomal assignment of CD1: an evidence for diferent evolutionary histories between classic CD1 and CD1D class genes. *J. Exp. Anim. Sci.* **41:** 87-90
18. **Brigl, M. and Brenner, M.B. (2004).** CD1: antigen presentation and T cell function. *Annu. Rev. Immunol.* **22:** 817-90
19. **Porcelli, S. (1995).** The CD1 family: a third lineage of antigen-presenting molecules. *Adv. Immunol.* **59:** 1-98
20. **Durandy, A., Thuillier, L., Forveille, M., and Fischer, A. (1990).** Phenotypic and functional characteristics of human newborns' B lymphocytes. *J. Immunol.* **144:** 60-65
21. **Delia, D., Cattoretti, G., Polli, N., Fontanella, E., Aiello, A., Giardini, R., Rilke, F., and Della Porta, G. (1988).** CD1c but neither CD1a nor CD1b molecules are expressed on normal, activated, and malignant human B cells: identification of a new B-cell subset. *Blood* **72:** 241-247
22. **Hiromatsu, K., Dascher, C.C., Sugita, M., Gingrish-Baker, C., Behar, S.M., LeClair, K.P., Brenner, M.B., and Porcelli, S.A. (2002).** Characterization of guinea-pig group 1 CD1 proteins. *Immunol.* **106:** 159-172
23. **Dover, L.G., Cerdeno-Tarraga, A.M., Pallen, M.J., Parkhill, J., and Besra, G.S. (2004).** Comparative cell wall core biosynthesis in the mycolated pathogens, *Mycobacterium tuberculosis* and *Corynebacterium diphtheriae. FEMS Microbiology Reviews* **28:** 225-250
24. **Willcox, B.E., Wilcox, C.R., Dover, L.G., and Besra, G.S.** Structures and functions of microbial lipid antigens presented by CD1. *Curr. Top. Microbiol. Immunol.* **314:** 73-110.

25. **Moody, D.B. (2006).** The surprising diversity of lipid antigens for CD1-restricted T cells*. Adv. Immunol.* **89:** 87-139
26. **Beckman, E.M., Porcelli, S.A., Morita, C.T., Behar, S.M., Furlong, S.T., and Brenner, M.B. (1994).** Recognition of a lipid antigen by CD1-restricted alpha beta+ T cells*. Nature* **372:** 691-4
27. **Zajonc, D.M., Crispin, M.D., Bowden, T.A., Young, D.C., Cheng, T.Y., Hu, J., Costello, C.E., Rudd, P.M., Dwek, R.A., Miller, M.J., Brenner, M.B., Moody, D.B., and Wilson, I.A. (2005).** Molecular mechanism of lipopeptide presentation by CD1a*. Immunity* **22:** 209-19
28. **Moody, D.B., Young, D.C., Cheng, T.-Y., Rosat, J.-P., Roura-Mir, C., O'Connor, P.B., Zajonc, D.M., Walz, A., Miller, M.J., Levery, S.B., Wilson, I.A., Costello, C.E., and Brenner, M.B. (2004).** T cell activation by lipopeptide antigens*. Science* **303:** 527-531
29. **Ratledge, C. and Snow, G.A. (1974).** Isolation and structure of nocobactin NA, a lipid-soluble iron-binding compound from *Nocardia asteroides. Biochem. J.* **139:** 407-13
30. **Compostella, F., Franchini, L., De Libero, G., Palmisano, G., Ronchetti, F., and Panza, L. (2002).** CD1a-binding glycosphingolipids stimulating human autoreactive T-cells: synthesis of a family of sulfatides differing in the acyl chain moiety*. Tet.* **58:** 8703-8708
31. **Moody, D.B., Reinhold, B.B., Guy, M.R., Beckman, E.M., Frederique, D.E., Furlong, S.T., Ye, S., Reinhold, V.N., Sieling, P.A., Modlin, R.L., Besra, G.S., and Porcelli, S.A. (1997).** Structural requirements for glycolipid antigen recognition by CD1b-restricted T cells*. Science* **278:** 283-286
32. **Yarkoni, E., Goren, M.B., and Rapp, H.J. (1979).** Regression of a transplanted guinea pig hepatoma after intralesional injection of an emulsified mixture of endotoxin and mycobacterial sulfolipid. *Infect. Immun.* **24:** 357-362
33. **Yarkoni, E., Goren, M.B., and Rapp, H.J. (1979).** Effect of sulfolipid I on trehalose-6,6'-dimycolate (cord factor) toxicity and antitumor activity. *Infect. Immun.* **24:** 586-588
34. **Sieling, P., Chatterjee, D., Porcelli, S., Prigozy, T., Mazzaccaro, R., Soriano, T., Bloom, B., Brenner, M., Kronenberg, M., and Brennan, P. (1995).** CD1-restricted T cell recognition of microbial lipoglycan antigens*. Science* **269:** 227-230
35. **Moody, D.B., Ulrichs, T., Mühlecker, W., Young, D.C., Gurcha, S.S., Grant, E., Rosat, J.-P., Brenner, M.B., Costello, C.E., Besra, G.S., and Porcelli, S.A. (2000).**

CD1c-mediated T-cell recognition of isoprenoid glycolipids in *Mycobacterium tuberculosis* infection. *Nature* **404:** 884-888

36. **Matsunaga, I., Bhatt, A., Young, D.C., Cheng, T.-Y., Eyles, S.J., Besra, G.S., Briken, V., Porcelli, S.A., Costello, C.E., Jacobs, W.R., Jr., and Moody, D.B. (2004).** *Mycobacterium tuberculosis* pks12 produces a novel polyketide presented by CD1c to T cells. *J. Exp. Med.* **200:** 1559-1569
37. **Willcox, B.E., Wilcox, C.R., Dover, L.G., and Besra, G.S. (2007).** Structures and functions of microbial lipid antigens presented by CD1. *Curr. Top. Microbiol. Immunol.* **314:** 73-110
38. **Kruszewska, J., Kubicek, C.P., and Palamarczyk, G. (1994).** Modulation of mannosylphosphodolichol synthase and dolichol kinase activity in *Trichoderma*, related to protein secretion. *Acta. Biochim. Pol.* **41:** 331-7
39. **Canchis, P., Bhan, A., Landau, S., Yang, L., Balk, S., and Blumberg, R. (1993).** Tissue distribution of the non-polymorphic major histocompatibility complex class I-like molecule, CD1d. *Immunol.* **80:** 561-565
40. **Racke, F.K., Clare-Salzer, M., and Wilson, S.B. (2002).** Control of myeloid dendritic cell differentiation and function by restricted (NK) T cells. *Frontiers in Bioscience* **7:** 978-985
41. **Creusot, R.J. and Mitchison, N.A. (2004).** How DCs control cross-regulation between lymphocytes. *Trends Immunol.* **25:** 126-31
42. **Brigl, M., Bry, L., Kent, S.C., Gumperz, J.E., and Brenner, M.B. (2003).** Mechanism of CD1d-restricted natural killer T cell activation during microbial infection. *Nat. Immunol.* **4:** 1230-7
43. **Schofield, L., McConville, M.J., Hansen, D., Campbell, A.S., Fraser-Reid, B., Grusby, M.J., and Tachado, S.D. (1999).** CD1d-restricted immunoglobulin G formation to GPI-anchored antigens mediated by NKT cells. *Science* **283:** 225-229
44. **Duthie, M.S., Wleklinski-Lee, M., Smith, S., Nakayama, T., Taniguchi, M., and Kahn, S.J. (2002).** During *Trypanosoma cruzi* Infection CD1d-restricted NK T cells limit parasitemia and augment the antibody response to a glycophosphoinositol-modified surface protein. *Infect. Immun.* **70:** 36-48
45. **Molano, A., Park, S.-H., Chiu, Y.-H., Nosseir, S., Bendelac, A., and Tsuji, M. (2000).** The IgG response to the circumsporozoite protein iMHC class II-dependent and CD1d-independent: exploring the role of GPIs in NK T cell activation and antimalarial responses. *J. Immunol.* **164:** 5005-5009
46. **Fischer, K., Scotet, E., Niemeyer, M., Koebernick, H., Zerrahn, J., Maillet, S., Hurwitz, R., Kursar, M., Bonneville, M., Kaufmann, S.H., and Schaible, U.E.**

(2004). Mycobacterial phosphatidylinositol mannoside is a natural antigen for CD1d-restricted T cells*. Proc. Natl. Acad. Sci. USA* **101:** 10685-90

47. **Kinjo, Y., Tupin, E., Wu, D., Fujio, M., Garcia-Navarro, R., Benhnia, M.R.-E.-I., Zajonc, D.M., Ben-Menachem, G., Ainge, G.D., Painter, G.F., Khurana, A., Hoebe, K., Behar, S.M., Beutler, B., Wilson, I.A., Tsuji, M., Sellati, T.J., Wong, C.-H., and Kronenberg, M. (2006).** Natural killer T cells recognize diacylglycerol antigens from pathogenic bacteria*. Nat. Immunol.* **7:** 978-986
48. **Bendelac, A., Lantz, O., Quimby, M., Yewdell, J., Bennink, JR, and Brutkiewicz, R. (1995).** CD1 recognition by mouse NK1+ T lymphocytes*. Science* **268:** 863-865
49. **Exley, M., Garcia, J., Balk, S.P., and Porcelli, S. (1997).** Requirements for CD1d recognition by human invariant Valpha24+ CD4-CD8- T cells*. J. Exp. Med.* **186:** 109-20
50. **Gumperz, J.E., Roy, C., Makowska, A., Lum, D., Sugita, M., Podrebarac, T., Koezuka, Y., Porcelli, S.A., Cardell, S., Brenner, M.B., and Behar, S.M. (2000).** Murine CD1d-restricted T cell recognition of cellular lipids*. Immunity* **12:** 211-21
51. **Christie, W.W. (2003).** Lipid analysis - third edition. The Oily Press, Bridgwater, UK.
52. **Joyce, S., Woods, A.S., Yewdell, J.W., Bennink, J.R., De Silva, A.D., Boesteanu, A., Balk, S.P., Cotter, R.J., and Brutkiewicz, R.R. (1998).** Natural ligand of mouse CD1d1: cellular glycosylphosphatidylinositol*. Science* **279:** 1541-1544
53. **De Silva, A.D., Park, J.J., Matsuki, N., Stanic, A.K., Brutkiewicz, R.R., Medof, M.E., and Joyce, S. (2002).** Lipid protein interactions: the assembly of CD1d1 with cellular phospholipids occurs in the endoplasmic reticulum*. J. Immunol.* **168:** 723-33
54. **Zhou, D., Mattner, J., Cantu, C., 3rd, Schrantz, N., Yin, N., Gao, Y., Sagiv, Y., Hudspeth, K., Wu, Y.P., Yamashita, T., Teneberg, S., Wang, D., Proia, R.L., Levery, S.B., Savage, P.B., Teyton, L., and Bendelac, A. (2004).** Lysosomal glycosphingolipid recognition by NKT cells*. Science* **306:** 1786-9
55. **Godfrey, D.I., McConville, M.J., and Pellicci, D.G. (2006).** Chewing the fat on natural killer T cell development*. J. Exp. Med.* **203:** 2229-2232
56. **Conzelmann, E. and Sandhoff, K. (1980).** The specificity of human N-acetyl-beta-D-hexosaminidases towards glycosphincolipids is determined by an activator protein. *Adv. Exp. Med. Biol.* **125:** 295-306
57. **Hava, D.L., Brigl, M., van den Elzen, P., Zajonc, D.M., Wilson, I.A., and Brenner, M.B. (2005).** CD1 assembly and the formation of CD1-antigen complexes*. Curr. Op. Immunol.* **17:** 88-94
58. **Xia, C., Yao, Q., Schumann, J., Rossy, E., Chen, W., Zhu, L., Zhang, W., De Libero, G., and Wang, P.G. (2006).** Synthesis and biological evaluation of [alpha]-

galactosylceramide (KRN7000) and isoglobotrihexosylceramide (iGb3). *Bioorg. Med. Chem. Lett.* **16:** 2195-2199

59. **Kobayashi, E., Motoki, K., Yamaguchi, Y., Uchida, T., Fukushima, H., and Koezuka, Y. (1996).** Enhancing effects of α-, β-monoglycosylceramides on natural killer cell activity. *Bioorg. Med. Chem.* **4:** 615–619
60. **Abrahamsson, S., Dahlén, B., and Pascher, I. (1977).** Molecular arrangements in glycosphingolipids: the crystal structure of glucosylphytosphingosine hydrochloride. *Acta. Cryst.* **B33:** 2008-2013
61. **Degroote, S., Wolthoorn, J., and van Meer, G. (2004).** The cell biology of glycosphingolipids. *Semin. Cell. Dev. Biol.* **15:** 375-87
62. **Pascher, I. (1976).** Molecular arrangements in sphingolipids conformation and hydrogen bonding of ceramide and their implication on membrane stability and permeability. *Biochim.Biophys. Acta - Biomembranes* **455:** 433-451
63. **Futerman, A.H. and van Meer, G. (2004).** The cell biology of lysosomal storage disorders. *Nat. Rev. Mol. Cell. Biol.* **5:** 554-65
64. **Morita, M., Kazuhiro, M., Akimoto, K., Natori, T., Sakai, T., Sawa, E., Yamaji, K., Koezuka, Y., Kobayahi, E., and Fukushima, H. (1995).** Structure-activity relationship of α-galactosylceramides against B16-bearing mice. *J. Med. Chem.* **38:** 2176-2187
65. **Wilson, M.T., Singh, A.K., and Van Kaer, L. (2002).** Immunotherapy with ligands of natural killer T cells. *Trend. Molec. Med.* **8:** 225-231
66. **Hammond, K.J.L. and Godfrey, D.I. (2002).** NKT cells: potential targets for autoimmune disease therapy? *Tissue Antigens* **59:** 353-363
67. **Bauer, A., Huttinger, R., Staffler, G., Hansmann, C., Schmidt, W., Majdic, O., Knapp, W., and Stockinger, H. (1997).** Analysis of the requirement for beta 2-microglobulin for expression and formation of human CD1 antigens. *Eur. J. Immunol.* **27:** 1366-73
68. **Moody, D.B. and Porcelli, S.A. (2003).** Intracellular pathways of CD1 antigen presentation. *Nat. Rev. Immunol.* **3:** 11-22
69. **Zeng, Z.-H., Castaño, A.R., Segelke, B.W., Stura, E.A., Peterson, P.A., and Wilson, I.A. (1997).** Crystal structure of mouse CD1: an MHC-like fold with a large hydrophobic binding groove. *Science* **277:** 339-345
70. **Moody, D.B. and Besra, G.S. (2001).** Glycolipid targets of CD1-mediated T-cell responses. *Immunol.* **104:** 243-251
71. **Koch, M., Stronge, V.S., Shepherd, D., Gadola, S.D., Mathew, B., Ritter, G., Fersht, A.R., Besra, G.S., Schmidt, R.R., Jones, E.Y., and Cerundolo, V. (2005).**

The crystal structure of human CD1d with and without α-galactosylceramide. *Nat. Immunol.* **6:** 819-826

72. **Kamada, N., Iijima, H., Kimura, K., Harada, M., Shimizu, E., Motohashi, S.-i., Kawano, T., Shinkai, H., Nakayama, T., Sakai, T., Brossay, L., Kronenberg, M., and Taniguchi, M. (2001).** Crucial amino acid residues of mouse CD1d for glycolipid ligand presentation to Vα14 NKT cells. *Int. Immunol.* **13:** 853-861
73. **Moody, D.B. (2006).** TLR gateways to CD1 function. *Nat. Immunol.* **7:** 811-817
74. **Gadola, S.D., Zaccai, N.R., Harlos, K., Shepherd, D., Castro-Palomino, J.C., Ritter, G., Schmidt, R.R., Jones, E.Y., and Cerundolo, V. (2002).** Structure of human CD1b with bound ligands at 2.3 A, a maze for alkyl chains. *Nat. Immunol.* **3:** 721-6
75. **Zajonc, D.M., Elsliger, M.A., Teyton, L., and Wilson, I.A. (2003).** Crystal structure of CD1a in complex with a sulfatide self antigen at a resolution of 2.15 A. *Nat. Immunol.* **4:** 808-15
76. **Sugita, M., Cernadas, M., and Brenner, M.B. (2004).** New insights into pathways for CD1-mediated antigen presentation. *Curr. Op. Immunol.* **16:** 90-95
77. **Moody, D.B. and Porcelli, S.A. (2001).** CD1 trafficking: invariant chain gives a new twist to the tale. *Immunity* **15:** 861-865
78. **Sullivan, B.A., Nagarajan, N.A., and Kronenberg, M. (2005).** CD1 and MHC II find different means to the same end. *Trends Immunol.* **26:** 282-288
79. **Major, A.S., Joyce, S., and Van Kaer, L. (2006).** Lipid metabolism, atherogenesis and CD1-restricted antigen presentation. *Trends. Mol. Med.* **12:** 270-278
80. **Kang, S.-J. and Cresswell, P. (2004).** Saposins facilitate CD1d-restricted presentation of an exogenous lipid antigen to T cells. *Nat. Immunol.* **5:** 175-181
81. **Park, J.J., Kang, S.J., De Silva, A.D., Stanic, A.K., Casorati, G., Hachey, D.L., Cresswell, P., and Joyce, S. (2004).** Lipid-protein interactions: biosynthetic assembly of CD1 with lipids in the endoplasmic reticulum is evolutionarily conserved. *Proc. Natl. Acad. Sci. USA* **101:** 1022-6
82. **Zhou, D., Cantu III, C., Sagiv, Y., Schrantz, N., Kulkarni, A.B., Qi, X., Mahuran, D.J., Morales, C.R., Grabowski, G.A., Benlagha, K., Savage, P., Bendelac, A., and Teyton, L. (2004).** Editing of CD1d-bound lipid antigens by endosomal lipid transfer proteins. *Science* **303:** 523-530
83. **Lydyard, P.M., Whelan, A., and Fanger, M.W. (2004).** Instant notes: immunology. Second ed. Abingdon: Garland Science/ BIOS Scientific Publishers, UK
84. **Roitt, I., Brostoff, J., and Male, D. (1996).** Immunology. Fourth Edition ed: Times Mirror International Publishers Ltd., UK.

85. **MacDonald, H. (1995).** NK1.1+ T cell receptor-alpha/beta+ cells: new clues to their origin, specificity, and function. *J. Exp. Med.* **182:** 633-638

86. **Matsuda, J.L. and Gapin, L. (2005).** Developmental program of mouse Vα14i NKT cells. *Curr. Op. Immunol.* **17:** 122-130

87. **Budd, R., Miescher, G., Howe, R., Lees, R., Bron, C., and MacDonald, H. (1987).** Developmentally regulated expression of T cell receptor beta chain variable domains in immature thymocytes. *J. Exp. Med.* **166:** 577-582

88. **Fowlkes, B.J., Kruisbeek, A.M., Ton-That, H., Weston, M.A., Coligan, J.E., Schwartz, R.H., and Pardoll, D.M. (1987).** A novel population of T-cell receptor αβ-bearing thymocytes which predominantly expresses a single Vβ gene family. *Nature* **329:** 251-254

89. **Ceredig, R., Lynch, F., and Newman, P. (1987).** Phenotypic properties, interleukin 2 production, and developmental origin of a "mature" subpopulation of Lyt-2- L3T4- mouse thymocytes. *Proc. Natl. Acad. Sci. USA* **84:** 8578-8582

90. **Kronenberg, M. (2005).** Toward an understanding of NKT cell biology: progress and paradoxes. *Annu. Rev. Immunol.* **26:** 877-900

91. **Park, Y.-K., Lee, J.-W., Ko, Y.-G., Hong, S., and Park, S.-H. (2005).** Lipid rafts are required for efficient signal transduction by CD1d. *Biochem. Biophys. Res. Comm.* **327:** 1143-1154

92. **Kjer-Nielsen, L., Borg, N.A., Pellicci, D.G., Beddoe, T., Kostenko, L., Clements, C.S., Williamson, N.A., Smyth, M.J., Besra, G.S., Reid, H.H., Bharadwaj, M., Godfrey, D.I., Rossjohn, J., and McCluskey, J. (2006).** A structural basis for selection and cross-species reactivity of the semi-invariant NKT cell receptor in CD1d/glycolipid recognition. *J. Exp. Med.* **203:** 661-673

93. **Shamshiev, A., Gober, H.-J., Donda, A., Mazorra, Z., Mori, L., and De Libero, G. (2002).** Presentation of the same glycolipid by different CD1 molecules. *J. Exp. Med.* **195:** 1013-1021

94. **Wu, D.Y., Segal, N.H., Sidobre, S., Kronenberg, M., and Chapman, P.B. (2003).** Cross-presentation of disialoganglioside GD3 to natural killer T cells. *J. Exp. Med.* **198:** 173-81

95. **Kawano, T., Cui, J., Koezuka, Y., Toura, I., Kaneko, Y., Motoki, K., Ueno, H., Nakagawa, R., Sato, H., Kondo, E., Koseki, H., and Taniguchi, M. (1997).** CD1d-restricted and TCR-mediated activation of Vα14 NKT cells by glycosylceramides. *Science* **278:** 1626-9

96. **Ortaldo, J.R., Young, H.A., Winkler-Pickett, R.T., Bere Jr, E.W., Murphy, W.J., and Wiltrout, R.H. (2004).** Dissociation of NKT stimulation, cytokine induction, and

NK activation *in vivo* by the use of distinct TCR-binding ceramides*. J. Immunol.* **172:** 943-953

97. **Naidenko, O.V., Maher, J.K., Ernst, W.A., Sakai, T., Modlin, R.L., and Kronenberg, M. (1999).** Binding and antigen presentation of ceramide-containing glycolipids by soluble mouse and human CD1d molecules*. J. Exp. Med.* **190:** 1069-1079
98. **Brossay, L., Naidenko, O., Burdin, N., Matsuda, J., Sakai, T., and Kronenberg, M. (1998).** Structural requirements for galactosylceramide recognition by CD1-restricted NK T cells*. J. Immunol.* **161:** 5124-8
99. **Sidobre, S., Hammond, K.J.L., Bénazet-Sidobre, L., Maltsev, S.D., Richardson, S.K., Ndoyne, R.M., Howell, A.R., Sakai, T., Besra, G.S., Porcelli, S.A., and Kronenberg, M. (2004).** The T cell antigen receptor expressed by Vα14*i* NKT cells has a unique mode of glycosphingolipid antigen recognition*. Proc. Natl. Acad. Sci. USA* **101:** 12254-12259
100. **Gadola, S.D., Koch, M., Marles-Wright, J., Lissin, N.M., Shepherd, D., Matulis, G., Harlos, K., Villiger, P.M., Stuart, D.I., Jakobsen, B.K., Cerundolo, V., and Jones, E.Y. (2006).** Structure and binding kinetics of three different human CD1d-α-galactosylceramide-specific T cell receptors*. J. Exp. Med.* **203:** 699-710
101. **Joyce, S. (2001).** CD1d and natural T cells: how their properties jump-start the immune system*. Cellular and Molecular Life Sciences* **58:** 442-469
102. **Hammond, K.J.L. and Kronenberg, M. (2003).** Natural killer T cells: natural or unnatural regulators of autoimmunity? *Curr. Op. Immunol.* **15:** 683-689
103. **Matsuda, J.L., Naidenko, O.V., Gapin, L., Nakayama, T., Taniguchi, M., Wang, C.-R., Koezuka, Y., and Kronenberg, M. (2000).** Tracking the response of natural killer T cells to a glycolipid antigen using CD1d tetramers*. J. Exp. Med.* **192:** 741-753
104. **Kita, H., He, X.-S., and Gershwin, M.E. (2003).** Application of tetramer technology in studies on autoimmune diseases*. Autoimmun. Rev.* **2:** 43-49
105. **Pear, W.S., Tu, L., and Stein, P.L. (2004).** Lineage choices in the developing thymus: choosing the T and NKT pathways*. Curr. Op. Immunol.* **16:** 167-173
106. **Benlagha, K., Weiss, A., Beavis, A., Teyton, L., and Bendelac, A. (2000).** In vivo identification of glycolipid antigen-specific T cells using fluorescent CD1d tetramers*. J. Exp. Med.* **191:** 1895-903
107. **Im, J.S., Yu, K.O.A., Illarionov, P.A., LeClair, K.P., Storey, J.R., Kennedy, M.W., Besra, G.S., and Porcelli, S.A. (2004).** Direct measurement of antigen binding properties of CD1 proteins using fluorescent lipid probes*. J. Biol. Chem.* **279:** 299-310

108. **Stanic, A.K., Shashidharamurthy, R., Bezbradica, J.S., Matsuki, N., Yoshimura, Y., Miyake, S., Young Choi, E., Schell, T.D., Van Kaer, L., Tevethia, S.S., Roopenian, D.C., Yamamura, T., and Joyce, S. (2003).** Another view of T cell antigen recognition: cooperative engagement of glycolipid antigens by Vα14Jα18 natural TCR*. J. Immunol.* **171:** 4539-4551

109. **Burdin, N., Brossay, L., and Kronenberg, M. (1999).** Immunization with alpha-galactosylceramide polarizes CD1-reactive NK T cells towards Th2 cytokine synthesis*. Eur. J. Immunol.* **29:** 2014-25

110. **Bendelac, A., Rivera, M.N., Park, S.H., and Roark, J.H. (1997).** Mouse CD1-specific NK1 T cells: development, specificity, and function*. Annu. Rev. Immunol.* **15:** 535-62

111. **Mercer, J.C., Ragin, M.J., and August, A. (2005).** Natural killer T cells: rapid responders controlling immunity and disease*. Int. J. Biochem. Cell Biol.*

112. **Bommhardt, U., Beyer, M., Hünig, T., and Reichardt, H. (2004).** Molecular and cellular mechanisms of T cell development*. Cell. Mol. Life Sciences* **61:** 263-280

113. **Bezbradica, J.S., Hill, T., Stanic, A.K., Van Kaer, L., and Joyce, S. (2005).** Commitment toward the natural T (iNKT) cell lineage occurs at the CD4+8+ stage of thymic ontogeny*. Proc. Natl. Acad. Sci. USA* **102:** 5114-9

114. **Arase, H., Arase, N., and Saito, T. (1996).** Interferon gamma production by natural killer (NK) cells and NK1.1+ T cells upon NKR-P1 cross-linking*. J. Exp. Med.* **183:** 2391-6

115. **Yang, Y., Ueno, A., Bao, M., Wang, Z., Im, J.S., Porcelli, S., and Yoon, J.-W. (2003).** Control of NKT cell differentiation by tissue-specific microenvironments*. J. Immunol.* **171:** 5913-5920

116. **Nelms, K., Keegan, A.D., Zaoran, J., Ryan, J.J., and Paul, W.E. (1999).** The IL-4 receptor: signaling mechanisms and biologic functions*. Annu. Rev. Immunol.* **17:** 701-738

117. **Van Kaer, L. (2005).** α-Galactosylceramide therapy for autoimmune diseases: prospects and obstacles*. Nat. Rev. Immunol.* **5:** 31-42

118. **Taniguchi, M., Harada, M., Kojo, S., Nakayama, T., and Wakao, H. (2003).** The regulatory role of Vα14 NKT cells in innate and acquired immune response*. Annu. Rev. Immunol.* **21:** 483-513

119. **Harada, M., Seino, K.-i., Wakao, H., Sakata, S., Ishizuka, Y., Ito, T., Kojo, S., Nakayama, T., and Taniguchi, M. (2004).** Down-regulation of the invariant Vα14 antigen receptor in NKT cells upon activation*. Int. Immunol.* **16:** 241-247

120. **Buckner, J.H. and Zielgler, S.F. (2004).** Regulating the immune system: the induction of regulatory T cells in the periphery*. Arthritis Res.Ther.* **6:** 215-222
121. **Shevach, E.M. (2000).** Regulatory T cells in autoimmmunity*. Annu. Rev. Immunol.* **18:** 423-449
122. **Sakaguchi, S., Toda, M., Asano, M., Itoh, M., Morse, S., and Sakaguchi, N. (1996).** T cell-mediated maintenance of natural self-tolerance: its breakdown as a possible cause of various autoimmune diseases*. J. Autoimmun.* **9:** 211-220
123. **Mosmann, T., Cherwinski, H., Bond, M., Giedlin, M., and Coffman, R. (1986).** Two types of murine helper T cell clone. I. Definition according to profiles of lymphokine activities and secreted proteins*. J. Immunol.* **136:** 2348-2357
124. **Jahromi, M., Millward, A., and Demaine, A. (2000).** A CA repeat polymorphism of the IFN-gamma gene is associated with susceptibility to type 1 diabetes*. J. Interferon Cytokine Res.* **20:** 187-190
125. **Szabo, S.J., Sullivan, B.M., Peng, S.L., and Glimcher, L.H. (2003).** Molecular mechanisms regulating T_H1 immune responses*. Annu. Rev. Immunol.* **21:** 713-758
126. **Mosmann, T.R. and Sad, S. (1996).** The expanding universe of T-cell subsets: Th1, Th2 and more*. Immunology Today* **17:** 138-146
127. **Constant, S.L. and Bottomly, K. (1997).** Induction of T_H1 and T_H2 $CD4^+$ responses: the alternative approaches*. Annu. Rev. Immunol.* **15:** 297-322
128. **Kidd, P. (2003).** Th1/Th2 Balance: the hypothesis, its limitations, and implications for health and disease*. Alt. Med. Rev.* **8:** 223-246
129. **Lafaille, J.J. (1998).** The role of helper T cell subsets in autoimmune diseases*. Cytokine Growth Factor Rev.* **9:** 139-51
130. **Pernis, A., Gupta, S., Gollob, K., Garfein, E., Coffman, R., Schindler, C., and Rothman, P. (1995).** Lack of interferon gamma receptor beta chain and the prevention of interferon gamma signaling in TH1 cells*. Science* **269:** 245-247
131. **Wensky, A., Marcondes, M.C., and Lafaille, J.J. (2001).** The role of IFN-gamma in the production of Th2 subpopulations: implications for variable Th2-mediated pathologies in autoimmunity*. J. Immunol.* **167:** 3074-81
132. **Linsen, L., Somers, V., and Stinissen, P. (2005).** Immunoregulation of autoimmunity by natural killer T cells*. Hum. Immunol.* **66:** 1193-1202
133. **Berkers, C.R. and Ovaa, H. (2005).** Immunotherapeutic potential for ceramide-based activators of iNKT cells*. Trends Pharmacol. Sciences* **26:** 252-257
134. **Godfrey, D.I., McCluskey, J., and Rossjohn, J. (2005).** CD1d antigen presentation: treats for NKT cells*. Nat. Immunol.* **6:** 754-756

135. **Mieza, M.A., Itoh, T., Cui, J.Q., Makino, Y., Kawano, T., Tsuchida, K., Koike, T., Shirai, T., Yagita, H., Matsuzawa, A., Koseki, H., and Taniguchi, M. (1996).** Selective reduction of Vα14$^+$ NK T cells associated with disease development in autoimmune-prone mice*. J. Immunol.* **156:** 4035-4040

136. **Wilson, M.T., Johansson, C., Olivares-Villagómez, D., Singh, A.K., Stanic, A.K., Wang, C.-R., Joyce, S., Wick, M.J., and Van Kaer, L. (2003).** The response of natural killer T cells to glycolipid antigens is characterised by surface receptor down-modulation and expansion*. Proc. Natl. Acad. Sci. USA* **100:** 10913-10918

137. **Burdin, N. and Kronenberg, M. (1999).** CD1-mediated immune responses to glycolipids*. Curr. Op. Immunol.* **11:** 326-31

138. **Pearson, C.I. and McDevitt, H.O. (1999).** Redirecting Th1 and Th2 responses in autoimmune disease. *Curr. Top. Microbiol. Immunol.* **238:** 79-122

139. **Singh, N., Hong, S., Scherer, D.C., Serizawa, I., Burdin, N., Kronenberg, M., Koezuka, Y., and Van Kaer, L. (1999).** Cutting Edge: activation of NK T cells by CD1d and α-galactosylceramide directs conventional T cells to the acquisition of a Th2 phenotype*. J. Immunol.* **163:** 2373-2377

140. **Wilson, S.B., Kent, S.C., Patton, K.T., Orban, T., Jackson, R.A., Exley, M., Porcelli, S., Schatz, D.A., Atkinson, M.A., Balk, S.P., Strominger, J.L., and Hafler, D.A. (1998).** Extreme Th1 bias of invariant Vα24JαQT cells in type 1 diabetes*. Nature* **391:** 177-181

141. **Lieberman, S.M. and DiLorenzo, T.P. (2003).** A Comprehensive guide to antibody and T-cell responses in type 1 diabetes*. Tissue Antigens* **62:** 359-377

142. **Dean, L. and McEntyre, J. (2001)** The genetic landscape of diabetes. NCBI Books.

143. **Kelly, M.A., Rayner, M.L., Mijovic, C.H., and Barnett, A.H. (2003).** Molecular aspects of type 1 diabetes*. J. Clin. Pathol.: Mol. Pathol.* **56:** 1-10

144. **Miyamoto, K., Miyake, S., and Yamamura, T. (2001).** A synthetic glycolipid prevents autoimmune encephalomyelitis by inducing T_H2 bias of natural killer T cells*. Nature* **413:** 531-534

145. **Sharif, S., Arreaza, G.A., Zucker, P., Mi, Q.-S., Sondhi, J., Naidenko, O.V., Kronenberg, M., Koezuka, Y., and Delovitch, T.L. (2001).** Activation of natural killer T cells by α-galactosylceramide treatment prevents the onset and recurrence of autoimmune Type 1 diabetes. *Nat. Med.* **7:** 1057-1062

146. **Araujo, L.M., Lefort, J., Nahori, M.A., Diem, S., Zhu, R., Dy, M., Leite-de-Moraes, M.C., Bach, J.F., Vargaftig, B.B., and Herbelin, A. (2004).** Exacerbated Th2-mediated airway inflammation and hyperresponsiveness in autoimmune diabetes-

prone NOD mice: a critical role for CD1d-dependent NKT cells. *Eur. J. Immunol.* **34:** 327-35

147. **Trembleau, S., Penna, G., Bosi, E., Mortara, A., Gately, M.K., and Adorini, L. (1995).** Interleukin 12 administration induces T helper type 1 cells and accelerates autoimmune diabetes in NOD mice. *J. Exp. Med.* **2:** 817-821
148. **Debray-Sachs, M., Carnaud, C., Boitard, C., Cohen, H., Gresser, I., Bedossa, P., and Bach, J.F. (1991).** Prevention of diabetes in NOD mice treated with antibody to murine IFN gamma. *J. Autoimmun.* **4:** 237-48
149. **Shaw, D. (2004)** Searching the Mouse Genome Informatics (MGI) resources for information on mouse biology from genotype to phenotype. *Curr. Protoc. Bioinformatics.* **Chapter 1:** Unit 1.7
150. **Wilson, S.B. and Delovitch, T.L. (2003).** Janus-like role of regulatory iNKT cells in autoimmune disease and tumour immunity. *Nat. Rev. Immunol.* **3:** 211-222
151. **Janeway Jr., C.A., Travers, P., Walport, M., and Shlomchik, M.J. (2001).** Immunobiology : the immune system in health and disease. 5 ed. New York: Garland Publishing.
152. **Sumida, T., Sakamoto, A., Murata, H., Makino, Y., Takahashi, H., Yoshida, S., Nishioka, K., Iwamoto, I., and Taniguchi, M. (1995).** Selective reduction of T cells bearing invariant Vα24JαQ antigen receptor in patients with systemic sclerosis. *J. Exp. Med.* **182:** 1163-1168
153. **Kotzin, B.L. (1996).** Systemic lupus erythematosus: review. *Cell* **85:** 303-306
154. **Pisetsky, D.S., Gilkeson, G., and St. Clair, E.W. (1997).** Systemic lupus erythematosus: diagnosis and treatment. *Med. Clin. North Am.* **81:** 113-129
155. **Sieling, P.A., Porcelli, S.A., Duong, B.T., Spada, F., Bloom, B.R., Diamong, B., and Hahn, B.H. (2000).** Human double-negative T cells in systemic lupus erythematosus provide help for IgH and are restricted by CD1c. *J. Immunol.* **165:** 5338-5344
156. **Oishi, Y., Sumida, T., Sakamoto, A., Kita, Y., Kurasawa, K., Nawata, Y., Takabayashi, K., Takahashi, H., Yoshida, S., Taniguchi, M., Saito, Y., and Iwamoto, I. (2001).** Selective reduction and recovery of invariant Vα24JαQ T cell receptor T cells in correlation with disease activity in patients with systemic lupus erythematosus. *J. Rheum.* **28:** 275-284
157. **Godfrey, D.I. and Kronenberg, M. (2004).** Going both ways: immune regulation via CD1d-dependent NKT cells. *J. Clin. Invest.* **114:** 1379-1388
158. **Singh, R.R. (2005).** SLE: translating lessons from model systems to human disease. *Trends Immunol.* **26:** 572-579

159. **Zeng, D., Liu, Y., Sidobre, S., Kronenberg, M., and Strober, S. (2003).** Activation of natural killer T cells in NZB/W mice induces Th1-type immune responses exacerbating lupus*. J. Clin. Invest.* **112:** 1211-1222

160. **Terabe, M., Matsui, S., Noben-Trauth, N., Chen, H., Watson, C., Donaldson, D.D., Carbone, D.P., Paul, W.E., and Berzofsky, J.A. (2000).** NKT cell-mediated repression of tumor immunosurveillance by IL-13 and the IL-4R-STAT6 pathway*. Nat. Immunol.* **1:** 515-520

161. **Poulton, L.D., Smyth, M.J., Hawke, C.G., Silveira, P., Shepherd, D., Naidenko, O.V., Godfrey, D.I., and Baxter, A.G. (2001).** Cytometric and functional analyses of NK and NKT cell deficiencies in NOD mice*. Int. Immunol.* **13:** 887-896

162. **Naumov, Y.N., Bahjat, K.S., Gausling, R., Abraham, R., Exley, M.A., Koezuka, Y., Balk, S.B., Strominger, J.L., Clare-Salzer, M., and Wilson, S.B. (2001).** Activation of CD1d-restricted T cells protect NOD mice from developing diabetes by regulating dendritic cell subsets*. Proc. Natl. Acad. Sci. USA* **98:** 13838-13843

163. **Wilson, S.B., Kent, S.C., Horton, H.F., Hill, A.A., Bollyky, P.L., Hafler, D.A., Strominger, J.L., and Byrne, M.C. (2000).** Multiple differences in gene expression in regulatory Vα24JαQ T cells from identical twins discordant for type 1 diabetes*. Proc. Natl. Acad. Sci. USA* **97:** 7411-7416

164. **Hong, S., Wilson, M.T., Serizawa, I., Wu, L., Singh, N., Naidenko, O.V., Miura, T., Haba, T., Scherer, D.C., Wei, J., Kronenberg, M., Koezuka, Y., and Van Kaer, L. (2001).** The natural killer T-cell ligand α-galactosylceramide prevents autoimmune diabetes in non-obese diabetic mice*. Nat. Med.* **7:** 1052-1056

165. **Hammond, K.J.L., Poulton, L.D., Palmisano, L.J., Silveira, P.A., Godfrey, D.I., and Baxter, A.G. (1998).** α/β-T cell receptor $(TCR)^+CD4^-CD8^-$ (NKT) thymocytes prevent insulin-dependent diabetes mellitus in nonobese diabetic (NOD)/ Lt mice by the influence of interleukin (IL)-4 and/or IL-10*. J. Exp. Med.* **187:** 1047-1056

166. **Kukreja, A., Cost, G., Marker, J., Zhang, C., Sun, Z., Lin-Su, K., Ten, S., Sanz, M., Exley, M., Wilson, B., Porcelli, S., and Maclaren, N. (2002).** Multiple immuno-regulatory defects in type-1 diabetes*. J. Clin. Invest.* **109:** 131-140

167. **van der Vliet, H.J.J., von Blomberg, B.M.E., Nishi, N., Reijm, M., Voskuyl, A.E., van Bodegraven, A.A., Polman, C.H., Rustemeyer, T., Lips, P., van den Eertwegh, A.J.M., Giaccone, G., Scheper, R.J., and Pinedo, H.M. (2001).** Rapid communication: circulating $V\alpha24^+$ $V\beta11^+$ NKT cell numbers are decreased in a wide variety of diseases that are characterized by autoreactive tissue damage*. Clin. Immunol.* **100:** 144-148

168. **Wang, B., Geng, Y.-B., and Wang, C.-R. (2001).** CD1-restricted NK T cells protect nonobese diabetic mice from developing diabetes*. J. Exp. Med.* **194:** 313-319

169. **Takeda, K. and Dennert, G. (1993).** The development of autoimmunity in C57BL/6 *lpr* mice correlates with the disappearance of natural killer type 1-positive cells: evidence for their suppressive action on bone marrow stem cell proliferation, B cell immunoglobulin secretion, and autoimmune symptoms*. J. Exp. Med.* **177:** 155-164

170. **Kojo, S., Adachi, Y., Keino, H., Taniguchi, M., and Sumida, T. (2001).** Dysfunction of T cell receptor AV24AJ18+,BV11+ double-negative regulatory natural killer T cells in autoimmune diseases*. Arthritis & Rheumatism* **44:** 1127-1138

171. **Jahng, A., Maricic, I., Aguilera, C., Cardell, S., Halder, R.C., and Kumar, V. (2003).** Prevention of autoimmunity by targeting a distinct, noninvariant CD1d-reactive T cell population reactive to sulfatide*. J. Exp. Med.* **199:** 947-957

172. **Lee, P.T., Putnam, A., Benlagha, K., Teyton, L., Gottlieb, P.A., and Bendelac, A. (2002).** Testing the NKT cell hypothesis of human IDDM pathogenesis*. J. Clin. Invest.* **110:** 793-800

173. **Laloux, V., Beaudoin, L., Jeske, D., Carnaud, C., and Lehuen, A. (2001).** NK T cell-induced protection against diabetes in Vα14-Jα281 transgenic nonobese diabetic mice is associated with a Th2 shift circumscribed regionally to the islets and functionally to islet autoantigen*. J. Immunol.* **166:** 3749-3756

174. **Yang, Y. and Santamaria, P. (2004).** T-cell receptor-transgenic NOD mice; a reductionist approach to understand autoimmune diabetes*. J. Autoimmun.* **22:** 121-129

175. **Rogers, P.R., Matsumoto, A., Naidenko, O., Kronenberg, M., Mikayama, T., and Kato, S. (2004).** Expansion of human Vα24$^+$ NKT cells by repeated stimulation with KRN7000*. J. Immunol. Methods* **285:** 197-214

176. **Mattner, J., Debord, K.L., Ismail, N., Goff, R.D., Cantu, C., 3rd, Zhou, D., Saint-Mezard, P., Wang, V., Gao, Y., Yin, N., Hoebe, K., Schneewind, O., Walker, D., Beutler, B., Teyton, L., Savage, P.B., and Bendelac, A. (2005).** Exogenous and endogenous glycolipid antigens activate NKT cells during microbial infections*. Nature* **434:** 525-9

177. **Xing, G.-W., Wu, D., Poles, M.A., Horowitz, A., Tsuji, M., Ho, D.D., and Wong, C.-H. (2005).** Synthesis and human NKT cell stimulating properties of 3-*O*-sulfo-α/β-galactosylceramides*. Bioorg. Med. Chem.* **13:** 2907-2916

178. **Zajonc, D.M., Maricic, I., Wu, D., Halder, R., Roy, K., Wong, C.-H., Kumar, V., and Wilson, I.A. (2005).** Structural basis for CD1d presentation of a sulfatide derived from myelin and its implications for autoimmunity*. J. Exp. Med.* **202:** 1517-1526

179. **Wu, D., Xing, G.W., Poles, M.A., Horowitz, A., Kinjo, Y., Sullivan, B., Bodmer-Narkevitch, V., Plettenburg, O., Kronenberg, M., Tsuji, M., Ho, D.D., and Wong, C.H. (2005).** Bacterial glycolipids and analogs as antigens for CD1d-restricted NKT cells*. Proc. Natl. Acad. Sci. USA* **102:** 1351-6

180. **Wu, D., Zajonc, D.M., Fujio, M., Sullivan, B.A., Kinjo, Y., Kronenberg, M., Wilson, I.A., and Wong, C.-H. (2006).** Design of natural killer T cell activators: structure and function of a microbial glycosphingolipid bound to mouse CD1d*. Proc. Natl. Acad. Sci. USA* **103:** 3972-3977

181. **Carnaud, C., Lee, D., Donnars, O., Park, S.-H., Beavis, A., Koezuka, Y., and Bendelac, A. (1999).** Cross-talk between cells of the innate immune system: NKT cells rapidly activate NK cells*. J. Immunol.* **163:** 4647-4650

182. **Tupin, E., Nicoletti, A., Elhage, R., Rudling, M., Ljunggren, H.-G., Hansson, G.K., and Paulsson Berne, G. (2004).** CD1d-dependent activation of NKT cells aggravates atherosclerosis*. J. Exp. Med.* **199:** 417-422

183. **Roep, B.O. (2003).** The role of T-cells in the pathogenesis of type 1 diabetes: from cause to cure*. Diabetologia* **46:** 305-321

184. **Sakai, T., Naidenko, O.V., Iijima, H., Kronenberg, M., and Koezuka, Y. (1999).** Syntheses of biotinylated α-galactosylceramides and their effects on the immune system and CD1 molecules*. J. Med. Chem.* **42:** 1836-1841

185. **Sakai, T., Morita, M., Matsunaga, N., Akimoto, K., Yokoyama, T., Iijima, H., and Koezuka, Y. (1999).** Effects of 3α- and 3β-galactosylated α-galactosylceramides on the immune system*. Bioorg. Med. Chem. Letts.* **9:** 697-702

186. **Baumruker, T. and Prieschl, E.E. (2002).** Sphingolipids and the regulation of the immune response*. Semin. Immunol.* **14:** 57-63

187. **Ito, Y., Tamiya-Koizumi, K., Koide, Y., Nakagawa, M., Kawade, T., Nishida, A., Murate, T., Takemura, M., Suzuki, M., and Yoshida, S. (2001).** Structural requirements of sphingosine molecules for inhibition of DNA primase: biochemical and computational analyses*. Biochemistry* **40:** 11571-11577

188. **De Libero, G., Moran, A.P., Gober, H.-J., Rossy, E., Shamshiev, A., Chelnokova, O., Mazorra, Z., Vendetti, S., Sacchi, A., Prendergast, M.M., Sansano, S., Tonevitsky, A., Landmann, R., and Mori, L. (2005).** Bacterial infections promote T cell recognition of self-glycolipids*. Immunity* **22:** 763-772

189. **Kolter, T. and Sandhoff, K. (1999).** Sphingolipids- their metabolic pathways and the pathobiochemistry of neurodegenerative diseases*. Angew. Chem. Int. Ed.* **38:** 1532-1568

190. **Yamamura, T., Miyamoto, K., Illes, Z., Pal, E., Araki, M., and Miyake, S. (2004).** NKT cell-stimulating synthetic glycolipids as potential therapeutics for autoimmune disease*. Curr. Top. Med. Chem.* **4:** 561-567

191. **Hermans, I.F., Silk, J.D., Gileadi, U., Salio, M., Mathew, B., Ritter, G., Schmidt, R., Harris, A.L., Old, L., and Cerundolo, V. (2003).** NKT cells enhance $CD4^+$ and $CD8^+$ T cell responses to soluble antigen *in vivo* through direct interaction with dendritic cells*. J. Immunol.* **171:** 5140-5147

192. **Oki, S., Chiba, A., Yamamura, T., and Miyake, S. (2004).** The clinical implication and molecular mechanism of preferential IL-4 production by modified glycolipid-stimulated NKT cells*. J. Clin. Invest.* **113:** 1631-1640

193. **Chiba, A., Oki, S., Miyamoto, K., Hashimoto, H., Yamamura, T., and Miyake, S. (2004).** Suppression of collagen-induced arthritis by natural killer T cell activation with OCH, a sphingosine-truncated analog of alpha-galactosylceramide*. Arthritis Rheum.* **50:** 305-13

194. **Lin, C.-C., Fan, G.-T., and Fang, J.-M. (2003).** A concise route to phytosphingosine from lyxose*. Tet. Lett.* **44:** 5281-5283

195. **Greene, T.W. and Wuts, P.G.M. (1999).** Protective groups in organic synthesis. Third ed: John Wiley & Sons, Inc.

196. **Reich, H.J. (2002).** Lithium Amide Bases-A Primer. A-7.

197. **Stock, L.M. (1988)** Studies of coupled chemical and catalytic coal conversion methods. University of Chicago, USA

198. **Plettenburg, O., Bodmer-Narkevitch, V., and Wong, C.-H. (2002).** Synthesis of α-galactosyl ceramide, a potent immunostimulatory agent*. J. Org. Chem.* **67:** 4559-4564

199. **Pagano, R.E. and Martin, O.C. (1988).** A series of fluorescent *N*-acylsphingosines: synthesis, physical properties, and studies in cultured cells*. Biochem.* **27:** 4439-4445

200. **Allmendinger, T., Dandois, C., and Walliser, B. (1991).** The hydrogenation of fluoroolefins*. Tet. Lett.* **32:** 2735-2736

201. **De Jonghe, S., Van Overmeire, I., Gunst, J., De Bruyn, A., Hendrix, C., Van Calenbergh, S., Busson, R., De Keukeleire, D., Philippé, J., and Herdewijn, P. (1999).** Synthesis and apoptogenic of fluorinated ceramide and dihydroceramide analogues*. Bioorg. Med. Chem. Letts.* **9:** 3159-3164

202. **Buchanan, G.W., Smits, R., and Munteanu, E. (2003).** Synthesis of a highly fluorinated fatty acid analog*. J. Fluor. Chem.* **119:** 207-209

203. **Pearson, D.E. and Buehler, C.A. (1974).** Potassium-*tert*-butoxide in Ssnthesis*. Chem. Reviews* **74:** 45-86

204. **McEwen, W.K. (1936).** A further study of extremely weak acids*. J. Am. Chem. Soc.* **58:** 1124-1129
205. **Reeves, R.R. (1985).** Recovery of alcohols. **US Patent 4594466**
206. **Flessner, T. and Doye, S. (1999).** Cesium carbonate: a powerful inorganic base in organic synthesis*. J. Prakt. Chem* **341:** 186-190
207. **Yamanoi, T., Akiyama, T., Ishida, E., Abe, H., Amemiya, M., and Inazu, T. (1989).** Horner-Wittig reaction of dimethyl 2,3-*O*-isopropylidene-D-glyceroylmethylphosphonate and its application to the formal synthesis of D-*erythro*-C_{18}-sphingosine*. Chem. Letts***:** 335-336
208. **Rauch, J., Gumperz, J., Robinson, C., Skölds, M., Roy, C., Young, D.C., Lafleur, M., Moody, D.B., Brenner, M.B., Costello, C.E., and Behar, S.M. (2003).** Structural features of the acyl chain determine self-phospholipid antigen recognition by a CD1d-restricted invariant NKT (iNKT) cell*. J. Biol. Chem.* **278:** 47508-47515
209. **Pasto, D.J. and Taylor, R.T. (1991).** Reduction with diimide, in organic reactions, John Wiley & Sons, Inc.: NY. p. 91-155.
210. **Hünig, S., Müller, H.R., and W, T. (1965).** The chemistry of diimine*. Angew Chem Int Ed* **4:** 271-382
211. **Hoffman jr, J. and Schlessinger, R. (1971).** Sodium metaperiodate: a mild oxidizing agent for the generation of di-imide from hydrazine*. J. Chem. Soc. D: Chem. Comms.***:** 1245-1246
212. **Hünig, S., Müller, H.R., and W, T. (1965).** The chemistry of diimine*. Angew. Chem. Int. Ed.* **4:** 271-382
213. **Cusack, N.J., Reese, C.B., Risius, A.C., and Roozpeikar, B. (1976).** 2,4,6-Tri-isopropylbenzenesulphonyl Hydrazide: A Convenient Source of Di-imide*. Tetrahedron.* **32:** 2157-2162
214. **Knight, D.W. and Sibley, A.W. (1997).** Total synthesis of (-)-slaframine from (2*R*,3*S*)-3-hydroxyproline*. J. Chem. Soc. Perkin Trans. 1***:** 2179-2187
215. **Nyffeler, P.T., Liang, C.-H., Koeller, K.M., and Wong, C.-H. (2002).** The chemistry of amine-azide interconversion: catalytic diazotransfer and regioselective azide reduction*. J. Am. Chem. Soc.* **124:** 10773-10778
216. **Timmer, M.S.M., Risseeuw, M.D.P., Verdoes, M., Filippov, D.V., Plaisier, J.R., van der Marel, G.A., Overkleeft, H.S., and van Boom, J.H. (2005).** Synthesis of functionalized heterocycles via a tandem Staudinger/aza-Wittig/Ugi multicomponent reaction*. Tet. Asym.* **16:** 177-185
217. **Du, W. and Gervay-Hague, J. (2005).** Efficient synthesis of α-galactosyl ceramide analogues using glycosyl iodide donors*. Org. Lett.* **7:** 2063-2065

218. **McCarthy, C., Shepherd, D., Fleire, S., Stronge, V.S., Koch, M., Illarionov, P.A., Bossi, G., Salio, M., Denkberg, G., Reddington, F., Tarlton, A., Reddy, B.G., Schmidt, R.R., Reiter, Y., Griffiths, G.M., van der Merwe, P.A., Besra, G.S., Jones, E.Y., Batista, F.D., and Cerundolo, V. (2007).** The length of lipids bound to human CD1d molecules modulates the affinity of NKT cell TCR and the threshold of NKT cell activation*. J. Exp. Med.* **204:** 1131-1144

219. **Burdin, N., Brossay, L., Degano, M., Iijima, H., Gui, M., Wilson, I.A., and Kronenberg, M. (2000).** Structural requirements for antigen presentation by mouse CD1*. Proc. Natl. Acad. Sci. USA* **97:** 10156-10161

220. **Sidobre, S., Naidenko, O.V., Sim, B.-C., Gascoigne, N.R.J., Garcia, K.C., and Kronenberg, M. (2002).** The Vα14 NKT cell TCR exhibits high-affinity binding to a glycolipid/CD1d complex*. J. Immunol.* **169:** 1340-1348

221. **Prigozy, T.I., Naidenko, O., Qasba, P., Elewaut, D., Brossay, L., Khurana, A., Natori, T., Koezuka, Y., Kulkarni, A., and Kronenberg, M. (2001).** Glycolipid antigen processing for presentation by CD1d molecules*. Science* **291:** 664-667

222. **Liu, Y., Goff, R.D., Zhou, D., Mattner, J., Sullivan, B.A., Khurana, A., Cantu III, C., Ravkov, E.V., Ibegbu, C.C., and Altman, J.D. (2006).** A modified α-galactosyl ceramide for staining and stimulating natural killer T cells*. Journal of Immunological Methods* **312:** 34-39

223. **Uchimura, A., Shimizu, T., Morita, M., Ueno, H., Motoki, K., Fukushima, H., Natori, T., and Koezuka, Y. (1997).** Immunostimulatory activities of monoglycosylated α-D-pyranosylceramides*. Bioorg. Med. Chem.* **5:** 2245-2249

224. **Costantino, V., Fattorusso, E., Mangoni, A., Di Rosa, M., and Ianaro, A. (1997).** Glycolipids from sponges. 6. Plakoside A and B, two unique prenylated glycosphingolipids with immunosuppressive activity from the marine sponge *Plakortis simplex. J. Am. Chem. Soc.* **119:** 12465-12470

225. **Motoki, K., Kobayahi, E., and Uchida, T. (1995).** Antitumor activities of α-, β-monogalactosylceramides and four diastereomers of an α-galactosylceramide*. Bioorg. Med. Chem. Letts.* **5:** 705-710

226. **Motoki, K., Morita, M., Kobayashi, E., Uchida, T., Akimoto, K., Fukushima, H., and Koezuka, Y. (1995).** Immunostimulatory and antitumor activities of monoglycosylceramides having various sugar moieties*. Biol. Pharm. Bull.* **18:** 1487-1491

227. **Singh, A.K., Wilson, M.T., Hong, S., Olivares-Villagomez, D., Du, C., Stanic, A.K., Joyce, S., Sriram, S., Koezuka, Y., and Van Kaer, L. (2001).** Natural killer T

cell activation protects mice against experimental autoimmune encephalomyelitis. *J. Exp. Med.* **194:** 1801-1811

228. **Kawano, T., Cui, J., Koezuka, Y., Toura, I., Kaneko, Y., Motoki, K., Ueno, H., Nakagawa, R., Sato, H., Kondo, E., Koseki, H., and Taniguchi, M. (1997).** CD1d-restricted and TCR-mediated activation of V_α14 NKT cells by glycosylceramides. *Science* **278:** 1626-1629
229. **Roeske-Nielsen, A., Fredman, P., Mansson, J.E., Bendtzen, K., and Buschard, K. (2004).** Beta-galactosylceramide increases and sulfatide decreases cytokine and chemokine production in whole blood cells. *Immunol. Lett.* **91:** 205-211
230. **Bruun, J.M., Roeske-Nielsen, A., Richelsen, B., Fredman, P., and Buschard, K. (2007).** Sulfatide increases adiponectin and decreases TNF-α, IL-6, and IL-8 in human adipose tissue in vitro. *Molecular and Cellular Endocrinology* **263:** 142-148
231. **Fais, F., Morabito, F., Stelitano, C., Callea, V., Zanardi, S., Scudeletti, M., Varese, P., Ciccone, E., and Grossi, C.E. (2004).** CD1d is expressed on B-chronic lymphocytic leukemia cells and mediates alpha-galactosylceramide presentation to natural killer T lymphocytes. *Int. J. Cancer.* **109:** 402-11
232. **Morita, M., Natori, T., Akimoto, K., Osawa, T., Fukushima, H., and Koezuka, Y. (1995).** Syntheses of α-, β-monoglycosylceramides and four diastereomers of an α-galactosylceramide. *Bioorg. Med. Chem. Letts.* **5:** 699-704
233. **Yang, G., Schmieg, J., Tsuji, M., and Franck, R.W. (2004).** The C-glycoside analogue of the immunostimulant α-galactosylceramide (KRN7000): synthesis and striking enhancement of activity. *Angew. Chem. Int. Ed.* **43:** 3818-3822
234. **Schmieg, J., Yang, G., Franck, R.W., and Tsuji, M. (2003).** Superior protetion against malaria and melanoma metastases by a *C*-glycoside analogue of the natural killer T cell ligand α-galacatosylceramide. *J. Exp. Med.* **198:** 1631-1641
235. **Davies, G.J., Gloster, T.M., and Henrissat, B. (2005).** Recent structural insights into the expanding world of carbohydrate-active enzymes. *Current Opinion in Structural Biology: Catalysis and regulation/Proteins* **15:** 637-645
236. **Lu, X., Song, L., Metelitsa, L.S. and Bittman, R. (2006).** Synthesis and Evaluation of an α-*C*-Galactosylceramide Analogue that Induces Th1-biased Responses in Human Natural Killer T Cells. *Chem. Bio. Chem.* **7:** 1750-1756
237. **Costantino, V., Fattorusso, E., Mangoni, A., Rosa, M.D., Ianaro, A., and Maffia, P. (1996).** Glycolipids from sponges. IV. Immunomodulating glycosyl ceramides from the marine sponge *agelas dispar*. *Tet.* **52:** 1573-1578
238. **Zhou, X.-T., Forestier, C., Goff, R.D., Li, C., Teyton, L., Bendelac, A., and Savage, P.B. (2002).** Synthesis and NKT cell stimulating properties of fluorophore-

and biotin-appended 6' '-amino-6' '-deoxy-galactosylceramides. *Org. Lett.* **4:** 1267-1270

239. **Flowers, H.M. (1981).** Chemistry and biochemistry of D- and L-fucose. *Adv. Carb. Chem. Biochem.* **39:** 279-345
240. **Jerud, E.S. (2006).** α-Fucosylceramide: characterization of the first reported antagonist/partial agonist of NKT cells in an NZB/W F1 lupus model. Meeting of Medical Fellows: Research Training Fellowships for Medical Students. HHMI Headquarters and conference center, Chevy Chase, Maryland, USA: Howard Hughes Medical Institute.
241. **Kim, J.H., Yang, H., Park, J., and Boons, G.-J. (2005).** A general strategy for stereoselective glycolsylations. *J Am Chem Soc* **127:** 12090-12097
242. **Paulsen, H. (1982).** Advances in selective chemical syntheses of complex oligosaccharides. *Angew. Chem. Int. Ed.* **21:** 155-173
243. **Schmid, U. and Waldmann, H. (1997).** *O*-Glycoside synthesis with glycosyl iodides under neutral conditions in 1 M $LiClO_4$ in CH_2Cl_2. *Liebigs. Ann.* **1997:** 2573-2577
244. **Bickley, J., Cottrell, J.A., Ferguson, J.R., Field, R.A., Harding, J.R., Hughes, D.L., Ravindanathan Kartha, K.P., Law, J.L., Scheinmann, F., and Stachulski, A.V. (2003).** Preparation, X-ray structure and reactivity of a stable glycosyl iodide. *Chem. Commun.* **2003:** 1266-1267
245. **Kartha, K.P.R., Aloui, M., and Field, R.A. (1996).** Iodine: A versatile reagent in carbohydrate chemistry III. Efficient activation of glycosyl halides in combination with DDQ. *Tet. Lett.* **37:** 8807-8810
246. **Lam, S.N. and Gervay-Hague, J. (2002).** Solution- and solid-phase oligosaccharide synthesis using glycosyl iodides: a comparative study. *Carbohydr. Res.* **337:** 1953-1965
247. **Hadd, M.J. and Gervay, J. (1999).** Glycosyl iodides are highly efficient donors under neutral conditions. *Carbohydr. Res.* **320:** 61-69
248. **Lemieux, R.U. and Hayami, J.-I. (1965).** The mechanism of the anomerization of the tetra-*O*-acetyl-D-glucopyranosyl chlorides. *Can. J. Chem.* **43:** 2162-2173
249. **Lemieux, R.U., Hendricks, K.B., Stick, R.V., and James, K. (1975).** Halide ion catalyzed glycosidation reactions. Syntheses of α-linked disaccharides. *J. Am. Chem. Soc.* **97:** 4056-4062
250. **Gervay, J. and Hadd, M.J. (1997).** Anionic additions to glycosyl iodides: highly stereoselective syntheses of *C*-, *N*-, and *O*-glycosides. *J. Org. Chem.* **62:** 6961-6967

251. **van Well, R.M., Kartha, R.K.P., and Field, R.A. (2005).** Iodine promoted glycosylation with glycosyl iodides: α-glycoside synthesis. *J. Carb. Chem.* **24:** 463-474
252. **Becker, D.J. and Lowe, J.B. (2003).** Fucose: biosynthesis and biological function in mammals. *Glycobiology* **13:** 41R-53
253. **Boons, G.-J. (1996).** Strategies in oligosaccharide synthesis. *Tet.* **52:** 1095-1121
254. **Uchiyama, T. and Hindsgaul, O. (1996).** Per-*O*-trimethylsilyl-α-L-fucopyranose iodide: a novel glycosylating agent for terminal α-L-fucosylation. *Synlett*. 499-501
255. **Brigl, M., van den Elzen, P., Chen, X., Meyers, J.H., Wu, D., Wong, C.-H., Reddington, F., Illarianov, P.A., Besra, G.S., Brenner, M.B., and Gumperz, J.E. (2006).** Conserved and heterogeneous lipid antigen specificities of CD1d-restricted NKT cell receptors. *J. Immunol.* **176:** 3625-3634
256. **Brossay, L., Tangri, S., Bix, M., Cardell, S., Locksley, R., and Kronenberg, M. (1998).** Mouse CD1-autoreactive T cells have diverse patterns of reactivity to CD1+ targets. *J. Immunol.* **160:** 3681-8
257. **Chiu, Y.H., Jayawardena, J., Weiss, A., Lee, D., Park, S.H., Dautry-Varsat, A., and Bendelac, A. (1999).** Distinct subsets of CD1d-restricted T cells recognize self-antigens loaded in different cellular compartments. *J. Exp. Med.* **189:** 103-10
258. **Spada, F.M., Koezuka, Y., and Porcelli, S.A. (1998).** CD1d-restricted recognition of synthetic glycolipid antigens by human natural killer T cells. *J. Exp. Med.* **188:** 1529-34
259. **Giabbai, B., Sidobre, S., Crispin, M.D.M., Sanchez-Ruiz, Y., Bachi, A., Kronenberg, M., Wilson, I.A., and Degano, M. (2005).** Crystal structure of mouse CD1d bound to the self ligand phosphatidylcholine: a molecular basis for NKT cell activation. *J. Immunol.* **175:** 977-984
260. **Zajonc, D.M., Cantu, C., Mattner, J., Zhou, D., Savage, P.B., Bendelac, A., Wilson, I.A., and Teyton, L. (2005).** Structure and function of a potent agonist for the semi-invariant natural killer T cell receptor. *Nat. Immunol.* **6:** 810-818
261. **Wilson, I.A. (1996).** Another twist to MHC-peptide recognition. *Science* **272:** 973-974
262. **Wilson, I.A. and Christopher Garcia, K. (1997).** T-cell receptor structure and TCR complexes. *Current Opinion in Structural Biology* **7:** 839-848
263. **Sakai, T., Ehara, H., and Koezuka, Y. (1999).** Synthesis of NBD-α-galactosylceramide and its immunologic properties. *Org. Letts.* **1:** 359-361

264. **Vo-Hoang, Y., Micouin, L., Ronet, C., Gachelin, G., and Bonin, M. (2003).** Total enantioselective synthesis and *in vivo* biological evaluation of a novel fluorescent BODIPY α-galactosylceramide*. Chem. Bio. Chem.* **4:** 27-33

265. **Ghidoni, R., Sala, G., and Giuliani, A. (1999).** Use of sphingolipid analogs: benefits and risks*. Biochemica et Biophysica Acta* **1439:** 17-39

266. **Yu, K.O., Im, J.S., Molano, A., Dutronc, Y., Illarionov, P.A., Forestier, C., Fujiwara, N., Arias, I., Miyake, S., Yamamura, T., Chang, Y.T., Besra, G.S., and Porcelli, S.A. (2005).** Modulation of CD1d-restricted NKT cell responses by using N-acyl variants of alpha-galactosylceramides*. Proc. Natl. Acad. Sci. USA* **102:** 3383-8

267. **Morrow, M.R., Singh, D., and Grant, C.W.M. (1995).** Glycosphingolipid acyl chain order profiles: substituent effects*. Biochem. Biophys. Acta.* **1235:** 239-248

268. **Hermans, I.F., Silk, J.D., Yang, J., Palmowski, M.J., Gileadi, U., McCarthy, C., Salio, M., Ronchese, F., and Cerundolo, V. (2004).** The VITAL assay: a versatile fluorometric technique for assessing CTL- and NKT-mediated cytotoxicity against multiple targets in vitro and in vivo*. J. Immunol. Methods* **285:** 25-40

269. **Moody, D.B., Briken, V., Cheng, T.-Y., Roura-Mir, C., Guy, M.R., Geho, D.H., L, T.M., Besra, G.S., and Porcelli, S.A. (2002).** Lipid length controls antigen entry into endosomal and nonendosomal pathways for CD1b presentation*. Nat. Immunol.* **3:** 435-442

270. **Park, J.-J., Kang, S.-J., De Silva, A.D., Stanic, A.K., Casorati, G., Hachey, D.L., Cresswell, P., and Joyce, S. (2004).** Lipid-protein interactions: Biosynthetic assembly of CD1 with lipids in the endoplasmic reticulum is evolutionarily conserved*. Proc. Natl. Acad. Sci. USA* **101:** 1022-1026

271. **Rauch, J., Gumperz, J., Robinson, C., Skold, M., Roy, C., Young, D.C., Lafleur, M., Moody, D.B., Brenner, M.B., Costello, C.E., and Behar, S.M. (2003).** Structural features of the acyl chain determine self-phospholipid antigen recognition by a CD1d-restricted invariant NKT (iNKT) cell*. J. Biol. Chem.* **278:** 47508-47515

272. **Forestier, C., Takaki, T., Molano, A., Im, J.S., Baine, I., Jerud, E.S., Illarionov, P., Ndonye, R., Howell, A.R., Santamaria, P., Besra, G.S., DiLorenzo, T.P., and Porcelli, S.A. (2007).** Improved outcomes in NOD mice treated with a novel Th2 cytokine-biasing NKT cell activator*. J. Immunol.* **178:** 1415-1425

273. **Griffith Cima, L. (1994).** Polymer substrates for controlled biological interactions*. J. Cell. Biochem.* **56:** 155-161

274. **Harris, J.M. and Zalipsky, S. (1992).** Polyethylene Glycol Chemistry: biotechnical and biomedical applications. Springer books, USA.

275. **Veronese, F.M. and Pasut, G. (2005).** PEGylation, successful approach to drug delivery. *Drug Discovery Today* **10:** 1451-1458

276. **Hammarstrom, S. (1971).** A convenient procedure for the synthesis of ceramides. *J. Lipid Res.* **12:** 760-765

277. **Heidlas, J.E., Lees, W.J., Pale, P., and Whitesides, G.M. (1992).** Gram-scale synthesis of uridine 5'-diphospho-N-acetylglucosamine: comparison of enzymic and chemical routes. *J. Org. Chem.* **57:** 146-151

278. **Lazarevic, D. and Thiem, J. (2002).** Syntheses of unnatural N-substituted UDP-galactosamines as alternative substrates for N-acetylgalactosaminyl transferases. *Carbohydr. Res.* **337:** 2187-2194

279. **Ong, D.E. and Brady, R.N. (1972).** Synthesis of ceramides using N-hydroxysuccinimide esters. *J. Lipid Res.* **13:** 819-822

280. **Shaw, D. (2004).** Searching the Mouse Genome Informatics (MGI) resources for information on mouse biology from genotype to phenotype. *Curr. Protoc. Bioinformatics.* **1:** 1.7

281. **Zajonc, D.M., Ainge, G.D., Painter, G.F., Severn, W.B., and Wilson, I.A. (2006).** Structural characterization of mycobacterial phosphatidylinositol mannoside binding to mouse CD1d. *J. Immunol.* **177:** 4577-4583

282. **Motoki, K. (2003).** *Composition for enhancing cellular immunogenicity comprising α-glycosylceramides*. **US 6,555,372 B1**

283. **Hobley, G., Stuttle, k., and Wills, M. (2003).** Studies of intramolecular alkylidene carbene reactions; an approah to heterocyclic nucleoside bases. *Tetrahedron* **59:** 4739-4748

284. **Yamamoto, T., Teshima, T., Saitoh, U., Hoshi, M., and Shiba, T. (1994).** Synthesis of ganglioside M5 from sea urchin egg. *Tet. Lett.* **35:** 2701-2704

285. **Bhat, A.S. and Gervay-Hague, J. (2001).** Efficient syntheses of β-cyanosugars using glycosyl iodides derived from per-*O*-silylated mono- and disaccharides. *Org. Lett.* **3:** 2081-2084

286. **Akimoto, K., Natori, T., and Morita, M. (1993).** Synthesis and stereochemistry of agelasphin-9b. *Tet. Lett.* **34:** 5593-5596

287. **Lapidot, Y., Rappoport, S., and Wolman, Y. (1967).** Use of esters of N-hydroxysuccinimide in the synthesis of N-acylamino acids. *J. Lipid Res.* **8:** 142-145

288. **Figueroa-Perez, S. and Schmidt, R.R. (2000).** Total synthesis of α-galactosyl cerebroside. *Carbohydr. Res.* **328:** 95-102

289. **Mitaku, S., Skaltsounis, A.-L., Tillequin, F., Koch, M., Rolland, Y., Pierre, A., and Atassi, G. (1996).** Synthesis and Anti-proliferative Activity of 2-Hydroxy-1,2-dihydroacronycine Glycosides. *Pharm. Res* **13:** 939-943

290. **Roberts, D.W., Williams, D.L., and Bethell, D. (1985).** Relative reactivity studies for olefin sulphonation with sulphur trioxide in Dichloromethane: evidence for concerted [2_s +2_s] cycloaddition. *J. Chem. Soc. Perkin Trans. 2* **3:** 389-394

291. **de la Fuente, J.M. and Penadés, S. (2002).** Synthesis of Le^x-neoglycoconjugate to study carbohydrate-carbohydrate associations and its intramolecular interaction. *Tet.: Asym.* **13:** 1879-1888

292. **Gadola, S.D., Dulphy, N., Salio, M., and Cerundolo, V. (2002).** Vα24-JαQ-independent, CD1d-restricted recognition of α-galactosylceramide by human CD4(+) and CD8$\alpha\beta$(+) T lymphocytes. *J. Immunol.* **168:** 5514-20

293. **Dunbar, P.R., Ogg, G.S., Chen, J., Rust, N., van der Bruggen, P., and Cerundolo, V. (1998).** Direct isolation, phenotyping and cloning of low-frequency antigen-specific cytotoxic T lymphocytes from peripheral blood. *Current Biology* **8:** 413-416

294. **Karadimitris, A., Gadola, S., Altamirano, M., Brown, D., Woolfson, A., Klenerman, P., Chen, J.-L., Koezuka, Y., Roberts, I.A.G., Price, D.A., Dusheiko, G., Milstein, C., Fersht, A., Luzzatto, L., and Cerundolo, V. (2001).** From the Cover: Human CD1d-glycolipid tetramers generated by in vitro oxidative refolding chromatography. *Proc. Natl. Acad. Sci. USA* **98:** 3294-3298

295. **Boulter, J.M., Glick, M., Todorov, P.T., Baston, E., Sami, M., Rizkallah, P., and Jakobsen, B.K. (2003).** Stable, soluble T cell receptor molecules for crystallization and therapeutics. *Protein Engineering* **16:** 707-711

296. **Willcox, B.E., Gao, G.F., Wyer, J.R., Ladbury, J.E., Bell, J.I., Jakobsen, B.K., and van der Merwe, P.A. (1999).** TCR binding to peptide-MHC stabilizes a flexible recognition interface. *Immunity* **10:** 357-365

297. **Jones, T.A., Zou, J.Y., Cowan, S.W., and Kjeldgaard, M. (1991).** Improved methods for building protein models in electron density maps and the location of errors in these models. *Acta. Crystallogr. A.* **47:** 110-119

298. **Lu, X., Song, L., Metelitsa, L.S., and Bittman, R. (2006).** Synthesis and evaluation of an α-*C*-galactosylceramide analogue that induces Th1-biased responses in human natural killer T cells. *ChemBioChem* **7:** 1750-1756